Synthetic Applications of Lithium(trimethylsilyl)diazomethane and Design of Fluorophores for Microscopy

BY

MATTHEW J. O'CONNOR

B.S., Northern Illinois University, DeKalb, Illinois, 2007

M.S., Northern Illinois University, DeKalb, Illinois, 2010

THESIS

Submitted as partial fulfillment of the requirements
for the degree of Doctor of Philosophy in Chemistry
in the Graduate College of the
University of Illinois at Chicago, 2016

Chicago, Illinois

Defense Committee: Daesung Lee, Advisor and Chair, Chemistry
Vladimir Gevorgyan, Chemistry
Duncan Wardrop, Chemistry
Justin Mohr, Chemistry
Karol Bruzik, Medicinal Chemistry and Pharmacognosy

For Andrew.

(November 30th 1986 – November 7th 2015)

ACKNOWLEDGEMENTS

I would like to express my sincere appreciation and gratitude to my advisor, Professor Daesung Lee. His patience, motivation, enthusiasm, and vast knowledge of organic chemistry are unparalleled. He is a true artist in the field, and I could not have asked for a better advisor over the years. Second, I would like to thank my family for their support and understanding of the sacrifice that obtaining a Ph.D. entails. Without their love and motivation, this journey would not have been possible.

I would also like to give special thanks to my committee members, Professor Vladimir Gevorgyan, Professor Duncan Wardrop, and Professor Justin Mohr from the Department of Chemistry, and Professor Karol Bruzik from the Department of Medicinal Chemistry and Pharmacognosy for their time, helpful comments and suggestions. Likewise, I would like to thank my group members: Chunrui Sun, Jingwei Li, Kung-Pern Wang, Sang Young Yun, Huaqing Liu, Ivan Volchkov, Venkata Sabbasani, Phani M., Rajdip Karmakar, Xinyu Guan, Hyunjin Lee, Sourav Ghorai, and our newest members Anh and Saswata. Finally, I'd like thank the chemistry department and staff for all of their help, support and encouragement throughout the years.

Last but not least, I would like to express my deepest gratitude to my beloved fiancée Madeleine for her unconditional love and support. She has truly been the positive influence in my life that made all of this possible. I look forward to sharing the rest of our lives together.

MJO

2015 in Chicago

CONTRIBUTION OF AUTHORS

Chapter I represents a published manuscript, O'Connor, M.; Sun, C.; Lee, D. *Angew. Chem. Int. Ed.* **2015**, *54*, 9963-9966, written by myself and Prof. Daesung Lee. I investigated the scope of the cycloaddition and worked through the initial route of amathaspiramides first developed by Dr. Chunrui Sun. The revised route was developed by myself and Prof. Daesung Lee, and I ran the experiments. Chapter II represents a series of my own unpublished experiments and approach to lactacystin. Chapter III represents published work that was developed with Dr. Chunrui Sun and Xinyu Guan: *Angew. Chem. Int. Ed.* **2016,** *55*, 2222–2225. This methodology was discovered by Dr. Sun, and I investigated the scope of benzylidene indanones with Dr. Sun; Xinyu Guan and Dr. Sun developed the chemistry of cyclohexenone derivatives. Venkata R. Sabbasani solved all of the X-ray structures for this chemistry. Chapter IV involves a collaborative project with Prof. Wonhwa Cho. This chapter contains both published and unpublished work. Myself and Prof. Lee did all of the synthetic work and fluorophore development, and the Cho lab ran all of the biochemical, microscopy and fluorescence experiments.

TABLE OF CONTENTS

CHAPTER PAGE

PART I

SYNTHETIC APPLICATIONS OF LITHIUM(TRIMETHYLSILYL)DIAZOMETHANE

TABLE OF CONTENTS (continued)

CHAPTER PAGE

TABLE OF CONTENTS (continued)

CHAPTER PAGE

LIST OF SCHEMES

LIST OF SCHEMES (continued)

LIST OF SCHEMES (continued)

SCHEME PAGE

LIST OF SCHEMES (continued)

SCHEME PAGE

LIST OF TABLES

LIST OF TABLES (continued)

TABLE PAGE

LIST OF TABLES (continued)

LIST OF FIGURES

LIST OF ABBREVIATIONS

Ac	Acetyl
AIBN	Azobisisobutyronitrile
Ar	Aryl
Boc	*t*-Butyloxycarbonyl
BOP	Bis(2-oxo-3-oxazolidinyl)phosphinic chloride
Bz	Benzoyl
Bn	Benzyl
Bu	Butyl
Cbz	Carbobenzyloxy
DABCO	1,4-Diazabicyclo[2.2.2]octane
DBU	1,8-Diazabicyclo[5.4.0]undec-7-ene
DCC	Dicyclohexylcarbodiimide
DCDHF	2-Dicyanomethylene-3-cyano-2,5-dihydrofuran
DCE	Dichloroethane
DCM	Dichloromethane
DDQ	2,3-Dichloro-5,6-dicyano-1,4-benzoquinone
DIAD	Diisopropyl azodicarboxylate
DIBAL	Diisobutylaluminum hydride
DIEA	*N*,*N*-Diisopropylethylamine
(+)-DIP-Cl	(−)-B-Chlorodiisopinocampheylborane
DMAB	4-Dimethylaminobenzaldehyde
DMAP	4-Dimethylaminopyridine
DME	Dimethoxyethane
DMF	Dimethylformamide

LIST OF ABBREVIATIONS (continued)

DMP	Dimethoxypropane
DMSO	Dimethyl sulfoxide
dr	Diastereomeric ratio
EDCI	*N*-(3-Dimethylaminopropyl)-*N′*-ethylcarbodiimide hydrochloride
EDT	Ethylenediaminetetraacetic acid
ee	Enantiomeric excess
EI	Electron impact
ESI	Electrospray ionization
EWG	Electron withdrawing group
FAB	Fast atom bombardment
HMPA	Hexamethylphosphoramide
HO	Highest occupied
HOMO	Highest occupied molecular orbital
HONR	Hydroxy Nile Red
IBX	2-Iodoxybenzoic acid
ITCF	Interrupted tricyanofuran
LA	Lewis acid
LAH	Lithium aluminum hydride ($LiAlH_4$)
LDA	Lithium diisopropylamide
LHMDS	Lithium hexamethyldisilazide ($LiN(SiMe_3)_2$)
LTMP	Lithium tetramethylpiperidide
LTMSD	Lithium(trimethylsilyl)diazomethene
LU	Lowest unoccupied
LUMO	Lowest unoccupied molecular orbital

LIST OF ABBREVIATIONS (continued)

MB	Molecular beacon
Ms	Methanesulfonyl (Mesyl, CH_3SO_2)
NIS	*N*-Iodosuccinimide
NLUMO	Next lowest unoccupied molecular orbital
NMM	*N*-Methylmorpholine
NMO	*N*-Methylmorpholine *N*-oxide
NMP	*N*-Methylpyrrolidone
NMR	Nuclear magnetic resonance
PCC	Pyridiniumchlorochromate
PDC	Pyridinium dichromate
Ph	Phenyl
PMB	4-Methoxybenzyl
PMP	4-Methoxyphenyl
PNB	4-Nitrobenzoyl
PNBA	4-Nitrobenzoic acid
py	Pyridine
rt	Room temperature
SQuID	Self-quenched intramolecular dimer
TBAF	Tetra-*n*-butylammonium fluoride
TBAT	Tetrabutylammonium difluorotriphenylsilicate
TBDMS	*t*-Butyldimethylsilyl
TBDPS	*t*-Butyldiphenylsilyl
TBS	*t*-Butyldimethylsilyl (also TBDMS)
TCF	Tricyanofuran

LIST OF ABBREVIATIONS (continued)

TEA	Triethylamine
TES	Triethylsilyl
Tf	Triflate (CF_3SO_2)
TFA	Trifluoroacetic
TFAA	Trifluoroacetic anyhdride
THF	Tetrahydrofuran
TIPS	Triisopropylsilyl
TLC	Thin layer chromatography
TMEDA	*N*,*N*,*N*',*N*'-Tetramethylethylenediamine
TMP	2,2,6,6-Tetramethylpiperidide
TMS	Tetramethylsilane (trimethylsilyl)
TMSD	(Trimethylsilyl)diazomethane
Trityl	Triphenylmethyl
Tol	Tolyl
Ts	Tosyl (*p*-$CH_3C_6H_4SO_2$)

SUMMARY

The following thesis involves several projects in two major areas. In the first, synthetic applications of lithium(trimethylsilyl)diazomethane (LTMSD) were investigated. These projects range from formal [3+2] cycloadditions with electron deficient olefins to sequential reactions involving multiple bond formations and fragmentations in a single flask. In the second research area, fluorophores were designed and synthesized for in vivo microscopy applications. Focus in this project was on analogs of two major classes: benzophenoxazines and 2-dicyanomethylen-3-cyano-4,5,5-trimethyl-2,5-dihydrofurans (TCF).

Chapter I focuses on the development and application of a formal [3+2] cycloaddition between LTMSD and α,β-unsaturated esters (enoates). The scope of this reaction was explored, and the protonolytic ring-opening of the newly generated Δ^2-pyraozlines leads to a new method for synthesizing the α-*tert*-alkyamino carboxylic ester functionality. This methodology was applied in a synthesis of the amathaspiramide family of natural products. Chapter II extends this methodology to two new classes of substrates, α-methylene- and α-benzylidene-β-hydroxy esters and α,β-unsaturated pseudoephedrine-derived amides. The hydroxy group proved to be a key controlling element in the diastereoselectivity of the reaction. Chapter III further explores the chemistry of LTMSD in tandem reaction processes involving Grob-type C–C fragmentations, alkylidene carbene-mediated Li–N insertions, and dipolar cycloadditions by controlling the reaction parameters. This chemistry was used to synthesize a variety of new heterocycles including pyrazoles, cyclic hemiaminals and diazepine derivatives.

Chapter IV involves the second area of research in which fluorophores were designed and synthesized for *in vitro* microscopy studies. The benzophenoxazine class of fluorophores were found to be superior to the tricyanofurans in the fluorescence assays in terms of their fluorescence intensity and behavior in the cell. A Nile Red-based fluorophore was successfully utilized in simultaneous *in situ* quantification of two cellular lipid pools.

CHAPTER I

FORMAL [3+2] CYCLOADDTION OF ENOATES WITH LITHIUM(TRIMETHYLSILYL)DIAZOMETHANE

1.1. Introduction*

The rapid and efficient synthesis of nonproteinogenic amino acids and their analogs is of significant merit in the molecular biology, biochemistry and medicinal chemistry fields.[1] These non-natural amino acids are of paramount importance in the design of enzymes, and particuarily, α,α-disubstituted α-amino acids (α-tert-alkylamino acids) can lead to increased rigidity, activity, and/or stability of these proteins.[2] These α-tert-alkylamino acids are sometimes enzyme inhibitors themselves,[3] and they serve as useful building blocks for biologically active natural products and pharmaceuticals. Several representative biologically active natural products and pharmaceuticals containing the α-tert-alkylamino acid functionality are shown below (**Figure 1.1**).[4]

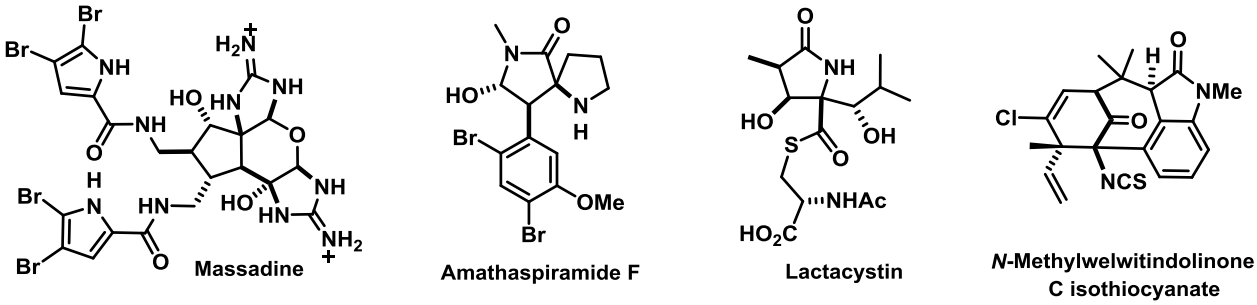

Figure 1.1. Select biologically active compounds containing the α-tert-alkylamino acid functionality

For construction of the α-*tert*-alkylamino group, it was envisioned that a facile two-step process involving a formal 1,3-dipolar cycloaddition with lithiated diazoalkane **1**, followed by protonolytic bond cleavage of the resulting pyrazoline would result in densely functionalized α,α-disubstituted α-amino acid derivatives (Eq. 1).[5]

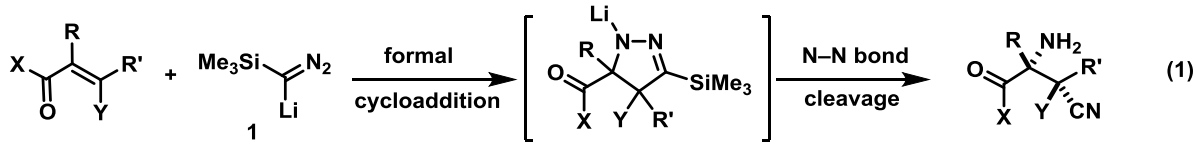

*Reproduced with permission from: O'Connor, M.; Sun, C.; Lee, D. *Angew. Chem. Int. Ed.* **2015**, *54*, 9963-9966.

1.1.1. Diazoalkane 1,3-Dipolar Cycloaddition

The 1,3-dipolar cycloaddition is a powerful synthetic tool for generating five-membered heterocycles and natural products.[6] These cycloadditions belong to a very large class of reactions, and this is due, in part, to the many different types of dipoles. Even if one is restricted to carbon, nitrogen and oxygen based dipoles, the possible combinations of unsymmetrical dipoles is quite large. Some of the most important 1,3-dipoles are shown in **Figure 1.2**.

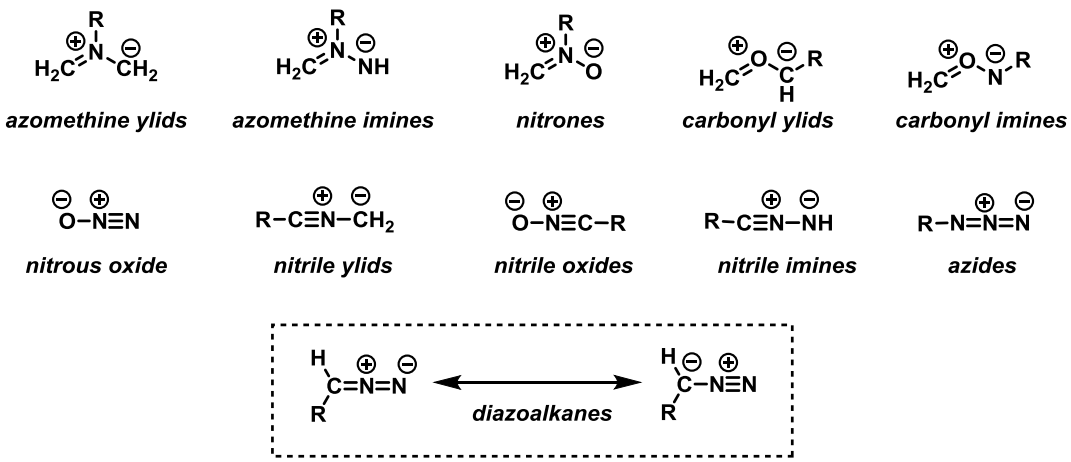

Figure 1.2. Selected Important 1,3-dipoles

This synthetic utility of this reaction is due largely in part to the high degrees of chemo-, regio-, and stereoselectivity in the [3+2] cycloaddition. Fundamentally, the 1,3-dipolar cycloaddition can be generalized in terms of the frontier orbitals of both reacting counterparts (**Figure 1.3**).[7]

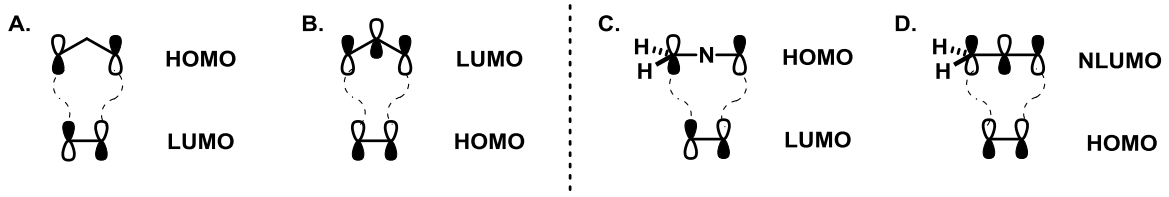

Figure 1.3. Frontier orbitals for 1,3-dipolar cycloadditions

Under normal electron-demand (dipole-HO controlled) 1,3-dipolar cycloadditions, the highest occupied molecular orbital (HOMO) of the 1,3-dipole overlaps with the lowest unoccupied molecular orbital (LUMO) of the dipolarophile (**Figure 1.3.A**). Alternatively, under inverse electron-demand (dipole-LU controlled), the LUMO of the 1,3-diopole overlaps with the HOMO of the dipolarophile (**Figure 1.3.B**). Under dipole-HO controlled interactions, linear 1,3-dipoles, such as diazomethane, have the proper HOMO/LUMO combinations for overlap (**Figure 1.3.C**), but the caveat is in the case of the dipole-LUMO controlled reaction where there is a node through the terminal carbon atom. In these cases, the LUMO is ignored, and the next lowest unoccupied orbital (NLUMO) is used (**Figure 1.3.D**).[7]

The diazoalkane 1,3-dipolar cycloaddition regioselectivity can be explained in terms of the orbital coefficients of the reacting counterparts, and this is expressed in terms of HOMO(dipole)-LUMO(dipolarophile) or LUMO(dipole)-HOMO(dipolarophile) interactions. The former, being cases where the dipolarophile is electron-deficient, is a dipole-HO controlled situation. This is the most common situation for the reactions of diazoalkanes because of their strong frontier orbital term (**Figure 1.4**).[7]

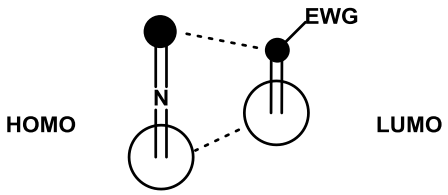

Figure 1.4. Regioselectivity of diazomethane reacting with electron-deficient olefins

A conventional approach when tuning reactivity in a 1,3-dipolar cycloaddition reaction is to enhance the reactivity of the dipolarophile by either a LUMO lowering (dipole-HO) or HOMO raising (dipole-LU) event, as shown in **Figure 1.5**.

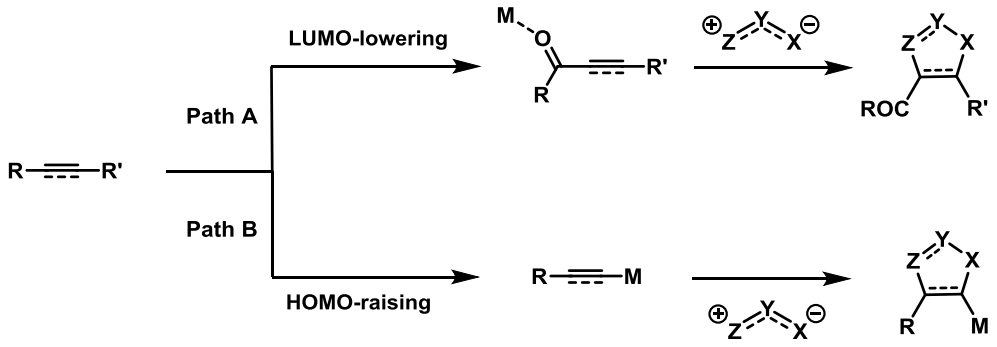

Figure 1.5. Tuning 1,3-dipolar cycloaddition reactivity via dipolarophile activation

This is commonly achieved by Lewis-acid activation of the dipolarophile, such as an ynone (**Path A**, **Figure 1.5**).[6] Alternatively, a dipolarophile such as alkyne, can be activated through a HOMO-raising event to generate a metal acetylide which can react with the 1,3-dipole to afford the cycloadduct, as commonly seen in "click" chemistry (**Path B**, **Figure 1.5**).[8]

Although the 1,3-dipolar cycloaddition is a large, well-studied class of reactions consisting of a seemingly endless variety of 1,3-dipole and dipolarophile combinations, one dipole class that stands out as underutilized and understudied is the diazoalkanes.[7] This is due largely to limitations in in generating diverse highly reactive diazoalkane dipoles, and a limited scope of reactive olefin counterparts. In order to overcome these limitations, it was surmised that diazoalkanes, such as commercially available (trimethylsilyl)diazomethane (TMSD), could be deprotonated with a strong base in a HOMO-raising event (**Scheme 1.1**).[9] This would not only create a more reactive, anionically activated dipole, but also expand the substrate scope of this [3+2] cycloaddition to less-reactive olefins.

Scheme 1.1. Lithium(trimethylsilyl)diazomethane (LTMSD): anionically activated dipole

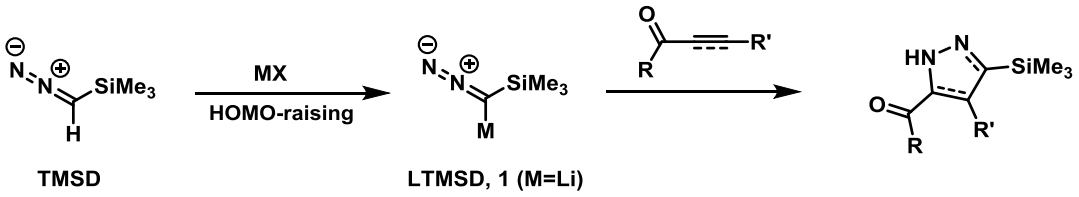

TMSD LTMSD, 1 (M=Li)

1.1.2. Lithium(trimethylsilyl)diazomethane: Anionically activated 1,3-dipole

The use of lithium(trimethylsilyl)diazomethane (LTMSD) **1** as a [C-N-N] synthon dates back over three decades to when Shioiri and Aoyama began their pioneering studies on this anionically activated dipole in the synthesis of 2-substituted 5-trimethylsilyltetrazoles **1-2** via reaction with methyl esters **1-1** (**Table 1.1**).[10]

Table 1.1. Tetrazoles from methyl esters and LTMSD

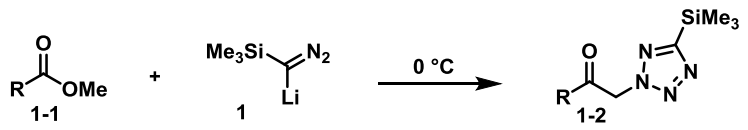

entry	R	base	yield (%)
1	phenyl	LDA	90
2	phenyl	*n*-BuLi	70
3	*p*-tolyl	LDA	88
4	*p*-tolyl	*n*-BuLi	73
5	*p*-chlorophenyl	LDA	88
6	*p*-anisyl	LDA	81
7	3-pyridyl	LDA	60
8	benzyl	LDA	49
9	ethyl	LDA	62

The author's observed that lithiumdiisopropylamide (LDA) was a superior base for this conversion when compared to *n*-butyllithium (*n*-BuLi) affording the tetrazoles **1-2** in 90% and 70% yields respectively (entries 1 and 2). Both electron donating and electron withdrawing aryl esters were well tolerated delivering products in good to excellent yields (73-88%, entries 3-6). Heteroaromatic 3-pyridyl methyl ester was also suitable for this reaction as well as benzyl and ethyl substituted methyl esters giving tetrazoles in fair to moderate yields (49-62%, entries 7-9). Mechanistically, this transformation can be explained by attack of **1** on the ester carbonyl carbon affording **1-1a** after elimination of lithium methoxide (**Scheme 1.2**). Another

molecule of **1** can then react with **1-1a′** via stepwise or direct 1,3-dipolar cycloaddition to give **1-2a** which leads to product **1-2** after treatment with water and elimination of trimethylsilanol.[11]

Scheme 1.2. Mechanism for tetrazole formation from LTMSD and methyl esters

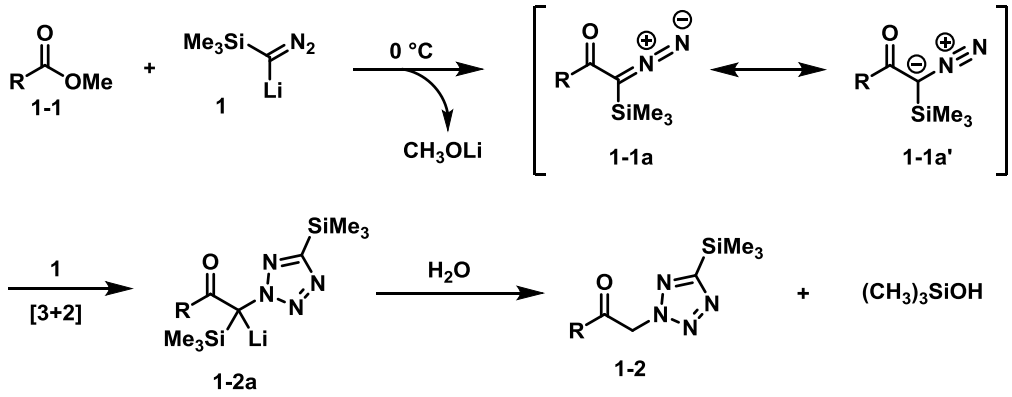

Shortly after, the same authors extended this chemistry to the reaction of **1** with nitriles **1-3** to generate 5-trimethylsilyl-1,2,3-triazoles **1-4** (**Table 1.2**).[11] The choice of base had no effect on the reaction yield, so *n*-BuLi was chosen as the preferred base for the study (entries 1 and 2). Aromatic nitriles provided excellent yields of the desired triazoles (90-93%, entries 1-5). Alkyl, benzyl and neryl nitriles were also well tolerated providing products **1-4** in good to high yields (75-96%, entries 6-9). Nitriles containing heteroatoms such as ethyltio, phenoxy and diethoxyphosphphinyl functionalities were also suitable, and they delivered products **1-4** in 90, 44, and 63% yields respectively (entries 10-12). Finally, cyanotrimethylsilane did not afford the desired triazole when exposed to **1**, and only bis(trimethylsilyl)diazomethane was isolated from the reaction in 87% yield (entry 13). This reaction proceeds either by a direct cycloaddition of **1** with the corresponding nitrile **1-3** or stepwise via nucleophilic attack of **1** on the nitrile carbon followed by cyclization, analogous to that shown in **Scheme 1.2**.[12] This early study demonstrated a convenient alternative approach in generating 1,2,3-triazoles while avoiding the use of explosive azides and acetylenes under forcing conditions.

Table 1.2. Triazoles from nitriles and LTMSD

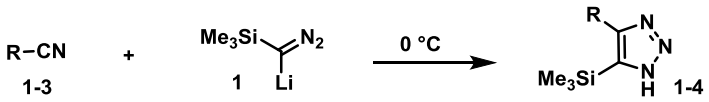

entry	R	base	yield (%)
1	phenyl	LDA	93
2	phenyl	*n*-BuLi	93
3	1-napthyl	*n*-BuLi	90
4	2-pyridyl	*n*-BuLi	92
5	1-isoquinolyl	*n*-BuLi	90
6	*n*-propyl	*n*-BuLi	90
7	*t*-butyl	*n*-BuLi	92
8	benzyl	*n*-BuLi	96
9	neryl	*n*-BuLi	75
10	ethylthio	*n*-BuLi	90
11	phenoxy	*n*-BuLi	44
12	diethoxyphosphinyl	*n*-BuLi	63
13	trimethylsilyl	*n*-BuLi	-

The use of LTMSD **1** as a [C-N-N] synthon was further showcased by Aoyama and Shioiri in 1984 when they reported a convenient synthesis of pyrazoles **1-6** from α,β-unsaturated nitriles **1-5** (**Table 1.3**).[12] Aliphatic nitriles reacted smoothly with **1** providing the desired pyrazoles **1-6** in good yields (65-82%, entries 1-3). In some cases, the 1,2,3-triazole by-product **1-7** was formed (entries 4-8). This is a result of a direct reaction of **1** with the nitrile carbon, analogous to their previous study (**Table 1-2**).[12] There was no difference in reactivity between *E*- or *Z*-isomers, and both produced the desired pyrazole in satisfactory yields with minimal amounts of tetrazole formation (entries 4 and 5). Aromatic nitriles were also well tolerated, and in these cases, the desired pyrazoles **1-6** were the sole products of the reaction (entries 9-11). Finally, the authors showed a single example of a reaction with an α,β-unsaturated ester, methyl (Z)-2-cyano-3-phenylacrylate, delivering **1-6** in 39% yield (entry 12). This report provided an alternate route to pyrazoles that delivered single regioisomers.

Table 1.3. Pyrazoles from α,β-unsaturated nitriles and LTMSD

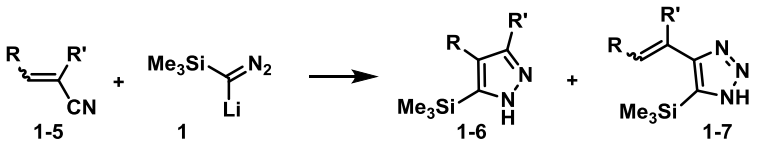

entry	R	R'	yield 1-6 (%)	yield 1-7 (%)
1	H	H	65	-
2	CH_3 (*E/Z* = 36/64)	H	82	-
3	H	CH_3	76	-
4	$CH_3(CH_2)_2$ (*E*)	H	66	7
5	$CH_3(CH_2)_2$ (*Z*)	H	68	5
6	$(CH_3)_3$ (*E/Z* = 55/45)	H	71	6
7	CH_3CH_2	$CH_3(CH_2)_2$	59	3
8	-CH_2CH(*t*-Bu)$(CH_2)_2$-		49	20
9	Ph	H	88	-
10	Ph	CN	82	-
11	*m*-Cl-Ph	CN	80	-
12	Ph	CO_2CH_3	39	-

Several years later, Aoyama and Shioiri investigated the reaction between **1** and ketenimines **1-8** (**Table 1.4**).[13] In this study, either tetrazoles **1-9** or pyrazoles **1-10** were formed in the reaction. In cases where the electron-withdrawing group was diethoxyphosphoryl (X = $(EtO)_2P$=O), pyrazoles **1-10** were formed in moderate yields (72-76%, entries 1-3). In one case, the dephosphorylated pyrazole was isolated as the major product along with **1-10** (67%, entry 3). Tetrazole **1-9** was isolated as the major product when R = Me and R' = Ph (entry 4). Acetyl ketenimines were also subjected to the reaction conditions, and either the pyrazole (R' = Et, entry 5) or tetrazole (R' = Ph, entry 6) were isolated as the sole products of the reactions. Ethoxycarbonyl substituted ketenimine also delivered pyrazole **1-10** albeit much lower yield (20%, entry 7). Finally, cyano-substituted ketenimine provided tetrazole **1-9** as the sole product of the reaction in just 43% yield (entry 8). This study further demonstrated the utility of **1** in generating a diverse array of products from common starting materials although the reaction is limited by yields.

Table 1.4. Pyrazoles or tetrazoles from ketenimines and LTMSD

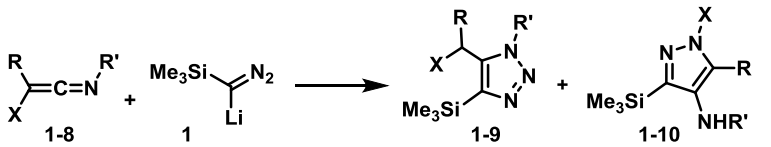

entry	X	R	R'	1-9 (%)	1-10 (%)
1	$(EtO)_2P(O)$	Me	Et	-	73
2	$(EtO)_2P(O)$	Ph	Et	-	72
3	$(EtO)_2P(O)$	Ph	Ph	-	9 (67[a])
4	$(EtO)_2P(O)$	Me	Ph	68	2
5	MeCO	Me	Et	-	48[a]
6	MeCO	Me	Ph	76	-
7	EtO_2C	Me	Et	-	20[a]
8	NC	Me	Me	43	-

[a]X = H in product 1-10

The Botta group studied the reaction of **1** with dimethyluracil derivatives **1-11** (**Table 1.5**).[14] The reaction or **1** with 1,3-dimethyluracil yielded Δ^2-pyrazoline **1-12** and pyrazolidine derivative **1-14** (entry 1). In the case of 5-fluoro-1,3-dimethyluracil, pyrazolidine **1-13** was the sole isolated product (68%, entry 2). Reaction of **1** with 5-brom-1,3-dimethyluracil generated pyrazole **1-14** (78%, entry 3). Finally, 5-nitro-1,3-dimethyluracil also produced **1-13** in low yield (entry 4).

Table 1.5. Reaction of LTMSD with dimethyluracil derivatives

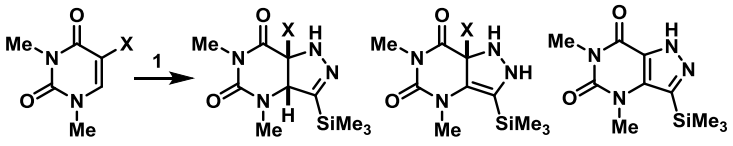

entry	X	1-12 (%)	1-13 (%)	1-14 (%)
1	H	58	29	-
2	F	-	68	-
3	Br	-	-	78
4	NO_2	-	7	-

The Aoyama group later demonstrated that indazoles **1-16** and **1-17** could be generated through the reaction of **1** with benzynes (**Table 1.6**).[15] In this study, the authors found that 2,2,6,6-tetramethylpyperidide (LTMP) was the optimal base for the conversion. Electron-donating groups in the R-position led to preferential formation of **1-16** in poor to moderate yields (26-61%, entries 1-5). Electron donating or withdrawing groups in the R‴-position lead to an equal regioisomeric mixture of **1-16** and **1-17** (entries 6-6). Finally, -OMe substitution at the R and R″ positions leads to exclusive formation of **1-16** (55%, entry 8).

Table 1.6. Reaction of LTMSD with benzyne

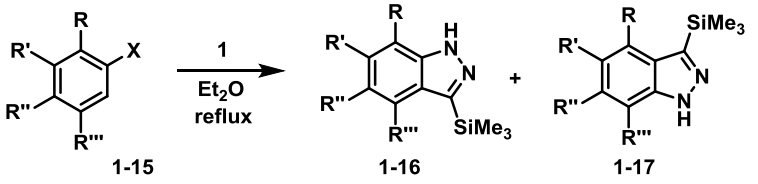

entry	X	R	R'	R''	R'''	yield (%) (ratio)
1	F	OMe	H	H	H	61 (73:27)
2	F	OBn	H	H	H	50 (75:25)
3	Br	NMe_2	H	H	H	36 (67:33)
4	Br	Br	H	H	H	49 (62:38)
5	F	*t*-BuO	H	H	H	26 (83:17)
6	F	H	H	H	OMe	75 (50:50)
7	F	H	H	H	CF_3	74 (50:50)
8	F	OMe	H	OMe	H	55 (100:0)

The mechanism for the above reaction can be explained by nucleophilic attack of **1** on benzyne followed by cyclization and hydrolysis (Scheme 1.3).[16]

Scheme 1.3. Proposed reaction mechanism of LTMSD with benzyne

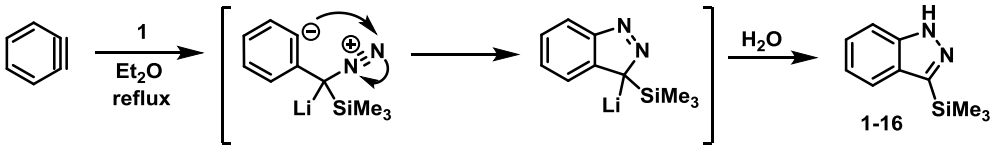

Regitz and Schurr demonstrated that **1** reacts with bis(trimethylsilyl)methylenechlorophosphine **1-18** to generate intermediate diazaphosphole **1-19** (Scheme 1.4).[16] Upon warming to room temperature, Me_3Si-shift occurs to yield **1-20**. Any attempts to purify **1-20** leads to rapid hydrolysis into **1-21**.

Scheme 1.4. Reaction of LTMSD with bis(trimethylsilyl)methylenechlorophosphine

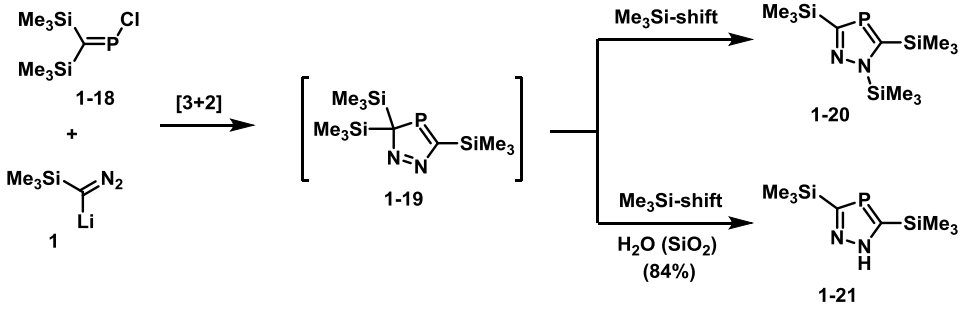

Shioiri and Aoyama also investigated the reaction of **1** with quinones **1-22** (**Table 1.7**).[17] When exposed to **1** at 0 °C for 4 hours, 1,4-naphthoquinone produced benzindazole derivative **1-23** in 89% yield (entry 1). Similarly, 5,8-diacetoxy-1,4-naphthoquinone and 5-acetoxy-1,4-naphthoquinone generated benzindazoles in 74 and 69% yields respectively (entries 2-3). With 2-acetoxy-1,4-naphthoquinone, the product was generated at room temperature and involved elimination of acetic acid from the intermediate cycloadduct to produce **1-23** (entry 4).

Table 1.7. Reaction of LTMSD with quinones

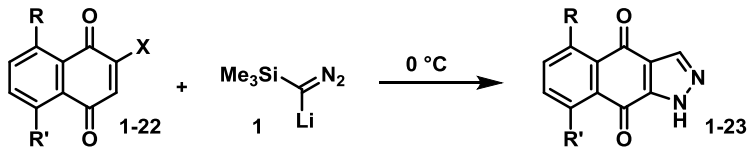

entry	X	R	R'	1-23 (%)
1	H	H	H	89
2	H	OAc	OAc	64
3	H	OAc	H	69
4	OAc	H	H	53

Asaki and Shioiri studied the reaction of **1** with α,β-unsaturated sulfones **1-24** (**Table 1.8**).[18] Alkyl substituted α,β-unsaturated sulfones cleanly produced pyrazoles **1-6** in good yields (74-86%, entries 1-4). Aryl α,β-unsaturated sulfones were also suitable for this reaction, and they delivered pyrazoles in good yields (59-71%, entries 5-7). Both *E*- and *Z*-α,β-unsaturated sulfones delivered the corresponding pyrazoles (entries 6-7), and methoxy substituted α,β-unsaturated sulfone was tolerated in the reaction although lower yield of **1-6** was obtained.

Table 1.8. Reaction of LTMSD with α,β-unsaturated sulfones

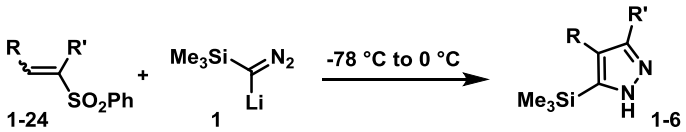

entry	R	R'	*E/Z*	1-6 (%)
1	H	H	-	85
2	CH_3	H	*E*	85
3	H	CH_3	-	74
4	$(CH_3)_3C$	H	*E*	86
5	Ph	H	*E*	84
6	4-Cl-Ph	H	*E*	93
7	Ph	Ph	*Z*	92
8	CH_3O	CH_3O	*E*	36

In another study on the reaction of **1** with ketenimines **1-25**, Shioiri and Aoyama showed that the pair react smoothly at 0 °C to deliver 1,2,3-triazoles **1-26** (**Table 1.9**).[19] Aryl substituted ketenimines **1-25** afforded **1-26** in good yields (67-74%, entries 1-3). The *N*-alkyl substituted ketenimine system was also tolerated and delivered **1-26** in 67% yield (entry 4). Dialkyl substitution at the terminal ketenimine carbon gave even higher yields of the desired products (82%, entries 5-6). In this particular study, diethyl ether was the solvent of choice, and reactions run in THF led to decreased yields of the 1,2,3-triazoles. Furthermore, desilylation could easily be achieved in 10% aqueous potassium hydroxide in methanol.[20]

Table 1.9. Reaction of LTMSD with ketenimines

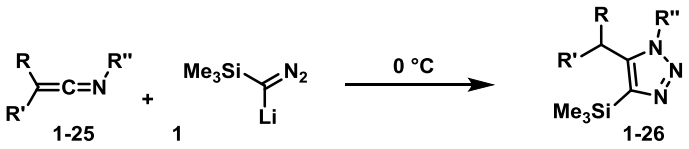

entry	R	R'	R''	1-26 (%)
1	Ph	Ph	*p*-Me-Ph	74
2	Ph	Ph	*p*-Br-Ph	69
3	Ph	Ph	*p*-MeO-Ph	68
4	Ph	Ph	*n*-C_4H_9	67
5	Me	Me	*p*-Me-Ph	82
6	C_2H_5	*n*-C_4H_9	*n*-C_4H_9	82

Shioiri and Aoyama further extended the dipolarophile scope with **1** to thioketones **1-27** to yield thiadiazolines **1-28** (**Table 1.10**).[20] Although limited, reported examples include cyclic thioketones which yielded **1-28** in 31 and 75% yields (entries 1-2). While alkyl substituted di-*tert*-butylthioketone yielded the desired azole in 82% (entry 3).

Table 1.10. Reaction of LTMSD with thioketones

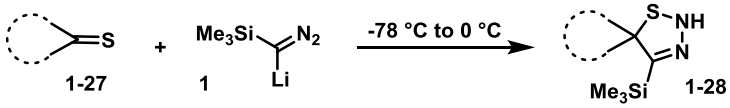

entry	substrate	solvent	1-28 (%)
1	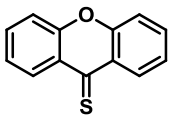	Et_2O	74
2	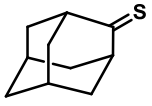	THF	31
3	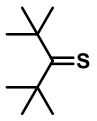	Et_2O	82

Aoyama and Shioiri also generated 1,2,3-thiadiazoles **1-30** from **1** and thionoesters or dithioesters **1-29** (**Table 1.11**).[21] Aryl esters delivered the desired thiadiazoles in good to excellent yields (69-90%, entries 1-2, 6), and a benzyl ester was also generated the azole in 83% yield (entry 3). Alkyl esters were also well tolerated yielding **1-30** in good yields (79-84%, entries 4-5). Finally *O*,*S*-diethyl carbonodithioate produced **1-30** in moderate yield (entry 7).

Table 1.11. Reaction of LTMSD with thionoesters and dithioesters

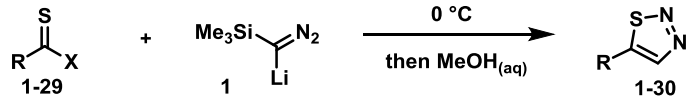

entry	X	R	1-30 (%)
1	OCH_3	Ph	90
2	SCH_3	Ph	82
3	OCH_3	$PhCH_2$	83
4	OCH_3	$CH_3(CH_2)_8$	79
5	SCH_3	$CH_3(CH_2)_8$	84
6	OCH_3	3-pyridyl	69
7	SC_2H_5	C_2H_5O	67

In another application, Aoyama and co-workers explored the reaction of **1** with isocyanates **1-31** to generate 5-hydroxy-1,2,3-triazoles **1-32** (**Table 1.12**).[22] Aromatic isocyanates were found to be more reactive than their alkyl-substituted counterparts, and the desired triazoles formed smoothly at 0 °C in good yields (79-83%, entries 1-3). As mentioned above, the alkyl substituted isocyanates required an elevated reaction temperature; *n*-butyl and cyclohexyl-substituted isocyanates required the reaction to be run at room temperature (entries 4 and 6). The sterically hindered *t*-butyl-substituted isocyanate required refluxing diethyl ether. It is worthwhile to note that the 1-aryl-5-hydroxy-1,2,3-triazoles are unstable to heat in solution, and they readily decompose to diazoacetamides.

Table 1.12. Reaction of LTMSD with isocyanates

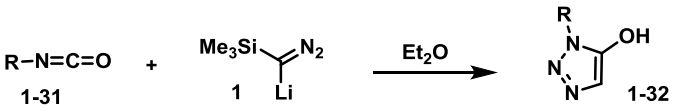

entry	R	T (°C)	yield (%)
1	Ph	0	79
2	4-Cl-Ph	0	83
3	1-naphthyl	0	83
4	*n*-butyl	-78 to 25	63
5	*t*-butyl	0 to 35	53
6	cyclohexyl	0 to 25	71

In a subsequent study, Aoyama studied the reaction of **1** with isothiocyanates **1-33** which gave 2-amino-1,3,4-thiadiazoles **1-34** (**Table 1-13**).[23] In the case of aryl isothiocyanates, the reaction proceeded in moderate to good yields at 0 °C, and diethyl ether was identified to be the solvent of choice (60-83%, entries 1-4). On the other hand, aliphatic substrates required room temperature and the use of hexane as the solvent (56-62%, entries 5-6). Finally, allyl- and benzyl-substituted isothiocyanates produced the desired 2-amino-1,3,4-thiadiazoles **1-34** in fair to moderate yields at 0 °C (40-57%, entries 7-8).

Table 1.13. Reaction of LTMSD with isothiocyanates

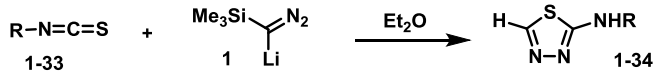

entry	R	T (°C)	yield (%)
1	Ph	0	83
2	4-Cl-Ph	0	83
3	1-naphthyl	0	60
4	2-napthyl	0	74
5	*n*-butyl	0 to 22	56
6	cyclohexyl	0 to 22	62
7	allyl	0	40
8	benzyl	0	57

As a follow-up study to that shown in **Table 1.13**; the authors disclosed a dramatic solvent effect when the solvent was changed from ether or hexane to THF (**Table 1.14**).[24] When isothiocyanates **1-33** were treated with **1** in THF followed by quenching with alkyl halides, 1-substituted 4-trimethylsilyl-5-alkylthio-1,2,3-triazoles **1-35** were formed. Aromatic isothiocyanates we well tolerated and produced the desired azoles **1-35** in excellent yields (98-99%, entries 1-2). Aliphatic substrates also generated satisfactory results, and products were generated in high yield (90-98%, entries 3-6). Allyl and benzyl systems were also well behaved under the conditions, and products were generated in 91% yields in both cases. Finally, the products **1-35** could be treated with aqueous potassium hydroxide to deliver 5-alkylthio-1,2,3-triazoles **1-36**.

Table 1.14. Reaction of LTMSD with isothiocyanates in THF

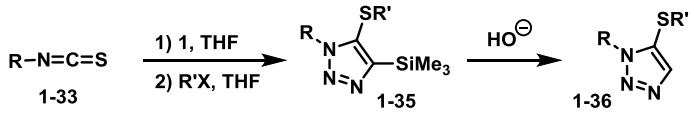

entry	R	R'X	1-35 (%)	1-36 (%)
1	Ph	MeI	98	94
2	Ph	BnBr	99	97
3	CH_3	MeI	96	100
4	CH_3	BnBr	90	98
5	$CH_3(CH_2)_3$	BnBr	97	95
6	cyclohexyl	BnBr	98	96
7	benzyl	BnBr	91	99
8	allyl	BnBr	91	83

Aoyama also studied the reaction β-amino-α,β-unsaturated ketones **1-37** with **1** (**Table 1.15**).[25] In cases where the substrate contained a methyl ketone, diazabicycloheptadiene **1-39** was isolated as the sole product in low to moderate yield (18-53%, entries 1 and 3). When methyl ketone of **1-37** is replaced with ethyl ketone, pyrazole **1-38** becomes the major product in this reaction along with **1-39** in a 2:1 ration respectively (entries 2 and 4).

Table 1.15. Reaction of LTMSD with β-amino-α,β-unsaturated ketones

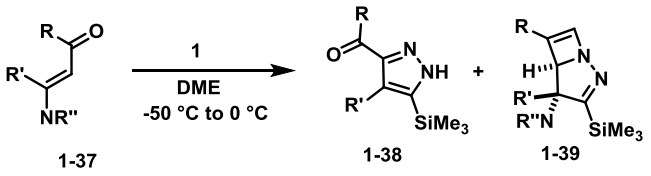

1-37 1-38 1-39

entry	R	R'	R"	1-38 (%)	1-39 (%)
1	CH_3	CH_3	$-(CH_2)_4-$	-	53
2	CH_2CH_3	CH_2CH_3	$-(CH_2)_4-$	27	14
3	CH_3	Ph	$-(CH_2)_4-$	-	18
4	CH_2CH_3	CH_2CH_3	Et_2	27	14

The formation of the products in **Table 1.15** can be explained through a stepwise addition of **1** on the β-carbon of **1-37** to generate **1-37′** followed by ring closure to **1-38′** or a direct [3+2] cycloaddition of **1** with **1-37** to generated **1-38′** (**Scheme 1.5**). Tautomerization and elimination of lithium pyrrolide gives **1-38**. Alternatively, 1,3-metal migration generates lithiated Δ^2-pyrazoline **1-39′** which can further undergo 1-2-addition and elimination of $LiOSiN_2$ to generate carbene **1-39′′**. Insertion of carbine **1-39′′** into the Li-N bond gives rise to the product **1-39** after protonation (**Scheme 1.5**). Applications of the tandem 1,4/1,2-addition of **1** will be discussed in Chapter 3.

Scheme 1.5. Mechanism for reaction of LTMSD with β-amino-α,β-unsaturated ketones

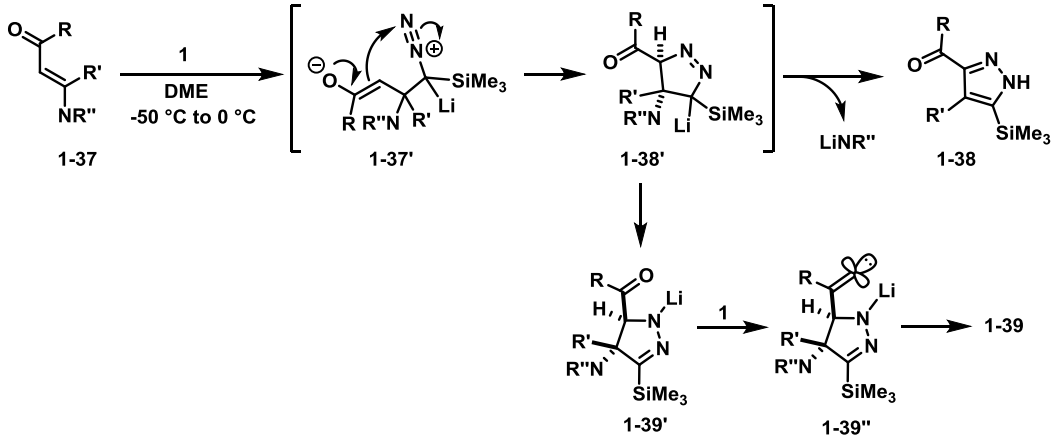

1-37 1-37' 1-38' 1-38 1-39' 1-39"

In a recent report by Lee and co-workers, the reaction of 1 with cyclic enones **1-40** was investigated (**Table 1.16**).[26] Bicyclic pyrazolines **1-41** were generated smoothly in the presence of **1** with endocyclic cyclohexene derivatives in good yields (68-82%, **1-41a** through **1-41e** and **1-41m-n**). Cyclopentene systems were also suitable under these conditions, and jasmone reacted cleanly to deliver **1-41f** in 65% yield. Exocyclic double bond containing enones were also subjected to **1**, and they produced the desired Δ^2-pyrazolines in fair to excellent yields (43-92%, **1-41g** through **1-41l**). In cases where there was substitution at the para-position of the benzylidene group yields were diminished where X = OMe and X = NO_2 (**1-41k** and **1-41l**). X-ray crystallography of **1-41j** unambiguously confirmed the spirocyclic nature of these bicyclic pyrazolines.

Table 1.16. Reaction of LTMSD with cyclic enones

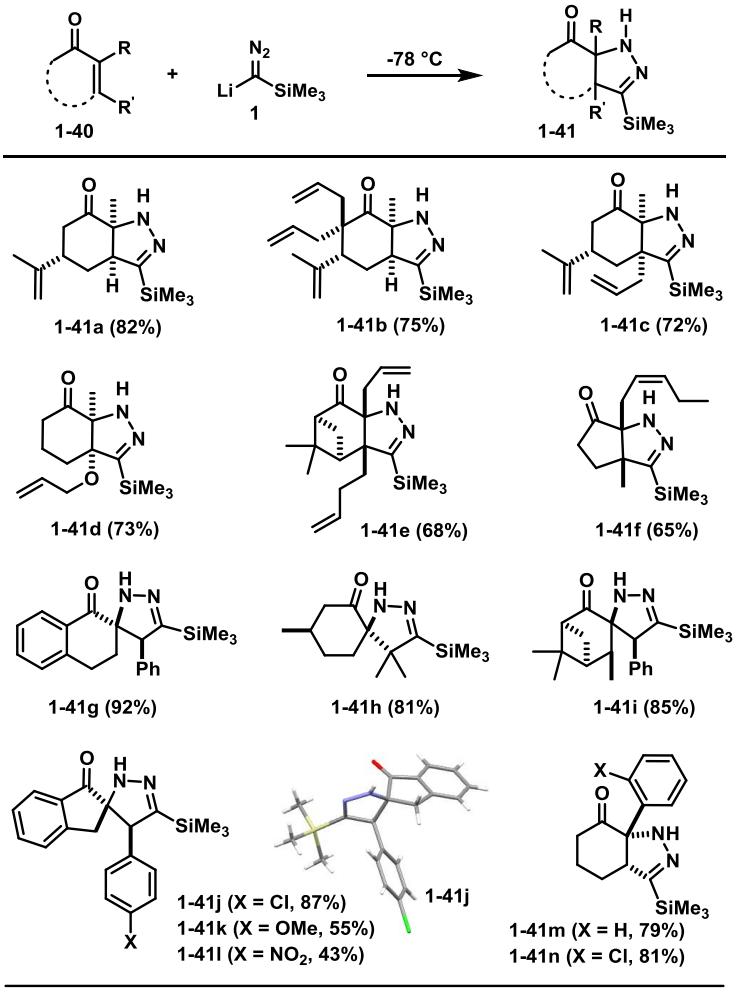

In the report, the authors demonstrated that the newly generated bicyclic pyrazolines could opened under protonolytic conditions to generate α-amino-β-cyano cyclic-ketones **1-41′**, constituting a formal α-amination process (**Scheme 1.6**).[5] On the contrary, in the case of acyclic enone **1-40**, enyne **1-42** was generated via Colvin rearrangement.

Scheme 1.6. Formal aminocyanation of enones utilizing LTMSD

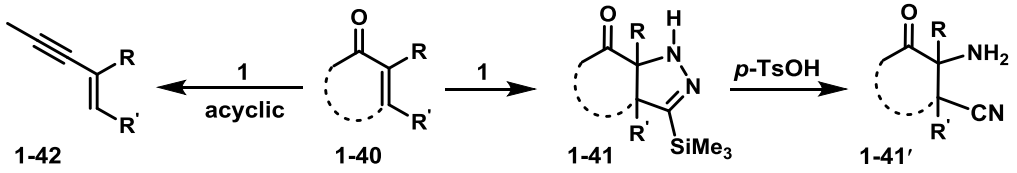

This study served as the inspiration for extending the reaction scope of **1** to acyclic and cyclic α,β-unsaturated esters (enoates) which were hypothesized to show preferential 1,4-addition/cyclization behavior. A similar protonolytic ring opening of the resulting Δ^2-pyrazolines would lead to densely substituted α,α-disubstituted-α-amino acid derivatives (α-*tert*-alkylamino acids) as shown in **Scheme 1.1**. Applications of this methodology could then be applied to the synthesis of biologically significant natural products (**Figure 1.1**).

1.2. Results and discussion

1.2.1. Reaction scope

One immediate concern regarding the chemoselectivity of this reaction is the reactivity of **1** with esters as reported by Shioiri and Aoyama, shown **Table 1.1** and **Scheme 1.2**.[11] To probe this selectivity issue, the study commenced by examining the reaction scope of the reaction of **1** with enoates **1-43** (**Table 1.17**).[27] Gratifyingly, in the case of methyl methacrylate **1-43a**, Δ^2-pyrazoline **1-44a** was the only observed product from the reaction demonstrating that 1,4-addition of **1** followed by ring closure, a formal [3+2] cycloaddition, was the preferred mode of reaction. Ethyl tiglate **1-43b** also reacted smoothly with **1** producing Δ^2-pyrazoline **1-44b** in a 4:1 mixture of diastereomers (82%, entry 2). Likewise, in the case of

E-enoates, the reaction was stereospecific, and ethyl cinnamate **1-43c** yielded **1-44c** in 85% yield in a 10:1 mixture of diastereomers. This structure was unambiguously confirmed by X-ray diffraction of **1-44c**.[28]

Table 1.17. Reaction of LTMSD with enoates

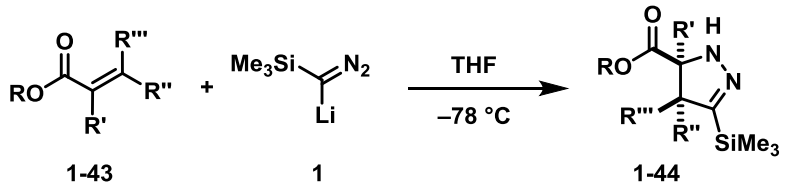

1-43 1 1-44

Entry	α,β-Unsaturated ester	Pyrazoline	Yield (%)	d.r.
1	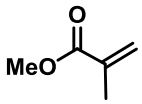 1-43a	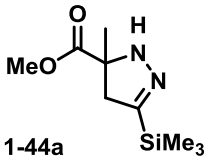 1-44a	91	–
2	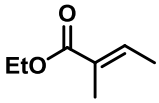 1-43b	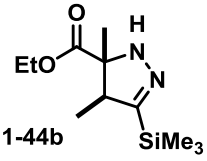 1-44b	82	4:1
3	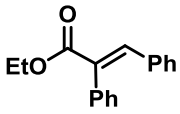 1-43c	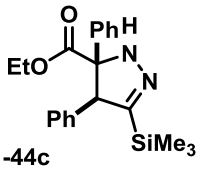 1-44c	85	10:1
4	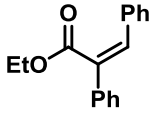 1-43d	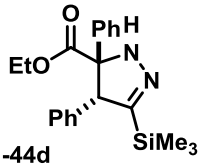 1-44d	80	1:1
5	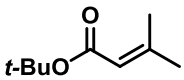 1-43e	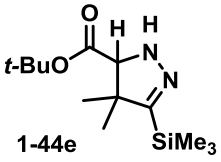 1-44e	75	–
6	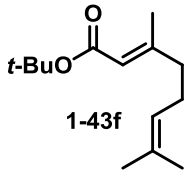 1-43f	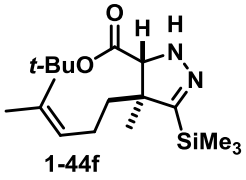 1-44f	71	9:1

In the case of *Z*-cinnamate **1-43d**, the reaction yielded a 1:1 mixture of diastereomers in an 80% yield (entry 4). Finally, β,β-disubstituted enoates **1-43e** and **1-43f** provided pyrazolines **1-44e** and **1-44f** in 75 and 71% yields, respectively, both containing all carbon quaternary centers. In both of these cases, methyl esters lead to preferential 1,2-addition of **1** to generate tetrazoles, so *t*-butyl esters were required.

Next, cyclic enoates **1-45** were investigated as substrates for this formal [3+2] cycloaddition reaction (**Table 1.18**).[27] In the prescence of **1**, cyclic enoates **1-45** reacted cleanly to generate bicyclic Δ^2-pyrazolines **1-46**. Methyl cyclopentene carboxylate **1-45a** delivered bicyclic pyrazoline **1-46a** in 71% yield (entry 1). Likewise, methyl myrtenate **1-45b** and methyl perillate **1-45c** produced Δ^2-pyrazolines **1-46b** and **1-46c** in 65 and 69% yields respectively (entries 2-3).

Table 1.18. Reaction of LTMSD with cyclic enoates

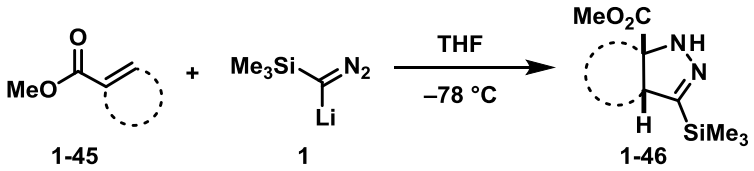

Entry	α,β-Unsaturated ester	Pyrazoline	Yield (%)	d.r.
1	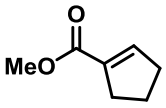 1-45a	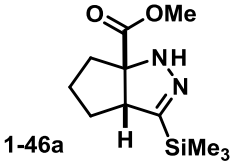 1-46a	71	1:0
2	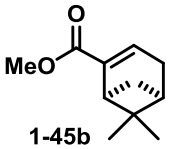 1-45b	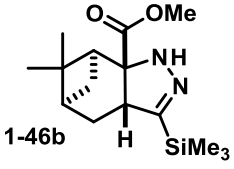 1-46b	65	1:0
3	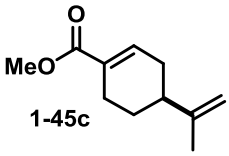 1-45c	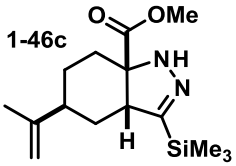 1-46c	69	1:0

1.2.2. Mechanistic considerations

Mechanistically, the reaction between enoates **1-43** and **1** can proceed via one of the two mechanistic scenarios shown in **Scheme 1.7**. In path A, a direct 1,3-dipolar cycloaddition between **1** and **1-43** would lead to lithiated Δ^1-pyrazoline **1-44'**. After 1,3-metal migration to **1-44''** and protonation; **1-44** is formed. Alternatively, a direct cycloaddition between **1'** and **1-43** can be envisioned leading directly to lithiated Δ^2-pyrazoline **1-44''**. In path B, **1** reacts directly with the β-carbon of enoate **1-43** generating 1,4-adduct **1-43'**. This intermediate can undergo endo-mode ring closure leading to **1-44''**. Based on the experimental results in **Table 1.17**, the mixtures of pyrazolines formed, from *Z*-enoates especially, strongly support the step-wise pathway. Also, in the cases of β,β-disubstituted enoates, 1,2-addition becomes the preferred mode of the reaction.[10,29] Likewise, the strong nucleophilic nature of **1** and its tendency to undergo 1,2-addition preferentially with acyclic α,β-unsaturated ketones also support this mechanism.

Scheme 1.7. Mechanistic scenario of LTMSD and enoates

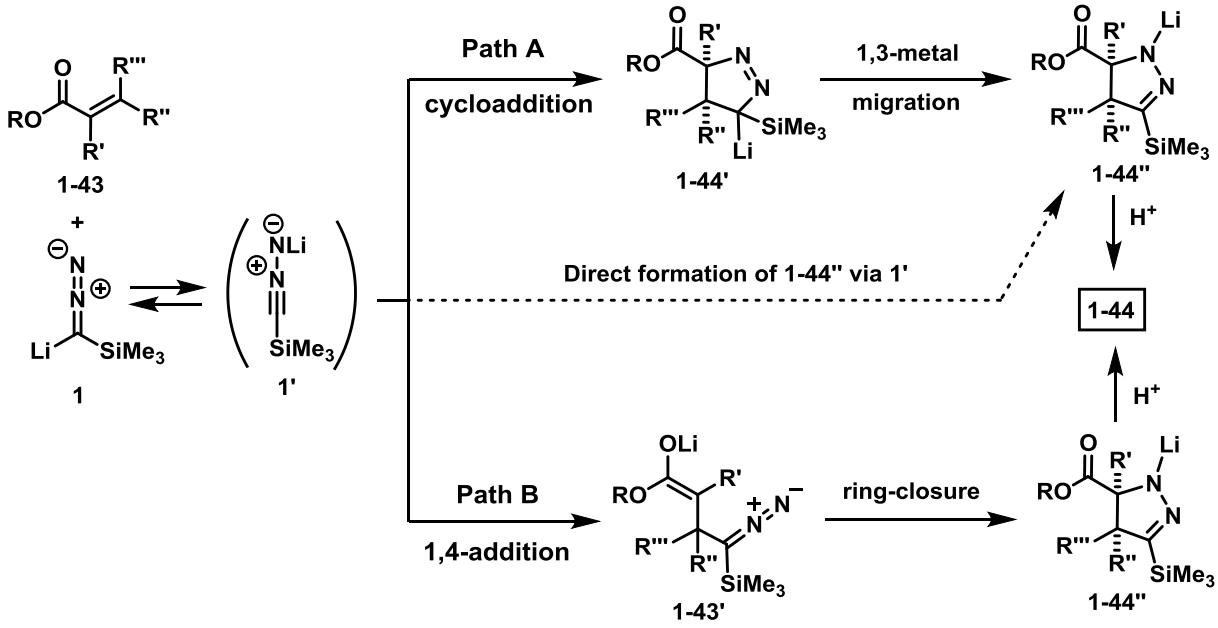

With the scope and selectivity of **1** with enoates **1-43** thoroughly investigated, application of this methodology was showcased in a synthesis of the amathaspiramides.[27]

1.3. Application in synthesis – amathaspiramides

The amathaspiramide family of natural products was isolated in 1999 from the marine bryozoan, *amathia wilsoni*, by the Prinsep group of the coast of New Zealand (**Figure 1.6**).[4c] They contain a wide range of biological activities including antiviral against the Polio virus Type 1, antibacterial against *Bacillus subtilis* (gram positive), and antifungal activity against *Trichophyton mentagrophytes*.

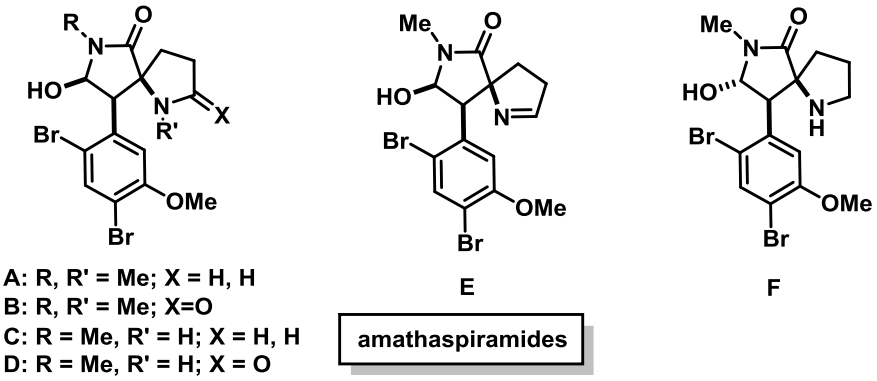

Figure 1.6. The amathaspiramide family of alkaloids

The amathaspiramide family of alkaloids contain many interesting structural features including a densely functionalized spirocyclic core containing a hemiaminal moiety (**Figure 1.6**). The hemiaminal ring is spiro-fused with either a pyrrolidine ring (amathaspiramides A, C, F), pyrrolidinone (amathaspiramides B, D), or pyrroline (amathaspiramide E).

1.3.1. Previous syntheses of amathaspiramides

1.3.1.1. Trauner synthesis of amathaspiramide F

In 2002, the Trauner group achieved the first total synthesis of amathaspiramide F (Scheme 1.8).[30] Starting from *L*-proline **1-47**, treatment with methylamine followed by pivaldehyde and trifluoroacetic acid (TFA) generated *N*,*N*-*t*-butyl acetal **1-48** in 50% yield. After extensive experimentation, the group was

Scheme 1.8. Trauner synthesis of amathaspiramide F

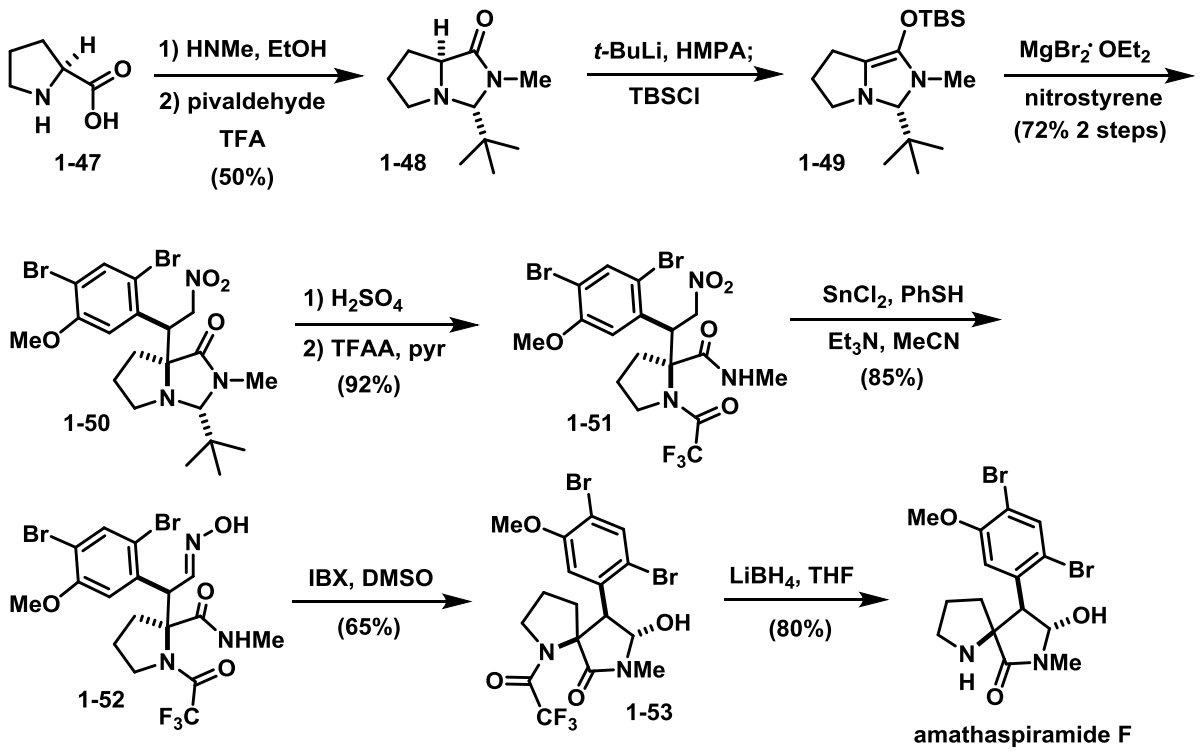

finally able to enolize **1-48** with t-butyllithium in the presence of hexamethylphosporamide (HMPA) followed by trapping with *tert*-butyldimethylsilyl chloride to generate **1-49**. Magnesium bromide catalyzed aldol reaction with the required nitrostyrene generated **1-50** in a 72% yield over two steps. A simple Nef reaction of **1-50** was unfruitful, so the scientists commenced with deprotection of the *N,N*-acetal followed by protection of the resulting pyrrolidine as its trifluoroacetamide **1-51** in 92% over two steps. Reduction of the nitro group in **1-51** to oxime **1-52** proceeded in 85% yield, and this compound was then oxidized to the aldehyde with IBX which cyclized directly to the desired hemiaminal **1-53**. Finally, reductive removal of the trifluoroacetamide protecting group generated amathaspiramide F in 80% yield.

1.3.1.2. Ohfune synthesis of amathaspiramide F

Several years later, the Ohfune group also tackled a synthesis of amathaspiramide F (**Scheme 1.9**).[31] Their approach commenced with ynone **1-54** which was reduced with (+)-DIP-Cl to propargyl alcohol

Scheme 1.9. Ohfune synthesis of amathaspiramide F

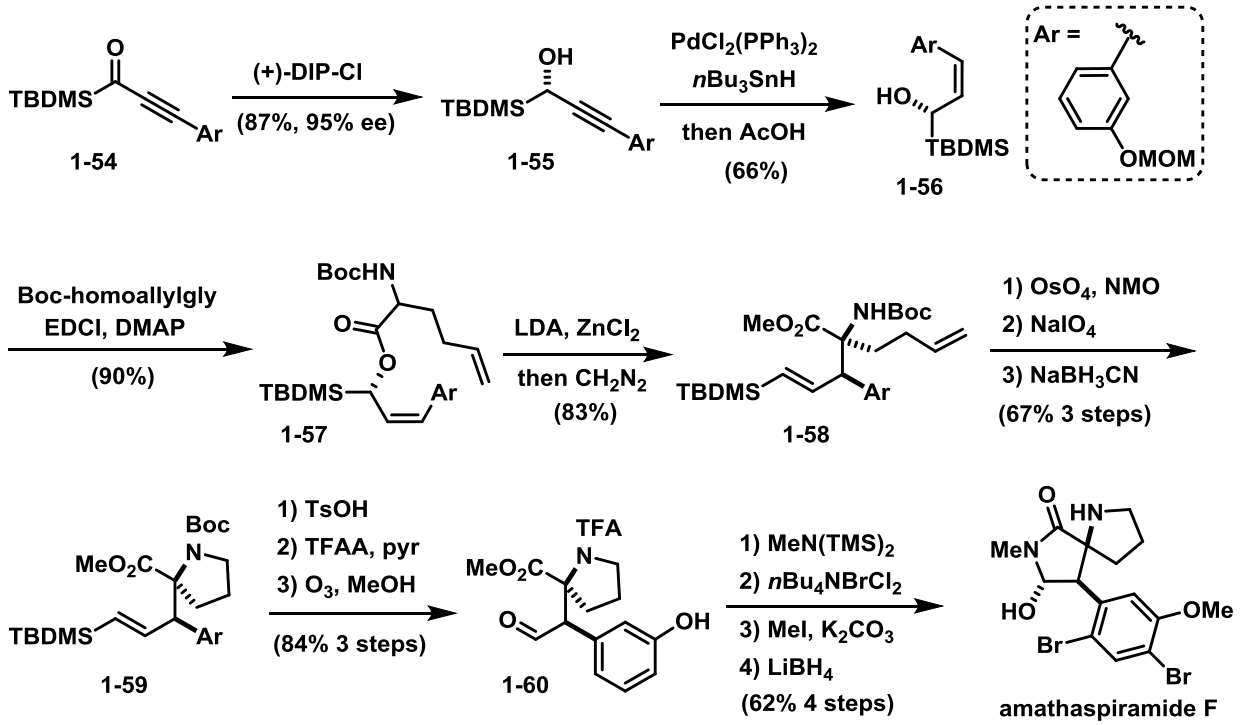

1-55. Reduction with tributyltin hydride in the presence of palladium led to *Z*-alkene **1-56** in 66% yield. Esterification with boc-homoallylglycine generated **1-57** in 90% yield, their precursor for the enolate Claisen rearrangement. Rearrangement of **1-57** to **1-58** via LDA in the presence of zinc chloride occurred in 58% yield. Oxidative cleavage of **1-58** followed by intramolecular reductive amination generated **1-59**. Removal of the Boc-group followed by protection as the trifluoroacetamide and ozonolysis produced aldehyde **1-60**. After extensive experimentation, the authors found that treatment of **1-60** with heptamethyldisilazane led to ring closure into the hemiaminal. Electrophilic bromination followed by phenol methylation and removal of the trifluoroacetamide group led to amathaspiramide F.

1.3.1.3. Fukuyama synthesis of all members of the amathaspiramides

In 2012, Fukuyama and co-workers disclosed a route to all members of the amathaspiramide family of alkaloids (**Scheme 1.10**).[32] Their general approach began with 2-Bromo-3′-methoxyacetophenone **1-61**

Scheme 1.10. Fukuyama approach to all members of the amathaspiramides

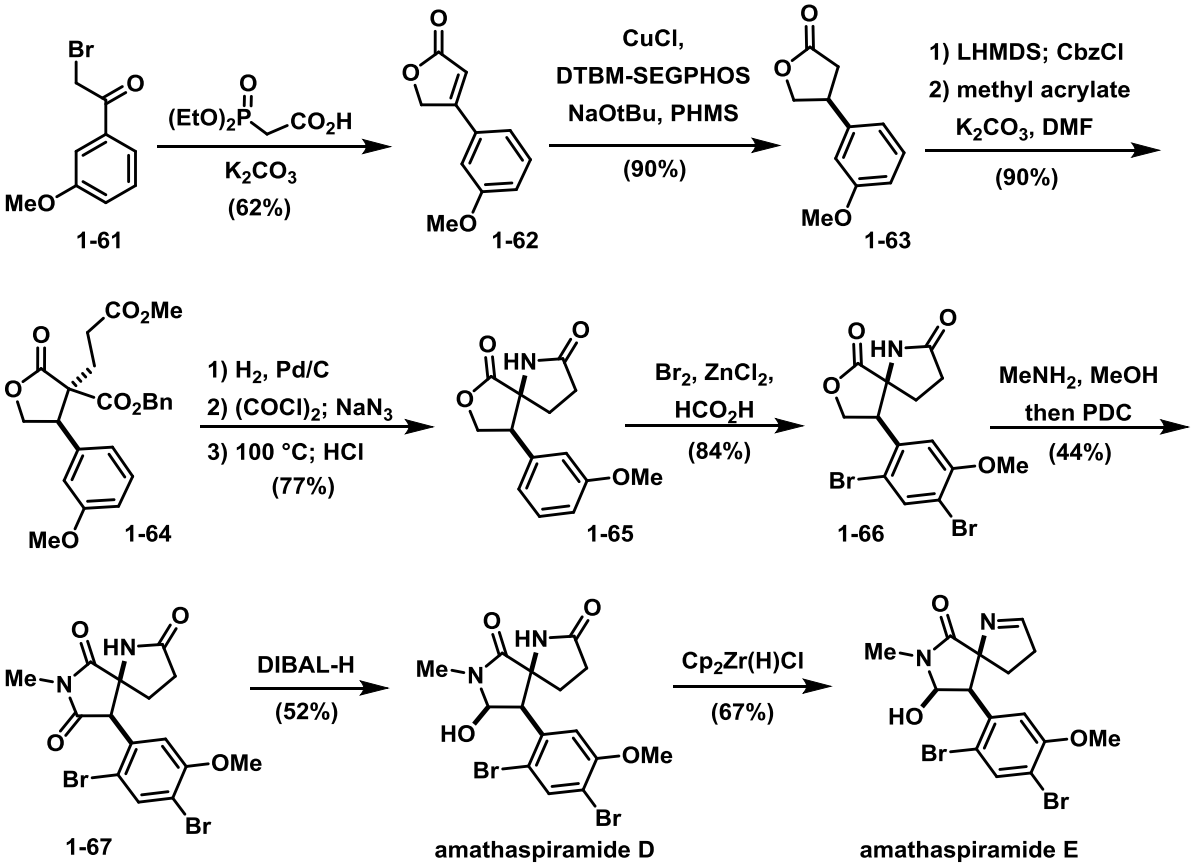

which was subjected to a Horner–Wadsworth–Emmons reaction with diethylphosphonoacetic acid to generate butenolide **1-62** after cyclization. Asymmetric reduction with DTBM-SEGPHOS in the presence of copper chloride generated lactone **1-63**. Alkylation with benzyl chloroformate followed by Michael addition to methyl acrylate produced **1-64**. Reduction of the benzoyl group followed by oxalyl chloride treatment and substitution with sodium azide led to their precursor for the Curtius rearrangement. Heating the acyl azide to 100 °C followed by reflux in aqueous hydrochloric acid produced the desired pyrrolidinone **1-65**. Bromination led to **1-66** which was treated with methyl amine followed by PDC yielding imide **1-67**, the precursor to all members of the amathaspiramide family. Imide **1-67** was reduce with DIBAL-H to amathaspiramide D in 52% yield. Amathaspiramide D could then be treated with Schwartz's reagent to provide amathaspiramide E in 67% yield.

1.3.1.4. Tambar synthesis of amathaspiramide F

In 2013, the Tambar research group disclosed a formal synthesis of amathaspiramide F (**Scheme 1.11**).[33] Their synthesis commenced with *L*-proline *tert*-butyl ester **1-68**, and prenylation led to **1-69**, the precursor for their allylic amination/2,3-Stevens rearrangement sequence. Treatment of **1-69** with olefin **1-70** in the presence of a palladium catalyst led to the rearranged product **1-71** in 70% yield. Reductive cleavage of the prenyl group led to **1-72** in which the tert-butylester was hydrolyzed with TFA to **1-73**. Methylation with trimethylsilyldiazomethane led to **1-74** in 14% yield over 3 steps, the same precursor that the Ohfune group during their synthesis of amathaspiramide F.[34]

Scheme 1.11. Tambar's formal synthesis of amathaspiramide F

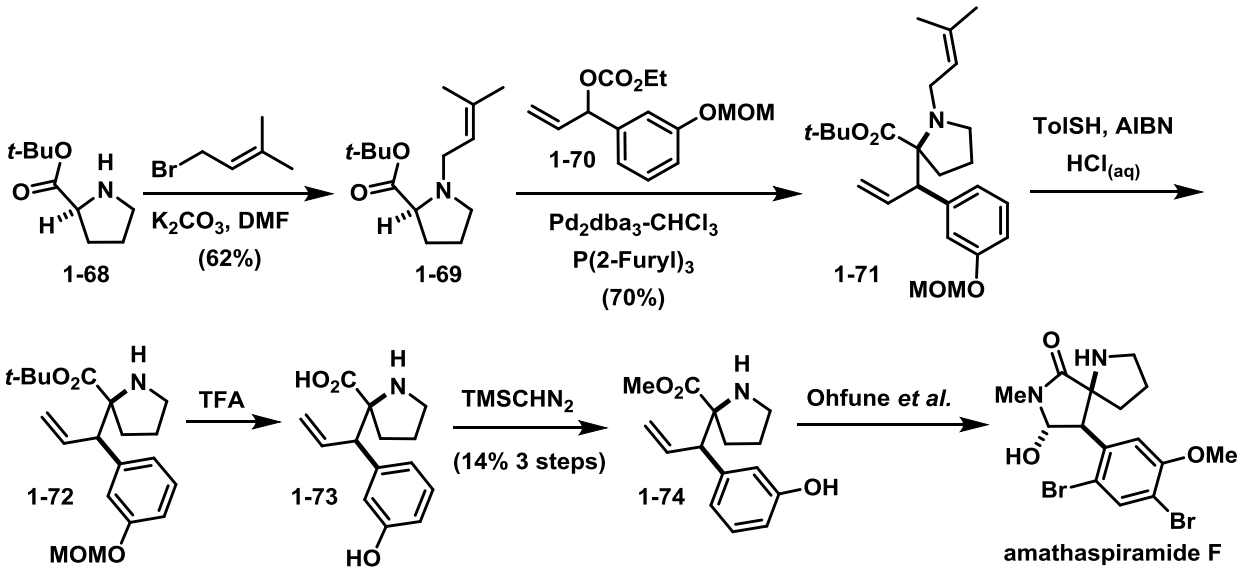

1.3.2. Synthesis of amathaspiramide C

1.3.2.1. Retrosynthesis of amathaspiramide C

It was envisioned that amathaspiramide C could be generated from imide **1-75** via reduction. Imide **1-75** could be realized through pyrrolidine **1-76**; which is the product of protonolytic ring opening of bicyclic pyrazoline **1-77**. Bicyclic Δ^2-pyrazoline **1-77** is the result of the tandem formal [3+2] cyclization

Scheme 1.12. Retrosynthesis of amathaspiramide C

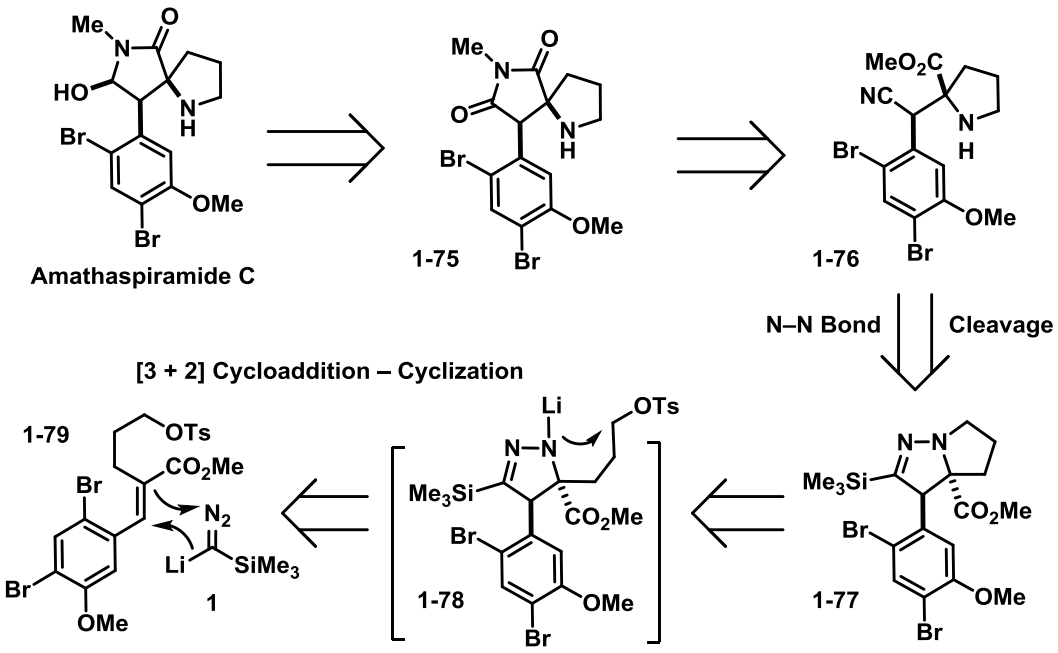

followed by cyclization of **1-78**. Monoadduct **1-78** is the direct result of the formal [3+2] cycloaddition of **1** with tosyl cinnamate **1-79**.

1.3.2.2. Forward synthesis of amathaspiramide C

The synthesis began with a Peterson olefination between **1-80** and aldehyde **1-81** which delivered a 1:1 mixture of *E*/*Z* isomers which were immediately treated with aqueous hydrochloric acid to deliver the primary alcohol which was converted to the required tosyl cinnamate **1-79**. When exposed to **1** at -78 C, **1-79** delivered a mixture of bicyclic pyrazolines **1-77**. Protonolytic ring opening of **1-77** with tosic acid in ethanol produced a mixture of pyrrolidines **1-76**. Gratifyingly, under basic hydrogen peroxide conditions in DMSO, **1-76b** was epimerized to the desired diastereomer **1-82**.[34] When imide **1-82** was subjected to Mitsunobu[35] conditions, penultimate intermediate **1-75** was isolated in 85% yield. Reduction with typical reducing agents ($LiAlH_4$, $NaBH_4$, K-selectride) led to the wrong chemoselectivity of **1-75** reduction giving the C6-carbonyl reduced product **1-83**. Finally, it was found that treatment of **1-75** with 3.5 equivalents DIBAL-H led to the formation of amathaspiramide C (31%) along with **1-83** in 45% yield.

Scheme 1.13. Forward synthesis of amathaspiramide C

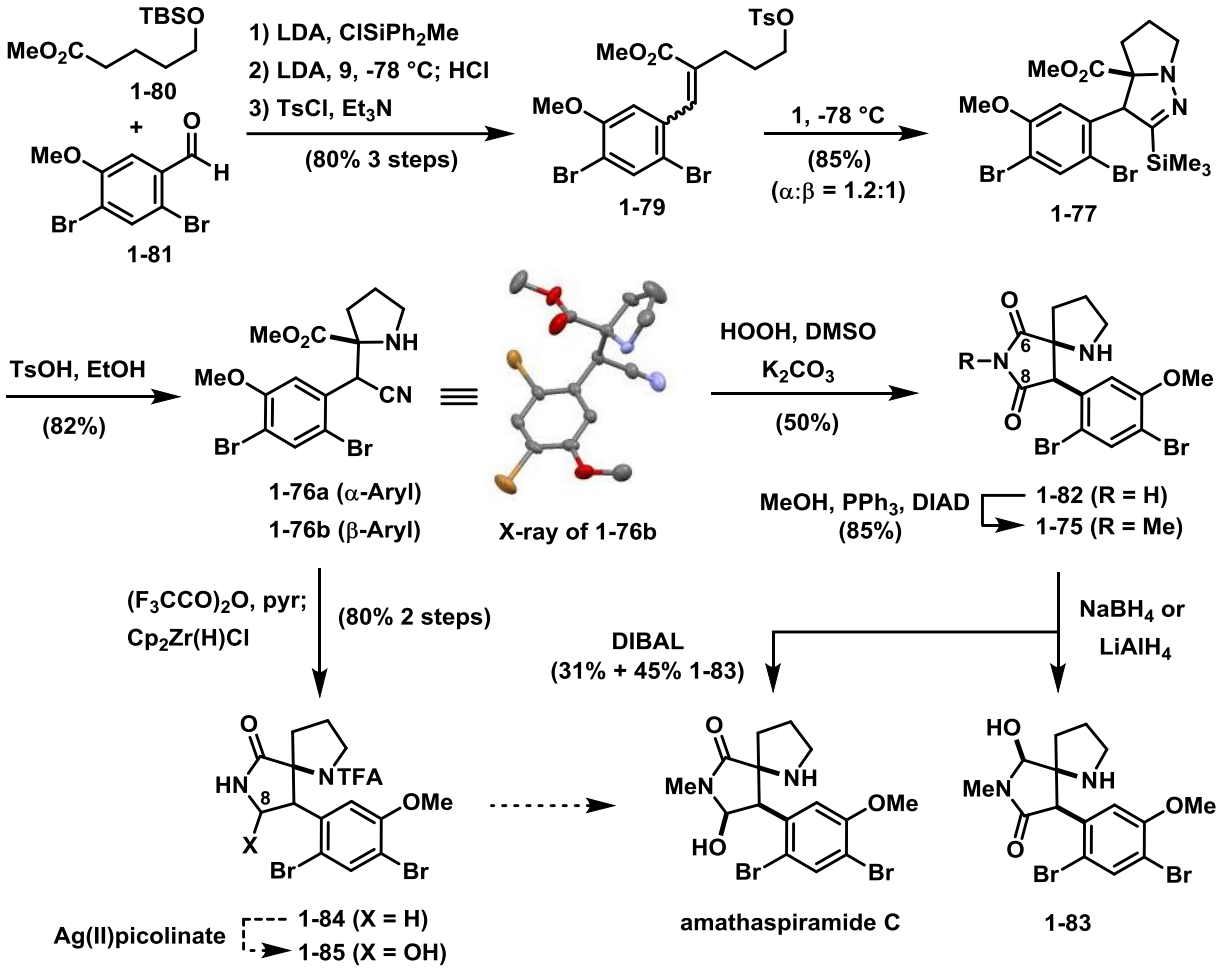

in order to circumvent the issues regarding the chemoselective reduction of **1-75**, pyrrolidine **1-76** was treated with trifluoroacetic anhydride to give its trifluoroacetamide, and this compound was treated with Schwartz's reagent which yielded only pyrrolidinone **1-84**. Compound **1-84** was treated with silver picolinate under known conditions,[36] but oxidation at C-8 to **1-85** was unfruitful.

1.3.3. Synthesis of all members of the amathaspiramides

1.3.3.1. Retrosynthesis of amathaspiramides

With the successful implementation of the newly developed methodology in the synthesis of amathaspiramide C, it was envisioned that a similar approach could be applied to the synthesis of all members of the amathaspiramide family (**Scheme 1.14**). Amathaspiramides A-F could be realized through

Scheme 1.14. Retrosynthesis of amathaspiramides

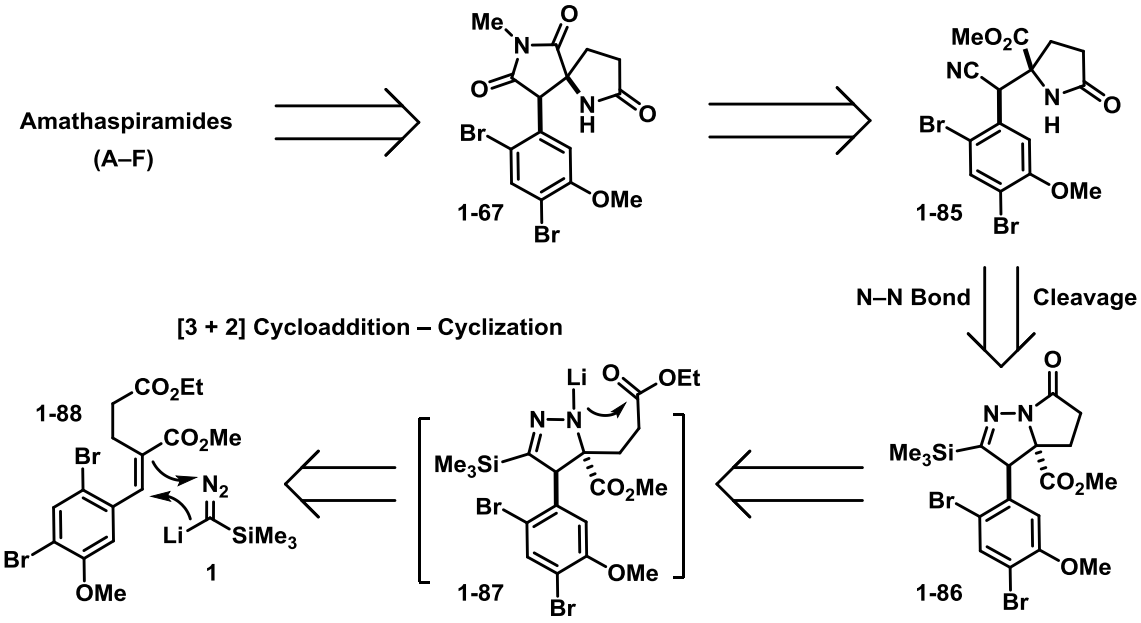

compound **1-67**, the same intermediate embraced by the Fukuyama group in their synthesis of the amathaspiramides.[32] Imide **1-67** could be synthesized via treatment of **1-85** with basic hydrogen peroxide, and pyrrolidinone **1-85** is the product of protonolytic ring opening of bicyclic Δ^2-pyrazoline **1-86**. Bicyclic pyrazoline **1-86** is the product of the ring closure of **1-87** formed via reaction of **1** with ester-tethered cinnamate **1-88**.

1.3.3.2. Forward synthesis of amathaspiramides

This new approach to all members of the amathaspiramide family commenced with a Baylis-Hillman reaction with aldehyde **1-89**, and the acquired allylic alcohol was then subjected to a Johnsen-Claisen rearrangement to give the desired cinnamate **1-88** in 55% over two steps in a 3:1 mixture of *E*/*Z* isomers.[37] Gratifyingly, the desired *E*-isomer could be selectively isolated via crystallization. Subjection

of **1-88** to **1** generated intermediate **1-87** which directly cyclized to **1-86** in a single operation. Protonolytic N-N bond cleavage occurred in refluxing ethanol to give **1-85** in 95% yield. In a similar sequence of events as in **Scheme 1.13**, pyrrolidinone **1-85** was converted to imide **1-90** in the presence of basic hydrogen pereoxide in DMSO.[38] Finally, methylation of **1-90** under typical Mitsunobu conditions was more challenging than that of **1-82**, but after extensive experimentation, it was found that polymer supported-

Scheme 1.15. Synthesis of amathaspiramides

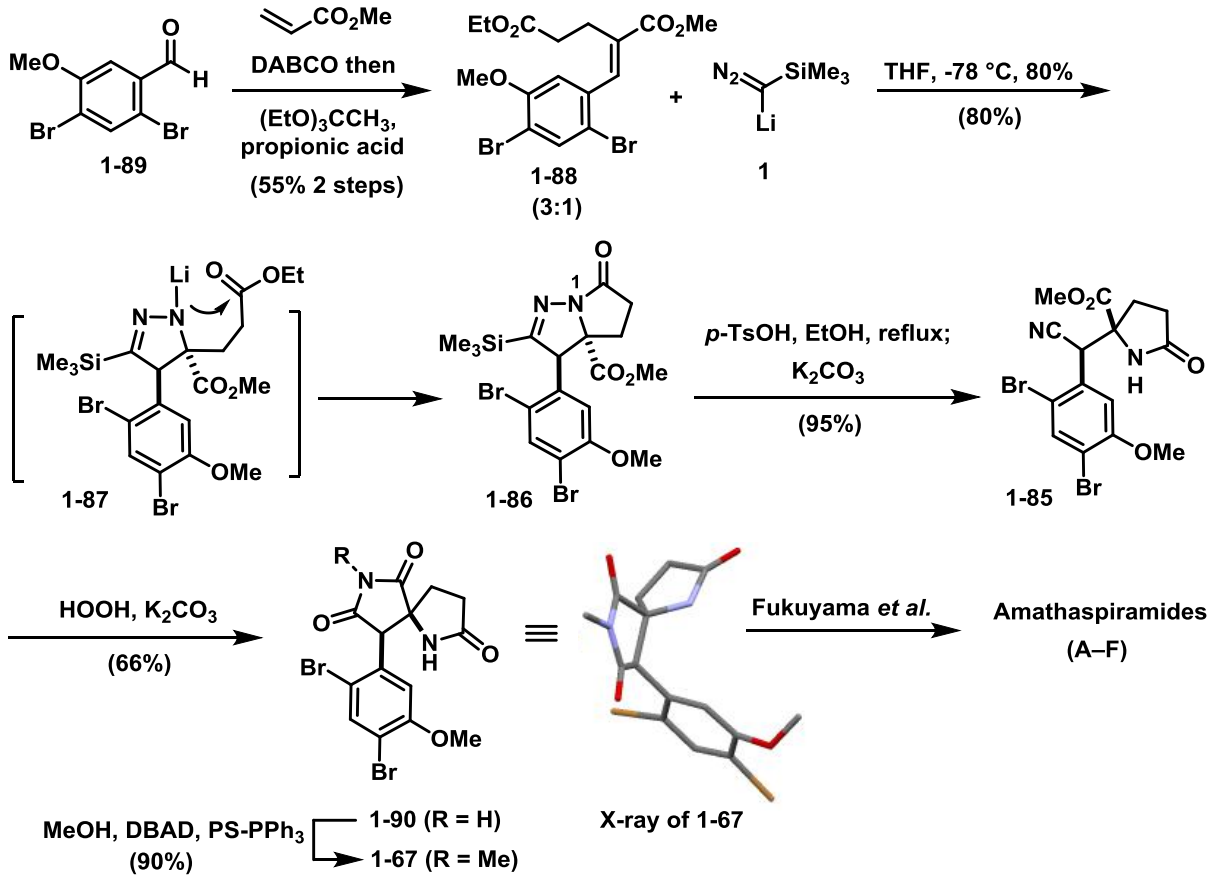

triphenylphosphine in the presence of di-*tert*-butyl azodicarboxylate (DBAD) led to the formation of **1-67** in 90% yield.[39] Because **1-67** was the intermediate that the Fukuyama group used to synthesize all members of the amathaspiramides, this constituted a formal synthesis of this dibrominated spirocyclic family of alkaloids.

1.4. Conclusion

In conclusion, a new method for the construction of structurally diverse Δ^2-pyrazolines was develovped relying on the reactivity of LTMSD **1** with acyclic and cyclic enoates. This method served as a convienent approach to constructing the α,α-disubstituted-α-amino acid moiety (α-tert-alkylamino group), and this was showcased in the synthesis of amatahaspiramide C in only 8 steps in an overall yield of 6.7%. The study was extended to a formal synthesis of all members of the amathaspiramides in 6 steps and 16% yield. Highlights of the synthesis include the diastereoselective cycloaddition of 1 with E-cinnamate **1-88** leading to *de novo* introduction of the Nitrogen atoms and the α-tert-alkylamino group in a single step. Likewise, protonolytic bond cleavage followed by nitrile hydrolysis led to facile construction of the spirocyclic core.

1.5. Experimental detail

1.5.1. General information

All reactions were carried out under an inert nitrogen atmosphere, unless otherwise indicated. Flasks were oven-dried and cooled under a stream of nitrogen. Compounds were purchased from Aldrich unless otherwise noted. CH_2Cl_2, THF, Et2O were purified based on standard procedures. Flash chromatography was performed using silica gel 60 Å (32-63 mesh) purchased from SiliCycle. Analytical thin layer chromatography (TLC) was performed on 0.25 mm SiliCycle precoated silica gel 60 (particle size 0.040-0.063 mm). 1H NMR and ^{13}C NMR spectra were recorded on a Bruker AV-500 spectrometer. ^{1}H and ^{13}C chemical shifts were referenced to internal solvent resonances and reported relative to SiMe4; multiplicities are indicated by s (singlet), d (doublet), t (triplet), q (quartet), qn (quintet), m (multiplet) and br (broad). Coupling constants, J, are reported in Hz (Hertz). Electrospray ionization (ESI) mass spectra were recorded on a Micromass LCT equipped with a time-of-flight analyzer on a Waters Micromass Q-Tof Ultima in the University of Illinois at Urbana-Champaign. Electron impact (EI) mass spectra were obtained using a Micromass AutoSpecTM. Fast atom bombardment (FAB) mass spectra were taken at the Mass

Spectrometry Laboratory in the University of Illinois at Urbana-Champaign, using a Micromass 70-VS-4F and 70-VSE for HRFAB and LRFAB, respectively. IR spectra were recorded using JASCO FT/IR-4100.

1.5.2. Procedure for preparation of pyrazolines

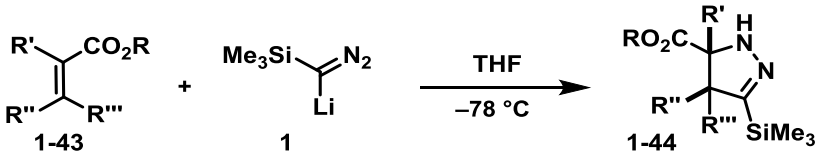

To a stirred solution of trimethylsilyldiazomethane **1**[40] (0.3 mL, 2.0 M in ether, 0.6 mmol) in anhydrous THF (2 mL) under an atmosphere of nitrogen and at –78 °C was added *n*-BuLi (0.24 mL, 2.5 M in hexanes, 0.65 mmol) dropwise over 1 minute. The solution went pale yellow and was allowed to stir for an additional 30 minutes at –78 °C. Enoate 6 (0.5 mmol), dissolved in THF (2 mL), was then added drop-wise over 30 seconds and the reaction was allowed to stir for a further 30 min until TLC showed the full consumption of the starting material. The reaction mixture was quenched with several drops of saturated NH_4Cl solution, allowed to warm to rt, and dried over $MgSO_4$. The drying reagent was filtered and solvent was removed under reduced pressure to give the crude product. Purification using flash chromatography with gradient elusion with hexane and ethyl acetate (20:1 to 6:1) to afford pure pyrazoline **7**.

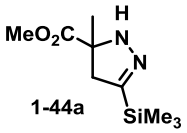

^{1}H NMR (500 MHz, $CDCl_3$) δ 3.72 (s, 3H), 3.24 (d, *J* = 16.9 Hz, 1H), 2.54 (d, *J* = 16.9 Hz, 1H), 1.45 (s, 3H), 0.16 (s, 9H) ^{13}C NMR (125 MHz, $CDCl_3$) δ 175.8, 159.7, 66.7, 52.6, 47.9, 23.6, -2.4. IR (neat) ν_{max} 2956, 1724, 1668, 1437, 1203, 845 cm^{-1}. HRMS (ESI) calc. for $C_9H_{19}N_2O_2Si$ $[M+H]^+$ 215.1216, found 215.1225.

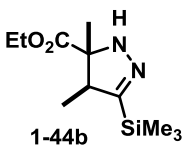

^{1}H NMR (500 MHz, $CDCl_3$) ppm 6.42 (s, 1H), 4.24-4.06 (m, 2H), 3.31 (q, *J* = 7.41, 7.40, 7.40 Hz, 1H), 1.31 (s, 3H), 1.23 (t, *J* = 7.11, 7.11 Hz, 3H), 1.02 (d, *J* = 7.43 Hz, 3H), 0.16 (s, 9H). ^{13}C NMR (125 MHz, $CDCl_3$) δ 176.1, 164.3, 69.4, 61.4, 49.8, 17.4, 14.1, 11.7, -

1.7. IR (neat) ν_{max} 3323, 2978, 1733, 1710, 1656, 1252, 843 cm^{-1}. HRMS (EI^+) calc. For $C_{11}H_{21}N_2O_2Si$ $[M]^+$ 241.13724, found 241.13637.

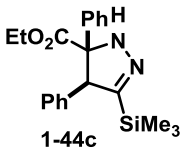

1-44c

^1H NMR (500 MHz, $CDCl_3$) δ 7.32-7.23 (m, 2H), 7.09-6.94 (m, 6H), 6.91-6.86 (m, 2H), 4.94 (s, 1H), 4.20 (dq, *J* = 7.11, 7.08, 7.08, 1.78 Hz, 2H), 1.22 (t, *J* = 7.12, 7.12 Hz, 3H), 0.01 (s, 9H). ^{13}C NMR (125 MHz, $CDCl_3$) δ 174.2, 163.8, 135.5, 135.2, 129.5, 127.7, 127.2, 126.9, 126.9, 77.5, 63.1, 62.2, 14.0, -1.9. IR (neat) ν_{max} 3281, 2956, 1720, 1213, 832 cm^{-1}. HRMS (ESI) calc. for $C_{21}H_{27}N_2O_2Si$ $[M+H]^+$ 367.1842, found 367.1846.

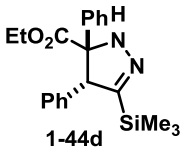

1-44d

^1H NMR (500 MHz, $CDCl_3$) δ 7.62-7.57 (m, 2H), 7.37 (t, *J* = 7.47, 7.47 Hz, 2H), 7.31 (t, *J* = 7.08, 7.08 Hz, 3H), 7.26 (m, 1H), 7.20 (d, *J* = 7.10 Hz, 2H), 6.75 (s, 1H), 4.52 (s, 1H), 3.65 (qdd, *J* = 53.66, 10.67, 7.11, 7.11, 7.09 Hz, 2H), 0.73 (t, *J* = 7.13, 7.13 Hz, 3H), -0.07 (s, 9H). IR (neat) ν_{max} 2924, 2850, 1728, 1250, 732. HRMS (ESI) calc. for $C_{21}H_{27}N_2O_2Si$ $[M+H]^+$ 367.1842, found 367.1833.

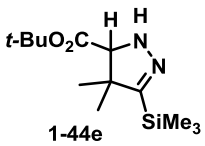

1-44e

^1H NMR (500 MHz, $CDCl_3$) δ 6.05 (s, 1H), 3.65 (d, *J* = 2.7 Hz, 1H), 1.46 (s, 9H), 1.30 (s, 3H), 1.13 (s, 3H), 0.22 (s, 9H). ^{13}C NMR (125 MHz, $CDCl_3$) 170.7, 165.5, 81.8, 71.5, 55.7, 28.1, 26.3, 20.7, -0.6. IR (neat) ν_{max} 3350, 3075, 2930, 1703, 1638, 1441, 1251, 914, 842, 688 cm^{-1}. HRMS (ESI) calc. for $C_{13}H_{27}N_2O_2Si$ $[M+H]^+$ 271.1842, found 271.1846.

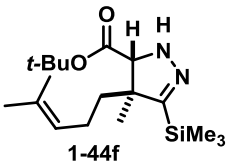

1-44f

^1H NMR (500 MHz, $CDCl_3$) δ 5.07 (m, 1H) ppm 3.74 (s, 1H) ppm 2.11 (s, 3H) ppm 1.84 (ddd, 2H, J=2.6Hz, J=4.0Hz, J=6.6Hz) ppm 1.68 (s, 3H) ppm 1.59 (s, 3H) ppm 1.47 (s, 9H) ppm 0.14 (s, 9H). HRMS (ESI) calc. for $C_{18}H_{35}N_2O_2Si$ $[M+H]^+$ 339.2468, found 339.2477.

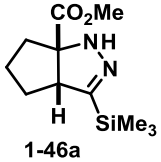

1-46a

^1H NMR (500 MHz, $CDCl_3$) δ 6.59 (bs, 1H), 3.72 (s, 3H), 3.69 (dd, *J* = 9.39, 2.60 Hz, 1H), 2.02 (dt, *J* = 12.04, 12.00, 6.32 Hz, 1H), 1.96-1.85 (m, 2H), 1.80-1.68 (m, 2H), 1.62-1.47 (m, 1H), 0.17 (s, 9H). ^{13}C NMR (125 MHz, $CDCl_3$) δ 175.9, 161.0, 76.4, 62.1, 52.6, 40.1,

32.1, 26.0, -1.6. IR (neat) ν_{max} 2956, 1730, 1438, 1258, 843 cm^{-1}. HRMS (ESI) calc. for $C_{11}H_{21}N_2O_2Si$ $[M+H]^+$ 241.1372, found 241.1379.

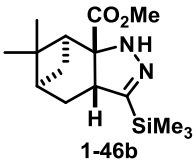

1-46b

^{1}H NMR (500 MHz, $CDCl_3$) δ 5.78 (brs, 1H), 3.96 (dd, *J* = 11.16, 3.05 Hz, 1H), 3.70 (s, 3H), 2.48 (t, *J* = 5.49, 5.49 Hz, 1H), 2.32-2.03 (m, 2H), 1.91 (brd, *J* = 4.24 Hz, 1H), 1.80 (td, *J* = 13.30, 3.37, 3.37 Hz, 1H), 1.21 (s, 3H), 0.92 (d, *J* = 10.68 Hz, 1H), 0.75 (s, 9H), 0.24 (s, 1H). ^{13}C NMR (125 MHz, $CDCl_3$) δ 174.5, 164.1, 71.8, 52.5, 47.1, 47.0, 39.6, 38.2, 28.9, 26.2, 24.5, 21.0, -1.0. IR (neat) ν_{max} 2950, 1730, 1708, 1249, 1206 cm^{-1}. HRMS (ESI) calc. for $C_{15}H_{27}N_2O_2Si$ $[M+H]^+$ 295.1842, found 295.1834.

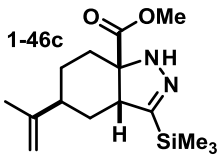

1-46c

^{1}H NMR (500 MHz, $CDCl_3$) δ 4.74 (m, 2H), 3.76 (s, 3H), 3.69 (d, 1H, J=8.9Hz), 3.41 (dd, 1H, J=2.8Hz, J=5.8Hz), 2.01 (m, 2H), 1.79 (ddd, 1H, J=5.4Hz, J=10.8Hz, J=12.0Hz), 1.72 (s, 3H), 1.63 (m, 1H), 1.48 (m, 1H), 1.22 (m, 1H), 0.24 (s, 9H). HRMS (ESI) calc. for $C_{15}H_{27}N_2O_2Si$ $[M+H]^+$ 295.1842, found 295.1834.

1.5.3. Synthesis of Amathaspiramide C

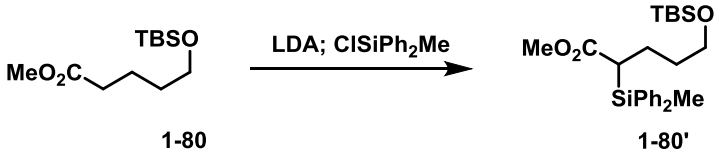

1-80 1-80'

A solution of *i*-Pr_2NH (1.8 mL, 13 mmol) in THF (10 mL) was treated with *n*-BuLi (4.8 mL, 12 mmol) at 0 °C and the solution was stirred at that temperature for 30 min and cooled to –78 °C followed by the slow addition of 8 (2.46 g, 10 mmol) in 5 mL THF. The resulting reaction mixture was stirred at –78 °C for 30 min followed by the addition of the $Ph_2MeSiCl$ (2.3 g, 10 mmol) in 5 mL of THF. The mixture was stirred at –78 °C for 1 hour and slowly warmed up to room temperature over 1 hour and quenched by 1 mL of saturated aqueous NH_4Cl solution. The cloudy solution was dried over $MgSO_4$, filtered and concentrated in vacuum to afford the crude product which was purified by column chromatography (Hex:EtOAc = 40:1) to

give final product **1-80'** containing 15% of an inseparable impurity (3.80 g, 86%). **1-80'**: colorless oil, ^{1}H NMR (500 MHz; $CDCl_3$): δ 7.56-7.52 (m, 4H), 7.40-7.33 (m, 6H), 3.59-3.55 (m, 1H), 3.54-3.50 (m, 1H), 3.40 (s, 3H), 2.62 (dd, *J* = 12.1, 2.1 Hz, 1H), 1.71-1.66 (m, 2H), 1.59-1.53 (m, 2H), 0.83 (s, 9H), -0.02 (d, *J* = 1.5 Hz, 6H). ^{13}C NMR (125 MHz; $CDCl_3$): δ 175.43, 134.82, 134.75, 129.62, 127.94, 62.47, 50.92, 36.01, 33.85, 33.39, 32.20, 25.98, -5.33, -5.51.

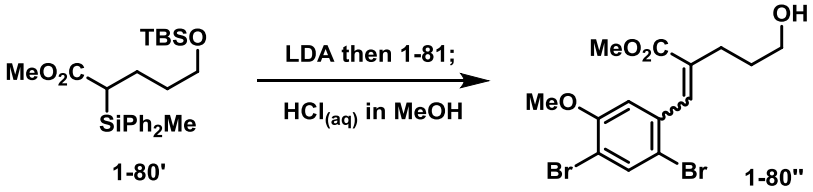

A solution of *i*-Pr_2NH (0.54 mL, 3.9 mmol) in THF (3 mL) was treated with *n*-BuLi (1.44 mL, 3.6 mmol) at 0 °C and the solution was stirred at that temperature for 30 min and cooled to –78 °C followed by the slow addition of **1-80'** (1.33 g, 3 mmol) in 3 mL THF. The resulting reaction mixture was stirred at –78 °C for 1 hour followed by the addition of 9 (0.88 g, 3 mmol) in 5 mL of THF. The mixture was slowly warmed up to room temperature over 2 hours, stirred at room temperature overnight, and quenched with 0.5 mL of saturated aqueous NH_4Cl solution. The cloudy solution was dried over $MgSO_4$, filtered and concentrated in vacuum to afford crude **1-80''**, which was purified by column chromatography (Hex:EtOAc = 40:1) to give **1-80''** as a 1:1 mixture of *E/Z* isomers, 1.29 g (78%). The above mixture was dissolved in MeOH and treated with a catalytic amount of 1 M HCl (0.5 mL) and the reaction mixture was kept at room temperature for 30 min and TLC showed the full consumption of the starting material. MeOH was removed under vacuum and CH_2Cl_2 was added. The solution was dried over $MgSO_4$, filtered and concentrated in vacuum to afford the crude **1-80''**, which was purified by column chromatography (Hex:EtOAc = 2:1) to give pure *Z*-80'' (453 mg) and *E*-s2 (449 mg) as a colorless liquid (95 %). ***Z*-80''**: colorless oil, ^{1}H NMR (500 MHz; $CDCl_3$): δ 7.68 (s, 1H), 6.74 (s, 1H), 6.67 (s, 1H), 3.81(s, 3H), 3.71 (t, *J* = 6.2 Hz, 2H), 3.57 (s, 3H), 2.54 (t, *J* = 7.3 Hz, 2H), 2.08-2.02 (bs, 1H), 1.80 (quintet, *J* = 7.0 Hz, 2H). ^{13}C NMR (125 MHz; $CDCl_3$): δ 169.06, 154.94, 137.05, 136.07, 135.80, 133.56, 113.69, 112.68, 111.60, 61.63, 56.47, 51.87, 31.32, 31.03.

***E*-80''**: colorless oil, ^{1}H NMR (500 MHz; $CDCl_3$): δ 7.76 (s, 1H), 7.59 (s, 1H), 6.83 (s, 1H), 3.90- 3.87 (s, 3H), 3.87-3.85 (s, 3H), 3.61 (td, *J* = 6.0, 3.3 Hz, 2H), 2.50 (dd, *J* = 9.9, 5.2 Hz, 2H), 1.76-1.71 (m, 2H), 1.68 (bs, 1H). ^{13}C NMR (125 MHz; $CDCl_3$): δ 168.26, 155.21, 138.50, 136.35, 136.10, 134.60, 114.37, 112.88, 112.39, 61.94, 56.58, 52.36, 31.97, 23.99. HRMS (ESI) calc. for $C_{14}H_{13}O_4Br_2$ $[M]^+$ 402.9181, found 402.9183.

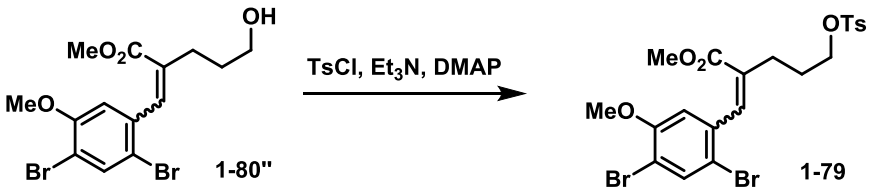

A solution of ***E*-80''** (449 mg, 1.1 mmol) in 5 mL CH_2Cl_2 was treated with TsCl (252 mg, 1.3 mmol), Et_3N (223 mg, 2.2 mmol) and a catalytic amount DMAP at room temperature. Then the solution was kept at room temperature for 3 h and TLC indicated the completion of the reaction. Water (5 mL) was added and the organic layer was separated and the aqueous layer was extracted with CH_2Cl_2 (3 x 3 mL). The combined organic extract was dried over $MgSO_4$, filtered and concentrated in vacuum to afford crude **1-79**, which was purified by column chromatography (Hex:EtOAc = 3:1) to give pure ***E*-1-79** (550 mg, 89 %). *E*-10: ^{1}H NMR (500 MHz; $CDCl_3$): δ 7.75 (s, 1H), 7.69 (d, *J* = 8.3 Hz, 2H), 7.58 (s, 1H), 7.31 (d, *J* = 7.9 Hz, 2H), 6.71 (s, 1H), 4.01 (t, *J* = 6.2 Hz, 2H), 3.87 (s, 3H), 3.81 (d, *J* = 4.5 Hz, 3H), 2.44 (s, 3H), 2.44-2.39 (m, 2H), 1.89-1.84 (m, 2H). ^{13}C NMR (125 MHz; $CDCl_3$): δ 167.50, 157.47, 144.82, 139.00, 136.42, 135.76, 133.44, 129.85, 127.78, 114.24, 112.60, 110.01, 69.88, 56.62, 52.30, 28.38, 24.21, 21.67. ***Z*-1-79**: ^{1}H NMR (500 MHz; CDCl3): δ 7.78 (d, J = 8.2 Hz, 2H), 7.68 (s, 1H), 7.31 (d, J = 8.0 Hz, 2H), 6.71 (s, 1H), 6.56 (s, 1H), 4.12 (t, J = 6.1 Hz, 2H), 3.81 (s, 3H), 3.56 (s, 3H), 2.50 (t, J = 7.2 Hz, 2H), 2.40 (s, 3H), 1.93 (quintet, J = 6.8 Hz, 2H). ^{13}C NMR (125 MHz; CDCl3): δ 168.22, 154.93, 144.87, 136.83, 135.77, 134.78, 134.48, 133.02, 129.89, 127.92, 113.58, 112.70, 111.72, 69.24, 56.49, 51.86, 30.74, 27.61, 21.64. IR (neat) ν_{max} 2923, 2851, 1713, 1465, 1360, 1192, 662 cm^{-1}. HRMS (ESI) calc. for $C_{21}H_{23}O_6SBr_2$ $[M+H]^+$ 560.9582, found 560.9582.

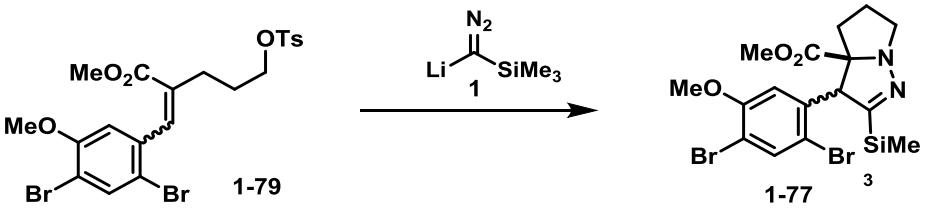

A solution of trimethylsilyldiazomethane (0.57 mL, 1.14 mmol, 2 M in Et_2O) in 2 mL THF was treated with *n*BuLi (0.49 mL, 1.22 mmol, 2.5 M in Hex) at -78 C and the reaction was stirred at -78 ^oC for 30 min, followed by the slow addtion of ***Z*-1-79** (530 mg, 0.94 mmol) in 2 mL of THF. Then the reaction mixture was slowly warmed up to 0 °C over 2 h and quenched with 0.5 mL of saturated aqueous NH_4Cl and was dried over $MgSO_4$, filtered and concentrated in vacuum to afford crude **1-77**, which was purified by column chromatography (Hex:EtOAc = 3:1) to give 407 mg of pure **1-77** (85 %). ^1H NMR (500 MHz, $CDCl_3$) δ 7.78 (s, 1H), 6.43 (s, 1H), 5.16 (s, 1H), 3.85 (s, 3H), 3.80 (s, 3H), 3.50 (dd, *J* = 12.3, 5.6 Hz, 1H), 3.38-3.36 (m, 1H), 2.04-2.02 (m, 1H), 1.78 (t, *J* = 6.3 Hz, 1H), 1.58 (t, *J* = 6.2 Hz, 2H), 0.09 (s, 9H). ^{13}C NMR (125 MHz; $CDCl_3$): δ 154.95, 143.34, 137.02, 136.79, 114.69, 85.40, 79.40, 63.79, 56.36, 54.05, 53.06, 29.49, 25.49, -0.91HRMS (ESI) calc. for $C_{18}H_{25}N_2O_3SiBr_2$ $[M+H]^+$ 503.0001, found 503.0001.

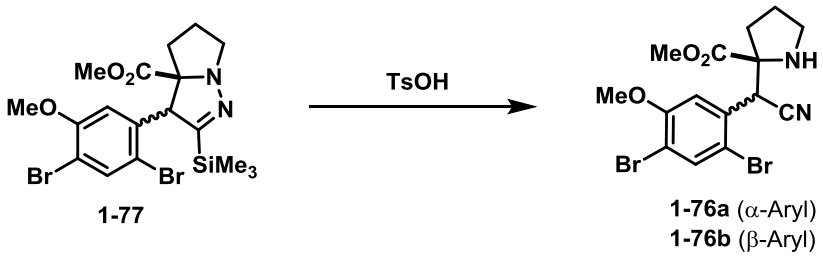

A solution of **1-77** (407 mg, 0.81 mmol) in 2 mL CH_2Cl_2 was treated with TsOH (184 mg, 0.97 mmol) and the reaction mixture was stirred under reflux until the TLC indicated the full consumption of the starting material. The mixture was cooled back to room temperature and 2 mL of saturated aqueous $NaHCO_3$ solution was carefully added to neutralize the reaction. The organic layer was separated and the aqueous layer was extracted with CH_2Cl_2 (3 x 2 mL). The combined organic extract was dried over $MgSO_4$, filtered and concentrated in vacuum to afford crude 12, which was purified by column chromatography

(Hex:EtOAc = 5:1) to give 287 mg of pure **1-76b** (82 %). ^{1}H NMR (500 MHz, $CDCl_3$) δ 7.68 (s, 1H), 7.64 (s, 1H), 4.82 (s, 1H), 3.92 (s, 3H), 3.61 (s, 3H), 3.16-3.11 (m, 2H), 2.41 (td, *J* = 8.7, 4.7 Hz, 1H), 2.31 (dt, *J* = 13.6, 7.9 Hz, 1H), 2.06-2.03 (m, 1H), 1.67 (dt, *J* = 12.3, 7.5 Hz, 1H). ^{13}C NMR (125 MHz; $CDCl_3$): δ 173.74, 155.58, 136.32, 132.85, 118.52, 114.21, 113.73, 113.36, 71.66, 56.68, 52.99, 47.93, 43.94, 36.91, 25.76. HRMS (ESI) calc. for $C_{15}H_{17}N_2O_3Br_2$ $[M+H]^+$ 430.9606, found 430.9599. **1-76a**: ^{1}H NMR (500 MHz, $CDCl_3$) δ 7.75-7.74 (s, 1H), 7.55 (s, 1H), 4.94 (s, 1H), 3.93-3.90 (s, 3H), 3.90-3.86 (s, 3H), 3.08-3.04 (m, 1H), 2.96-2.88 (bs, 1H), 2.72-2.68 (m, 1H), 1.99 (dt, *J* = 13.8, 6.9 Hz, 1H), 1.75 (td, *J* = 11.6, 5.9 Hz, 1H), 1.59-1.50 (m, 1H), 1.23-1.15 (m, 1H). 13C NMR (125 MHz; $CDCl_3$): δ 174.97, 155.37, 135.90, 132.12, 118.94, 115.76, 115.31, 113.27, 72.09, 56.68, 53.58, 47.28, 42.71, 33.73, 25.70. HRMS (ESI) calc. for $C_{15}H_{17}N_2O_3Br_2$ $[M+H]^+$ 430.9606, found 430.9599.

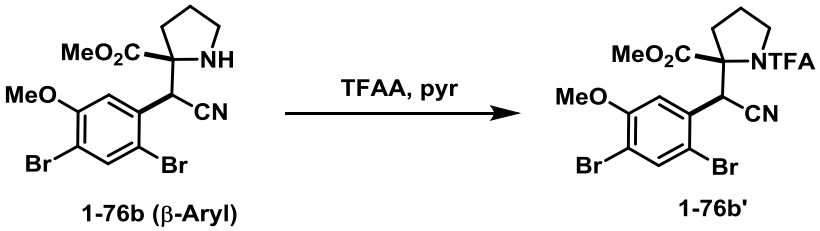

1-76b (β-Aryl) **1-76b'**

A solution of **1-76b** (75 mg, 0.17 mmol) in 1 mL CH_2Cl_2 was treated with TFAA (0.036 mL, 0.26 mmol) and pyridine (0.021 mL, 0.26 mmol) at room temperature and the resulting mixture turned bright yellow and was stirred at room temperature for 1 h until the TLC indicated the consumption of the starting material. The reaction was neutralized by the addition of 1 mL of 1 M HCl carefully and the organic layer was separated and the aqueous layer was extracted with CH_2Cl_2 (3 x 1 mL). The combined organic extract was dried over $MgSO_4$, filtered and concentrated in vacuum to afford crude s3, which was purified by column chromatography (Hex:EtOAc = 4:1) to give the pure **1-76b'** (81 mg, 90 %). s3: white solid, ^{1}H NMR (500 MHz; $CDCl_3$): δ 7.75 (s, 1H), 7.38 (s, 1H), 5.33 (s, 1H), 3.98-3.97 (m, 1H), 3.95 (s, 3H), 3.81-3.79 (m, 1H), 3.78-3.77 (s, 3H), 2.60 (dt, *J* = 13.4, 6.8 Hz, 1H), 2.40 (dt, *J* = 13.5, 6.9 Hz, 1H), 2.16-2.06 (m, 2H). ^{13}C NMR (125 MHz; $CDCl_3$): δ 168.62, 156.65, 155.81, 136.30, 131.60, 117.85, 115.69, 114.31, 113.90, 72.50, 56.55, 53.48, 49.10, 40.92, 35.69, 23.74.

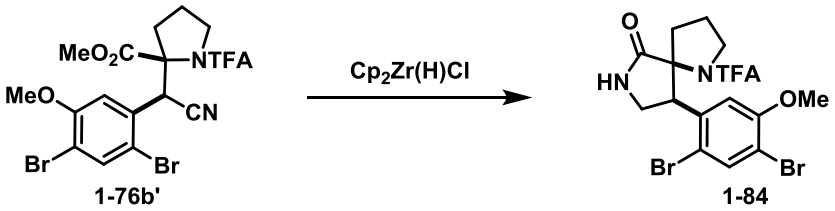

A solution of **1-76b'** in CH_2Cl_2 (40 mg, 0.08 mmol) was treated with Cp_2ZrCl (59 mg, 0.24 mmol) at room temperature and the solution was kept at room temperature overnight; CH_2Cl_2 was removed under vacuum, and the residue was purified by column chromatography (EtOAc) to give pure **1-84** (30 mg, 80 %). 16: white solid, ^{1}H NMR (500 MHz; $CDCl_3$): δ 7.77 (s, 1H), 6.89 (s, 1H), 6.16 (s, 1H), 4.31 (t, *J* = 9.0 Hz, 1H), 3.82-3.77 (m, 4H), 3.70-3.65 (m, 1H), 3.61 (t, *J* = 8.7 Hz, 1H), 3.32-3.28 (m, 1H), 2.56 (td, *J* = 12.3, 7.1 Hz, 1H), 2.39 (ddd, *J* = 12.7, 6.4, 2.9 Hz, 1H), 2.08-2.03 (m, 1H), 1.88-1.85 (m, 1H). ^{13}C NMR (125 MHz; $CDCl_3$): δ 173.10, 156.72, 155.62, 136.61, 136.06, 115.81, 114.88, 112.82, 112.03, 71.41, 56.10, 50.17, 48.83, 47.28, 38.43, 24.09.

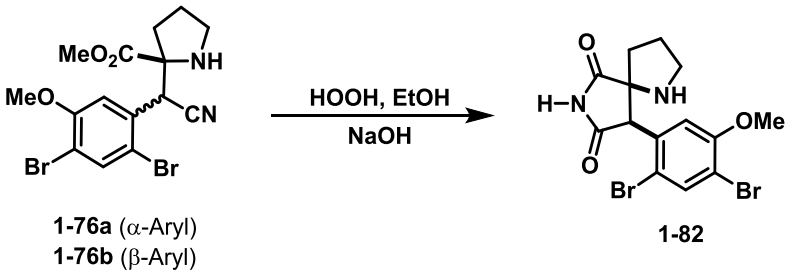

A solution of **1-76a** (50 mg, 0.12 mmol) in 1 mL EtOH was treated with H_2O_2 (30% wt. in H_2O, 95 mg, 0.84 mmol) and solid NaOH (1.5 mg, 0.06 mmol) and the reaction mixture was stirred until the TLC indicated the consumption of the starting material. Then EtOH was removed under vacuum and the residue was treated with 1 mL of sat. aq. NH_4Cl, 1 mL of CH_2Cl_2 and then carefully neutralized with aqueous HCl (1M). Then the organic layer was separated and the aqueous layer was extracted with CH_2Cl_2 (3 x 1 mL). The combined organic extract was dried over $MgSO_4$, filtered and concentrated in vacuum to afford crude **1-82**, which was purified by column chromatography (Hex:EtOAc = 2:1) to give the pure **1-82** (24 mg, 50 %). Similar procedure with 1.5 equivalents of the NaOH was applied to a 1:1 mixture of **1-76a** and **1-**

76b and isolated **1-82** in 38% yield. ^{1}H NMR (500 MHz, $CDCl_3$) δ 7.78 (s, 1H), 6.67 (s, 1H), 4.61 (s, 1H), 3.85 (s, 3H), 3.05 (dt, *J* = 10.5, 7.1 Hz, 1H), 2.75 (ddd, *J* = 10.6, 7.5, 5.5 Hz, 1H), 2.39-2.33 (m, 1H), 2.26-2.21 (m, 1H), 2.04-1.98 (m, 1H), 1.89-1.81 (m, 1H). ^{13}C NMR (125 MHz; $CDCl_3$): δ 180.98, 175.88, 155.63, 136.54, 133.32, 116.77, 113.41, 112.82, 70.58, 57.87, 56.68, 47.75, 37.58, 26.17. IR (neat) ν_{max} 2933, 2852, 1772, 1708, 1671, 1580, 1469, 1366, 1050 cm^{-1}. HRMS (ESI) calc. for $C_{14}H_{15}N_2O_3Br_2$ $[M+H]^+$ 416.9449, found 416.9447.

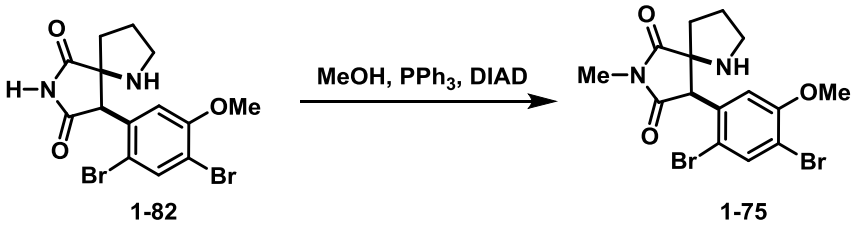

1-82 **1-75**

A solution of **1-82** (50 mg, 0.12 mmol) in 1 mL THF was treated with PPh_3 (47 mg, 0.18 mmol), DIAD (36 mg, 0.18 mmol) and MeOH (0.01 mL) under an atmosphere N_2 at 0 °C. The reaction mixture was stirred at room temperature for 1 h and THF was removed under vacuum and the residue was purified by column chromatography (Hex:EA = 2:1) to give the pure **1-75**(44 mg, 85 %). **1-75**: white solid, ^{1}H NMR (500 MHz, $CDCl_3$) δ 7.80 (s, 1H), 6.55 (s, 1H), 4.61 (s, 1H), 3.86 (s, 3H), 3.13 (s, 3H), 3.05 (dt, *J* = 10.7, 7.2 Hz, 1H), 2.71-2.66 (m, 1H), 2.40-2.34 (m, 1H), 2.25-2.19 (m, 1H), 2.06-2.00 (m, 1H), 1.90-1.81 (m, 1H). ^{13}C NMR (125 MHz, $CDCl_3$) δ 180.61, 155.44, 136.47, 133.51, 116.85, 113.61, 69.64, 62.35, 56.85, 56.59, 47.83, 37.07, 26.36. HRMS (ESI) calc. for $C_{15}H_{17}N_2O_3Br_2$ $[M+H]^+$ 430.9606, found 430.9602.

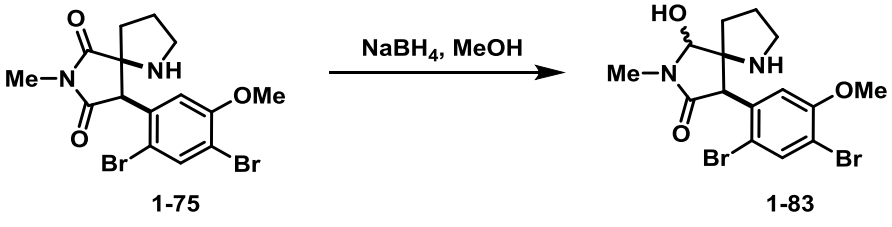

1-75 **1-83**

A solution of **1-75** (10 mg, 0.02 mmol) in 1 mL CH_2Cl_2/EtOH (v/v 1/1) was treated with $NaBH_4$ (1.2 mg, 0.03 at room temperature. The reaction mixture was stirred at 0 °C for 30 min and the solvent was removed

under vacuum and the residue was purified by column chromatography (EtOAc:EtOH = 4:1) to give pure **1-83** and ***epi*-1-83**. ^{1}H NMR (500 MHz, $CDCl_3$) δ 7.77 (s, 1H), 6.63 (s, 1H), 4.54 (s, 1H), 4.31 (s, 1H), 3.84 (s, 3H), 3.04 (s, 3H), 2.86-2.83 (m, 2H), 2.30-2.26 (m, 1H), 2.08-2.03 (m, 1H), 1.85-1.81 (m, 1H), 1.76-1.72 (m, 1H). HRMS (ESI) calc. for $C_{15}H_{19}N_2O_3Br_2$ $[M+H]^+$ 432.9762, found 432.9742. ^{1}H NMR (500 MHz, $CDCl_3$) δ 7.77 (s, 1H), 6.72 (s, 1H), 4.70 (s, 1H), 4.60 (s, 1H), 3.85 (s, 3H), 3.02 (s, 3H), 2.85-2.80 (m, 2H), 2.35-2.30 (m, 1H), 2.07-1.99 (m, 1H), 1.87-1.80 (m, 1H), 1.77-1.71 (m, 1H). HRMS (ESI) calc. for $C_{15}H_{19}N_2O_3Br_2$ $[M+H]^+$ 432.9762, found 432.9755.

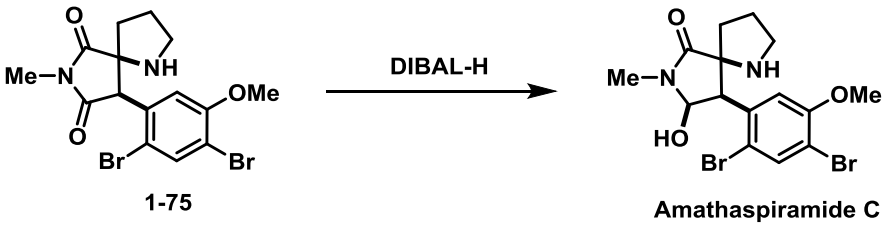

1-75 **Amathaspiramide C**

A solution of **1-75** (10 mg, 0.02 mmol) in 1 mL CH_2Cl_2 was treated with DIBAL-H (1 M in toluene, 0.16 mL) at -78 ^{o}C. The reaction mixture was slowly warmed to room temperature in 1 hour and was quenched by the slow addition of MeOH followed by the saturated aqueous solution of sodium potassium tartrate. Then the organic layer was separated and the aqueous layer was extracted with CH_2Cl_2 (3 x 1 mL). The combined organic extract was dried over $MgSO_4$, filtered and concentrated in vacuum to afford the crude amathaspiramide C, which was purified by column chromatography (EtOAc:EtOH = 19:1).

Synthetic: R*f* = 0.31 (EtOAc:EtOH = 9:1, UV, ninhydrin) IR (neat, cm^{-1}) 3346 (br), 2923, 1674, 1464, 1253, 1054; ^{1}H NMR (500 MHz, $CDCl_3$) δ 7.77 (s, 1H), 7.75 (s, 1H), 5.07 (d, *J* = 5.0 Hz, 1H), 3.91 (d, *J* = 5.0 Hz, 1H), 3.87 (s, 3H), 3.11-3.06 (m, 1H), 3.01 (s, 3H), 2.63-2.61 (m, 1H), 2.17 (m, 1H), 1.86-1.85 (m, 1H), 1.74-1.70 (m, 1H), 1.64-1.61 (m, 1H). HRMS (ESI) calc. for $C_{15}H_{19}N_2O_3Br_2$ $[M+H]^+$ 432.9762, found 432.9768.

Natural (lit.)[4c]: R*f* = 0.49 (EtOAc:acetone = 5:1, UV); IR(neat, cm^{-1}) 3422 (br), 1682, 1474, 1441, 1208, 1139, 1054; ^{1}H NMR ($CDCl_3$, 300 MHz) δ 7.77 (s, 1H), 7.75 (s, 1H), 7.70 (br-s, 1H), 5.07 (d, *J* = 4.8 Hz,

1H), 3.90 (d, *J* = 4.8 Hz, 1H), 3.87 (s, 3H), 3.08 (m, 1H), 3.01 (s, 3H), 2.62 (m, 1H), 2.17 (m, 1H), 1.87 (m, 1H), 1.73 (m, 1H), 1.62 (m, 1H); ^{13}C NMR ($CDCl_3$, 75 MHz) δ 176.7, 155.0, 136.1, 134.3, 117.6, 115.2, 112.0, 84.2, 70.2, 56.5, 51.5, 48.1, 36.5, 34.0, 27.7, 26.6; HRMS (FAB) calcd for $C_{15}H_{19}{}^{81}Br_2N_2O_3$ ($[M+H]^+$) 436.9721, found 436.9738, calcd for $C_{15}H_{19}{}^{79}Br^{81}BrN_2O_3$ ($[M+H]^+$) 434.9742, found 434.9738, calcd for $C_{15}H_{19}{}^{79}Br_2N_2O_3$ ($[M+H]^+$) 432.9762, found 432.9732.

1.5.4. Synthesis of Amathaspiramides A-F

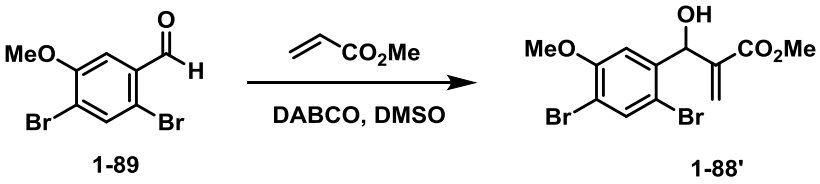

1-89 **1-88'**

A solution of **1-89** (1 g, 3.4 mmol) in 3 mL DMSO was treated with methyl acrylate (1 mL, 10.2 mmol) followed by 1 equivalent phenol (320 mg, 3.4 mmol). DABCO (760 mg, 6.8 mmol) was added, and the solution was allowed to to stir at room temperature until TLC showed full consumption of 9 (10 h). The solution was diluted with 100 mL of 0.5 M HCl and ethyl acetate (100 mL). The aqueous layer is back extracted with 3 x 20 mL ethyl acetate. The combined organic layers were washed with 100 mL of 0.5M NaOH solution, H_2O (3 x 100 mL), and brine (1 x 100 mL). The organic layer was then dried (Na_2SO_4), filtered and the solvent was removed under reduced pressure. The gummy residue was purified by column chromatography (Hex:EA = 4:1) **1-88'**: ^{1}H NMR (500 MHz, $CDCl_3$) δ 7.70 (s, 1H), 7.15 (s, 1H), 6.32 (s, 1H), 5.83 (d, J = 2.83 Hz, 1H), 5.47 (s, 1H), 3.89 (s, 3H), 3.81 (s, 3H), 3.44 (d, J = 3.78 Hz, 1H). ^{13}C NMR (125 MHz, $CDCl_3$) δ 167.1, 155.7, 140.2, 140.1, 136.2, 127.4, 113.2, 111.7, 111.6, 71.1, 56.5, 52.3. IR (neat) ν_{max} 3430, 1712, 1464, 1365, 1246, 1140, 1061, 964 cm^{-1}. HRMS (ESI) calc. for $C_{12}H_{12}O_4Br_2Na$ $[M+Na]^+$ 400.9000, found 400.8999.

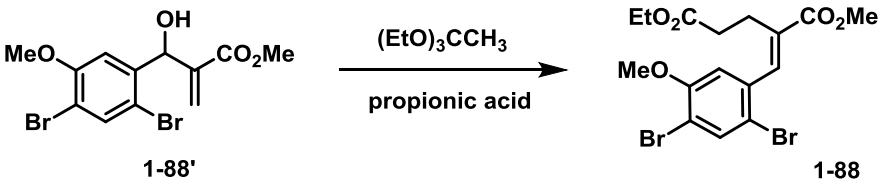

Compound **1-88'** (1 g, 2.63 mmol) was dissolved in 5 equivalents triethyl orthoacetate (2.13 mL, 13.2 mmol) and 6 drops of propionic acid was added with stirring. The resulting solution was refluxed overnight and then the excess triethylorthoacetate was removed under reduced pressure. The resulting gum was purified using column chromatography (Hex:EA = 19:1). **1-88**: ^{1}H NMR (500 MHz, $CDCl_3$) δ 7.67 (s, 1H), 6.73 (s, 1H), 6.70 (s, 1H), 4.13 (q, J = 7.14, 7.14, 7.14 Hz, 2H), 3.80 (s, 3H), 3.58 (s, 3H), 2.75 (t, J = 7.59, 7.59 Hz, 2H), 2.57 (t, J = 7.55, 7.55 Hz, 2H), 1.24 (t, J = 7.14, 7.14 Hz, 2H). *E*-2: ^{1}H NMR (500 MHz, $CDCl_3$) δ 7.76 (s, 1H), 7.61 (s, 1H), 6.86 (s, 1H), 4.08 (q, J = 7.13, 7.13, 7.13 Hz, 2H), 3.89 (s, 3H), 3.84 (s, 3H), 2.80-2.61 (m, 2H), 2.57-2.46 (m, 2H), 1.21 (t, J = 7.13, 7.13 Hz, 3H). ^{13}C NMR (125 MHz, $CDCl_3$) δ 172.3, 168.2, 154.9, 136.8, 135.9, 134.7, 113.7, 112.7, 111.8, 60.6, 56.5, 51.9, 33.3, 30.0, 14.3. IR (neat) ν_{max} 2949, 1727, 1465, 1368, 1218 cm^{-1}. HRMS (ESI) calc. for $C_{16}H_{19}O_5Br_2$ $[M+H]^+$ 448.9599, found 448.9594.

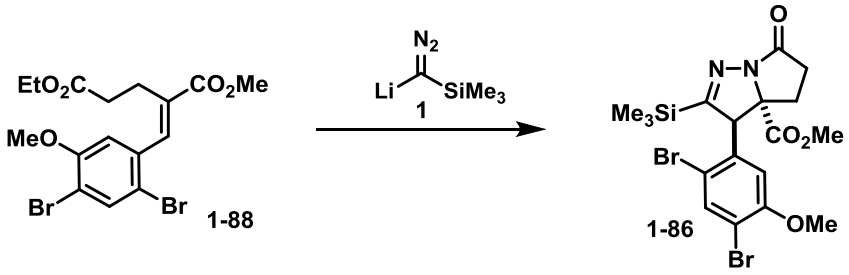

The general procedure for preparation of pyrazolines **1-44** was followed. ^{1}H NMR (500 MHz, $CDCl_3$) δ 7.82(s, 1H), 6.09 (s, 1H), 5.05 (s, 1H), 3.83 (s, 1H), 3.76 (s, 1H), 3.06 (ddd, J = 16.95, 11.55, 8.60 Hz, 1H), 2.43 (dd, J = 16.97, 8.99 Hz, 1H), 2.19 (dd, J = 13.45, 8.34 Hz, 1H), 1.30 (ddd, J = 13.23, 11.64, 9.31 Hz, 1H), 0.13 (s, 1H). ^{13}C NMR (125 MHz, $CDCl_3$) δ 174.8, 171.9, 168.9, 155.9, 137.3, 133.0, 115.4, 112.8, 112.5, 72.8, 59.2, 56.6, 53.4, 35.3, 24.7, -1.7. IR (neat) ν_{max} 2953, 1730, 1472, 1248, 1054, 841 cm^{-1}. HRMS (ESI) calc. for $C_{20}H_{29}N_2O_5SiBr_2$ $[M+H]^+$ 563.0212, found 563.0210.

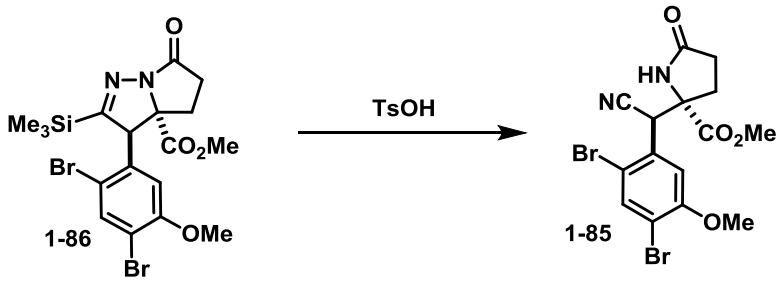

A solution of **1-86** (500 mg, 0.79 mmol) in 4 mL EtOH was treated with TsOH (190 mg, 1 mmol) and the reaction mixture was stirred at room temperature until the TLC indicated the full consumption of the starting material. The solvent was removed and the semisolid was diluted with 5 mL CH_2Cl_2 and 2 mL of saturated aqueous $NaHCO_3$ solution was added to neutralize the reaction. The organic layer was separated and the aqueous layer was extracted with CH_2Cl_2 (3 x 2 mL). The combined organic extract was dried over $MgSO_4$, filtered and concentrated in vacuum to afford crude **1-85**, which was purified by column chromatography (Hex:EA = 4:1) to give pure **1-85** (352 mg, 80 %). ^{1}H NMR (500 MHz, $CDCl_3$) δ 7.82 (s, 1H), 7.04 (s, 1H), 6.70 (s, 1H), 5.09 (s, 1H), 3.93 (s, 1H), 3.90 (s, 1H), 2.29 (t, J = 7.93, 7.93 Hz, 1H), 2.23-2.09 (m, 1H), 1.50 (td, J = 17.50, 8.84, 8.84 Hz, 1H). ^{13}C NMR (125 MHz, $CDCl_3$) δ 177.0, 171.1, 156.1, 137.0, 129.6, 117.3, 115.1, 114.6, 113.7, 67.9, 56.9, 54.0, 42.5, 29.3, 28.2. HRMS (ESI) calc. for $C_{15}H_{15}N_2O_4Br_2$ $[M+H]^+$ 444.9399, found 444.9399.

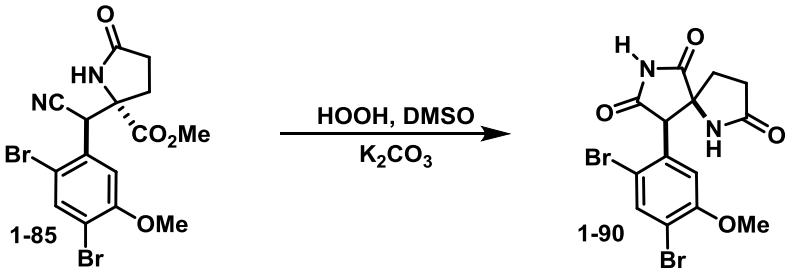

A solution of **1-85** (65 mg, 0.015 mmol) in 2 mL DMSO was treated with H_2O_2 (30% wt. in H_2O, 116 µL, 10 equiv) and solid K_2CO_3 (40 mg, 0.03 mmol) and the reaction mixture was stirred until the TLC indicated

the consumption of the starting material. The reaction was then diluted with $CHCl_3$ and saturated NH_4Cl. The pH was then neutralized with 1 M HCl. Then the organic layer was separated and the aqueous layer was extracted with CH_2Cl_2 (3 x 1 mL). The combined organic extract was dried over $MgSO_4$, filtered and concentrated in vacuum to afford the crude **1-90**, which was purified by column chromatography (Hex:EA = 1:1 to Hex:EA = 0:1) to give the pure **1-90** (41 mg, 66 %). ^{1}H NMR (500 MHz, $CDCl_3$) δ 10.30 (s, 1H), 7.75 (s, 1H), 7.31 (s, 1H), 6.55 (s, 1H), 4.60 (s, 1H), 3.73 (s, 3H), 2.53 (ttd, J = 23.62, 10.39, 10.39, 5.01, 5.01 Hz, 4H). ^{13}C NMR (125 MHz, $CDCl_3$) δ 179.3, 178.9, 174.9, 156.1, 136.7, 132.3, 116.3, 113.0, 112.6, 67.0, 57.1, 56.5, 32.5, 29.6. HRMS (ESI) calc. for $C_{14}H_{13}N_2O_4Br_2$ $[M+H]^+$ 430.9242, found 430.9241.

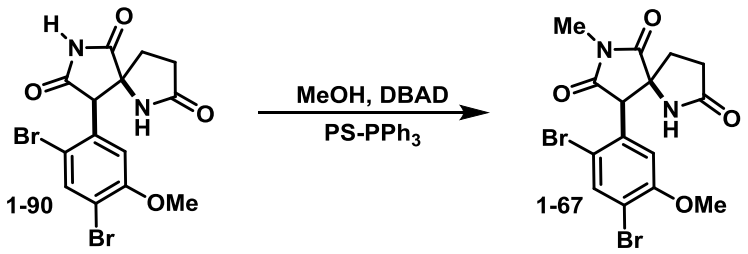

Compound **1-90** (46 mg, 0.0106 mmol) was dissolved in $CDCl_3$ (1 mL) and MeOH (9 µL, 0.02 mmol) was added with stirring followed by PS-PPh_3 (88 mg, 0.025 mmol). The resulting suspension is cooled to 0 °C, and DBAD (49 mg, 0.02 mmol) is added as a single portion. The progress of the reaction is followed by TLC then 100 mg of SiO_2 is added and the solvent was removed under reduced presusre. The resulting solids were purified using column chromatography (Hex:EA = 1:1) to yield 5 (27 mg, 58%).

Compound 1-67: ^{1}H NMR(500 MHz, DMSO-*d*6) δ 7.95 (s, 1H), 7.89 (s, 1H), 6.80 (s, 1H), 4.84 (s, 1H), 3.78 (s, 3H), 2.98 (s, 3H), 2.27-2.21 (m, 1H), 2.12-2.06 (m, 1H). ^{13}C NMR (125 MHz, DMSO-*d*6) δ 178.0, 176.9, 175.7, 155.3, 135.9, 134.1, 116.4, 116.2, 111.9, 66.0, 57.2, 55.9, 30.5, 29.7, 25.8. HRMS (ESI) calcd. For $C_{15}H_{15}N_2O_4Br_2$ $[M+H]^+$ 444.9399, found 444.9398.

Fukuyama Intermediate:[32] R*f* = 0.67 (toluene/acetone = 1:1, UV, Ce-PMA); Mp 116.3–116.6 °C (CH_2Cl_2) IR (neat, cm^{-1}) 1785, 1703, 1584, 1437, 1367; 1H NMR (DMSO-*d*6, 400 MHz) δ 7.96 (s, 1H), 7.90 (s, 1H),

6.83 (s, 1H), 4.85 (s, 1H), 3.81 (s, 3H), 3.00 (s, 3H), 2.59 (ddd, *J* = 13.3, 10.1, 7.8 Hz, 1H), 2.45 (ddd, *J* = 13.7, 9.6, 5.5 Hz, 1H), 2.26 (ddd, *J* = 15.1, 10.1, 5.5 Hz, 1H), 2.11 (ddd, *J* = 16.9, 9.6, 7.8 Hz, 1H); 13C NMR (DMSO-*d*6, 100 MHz) δ 177.5, 176.4, 175.2, 154.8, 135.4, 133.6, 116.0, 115.7, 111.4, 65.5, 56.7, 55.5, 30.0, 29.2, 25.3; HRMS (ESI) calcd for $C_{15}H_{14}{}^{79}Br_2N_2O_4Na$ ($[M+Na]^+$) 466.92180, found 466.92185.

1.5.5. ORTEPS

ORTEP of 1-44c (CCDC 1044098)

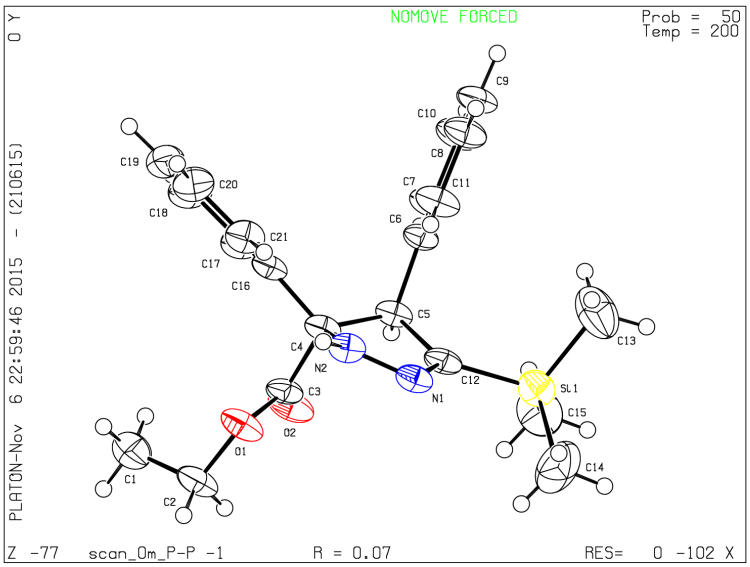

ORTEP of 1-76b (CCDC 1044017)

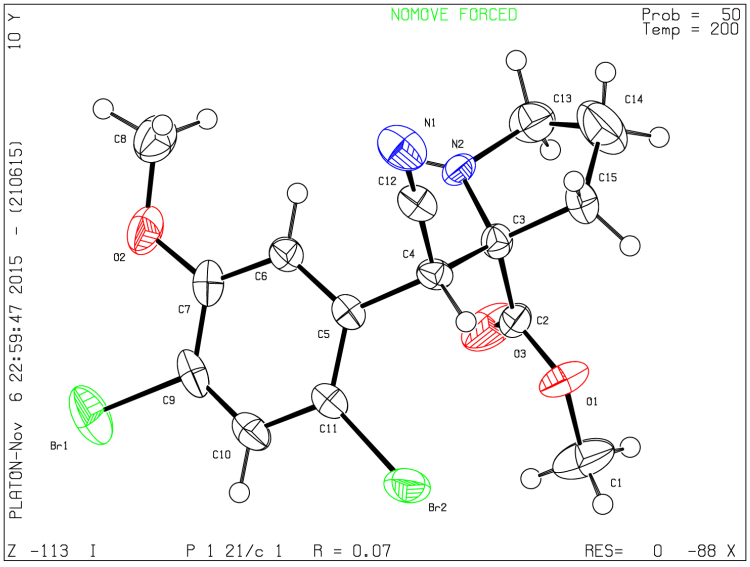

ORTEP of 1-67 (CCDC 1044018)

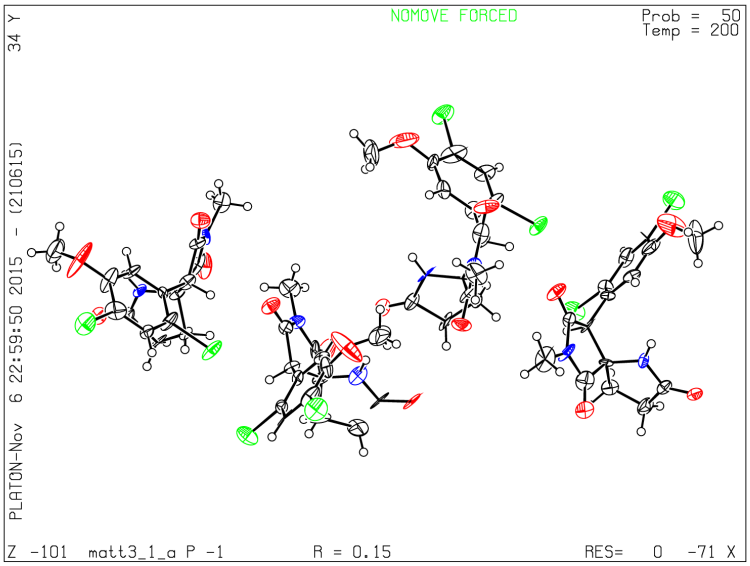

1.6. References

[1] For reviews, see: a) Heck, T.; Geueke, B.; Kohler, H. P. E. *Chem. Biodiversity* **2012**, *9*, 2388; b) Jamieson, A. G.; Boutard, N.; Sabatino, D.; Lubell, W. D. *Chem. Biol. Drug Des.* **2013**, *81*, 148; c) Kwon, I.; Lim, S. I. *Macromol. Chem. Phys.* **2013**, *214*, 1295; d) Vasudev, P. G.; Chatterjee, S.; Shamala, N.; Balaram, P. *Chem. Rev.* **2011**, *111*, 657.

[2] a) Balaram, P. *Curr. Opin. Struct. Biol.* **1992**, *2*, 845; b) Benedetti, E.; Gavuzzo, E.; Santini, A.; Kent, D. R.; Zhu, Y.-F.; Zhu, Q.; Mahr, C.; Goodman, M. *J. Pept. Sci.* **1995**, *1*, 349; c) Dry, O.; Josien, H.; Grassi, J.; Chassaing, G.; Couraud, J. Y.; Lavielle, S. *Biopolymers* **1996**, *39*, 67; d) Cativiela, C. Díaz-de-Villegas, M. D. *Tetrahedron: Asymmetry* **1998**, *9*, 3517. e) Toniolo, C.; Crisma, M.; Formaggio, F.; Peggion, C. *Biopolymers* **2001**, *60*, 396. f) Maity, P.; König, B. *Biopolymers* **2008**, *90*, 8.

[3] a) Sourkers, T. L.; Arch. *Biochem. Biophys.* **1945**, *51*, 444. b) Zhelyaskov, D. K.; Levitt, M.; Uddenfriend, S. *Mol. Pharmacol.* **1968**, *4*, 445; c) Pellicciari, R.; Luneia, R.; Costantino, G.; Marinozzi, M.; Natalini, B.; Jakobsen, P.; Kanstrup, A.; Lombardi, G.; Moroni, F.; Thomsen, C. *J. Med. Chem.* **1995**, *38*, 3717 – 3719; d) Schoepp, D. D.; Jane, D. E.; Monn, J. A. *Neuropharmacology* **1999**, 38, 1431.

[4] a) Nishimura, S.; Matsunaga, S.; Shibazaki, M.; Suzuki, K.; Furihata, K.; van Soest, R. W. M.; Fusetani, N. *Org. Lett*. **2003**, *5*, 2255. b) Grube, A.; Immel, S.; Baran, P. S.; Kock, M. *Angew. Chem., Int. Ed.* **2007**, *46*, 6721. c) Morris, B. D.; Prinsep, M. R. *J. Nat. Prod.* **1999**, *62*, 688. d) Omura, S.; Fujimoto, T.; Otoguro, K.; Matsuzaki, K.; Moriguchi, R.; Tanaka, H.; Sasaki, Y. *J. Antibiot.* **1991**. *44*, 113-116. e) Stratmann, K.; Moore, R. E.; Bonjouklian, R.; Deeter, J. B.; Patterson, G. M. L.; Shaffer, S.; Smith, C. D.; Smitka, T. A. *J. Am. Chem. Soc.* **1994**, *116*, 9935; f) Jimenez, J. I.; Huber, U.; Moore, R. E.; Patterson, G. M. L.; *J. Nat. Prod*. **1999**, *62*, 569.

[5] For the installation of α-tert-alkylamino functionality: a) Kang, S. H.; Kang, S. Y.; Lee, H.-S.; Buglass, A. J. *Chem. Rev.* **2005**, *105*, 4537; b) Ohfune, Y.; Shinada, T. Eur. *J. Org. Chem.* **2005**, 5127; c) Cativiela, C.; Diaz-de-Villegas, M. D. *Tetrahedron: Asymmetry* **2007**, *18*, 569; d) Vogt, H.; Brase, S. *Org. Biomol. Chem.* **2007**, *5*, 406; e) Frey, G.; Luu, H.-T.; Bichovski, P.; Feurer, M.; Streuff, J. *Angew. Chem. Int. Ed.* **2013**, *52*, 7131; *Angew. Chem.* **2013**, *125*, 7271; f) Li, K.; Tan, G.; Huang, J.; Song, F.; You, J. *Angew. Chem. Int. Ed.* **2013**, *52*, 12942; *Angew. Chem.* **2013**, *125*, 13180; g) Sun, F.-G.; Ye, S. *Org. Biomol. Chem.* **2011**, *9*, 3632; h) Wu, K.-J.; Li, G.-Q.; Li, Y.; Dai, L.-X.; You, S.-L. *Chem. Commun.* **2011**, *47*, 493; for asymmetric α-aminations: i) Greck, C.; Drouillat, B.; Thomassigny, C. *Eur. J. Org. Chem.* **2004**, 1377; j) Janey, J. M. *Angew. Chem. Int. Ed.* **2005**, *44*, 4292; *Angew. Chem.* **2005**, *117*, 4364; For other methods: k) Guillena, G.; Ramon, D. J. *Tetrahedron: Asymmetry* **2006**, *17*, 1465; l) Russo, A.; Fusco, C. D.; Lattanzi, A. *RSC Adv.* **2012**, *2*, 385; for reviews: m) Najera, C.; Sansano, J. M. *Chem. Rev.* **2007**, *107*, 4584; n) Smith, A. M. R.; Hii, K. K. *Chem. Rev.* **2011**, *111*, 1637.

[6] For a comprehensive review of 1,3-dipolar cycloadditions, see: (a) *Synthetic Applications of 1,3-Dipolar Cycloaddition Chemistry toward Heterocycles and Natural Products*; Padwa, A.; W. H. Pearson, Eds.; John Wiley and Sons: Hoboken, NJ, **2003**; (b) Nájera, C. ; Sansano, J. M. *Curr. Org. Chem.* **2003**, *7*, 1105; (c) Kanemasa, S. *Synlett* **2002**, 1371; (d) Gothelf, K. V. In *Cycloaddition Reactions in Organic Synthesis*; Kobayashi, S. ; Jørgensen, K. A. Wiley-VCH: Weinheim, Germany, **2002**; 211–245 ; (d) Maas, G. in "The Chemistry of Heterocyclic Compounds, Vol. 59: Synthetic Application of 1,3-Dipolar Cycloaddition Chemistry Toward Heterocycles and Natural products" Padwa, A.; W. H. Pearson, Ed.; John Wiley & Sons, Inc., **2002**; 539–621; (e) Kanemasa, S.; Kanai, T. *J. Am. Chem. Soc.* **2000**, *122*, 10710; (f) Kano, T.; Hashimoto, T.; Maruoka, K. *J. Am. Chem. Soc.* **2006**, *128*, 2174; (g) Sibi, M. P.; Stanley, L. M.; Soeta, T. *Org. Lett.* **2007**, *9*, 1553.

[7] *Frontier Orbitals and Organic Chemical Reactions*; Fleming, I. John Wiley & Sons Ltd: West Sussex, England, **1976**.

[8] Kolb, H. C.; Finn, M. G.; Sharpless, K. B. *Ange. Chem., Int. Ed*. **2001**, *40*, 2004-2021.

[9] For the structural study of **1**, see: Boche, G.; Lohrenz, J. C. W.; Schubert, F. Tetrahedron **1994**, *50*, 5889. Reviews: (a) Shioiri, T.; Aoyama, T. *Synth. Org. Chem. Jpn*. **1996**, *54*, 918; (b) Saladino, R.; Stasi, L.; Crestini, C.; Nicoletti, R.; Botta, M. *Tetrahedron* **1997**, *53*, 7045; (c) Shioiri, T.; Aoyama, T. In Science of Synthesis; Fleming, I., Ed.; Georg Thieme: Stuttgart, **2002**; *4*, 569–577.

[10] Aoyama, T.; Shioiri, T. *Chem. Pharm. Bull*. **1982**, *30*, 3450.

[11] Aoyama, T.; Sudo, K.; Shioiri, T. *Chem. Pharm. Bull*. **1982**, *30*, 3849.

[12] Aoyama, T,; Inoue, S.; Shioiri, T. *Tetrahedron Lett.* **1984**, *25*, 433.

[13] Aoyama, T.; Nakano, T.; Marumo, K.; Uno, Y.; Shioiri, T. *Synthesis* **1991**, 1163.

[14] Saladino, S.; Stasi, L.; Crestini, C.; Nicoletti, R.; Botta, M. *Tetrahedron* **1997**, *53*, 7045.

[15] Shoji, Y.; Hari, Y.; Aoyama, T. Tetrahedron Lett. **2004**, *45*, 1769.

[16] Schnurr, W.; Regitz, M. *Synthesis* **1989**, 511.

[17] Aoyama, T.; Nakano, T.; Nishigaki, S.; Shioiri, T. *Heterocycles* **1990**, *30*, 375.

[18] Asaki, T.; Aoyama, T.; Shioiri, T. *Heterocycles* **1988**, *27*, 343.

[19] Aoyama, T.; Katsuta, S.; Shioiri, T. *Heterocycles* **1989**, *28*, 133.

[20] Shioiri, T.; Iwamoto, Y.; Aoyama, T. *Heterocycles* **1987**, *26*, 1467.

[21] Aoyama, T.; Iwamoto, Y.; Shioiri, T. *Heterocycles* **1986**, *24*, 589.

[22] Aoyama, T.; Kabeya, M.; Fukushima, A.; Shioiri, T. *Heterocycles* **1985**, *23*, 2363.

[23] Aoyama, T.; Kabeya, M.; Fukushima, A.; Shioiri, T. *Heterocycles* **1985**, *23*, 2367.

[24] Aoyama, T.; Kabeya, M.; Shioiri, T. *Heterocycles* **1985**, *23*, 2371.

[25] Ito, T.; Hatano, K.; Kurono, Y.; Aoyama, T.; Shioiri, T. *Heterocycles* **1993**, *35*, 41.

[26] Sun, C.; O'Connor, M. J.; Lee, D.; Wink, D. J.; Milligan, R. D. *Angew. Chem. Int. Ed*. **2014**, *53*, 3197; *Angew. Chem.* **2014**, *126*, 3261.

[27] O'Connor, M. J.; Sun, C.; Lee, D. *Angew. Chem. Int. Ed.* **2015**, *54*, 9963–9966.

[28] CCDC-1044098, 1044017 and 1044018 contains the supplementary crystallographic data for this study. This data is provided free of charge by The Cambridge Crystallographic Data Centre.

[29] This was also the case with substrates **1-43e** and **1-43f** in **Table 1.17**.

[30] Hughes, C. C.; Trauner, D. *Angew. Chem., Int. Ed*. **2002**, *41*, 4556

[31] Sakaguchi, K.; Ayabe, M.; Watanabe, Y.; Okada, T.; Kawamura, K.; Shiada, T.; Ohfune, Y. *Org. Lett*. **2008**, *10*, 5449.

[32] Chiyoda, K.; Shimokawa, J.; Fukuyama, T. *Angew. Chem., Int. Ed*. **2012**, *51*, 2505

[33] Soheili, A.; Tambar, U. K. *Org. Lett*. **2013**, *15*, 5138.

[34] Nagata, K.; Sano, D.; Shimizu, Y.; Miyazaki, M.; Kanemitsu, T.; Itoh, T. *Tetrahedron: Asymmetry* **2009**, *20*, 2530.

[35] Kiankarimi, M.; Lowe, R.; McCarthy, J. R.; Whitten, J. P. *Tetrahedron Lett.* **1999**, *40*, 4497.

[36] Seiple, I. B.; Su, S.; Young, I. S.; Nakamura, A.; Yamaguchi, J.; Jørgensen, L.; Rodrigues, R. A.; O'Malley, D. P.; Gaich, T.; Köck, M. Baran, P. S. *J. Am. Chem. Soc.* **2011**, *133*, 14710.

[37] For a recent reviews of the Baylis-Hillman reaction, see: a) Basavaiah, D.; Rao, A. J. ; Satyanarayana, T. Chem. Rev. **2003**, *103*, 811. b) Basavaiah, D.; Rao, P. D.; Hyma, R. S. Tetrahedron **1996**, *52*, 8001; For the Johnson-Claisen rearrangement of Baylis-Hillman adducts, see c) Basavaiah, D.; Pandiaraju, S. *Tetrahedron Lett.* **1995**, *36*, 757; d) Basavaiah, D.; Pandiaraju, S.; Krishnamacharyulu, M. *Synlett* **1996**, 747.

[38] Nagata, K.; Sano, D.; Shimizu, Y.; Miyazaki, M.; Kanemitsu, T.; Itoh, T. *Tetrahedron: Asymmetry* **2009**, *20*, 2530.

[39] Kiankarimi, M.; Lowe, R.; McCarthy, J. R.; Whitten, J. P. *Tetrahedron Lett.* **1999**, *40*, 4497.

[40] Caution! Trimethylsilyldiazomethane should be regarded extremely toxic and all operations must on carried out only in a well-ventilated fume hood and all skin contact should be avoided, see: (a) Shioiri, T.; Aoyama, T.; Mori, S.; *Org. Synth., Coll. Vol.* **1993**, *8*, 612. (b) Barnhart, R.; Dale, D. J.; Ironside, M. D.; Vogt, P. F. *Org. Process Res. Dev.* **2009**, *13*, 1388. (c) Kemsley, J., *Chem. Eng. News* **2011**, *89(19)*, 15.

CHAPTER II

HYDROXY-CONTROLLED DIASTEREOSELECTIVE [3+2] CYCLOADDITIONS WITH $TMSCLiN_2$

2.1. Introduction

When considering the control of diastereoselectivity in a chemical reaction where a controlling stereocenter and prochiral group are on the same molecule and separated by one or two bonds, for acyclic, open-chain systems, there are two major criteria that must be met.[1] First, only one conformation of the bonds connecting the chiral and prochiral groups should be available at the transition state of the reaction. Second, the diastereotopic faces of the prochiral group should be differentiated by the substituents attached to the controlling stereocenter (**Figure 2.1**).

Figure 2.1. Conformation in asymmetric induction

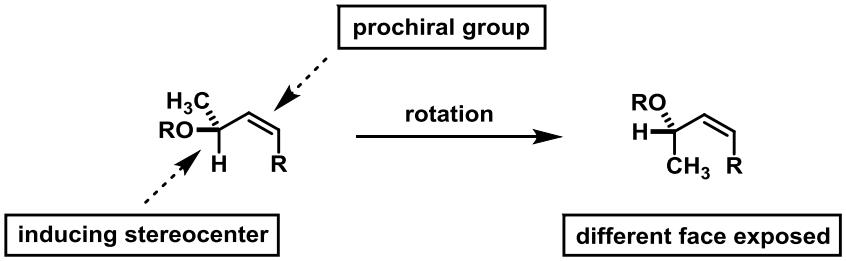

The latter mentioned differentiation can be one of two scenarios, as designated by Winterfeldt.[2] In the first, a bulky group attached to the inducing stereocenter should shield one side of the reacting prochiral group from approach (**Figure 2.2a**); this is referred to as "inert volume". In the second, coordination of the incoming reagent with a directing element at the controlling stereocenter delivers to a discrete face of the prochiral group; this is referred to as "active volume" (**Figure 2.2b**).

The obstacle of restricting conformation around the bonds that connect the inducing stereocenter and the prochiral group in acyclic systems can be overcome by taking advantage of the conformational preference of vinylic bonds possessing highly substituted allylic positions.[1] This principle was first identified and described by Johnson nearly 50 years ago when he conceived the concept of allylic 1,3-

Figure 2.2. Inert volume versus active volume at controlling stereocenters

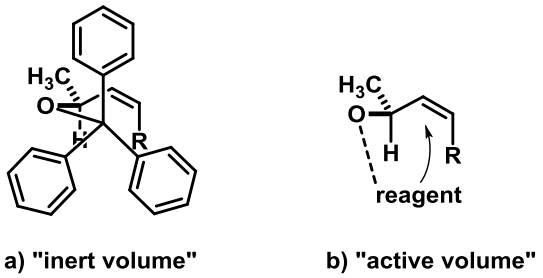

Strain (**Figure 2.3**).[3] This concept, confirmed by ab initio calculations, is purely steric in origin.[4] For *E*-alkenes, two conformations, **A** and **B**, are favored (**Figure 2.3**) with **A** being preferential due to the eclipsed nature of the H-atom and double bond. On the other hand, *Z*-alkenes are essentially "locked" into conformation **C** by over 4 kcal/mol energy (relative to **D**) due to the steric requirements of the double bond positioning the smallest group (H-atom) into the alkene plane. In the case of allylic alcohols and ethers, stereoelectronic effects compete with the steric factors.[5] Conformation **G**, with methyl group eclipsing the double bond, is higher in energy than counterpart **B** due to less favorable orbital interactions of the C-O bond and π-system when compared to those in **F**. The consequence is only a small energy difference between favorable conformations **E** and **F** in 3-buten-2-ol (**Figure 2.3**).

Figure 2.3. 1,3-Allylic strain

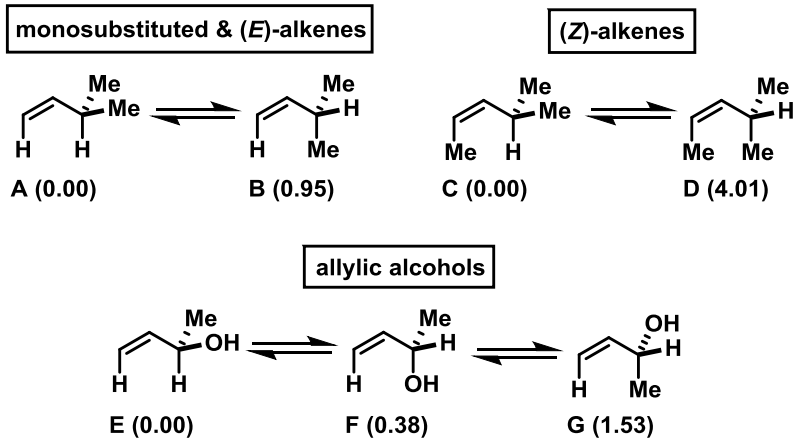

The second challenge of controlling the facial selectivity of the reaction via "active" or "inert" volume can be accomplished by using allylic alcohols, as shown in **Figure 2.2**. The utilization of these concepts has often been used in successfully controlling the stereoselectivity of [3+2] cycloaddition reactions.

2.1.1. Allylic alcohols as dipolarophiles in 1,3-dipolar cycloadditions

2.1.1.1. Nitrile oxide dipoles

Early work by Houk focused on developing a model to describe the reactivity trends of nitrile oxides with substituted alkenes.[6] Based on the reactivity of chiral dipolarophiles and calculated data, the concept of the "inside alkoxy" effect was conceived (**Figure 2.4**). The calculated relative energies (in kcal/mol) showed that methyl group favors the sterically least congested *anti* position, hydroxyl group favors *outside* position to maximize hydrogen bonding,[7] and ethers prefer the *inside* position as shown in **Figure 2.3**. This "inside alkoxy" effect served to be useful for predicting the stereoselectivities nitrile oxide cycloadditions with chiral allylic alcohols and ethers experimentally, as shown in **Table 2.1**.

Figure 2.4. Houk's "Inside Alkoxy" effect

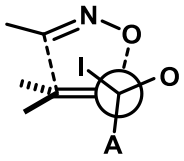

	Me	OH	OR
Anti (A)	0.0	4.9	0.7
Inside (I)	1.1	0.8	0.0
Outside (O)	0.6	0.0	2.9

In cases where allylic alcohols **2-1** were used as dipolarophiles, though, the selectivity was marginal (entries 1-2, 4-6, 8) when compared to that of their silyl ether counterparts (entries 3 and 7) in generating isoxazolines **2-2** and **2-3**. Two of the main factors contributing to the lower diastereoselectivities are competitive hydrogen bonding participation from solvent with the nitrile oxide dipole[8] and the competing "inside alkoxy" transition state which is only 0.8 kcal/mol different in energy.

Table 2.1. Houk's nitrile oxide experimental ratios

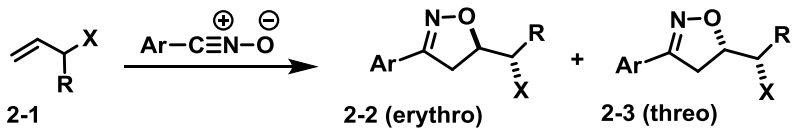

entry	Ar	R	X	2-2:2-3
1	Ph	Me	OH	40:60
2	*p*-NO_2Ph	Me	OH	45:55
3	Ph	Me	OTBS	72:28
4	*p*-NO_2Ph	Ph	OH	44:56
5	*p*-NO_2Ph	Et	OH	36:64
6	*p*-NO_2Ph	*t*-Bu	OH	35:65
7	*p*-NO_2Ph	*t*-Bu	OTMS	95:5
8	*p*-NO_2Ph	Me	OH	50:50

In early days, Jäger[6] explored the selectivity of the 1,3-dipolar cycloaddition of benzonitrile oxide **2-5** with allylic alcohol derivatives **2-4** (**Table 2-2**). In this study, 1,2-diols and their corresponding ethers **2-4** were examined, and in all cases, the erythro products **2-6** were found to be the major products from the reaction (entries 1-3). In these cases, the experimental data on the free alcohols did not align

Table 2.2. Early study of nitrile oxides and allylic alcohols by Jager

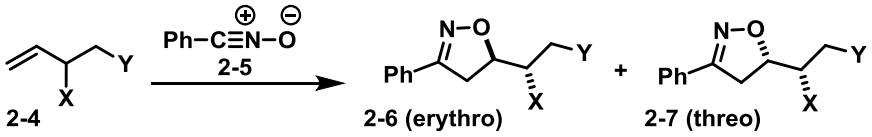

entry	X	Y	Yield (%)	2-6:2-7
1	OH	OH	67	61:39
2	O-trityl	OH	100	54:46
3	OTMS	OTMS	65	75:25
4	-O-CO-O-		88	85:15

well with Houk's calculations, which were based on simple allylic alcohols, and the threo products **2-7** were found as the minor epimers (entries 1 and 2).

Later, the group of Curran[9] studied cyclopentene systems **2-8** with benzonitrile oxide **2-5** (**Table 2-3**). In Curran's study, the effect of hydrogen bonding was rationalized with the use of 2° amides. In the cases of R = alkyl, isoxazoline **2-11** was isolated as the major product of the reaction (entry 1). On the other hand when R = NMe_2, OMe, or OAc, the regiochemistry was reversed, and bicyclic isoxazoline **2-12** was the major product (entries 2-4). Expectedly, in cases of allylic alcohol **2-8**, a hydrogen-bonding effect was possible, and more of a directed β–face approach of the dipole was observed with the formation of isoxazoline **2-9** in greater amounts (entries 5 and 6). Finally, in the case the 2° amide, an even better H-bond donor, product **2-9** was formed in 90% yield (entry 7). This report served as one of the earliest examples of a direct correlation between H-bonding effect in controlling the chemo-, regio-, and stereoselectivity of an olefin/nitrile oxide 1,3-dipolar cycloaddition.

Table 2.3. Curran's H-bonding study

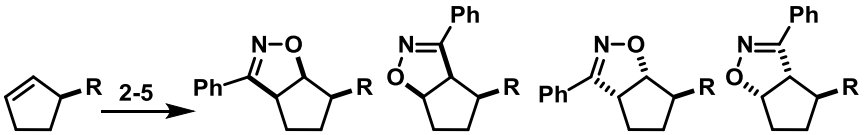

2-8 2-9 2-10 2-11 2-12

entry	R	solv.	2-9	2-10	2-11	2-12
1	Me	Et_2O	3	1	63	33
2	NMe_2	Et_2O	7	0	23	70
3	OMe	Et_2O	3	4	22	71
4	OAc	Et_2O	5	3	15	77
5	OH	Et_2O	30	5	12	53
6	OH	PhH	50	-	17	33
7	NHCOPh	PhH	90	-	-	10

The Raimondi group studied the reaction of Baylis-Hillman adducts **2-13** towards benzonitrile oxides (**Table 2-4**).[10] In this study, moderate to excellent selectivities were observed favoring the threo isomers **2-14** over their erythro counterparts **2-15** (entries 1-4). Silyl allylic ethers were also selective for the threo epimers in good yield (entries 5-6), and even lower selectivity was observed in the case of allylic acetates; the lowest still favoring the syn-isomer **2-14** (55:45, entries 7-8).

Table 2.4. Reaction of nitrile oxides with Baylis-Hillman adducts

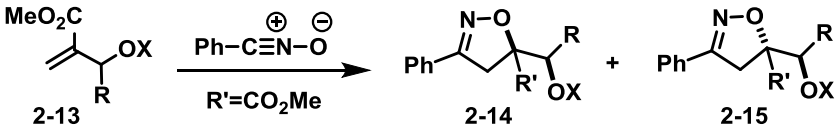

entry	R	X	yield (%)	2-17:2-18
1	Me	H	98	74:26
2	*n*-Pr	H	93	94:6
3	*i*-Pr	H	70	97:3
4	Ph	H	51	70:30
5	Me	TBS	94	86:14
6	*n*-Pr	TBS	91	87:13
7	Me	Ac	92	55:45
8	*n*-Pr	Ac	96	77:23

A big breakthrough in controlling the stereochemistry of the 1,3-dipolar cycloaddition between nitrile oxides an allylic alcohols came from the Kanemasa group a few years later.[11] In their study, Kanemasa and co-workers utilized a metal coordination approach to not only control the stereo- and regiochemistry of the reaction but also the reaction rate. Utilizing metal alkoxides, such as magnesium alkoxides, nearly complete diastereoselectivity was observed with terminal allylic alcohols **2-13** in excellent yields (**Table 2.5,** entries 1-2, 4-6). Only a slight drop in diastereoselectivity was observed in the case where R = R' = Ph (89:11, entry 3). The success of this approach relies in the ability of the magnesium ion to chelate to both the nitrile oxide dipole and the allylic alcohol **2-13** turning the reaction mode from an

inter- to intramolecular process. The authors also observed a noticeable solvent effect in which selectivity was reduced in THF solution to 60:40 mixture of **2-14**:**2-15** which is contributed to the competing complexation of the magnesium metal to the oxygen atom in THF. This report by Kanemasa served as an elegant, first successful metal-coordination controlled 1,3-dipolar cycloaddition to allylic alcohols utilizing nitrile oxide dipoles.

Table 2.5. Kamemasa's metal coordination study

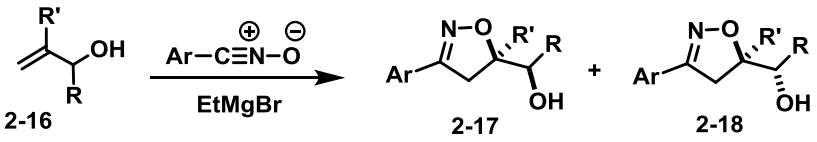

entry	Ar	R	R'	yield (%)	2-14:2-15
1	Ph	Et	H	92	>99:1
2	Ph	Me	H	95	96:4
3	Ph	Ph	H	94	89:11
4	*p*-OMe-Ph	Et	H	92	>99:1
5	Ph	*i*-Pr	H	95	97:3
6	Ph	*n*-Bu	Me	85	96:4

2.1.1.2. Nitrone dipoles

One class of dipoles that stands out as one of the most exploited in area of 1,3-dipolar cycloadditions to allylic alcohols is the nitrones. In one of the earliest studies, cyclic nitrone **2-19** and *cis*-1,2-disubstituted butene derivatives **2-20** were investigated.[12] In the case where X = Cl, the cycloaddition was *syn* selective in the formation of **2-21** (entry 1, 96% yield). Similarly, when the allylic alcohol analog of **2-20** was used, exclusive formation ***syn*-2-21** was observed. In cases where the cyclobutene was ester or anhydride substituted, the *anti*-isomer became the major product in the reaction, entries 3 and 4 respectively (**Table 2.6**). This reversal of selectivity can be attributed to the less-effective hydrogen

bonding nature of these substrates, when compared to that of entries 1 and 2, which are more capable of undergoing hydrogen-bond interactions during the cycloaddition. This early study inspired later work which investigated the 1,3-dipolar cycloaddition of nitrones and allylic alcohols in more detail.

Table 2.6. Nitrone cycloaddition with cyclobutene derivatives

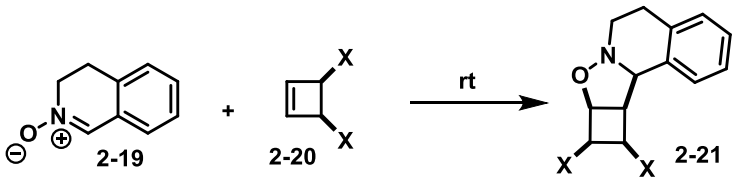

entry	X	yield (%)	syn:anti
1	Cl	96	78:22
2	OH	92	100:trace
3	CO_2Me	-[a]	syn < anti[b]
4	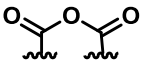	-[a]	1:100

[a]Yield not given. [b]Exact ratio not provided.

Unsurprisingly, because of her continued interest the reactions of 1,3-dipoles with allylic alcohols and ethers, Prof. Raimondi also extensively studied this cycloaddition with nitrones. The Raimondi group studied the reaction of formaldehyde *N*-benzyl nitrone **2-22** with allylic alcohols and ethers **2-23** to yield isoxazolidines **2-24** and **2-25** (**Table 2.7**).[13] In examples where allylic alcohol **2-23** was used, the *syn* stereoisomers **2-25** were favored over the ***anti*-2-24** although the selectivity was low (29:71 to 24:76, entries 1 to 3). Increasing the steric bulk at the allylic center had little influence on the diastereoselectivity of the reaction, and switching from methyl- to isopropyl- to 2-(1,3-dithiane) varied the selectivity in negligible amounts (entries 1 to 3). In the cases where R is large or allylic ethers were used, the *anti*-isomer **2-24** predominates, in agreement with Houk's "inside alkoxy" effect model[4]. It is worthwhile to note that, in the cases of these *tert*-butyldimethylsilyl ethers, low to fair yields of the products were observed (entries 4-6).

Table 2.7. Raimondi's nitrone study

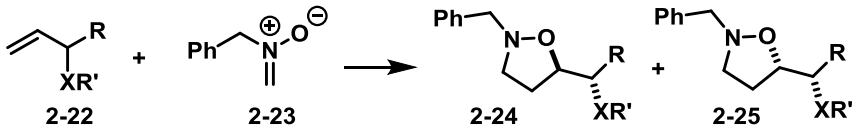

2-22 2-23 2-24 2-25

entry	X	R	R'	yield (%)	2-24:2-25
1	O	Me	H	68	29:71
2	O	*i*-Pr	H	70	27:73
3	O	1,3-dithiane	H	66	24:76
4	O	Me	TBS	47	63:37
5	O	*i*-Pr	TBS	23	90:10
6	O	1,3-dithiane	TBS	42	76:24

In a metallic-base induced nitrone cycloaddition to allylic alcohols **2-27**, the Kanemasa and Wada group generated *exo*-isoxazolidines **2-28** as the major products when reacted with nitrone **2-26** in the presence of Lewis-acid additives (**Table 2.8**).[14] In the absence of any metal additives, the reaction still proceeded in high diastereoselectivity favoring *exo* product **2-28** and 78% yield after 24 hours (97:3, entry 1). When Lewis acid additives were added to the reaction, the selectivity (up to 100:0) and rate of reaction increased providing the *exo* products in only 1 to 5 hours (entries 2-5). Interestingly, with β-substituted allylic alcohols in the absence of any Lewis acid additive, the selectivity was reversed in favor of the *endo* product in 94% yield (18:82, entry 6). Adding ethylmagnesium bromide to the reaction medium led to a switch in selectivity back to the *exo* product **2-28** in 97% yield (97:3, entry 7). Even more effective, when diethylzinc was used as the Lewis acid additive, the *exo* product formed exclusively, albeit lower yield (100:0, 57%, entry 8). Finally, a catalytic process was developed relying on the use of chlorotriisopropoxytitanium; this catalyst provided the *exo* product exclusively in 58% with a 10 mol % loading in the reaction mixture (entry 9).

Table 2.8. Metallic-base induced Lewis acid-catalyzed nitrone cycloaddition

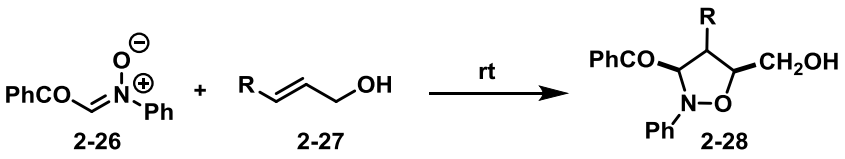

entry	R	additive	yield (%)	exo:endo
1	H	-	78	97:3
2	H	EtMgBr	93	98:2
3	H	Et_2Zn	57	100:0
4	H	$MgBr_2$	81	100:0
5	H	$ZnBr_2$	65	100:0
6	Me	-	94	18:82
7	Me	EtMgBr	97	98:2
8	Me	Et_2Zn	57	100:0
9	Me	$TiCl(O\textit{i}\text{-}Pr)_3$	58	100:0

In a follow-up report, Kanemasa studied a magnesium and zinc ion mediated nitrone cycloaddition of allylic alcohols **2-29** containing additional substitution at the allylic position (**Table 2.9**).[15] Unlike their previous study,[12] reaction of allylic alcohols **2-29** with nitrone **2-26** produced mixtures of epimers **2-30** and **2-31** in the absence of any Lewis acid additive (100% yield, 53:47, entry 1). The addition of $MgBr_2$ or $ZnBr_2$ to the reaction mixture led to an increase in diastereoselectivity to 84:16 and 73:27, respectively, albeit lower yields (73-89%, entries 2-3). Replacement of the methyl group in **2-29** with propyl or phenyl group did not change the outcome of the significantly, and similar diastereoselectivities were observed in both the absence and presence of the Lewis acid additives (entries 4-6). Substitution at the β-position of the allylic alcohol **2-29** enhanced the diastereoselectivity even further in the presence of the magnesium bromide catalyst, and isoxazolidines **2-30** were isolated in 96:4 (R = Me) and 100:0 (R = *i*-Pr) ratios (entries 7 and 8).

Table 2.9. Magnesium and zinc-ion mediated nitrone cycloaddition

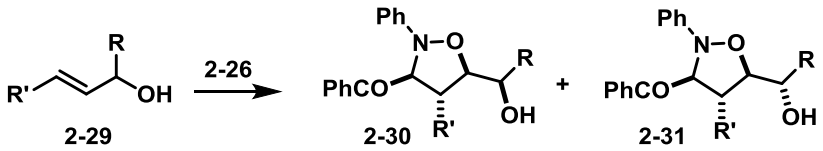

entry	R	R'	additive	yield (%)	2-30:2-31
1	Me	H	-	100	53:47
2	Me	H	$MgBr_2$	89	84:16
3	Me	H	$ZnBr_2$	73	73:27
4	*n*-Pr	H	-	95	55:45
5	*n*-Pr	H	$MgBr_2$	96	85:15
6	Ph	H	$MgBr_2$	91	88:12
7	Me	Me	$MgBr_2$	85	96:4
8	*i*-Pr	Me	$MgBr_2$	47	100:0

Shortly after, the Kanemasa group disclosed a magnesium bromide promoted *E/Z*-isomerization of carbonyl-conjugated nitrones **2-32** followed by tandem 1,3-dipolar cycloaddition with allylic alcohol **2-27** in a one-pot procedure (**Table 2-10**).[16] In the absence of the magnesium bromide additive, a 69:31 mixture of epimers is obtained favoring the hydroxyl-methyl group in

Table 2.10. Magnesium bromide-promoted nitrone *E/Z*-isomerization and cycloaddition

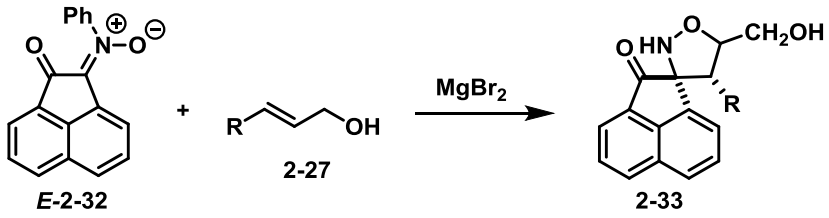

entry	R	T (°C)	yield (%)	α:β
1	H	110	65	69:31[a]
2	H	61	82	100:0
3	Me	61	50	100:0

[a]Reaction run in the absence of $MgBr_2$

α-orientation. When ***E*-2-32** is exposed to magnesium bromide under refluxing conditions in DCE, it completely isomerizes to ***Z*-2-32**. Under these $MgBr_2$ catalyzed conditions, **2-32** reacted cleanly with **2-27** producing the **α-2-33** as the exclusive product (entries 2 and 3). This study served as the first report of a Lewis acid-catalyzed *E*- to *Z*-isomerization of carbonyl-conjugated nitrones, and displayed their enhanced reactivity toward allylic alcohols in 1,3-dipolar cycloaddition.

Piniella and co-workers examined the reaction of 1,2-disubstituted electron-deficient olefins bearing an allylic stereocenter **2-34** with cyclic nitrones **2-35** (**Table 2.11**).[17] In all cases, the selectivity of the reaction of cyclic nitrone **2-35** with allylic alcohols was endo selective (entries 1-5). With regards to the relative stereochemistry of the product with the allylic stereocenter, the reaction only displayed marginal selectivities, and anti-relationship between the groups was observed as the major epimers **2-36** where R = benzyl or methyl ethers (entries 1, 3, 4). On the other hand, when R contained free hydroxyl group (entries 2 and 5) the endo product **2-37** was the major product from the reaction. These findings also agreed with Houk's "inside alkoxy" model, and hydrogen bonding still cannot be neglected as an additional controlling factor in the reaction.

Table 2.11. Cyclic nitrone study

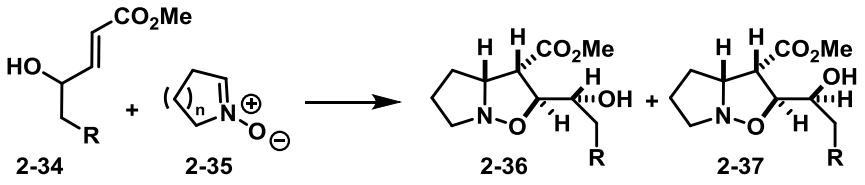

2-34 2-35 2-36 2-37

entry	R	n	2-36 (%)[a]	2-37 (%)[a]
1	CH_2OCH_2Ph	1	60	22
2	OH	1	34	49
3	CH_2OCH_2Ph	2	52	22
4	CH_2OCH_3	2	44	23
5	OH	2	35	42

[a]Minor amounts of *exo*-adducts also formed

In order to create a more ridged 1,3-dipole, chelation controlled cycloaddition reactions have been devised. One such study by the Hanselmann group relied on the chelation of a chiral, in situ, generated dipole **2-41** to a magnesium bromide Lewis acid which could further react with allylic alcohol **2-29** to form isoxazolidine **2-40** (**Scheme 2.1**).[18] A diastereomeric ratio of up to 97:3 was possible using this methodology with a variety of aldehydes including those containing allyl ether tethers in cyclic and acyclic systems.

Scheme 2.1. Chelation-controlled nitrone 1,3-dipolar cycloaddition

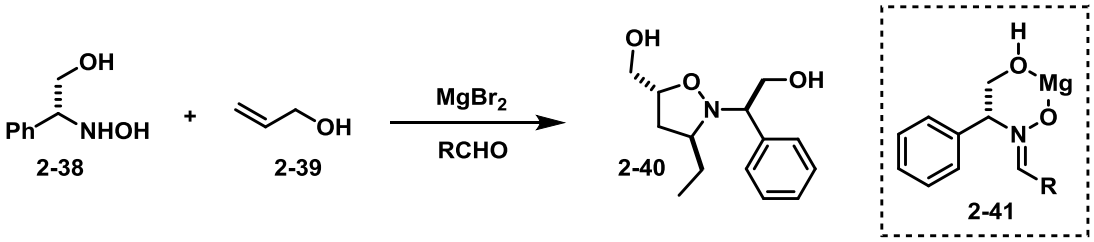

Shortly after, the Lopez group used a similar chelation approach involving metal chelated nitrone **2-44** and allylic alcohol **2-39** (**Scheme 2.2**).[19] In this study, the N-benzyl C-(2-pyridyl) nitrone **2-44**, generated from **2-42** and metal salts, reacted with allyl alcohol **2-39** to generate isoxazolidine **2-43** with a variety of Lewis acids including zinc and silver salts. In all cases, the diastereoselectivity of the reaction was greater than 95:5 in favor of the cis-cycloadduct, although the substrate scope of this transformation was not thoroughly investigated.

Scheme 2.2. Chelation control Lopez

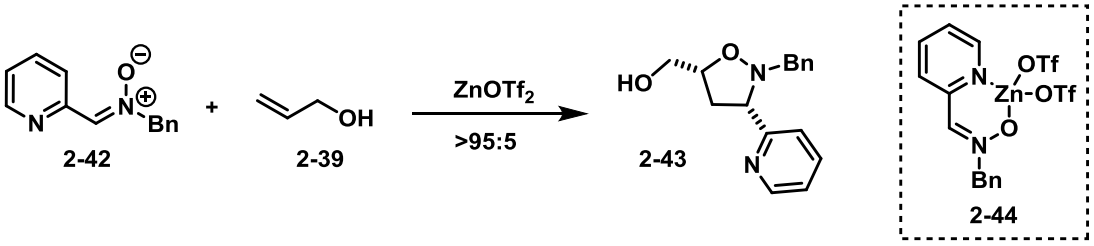

In an application of the 1,3-dipolar cycloaddition of nitrones to allyl alcohol, a route to deoxycastanospermine analogs was developed by the Dhavale group (**Scheme 2.3**).[20] In their approach, 1,2-*O*-isopropylidene-3-*O*-benzyl-α-D-*xylo*-pento-dialdose **2-45** was prepared readily from α-D-glucose, and then treated with *N*-benzyl hydroxylamine to generate *Z*-nitrone **2-46**. Nitrone **2-46** underwent a 1,3-dipolar cycloaddition with allyl alcohol **2-39**, and then it was converted to the tosylate **2-47**. Hydrogenation of **2-47** followed by selective amine protection with benzyl chloroformate led to diol **2-48**. This one-pot three-step hydrogenation reaction achieved N-O bond cleavage, intramolecular aminocyclization to deliver the pyrrolidine and removal of the *N*- and *O*-benzyl groups. The synthesis was completed by removal of the 1,2-acetonide followed by hydrogenation to deliver 2-hydroxy-1-deoxycastenospermine. The authors synththesized several other analogs using this method, and all were characterized by conversion to their corresponding acetyl derivatives by treatment with acetic anhydride and pyridine.

Scheme 2.3. Synthesis of 2-hydroxy-1-deoxycastanospermine analogs

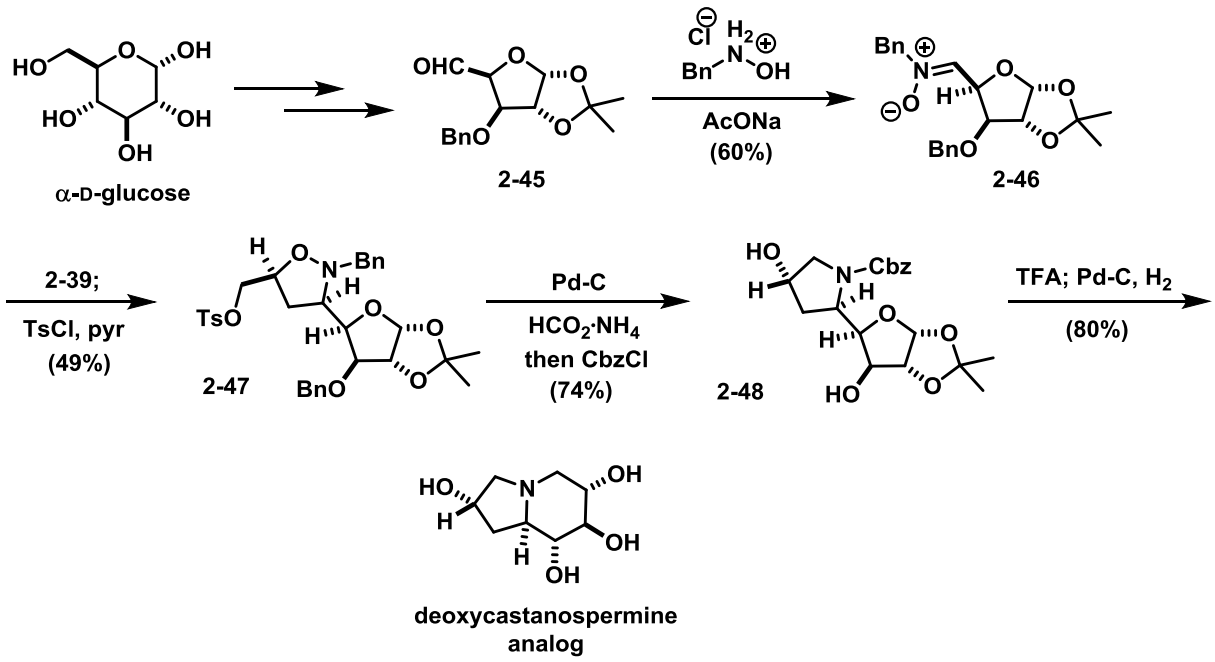

2.1.1.3. Diazoalkane dipoles

One of the least studied classes of dipoles in their 1,3-dipolar cycloaddition reaction with allylic alcohols is the diazoalkanes. Early work investigated the reaction of diazoalkanes with *cis*-3,4-dichlorobutene **2-20** (**Table 2.12**).[21] In the case of 2-diazopropane **2-49** (R = R' = Me), a quantitative reaction occurred leading to a 29:71 diastereomeric mixture of **2-50** and **2-51** (entry 1). On the contrary, when diazoethane or diazomethane were exposed to the reaction condition, syn-isomers **2-50** formed exclusively in an **80** and 90% yields respectively (entries 2 and 3). In the case of cyclobutenedicarboxylate, selectivity was reversed, and bicyclic Δ^1-pyrazoline **2-51** formed exclusively in 85% yield (entry 4).

Table 2.12. Reaction of cyclobutene with diazoalkanes

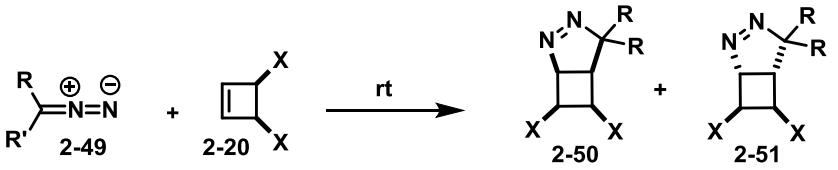

entry	R	R'	X	yield (%)	2-50:2-51
1	Me	Me	Cl	100	29:71
2	H	Me	Cl	80	100:0
3	H	H	Cl	90	100:0
4	Me	Me	CO_2Me	85	0:100

Unsurprisingly, the Raimondi group also investigated the reaction of diazomethane with Baylis-Hillman adducts **2-16** during their study with nitrile oxides (**Table 2.13**). In all cases, the reaction was *syn* selective delivering Δ^1-pyrazolines **2-52** and **2-53**. This cycloaddition was limited by yields, and only moderate to good quantities of the pyrazolines were isolated when reacted with the free allylic alcohols **2-16** were used in the cycloaddition (40-77%, entries 1-3). In the case where R = phenyl, no cycloaddition occurred, and only decomposition products were observed (entry 4). In the cases of silyl ether substrates, selectivity dropped, although still favoring the syn Δ^1-pyraozlines **2-52** (62:38 and 76:24, entries 5-6). Finally, in the cases of acetate protected allylic alcohols, high yields were achieved, but the selectivity

further dropped (90-95%, 58:42 to 74:26). Based on this study, a few generalizations could be made. For one, the smaller the X group, the higher the *syn* selectivity of the reaction, and second, the cycloadducts were quite unstable which lowered the chemical yields.

Table 2.13. Diazomethane reactivity with Baylis-Hillman adducts

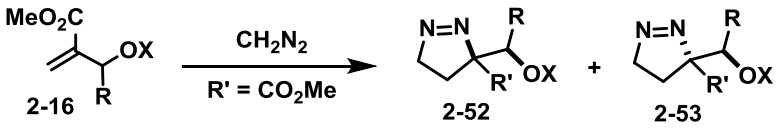

entry	R	X	yield (%)	
1	Me	H	50	85:15
2	*n*-Pr	H	77	80:20
3	*i*-Pr	H	40	98:2
4	Ph	H	-[a]	-[a]
5	Me	TBS	98	62:38
6	*n*-Pr	TBS	73	76:24
7	Me	Ac	90	58:42
8	*n*-Pr	Ac	95	74:26

[a]Decomposition

2.1.2. Pseudoephedrine auxiliary

One of the most powerful methods for inducing asymmetric induction in chemical reactions via chiral auxiliary approach is utilizing pseudoephedrine. This method was envisioned to compliment the methods discussed in **Section 2.1.1** as an additional use of the hydroxyl group as a controlling element in cycloaddition reactions where the inducing stereocenter and prochiral group are more than one or two bonds apart. This chemistry was first developed and exploited by the Myers group in asymmetric alkylation reactions.[22]

2.1.2.1. Alkylation

In Myers' seminal report, an efficient and highly diastereoselective alkylation reaction of pseudoephedrine amides **2-54** was disclosed (**Table 2.14**).[22] By treating **2-54** with two equivalents of LDA in the presence of at least four equivalents of lithium chloride, the dianion of the carboxamide is formed which can then be alkylated with a variety of alkyl and benzyl halides to generate α-alkylation product **2-55**. In many cases, the isolated de of the reaction is greater than 99% (entries 1-2, 6-8). Likewise, the crystalline nature of the products makes isolation and purification expeditious. Amides containing alkyl, benzyl, phenyl and even alkyl halide R substituents were well tolerated in the reaction. In general, utilizing iodomethane as the alkylating agent led to reduced de values (entries 3 and 5) although these de values were still greater than or equal to 94%. This study served as the catalyst for exploring pseudoephedrine as a chiral auxiliary in organic synthesis.

Table 2.14. Myers' early report

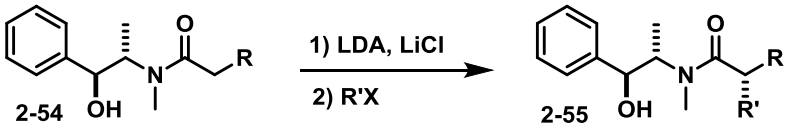

entry	R	R'X	de (%)	yield (%)
1	Me	BnBr	>99	90
2	Me	*n*-BuI	>99	80
3	Bn	MeI	94	99
4	Bn	*n*-BuI	98	90
5	*n*-Bu	MeI	94	94
6	*n*-Bu	BnBr	>99	87
7	Ph	EtI	>99	92
8	Cl	BnBr	>99	88

A few years later, the Myers group extended their alkylation chemistry to pseudoephedrine glycinamide **2-56** (**Table 2.15**).[23] In this report, high diastereoselectivities were observed with a variety of

Table 2.15. Myers alkylation of pseudoephedrine glycinamide

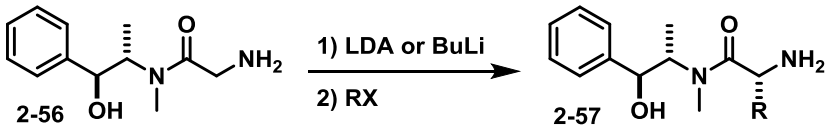

entry	RX	time (h)	de (%)	yield (%)
1	EtI	1.5	>99	76
2	AllylBr	0.3	>99	69
3	*i*-BuI	48	94	99
4	MeI	5	94	61
5	*c*-propylI	10	99	66
6	BnBr	1	99	65
7	*o*-MeO-BnBr	2	91	83
8	$(CH_3)_3SiCH_2Br$	22	>99	57

electrophiles including alkyl, allyl and benzyl halides in moderate to good yields (65-99%, entries 1-7). The reaction conditions also tolerated (Trimethylsilyl)methyl bromide as an electrophile, and the alkylation product **2-57** was isolated in moderate yield after 22 hours in >99% de (57%, entry 8). Based on the reactivity trend observed during their studies, Myers proposed a mnemonic to account for the observed stereochemical outcome of the reaction (**Scheme 2.4**). As depicted in **Scheme 2.4**, the electrophile enters from the same face as the methyl group of the pseudoephedrine auxiliary when the (putative) *Z*-enolate is drawn in a planar extended conformation.[23]

Scheme 2.4. Mnemonic for enolate alkylation

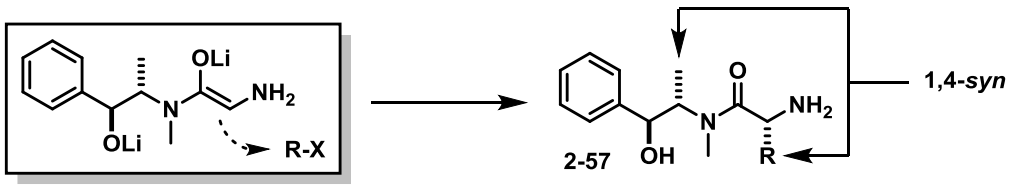

Myers' pseudoephedrine glycinamide study was followed up shortly by alkylation using β-branched electrophiles (**Table 2.16**).[24] The enhanced nucleophilicity and stability of pseudoephedrine enolates make alkylation possible at room temperature with β-branched primary iodides. High ratios of diastereomers were obtained ranging from 41:1 to 142:1 in good to excellent yields (89-97%, entries 1-4). In cases where the 1,3-syn or 1,3,5-syn products were obtained, selectivities were slightly higher, which suggests "matched" cases (entries 2 and 4). Another merit to this methodology is that 1,3,5,*n*(odd)-polyalkyl-substituted carbon chains of any configuration could be generated. This technology not only complimented Evans' and Heath's existing prolinol alkylation chemistry at the time,[25] but also provided some significant advances.

Table 2.16. Alkylation utilizing β-branched electrophiles

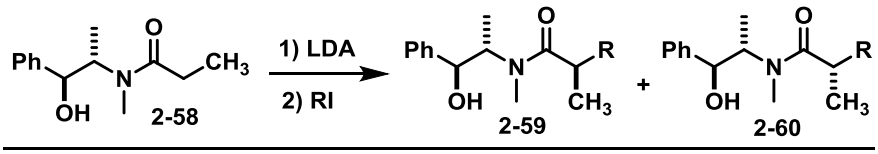

entry	RI	yield (%)	2-59:2-60
1	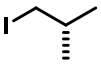	94	62:1
2	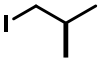	89	86:1
3	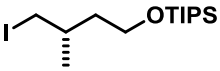	96	41:1
4		93	142:1

2.1.2.2. Conjugate addition

Myers first demonstrated the use of pseudoephedrine derived enolates in the Michael reaction during his synthesis of HIV protease inhibitors (**Scheme 2.5**).[26] In this study, the lithium enolate of pseudoephedrine α-fluoroacetamide **2-61** was treated with a solution of the appropriate Michael acceptor, either nitroalkene or vinylsulfoxide, to yield amides **2-62** or **2-63** respectively. Either of these Michael

Scheme 2.5. Conjugate addition of pseudoephedrine α-fluoroacetamide

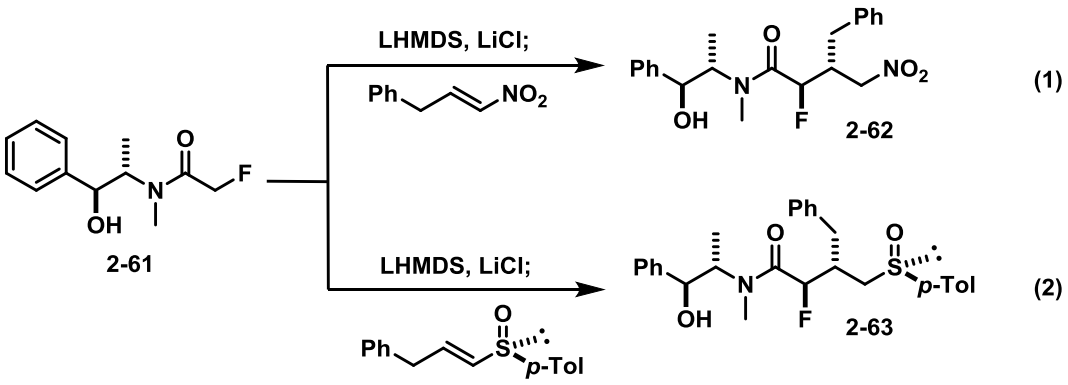

adducts could be isolated as pure diastereomers after recrystallization although yields were limited by yields do to deprotonation of the electrophile. This served as the first example of the use of pseudoephedrine as an auxiliary for the donor nucleophile in the Michael reaction.

Simultaneously, as Myers published the above work, the use of pseudoephedrine in the asymmetric Michael reaction was being investigated by a Merck process team in 2003 (**Table 2.17**).[27] In their report, a variety of Michael acceptors were examined in their reaction with the lithium enolate of **2-64**. Benzyl and PMP ether substitutions on the acceptor as well as simple methyl and phenyl substitutions were well

Table 2.17. Asymmetric Michael reaction with pseudoephedrine developed by Merck

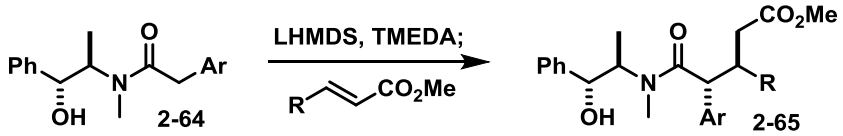

entry	Ar	R	ee (%)[a]	yield (%)
1	Ph	CH_2OBn	91	80
2	Ph	CH_2OPMP	98	76
3	Ph	CH_3	91	85
4	Ph	$(CH_2)_2Ph$	87	78
5	Ph	Ph	83	89

[a]Determined after reduction and hydrolysis.

tolerated in the reaction (**Table 2.17**, entries 1-5). In all cases, good to excellent ee values of the resulting lactones from reduction and acidic hydrolysis of **2-65** were obtained (83-98%).

That same year, the Carrillo group utilized the pseudoephedrine auxiliary in an *aza*-Michael reaction onto α,β-unsaturated amides (**Table 2-18**).[28] Contrary to the previous studies, this report utilized the pseudoephedrine auxiliary on the Michael acceptor **2-66**. In this study, the authors found that simple amines such as benzylamine, dibenzylamine or *N*-methylbenzylamine did not afford any of the desired Michael adducts. On the contrary, when they switched to the more reactive nitrogenous nucleophiles, such as linhium *N*,*N*-dibenzylamide, the Michael adducts **2-67** and **2-68** were obtained in moderate diastereoselectivity in THF (**Table 2.18**, entries 1-2). By simply switching to a non-coordinating solvent, such as toluene, higher diastereoselectivity was obtained albeit lower yield (79:21, 30%, entry 3). Lowering reaction temperature even further led to essentially complete diastereoselectivity in moderate to good yields (>99:1, 60-88%, entries 4-6). This study served as one of the earliest reports of the use of pseudoephedrine as an auxiliary on the conjugate acceptor in the asymmetric conjugate addition reaction, and it demonstrated an effective 1,5-asymmetric induction process in the formation *aza*-Michael adducts.

Table 2.18. *Aza*-Michael reaction utilizing pseudoephedrine

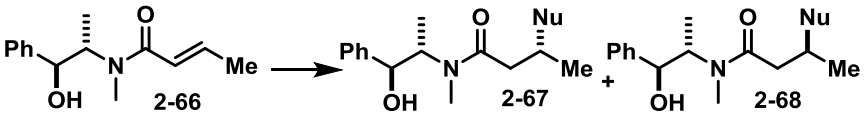

entry	Nu	Solvent	T (°C)	2-64:2-65	yield (%)
1	Bn_2NLi	THF	–78	70:30	67
2	Bn_2NLi	THF	–105	72:28	81
3	Bn_2NLi	$PhCH_3$	–78	79:21	30
4	Bn_2NLi	$PhCH_3$	–90	>99:1	60
5	Bn_2NLi	$PhCH_3$	–90	>99:1	85
6	BnMeNLi	$PhCH_3$	–90	>99:1	88

Two years later, the Carrillo group disclosed a tandem asymmetric conjugate addition/α-alkylation sequence using the (*S*,*S*)-(+)-pseudoephedrine auxiliary (**Table 2.19**).[29] In this study, the authors treat amide **2-66** with an alkyl or aryl lithium nucleophile to generate the Michael adduct which is then exposed to excess electrophile generating the tandem conjugate addition – alkylation product **2-69** in a single-flask operation. In the case of phenyllithium as the nucleophile, methyl, ethyl, allyl and benzyl halide electrophiles all led to the tandem product **2-69** in good to excellent yields and dr values (77-96%, up to 95:5:<1:<1, entries `1-4). When normal butyl lithium was utilized as the nucleophile, yields and diastereoselectivities were lower than that of phenyllithium but still synthetically useful (67-73%, up to 91:5:3:<1, entries 5-7). This study demonstrated very elegantly the utility of pseudoephedrine auxiliary in both conjugate addition and alkylation in a tandem one-pot process.

Table 2.19. Asymmetric conjugate addition/α-alkylation using pseudoephedrine

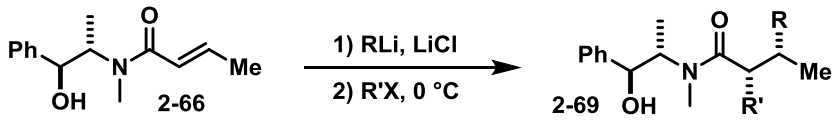

entry	R	R'	yield (%)	dr
1	Ph	Me	77	93:4:3:<1
2	Ph	Et	96	95:5:<1:<1
3	Ph	allyl	70	93:4:2:1
4	Ph	Bn	78	94:4:<1:<1
5	*n*-Bu	Me	67	91:5:3:<1
6	*n*-Bu	Et	73	91:6:2:<1
7	*n*-Bu	allyl	71	86:10:4:<1

Shortly after, the Myers group reported construction of quaternary carbon centers utilizing pseudoephedrine auxiliary (**Table 2.20**).[30] In this study, acrylamide **2-70** is deprotonated with methyllithium followed by treatment with an alklyl- or phenyllithium to promote conjugate addition, and this adduct is then treated with an appropriate electrophile generating the new quaternary center containing

Table 2.20. Myers' quaternary carbon center construction

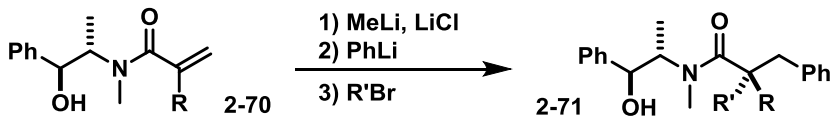

entry	R	R'	yield (%)	dr
1	Et	Me	89	19:1
2	*s*-But	Me	91	19:1
3	cyclopropyl	Me	92	19:1
4	Me	allyl	95	19:1

pseudoephedrine amide **2-71** in a single flask. In this report, a variety of substituted acrylamides **2-70** were investigated including R = Et, *s*-but, cyclopropyl and Me (entries 1-4). Likewise, a number of electrophiles were examined including, but not limited to, iodomethane and allylbromide. In all cases, the reaction was highly diastereoselective, and only single diastereomers were visible in the NMR spectrum of the crude reaction mixture. This and the above reports inspired the ensuing investigations on utilizing hydroxyl group as a controlling element, via 1,2- or 1,5-indution, in the formal [3+2] cycloaddition of lithiumtrimethylsilyldiazomethane **1** with hydroxyl-containing α,β-unsaturated carbonyl compounds.

2.2. Results and Discussion

2.1.1. α-Alkylidene and α-benzylidene-β-hydroxy esters

2.1.1.1. Optimization

To test the feasibility of the hydroxyl-controlled cycloaddition, α-alkyidene-β-hydroxy esters were first explored as substrates. Expectedly, initial experiments showed that unlithiated **1** gave no reaction with **2-72a**, and an additional equivalent of *n*-BuLi was required for the formation of the Δ^2-pyrazoline adduct **2-73a** (**Table 2-21**, entries 1 and 2). Only modest yields were observed even with 2.2 equivalents of **1** and increased reaction temperatures and time (entries 3 and 4) although the reaction showed complete

diastereoselectivity based on NMR analysis of the crude reaction mixture. Gratifyingly, the addition of five equivalents of lithium chloride[31] led to complete conversion into **2-73a** as a single diastereomer based on NMR analysis (entries 5 and 6).

Table 2.21. Optimization of reaction conditions

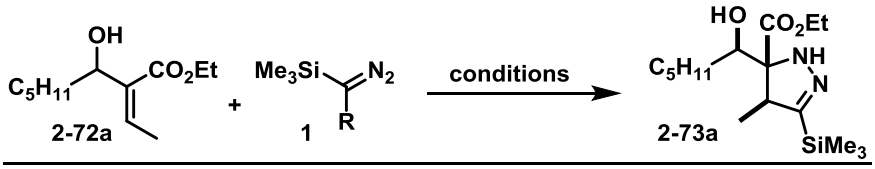

entry	R	Equiv 2	Additive	Time (h)	T (°C)	yield (%)	dr
1	H	2.2	none	60	22	nr	-
2	Li	1.2	BuLi (1.1)	16	-78	41	19:1
3	Li	2.2	none	16	-78	43	19:1
4	Li	2.2	none	16	-78 to rt	51	19:1
5	Li	2.2	LiCl (5)	2	-78	82	19:1
6	Li	1.2	BuLi (1.1) LiCl (5)	2	-78	80	19:1

2.2.1.2. Scope

The scope of the annulation between **1** and β-hydroxy-α-methylene esters **2-72** was examined next (**Table 2.22**). Allylic alcohols containing terminal double bonds **2-72b** through **2-72d** reacted cleanly with **1** producing Δ^2-pyrazolines **2-73** in good yields and selectivities (10:1). As anticipated, β-alkyl or -aryl substitution at the methylene position of α,β-unsaturated esters, **2-73e** through **2-73l**, delivered even higher selectivites (>19:1) with good to excellent yields. In all cases, only single diastereomers were visible in the NMR of the crude reaction mixture. The formal cycloaddition reaction was also stereospecific. Ester **2-27g** produced a single diastereomer **2-73g** whose structure was distinct from that of **2-73h** based on NOE and X-ray analysis. Sterically hindered substrate **2-72l** provided Δ^2-pyrazoline **2-73l** as the sole product albeit lower yield with recovered starting material.

Table 2.22. Reaction scope of **1** with α-Alkylidene and α-benzylidene -β-hydroxy esters

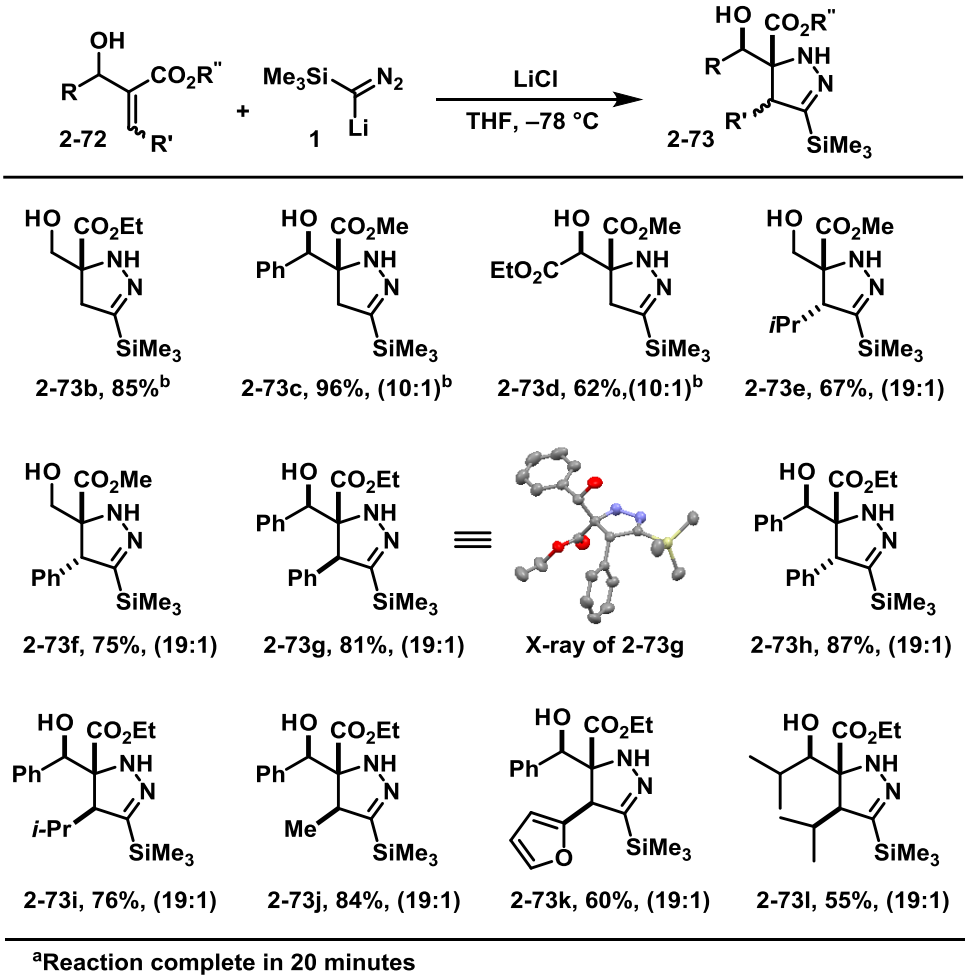

[a]Reaction complete in 20 minutes

2.2.1.3. Mechanistic considerations

The relative stereochemical outcome of this reaction is governed by the underlying mechanism as well as the role of LiCl. Based on NMR and X-ray analysis of **2-73g**, α-face attack of the dipole **1** with **2-72g** can occur through α-face attack of **1** on the lithium chelate of **2-72g** via concerted or step-wise mechanism (**Scheme 2.6**). Based on the observed increase rate and yield in the presence of lithium chloride, this salt improves chelation and slows down C-C bond rotation. An additional role of lithium chloride is in solvating or breaking up enolate type aggregates. Both of these observations would favor a step-wise

mechanism and **TS-1**. Likewise, bond rotation could occur in unchelated **TS-2** leading to the diastereomers of **2-73g**, but neither of these diastereomers are observed.

Scheme 2.6. Plausible mechanistic pathways

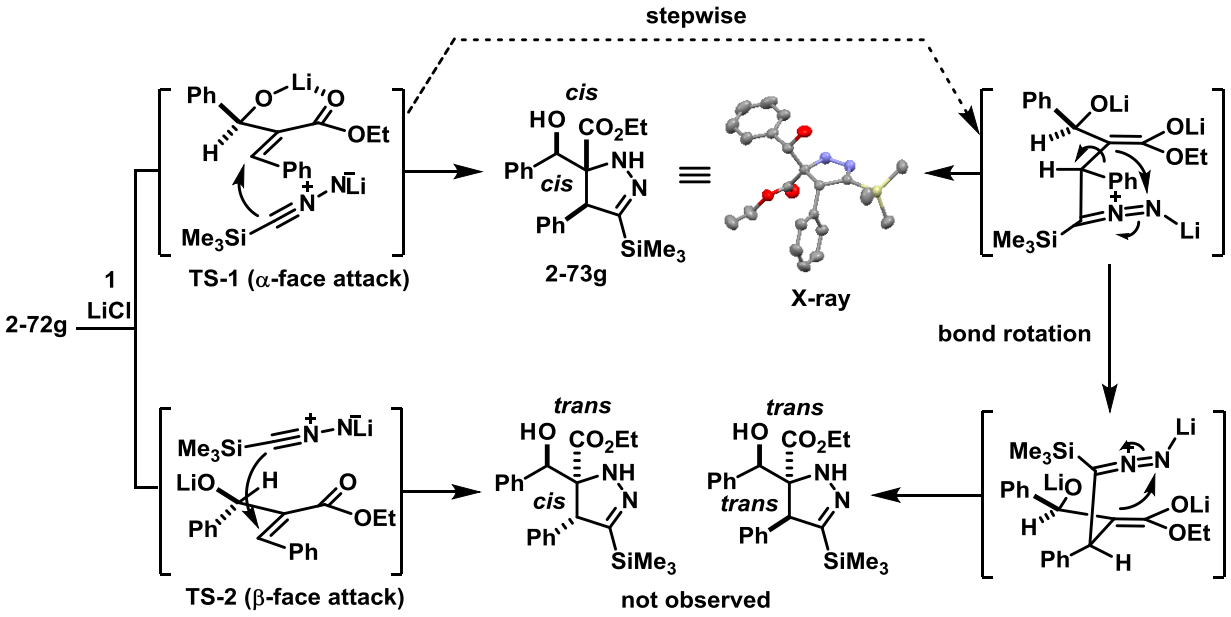

To further confirm the stepwise nature of this process, the hydroxyl groups of **2-72g** and **2-72h** were protected as their TBS ethers affording **2-72g′** and **2-72h′** (**Scheme 2.7**). In both cases, when **2-72g′** or **2-72h′** were exposed to the standard reaction conditions, diastereomeric mixtures of products were obtained (**Schemes 2.7**, eq 1 and 2). These studies suggest, that lithium plays a key role in "locking" the alkoxides of **2-72** in conformation and preventing any bond rotation of the initial 1,4-adduct (**Scheme 2.6**, TS-1). The lithium chelate effect fixes the conformation of the chiral and prochiral groups in substrate **2-72** resulting in only one available conformation at the transition state of the reaction, one of the key requirements for 1,2-asymmetric induction as mentioned in **Section 2.1**. Second, the R group on **2-72** shields the β-face of the chelate in an "inert volume" type effect leading to preferential approach of lithium(trimethylsilyl)diazomethane **1** from the α-face, as shown in **Scheme 2.6**. Both of these effects work synergistically in controlling the diastereoselectivity of the cycloaddition.

Scheme 2.7. Control experiments

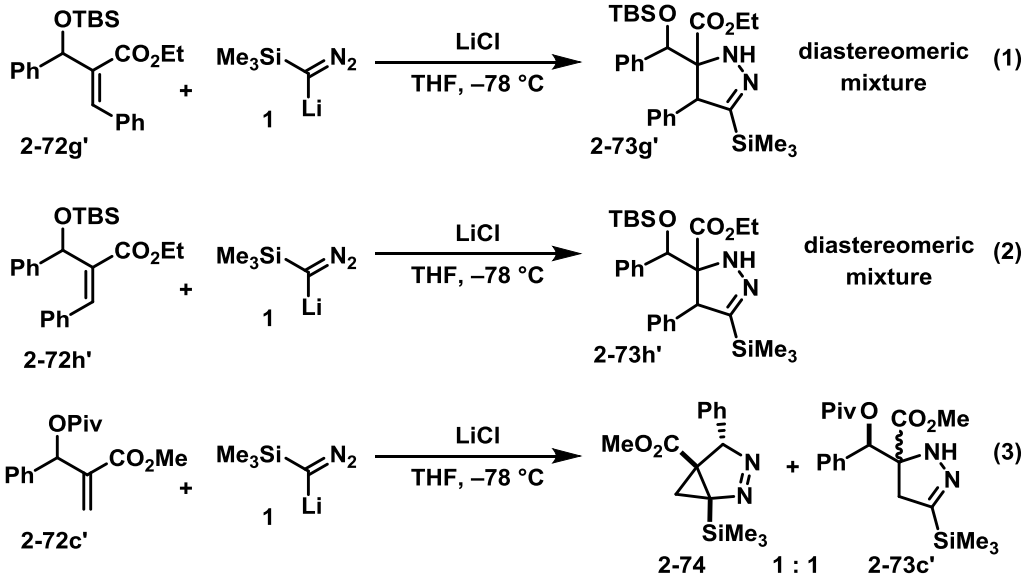

Furthermore, when pivalate **2-72c′** is exposed to the reaction condition, both the elimination product **2-74** and cycloadducts **2-73′** formed as a 1 : 1 mixture when exposed to the reaction conditions (**Scheme 2.6**, eq 3). This simple mechanistic probe further demonstrates that a 1,4-addition/cyclization process is operating under the reaction conditions. With an efficient, 1,2-asymmetric induction process developed, the chemistry was further extended to a 1,5-asymmetric induction reaction utilizing pseudoephedrine derived α,β-unsaturated amides.

2.2.2. Pseudoephedrine derived α,β-unsaturated amides

To probe the feasibility of the formal 1,3-dipolar cycloaddition process of **1** with pseudoephedrine derived α,β-unsaturated amides **2-75**, nerol analog **2-75a** was treated with five equivalents lithium chloride and lithium(trimethylsilyl)diazomethane **1** at −78 °C (**Scheme 2.8**). Delightfully, a single diastereomer **2-76a** was isolated from the reaction mixture in 71% yield. Existing as highly crystalline compounds, the structure of Δ^2-pyrazoline **2-76a** was further confirmed by X-ray diffractive analysis (S**cheme 2.8**).

Scheme 2.8. Initial reaction with α,β-unsaturated pseudoephedrine amide

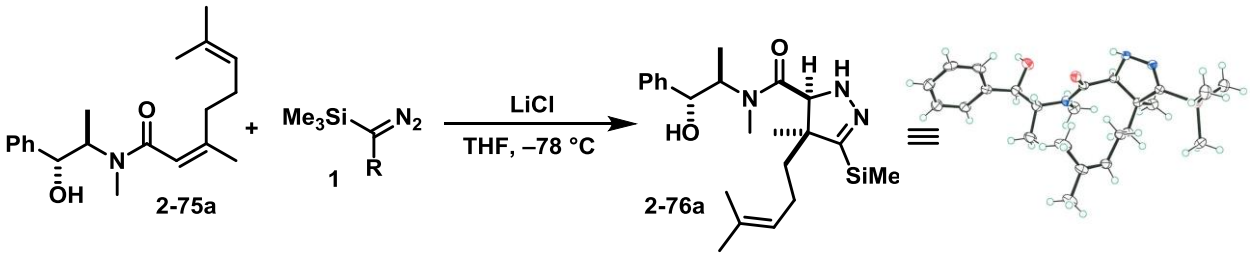

2.2.2.1. Scope

Encouraged by the result of forming Δ^2-pyrazoline from α,β-unsaturated amide **2-75a**, containing β,β-disubstitution, as a single diastereomer, the scope of the pseudoephedrine auxiliary-based cycloaddition was examined (**Table 2.23**). Both methyl- and phenylacrylamides **2-75b** and **2-75c** produced Δ^2-pyrazolines in 79 and 75% yields respectively as the sole isolated products from the reaction mixture (entries 1 and 2). Likewise, tiglamide-derived pseudoephedrine amide **2-75d** generated the desired Δ^2-pyrazoline **2-76d** as a single diastereomer (entry 3). Geranic acid derivative **2-75e** also reacted cleanly with **1**, generating the pyrazoline **2-76e** in 71% yield (entry 4). Finally, cyclic pseudoephedrine amides were tolerated under the reaction conditions. Cyclopentene-substituted pseudoephedrine amide **2-75f** produced bicyclic Δ^2-pyrazoline **2-76f** in moderate yield with excellent selectivity (67%, 19:1). Similarly, cyclohexene analog **2-75g**, produced the desired bicyclic pyrazoline **2-76g** whose structure was further confirmed by X-ray crystallography (**Scheme 2.9**).

Scheme 2.9. Formation of bicyclic Δ^2-pyrazoline utilizing pseudoephedrine auxiliary

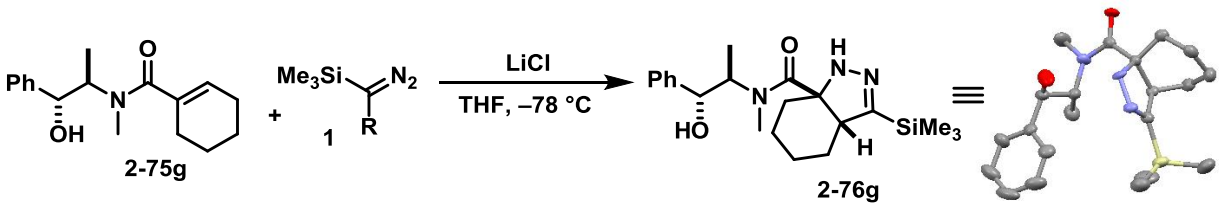

Table 2.23. Reaction scope of **1** with pseudoephedrine-derived α,β-unsaturated amides

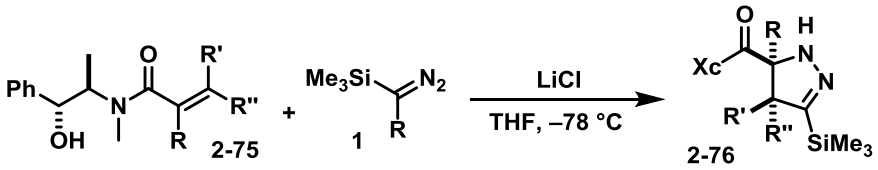

Entry	α,β-Unsaturated amide	Pyrazoline	Yield (%)	dr
1	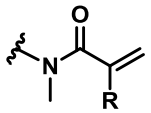	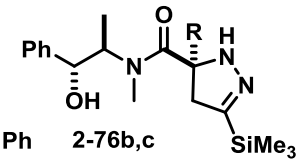	79	19:1
2	2-75b,c R = Me, Ph	2-76b,c	75	19:1
3	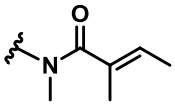 2-75d	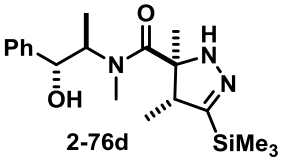 2-76d	70	19:1
4	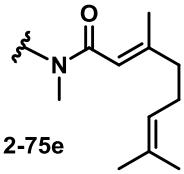 2-75e	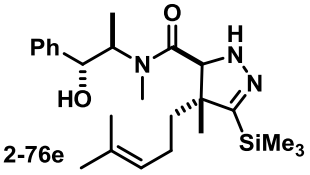 2-76e	71	19:1
5	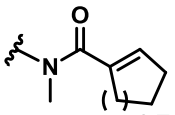 n = 1,2	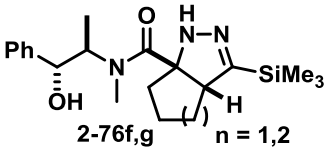 n = 1,2	67	19:1
6	2-75f,g	2-76f,g	70	19:1

2.2.2.2. Mechanistic considerations

When considering the mechanism for formation of pyrazolines **2-76** from the pseudoephedrine α,β-unsaturated amides **2-75**, the conformation of the of the tertiary amide starting material as well as approach of the 1,3-dipole **1** need to be considered. Regarding the former, there are four possible conformers of the pseudoephedrine amide, two *s-cis* and two *s-trans* (**Scheme 2.10**). It has been demonstrated that nucleophiles react with *E*-α,β-unsaturated acceptors exclusively in the *s-cis* conformation, so these were the conformers considered when conspiring plausible pathways to account for the observed selectivity.[32]

Scheme 2.10. The four possible conformers of pseudoephedrine amides

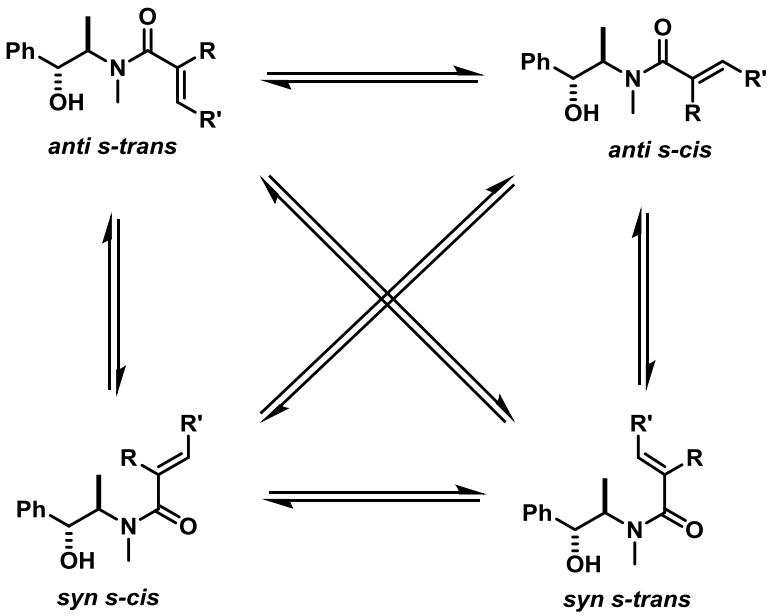

The reactive conformation of pseudoephedrine glycinamide, as determined by Myers' X-ray studies,[23] adopts an *anti s-cis* conformation. By adopting this conformation with the pseudoephedrine-derived α,β-unsaturated amide, a model can be constructed to account for the observed diastereoselectivity (**Scheme 2-11**). When deprotonated into its lithium alkoxide, the *Si*-face of the amide is screened by solvent molecules and lithium cation leading to approach of the dipole from the *Re*-face (**Scheme 2.11**).

Scheme 2.11. Stereochemical model for observed facial selectivity *anti-s*-cis

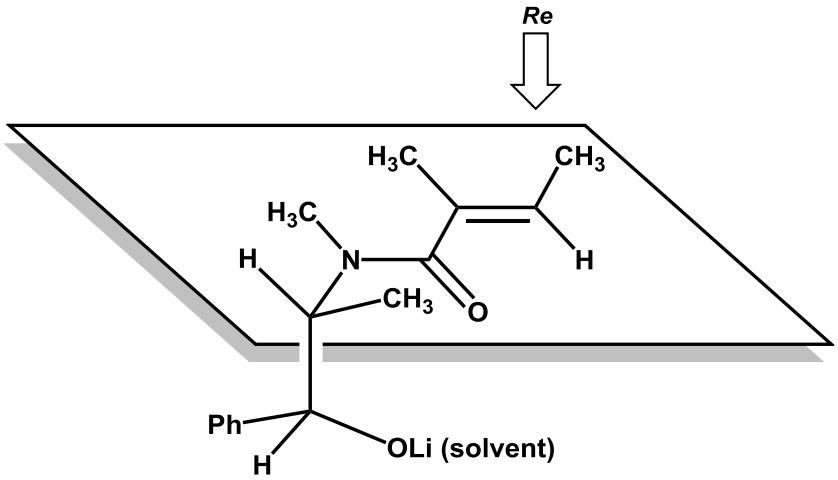

In an alternative view, the Badia group argues that the *syn-s-cis* conformation is the reactive conformer of the pseudoephedrine α,β-unsaturated amides in conjugate addition reactions.[33] This idea was inspired by the work of Davies who demonstrated that, using the concept of matched and mismatched pairings, reactive conformations of Michael acceptors were be determined to be *syn-s-cis*.[34] Also, this *syn-s-sys* conformation would allow for a "directing effect" of **1** with the lithium alkoxide to the *Re*-face via coordination (**Scheme 2.12**). This postulate was based on the well know directing effect of lithium alkoxides in 1,4-conjugate addition reactions.[29,32,35]

Scheme 2.12. Stereochemical model for observed facial selectivity *syn-s*-cis

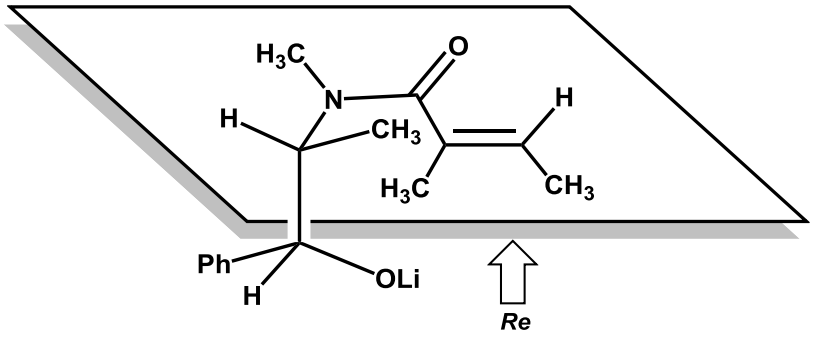

One final view, proposed by Mukaiyama during his seminal report on the conjugate addition of Grignard reagents to α,β-unsaturated amides derived from ephedrine, relies on chelation followed by attack at the least hindered face of the double bond (**Scheme 2.13**).[36] In this fundamental view, lithium chelation with both the alkoxide and amide oxygen atoms leads to a rigid structure with one exposed face for nucleophilic attack.

Scheme 2.13. Adaptation of Mukaiyama's model for facial selectivity

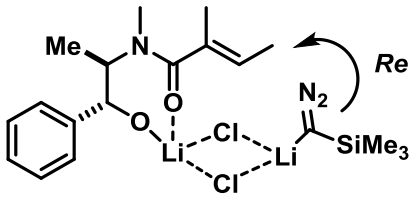

2.3. Application in synthesis - lactacystin

With the new modes of asymmetric induction realized in the formal [3+2] cycloaddition of **1** with α,β-unsaturated pseudoephedrine amides **2-75** and α-methylene-β-hydroxy esters **2-72**, a synthesis of lactacystin was commenced. Isolated from *Streptomyces* in 1991 by Omura, lactacystin was found to be a potent 20s proteasome inhibitor which is now used widely in biochemistry and cellular biology.[37] Numerous sophisticated and efficient total syntheses of lactacystin have been developed to date. Two of them will be discussed here; one classic and one modern approach.

2.3.1. Select previous syntheses of lactacystin

2.3.1.1. Corey synthesis of lactacystin

Shortly after its isolation, a synthesis of lactacystin was reported by E. J. Corey (**Scheme 2.14**).[38]

Scheme 2.14. Corey synthesis of lactacystin

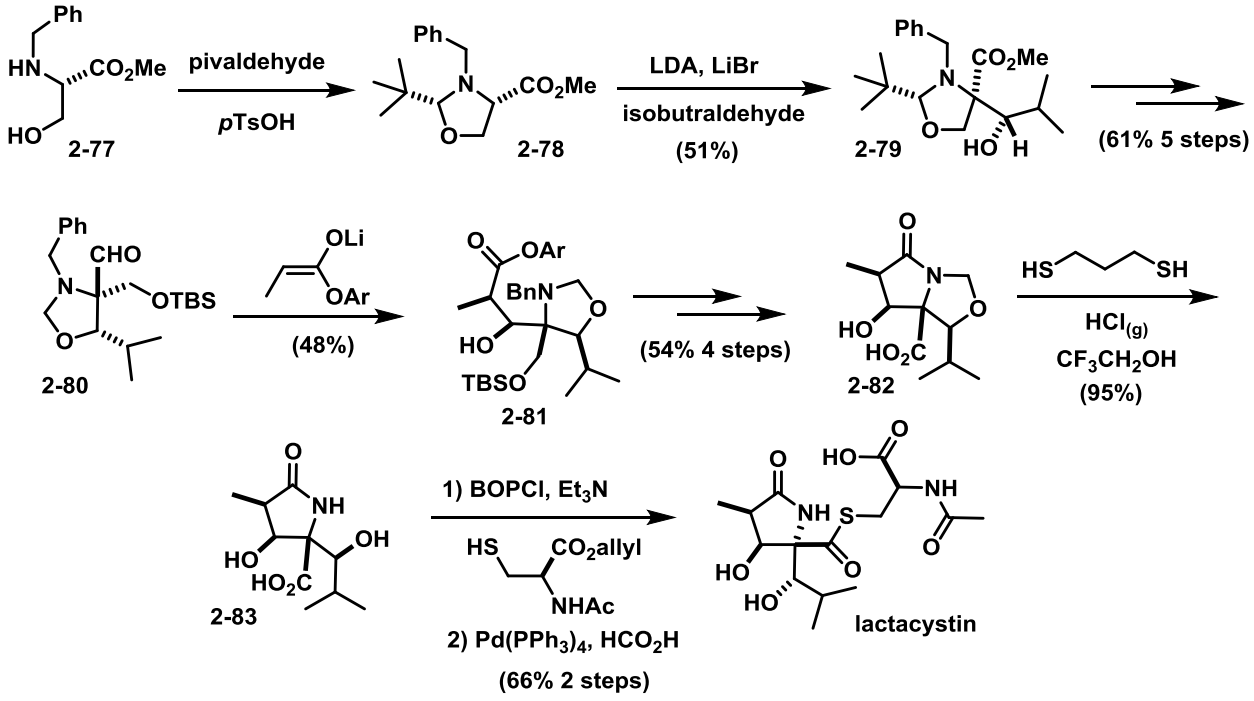

Starting from *N*-benzylserine methyl ester **2-77**, *N,O*-acetonide **2-78** was generated in the presence of pivaldehyde and trifluoroacetic acid. Aldol reaction between **2-78** and isobutraldehyde led to secondary alcohol **2-79** which was converted to key aldehyde **2-80** after a series of protecting group manipulations and oxidation. The key aldol reaction, under Heathcock conditions,[39] led to compound **2-81** in 48% yield. Deprotection and oxidation led to compound **2-82** which was treated with 1,3-propanedithiol in hydrochloric acid to remove the *N,O* methylene bridge. Finally, the allyl ester of lactacystin was generated via BOP-Cl treatment followed by *N*-acetylcysteine allyl ester. Removal of the allyl group under Pd(0) conditions led to lactacystin in 84% yield. Although lengthy, this report served as the first total synthesis of lactacystin.

2.3.1.2. Wardrop synthesis of lactacystin

More recently, the Wardrop and Bowen disclosed an elegant synthesis of lactacystin (**Scheme 2.15**).[40] In their approach, epoxy alcohol **2-84** was opened with sodium azide under acidic conditions

Scheme 2.15. Wardrop synthesis of lactacystin

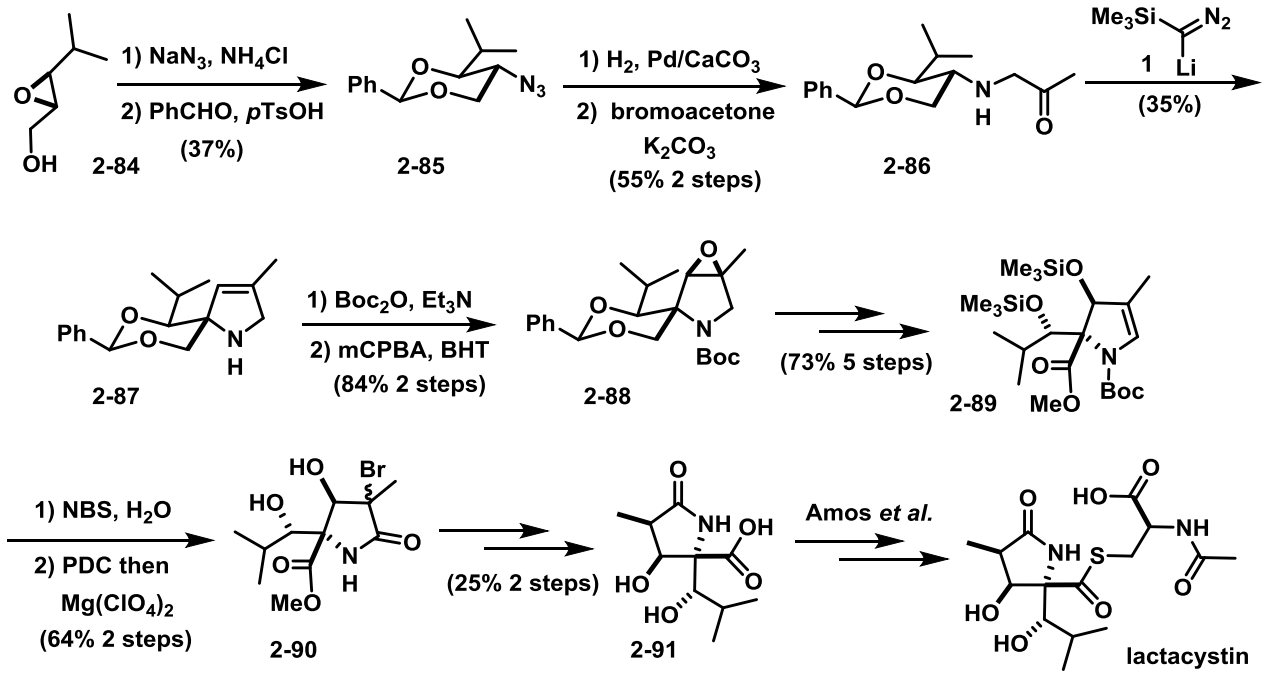

followed by protection of the resulting diol as benzylidene acetal **2-85**. Hydrogenation of the azide followed by alkylation with bromoacetone led to key intermediate **2-86**. Gratifyingly, when α-amino ketone **2-86** was exposed to **1**, the desired pyrroline **2-87** was isolated in 35% yield. The efficiency of this carbene insertion could be further increased to 67% by using an alternative α-elimination protocol for generation of the alkylidene carbene. Protection with Boc anhydride followed by epoxidation with *m*-CPBA from the less hindered β-face led to **2-88** in 84% over two steps. A sequence involving hydrogenation, oxidation and opening of the epoxide under basic conditions led the hydroxyl enamide which was protected as its bistrimethylsilyl ether **2-89**. Hydrobromination of **2-89** with aqueous NBS led to a mixture of α-brominated diastereomers which were then oxidized to the pyrrolidinone **2-90** with PDC in 64% followed by BOC removal with magnesium perchlorate. Endgame consisted of removal of the silyl ether protecting groups followed by samarium diiodide reduction of the α-bromo ester leading to an epimeric mixture of **2-91**, the β-epimer of which was previously converted to lactacystin by Smith and co-workers.[41]

2.3.2. Initial route to lactacystin

It was envisioned that lactacystin could be obtained via oxidation and thiolation of γ-lactam **2-92** (**Scheme 2-16**). Lactam **2-92** could be generated by protonolytic ring-opening of Δ^2-pyrazoline **2-93**.

Scheme 2.16. Retrosynthesis of lactacystin

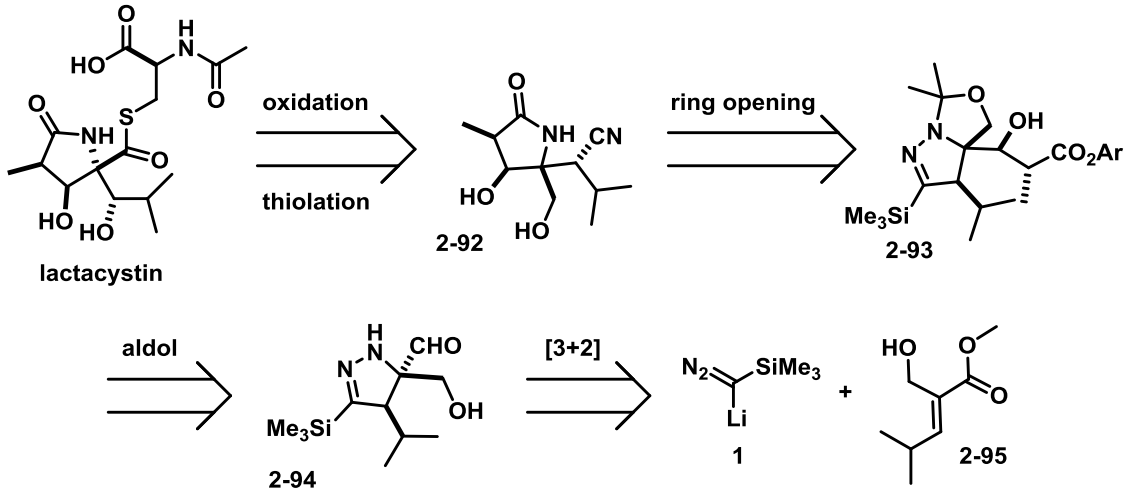

Pyrazoline **2-93** could be accessed through an aldol reaction with **2-94**, the redox adjusted Δ^2-pyrazoline generated from **1** and allylic alcohol **2-95**.

The synthesis commenced with a Baylis-Hillman reaction of isobutraldehyde with methyl acrylate generating allylic alcohol **2-96** (**Scheme 2.17**). Alcohol **2-96** was subjected to Mitsunobu conditions leading to *p*-nitrobenzoyl ester **2-97** via S_N2' reaction.[42] Removal of the benzoyl group of **2-97** generated key allylic alcohol **2-95** which was subjected to **1** generating Δ^2-pyrazoline **2-98** as a single diastereomer from the reaction. Protection of Δ^2-pyrazoline as its *N*,*O*-acetonide **2-99** followed by reduction and oxidation gave **2-100**. Aldol reaction of **2-100** was not selective and produced a mixture of diastereomers (1:1:1.3) of which, **2-93** gave a crystal suitable for X-ray crystallographic analysis. Treatment of **2-93** with tosic acid in refluxing ethanol led to the ring opened product although the *N*,*O*-acetonide was left intact, and cyclization to the lactam did not occur. This is contributed to the steric hindrance of the acetonide methyl groups. The *N*,*O*-acetonide turned out to be quite stable, and **2-101** did not deprotect or cyclize under strongly acidic or basic conditions. Because of the stereoselectivity issues with the aldol reaction of **2-100** and the above mentioned issues with of nitrile **2-101**, a revised synthesis was devised.

Scheme 2.17. Initial route to lactacystin

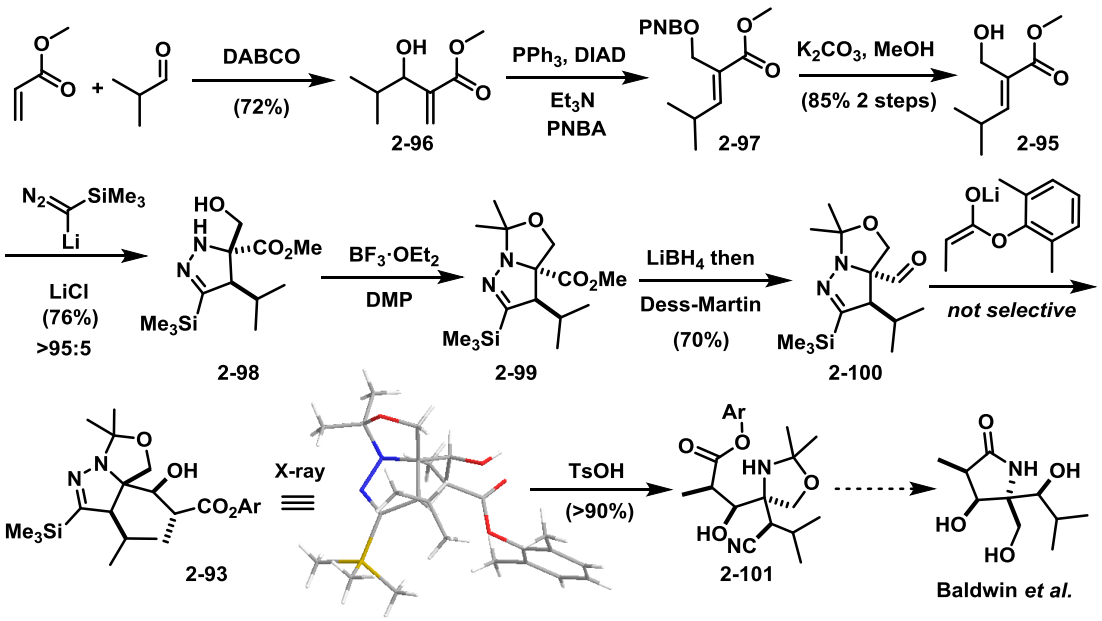

2.3.3. Revised route to lactacystin

In the revised route, lactacystin could be generated from Wardrop's and Amos' intermediate **2-102** which is the direct result of an intramolecular aldol reaction of **2-103** (**Scheme 2.18**). Aldehyde **2-103** could be generated via proponylation and homologation of nitrile **2-104**. Nitrile **2-104** is the result of *N*,*O*-methylene bridge installation and protonolytic ring opening of Δ^2-pyrazoline **2-105**.

Scheme 2.18. Revised retrosynthesis of lactacystin

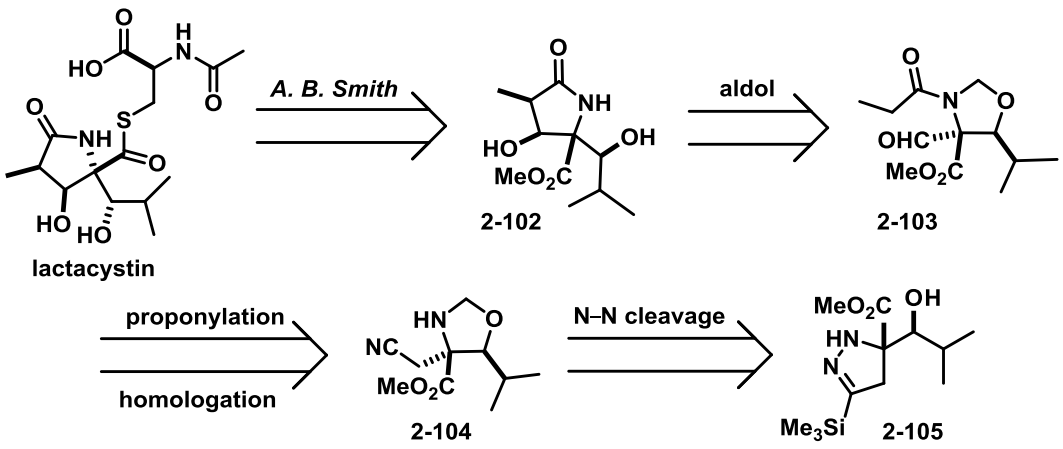

The revised synthesis commenced with a formal cycloaddition between **1** and allylic alcohol **2-96** producing Δ^2-pyrazoline **2-105** in 86% yield as a single diastereomer after recrystallization (**Scheme 2.19**). Treatment of **2-105** with aqueous formaldehyde in THF led to the bicyclic pyrazoline which was opened up under protonolytic conditions to nitrile **2-104**. Proponylation with proponyl chloride in DMF in the presence of pyridine and DMAP at 75 °C led to amide **2-106**. Reduction of the nitrile with Raney-Nickel led to aldehyde **2-107**.[43] Conversion of **2-107** to its lower homolog was then accomplished using the protocol developed by Cossy to generate the key intramolecular aldol precursor **2-103**.[44] Aldol reaction of **2-103**, led to lactam

Scheme 2.19. Revised synthesis of lactacystin

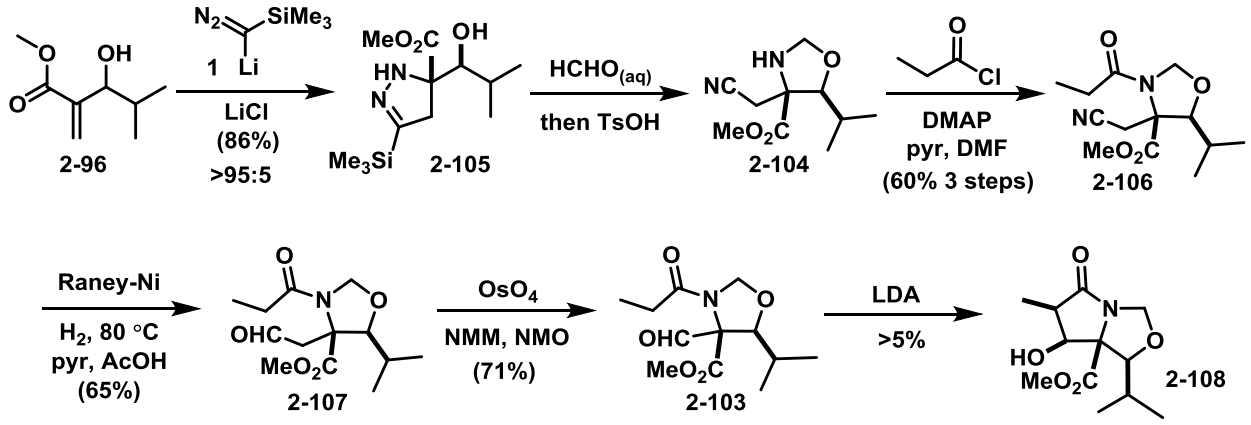

2-108, containing all of the required stereochemistry of lactacystin, although it was generated in only 5% yield with the majority of **2-103** decomposing under the conditions.

2.4. Conclusion

In summary, a selective and efficient, formal [3+2] cycloaddition reaction was developed with both α-methylene and α-benzylidine hydroxy esters **2-72** and pseudoephedrine-derived amides **2-75** with lithium(trimethymsilyl)diazomethane **1**. Utilizing this methodology, a concise approach to lactacystin was devised relying on the selective installation of the α-tert-alkylamino acid moiety in a two-step process involving the formal cycloaddition and protonolytic bond cleavage.

2.5. Experimental

2.5.1. General information

All reactions were carried out under an inert nitrogen atmosphere, unless otherwise indicated. Flasks were oven-dried and cooled under a stream of nitrogen. Compounds were purchased from Aldrich unless otherwise noted. CH_2Cl_2, THF, Et_2O were purified based on standard procedures. Flash chromatography was performed using silica gel 60 Å (32-63 mesh) purchased from SiliCycle.

Analytical thin layer chromatography (TLC) was performed on 0.25 mm SiliCycle precoated silica gel 60 (particle size 0.040-0.063 mm). 1H NMR and ^{13}C NMR spectra were recorded on a Bruker AV-500 spectrometer. ^{1}H and ^{13}C chemical shifts were referenced to internal solvent resonances and reported relative to $SiMe_4$; multiplicities are indicated by s (singlet), d (doublet), t (triplet), q (quartet), qn (quintet), m (multiplet) and br (broad). Coupling constants, J, are reported in Hz (Hertz). Electrospray ionization (ESI) mass spectra were recorded on a Micromass LCT equipped with a time-of-flight analyzer on a Waters Micromass Q-Tof Ultima in the University of Illinois at Urbana-Champaign. Electron impact (EI) mass spectra were obtained using a Micromass AutoSpecTM. Fast atom bombardment (FAB) mass spectra were taken at the Mass Spectrometry Laboratory in the University of Illinois at Urbana-Champaign, using a Micromass 70-VS-4F and 70-VSE for HRFAB and LRFAB, respectively. IR spectra were recorded using JASCO FT/IR-4100.

2.5.2. General procedure for preparation of pyrazolines

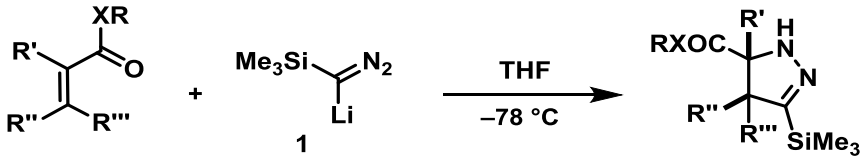

To a stirred solution of trimethylsilyldiazomethane[1] **1** (0.3 mL, 2.0 M in ether, 0.6 mmol) in anhydrous THF (2 mL) under an atmosphere of nitrogen and at –78 °C was added *n*-BuLi (0.24 mL, 2.5 M in hexanes, 0.65 mmol) dropwise over 1 minute. The solution went pale yellow and was allowed to stir for an additional 30 minutes at –78 °C. The α,β-unsaturated compound (0.5 mmol) and LiCl, dissolved in THF (5 mL), was then added drop-wise over 30 seconds and the reaction was allowed to stir for a further 30 min until TLC

[1] Caution! Trimethylsilyldiazomethane should be regarded extremely toxic and all operations must on carried out only in a well-ventilated fume hood and all skin contact should be avoided, see: (a) Shioiri, T.; Aoyama, T.; Mori, S.; *Org. Synth., Coll. Vol.* **1993**, *8*, 612. (b) Barnhart, R.; Dale, D. J.; Ironside, M. D.; Vogt, P. F. *Org. Process Res. Dev.* **2009**, *13*, 1388. (c) Kemsley, J., *Chem. Eng. News* **2011**, *89(19)*, 15.

showed the full consumption of the starting material. The reaction mixture was quenched with several drops of saturated NH_4Cl solution, allowed to warm to rt, and dried over $MgSO_4$. The drying reagent was filtered and solvent was removed under reduced pressure to give the crude product. Purification using flash chromatography with gradient elusion with hexane and ethyl acetate (20:1 to 6:1) to afford pure pyrazoline.

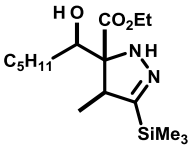

^{1}H NMR (500 MHz, $CDCl_3$) δ 4.21 (m, 2H) ppm 3.74 (m, 1H) ppm 3.58 (q, 1H, J=7.6Hz) ppm 1.37 (dd, 2H, J=7.0Hz, J=14.1Hz) ppm 1.28 (m, 9H) ppm 1.16 (d, 3H, J=7.6Hz) ppm 0.88 (t, 3H, J=7.0Hz) ppm 0.20 (s, 9H). ^{13}C NMR (125 MHz, $CDCl_3$) δ 172.3, 164.6, 77.6, 72.2, 61.4, 52.4, 33.9, 31.6, 25.8, 22.5, 14.3, 14.0, -0.4, -1.5.

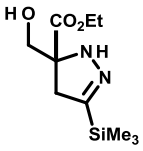

^{1}H NMR (500 MHz, $CDCl_3$) ppm 6.70 (s, 1H) ppm 4.23 (q, 2H, J=7.1Hz) ppm 3.81 (d, 1H, J=10.4Hz) ppm 3.69 (m, 1H) ppm 3.12 (d, 1H, J=17.4Hz) ppm 2.89 (d, 1H, J=17.4Hz) ppm 2.53 (s, 1H) ppm 1.28 (t, 3H, J=7.1Hz) ppm 0.19 (s, 9H) ^{13}C NMR (125 MHz, $CDCl_3$) δ 173.8, 160.6, 70.7, 64.9, 62.0, 44.4, 14.1, -2.3.

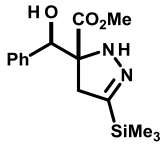

^{1}H NMR (500 MHz, $CDCl_3$) δ ppm 7.30 (m, 5H) ppm 4.98 (s, 1H) ppm 3.67 (s, 3H) ppm 2.95 (m, 2H) ppm 0.10 (s, 9H). ^{13}C NMR (125 MHz, $CDCl_3$) 173.9, 161.1, 138.6, 128.3, 128.3, 126.6, 75.6, 74.7, 52.7, 41.4, -2.4. HRMS (ESI) calc. for $C_{15}H_{23}N_2O_3Si$ $[M+H]^+$ 307.1478, found 307.1476.

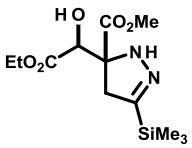

^{1}H NMR (500 MHz, $CDCl_3$) δ ppm 6.57 (bs, 1H) ppm 4.39 (d, 1H, J=8.9Hz) ppm 4.22 (q, 2H, J=7.2Hz) ppm 3.75 (s, 1H) ppm 3.25 (s, 1H) ppm 3.07 (d, 1H, J=17.6Hz) ppm 2.16 (s, 1H) ppm 1.28 (t, 3H, J=7.1Hz) ppm 0.18 (s, 9H). ^{13}C NMR (125 MHz, $CDCl_3$) δ 173.0, 171.4, 160.1, 72.3, 62.1, 52.9, 45.6, 14.1, -2.3. HRMS (ESI) calc. for $C_{21}H_{27}N_2O_2Si$ $[M+H]^+$ 303.1376, found 303.1382.

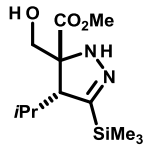

^{1}H NMR (500 MHz, $CDCl_3$) δ ppm 4.14 (d, 1H, J=10.7Hz) ppm 3.96 (d, 1H, J=10.7Hz) ppm 3.74 (s,3H) ppm 3.25 (d, 1H, J=2.3Hz) ppm 1.98 (qd, 1H, J=4.3Hz, J=6.6Hz) ppm 1.03 (d, 3H, J=7.1Hz) ppm 0.94 (d, 3H, J=6.9Hz) ppm 0.20 (s, 9H). ^{13}C NMR (125 MHz, $CDCl_3$) δ 175.7, 162.2, 74.8, 63.1, 61.8, 52.9, 27.1, 22.3, 19.1, -1.0. HRMS (ESI) calc. for $C_{21}H_{27}N_2O_2Si$ $[M+H]^+$ 273.1634, found 273.1633.

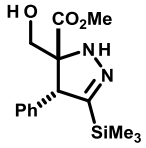

^{1}H NMR (500 MHz, $CDCl_3$) δ 7.26 (m, 3H) ppm 7.07 (d, 2H, J=7.1Hz) ppm 6.90 (s, 1H) ppm 4.44 (s, 1H) ppm 3.79 (s, 3H) ppm 3.61 (d, 1H, J=11.0Hz) ppm 3.33 (d, 1H, J=11.1Hz) ppm -0.04 (s, 9H). ^{13}C NMR (125 MHz, $CDCl_3$) δ 175.0, 162.5, 133.9, 129.3, 128.7, 128.0, 73.9, 64.9, 62.0, 53.0, -1.4. HRMS (ESI) calc. for $C_{15}H_{23}N_2O_3Si$ $[M+H]^+$ 307.1478, found 307.1473.

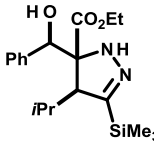

^{1}H NMR (500 MHz, $CDCl_3$) δ ppm 7.35 (d, 2H, J=6.6Hz) ppm 7.27 (m, 3H) ppm 6.42 (s, 1H) ppm 4.74 (d, 1H, J=9.6Hz) ppm 4.01 (tt, 1H, J=7.2Hz, J=14.3Hz) ppm 3.90 (m, 1H) ppm 3.65 (d, 1H, J=1.7Hz) ppm 3.15 (d, 1H, J=9.7Hz) ppm 2.34 (dtd, 1H, J=2.4Hz, J=7.1Hz, J=14.3Hz) ppm 1.12 (t, 3H, J=7.2Hz) ppm 0.99 (d, 6H, J=7.2Hz) ppm 0.22 (s, 9H). ^{13}C NMR (125 MHz, $CDCl_3$) δ 172.1, 163.0, 139.8, 128.1, 128.0, 127.6, 77.1, 76.0, 65.2, 61.7, 27.8, 20.8, 18.9, 13.7, -0.7. HRMS (ESI) calc. for $C_{19}H_{31}N_2O_3Si$ $[M+H]^+$ 363.2104, found 363.2099.

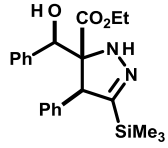

^{1}H NMR (500 MHz, $CDCl_3$) δ ppm 7.34 (m, 3H) ppm 7.25 (m, 7H) ppm 6.48 (s, 1H) ppm 4.93 (s, 1H) ppm 4.74 (s, 1H) ppm 3.45 (qd, 1H, J=7.2Hz, J=10.7Hz) ppm 3.25 (qd, 2H, J=7.2Hz, J=10.6Hz) ppm 0.63 (t, 3H, J=7.2Hz) ppm -0.04 (s, 9H). ^{13}C NMR (125 MHz, $CDCl_3$) δ 170.7, 163.2, 140.0, 137.5, 129.4, 128.4, 128.2, 128.1, 127.7, 127.3, 79.7, 76.5, 66.4, 61.2, 13.2, -1.4. HRMS (ESI) calc. for $C_{22}H_{29}N_2O_3Si$ $[M+H]^+$ 397.1947, found 397.1946.

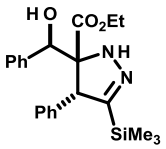

^{1}H NMR (500 MHz, $CDCl_3$) δ 7.34 (m, 3H) ppm 7.26 (d, 2H, J=5.0Hz) ppm 7.21 (m, 3H) ppm 7.02 (m, 2H) ppm 6.93 (s, 1H) ppm 4.72 (s, 1H) ppm 4.58 (s, 1H) ppm 3.96 (qd, 1H, J=7.1Hz, J=10.8Hz) ppm 3.85 (qd, 1H, J=7.1Hz, J=10.8Hz) ppm 3.10 (bs, 1H) ppm 1.06 (t, 3H, J=7.1Hz) ppm -0.02 (s, 9H) ^{13}C NMR (125 MHz, $CDCl_3$) δ 173.3, 164.7, 140.2, 134.3, 130.3, 128.6, 128.1, 128.0, 128.0, 126.8, 72.5, 63.1, 61.9, 13.8, -1.8. HRMS (ESI) calc. for $C_{22}H_{29}N_2O_3Si$ $[M+H]^+$ 397.1947, found 397.1947.

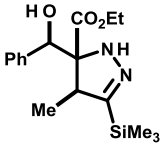

^{1}H NMR (500 MHz, $CDCl_3$) δ 7.27 (m, 5H) ppm 6.39 (s, 1H) ppm 4.83 (s, 1H) ppm 4.02 (qd, 1H, J=7.1Hz, J=10.6Hz) ppm 3.91 (m, 1H) ppm 3.73 (q, 1H, J=7.6Hz) ppm 3.18 (s, 1H) ppm 2.36 (s, 1H) ppm 1.26 (d, 3H, J=7.6Hz) ppm 1.11 (t, 3H, J=7.1Hz) ppm 0.22 (s, 9H). ^{13}C NMR (125 MHz, $CDCl_3$) δ 171.1, 165.0, 140.4, 128.2, 128.2, 127.2, 78.2, 76.5, 74.3, 61.4, 53.2, 14.3, 14.0, -1.5. HRMS (ESI) calc. for $C_{17}H_{27}N_2O_3Si$ $[M+H]^+$ 335.1791, found 335.1779.

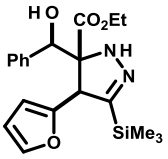

^{1}H NMR (500 MHz, $CDCl_3$) δ 7.28 (m, 5H) ppm 6.54 (s, 1H) ppm 6.36 (dd, 1H, J=1.8Hz, J=3.1Hz) ppm 6.26 (d, 1H, J=3.2Hz) ppm 4.95 (s, 1H) ppm 4.91 (s, 1H) ppm 3.70 (qd, 1H, J=7.1Hz, J=10.7Hz) ppm 3.58 (tt, 1H, J=7.2Hz, J=10.7Hz) ppm 3.15 (s, 1H) ppm 0.90 (t, 3H, J=7.2Hz) ppm 0.02 (s, 9H). ^{13}C NMR (125 MHz, $CDCl_3$) δ 170.5, 160.6, 149.9, 142.4, 139.9, 128.3, 128.3, 127.1, 111.0, 109.4, 78.3, 75.1, 61.8, 58.8, 13.5, -2.2. HRMS (ESI) calc. for $C_{20}H_{27}N_2O_4Si$ $[M+H]^+$ 387.1740, found 387.1740.

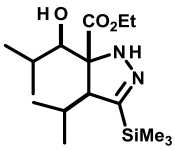

^{1}H NMR (500 MHz, $CDCl_3$) δ 4.21 (d p, 2H, J=3.8Hz, J=6.7Hz) ppm 3.63 (d, 1H, J=0.6Hz) ppm 3.55 (d, 1H, J=2.4Hz) ppm 2.36 (dtd, 1H, J=2.2Hz, J=7.0Hz, J=14.0Hz) ppm 1.72 (dtd, 1H, J=2.2Hz, J=6.9Hz, J=13.8Hz) ppm 1.32 (t, 3H, J=7.2Hz) ppm 0.97 (m, 9H) ppm 0.81 (d, 3H, J=6.8Hz) ppm 0.23 (s, 9H). ^{13}C NMR (125 MHz, $CDCl_3$) δ 173.0, 162.9, 78.2, 75.6, 67.3, 61.7, 30.7, 27.3, 21.9, 20.9, 18.9, 16.0, 13.9, -0.7. HRMS (ESI) calc. for $C_{16}H_{33}N_2O_3Si$ $[M+H]^+$ 329.2260, found 329.2259.

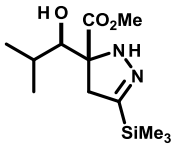

^{1}H NMR (500 MHz, $CDCl_3$) δ 6.54 (s, 1H) ppm 3.76 (s, 1H) ppm 3.66 (dd, 1H, J=3.1Hz, J=11.3Hz) ppm 3.17 (q, 2H, J=17.6Hz) ppm 2.28 (d, 1H, J=11.3Hz) ppm 1.54 (dtd, 1H, J=3.1Hz, J=6.7Hz, J=13.5Hz) ppm 0.98 (d, 3H, J=6.8Hz) ppm 0.84 (d, 3H, J=6.8Hz) ppm 0.18 (s, 9H). ^{13}C NMR (125 MHz, $CDCl_3$) δ 174.8, 161.1, 76.2, 73.7, 52.7, 48.1, 31.6, 21.2, 15.8, -2.3.

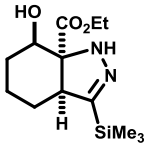

^{1}H NMR (500 MHz, $CDCl_3$) δ 6.79 (bs, 1H) ppm 4.12 (d p, 2H, J=3.6Hz, J=7.5Hz) ppm 4.03 (dd, 1H, J=4.8Hz, J=11.3Hz) ppm 3.10 (dd, 1H, J=6.5Hz, J=11.5Hz) ppm 2.90 (bs, 1H) ppm 1.80 (m, 1H) ppm 1.67 (m, 2H) ppm 1.53 (dq, 1H, J=3.1Hz, J=12.3Hz) ppm 1.26 (ddd, 1H, J=3.3Hz, J=9.8Hz, J=9.2Hz) ppm 1.17 (t, 3H, J=7.1Hz) ppm 0.81 (m, 1H) ppm 0.10 (s, 9H). ^{13}C NMR (125 MHz, $CDCl_3$) δ 175.7, 164.0, 74.3, 71.9, 61.7, 52.6, 29.8, 26.5, 21.9, 14.2, -1.8.

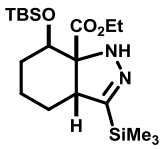

^{1}H NMR (500 MHz, $CDCl_3$) δ 6.42 (bs, 1H) ppm 4.05 (td, 3H, J=5.6Hz, J=9.7Hz) ppm 3.37 (dd, 1H, J=6.9Hz, J=9.6Hz) ppm 1.82 (ddd, 1H, J=5.8Hz, J=9.7Hz, J=12.2Hz) ppm 1.64 (m, 3H) ppm 1.28 (m, 1H) ppm 1.21 (t, 3H, J=7.1Hz) ppm 1.11 (m, 1H) ppm 0.82 (s, 9H) ppm 0.16 (s, 9H) ppm 0.01 (s, 3H) ppm -0.03 (s, 3H). ^{13}C NMR (125 MHz, $CDCl_3$) δ 173.6, 166.2, 73.5, 69.8, 61.0, 48.0, 29.1, 25.6, 25.2, 17.9, 17.0, 14.0, -1.7, -4.2, -5.3.

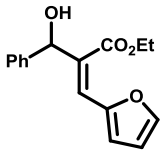

^{1}H NMR (500 MHz, $CDCl_3$) δ 7.41 (dd, 3H, J=4.3Hz, J=8.1Hz) ppm 7.35 (t, 2H, J=7.4Hz) ppm 7.29 (t, 1H, J=7.2Hz) ppm 6.84 (d, 1H, J=3.4Hz) ppm 6.74 (s, 1H) ppm 6.43 (dd, 1H, J=1.7Hz, J=3.3Hz) ppm 5.57 (d, 1H, J=3.9Hz) ppm 4.18 (q, 2H, J=7.1Hz) ppm 2.98 (d, 1H, J=5.2Hz) ppm 1.16 (t, 3H, J=7.1Hz). ^{13}C NMR (125 MHz, $CDCl_3$) δ 167.6, 150.2, 143.6, 141.3, 131.3, 128.5, 128.0, 126.7, 122.4, 114.1, 112.0, 75.3, 60.9, 14.1. HRMS (ESI) calc. for $C_{16}H_{16}O_4Na$ $[M+Na]^+$ 295.0946, found 295.0952.

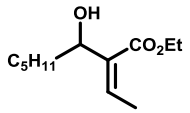

^{1}H NMR (500 MHz, $CDCl_3$) δ 6.18 (q, 1H, J=6.6Hz) ppm 4.21 (dd, 2H, J=7.1Hz, J=14.3Hz) ppm 4.18 (bs, 1H) ppm 2.77 (bs, 1H) ppm 1.93 (d, 3H, J=7.1Hz) ppm 1.55 (m, 2H) ppm 1.36 (dd, 1H, J=4.2Hz, J=6.4Hz) ppm 1.27 (dd, 8H, J=9.9Hz, J=17.0Hz) ppm 0.83 (t, 3H, J=6.7Hz). ^{13}C NMR (125 MHz, $CDCl_3$) δ 167.7, 136.5, 135.4, 74.3, 60.3, 36.5, 31.6, 25.7, 22.5, 15.4, 14.2, 14.0. HRMS (ESI) calc. for $C_{12}H_{22}O_3Na$ $[M+Na]^+$ 237.1467, found 237.1476.

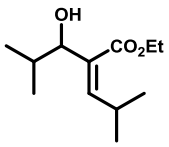

^{1}H NMR (500 MHz, $CDCl_3$) δ 65.77 (d, 1H, J=9.9Hz) ppm 4.21 (q, 2H, J=7.1Hz) ppm 3.76 (d, 1H, J=7.4Hz) ppm 3.00 (m, 1H) ppm 2.72 (bs, 1H) ppm 1.78 (m, 1H) ppm 1.28 (t, 3H, J=7.1Hz) ppm 0.99 (dd, 6H, J=4.7Hz, J=6.5Hz) ppm 0.94 (d, 3H, J=6.6Hz) ppm 0.80 (d, 3H, J=6.8Hz). ^{13}C NMR (125 MHz, $CDCl_3$) δ 168.1, 148.9, 131.0, 80.6, 60.4, 33.2, 28.5, 22.6, 22.6, 19.6, 18.4, 14.2.

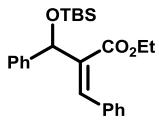

^{1}H NMR (500 MHz, $CDCl_3$) δ 7.44 (d, 2H, J=7.3Hz) ppm 7.35 (t, 2H, J=7.5Hz) ppm 7.29 (m, 6H) ppm 6.90 (d, 1H, J=0.9Hz) ppm 5.68 (s, 1H) ppm 4.05 (q, 2H, J=7.1Hz) ppm 1.01 (t, 3H, J=7.1Hz) ppm 0.95 (s, 9H) ppm 0.16 (s, 3H) ppm -0.02 (s, 3H). ^{13}C NMR (125 MHz, $CDCl_3$) δ 168.6, 142.0, 138.3, 135.9, 131.4, 128.4, 128.2, 128.1, 127.9, 127.7, 127.1, 75.5, 60.6, 25.9, 18.3, 13.7, -4.7, -4.9.

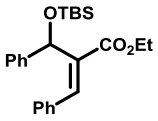

^{1}H NMR (500 MHz, $CDCl_3$) δ 7.86 (s, 1H) ppm 7.44 (dd, 4H, J=2.4Hz, J=5.2Hz) ppm 7.32 (m, 5H) ppm 7.23 (t, 1H, J=7.3Hz) ppm 6.14 (s, 1H) ppm 4.16 (m, 2H) ppm 1.18 (t, 3H, J=7.1Hz) ppm 0.87 (s, 9H) ppm -0.07 (s, 3H) ppm -0.13 (s, 3H). ^{13}C NMR (125 MHz, $CDCl_3$) δ 167.4, 143.3, 140.7, 135.2, 134.7, 129.7, 128.9, 128.3, 127.9, 126.5, 125.5, 69.1, 60.7, 25.8, 18.2, 14.1, -4.8, -5.2.

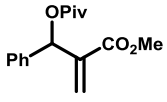

^{1}H NMR (500 MHz, $CDCl_3$) δ 7.32 (m, 5H) ppm 6.64 (s, 1H) ppm 6.37 (s, 1H) ppm 5.81 (s, 1H) ppm 3.72 (s, 3H) ppm 1.21 (s, 9H). ^{13}C NMR (125 MHz, $CDCl_3$) δ 176.7, 165.6,

140.2, 138.1, 128.4, 128.2, 127.4, 125.8, 72.8, 52.0, 38.8, 27.1.

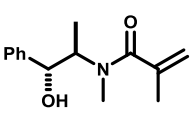

^{1}H NMR (1.2:1 rotamer ratio, asterisks denote distinguishable minor rotamer peaks, 500 MHz, $CDCl_3$) δ 7.34-7.31 (m) ppm 5.28* (bs, 2H) ppm 5.12 (bs, 2H) ppm 4.99* (bs, 1H) ppm 4.89 (bs, 1H) ppm 4.66 (bd, 1H, J=6.1Hz) ppm 4.52* (bd, 1H, J=7.9Hz) ppm 4.33 (bt, 1H) ppm 4.21* (bt, 1H) ppm 2.94* (bs, 3H) ppm 2.79 (bs, 3H) ppm 1.96* (bs, 3H) ppm 1.86 (bs, 3H) ppm 1.18 (bs, 3H) ppm 0.96* (bs, 3H) ^{13}C NMR (125 MHz, $CDCl_3$) δ 174.7, 142.4, 141.5, 141.1, 128.7, 128.4, 127.6, 127.0, 126.3, 115.7, 114.7*, 76.2, 75.2*, 59.6, 58.8*, 35.0, 27.3, 27.1, 26.3, 20.9*, 20.0, 15.3*, 14.2. HRMS (ESI) calc. for $C_{14}H_{20}O_2N$ $[M+]^+$ 234.1494, found 234.1497.

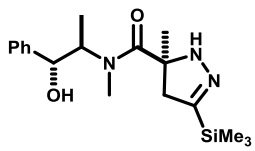

^{1}H NMR (500 MHz, $CDCl_3$) δ 7.28 (m, 5H), 5.85 (bs, 1H), 4.61 (bs, 1H), 4.43 (bd, 1H, J=9.4Hz), 3.38 (m, 1H) ppm 3.00 (d, 1H, J=18.0Hz), 2.93 (s, 3H), 2.76 (bd, 1H, J=18.2Hz), 1.40 (bs, 3H), 0.81 (bd, 3H, J=5.7Hz), 0.17 (s, 9H). ^{13}C NMR (125 MHz, $CDCl_3$) δ 174.4, 161.6, 142.3, 128.5, 127.9, 127.0, 75.5, 63.9, 57.4, 52.6, 28.0, 27.3, 21.0, 15.5, 14.2, -2.2. HRMS (ESI) calc. for $C_{18}H_{30}N_3O_2Si$ $[M+H]^+$ 348.2107, found 348.2104.

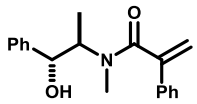

^{1}H NMR (2:1 rotamer ratio, asterisks denote distinguishable minor rotamer peaks, 500 MHz, $CDCl_3$) δ 7.48 (d, J=7.3Hz) ppm 7.41 (d, J=7.3Hz) ppm 7.35 (m) ppm 7.29 (m) ppm 7.09 (m) ppm 5.71* (s, 1H) ppm 5.69 (s, 1H) ppm 5.31* (s, 1H) ppm 5.21 (s, 1H) ppm 4.72 (d, 1H, J=7.4Hz) ppm 4.52 (m, 1H) ppm 4.46* (d, 1H, J=8.8Hz) ppm 4.04* (qd, 1H, J=6.8Hz, J=13.6Hz) ppm 3.04* (s, 3H) ppm 2.72 (s, 3H) ppm 1.24 (d, 3H, J=7.0Hz) ppm 0.82* (d, 3H, J=6.7Hz). ^{13}C NMR (125 MHz, $CDCl_3$) δ 172.7, 172.0*, 145.4, 145.4*, 142.4, 141.6*, 136.1*, 135.1, 128.9, 128.8, 128.6, 128.6, 128.5, 128.3, 127.7, 126.9, 126.3, 126.0, 125.6, 114.6*, 114.1, 76.0, 75.5*, 59.4, 58.7*, 34.9*, 26.6, 15.0*, 14.2 .

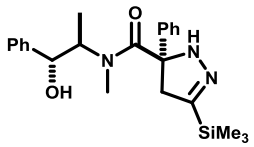

^{1}H NMR (500 MHz, $CDCl_3$) δ 7.41 (m, 5H, J=6.6Hz, J=26.7Hz, J=23.2Hz), 4.90 (d, 1H, J=7.8Hz), 3.54 (m, 1H, J=6.2Hz, J=12.5Hz), 2.86 (s, 3H), 2.44 (dd, 2H, J=22.1Hz, J=39.9Hz), 1.36 (d, 3H, J=6.2Hz), 0.13 (s, 9H). ^{13}C NMR (125 MHz, $CDCl_3$) δ 171.8, 158.2, 146.1, 141.8, 128.9, 128.6, 125.5, 128.2, 127.4, 126.6, 125.9, 124.4, 82.5, 74.9, 71.8, 61.3, 57.9, 53.6, 27.4, 17.3, 13.4, -2.3.

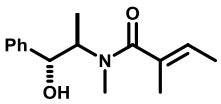

^{1}H NMR (500 MHz, $CDCl_3$) δ 7.34 (bs, 5H), 5.54 (bs, 1H), 4.96 (bs, 1H), 4.64 (bs, 1H), 4.27 (bs, 1H), 2.90 (bd, 3H), 1.77 (bs, 3H), 1.67 (bs, 3H), 1.17 (bd, 3H). ^{13}C NMR (125 MHz, $CDCl_3$) δ 175.9, 142.6, 132.7, 128.3, 127.6, 126.3, 76.2, 59.0, 35.1, 35.0, 14.2, 13.8, 13.7, 13.2. HRMS (ESI) calc. for $C_{15}H_{22}N_3O_2$ $[M+H]^+$ 248.1651, found 248.1658.

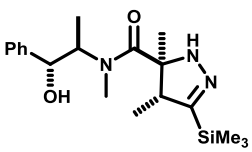

^{1}H NMR (500 MHz, $CDCl_3$) δ 7.38-7.30 (m, 5H), 4.66 (bs, 1H), 4.51 (bs, 1H), 3.70 (bs, 1H), 3.37 (bs, 1H), 2.96 (bd, 3H), 1.34 (bs, 3H), 1.22 (bd, 3H), 0.24 (s, 9H). HRMS (ESI) calc. for $C_{19}H_{32}N_3O_2Si$ $[M+H]^+$ 362.2264, found 362.2269.

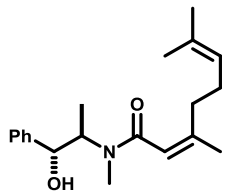

^{1}H NMR (500 MHz, $CDCl_3$) δ 7.15 (m, 10H), 5.58 (s, 1H), 5.53 (s, 1H), 4.96 (m, 2H), 4.40 (td, 4H, J=8.3Hz, J=16.7Hz), 3.96 (m, 1H), 2.76 (s, 3H), 2.66 (s, 3H), 1.99 (m, 9H), 1.65 (s, 3H), 1.60 (s, 3H), 1.55 (s, 3H), 1.52 (s, 3H), 1.50 (s, 3H), 1.48 (s, 3H), 0.94 (d, 2H, J=6.8Hz), 0.85 (d, 3H, J=6.8Hz). ^{13}C NMR (125 MHz, $CDCl_3$) δ 170.8, 170.6, 149.2, 146.5, 143.0, 142.8, 132.3, 132.1, 128.6, 128.5, 128.0, 127.7, 127.2, 126.8, 124.0, 123.8, 119.8, 118.9, 76.2, 75.6, 59.4, 57.6, 39.9, 39.5, 33.2, 27.1, 26.34, 26.28, 26.0, 18.73, 18.70, 18.0, 15.9, 14.6. HRMS (ESI) calc. for $C_{20}H_{30}NO_2$ $[M+H]^+$ 316.2277, found 316.2276.

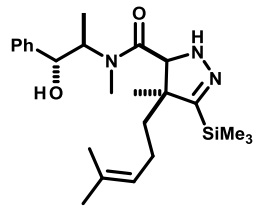

^{1}H NMR (500 MHz, $CDCl_3$) δ 7.34 (m, 5H), 6.24 (bs, 1H), 4.91 (bdt, 1H, J=1.2Hz, J=5.9Hz), 4.82 (m, 1H), 4.55 (bt, 1H, J=8.4Hz), 4.15 (s, 1H), 3.38 (bs, 1H), 3.04 (s, 3H), 2.07 (m, 1H), 1.67 (m, 3H), 1.61 (s, 3H), 1.54 (s, 3H), 1.36 (s, 3H), 0.95 (d, 3H, J=7.0Hz), 0.25 (s, 9H). ^{13}C NMR (125 MHz, $CDCl_3$) δ 174.2, 142.3, 129.2, 129.0, 128.9, 128.5, 127.7, 127.2, 124.4, 76.7, 67.9, 61.8, 35.9, 26.5, 26.0, 24.4, 18.3, 15.0, -0.2. HRMS (ESI) calc. for $C_{24}H_{40}N_3O_2Si$ $[M+H]^+$ 430.2890, found 430.2882.

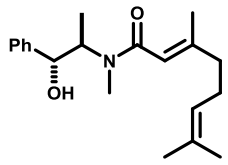

^{1}H NMR (2:1 rotamer ratio, asterisks denote distinguishable minor rotamer peaks, 500 MHz, $CDCl_3$) δ 7.37-7.25 (m, 7H), 5.76* (s, 1H), 5.70 (s, 1H), 5.11-5.05 (m), 4.58 (d, 1H, J=7.8Hz), 4.50* (d, 1H, J=8.2Hz), 4.44-4.41 (m), 4.26 (bs, 1H), 4.09 (tt, 1H, J=7.0Hz, J=14.3Hz), 2.93* (s, 3H), 2.87 (s, 3H), 2.15-2.11 (m), 1.83 (s, 3H), 1.78* (s, 3H), 1.67 (s, 3H), 1.64* (s, 3H), 1.62* (s, 3H), 1.59 (s, 3H), 1.09 (d, 3H, J=7.0Hz), 0.95 (d, 3H, J=6.8Hz). ^{13}C NMR (125 MHz, $CDCl_3$) δ 180.13, 170.90, 170.35, 149.73, 146.89, 142.62, 142.53, 141.77, 132.17, 128.28, 127.58, 127.50, 126.85, 126.50, 126.40, 123.58, 123.43, 119.12, 118.33, 76.37, 76.14, 75.50, 59.07, 58.33, 39.68, 39.26, 39.20, 33.43, 28.25, 26.59, 26.04, 25.95, 25.68, 18.50, 17.71, 15.41, 14.48, 14.43. HRMS (ESI) calc. for $C_{20}H_{30}NO_2$ $[M+H]^+$ 316.2277, found 316.2268.

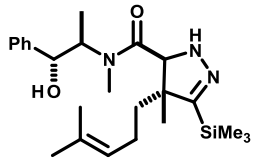

^{1}H NMR (500 MHz, $CDCl_3$) δ 7.40-7.30 (m, 5H), 6.34 (bs, 1H), 5.07 (m, 1H), 4.73 (bs, 1H), 4.61-4.60 (m, 1H), 4.24 (s, 1H), 3.70 (bs, 1H), 2.99 (s, 3H), 2.13-2.09 (m, 2H), 1.82-1.79 (m, 2H), 1.70 (s, 3H), 1.61 (s, 3H), 1.05, bs, 6H), 0.24 (s, 9H). ^{13}C NMR (125 MHz, $CDCl_3$) δ 173.83, 162.75, 141.97, 132.13, 128.77, 128.51, 127.93, 127.81, 127.28, 126.59, 126.25, 123.49, 75.88, 65.14, 61.61, 40.51, 25.70, 23.28, 21.43, 17.78, 14.67, -0.40. HRMS (ESI) calc. for $C_{24}H_{40}N_3O_2Si$ $[M+H]^+$ 430.2890, found 430.2882.

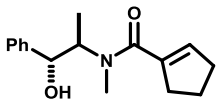

^{1}H NMR (500 MHz, $CDCl_3$) δ 7.13-7.08 (m, 5H), 5.58 (bs, 1H), 5.01 (bs, 1H), 4.52 (bs, 1H), 4.41-4.33 (m, 2H), 4.00 (bs, 1H), 2.73 (bs, 3H), 2.65* (bs, 3H), 2.23* (bs, 4H), 2.24 (bs, 4H), 1.71-1.68 (m, 2H), 0.91* (bs, 3H), 0.81-0.80 (bd, 3H). ^{13}C NMR (125 MHz, $CDCl_3$) δ 171.58, 171.49, 142.88, 139.32, 139.24, 133.40, 131.07, 128.56, 128.37, 127.91, 127.62, 127.11, 126.77, 75.80, 75.12, 60.61, 59.52, 57.21, 57.06, 34.92, 34.22, 33.51, 27.12, 23.24, 23.11, 15.92, 14.34. HRMS (ESI) calc. for $C_{16}H_{22}NO_2$ $[M+H]^+$ 260.1651, found 260.1649.

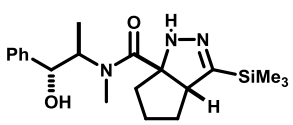

^{1}H NMR (500 MHz, $CDCl_3$) δ 7.99 (bs, 1H), 7.47 (bs, 1H), 7.33-7.27 (m, 10H), 6.23 (bs, 1H), 5.17 (bs, 1H), 4.57-4.55 (m, 1H), 4.39-4.37 (m, 1H), 4.23 (bs, 1H), 3.68 (bs, 1H), 3.55 (bs, 1H), 3.19 (bs, 1H), 2.87 (bs, 3H), 2.84 (bs, 3H), 1.85-1.79 (m, 2H), 1.58-1.56 (m, 2H), 1.38 (m, 2H), 0.87 (d, 3H, J=5.1Hz), 0.81 (d, 3H, J=5.3Hz), 0.16 (s, 9H), 0.14 (s, 3H). ^{13}C NMR (125 MHz, $CDCl_3$) δ 173.78, 173.40, 164.09, 162.73, 142.15, 141.90, 128.84, 128.61, 128.46, 128.26, 127.83, 127.33, 127.17, 75.29, 74.82, 74.50, 64.41, 62.70, 57.97, 57.02, 42.37, 41.31, 31.94, 30.84, 28.14, 27.42, 25.56, 24.10, 15.75, 15.43, -1.34, -1.50. HRMS (ESI) calc. for $C_{20}H_{32}N_3O_2Si$ $[M+H]^+$ 374.2264, found 374.2259.

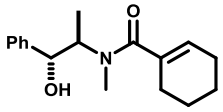

^{1}H NMR (500 MHz, $CDCl_3$) δ 7.32 (bm, 5H), 5.70 (bs, 1H), 4.63 (bs, 1H), 4.24 (bs, 1H), 2.79 (bs, 3H), 2.14-2.06 (m, 4H), 1.66 (bs, 2H), 1.60 (bs, 2H), 1.19-0.96 (m, 3H). ^{13}C NMR (125 MHz, $CDCl_3$) δ 174.99, 142.34, 141.93, 136.73, 134.90, 128.94, 128.82, 128.24, 127.49, 127.31, 126.81, 126.38, 75.96, 75.84, 74.96, 59.62, 58.04, 57.57, 34.57, 30.36, 29.63, 26.05, 25.78, 25.42, 24.57, 23.86, 22.06, 21.83, 21.61, 21.17, 15.32, 14.10, 13.08. HRMS (ESI) calc. for $C_{17}H_{24}NO_2$ $[M+H]^+$ 274.1807, found 274.1819.

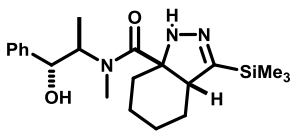

^{1}H NMR (500 MHz, $CDCl_3$) δ 7.31 (bs, 5H), 6.27 (bs, 1H), 4.52 (bs, 1H),2.90 (s, 3H), 1.87-1.85 (m, 1H), 1.53-1.42 (m, 4H), 1.42 (bs, 3H), 0.92 (m, 4H). ^{13}C NMR (125 MHz, $CDCl_3$) δ 143.3, 128.5, 127.9, 126.8, 75.7, 57.3, 50.8, 30.2, 28.3, 25.4, 23.8, 21.3, 20.2,

18.8, 15.5, 14.5, -1.6. HRMS (ESI) calc. for $C_{21}H_{34}N_3O_2Si$ $[M+H]^+$ 388.2420, found 388.2417.

2.5.3. Approach to lactacystin

A. Initial Approach

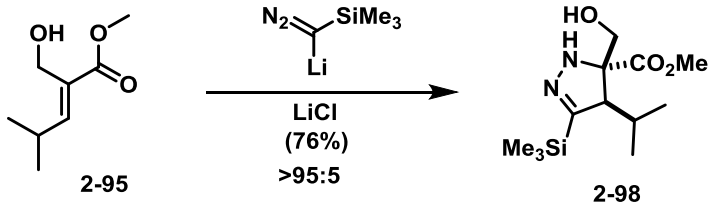

A solution of trimethylsilyldiazomethane (2 mmol) in 5 mL THF was treated with *n*-BuLi (2 mmol) at -78 °C and the reaction was stirred at -78 °C for 30 min, followed by the slow addtion of **2-95** and LiCl in 5 mL of THF. Then the reaction mixture was slowly warmed up to 0 °C over 1 h and quenched with 0.5 mL of saturated aqueous NH_4Cl and was dried over $MgSO_4$, filtered and concentrated in vacuum to afford crude **2-98**, which was purified by column chromatography to give pure **2-98** (76 %). 4.14 (d, 1H, J=10.7Hz), 3.96 (d, 1H, J=10.7Hz), 3.74 (s, 3H), 3.25 (d, 1H, J=2.3Hz), 1.98 (m, 1H), 1.03 (d, 3H, J=7.1Hz), 0.94 (d, 3H, J=6.9Hz), 0.20 (s, 9H). ^{13}C NMR (125 MHz; $CDCl_3$): δ 175.7, 162.2, 74.8, 63.1, 61.8, 52.8, 27.1, 22.2, 19.1, -1.1.

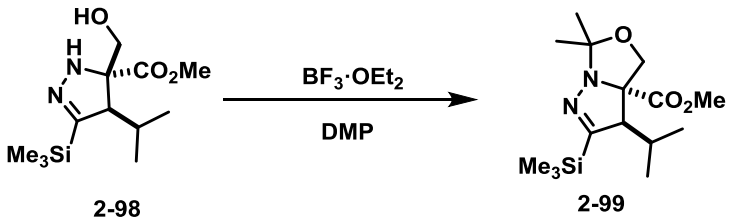

A solution of 2,2-dimethoxypropane (8 mmol) and **2-98** (1 mmol) in 5 mL acetone was treated with BF_3 etherate (0.1 mmol) at 0 °C and the solution was allowed to warm to room temperature until the TLC indicated the full consumption of the starting material. The mixture was quenched with 5 drops Et_3N and extracted into ether. The combined organic extract was washed with $NaHCO_3$, dried over $MgSO_4$, filtered

and concentrated in vacuum to afford crude **2-99**, which was pure enough to carry on to the next step. ^{1}H NMR (500 MHz, $CDCl_3$) δ 3.80 (d, 1H, J=22.0Hz) ppm 3.75 (s, 3H) ppm 3.27 (d, 1H, J=18.2Hz) ppm 3.03 (d, 1H, J=9.7Hz) ppm 2.80 (d, 1H, J=18.2Hz) ppm 1.71 (m, 1H) ppm 1.66 (s, 3H) ppm 1.32 (s, 3H) ppm 1.00 (d, 3H, J=6.4Hz) ppm 0.91 (d, 3H, J=6.6Hz) ppm 0.18 (s, 1H). ^{13}C NMR (125 MHz; $CDCl_3$): δ 173.2, 161.0, 98.1, 86.6, 78.0, 52.7, 45.9, 30.0, 29.1, 24.0, 21.2, 19.1, -1.8.

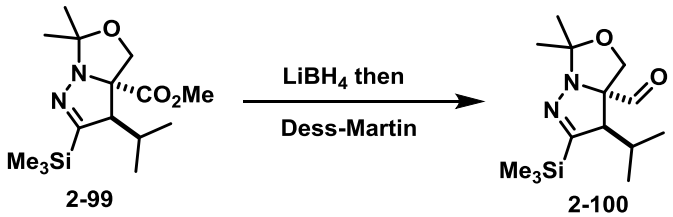

A solution of **2-99** (1 mmol) in 4 mL THF:MeOH (3:1) was treated with $LiBH_4$ (5 mmol); the reaction was followed by TLC and then quenched with NH_4Cl(sat) and extracted with EtOAc. The solvent was removed and the crude material was used directly in the oxidation reaction. Crude alcohol was dissolved in CH_2Cl_2 and $NaHCO_3$ (3 mmol) was added. The Dess-Martin reagent (1.3 mmol) was added and the reaction was followed by TLC. The reaction mixture was diluted with ether and then filtered. The filtrate was dried over $MgSO_4$, filtered and concentrated in vacuum to afford crude **2-100**, which was purified by column chromatography to give the pure **2-100** ^{1}H NMR (500 MHz; $CDCl_3$): δ 9.56 (s, 1H) ppm 4.36 (d, 1H, J=8.8Hz) ppm 3.70 (d, 1H, J=8.7Hz) ppm 3.23 (d, 1H, J=8.0Hz) ppm 2.09 (dt, 1H, J=6.8Hz, J=13.7Hz) ppm 1.58 (s, 3H) ppm 1.25 (s, 3H) ppm 1.10 (d, 3H, J=6.6Hz) ppm 0.82 (d, 3H, J=6.9Hz) ppm 0.26 (s, 1H)^{13}C NMR (125 MHz; $CDCl_3$): δ 200.11, 99.12, 83.73, 64.72, 61.32, 28.16, 27.79, 24.61, 24.05, 22.15, -0.31.

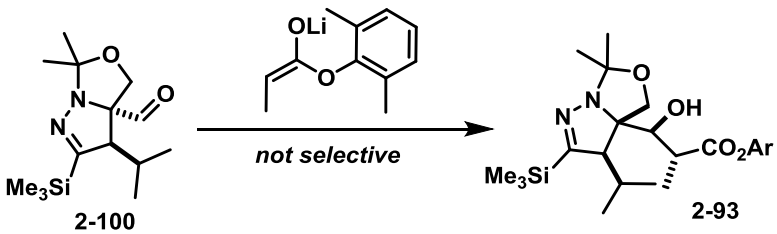

A solution of DIPA (1.5 mmol) in 5 mL THF is treated with *n*-BuLi (1.5 mmol) at 0 °C, and the solution is stirred for 45 minutes. After cooling to -78 °C, a solution of aldehyde 2-100 (1 mmol) in 3 mL THF is added, and it was fully consumed over 30 minutes. The solution was quenched with NH_4Cl (sat. aq.) and extracted into EtOAc. After removal of solvent, crude NMR showed a 1:1:1.5 mixture of 3 distinguishable diastereomers. Isomer A: ^{1}H NMR (500 MHz; $CDCl_3$): δ 7.06 (s, 3H) ppm 4.16 (d, 1H, J=10.1Hz) ppm 3.96 (d, 1H, J=10.0Hz) ppm 3.81 (m, 1H) ppm 3.18 (d, 1H, J=4.5Hz) ppm 3.12 (d, 1H, J=2.7Hz) ppm 2.86 (m, 1H, J=7.0Hz) ppm 2.16 (s, 6H) ppm 1.52 (s, 3H) ppm 1.47 (d, 3H, J=7.1Hz) ppm 1.44 (s, 3H) ppm 1.08 (d, 3H, J=7.2Hz) ppm 1.03 (d, 3H, J=7.0Hz) ppm 0.27 (s, 9H). ^{13}C NMR (125 MHz; $CDCl_3$): δ 173.71, 165.15, 147.93, 130.12, 128.66, 128.54, 125.97, 97.39, 78.85, 77.75, 66.75, 61.86, 42.92, 29.34, 27.03, 24.12, 21.67, 20.01, 17.17, 16.48, -0.41. Isomer B: ^{1}H NMR (500 MHz; $CDCl_3$): δ 7.04 (s, 3H) ppm 4.09 (d, 1H, J=10.1Hz) ppm 3.93 (dd, 1H, J=2.1Hz, J=9.0Hz) ppm 3.82 (d, 1H, J=10.0Hz) ppm 3.15 (d, 1H, J=2.1Hz) ppm 2.98 (d, 1H, J=2.1Hz) ppm 2.87 (m, 1H) ppm 2.19 (s, 6H) ppm 1.49 (d, 6H, J=5.1Hz) ppm 1.37 (d, 3H, J=7.1Hz) ppm 1.18 (d, 3H, J=7.3Hz) ppm 1.02 (d, 3H, J=7.1Hz) ppm 0.26 (s, 9H). ^{13}C NMR (125 MHz; $CDCl_3$): δ 172.56, 165.42, 147.93, 130.48, 128.59, 125.84, 97.14, 79.56, 79.07, 65.94, 60.74, 42.47, 29.14, 26.33, 24.31, 22.18, 19.51, 16.42, 15.18, -0.33. Isomer C: ^{1}H NMR (500 MHz; $CDCl_3$): δ 7.04 (s, 3H) ppm 4.09 (d, 1H, J=10.0Hz) ppm 3.93 (dd, 1H, J=1.8Hz, J=9.0Hz) ppm 3.82 (d, 1H, J=10.0Hz) ppm 3.15 (d, 1H, J=1.9Hz) ppm 2.98 (d, 1H, J=1.8Hz) ppm 2.87 (m, 1H) ppm 2.19 (s, 6H) ppm 1.49 (d, 6H, J=5.0Hz) ppm 1.37 (d, 3H, J=7.0Hz) ppm 1.18 (d, 3H, J=7.2Hz) ppm 1.02 (d, 3H, J=7.0Hz) ppm 0.26 (s, 9H). ^{13}C NMR (125 MHz; $CDCl_3$): δ 172.57, 165.43, 147.92, 130.48, 128.59, 125.84, 97.14, 79.56, 79.07, 65.94, 60.74, 42.47, 29.14, 26.33, 24.31, 22.17, 19.51, 16.41, 15.18, -0.33.

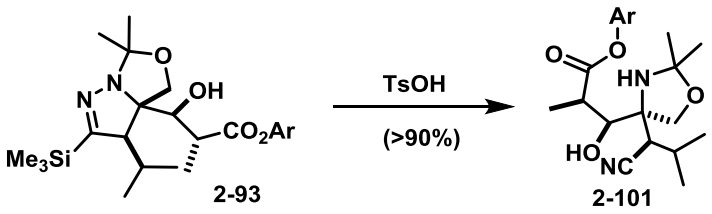

A solution of **2-93** (0.5 mmol) was dissolved in 5 mL EtOH and *p*-TsOH was added. The solution was heated at reflux until NMR showed full consumption of the starting material. The solvent was removed, and the mixture was partitioned between aq. K_2CO_3 and DCM. The mixture was extracted with DCM (3x5 mL) and organic layers dried and filtered. After removal of the solvent, the crude oil **2-101** was purified using column chromatography. ^{1}H NMR (500 MHz, $CDCl_3$) δ 7.05 (s, 3H) ppm 4.25 (d, 1H, J=10.6Hz) ppm 4.03 (d, 1H, J=11.3Hz) ppm 3.89 (d, 1H, J=11.3Hz) ppm 3.10 (qd, 1H, J=6.7Hz, J=10.7Hz) ppm 2.93 (d, 1H, J=2.3Hz) ppm 2.66 (dtd, 1H, J=2.2Hz, J=6.8Hz, J=13.7Hz) ppm 2.19 (s, 6H) ppm 1.59 (d, 3H, J=6.7Hz) ppm 1.36 (s, 3H) ppm 1.31 (s, 3H) ppm 1.15 (d, 3H, J=7.0Hz) ppm 1.07 (d, 3H, J=6.7Hz). ^{13}C NMR (125 MHz; $CDCl_3$): δ 171.97, 148.02, 130.43, 128.59, 125.86, 118.97, 91.93, 79.50, 67.57, 60.58, 40.50, 39.52, 30.03, 27.81, 26.26, 23.03, 19.29, 16.44, 14.76.

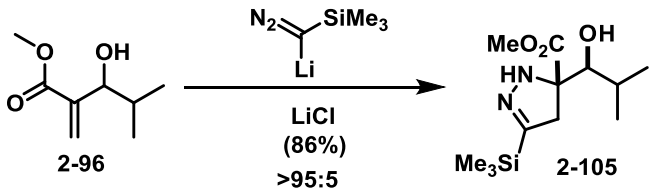

A solution of trimethylsilyldiazomethane (2 mmol) in 5 mL THF was treated with *n*-BuLi (2 mmol) at -78 °C and the reaction was stirred at -78 °C for 30 min, followed by the slow addtion of **2-96** and LiCl in 5 mL of THF. Then the reaction mixture was slowly warmed up to 0 °C over 1 h and quenched with 0.5 mL of saturated aqueous NH_4Cl and was dried over $MgSO_4$, filtered and concentrated in vacuum to afford crude **2-105** (86 %), which was pure enough to use in the following step without purification. ^{1}H NMR (500 MHz, $CDCl_3$) δ 6.54 (s, 1H) ppm 4.77 (bs, 1H) ppm 3.76 (s, 3H) ppm 3.67 (dd, 1H, J=2.8Hz, J=11.1Hz) ppm 3.17 (q, 2H, J=17.8Hz) ppm 2.27 (d, 1H, J=11.2Hz) ppm 1.54 (m, 1H) ppm 0.98 (d, 3H, J=6.8Hz) ppm 0.84 (d, 3H, J=6.7Hz) ppm 0.18 (s, 9H). ^{13}C NMR (125 MHz, $CDCl_3$) δ 175.19, 161.44, 76.60, 74.08, 53.11, 48.54, 31.97, 21.56, 16.19, -1.91.

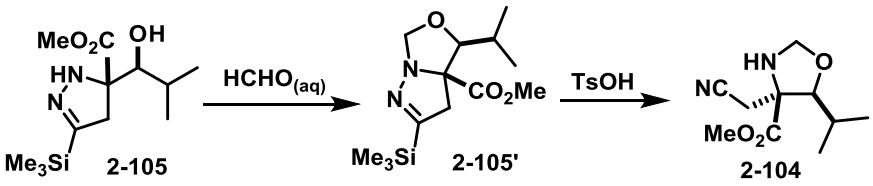

A solution of **2-105** (1 mmol) in THF was treated with aqueous HCHO (1 mmol), and the solution was stirred for 30 minutes. One gram of silica gel was then added, and the solvent removed under reduced pressure. The solid residue was then purified on SiO_2 to yield **2-105'**. ^{1}H NMR (500 MHz, $CDCl_3$) δ 5.16 (d, 1H, J=5.6Hz) ppm 5.05 (d, 1H, J=5.6Hz) ppm 3.75 (s, 3H) ppm 3.29 (d, 1H, J=17.6Hz) ppm 3.01 (d, 1H, J=9.7Hz) ppm 2.91 (d, 1H, J=17.6Hz) ppm 1.67 (tdd, 1H, J=6.6Hz, J=9.9Hz, J=13.1Hz) ppm 1.02 (d, 3H, J=6.5Hz) ppm 0.87 (d, 3H, J=6.6Hz) ppm 0.18 (s, 9H). ^{13}C NMR (125 MHz, $CDCl_3$) δ 170.90, 162.30, 87.05, 86.72, 77.50, 52.38, 45.97, 30.10, 21.04, 18.49, -2.42. Compound **105'** (1 mmol) was dissolved in DCM (5 mL), and *p*-TsOH was added. The solution was then refluxed for 1 hour, cooled to room temperature and then quenched with $NaHCO_3$ (sat. aq.). The solution is extracted with DCM (3x5 mL), organic layers dried and filtered. After removing the solvent, compound **2-105** was sufficiently pure to use in the next step. ^{1}H NMR (500 MHz, $CDCl_3$) δ 6.78 (s, 1H) ppm 5.04 (s, 2H) ppm 3.75 (s, 3H) ppm 3.32 (dd, 1H, J=1.0Hz, J=18.0Hz) ppm 3.15 (d, 1H, J=9.8Hz) ppm 2.88 (dd, 1H, J=1.6Hz, J=18.0Hz) ppm 1.66 (sext.t, 1H, J=6.6Hz, J=13.1Hz) ppm 1.00 (d, 3H, J=6.5Hz) ppm 0.86 (d, 3H, J=6.7Hz). ^{13}C NMR (125 MHz, $CDCl_3$) δ 170.48, 144.96, 87.16, 86.70, 77.43, 52.47, 41.75, 30.07, 20.99, 18.40.

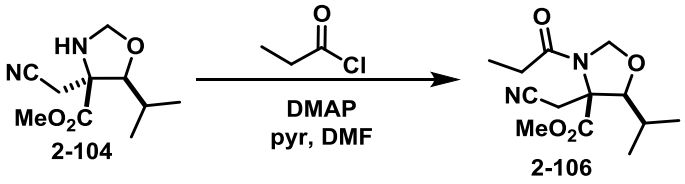

A solution of 2-104 (1 mmol) in DMF was sequentially treated with pyridine, DMAP, and propionyl chloride. The solution is heated at 80 °C and followed by TLC. When complete, the reaction is cooled to room temperature, diluted with water and the aqueous solution extracted with EtOAc. Then the organic layer was separated and the aqueous layer was extracted with CH_2Cl_2 (3 x 5 mL). The combined organic

extract was dried over $MgSO_4$, filtered and concentrated in vacuum to afford crude **2-106**, which was purified by column chromatography. ^{1}H NMR (500 MHz, $CDCl_3$) δ 5.24 (d, 1H, J=3.6Hz) ppm 5.01 (d, 1H, J=3.6Hz) ppm 3.91 (d, 1H, J=17.6Hz) ppm 3.87 (d, 1H, J=9.4Hz) ppm 3.74 (s, 3H) ppm 2.99 (d, 1H, J=17.6Hz) ppm 2.27 (m, 2H) ppm 1.73 (m, 1H) ppm 1.16 (t, 3H, J=7.4Hz) ppm 1.07 (d, 3H, J=6.5Hz) ppm 1.01 (d, 3H, J=6.7Hz). ^{13}C NMR (125 MHz, $CDCl_3$) δ 171.10, 169.09, 116.77, 89.71, 78.90, 66.15, 52.97, 29.36, 28.31, 22.75, 20.16, 18.64, 8.46

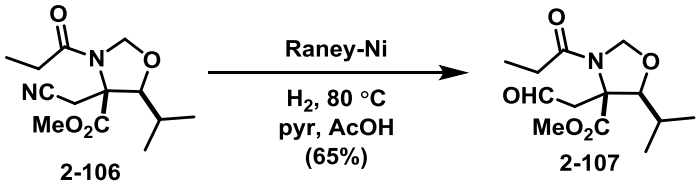

2-106 2-107

A solution of **2-106** (1 mmol) in pyridine:AcOH:H_2O (8 mL, 2:1:1) is heated at 80 °C under an atmosphere of H_2 (bubbling) overnight in the presence of Raney-Ni slurry (50%, in H_2O, 1.5 mL). After cooling, the solution is diluted with EtOAc, filtered and absorbed onto SiO_2. The solids are purified using 3:1 Hex:EtOAc to yield **2-107**. ^{1}H NMR (500 MHz, $CDCl_3$) δ 9.72 (d, 1H, J=1.5Hz) ppm 5.22 (d, 1H, J=3.2Hz) ppm 5.03 (d, 1H, J=3.4Hz) ppm 3.80 (d, 1H, J=17.5Hz) ppm 3.75 (s, 3H) ppm 2.88 (dd, 1H, J=2.1Hz, J=17.5Hz) ppm 2.19 (m, 2H) ppm 1.70 (m, 1H) ppm 1.11 (t, 3H, J=7.4Hz) ppm 1.02 (d, 3H, J=6.5Hz) ppm 0.99 (d, 3H, J=6.7Hz)^{13}C NMR (125 MHz, $CDCl_3$) δ 198.84, 109.99, 90.03, 78.54, 52.64, 46.06, 29.69, 29.40, 28.16, 20.12, 19.14.

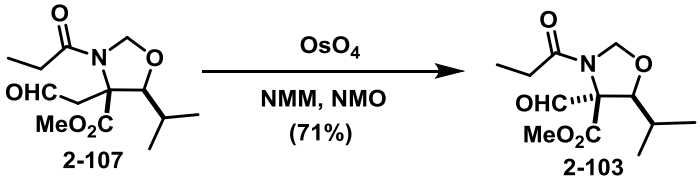

2-107 2-103

A solution of **2-107** (1 mmol) in 11 mL acetone:H_2O (10:1) was treated sequentially with NMO (2 mmol), NMM (1 mmol) and OsO_4 solution (10 μL, 1g/20 mL). The reaction mixture was stirred at room temperature for 96 h and then diluted with acetone and filtered. Absorption onto SiO_2 and purification lead

to 2-103 in 62% yield. ^{1}H NMR (500 MHz, $CDCl_3$) δ 10.14 (s, 1H) ppm 5.20 (d, 1H, J=2.7Hz) ppm 5.07 (d, 1H, J=2.7Hz) ppm 3.82 (s, 3H) ppm 3.79 (d, 1H, J=10.1Hz) ppm 2.21 (m, 2H) ppm 1.66 (tdd, 1H, J=6.6Hz, J=10.3Hz, J=13.1Hz) ppm 1.12 (t, 3H, J=7.4Hz) ppm 1.02 (d, 2H, J=6.5Hz) ppm 0.87 (d, 2H, J=6.6Hz). ^{13}C NMR (125 MHz, $CDCl_3$) δ 194.76, 91.90, 78.86, 73.01, 52.92, 28.96, 27.10, 19.39, 18.65, 8.22.

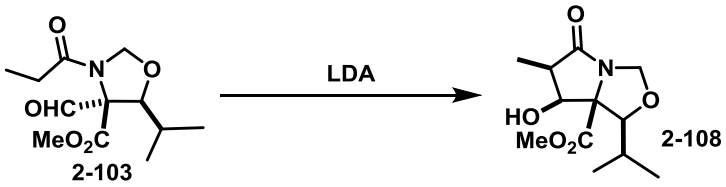

A solution of **2-103** (22 mg, 0.0855 mmol) in 1 mL THF was added dropwise to a solution of LDA (0.1 mmol) in THF (2 mL) at -78 °C. The starting material was consumed over 2 hours at this temperature and then quenched with saturated ammonium chloride solution (0.1 mL). The volatiles were removed, and the mixture was purified to yield compound **2-108** (ca 1 mg, ~5% yield) along with an aldehyde decomposition product. ^{1}H NMR (500 MHz, $CDCl_3$) δ 5.23 (d, 1H, J=4.0Hz) ppm 4.91 (d, 1H, J=4.2Hz) ppm 4.32 (d, 1H, J=9.4Hz) ppm 3.70 (s, 3H) ppm 3.36 (d, 1H, J=11.3Hz) ppm 2.80 (d, 1H, J=13.1Hz) ppm 2.23 (s, 3H) ppm 1.38 (d, 3H, J=6.5Hz) ppm 1.34 (d, 3H, J=6.3Hz) ppm 1.02 (d, 3H, J=6.4Hz) ppm 0.97 (d, 3H, J=6.6Hz). HRMS (ESI) calc. for $C_{12}H_{20}NO_5$ $[M+H]^+$ 258.1341, found 258.1342.

2.5.4. ORTEPS

ORTEP of 2-73g

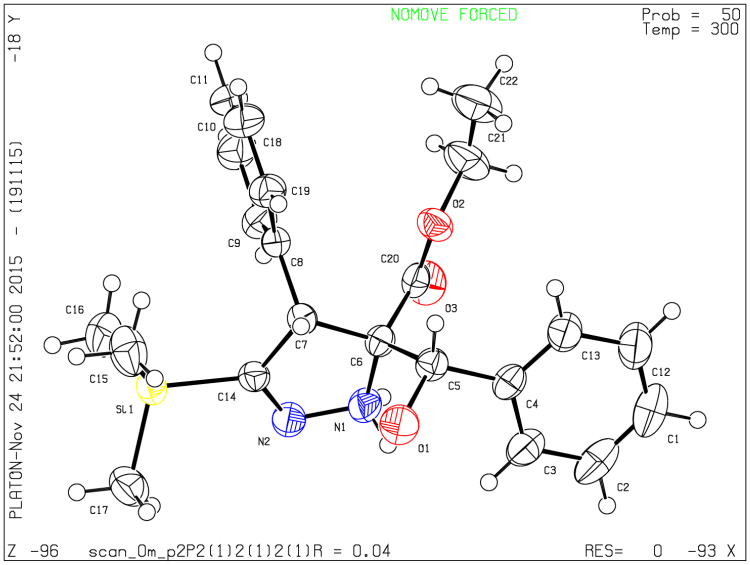

ORTEP of 2-76g

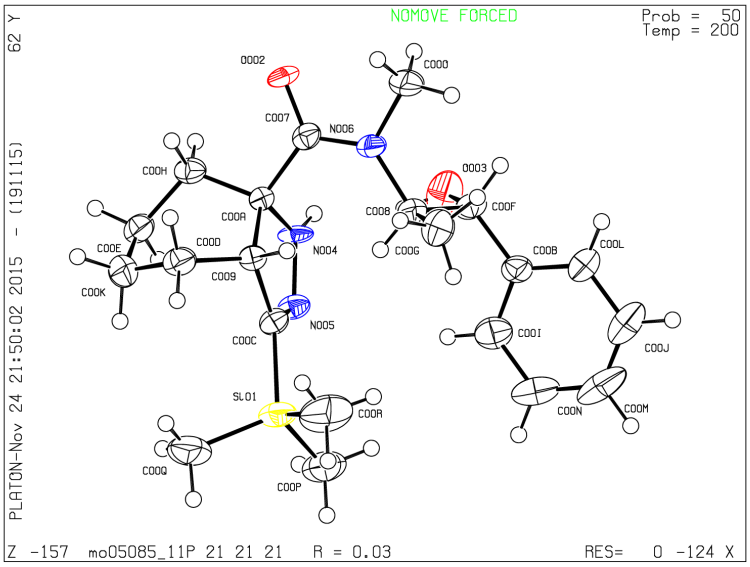

2.6. References

[1] Hoffmann, R. W. *Chem. Rev.* **1989**, *89*, 1841.

[2] Winterfeldt, E. *Prinzipien und Methoden der Stereoselektiuen Synthese;* F. Vieweg & Sohn: Verlagsgesellschaft/ Braunschwe', **1988**, 1.

[3] Johnson, F. *Chem. Rev.* **1968**, *68*, 375.

[4] a) Broeker, J. L.; Hoffmann, R. W.; Houk, K. N. *J. Am. Chem. Soc.* **1991**, *113*, 5006; b) Petterson, I.; Gundertofte, K. *J. Comput. Chem.* **1991**, *12*, 839; c) Wiberg, K. B.; Martin, E. *J. Am. Chem. Soc.* **1985**, *107*, 5035.

[5] a) Gung, B. W.; Melnick, J. P.; Wolf, M. A.; King, A. *J. Org. Chem.* **1995**, *60*, 1947; b) Gung, B. W.; Wolf, M. A.; *J. Org. Chem.* **1993**, *58*, 7038; c) Gung, B. W.; Wolf, M. A.; Zhu, Z. *J. Org. Chem.* **1993**, *58*, 3350; d) Kahn, S. D.; Pau, C. F.; Chamberlain, A. R.; Hehre, W. J. *J. Am.Chem. Soc.* **1987**, *109*, 650.

[6] Houk, K. N.; Moses, S. R.; Wu, Y. D.; Rondan, N. G.; Jager, V.; Schohe, R.; Fronczek, F. R. *J. Am. Chem. Soc.* **1984**, *106*, 3880.

[7] a) Caramella, P.; Cellerino, G. *Tetrahedron Lett.* **1974,** 229. b) McAlduff, E. J.; Caramella, J.; Houk, K. N. *J. Am. Chem. Soc.* **1978**, *100*, 105. c) Bianchi, G.; De Micheli, C.; Gamba, A.; Gandolfi, R. *J. Chem. Soc., Perkin Trans.1* **1974**, 137. d) De Micheli, D.; Gamba Invernizzi, A.; Gandolfi, R.; Scevola, L. *J. Chem. Soc., Chem. Commun.* **1976**, 246.

[8] Jäger, V.; Schohe, R.; Paulus, E. F. *Tetrahedron Lett.* **1983**, *24***,** 5501.

[9] Curran, D.; Choi, S.M.; Hothe, S.A.; Lin, F.T. *J. Org. Chem.* **1990**, *55*, 3710.

[10] Annunziata, R.; Benaglia, M.; Cinquini, M.; Cozzi, F.; Raimondi, L. *J. Org. Chem.* **1995**, *60*, 4697.

[11] Kanemasa, S.; Nishiuchi, M.; Kamimura, A.; Hori, K. *J. Am. Chem. Soc.* **1994**, *116*, 2324.

[12] Micheli, C.; Gamba-Invernizzi, A.; Gandolfi, R. *Tetrahedron Lett.* **1975**, 2493; b) Micheli, C.; Gamba-Invernizzi, A.; Gandolfi, R.; Scevola, L. *J. Chem Soc. Chem. Comm.* **1976**, 246.

[13] Annunziata, R.; Cinquini, M.; Cozzi, F.; Giaroni, P.; Raimondi, L. *Tetrahedron Lett.* **1991**, *32*, 1659.

[14] Kanemasa, S.; Tsuruoka, T.; Wada, E. *Tetrahedron Lett.* **1993**, *34*, 87.

[15] Kanemasa, S.; Tsuruoka, T.; Yamamoto, H. *Tetrahedron Lett.* **1995**.

[16] Kanemasa, S.; Tsuruoka, T. *Chem. Lett.* **1995**, 49.

[17] Busque, F.; de March, P.; Figueredo, M.; Font, J.; Monsalvatje, M.; Virgili, A.; Alvarez-Larena, A.; Piniella, J. F. *J. Org. Chem.* **1996**, *61*, 8578.

[18] Hanselmann, R.; Zhou, J. ; Ma, P.; Confalone, P. N. *J. Org. Chem.* **2003**, *68*, 8739.

[19] Merino, P.; Tejero, T.; Laguna, M.; Cerrada, E.; Moreno, A.; Lopez, J. A. *Org. Biomol. Chem.* **2003**, *1*, 2336.

[20] Karanjule, N. S.; Markad, S. D.; Sharma, T.; Sabharwal, S. G.; Puranik, V. G.; Dhavale, D. D. *J. Org. Chem.* **2005**, *70*, 1356.

[21] a) Franck-Neumann, M. *Angew. Chem., Int. Ed.* **1969**, *8*, 210; b) Franck-Neumann, M. *Tetrahedron Lett.* **1962**, 2979.

[22] Myers, A.; Yang, B. H.; Chen, H.; Gleason, J. L. *J. Am. Chem. Soc.* **1994**, *116*, 9361.

[23] Myers, A. G.; Gleason, J. L.; Yoon, T.; Kung, D. W. *J. Am. Chem. Soc.* **1997**, *119*, 656.

[24] Myers, A. G.; Yang, B. H.; Chen, H.; McKinstry, L.; Kopecky, D. J.; Gleason, J. L. *J. Am. Chem. Soc.* **1997**, *119*, 6496.

[25] a) Evans, D. A.; Takacs, J. M. *Tetrahedron Lett*. **1980**, *21*, 4233. b) Sonnet, P.; Heath, R. R. *J. Org. Chem*. **1980**, *45*, 3137.

[26] Myers, A. G.; Barbay, J. K.; Zhong, B. J. *J. Am. Chem. Soc.* **2001**, *123*, 7207.

[27] Smitrovich, J. H.; Boice, G. N. ; Qu, C.; DiMichele, L.; Nelson, T. D.; Huffman, M. A.; Murry, J.; McNamara, J.; Reider, P. J. *Org. Lett.* **2002**, *4*, 1963.

[28] Etxebarria, J. ; Vicario, J. L.; Badia, D. ; Carrillo, L. *J. Org. Chem.* **2004**, *69*, 2588.

[29] Reyes, E.; Vicario, J. L. ; Carrillo, L.; Badia, D.; Iza, A.; Uria, U. *Org. Lett.* **2006**, *8*, 2535.

[30] Krummer, D. A.; Chain, W. J.; Morales, M. R.; Quiroga, O.; Myers. A. G. *J. Am. Chem. Soc.* **2008**, *130*, 13231.

[31] a) Seebach, D. *Angew. Chem., Int. Ed. Engl.* **1988**, *27*, 1624. b) Seebach, D.; Bossler, H.; Grundler, H. ; Shoda, S. I. *Helv Chim.Acta* **1991**, *74*, 197. c) Miller, S. A.; Griffiths, S. L. ; Seebach, D. *Helv. Chim. Acta* **1993**, *76*, 563. d) Bossler, H. G.; Seebach, D. *Helv. Chim. Acta* **1994**, *77*, 1124.

[32] a) Davies, S. G. ; Walters, I. A. S. *J. Chem. Soc., Perkin Trans. 1* **1994**, 1129. b) Asao, N.; Uyehara, T. ; Yamamoto, Y. *Tetrahedron* **1990**, *46*, 4563. c) Nicholas, E.; Russell K. C. ; Hruby, V. J. *J. Org. Chem.*, **1993**, *58*, 766; Lou, B-S.; Li, G. ; Lung F-D. ; Hruby, V. J. *J. Org. Chem.*, **1995**, *60*, 5509. d) Williams, D. R. ; Kissel, W. S.; Li, J. J. *Tetrahedron Lett.*, **1998**, *39*, 8593.

[33] a) Etxebarria, J. ; Vicario, J. L.; Badia, D. ; Carrillo, L. ; Ruiz, N. *J. Org. Chem.* **2005**, *70*, 8790. b) Myers, A. G.; McKinstry, L .*J. Org. Chem.* **1996**, *61*, 2428.

[34] Davies, S. G. ; Hermann, G. J.; Sweet, M. J.; Smith, A. D. *Chem. Comm.* **2004**, 1128.

[35] The stereodirecting power of the lithium alkoxide in other reactions of amides derived from chiral amino alcohols has also been invoked by other authors to account for the observed diastereoselectivity. See, for example: Askin, D.; Volante, R. P.; Ryan, K. M.; Reamer, R. A. ; Shinkai, I. *Tetrahedron Lett.* **1988**, *29*, 4245. b) Vicario, J.; Badıa, L.; Carrillo, D. L. *J. Org. Chem.* **2001**, *66*, 5801.

[36] Mukaiyama, T.; Iwasawa, N. *Chem. Lett.* **1981**, 913.

[37] Omura, S.; Fujimoto, T. ; Otoguro, K. ; Matsuzaki, K.; Moriguchi, R.; Tanaka, H.; Sasaki, Y. *J. Antibiot.* **1991**, *44*, 113.

[38] Corey, E. J. ; Reichard, G. A. *J. Am. Chem. Soc*. **1992**, *114*, 10677.

[39] Pirrung, M. C.;Heathcock, C. H. *J. Org. Chem.* **1980**. *45*, 1727-1728.

[40] Wardrop, D. J.; Bowen, E. G. *Chem. Commun*. **2005**, 5106.

[41] Nagamitsu, T.; Sunazuka, T.; Tanaka, H.; Omura, S.; Sprengeler, P. A.; Smith, A. B. *J. Am. Chem. Soc.*, **1996**, *118*, 3584.

[42] Charette, A. B.; Cote, B.; Monroc, S.; Prescott, S. *J. Org. Chem.* **1996**, *60*, 6888.

[43] Staskun, B.; van Es, T. *S. Afr. J. Chem.* **2008**, *61*, 144.

[44] Belotti, D.; Andreatta, G.; Pradaux, F.; BouzBouz, S.; Cossy, J. *Tetrahedron Lett.* **2003**, *44*, 3613.

CHAPTER III

SEQUENTIAL 1,4- AND 1,2-ADDITION OF TMSCLiN_2 ONTO α,β-UNSATURATED KETONES

3.1. Introduction*

Inventing synthetic methods that reduce time, cost and chemical waste is instrumental in developing a synthetically useful process. In this regard, tandem processes involve the execution of two or more chemical reactions in a single experimental protocol.[1] Some tandem processes include domino reactions, which occur without altering experimental conditions,[2] and sequential/consecutive reactions that which require additional energy or reactants.[3] One classic example of a tandem process is Robert Robinson's tropinone **3-1** synthesis in which this bicyclic alkaloid was synthesized in single flask (**Scheme 3.1**).[4] In this sequential reaction, succinaldehyde, methylamine and acetonedicarboxylic acid were simply mixed and allowed to sit overnight followed by acid treatment and heating to induce decarboxylation.

Scheme 3.1. Robinson's tropinone synthesis

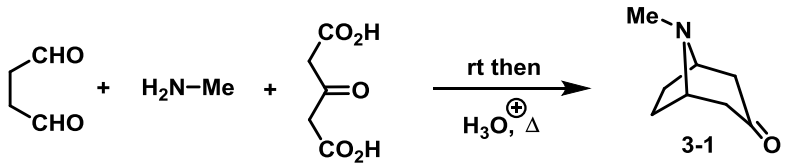

Nearly a century since Robinson's efficient and direct synthesis of tropinone, tandem reactions have developed into a broad field of organic chemistry, and one class of tandem reactions that allows access to complex and diverse molecular architectures in a rapid fashion is the nucleophilic addition/fragmentation reaction.

3.1.1. Nucleophilic addition/fragmentation reactions

The Dudley group has studied the tandem nucleophilic addition/fragmentation reaction extensively in their work with vinylogous acyl triflates (**Table 3.1**).[5] Triflate **3-2** was treated with various aryl Grignard reagents to inducing a tandem 1,2-addition/fragmentation producing aryl ketones containing an alkyne

*Reproduced, with permission from: O'Connor, M.; Sun, C.; Guan, X.; Sabbasani, V.; Lee, D. *Angew. Chem., Int. Ed.*, **2016**, *55*, 2222–2225.

Table 3.1. Reaction of vinylogous acyl triflate with Grignard reagents

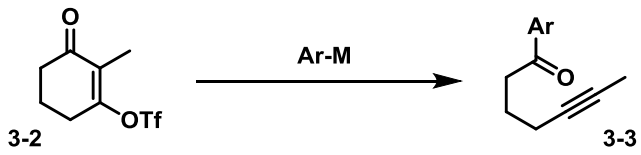

entry	Ar-M	conditions	yield (%)
1	PhMgBr	0 °C to rt	80
2	(*p*-MeO)C_6H_4MgBr	0 °C to rt	86
3	(*m*-MeO)C_6H_4MgBr	0 °C to rt	57
4	(*o*-MeO)C_6H_4MgBr	0 °C to rt	34
5	(*p*-Cl)C_6H_4MgBr	0 °C to 60 °C	61
6	(2-thienyl)MgBr	0 °C to 60 °C	63

tether **3-3**. Phenymagnesium bromide and electron donating and aryl nucleophiles work in the fragmentation reaction (entries 1-4, 34-80% yield). The lower yields in the can be attributed the sterically congested ortho-substituted Grignard reagents. Electron withdrawing *p*-chloro gives the cleavage product **3-3** although the reaction requires an increase in temperature (61 °C, entry 5). Finally, 2-thienylmagnesium bromide also produces the ynone **3-3** in moderate yield with an increase in temperature required (63%, 60 °C, entry 6). In the same report, Dudley extended the application of this cleavage process to generate a diverse array of functionalized products (**Scheme 3.2**).

Scheme 3.2. Utility of tandem fragmentation reaction

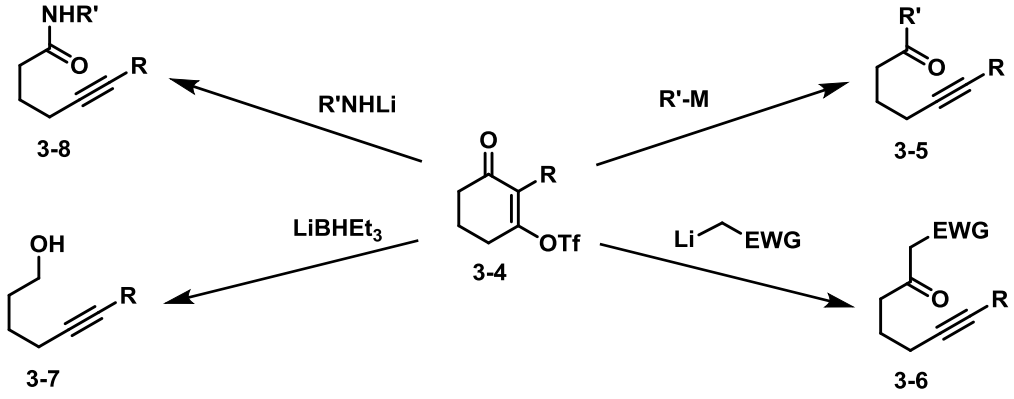

When lithium amides were used as the nucleophile with vinylogous acyl triflate **3-4**, secondary amides **3-8** were generated in the reaction (**Scheme 3.2**). Both alkyllithium and alkyl Grignard reagents were also effective in this protocol, and alkyl ketones **3-5** were generated in good yields (**Scheme 3.2**). In these cases, it was found that reagent and solvent purity was vital to obtaining satisfactory results. Lithium enolates and their analogs were also suitable nucleophiles which generated 1,3-diketone-type compounds with tethered alkynes **3-6** when reacted with triflate **3-4** (**Scheme 3.2**). Finally, it was demonstrated that reducing agents could be used in the reaction to generate alcohols **3-7** from triflate **3-4** (**Scheme 3.2**). In this reductive ring-opening strategy, Super-Hydride ($LiBHEt_3$) gave the primary alcohol **3-7** upon warming the reaction from -78 °C to 60 °C. The broad range of product classes generated in this tandem fragmentation reaction as well as the mild reaction conditions and ease of starting material synthesis make it an attractive process for synthetic chemists.

Scheme 3.3. Pathway for fragmentation

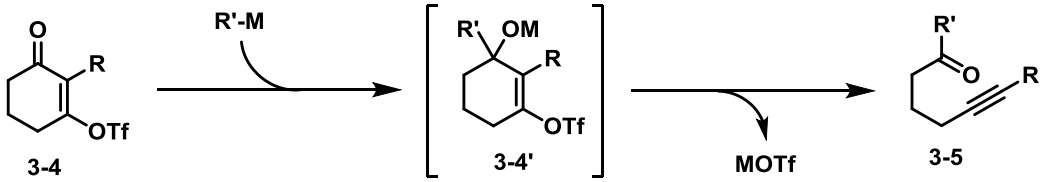

The mechanism of this reaction in explained in **Scheme 3.3**. The metal alkoxide **3-4′**, formed from 1,2-addition of the nucleophile to triflate **3-4**, collapses and subsequently induces C-C bond cleavage in a Grob-type[6] fragmentation process with expulsion of the triflate leaving group. In all cases, the ketone product containing tethered alkyne **3-5** was the major product form the reaction, and the only observed by-product was the cyclic alkene formed via 1,4-addition.

Shortly after, the Dudley group extended this methodology to dihydropyridone triflates **3-9** (**Table 3.2**).[7] In this methodology, it was found that *n*-Butyllithium was the optimal nucleophile, and when dihydropyridone triflates **3-9** were treated with this reagent at −78 °C and then warmed to room temperature, homopropargyl amides **3-10** were generated in good to excellent yields (**Table 3.2**). Various substitution

patterns on **3-9** were tolerated including R = alkyl and aryl (**Table 3.2**, enties 1-5). Dihydropyridones containing *N*-aryl substitution gave the best results, and electron donating or withdrawing groups led to the desired homopropargyl amides **3-10** in good yield (81-88%, entries 2-3). The mechanism for this transformation is analogous to that shown in **Scheme 3.3** in which collapse of the tetrahedral intermediate after initial 1,2-addition leads to cleavage and elimination of triflate producing the product **3-10**.

Table 3.2. Dihydropyridone triflate fragmentation

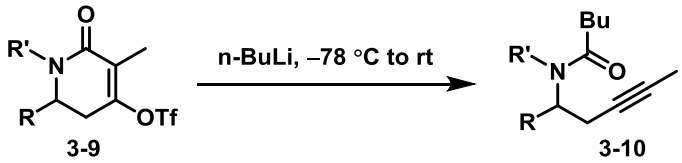

3-9 3-10

entry	R	R'	yield (%)
1	Me	Ph	97
2	Me	(*p*-MeO)C_6H_4	81
3	Me	(*p*-Cl)C_6H_4	88
4	*i*-Pr	Ph	80
5	Ph	Ph	77

3.1.2. Sequential reactions involving Grob-type fragmentations

The Charette group developed a tandem Grob fragmentation/nucleophilic trapping protocol utilizing Grignard reagents mediated by silver ion (**Table 3.3**).[8] In this study, enantiopure aza-bicyclo[2.2.2]octane **3-11** was exposed to silver ion generating dihydropyridinium salt which was subsequently trapped with Grignard reagents to generate 2,3,6-trisubstituted piperidines **3-12**. Alkyl Grignard reagents were tolerated in the reaction and generated the piperidine products **3-12** in moderate to good yields (55-88%, entries 1-3). The drop in yield for entry 3 can be attributed to the sterically congested isopropylmagnesium chloride nucleophile. Allyl-, vinyl- and phenylmagnesium salts also produced the tandem fragmentation/nucleophilic addition product in good yields (75-82%, entries 4-6). In all cases,

Table 3.3. Grob fragmentation with Grignard reagent trapping

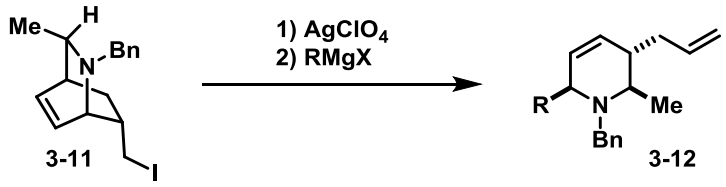

entry	R	X	yield (%)[a]
1	Me	Br	88
2	*n*-Pr	Br	88
3	*i*-Pr	Cl	55
4	allyl	Cl	77
5	vinyl	Br	75
6	Ph	Br	82

[a]dr >95:5

single diastereomers were formed in the reaction. The mechanism for this tandem fragmentation process is depicted in **Scheme 3.4**. For fragmentation, the required fixed antiperiplanar relationship of the nitrogen lone pair with the C(β)-C(γ) and C(α)-I bonds was confirmed by nOe, so proper orbital alignment was anticipated. Coordination of silver ion to the alkyl iodide moiety in **3-11** induces the fragmentation process through transition state **3.11′** generating dihydropyridinium salt **3-12′** which is subsequently trapped with the Grignard reagent producing 2,3,6-trisubstituted piperidine **3-12.**

Scheme 3.4. Grob fragmentation mechanism

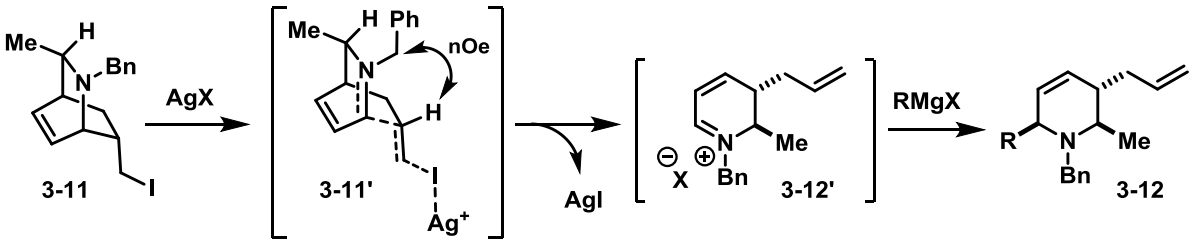

Shortly after, Prof. Charette extended the tandem Grob fragmentation/addition reaction to a triflic

anhydride activated process (**Scheme 3.5**).[9] In this superior synthetic process, the additional step of converting primary alcohol to primary alkyl iodide could be omitted in favor of the metal-free conversion. When aza-bicyclo[2.2.2]octane **3-13** was treated with triflic anhydride followed by triethylamine, dihydropyridinium salt of type **3-12′** (**Scheme 3.4**) is formed which is then trapped by the Grignard reagent. In all cases, good to excellent yields and diastereoselectivities were observed (77-99%, 6.3:1 to >95:5).

Scheme 3.5. Tandem Tf_2O-mediated Grob fragmentation

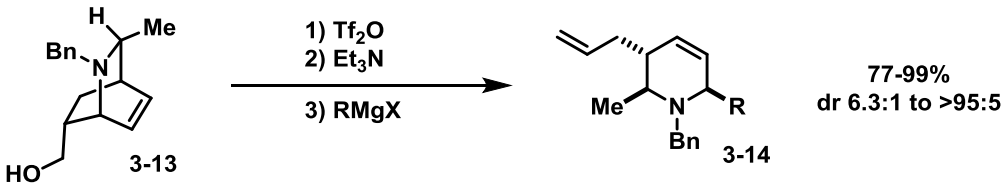

Charette and co-workers further demonstrated the utility of this tandem fragmentation process in a brief synthesis of the indolizidine alkaloids (−)-209I and (−)-209J (**Scheme 3.6**).[9] Starting from aza-bicyclo[2.2.2]octane **3-15**, the tandem Grob-fragmentation/Grignard addition process was achieved utilizing triflic anhydride and triethylamine to generate 2,3,6-trisubstituted piperidine **3-16**. The alkenes of **3-16** were hydrogenated utilizing Adam's catalyst and hydrogen gas followed by removal of the benzyl groups with Pearlman's catalyst in the presence of trifluoroacetic acid and hydrogen gas at 400 psi. Finally,

Scheme 3.6. Synthesis of (−)-209I and (−)-223J

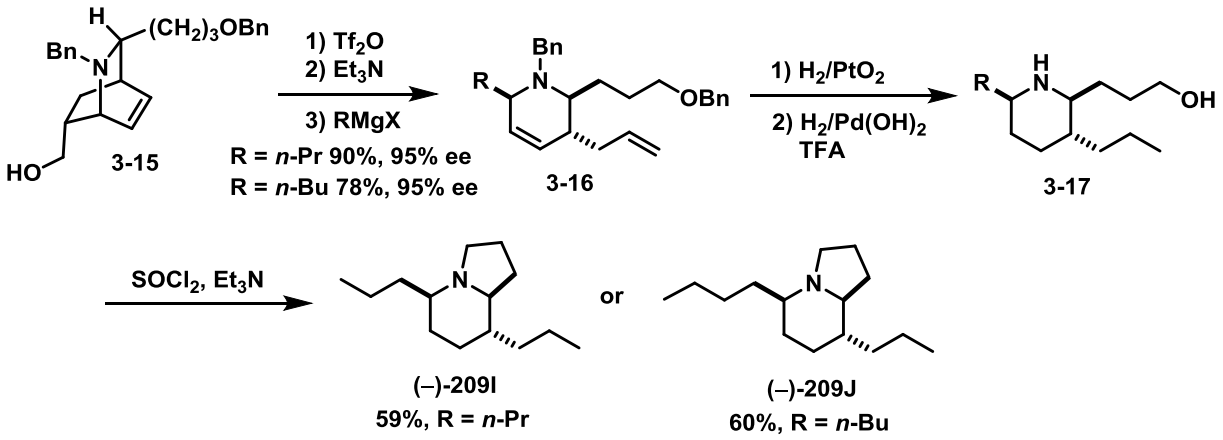

the primary alcohol was treated with thionyl chloride and triethylamine producing the natural products (−)-209I (R = *n*-Pr) and (−)-209J (R = *n*-Bu) in 59 and 60% yields respectively.

Charette and co-workers later disclosed a report on the synthesis of a variety of polysubstituted piperidines utilizing cuprates and other soft nucleophiles in the tandem Grob fragmentation sequence (**Scheme 3.7**).[10] Alkynyl piperidines of type **3-19** could be generated via triflic anhydride activation followed by subsequent cuprate addition followed by copper-catalyzed alkyne coupling in a "one-pot" sequential process. Cuprate addition followed by tetrahydropyridine reduction with sodium borohydride led to piperidines **3-20** which could be further elaborated to **3-22** via RCM of **3-12** through a sequence analogous to that shown in **Scheme 3.5**. Finally, in a tandem, sequential, one-pot procedure, octahydroisoquinolinone **3-21** could be synthesized. It was envisioned that the dihydropyridinium salt could function as a reactive dienophile in the Diels-Alder reaction with siloxy diene counter-partners, and indeed, when treated with 4-phenyl-2-trimethylsilylbutadiene, octahydroisoquinolinone **3-21** formed after subsequent reduction and acid treatment of the Diels-Alder adduct with $NaBH_3CN$/TFA.

Scheme 3.7. Polysubstituted piperidines via tandem Grob fragmentation sequence

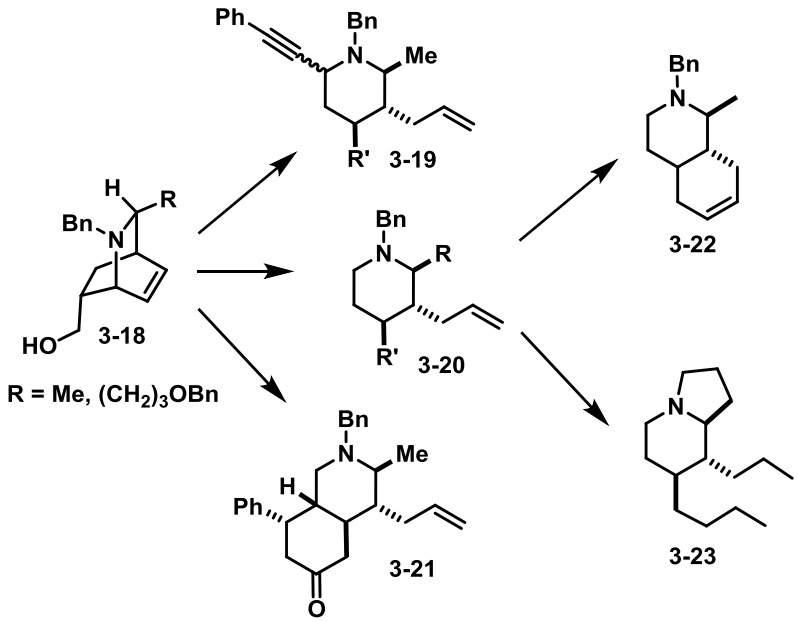

The Molander lab reported a tandem Barbier cyclization/Grob fragmentation in their synthesis of carbocycles (**Scheme 3.8**).[11] In this ring expansion strategy, keto mesylates bearing iodoalkyl, -allyl or benzyl side chains **3-24** were subjected to Barbier-type reductive conditions using samarium(II)iodide to yield medium-sized carbocycles **3-26** . After the initial reductive intramolecular coupling of **3-24**, the intermediated bicyclic metal alkoxide **3-25** underwent a Grob fragmentation via C-C bond cleavage and elimination of mesylate to generate the ring-expanded product **3-26**. In general, the reaction proceeded with moderate to excellent yields (42-92%) under mild conditions.

Scheme 3.8. Molander's tandem Barbier cyclization/Grob fragmentation

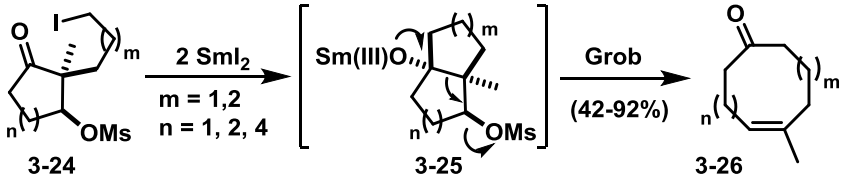

3.1.3. Other tandem fragmentation reactions

Prof. Matsubara recently reported a tandem 1,4-addition/acylation/fragmentation sequence (**Table 3.4**).[12] In this study, γ-acyloxy-α,β-unsaturated ketones **3-27** were converted to the corresponding 1,3-

Table 3.4. Tandem fragmentation reaction for 1,3-diketone formation

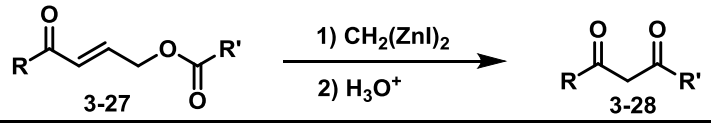

entry	R	R'	yield (%)
1	Ph	Me	91
2	Ph	*i*-Pr	91
3	2-napthyl	Me	91
4	$PhCH_2CH_2$	(*p*-MeO)C_6H_4	69
5	Me	(*p*-CF_3)C_6H_4	51

diketones in a bis(iodozincio)methane mediated process. Aryl enones generated the 1,3-diketones **3-27** in excellent yields (91%, entries 1-3); while alkyl enones produced the product in only moderate yields (51-69%, entries 4-5). Substitution at the acyloxy group was also investigated, and alkyl as well as aryl groups were well tolerated under the reaction conditions. A plausible reaction pathway is shown in **Scheme 3.9**; bis(iodozinco)methane adds to γ-acyloxy-α,β-unsaturated ketone **3-27** via 1,4-addition, and this is followed by attack of the zinc enolate **3-29** on the ester moiety in an intramolecular condensation reaction generating **3.30**. Finally, Grob-type fragmentation occurs leading to the enolate of the diketone **3-31** and zinc alkoxide of allyl alcohol. Protonation leads to the final products.

Scheme 3.9. Plausible pathway for fragmentation

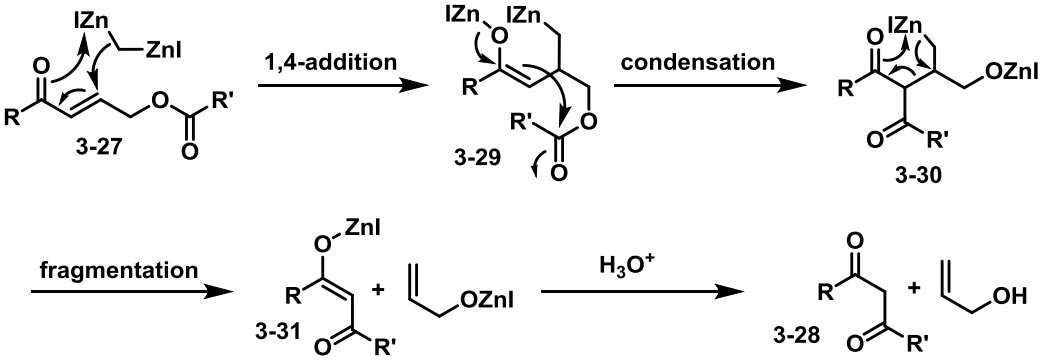

The alkylative fragmentation of tosylhydrazones was investigated by the group of Chandrasekhar (**Table 3.5**).[13] In their study, cyclic ethers containing tosylhydrazones at the α-position **3-32** were subjected to excess amounts of Grignard reagents which generated cleavage product **3-33** and addition product **3-34**. When phenylmagnesium bromide was used as the nucleophile, the fragmentation product **3-33** was formed as the sole product of the reaction in 59% yield (entry 1). When the Grignard reagent was changed to methylmagnesium iodide, formation of vinyl ether **3-34** was also detected as the minor product (entry 2, 3:1). When the more sterically demanding isopropylmagnesium bromide was used, the vinyl ether **3-34** became the major product of the reaction (entry 3). A plausible mechanism for formation of the products can be seen in **Scheme 3.10**.

Table 3.5. Alkylative fragmentation of tosylhydrazones of cyclic ethers

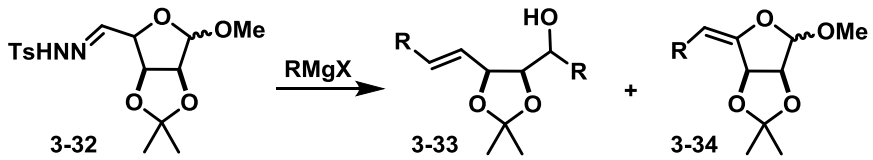

entry	R	X	3-33:3-34	yield (%)
1	Ph	Br	1:0	59
2	Me	I	3:1	86
3	*n*-Pr	Br	1:2	72

Initial deprotonation of the and nucleophilic attack of the Grignard reagent on the tosylhydrazone **3-32** leads to intermediate **3-35** of which elimination occurs leading to the addition product **3-34**. The fragmentation product **3-33** generates via Grob-type fragmentation of **3-35** which produces aldehyde **3-36**. Subsequent nucleophilic attack of the Grignard reagent on **3-36** leads to the final product **3-33**. The tandem ring-opening products **3-33** generated from fragmentation serve as useful building blocks for C-glycoside synthesis.

Scheme 3.10. Alkylative fragmentation of tosylhydrazones of cyclic ethers

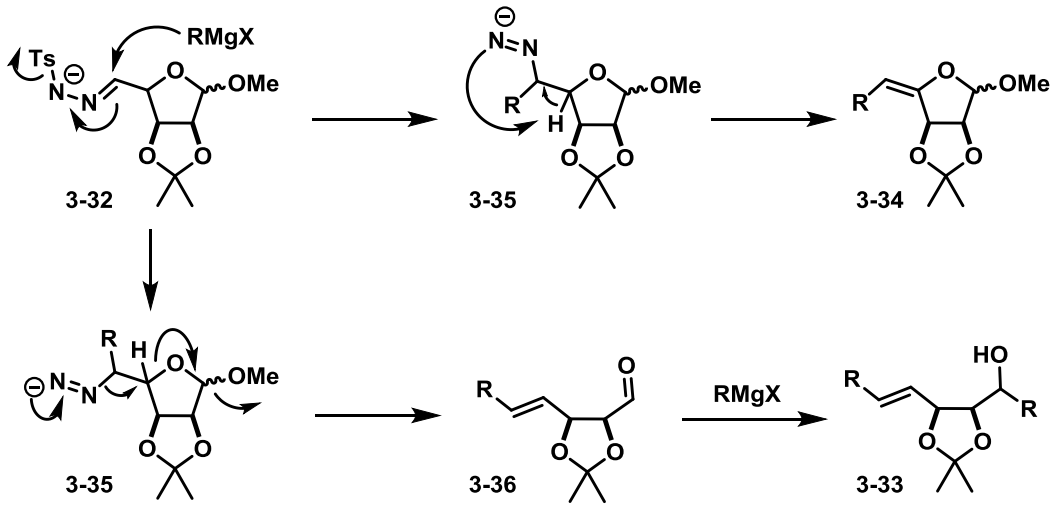

3.1.4. Tandem addition reactions involving enones/enals

Reactions involving two consecutive additions of strong nucleophiles to α,β-unsaturated ketones (enones) are rare. This is because the first reaction in 1,2-addition or 1,4-addition mode would convert the electrophilic nature of the starting enone to the corresponding alkoxide or enolate, respectively. For consecutive double additions to be feasible, the first addition must occur in 1,4- fashion, and the resulting 1,4-adduct should exist in its keto-, non-enolate, form (**Scheme 3.11**). However, under typical reaction conditions, in situ conversion of the enolate to the corresponding keto-form is not feasible due to the incompatibility of typical electrophiles with strong nucleophiles.

Scheme 3.11. Tandem 1,4/1,2-addition to α,β-unsaturated enones

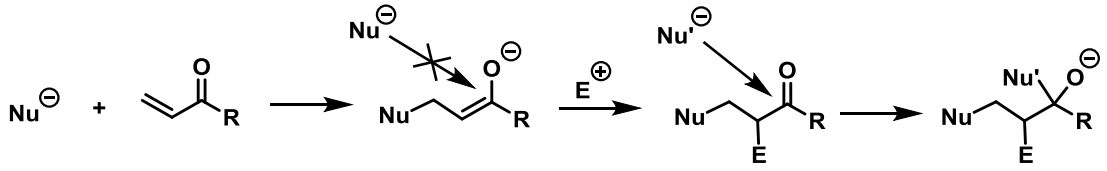

To overcome this inherent reactivity of α,β-unsaturated enones, sequential reactions involving nucleophiles containing an acidic proton capable of protonating the resulting enolate of the Michael addition can be used. In one such report by Cozzi and Umani-Ronchi, the reaction of indole **3-38** with α,β-

Table 3.6. Sequential $InBr_3$-catalyzed 1,4- then 1-2-nucleohpilic addition to enones

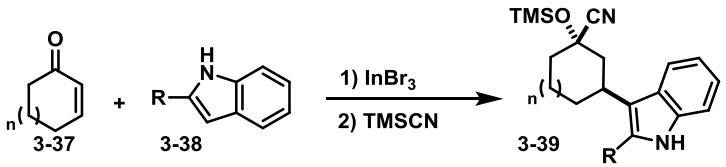

entry	R	n	yield (%)	*cis:trans*
1	H	0	52	50:50
2	H	1	47	50:50
3	Me	0	55	74:26
4	Me	1	87	84:16

unsaturated enones **3-37** in the presence of indium(III)bromide was studied (**Table 3.6**).[14] When cyclic enone **3-37** is mixed with indole **3-38** in the presence of indium(III)bromide, the initial 1,4-Michael adduct is formed. The mixture is then treated with trimethylsilyl cyanide to complete the sequential addition process generating the tandem 1,4/1,2-addition product **3-39**. Both cyclopentenone and cyclohexenone were tolerated in the reaction producing **3-39** in fair to good yields 47-87% (**Table 3.6**, entries 1-4). It is worthwhile to note that in the case 2-methylindole as the nucleophile, some diastereoselectivity was observed (74:26 to 84:16, entries 3-4).

With regards to tandem addition reactions involving enones and enals, (trimethsilyl)diazomethane is a convenient reagent for this purpose because of its ability to function as a nucleophile, electrophile or pure 1,3-dipole depending on the reaction conditions. In a recent report, the Aoyama group demonstrated that the magnesium salt of trimethylsilyldiazomethane can be added to aldehydes and ketones **3-40** and subsequently protonated with acetic acid; then in a sequential process, the generated 2-diazo-2-(trimethylsilyl)ethanol is reacted with electron deficient alkynes in a cycloaddition reaction (**Table 3.7**).[15] In their study, both electron rich and electron deficient aldehydes were tolerated under the reaction

Table 3.7. Pyrazole synthesis via tandem reaction with $TMSC(MgBr)N_2$

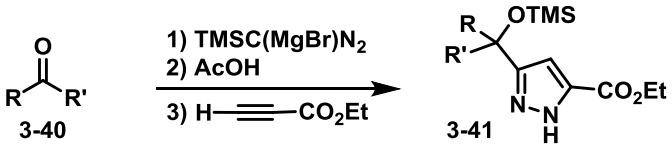

entry	R	R'	yield (%)
1	(*p*-Cl)C_6H_4	H	81
2	Ph	H	65
3	(*p*-MeO)C_6H_4	H	78
4	*t*-Bu	H	66
5	Ph	Me	77
6	$PhCH_2CH_2$	Me	92

conditions providing good yields of the pyrazoles **3-41** (65-81%, entries 1-3). Alkyl substitution (R = *t*-Bu) also worked under the reaction conditions producing the pyrazole in 66% yield (entry 4). Finally, ketones were also studied, which delivered the expected pyrazoles in good to excellent yield (77-92%, entries 5-6). This served as an early example of utilizing trimethylsilyldiazomethane in a 1,2-addition fashion followed by a sequential intermolecular cycloaddition process.

In a study on the tandem reactive behavior of trimethylsilyldiazomethane, Lee and co-workers investigated its Lewis base-catalyzed reaction with 4-alkenyl ketones and aldehydes (**Scheme 3.12**).[16] In the case of acyclic 4-alkenyl ketones and aldehydes **3-42**, bicyclic pyrazolines **3-43** were generated when reacted with trimethylsilyldiazomethane and a catalytic amount of TBAT or potassium *t*-butoxide in 37-92% yield. When cyclic ketones containing a tethered alkene **3-44** were subjected to the reaction conditions, tricyclic Δ^1-pyrazolines were generated in fair to excellent yields and diastereoselectivities (43-82%, up to 19:1 dr). When cyclic alkenes containing tethered ketone **3-46** were subjected to the reaction conditions, tricyclic pyrazolines were generated in good yield (74-83%). Although diastereoselectivity for the carbonyl addition step could not be controlled, the facial selectivity of the cycloaddition was high, and only two diastereomers were formed in all cases.

Scheme 3.12. Sequential reactions of $TMSCHN_2$ with 4-alkenyl ketones and aldehydes

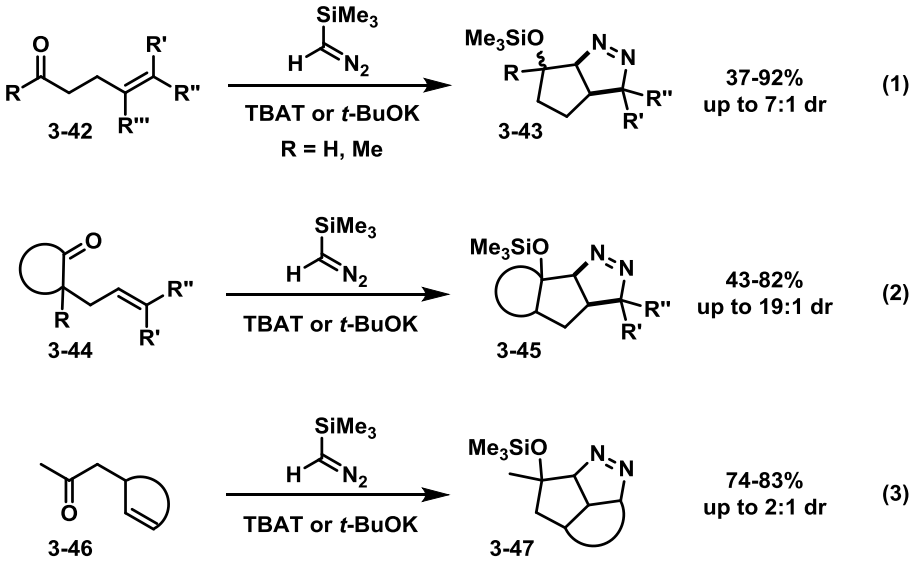

The earliest report of utilizing lithium(trimethylsilyl)diazomethane **1** in a tandem 1,4/1,2-addition, C-C bond fragmentation, and Li-N alkylidene carbene insertion was that of Aoyama and Shioiri in their study on enamino ketones (**Schemes 1.5**, **3.13** and **Table 1.15**).[17] When β-pyrrolidine-substituted α,β-unsaturated ketone **3-48** is exposed to lithium(trimethylsilyl)diazomethane **1**, initial 1,4-addition/cyclization product, Δ^2-pyrazoline, is formed regenerating the carbonyl functionality. A subsequent 1,2-addition of **1** followed by warming to 0 °C leads to alkylidene carbene **3-49** which inserts into the N-Li bond forming bicyclic Δ^2-pyrazoline **3-50** in moderate yield (53%). Although only a few examples were reported, this study demonstrated that LTMSD **1** has ideal characteristics for double 1,4/1,2-addition to enones.

Scheme 3.13. Tandem reaction of LTMSD with enamino ketones

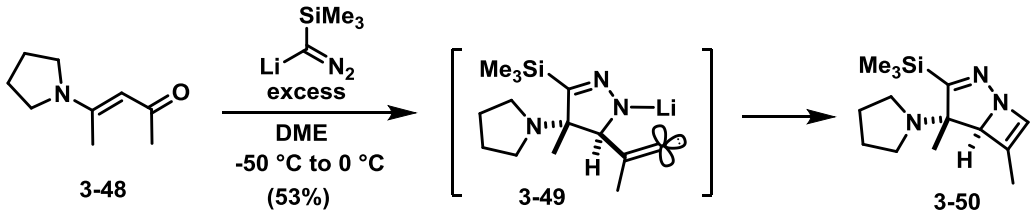

3.2. Results and discussion

On the basis of the known reaction between **1** and cyclic enones **3-51/3-51′** to generate pyrazolines **3-53/3-53′**,[18] most likely via protonation of putative intermediate **3-52/3-52′**, we envision these intermediates can further react with **1** if 2 equivalents of LTMSD is employed from the start of the reaction (**Scheme 3.14**). Once 1,2-addition between **1** and **3-52/3-52′** occurs, the resulting alkoxide of the 1,2-adduct would induce a C→O silyl migration (1,3-Brook rearrangement)[19] and elimination of $LiOSiMe_3$ and N_2 to generate a new intermediate **3-54/3-54′**. We expect that, depending the structural characteristics of the carbon skeleton of these intermediates and reaction conditions, they would lead to different end products via Li-N insertion[20] or Grob-type fragmentation[6] pathways. Herein, we report the formation of various novel heterocycles from these putative intermediates, which are in turn derived from 1,4/1,2-double addition of **1** with *exo*- and *endo*-cyclic α,β-unsaturated ketones.

Scheme 3.14. Sequential 1,4-/1,2-addition of **1** with cyclic ketones

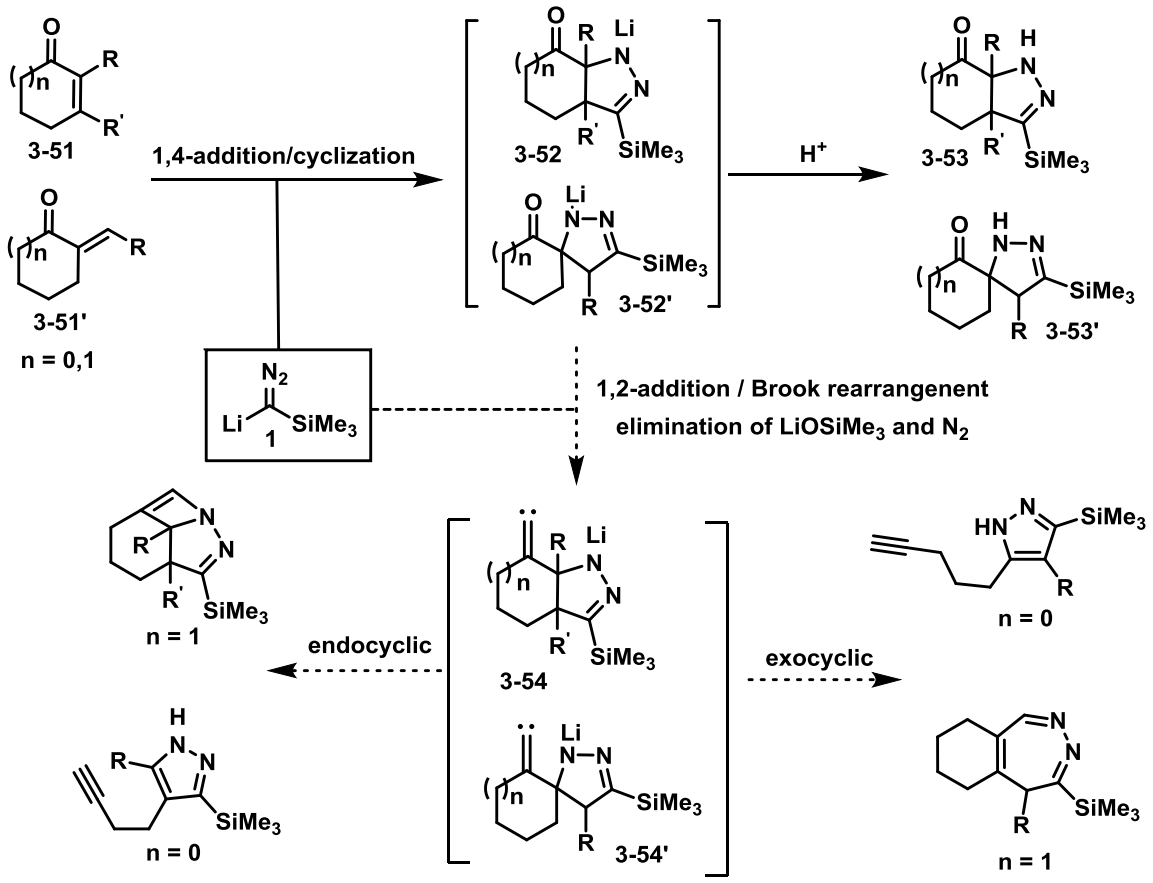

3.2.1. Reaction of $TMSCLiN_2$ with systems containing exocyclic double bonds

3.2.1.1. Alkynyl pyrazoles from indanone benzylidenes

The feasibility of the proposed double 1,4/1,2-addition-based multistep transformation was first examined with benzylidene indanones (**Table 3.8**). Treatment of methylidene indanone **3-55a** (R = H) with **1** (2.2 equiv) at –78 °C followed by slow warming up to room temperature provided pyrazole **3-56a** in 62% yield. Benzylidene indanone **3-55b** (R = Ph), under identical conditions provided pyrazole **3-56b** in 81% yield. Similarly, 4-Cl and 4-OMe-substituted benzylidene indanones (**3-55c** and **3-55d**) provided pyrazoles **3-56c** and **3-56d** in 83% and 78% yield, respectively. Furthermore, reaction with 1-allyloxy, 1,6-dichloro, 3,4-methlenedioxy, and 2,3,4-trimethoxy-substituted benzylidene indanones (**3-55e**–**3-55g**) afforded

pyrazoles **3-56e**–**3-56h** with yields in the range of 60–80%. This fragmentation reaction is not limited to the indanone system. Thus, under the same conditions, *bis*-benzylidene cyclopentanone **3-55i** delivered enyne **3-56i** in 60% yield.

Table 3.8. Alkynyl pyrazoles from indanone benzylidenes and **1**

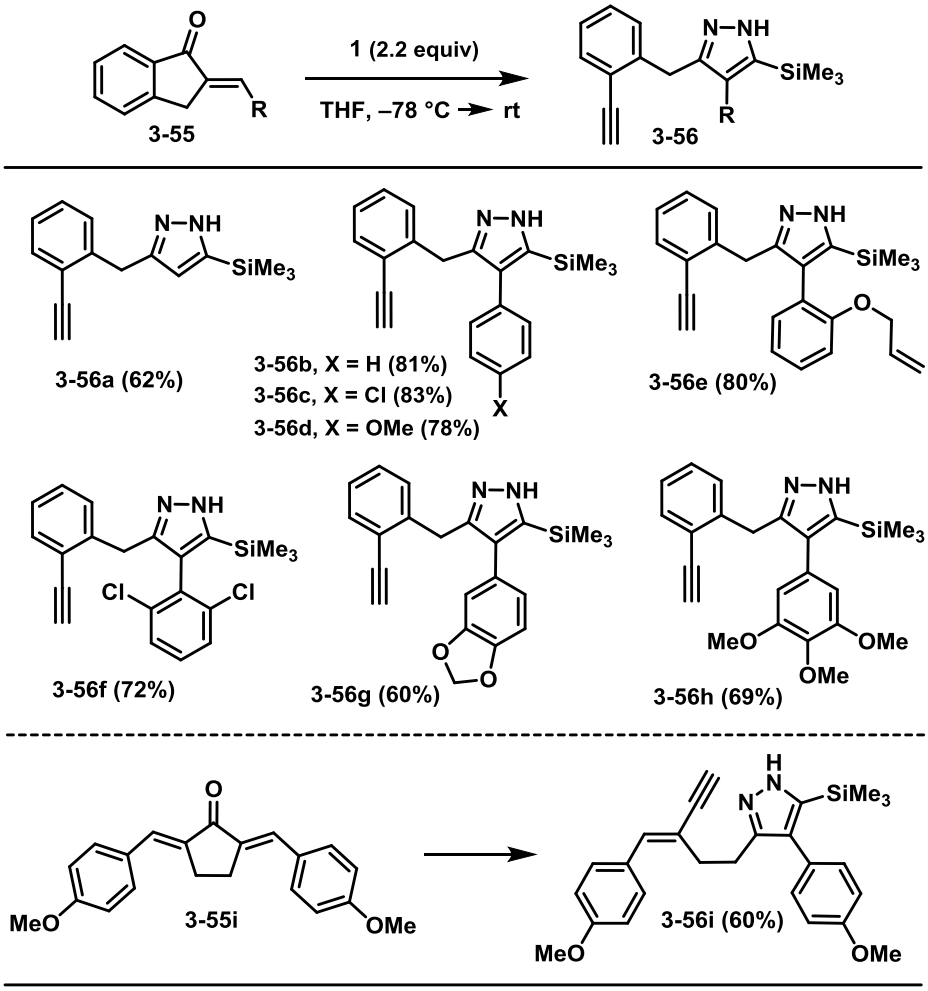

3.2.1.2. Tricyclic Hemiaminals from indanone benzylidenes

Having observed this novel pyrazole formation via tandem 1,4/1,2-addition events, we expected that the reaction path leading to pyrazoles could be diverted to generate different final products. This assumption is based on the predicted multiple chelation on the putative 1,4/1,2-adduct **3-57**, where the elimination of lithiumsilanolate ($LiOSiMe_3$) could be modulated by temperature, time, additives, and solvent (**Scheme 3.15**).

Depending on the reaction conditions, benzylidene indanone **3-55b**, **3-55d**, and **3-55h** afforded pyrazoles **3-56b**, **3-56d**, and **3-56h** through Grob-type fragmentation of **3-58** to generate putative intermediate lithium acetylide **3-59**, or alternatively, different pyrazoles **3-56b′**, **3-56d′**, and **3-56h′** form via protonation of **3-57** to **3-60** followed by fragmentation to **3-61** of which keto-form **3-62** is trapped generating the desired hemiaminal. While typical slow warming up of the reaction to room temperature after the addition of **1** predominantly provided pyrazoles **3-56b**, **3-56d**, and **3-56h**, quenching the reaction with silica gel at around –40 °C before warming up yielded pyrazoles **3-56b′**, **3-56d′**, and **3-56h′** as predominant products.

Scheme 3.15. Mechanism for different C-C fragmentations

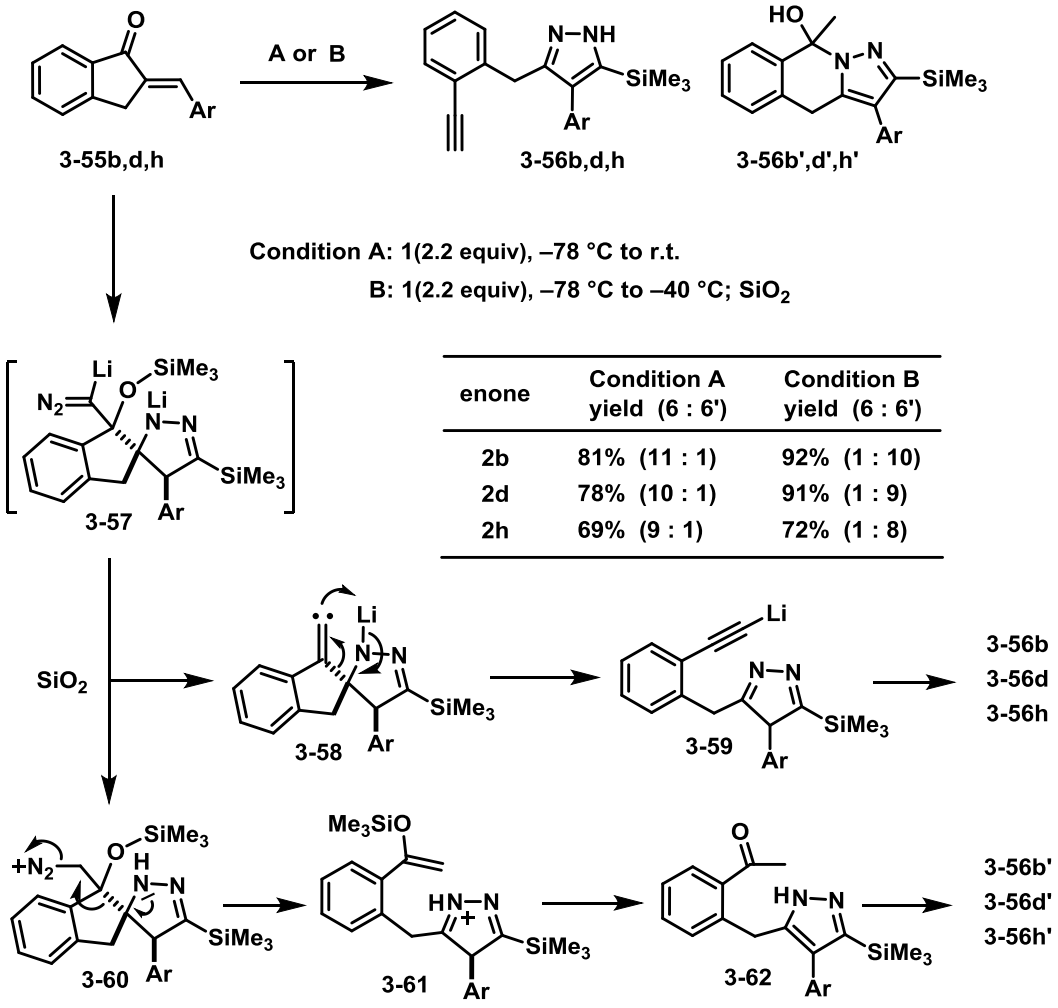

enone	Condition A yield (6 : 6')	Condition B yield (6 : 6')
2b	81% (11 : 1)	92% (1 : 10)
2d	78% (10 : 1)	91% (1 : 9)
2h	69% (9 : 1)	72% (1 : 8)

The yields and ratios of these structurally different pyrazoles are strongly dependent on the temperature and timing of quenching with SiO_2. Under optimized conditions, excellent yields and ratios of **3-56b/3-56b′**, **3-**

56d/3-56d′, and **3-56h/3-56h′** were obtained. The identity of these pyrazoles was unambiguously established via X-ray diffraction analyses (**Figure 3.1**).

Figure 3.1. X-ray structures of select pyrazoles

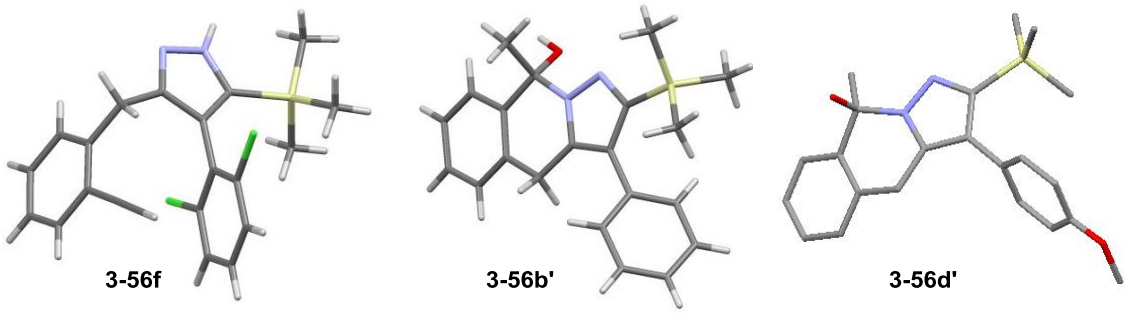

3.2.1.3. Tandem 1,4/1,2-Additions of $TMSCLiN_2$ with cyclohexenone derivatives

The reaction of 6- and 7-membered cyclic ketones of a conjugated exocyclic double with **1** (2.2 equiv, –78 °C → 25 °C) provided completely different behavior compared to that of the corresponding 5-membered counterpart (**Table 3.9**). The reaction of pulegone **3-63** afforded bicyclic 4*H*-1,2-diazepine derivatives **3-64** in excellent yield (entry 1), which is the result of N–Li insertion followed by cycloreversion. Under the same conditions, however, **3-65** afforded cyanohydrin **3-66** in 67% yield via an initial 1,2-addition followed by an oxidative deamination (entry 2), while the corresponding tetralone derivative **3-67** afforded Grob fragmentation product **3-68** exclusively (entry 3). Also, the reaction of benzylidene cycloheptanone **3-69** afforded 4*H*-1,2-diazepine derivative **3-70** in slightly lower yield (51%, entry 4).

In stark contrast, cyclohexenone derivatives of an endocyclic double take various reaction courses depending on the substituent on the system (**Table 3.10**). Carvone **3-71** and dihydrocarvone **3-73** produced a mixture of carbene-inserted pyrazole and Grob fragmentation product in 87% (**3-72**:**3-72′** = 5:1) and 75% (**3-74**:**3-74′** = 3:1) yield, respectively (entries 1 and 2). 1-Methyl-2-allyl-2-cyclohexenone containing isopropenyl group at 4-position **3-75** provided **3-76** as a sole product (entry 3), whereas **3-77** devoid of the

Table 3.9. Reaction of **1** with cyclohexenone derivatives

entry	enone	products	yield (%)
1	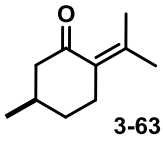 3-63	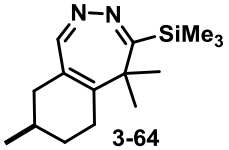 3-64	89
2	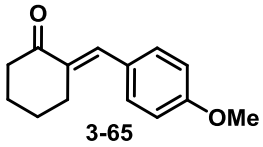 3-65	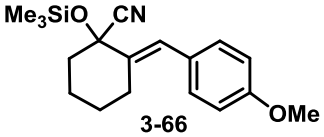 3-66	67
3	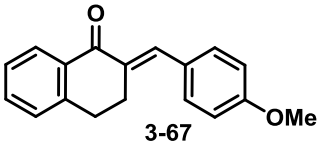 3-67	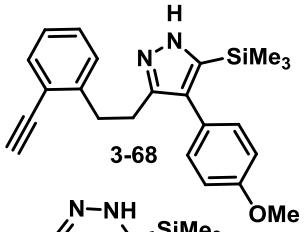 3-68	65
4	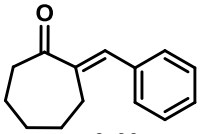 3-69	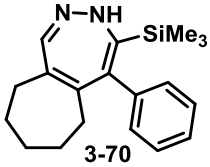 3-70	51

isopropenyl group afforded a mixture of **3-78** and a mono-adduct **3-78′** in a 3:1 ratio (entry 4). 2-Cyclohexenone **3-79** with a methoxymethyl(MOM)-protected hydroxymethyl group delivered two products; insertion product **3-80** and tetrahydrofuran-containing product **3-80′** in 81 % yield with a 1:1 ratio (entry 5). The formation of **3-80′** is the consequence of slow elimination of $LiOSiMe_3$ from the bis-adduct of **1** due to strong chelation of C–Li moiety by the MOM group. The reaction of verbenone **3-81** provided product **3-82** and **3-82′** in 87% yield with a 1:1 ratio (entry 6). The sterically hindered nature of the mono-adduct of **3-82** with **1** slowed down both the second addition of **1** and the elimination of $LiOSiMe_3$ from the bis-adduct.

From the reaction in Tables **3.10** and **3.11**, a general trend can be identified. Alkylidene carbene **3-54** of a 6-membered fused bicycle can undergo either fragmentation or insertion on to

Table 3.10. 1,4/1,2-Additions of **1** with cyclohexenone derivatives

entry	enone	products			yield (%)
1	R =  3-71	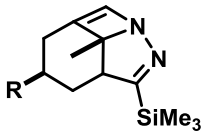 3-72	(5:1)	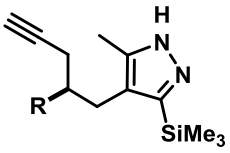 3-72'	87
2	R =  3-73	3-74	(3:1)	3-74'	75
3	R =  3-75	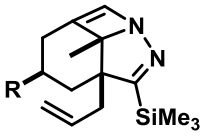 3-76	(1:0)	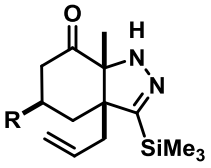 3-76'	72
4	R = H 3-77	3-78	(3:1)	3-78'	87
5	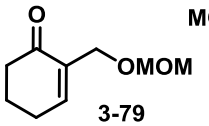 3-79	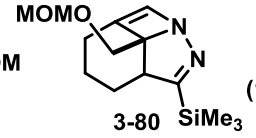 3-80	(1:1)	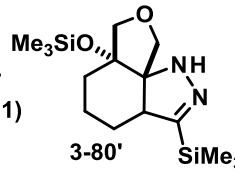 3-80'	81
6	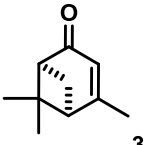 3-81	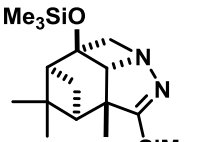 3-82	(3:1)	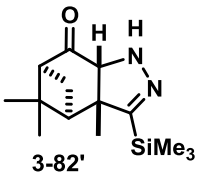 3-82'	82

N–Li bond to generate **3-72,74,76,78,** or **80** respectively (**Scheme 3.16**). The Grob-type fragmentation of **3-54** happened only when R′ = H, otherwise N–Li insertion is more favorable. This may imply that the aromatization to form pyrazole is the ultimate driving force for the C–C bond cleavage. On the other hand, the fate of alkylidene carbene **3-54′** of 5- and 6-membered spirobicycles depends on its ring size. From spirocycle (n = 0) **3-54′**, only fragmentation occurred to generate **3-56a** to **3-56i**, but product **3-85**, derived from putative intermediate **3-83,** did not form, which is most likely due to the high strain of **3-83**. For spirocycle (n = 1) **3-54′**, both the C–C fragmentation and N–Li insertion occurred to generate **3-68** and **3-84**, and the cycloreversion of

the latter afforded **3-64** (after tautomerization). In case of spirocycle (n = 2) **3-54′**, only N–Li insertion occurred to generate **3-70**.

Scheme 3.16. General trend in consecutive additions of **1** to enones

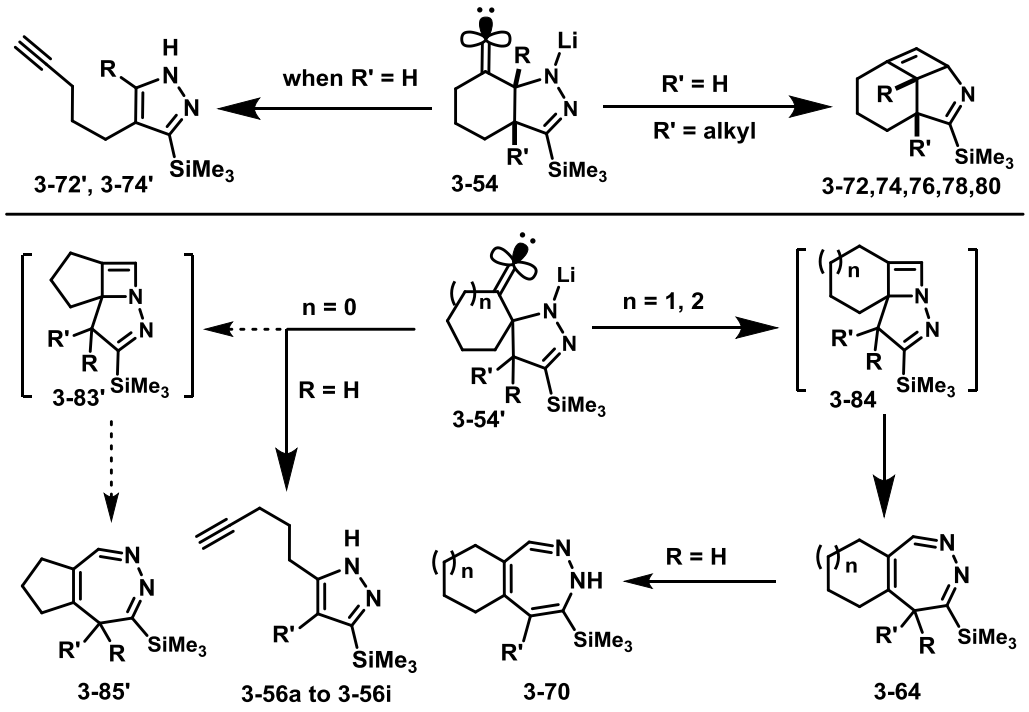

3.3. Conclusion

In conclusion, we discovered sequential 1,4-/1,2-addition of LTMSD **1** with exo- and endocyclic enones followed by subsequent transformations involving Grob-type C–C fragmentation or alkylidene carbene-mediated Li–N insertion depending on reaction conditions and quenching procedures. These multiple domino processes are made possible by the unique reactivity of LTMSD that selectivity undergoes 1,4-addition, leaving the free carbonyl group for the subsequent 1,2-addition. The fate of the lithiated diazomethane moiety containing an α-silyloxy group at different stages of intermediates can be controlled by temperature and its protonation states. By choosing right combinations of these two reaction parameters

in combination with different structural characteristics of substrates, diverse arrays of unique molecular structures can be synthesized in a single operational step from terpenes and their derivatives.

3.4. Experimental details

3.4.1. General information

All reactions were carried out under an inert nitrogen atmosphere, unless otherwise indicated. Flasks were oven-dried and cooled under a stream of nitrogen. Compounds were purchased from Aldrich unless otherwise noted. CH2Cl2, THF, Et2O were purified based on standard procedures. Flash chromatography was performed using silica gel 60 Å (32-63 mesh) purchased from SiliCycle. Analytical thin layer chromatography (TLC) was performed on 0.25 mm SiliCycle precoated silica gel 60 (particle size 0.040-0.063 mm). 1H NMR and 13C NMR spectra were recorded on a Bruker AV-500 spectrometer. 1H and 13C chemical shifts were referenced to internal solvent resonances and reported relative to SiMe4; multiplicities are indicated by s (singlet), d (doublet), t (triplet), q (quartet), qn (quintet), m (multiplet) and br (broad). Coupling constants, J, are reported in Hz (Hertz). Electrospray ionization (ESI) mass spectra were recorded on a Micromass LCT equipped with a time-of-flight analyzer on a Waters Micromass Q-Tof Ultima in the University of Illinois at Urbana-Champaign. Electron impact (EI) mass spectra were obtained using a Micromass AutoSpecTM. Fast atom bombardment (FAB) mass spectra were taken at the Mass Spectrometry Laboratory in the University of Illinois at Urbana-Champaign, using a Micromass 70-VS-4F and 70-VSE for HRFAB and LRFAB, respectively. IR spectra were recorded using JASCO FT/IR-4100.

3.4.2. General procedures

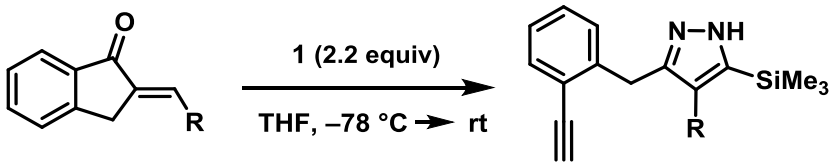

Method A: To a stirred solution of trimethylsilyldiazomethane[1] **1** (0.3 mL, 2.0 M in ether, 0.6 mmol) in anhydrous THF (2 mL) under an atmosphere of nitrogen and at –78 °C was added *n*-BuLi (0.3 mL, 2.0 M in hexanes, 0.6 mmol) dropwise over 1 minute. The solution went pale yellow and was allowed to stir for an additional 30 minutes at –78 °C. Enone (0.27 mmol), dissolved in THF (2 mL), was then added drop-wise over 30 seconds and the reaction was allowed to stir for a further 30 min until TLC showed the full consumption of the starting material. The reaction allowed to warm to rt, and the mixture was quenched with several drops of saturated NH_4Cl solution, and dried over $MgSO_4$. The drying reagent was filtered and solvent was removed under reduced pressure to give the crude product. Purification using flash chromatography with gradient elusion with hexane and ethyl acetate (20:1 to 6:1) to afford pure pyrazoles.

Method B: For hemiaminal synthesis. Same as the above conditions except the reaction is quenched with 0.5 g of SiO_2 at −40 °C before warming to rt.

3.4.3. Characterization Data

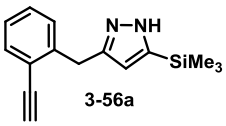

3-56a

^{1}H NMR (500 MHz, $CDCl_3$) δ 7.51 (d, 1H, J=7.7Hz), 7.26 (m, 2H), 7.17 (m, 1H), 6.22 (s, 1H), 4.25 (s, 2H), 3.29 (s, 1H), 0.27 (s, 9H) ^{13}C NMR (125 MHz, $CDCl_3$) δ 151.2, 143.9, 142.6, 132.8, 129.3, 129.0, 126.1, 112.0, 82.4, 81.2, 32.4, -1.2. HRMS (ESI) calc. for $C_{15}H_{19}N_2Si$ $[M+H]^+$ 255.1318, found 255.1318.

[1] Caution! Trimethylsilyldiazomethane should be regarded extremely toxic and all operations must on carried out only in a well-ventilated fume hood and all skin contact should be avoided, see: (a) Shioiri, T.; Aoyama, T.; Mori, S.; *Org. Synth., Coll. Vol.* **1993**, *8*, 612. (b) Barnhart, R.; Dale, D. J.; Ironside, M. D.; Vogt, P. F. *Org. Process Res. Dev.* **2009**, *13*, 1388. (c) Kemsley, J., *Chem. Eng. News* **2011**, *89(19)*, 15.

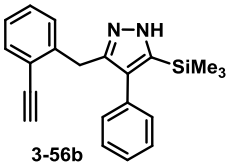

3-56b

^{1}H NMR (500 MHz, $CDCl_3$) δ 7.44 (dd, *J* = 7.9, 1.3 Hz, 1H), 7.35-7.29 (m, 3H), 7.23-7.20 (m, 3H), 7.14-7.11 (m, 2H), 4.18 (s, 2H), 3.14 (s, 1H), 0.15 (s, 9H). ^{13}C NMR (125 MHz, $CDCl_3$) δ 142.62, 134.54, 132.65, 130.38, 129.06, 128.84, 127.99, 126.93, 121.56, 82.34, 81.17, 30.35, -0.93. HRMS (ESI) calc. for $C_{21}H_{23}N_2Si$ $[M+H]^+$ 331.1631, found 331.1631.

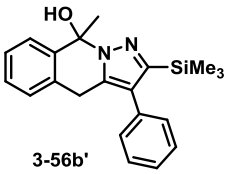

3-56b'

^{1}H NMR (500 MHz, $CDCl_3$) δ 7.83 (d, *J* = 7.7 Hz, 1H), 7.46-7.33 (m, 7H), 7.25 (d, *J* = 7.4 Hz, 1H), 4.45 (s, 1H), 4.09 (q, *J* = 16.4 Hz, 2H), 2.07 (s, 3H), 0.20 (s, 9H).^{13}C NMR (125 MHz, CDCl3) δ 151.05, 138.16, 134.85, 132.72, 129.96, 128.29, 128.22, 128.10, 127.27, 126.79, 125.81, 84.72, 32.30, 26.58, -0.29. HRMS (ESI) calc. for $C_{21}H_{25}N_2OSi$ $[M+H]^+$ 349.1736, found 349.1728.

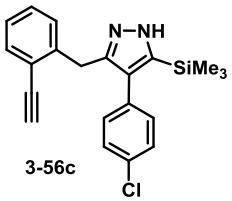

3-56c

^{1}H NMR (500 MHz, $CDCl_3$) δ 7.44-7.43 (m, 1H), 7.31-7.29 (m, 2H), 7.21 (dd, *J* = 7.6, 1.3 Hz, 1H), 7.14-7.10 (m, 4H), 4.16 (s, 2H), 3.15 (s, 1H), 0.14 (d, *J* = 3.4 Hz, 9H). ^{13}C NMR (125 MHz, $CDCl_3$) δ 142.34, 133.12, 132.88, 132.70, 131.65, 128.96, 128.85, 128.22, 127.81, 126.02, 121.54, 82.23, 81.32, 30.33, -0.89. HRMS (ESI) calc. For $C_{21}H_{22}N_2SiCl$ $[M+H]^+$ 365.1241, found 365.1234.

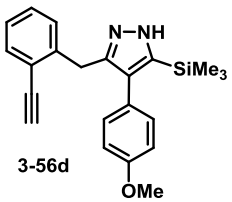

3-56d

^{1}H NMR (500 MHz, CDCl3) δ 7.45-7.43 (m, 1H), 7.21 (d, *J* = 7.5 Hz, 1H), 7.13-7.11 (m, 4H), 6.88 (d, *J* = 8.6 Hz, 2H), 4.18 (s, 2H), 3.82 (s, 3H), 3.17 (s, 1H), 0.12 (s, 9H).^{13}C NMR (125 MHz, $CDCl_3$) δ 158.62, 142.78, 132.62, 131.43, 128.99, 128.83, 126.79, 125.87, 121.55, 113.44, 82.37, 81.30, 55.24, 30.33, -0.88. HRMS (ESI) calc. for $C_{22}H_{25}N_2OSi$ $[M+H]^+$ 361.1736, found 361.1734.

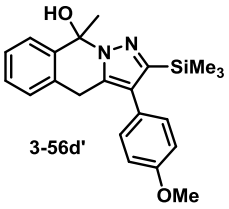

3-56d'

^{1}H NMR (500 MHz, CDCl3) δ 7.82 (d, *J* = 7.7 Hz, 1H), 7.42-7.23 (m, 6H), 6.99 (d, *J* = 8.5 Hz, 2H), 4.37 (s, 1H), 4.06 (q, *J* = 16.3 Hz, 2H), 3.89 (s, 3H), 2.06 (s, 3H), 0.17 (s, 9H). ^{13}C NMR (125 MHz, $CDCl_3$) δ 158.60, 151.13, 138.22, 132.66, 131.03, 130.00, 128.24, 128.10, 127.09, 127.09, 125.80, 125.36, 113.66, 84.65, 55.28, 32.25, 26.55, -0.30. HRMS (ESI) calc. for $C_{22}H_{27}N_2O_2Si$ $[M+H]^+$ 379.1842, found 379.1828.

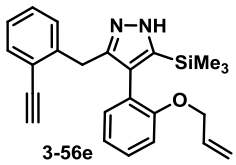

3-56e

^{1}H NMR (500 MHz, $CDCl_3$) δ 7.37 (d, 1H, J=7.6Hz) 7.25 (m, 1H, J=1.1Hz, J=14.2Hz) 7.15 (t, 1H, J=7.5Hz) 7.08 (dd, 3H, J=7.2Hz, J=14.5Hz) 6.90 (t, 1H, J=7.4Hz) 6.85 (d, 1H, J=8.2Hz) 5.86 (ddd, 1H, J=5.0Hz, J=10.3Hz, J=22.2Hz) 5.17 (ddd, 2H, J=1.4Hz, J=13.9Hz, J=12.0Hz) 4.39 (d, 2H, J=1.5Hz) 4.07 (s, 2H) 3.09 (s, 1H) 0.09 (s, 9H). ^{13}C NMR (125 MHz, $CDCl_3$) δ 156.9, 142.6, 133.5, 132.9, 132.4, 129.3, 128.7, 128.6, 125.7, 123.6, 121.5, 120.1, 116.8, 111.9, 82.4, 80.8, 68.7, 30.7, -1.3. HRMS (ESI) calc. for $C_{24}H_{27}N_2OSi$ $[M+H]^+$ 387.1893, found 387.1890.

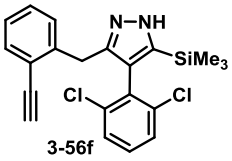

3-56f

^{1}H NMR (500 MHz, $CDCl_3$) δ 7.36 (d, 1H, J=7.5Hz) 7.31 (d, 2H, J=8.0Hz) 7.19 (dd, 1H, J=7.7Hz, J=8.4Hz) 7.15 (d, 2H, J=5.5Hz) 7.09 (m, 1H) 4.03 (s, 2H) 3.07 (s, 1H) 0.10 (s, 9H) ^{13}C NMR (125 MHz, $CDCl_3$) δ 141.3, 137.5, 132.9, 132.4, 129.7, 129.4, 128.7, 127.7, 126.0, 123.0, 121.6, 82.0, 80.7, 30.8, -1.7. HRMS (ESI) calc. for $C_{21}H_{21}N_2SiCl_2$ $[M+H]^+$ 399.0851, found 399.0854.

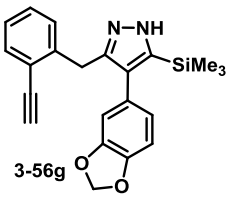

3-56g

^{1}H NMR (500 MHz, $CDCl_3$) δ 7.43 (d, 1H, J=7.5Hz), 7.20 (t, 1H, J=7.4Hz), 7.12-7.09 (m, 2H), 6.77 (d, 1H, J=7.8Hz), 6.65-6.62 (m, 2H), 5.96 (s, 2H), 4.16 (s, 2H), 3.18 (s, 1H), 0.15 (s, 9H). ^{13}C NMR (125 MHz, $CDCl_3$) δ 147.2, 146.6, 142.6, 132.6,

129.0, 128.8, 128.7, 128.2, 125.9, 123.8, 121.6, 110.8, 107.9, 100.9, 82.4, 81.2, 30.3, 0.9. HRMS (ESI) calc. for $C_{22}H_{23}N_2O_2Si$ $[M+H]^+$ 375.1529, found 375.1527.

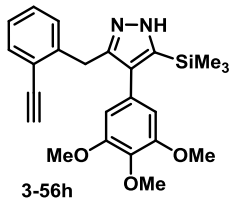

3-56h

^{1}H NMR (500 MHz, $CDCl_3$) δ 7.41 (d, 1H, J=6.8Hz) 7.21 (dt, 1H, J=1.3Hz, J=7.6Hz) 7.10 (t, 2H, J=8.0Hz), 6.31 (s, 2H), 4.17 (s, 2H), 3.86 (s, 3H), 3.71 (s, 6H), 3.16 (s, 1H), 0.18 (s, 9H). ^{13}C NMR (125 MHz, $CDCl_3$) δ 152.6, 142.6, 137.0, 132.6, 129.0, 128.8, 125.9, 121.6, 107.6, 82.2, 81.3, 60.9, 55.9, 30.5, 0.9. HRMS (ESI) calc. for $C_{24}H_{29}N_2O_3Si$ $[M+H]^+$ 421.1947, found 421.1965.

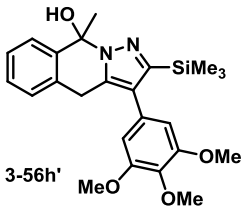

3-56h'

^{1}H NMR (500 MHz, $CDCl_3$) δ 7.79 (d, 1H, J=7.3Hz), 7.37 (t, 1H, J=6.8Hz), 7.32 (dt, 1H, J=1.2Hz, J=7.4Hz), 7.24 (d, 1H, J=7.1Hz), 6.53 (s, 2H), 4.07 (dd, 1H, J=18.9Hz, J=38.2Hz), 3.91 (s, 3H), 3.87 (s, 6H), 2.04 (s, 3H), 0.20 (s, 9H). ^{13}C NMR (125 MHz, $CDCl_3$) δ 152.9, 150.9, 138.0, 137.0, 132.7, 130.3, 129.7, 128.3, 128.1, 127.3, 125.8, 107.2, 84.7, 61.0, 56.2, 32.2, 26.6, 0.3. HRMS (ESI) calc. for $C_{24}H_{31}N_2O_4Si$ $[M+H]^+$ 439.2053, found 439.2035.

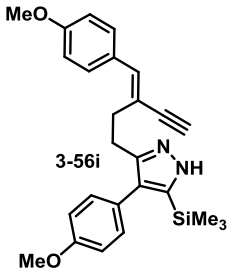

3-56i

^{1}H NMR (500 MHz, $CDCl_3$) δ 7.11 (d, 2H, J=8.6Hz) 7.02 (d, 2H, J=8.6Hz) 6.88 (d, 2H, J=8.6Hz) 6.82 (s, 1H) 6.78 (d, 2H, J=8.7Hz) 3.84 (s, 3H) 3.80 (s, 3H) 2.93 (dd, 2H, J=6.7Hz, J=9.7Hz) 2.91 (s, 1H) 2.63 (m, 2H) 0.13 (s, 9H). ^{13}C NMR (125 MHz, $CDCl_3$) δ 158.8, 158.6, 150.3, 141.1, 137.3, 131.4, 130.1, 128.8, 128.2, 126.8, 121.8, 113.7, 113.5, 86.1, 76.7, 55.2, 55.2, 31.4, 24.9, -1.0.

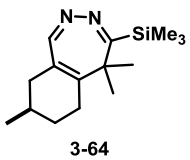

3-64

^{1}H NMR (500 MHz, $CDCl_3$) δ 6.43 (s, 1H), 2.31 (d, 1H, J=14.9Hz), 2.14-2.05 (m, 2H), 1.86-1.78 (m, 2H), 1.72 (m, 1H), 1.28 (dtd, 2H, J=6.1Hz, J=10.5Hz, J=16.3Hz), 1.06 (d, 6H, J=6.1Hz), 1.00 (d, 3H, J=6.6Hz), 0.16 (s, 9H). ^{13}C NMR (125 MHz,

$CDCl_3$) δ 156.3, 153.8, 141.8, 133.8, 56.4, 32.5, 31.3, 29.3, 22.9, 22.8, 21.7, 21.3, 0.19. HRMS (ESI) calc. for $C_{15}H_{27}N_2Si$ $[M+H]^+$ 263.1944, found 263.1933.

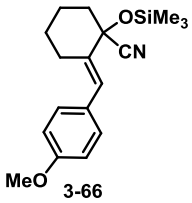

3-66

^1H NMR (500 MHz, $CDCl_3$) δ 7.16 (d, 2H, J=8.5Hz), 6.89 (d, 2H, J=8.7Hz), 6.83 (s, 1H), 3.82 (s, 3H), 2.57 (m, 1H), 2.45 (ddd, 1H, J=4.1Hz, J=7.8Hz, J=17.4Hz), 2.11 (ddd, 1H, J=4.0Hz, J=8.0Hz, J=12.4Hz), 2.02 (m, 1H), 1.88 (dtd, 1H, J=3.7Hz, J=7.7Hz, J=15.5Hz), 1.75 (dddd, 1H, J=3.9Hz, J=7.9Hz, J=12.2Hz, J=17.9Hz), 1.53 (m, 2H), 0.29 (s, 9H). ^{13}C NMR (125 MHz, $CDCl_3$) δ 158.6, 138.0, 130.1, 124.1, 113.7, 55.3, 42.3, 26.6, 25.6, 22.0, 1.3. HRMS (ESI) calc. for $C_{19}H_{27}N_2OSi$ $[M+H]^+$ 327.1893, found 327.1906.

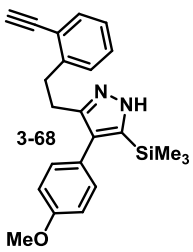

3-68

^1H NMR (500 MHz, $CDCl_3$) δ 7.41 (d, 1H, J=7.6Hz), 7.21 (t, 1H, J=7.7Hz), 7.13-7.10 (m, 4H), 6.89 (d, 2H, J=8.6Hz), 3.84 (s, 3H), 3.07 (t, 2H, J=7.6Hz), 3.04 (s, 1H), 2.90 (t, 2H, J=7.6Hz), 0.15 (s, 9H). ^{13}C NMR (125 MHz, $CDCl_3$) δ 158.7, 144.6, 132.8, 131.5, 128.8, 125.8, 121.5, 113.4, 82.00, 80.6, 55.2, 34.5, 29.7, 27.1, 1.0. HRMS (ESI) calc. for $C_{23}H_{27}N_2OSi$ $[M+H]^+$ 375.1893, found 375.1895.

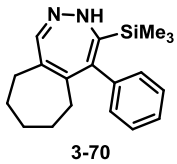

3-70

^1H NMR (500 MHz, $CDCl_3$) δ 7.40 (bs, 1H), 7.35 (m, 5H), 7.23 (td, 1H, J=2.1Hz, J=8.5Hz) 2.90 (t, 2H, J=6.6Hz) 2.83 (t, 2H, J=6.8Hz) 1.79 (m, 2H) 1.73 (m, 2H) 1.57 (m, 2H) 0.34 (s, 9H). ^{13}C NMR (125 MHz, $CDCl_3$) δ 138.1, 134.7, 128.9, 128.1, 127.0, 126.4, 125.3, 28.6, 28.5, 27.4, 24.2, 23.8, -1.1. HRMS (ESI) calc. for $C_{19}H_{27}N_2Si$ $[M+H]^+$ 311.1944, found 311.1943.

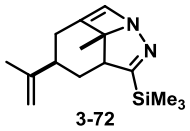

3-72

^{1}H NMR (500 MHz, $CDCl_3$) δ 6.52 (d, 1H, J=0.9Hz), 4.73 (d, 1H, J=13.1Hz), 2.73 (m, 2H), 2.22 (m, 1H), 2.07 (m, 2H), 1.76 (t, 1H, J=11.2Hz), 1.71 (s, 3H), 1.60 (ddd, 1H, J=6.2Hz, J=12.7Hz, J=14.6Hz), 1.49 (s, 3H), 0.22 (s, 9H). ^{13}C NMR (125 MHz, $CDCl_3$) δ 178.4, 148.0, 147.4, 144.6, 110.3, 73.2, 55.2, 49.3, 29.9, 28.3, 20.6, 20.0, -1.6. HRMS (ESI) calc. for $C_{15}H_{25}N_2Si$ [M+H]+ 261.1787, found 261.1782.

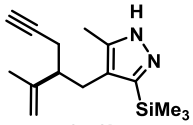

3-72'

^{1}H NMR (500 MHz, $CDCl_3$) δ 4.85 (s, 1H), 4.76 (s, 1H), 2.61 (qd, *J* = 15.8, 7.5 Hz, 2H), 2.44-2.39 (m, 1H), 2.31-2.18 (m, 5H), 1.97-1.95 (m, 1H), 1.74 (s, 3H), 0.35-0.30 (s, 9H).^{13}C NMR (125 MHz, $CDCl_3$) δ 146.34, 124.01, 112.08, 83.09, 69.42, 47.92, 28.45, 22.07, 20.04, 11.85, -0.82. HRMS (ESI) calc. for $C_{15}H_{25}N_2Si$ [M+H]+ 261.1787, found 261.1782.

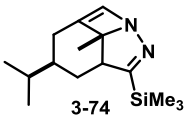

3-74

^{1}H NMR (500 MHz, $CDCl_3$) δ 6.50 (s, 1H), 2.72 (d, 1H, J=4.7Hz), 2.21 (dd, 1H, J=3.1Hz, J=12.3Hz), 2.04 (d, 1H, J=13.8Hz), 1.52 (t, 2H, J=11.1Hz), 1.47 (s, 3H), 1.40 (dd, 1H, J=6.0Hz, J=14.0Hz), 1.36-1.34 (m, 1H), 0.91 (dd, 6H, J=4.4Hz, J=6.6Hz), 0.23 (s, 9H). ^{13}C NMR (125 MHz, $CDCl_3$) δ 178.7, 146.9, 145.5, 55.4, 48.5, 33.1, 28.1 26.4, 20.0, 19.9, 19.6, -1.6. HRMS (ESI) calc. for $C_{15}H_{27}N_2Si$ $[M+H]^+$ 263.1944, found 263.1955.

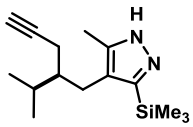

3-74'

^{1}H NMR (500 MHz, $CDCl_3$) δ 2.56 (dd, J = 14.5, 5.9 Hz, 1H), 2.44 (dd, J = 14.5, 9.5 Hz, 1H), 2.25 (s, 3H), 2.09 (ddd, J = 6.3, 3.7, 2.7 Hz, 2H), 1.93 (t, J = 2.6 Hz, 2H), 1.63 (ddd, J = 9.5, 5.9, 4.7 Hz, 1H), 0.99 (d, J = 6.9 Hz, 3H), 0.95 (d, J = 6.9 Hz, 3H), 0.33 (s, 9H).^{13}C NMR (125 MHz, $CDCl_3$) δ 124.42, 83.81, 69.40, 45.03, 28.84, 24.96, 19.44, 19.22, 11.93, 0.81. HRMS (ESI) calc. for $C_{15}H_{27}N_2Si$ $[M+H]^+$ 263.1944, found 263.1945.

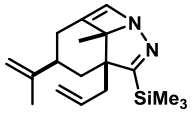

3-76

^{1}H NMR (500 MHz, $CDCl_3$) δ ppm 6.49 (s, 1H) ppm 5.55 (m, 1H) ppm 5.02 (m, 1H) ppm 4.73 (d, 2H, J=17.4Hz) ppm 2.23 (dd, 2H, J=6.7Hz, J=11.3Hz) ppm 2.17 (dd, 2H, J=3.7Hz, J=12.4Hz) ppm 2.07 (m, 1H) ppm 1.96 (dd, 1H, J=2.6Hz, J=14.4Hz) ppm 1.71 (s, 3H) ppm 1.47 (s, 3H) ppm 1.33 (ddd, 2H, J=9.0Hz, J=15.6Hz, J=14.5Hz) ppm 0.23 (s, 9H). ^{13}C NMR (125 MHz, $CDCl_3$) δ 178.9, 147.7, 147.0, 146.4, 134.3, 117.7, 110.4, 75.6, 59.9, 47.8, 40.0, 37.4, 27.7, 20.7, 15.6, -0.4. HRMS (ESI) calc. for $C_{18}H_{29}N_2Si$ $[M+H]^+$ 301.2100, found 301.2096.

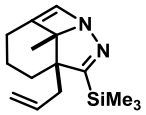

3-78

^{1}H NMR (500 MHz, $CDCl_3$) δ 6.45 (d, 1H, J=1.5Hz), 5.98-5.90 (m, 2H), 5.09 (dd, 1H, J=1.3Hz, J=17.1Hz), 5.05 (dd, 1H, J=0.7Hz, J=10.1Hz), 2.63 (dd, 1H, J=6.1Hz, J=14.4Hz)\, 2.35 (dd, 1H, J=8.2Hz, J=14.4Hz), 2.13 (td, 1H, J=4.9Hz, J=8.7Hz), 1.86-1.83 (m, 3H), 1.47-1.39 (m, 2H), 1.07 (s, 3H), 0.23 (s, 9H). ^{13}C NMR (125 MHz, $CDCl_3$) δ 181.7, 145.9, 144.0, 135.1, 116.8, 55.6, 34.8, 33.8, 27.3, 23.0, 21.4. HRMS (ESI) calc. for $C_{15}H_{25}N_2Si$ $[M+H]^+$ 261.1787, found 261.1785.

3-78'

^{1}H NMR (500 MHz, $CDCl_3$) δ 6.88 (s, 1H), 5.58 (tdd, 1H, J=7.5Hz, J=9.4Hz, J=20.1Hz), 5.04 (d, 1H, J=0.9Hz), 5.01 (d, 1H, J=3.2Hz), 2.37 (m, 3H), 2.23 (dt, 1H, J=5.6Hz, J=13.5Hz), 2.06 (td, 1H, J=4.4Hz, J=14.4Hz), 1.93-1.87 (m, 1H), 1.72-1.66 (m, 1H), 1.58-1.49 (m, 1H), 1.06 (s, 3H), 0.18 (s, 9H). ^{13}C NMR (125 MHz, $CDCl_3$) δ 214.2, 165.8, 132.9, 118.8, 76.4, 60.6, 38.8, 32.2, 29.2, 22.8, 20.0, 0.5. HRMS (ESI) calc. for $C_{14}H_{25}N_2O_2Si$ $[M+H]^+$ 265.1736, found 265.1734.

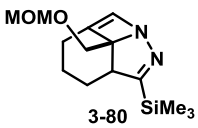

3-80

^{1}H NMR (500 MHz, $CDCl_3$) δ 6.54 (d, 1H, J=1.6Hz), 4.67 (s, 2H), 3.82 (q, 2H, J=10.6Hz), 3.36 (s, 3H), 2.93 (dd, 1H, J=4.4Hz, J=6.5Hz), 2.19 (td, 1H, J=5.0Hz, J=13.3Hz), 2.00 (dddd, 1H, J=2.1Hz, J=4.8Hz, J=8.7Hz, J=15.2Hz), 1.90 (ddd, 1H,

J=5.2Hz, J=10.1Hz, J=14.0Hz), 1.82-1.76 (m, 2H), 1.60-1.52 (m, 1H), 0.22 (s, 9H). ^{13}C NMR (125 MHz, $CDCl_3$) δ 179.1, 147.3, 142.3, 96.7, 74.9, 68.9, 55.3, 51.2, 28.0, 25.0, 23.2, 1.7. HRMS (ESI) calc. for $C_{14}H_{25}N_2O_2Si$ $[M+H]^+$ 281.1685, found 281.1683.

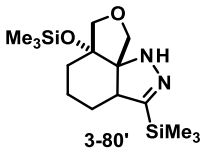

3-80'

^{1}H NMR (500 MHz, $CDCl_3$) δ3.94 (d, 1H, J=9.5Hz), 3.79 (d, 1H, J=7.4Hz), 3.55 (d, 1H, J=9.5Hz), 3.49 (d, 1H, J=7.4Hz), 2.93 (t, 1H, J=6.4Hz), 1.95 (ddd, 2H, J=5.8Hz, J=11.3Hz, J=13.1Hz), 1.68 (tdd, 2H, J=6.7Hz, J=11.4Hz, J=19.0Hz), 1.47 (ddd, 1H, J=6.2Hz, J=12.2Hz, J=13.4Hz), 1.08 (ddd, 1H, J=5.1Hz, J=7.6Hz, J=18.0Hz), 0.20 (s, 9H), 0.15 (s, 9H). ^{13}C NMR (125 MHz, $CDCl_3$) δ 165.5, 80.8, 76.8, 76.1, 74.8, 47.2, 27.1, 23.6, 17.1, 1.8, 1.6. HRMS (ESI) calc. for $C_{15}H_{31}N_2O_2Si_2$ $[M+H]^+$ 327.1924, found 327.1918.

3-82

^{1}H NMR (500 MHz, $CDCl_3$) δ 3.93 (d, *J* = 11.1 Hz, 1H), 3.81 (s, 1H), 3.66 (d, *J* = 11.0Hz, 1H), 2.28 (dt, *J* = 11.6, 6.7 Hz, 1H), 1.82 (dd, *J* = 6.2, 4.6 Hz, 1H), 1.77-1.74 (m,1H), 1.36 (s, 3H), 1.28 (s, 3H), 1.05 (d, *J* = 11.6 Hz, 1H), 0.98 (s, 3H), 0.19 (s, 9H), 0.14-0.10 (s, 9H). ^{13}C NMR (125 MHz, $CDCl_3$) δ 174.76, 78.01, 65.48, 63.07, 49.17, 46.47, 42.91, 28.43, 28.14, 25.43, 24.10, 1.90, -0.53. HRMS (ESI) calc. for $C_{15}H_{27}N_2OSi$ $[M+H-TMS]^+$ 279.1893, found 279.1899.

3.4.4. ORTEPS

ORTEP of 3-56f (CCDC 1433828)

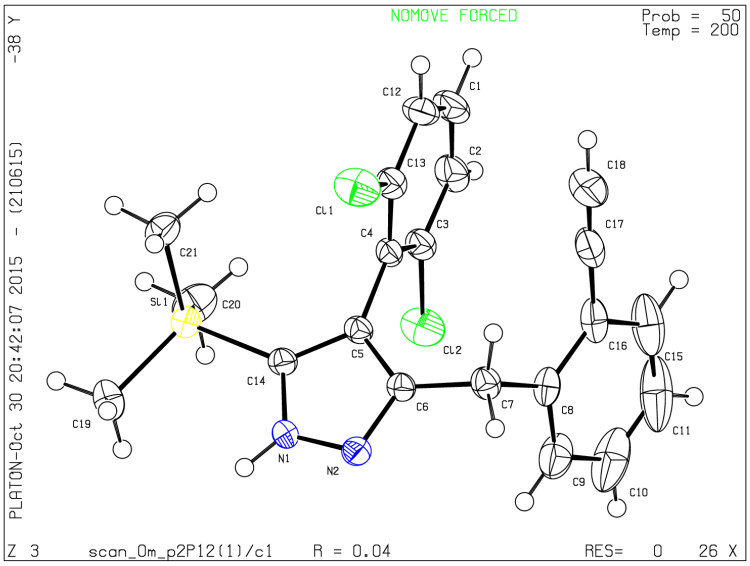

ORTEP of 3-56b′ (CCDC 1433827)

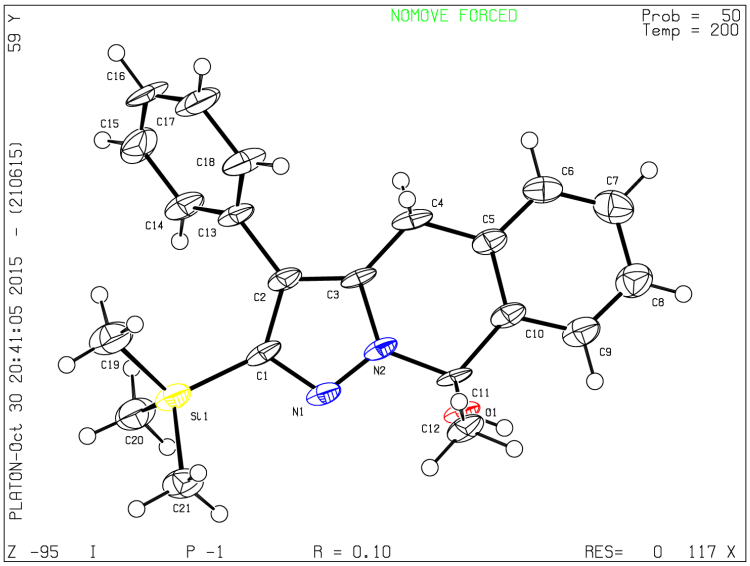

ORTEP of 6b

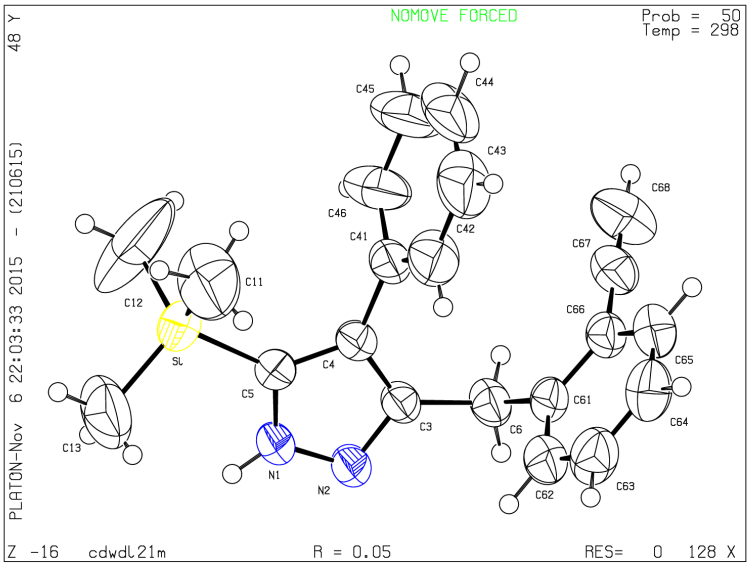

ORTEP of 6d′

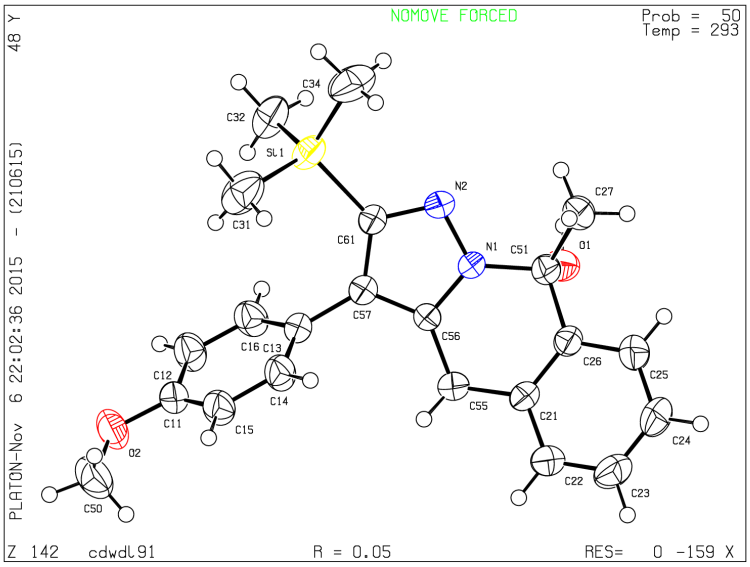

3.5. References

[1] Ho, T. *Tandem Organic Reactions;* Wiley-Interscience: New York, **1992**.

[2] (a) Tietze, L. F.; Beifuss, U. *Angew. Chem., Int. Ed. Engl.***1993**, *32*, 131. (b) Tietze, L. F. *Chem. Rev.* **1996**, *96*, 115. (c) Tietze, L. F.; Brasche, G.; Gericke, K. M. *Domino Reactions in Organic Synthesis;* Wiley-VCH: Weinheim, **2006**.

[3] (a) Denmark, S. E.; Thorarensen, A. *Chem. Rev.* **1996**, *96*, 137. (b) Wasilke, J.-C.; Obrey, S. J.; Baker, R. T.; Bazan, G. C. *Chem. Rev.* **2005**, *105*, 1001. (c) Li, J.; Lee, D. *Eur. J. Org. Chem.* **2011**, 4269.

[4] Robinson, R. *J. Chem. Soc. Trans.*, **1917**, 111, 762.

[5] Kamijo, S.; Dudley, G. B. *J. Am. Chem. Soc.* **2005**, *127*, 5028; b) Kamijo, S.; Dudley, G. B. Org. Lett. **2006**, *8*, 175; c) Shin Kamijo and Gregory B. Dudley, *J. Am. Chem. Soc.* **2006**, *128*, 6499.

[6] a) Grob, C. A.; Schiess, P.W. *Angew. Chem., Int. Ed. Engl.* **1967**, *6*, 1; b) Grob, C. A. *Angew. Chem., Int. Ed. Engl.* **1969**, *8*, 535; c) Prantz, K.; Mulzer, J. *Chem. Rev.* **2010**, *110*, 3741–3766.

[7] Tummatorn, J.; Dudley, G. B. *Org. Lett.* **2010**, *13*, 158.

[8] Barbe, G.; St-Onge, M.; Charette, A. B. *Org. Lett*. **2008**, *10*, 5497.

[9] Lemonnier, G.; Charette, A. B. *J. Org. Chem.* **2010**, *75*, 7465.

[10] Lemonnier, G.; Charette, A. B. *J. Org. Chem.* **2012**, *77*, 5832.

[11] Molander, G. A.; Huerou, Y. L.; Brown, G. A. *J. Org. Chem.* **2001**, *66*, 4511.

[12] Sada, M.; Matsubara, S. *J. Am. Chem. Soc.* **2010**, *132*, 432.

[13] Chandrasekhar, S.; Venkat Reddy, M.; Taki, M. *Tetrahedron Lett.* **1998**, *39*, 6535.

[14] Bandini, M.; Cozzi, P. G.; Giacomini, M.; Melchiorre, P.; Selva, S.; Umani-Ronchi, A. *J. Org. Chem.* **2002**, *67*, 3700.

[15] Hari, Y.; Tsuchida, S.; Sone, R.; Aoyama, T. *Synthesis* **2007**, *21*, 3371.

[16] Liu, H.; O'Connor, M. J.; Sun, C.; Wink, D.; Lee, D. *Org. lett*. **2013**, *15*, 2974.

[17] Ito, T.; Hatano, K.; Kurono, Y.; Aoyama, T.; Shioiri, T. Heterocycles **1993**, *35*, 41.

[18] a) Sun, C.; O'Connor, M. J.; Lee, D.; Wink, D. J.; Milligan, R. D. *Angew. Chem., Int. Ed.* **2014**, *53*, 3197–3200; b) O'Connor, M. J.; Sun, C.; Lee, D. *Angew. Chem., Int. Ed.*, **2015**, *54*, 9963–9966.

[19] a) Brook, A. G. *J. Am. Chem. Soc.*, **1957**, *79*, 4373; b) Brook, A. G.; Quigley, M. A. ; Peddle, G. J. D.; Schwartz, N. V. ; Warner, C. M. *J. Am. Chem. Soc.*, **1960**, *82*, 5102; c) Moser, W. H. *Tetrahedron* **2001**, *57*, 2065–2084.;

[20] For reviews on carbene insertion, see: a) Zhang, Z.; Wang, J. *Tetrahedron* **2008**, 64, 6577–6605; b) Doyle, M. P.; Duffy, R.; Ratnikov, M.; Zhou, L. *Chem. Rev.* **2010**, 110, 704–724; c) Arduengo III, A. J.; Calabrese, J. C.; Davidson, F.; Rasika Dias, H. V.; Goerlich, J. R.; Krafczyk, R.; Marshall, W. J.; Tamm, M.; Schmutzler, R. *Helv. Chim. Acta* **1999**, *82*, 2348–2364.

CHAPTER IV

DESIGN AND SYNTHESIS OF FLUOROPHORES FOR MICROSCOPY APPLICATIONS

4.1. Introduction

The ability to track biomolecules such as proteins, peptides, amino acids or antibodies is a useful tool that is often instrumental in studying biological processes. In this regard, the use of fluorescent labeling is one of the most powerful techniques for this purpose due to its high sensitivity and non-deleterious nature. Furthermore, the use of fluorescence labeling techniques often requires only small measurement volumes and low concentrations of the fluorescent material.[1] Several factors need to be considered when designing fluorescent probes including the size and stability of the probe. There should also be minimal interference with the folding or biological function of the target. Furthermore, the labeling process should be adaptable and efficient; this includes the preferable formation a covalent bond with the target (**Figure 4.1**).[1]

Figure 4.1. Schematic representation of labeling of biomolecule with fluorophore

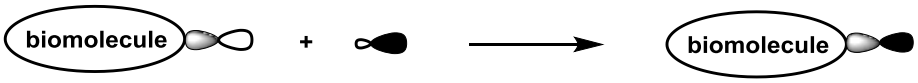

Because of their favorable fluorescent properties, including high fluorescence quantum yields and their tendency to fluoresce at long wavelengths, the benzophenoxazine-based fluorescent dyes have the potential to serve as useful labels for biomolecules (**Figure 4.2**).[2]

Figure 4.2. Benzophenoxazine fluorescent dyes

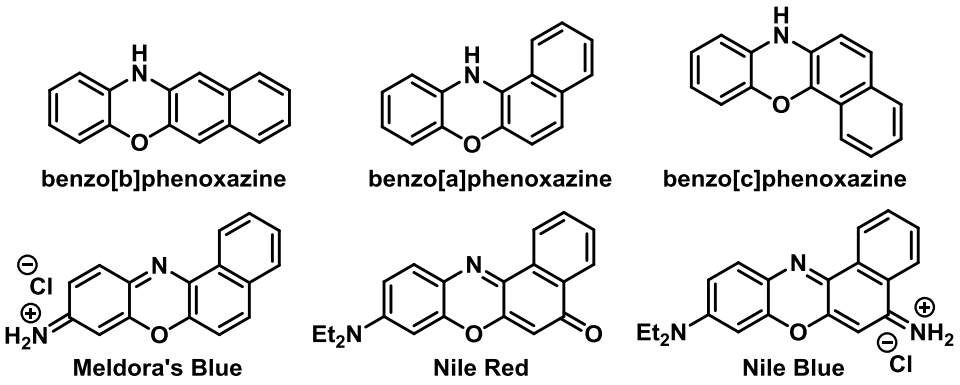

4.1.1. Benzophenoxazine-based fluorophores

As shown in **Figure 4.2**, the benzophenoxazines can take an angular benzo[a/c]phenoxazine or linear benzo[b]phenoxazine shape depending the ring fusion. When electron donating and/or electron withdrawing substituents are added to the benzophenoxazine core, these ring systems can often fluoresce. One example of such compound is Meldola's blue.

4.1.1.1. Meldola's blue

Although it is the oldest of the three most well know benzophenoxazines, Meldola's Blue is the least studied. Mostly used in paints, textiles and paper, this penzo[a]phenoxazine's use is limited to do its poor water solubility. The first synthesis of Meldola's Blue was accomplished in 1979 through the condensation of nitroso compound **4-1** and 2-napthol **4-2** (**Scheme 4.1**). The exact reaction conditions and yield were never reported by Meldola, but a subsequent synthesis has been disclosed relying on a Lewis

Scheme 4.1. First Synthesis of Meldola's Blue

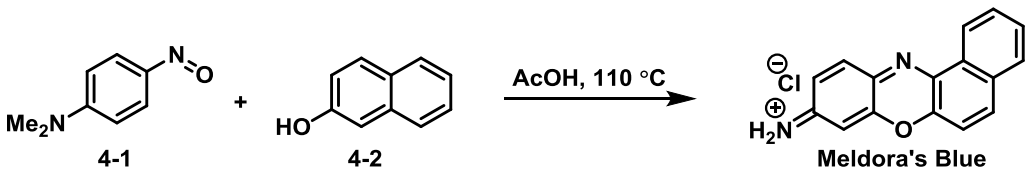

acid approach.[3] The incorporation of the dimethyl amino group into its core evokes a shift in absorption and emission characteristics into a useful range ($\lambda_{max\ abs}$ 540 nm, $\lambda_{max\ emiss}$ 568).[4] The main use of Meldora involves its use as a redox sensor for detection of NADH, pyruvates, glucose, or hydrogen peroxide.[5]

4.1.1.2. Nile Red

One of Nile Blue's most studied relatives is the oxidized, neutral, Nile Red **4-3** (**Scheme 4.2**). The fluorescent properties of this fluorophore are due to the ability of the diethylamino group to donate electron density across the ring system into the carbonyl group as shown in **Scheme 4.2**.

Scheme 4.2. Nile Red electron delocalization

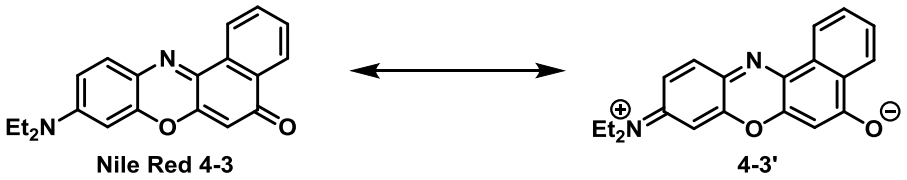

Nile Red was first synthesized through a condensation reaction of 5-amiono-2-nitrosophenol **4-4** with 1-naphthol **4-5** as shown in **Scheme 4.3.1**. Alternatively, Nile Red can be synthesized directly from Nile Blue **4-6** via hydrolysis under acidic conditions (**Scheme 4.3.2**).

Scheme 4.3. Nile Red Synthesis

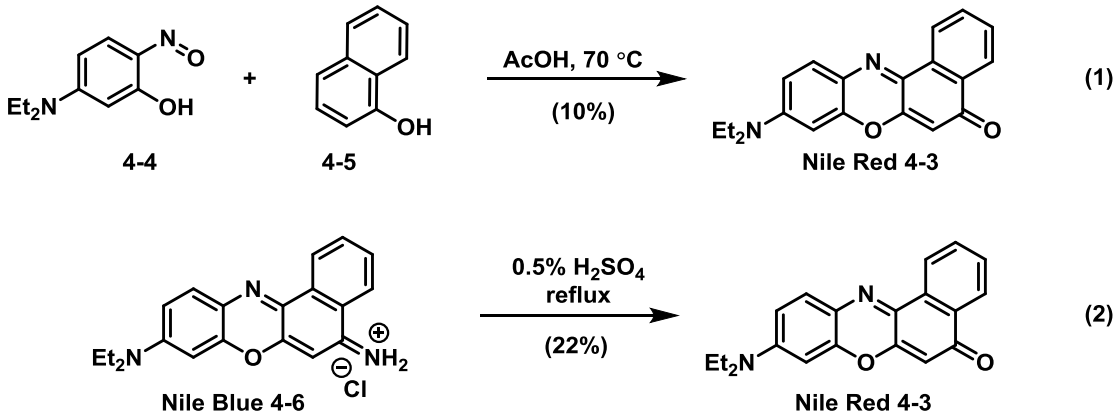

Due to Nile Red's low solubility in water, several analogs have been constructed to increase water solubility and provide sufficient handles for attachment to biomolecules. For example, 6-carboxy ethyl analogs **4-7** were synthesized containing tethered hydroxyl groups or morpholine rings appended to the benzophenoxazine core in 24-60% (**Scheme 4.4**).[6]

Scheme 4.4. 6-carboxy Nile Red derivatives

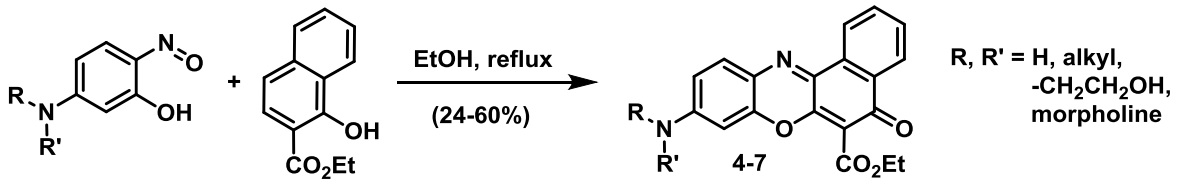

Significant advances in Nile Red analogs came with the introduction of 1- and 2-hydroxy Nile Red (**4-9** and **4-11** respectively) by Briggs (**Scheme 4.5**).[7] Starting from 5-amiono-2-nitrosophenol **4-4** and 1,5-dihydroxynaphthalene **4-8**, 1-hydroxy Nile Red **4-9** (1-HONR) could be isolated in 70% yield. Similarly, **4-4** and 1,6-dihydroxynaphthalene **2-10** can be mixed in DMF at refluxing temperatures to generate 2-hydroxy Nile Red (2-HONR) **4-11** in 65% yield (**Scheme 4.5.2**). The hydroxyl group on these Nile Red analogs serves as an effective handle for further functionalization of the fluorophore.

Scheme 4.5. Hydroxy Nile Red analogs

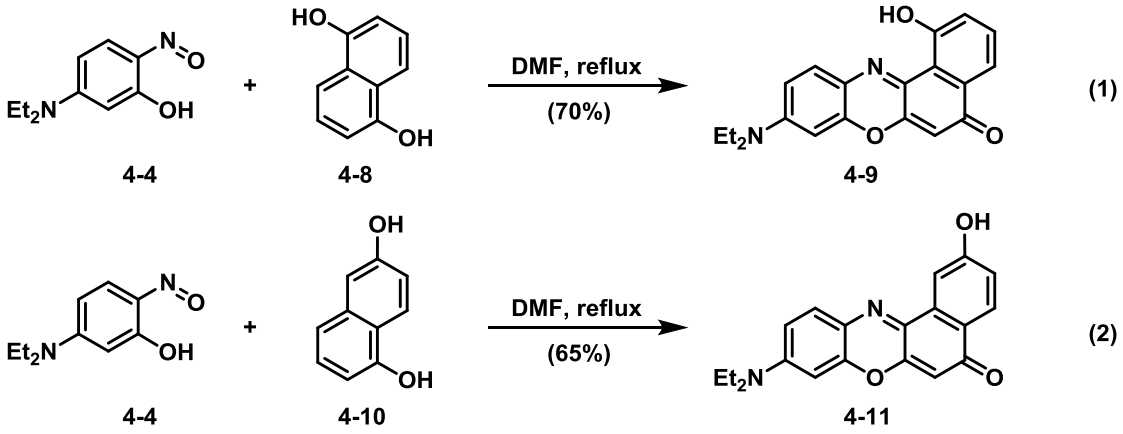

Briggs and co-workers showed that 2-HONR **4-11** could be further functionalized via alkylation followed by hydrolysis with PLE into acid **4-12**. Likewise, acylation with adipic anhydride in the presence of DMAP leads to Nile Red analog **4-13**.[7] Significant breakthroughs in the appendage of biomolecules came with the transformation of 2-HONR into thiol-selective analogs **4-14** and **4-15**. The synthesis of α-iodoacetamide **4-14**, was accomplished in a three step sequence via alkylation with *N*-(2-bromoethyl)-phthalimide, aminolysis and treatment with iodoacetic anhydride.[8] Finally, Nile Red maleimide **4-15** was synthesized by the Moerner group in three steps from 2-HONR via alkylation followed by retro-Diels-Alder reaction to liberate the free maleimide.[9]

Scheme 4.6. Further transformations of 2-hydroxyl Nile red

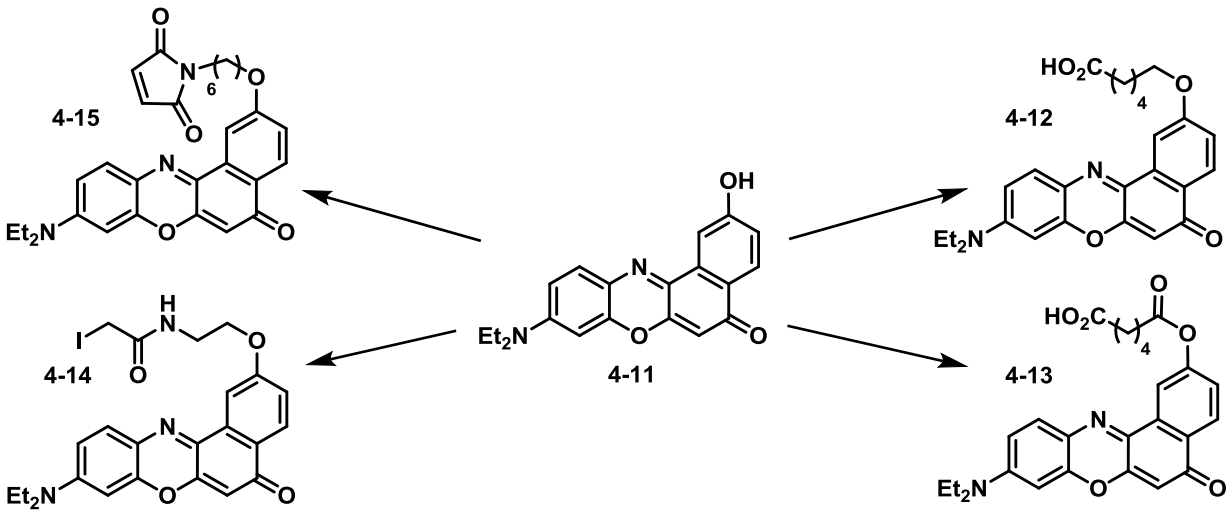

Several fluorinated Nile Red derivatives were synthesized, and one such example is shown in **Scheme 4.7**.[10] Starting from diethylamino phenol and tetrafluoronaphthalene **4-16**, a series of S_NAr reactions leads to compound **4-18** after oxidation. Reduction with zinc under acidic conditions yields the phenoxazine core of fluorinated analog **4-19**. The properties of these analogs changed the spectroscopic properties of this benzophenoxazine only slightly when compared to that of Nile Red.

Scheme 4.7. Preparation of 6-fluoro Nile Red

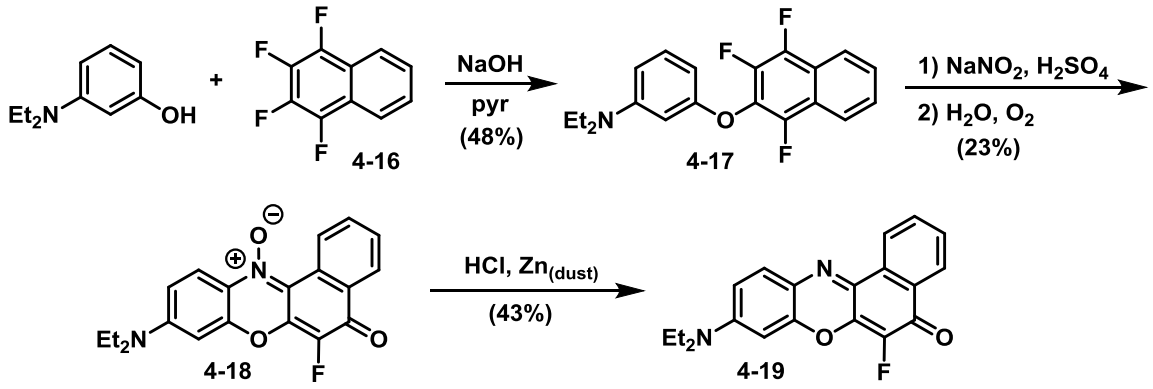

Leading to their non-fluorescent nature, the FLAsH dyes contain a bisarsenic moiety which quenches the excited state by way of intramolecular energy transfer (**Scheme 4.8**).[11] This class of Nile Red

Scheme 4.8. Preparation of FLAsH system

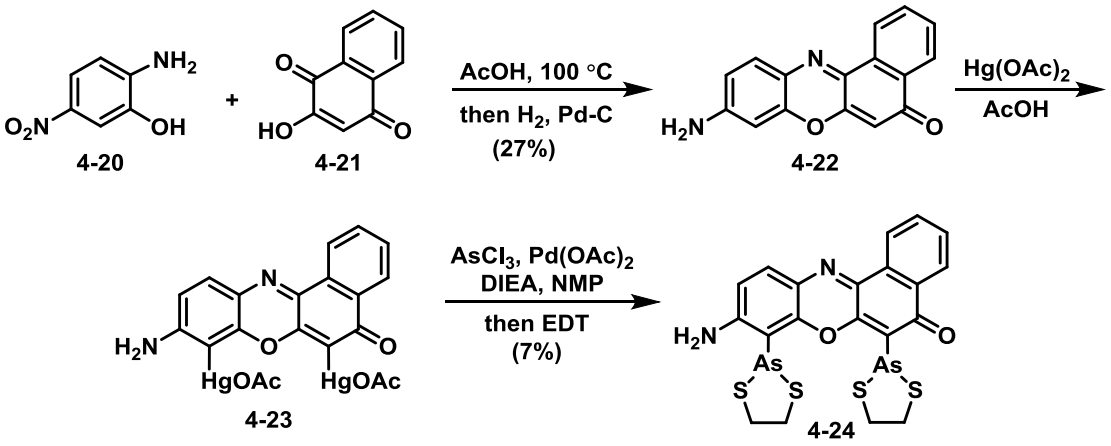

dye is synthesized via condensation to the benzophenoxazine core in absence of the *N*,*N*-diethylamino group. Mercuration with mercury(II)acetate gives compound **4-23** which is converted into the 'FLAsH dye' **2-24** with 1,2-ethanedithiol after treatment with $AsCl_3$ in the presence of a palladium(II)acetate. This particular class of dye reacts with specially engineered proteins containing dicysteine residues which has two effects. The first is alternating the oxidation potential at the arsenic center, and the second is restricting the rotation around the C-As bond. These structural changes render the dye-protein complex fluorescent.

Table 4.1. Other Water soluble Nile Red analogs by Burgess[12]

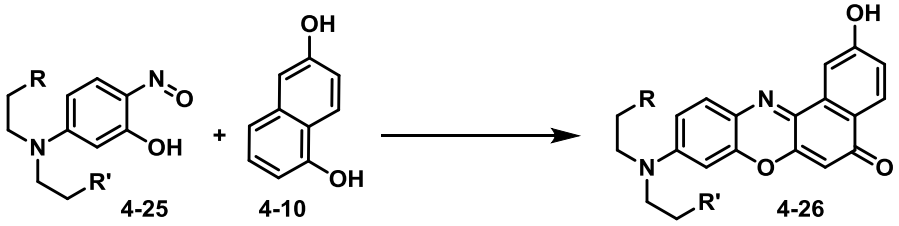

entry	R	R'	additive	solvent	T (°C)	yield (%)
1	CH_2OH	CH_2OH	none	DMF	153	54
2	CO_2Me	CO_2Me	$HCl_{(aq)}$	MeOH	65	53
3	CH_2SO_3H	CO_2H	none	DMF	153	53

4.1.1.3. Nile Blue

Red Red's not too distant cousin is the oxidized, positively charged, phenoxazinium, Nile Blue. First synthesized in 1986 through the condensation of 5-amino-2-nitrosophenol **4-4** with 1-aminonaphthalene **4-27**, the yield of Nile Blue **4-28** was only 3%.[13] An increase in yield was achieved with the use of perchloric acid in ethanol (**Scheme 4.9**).[14] Nile Blue **4-28** has significantly better water solubility than Nile Red, and this increase in solubility is due to its cationic nature when compared to its neutral relative **4-3**.

Scheme 4-9. First synthesis of Nile Blue

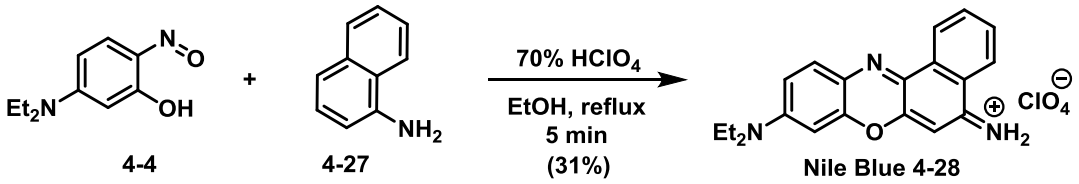

Derivatives of Nile Blue have been made utilizing 8-hydroxyjulolidine **4-29** (**Scheme 4.10**).[14] This amine is "privileged" in dye synthesis because it locks the nitrogen lone pair into conjugation with the aromatic ring skeleton. One drawback is that the julolidine moiety is quite hydrophobic, so solubility is low in aqueous media. For the synthesis, 8-hydroxyjulolidine **4-29** is not sufficiently reactive, so the more reactive azo-functionalized counterpart **4-30** is required. Several analogs containing the 8-hydroxyjulolidine **4-29** moiety were constructed, but like most chemistry of the benzophenoxazines, the applicability was limited by yields.

Scheme 4.10. 8-Hydroxyjulolidine-based Nile Blue Analogs

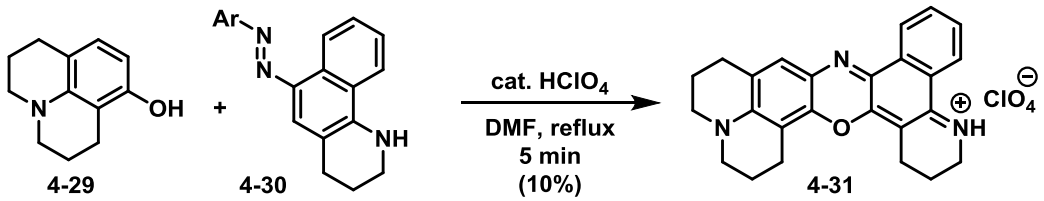

Other modifications to Nile Blue involve efforts to increase water solubility. Several Nile Blue analogs containing sulfonic acid groups have been synthesized (**Scheme 4.11**).[15] Treatment of 5-amino-2-nitrosophenol **4-4** with prefunctionalized β-amino acid **4-32** under acidic condition led to Nile Blue derivative **4-33**. Alternatively, phenol **4-34** could be treated with nitroso compound **4-35** to yield **4-36** in 10% yield after treatment with hydrochloric acid. Finally, similar to the synthesis of Nile Blue, nitrosophenol **4-37** could be condensed with 1-amino naphthalene **4-27** to yield sulfonic acid Nile Blue analog **4-38** in 64% yield (**Scheme 4.11.3**). Compounds **4-33** and **4-36** are the so-called EVO Blue dyes which are more stable than rhodamine and BODIPY dyes under acidic conditions. Applications of dyes of this type could find potential uses in high throughput screening processes and solid phase synthesis where cleavage of compounds from resins is accomplished using acidic conditions.

Scheme 4.11. Water soluble Nile Blue analogs

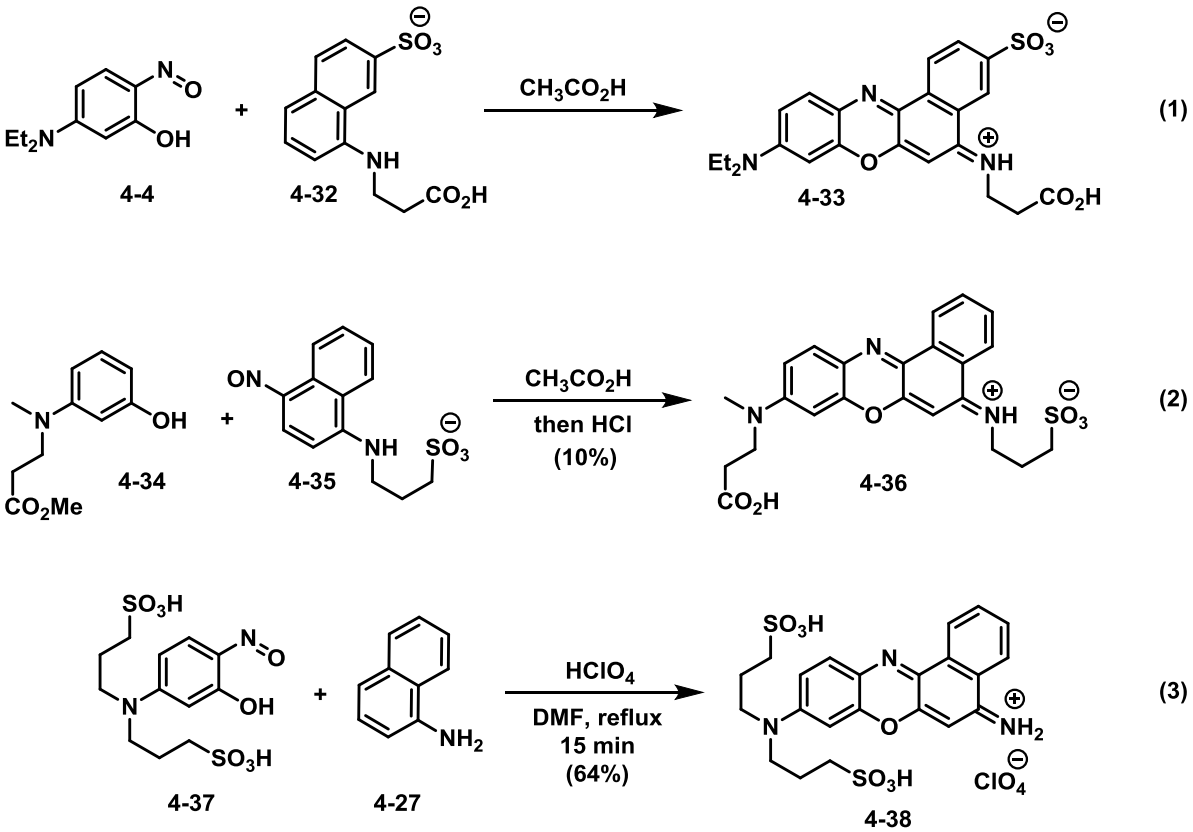

Scheme 4.12. Halogenation of Nile Blue

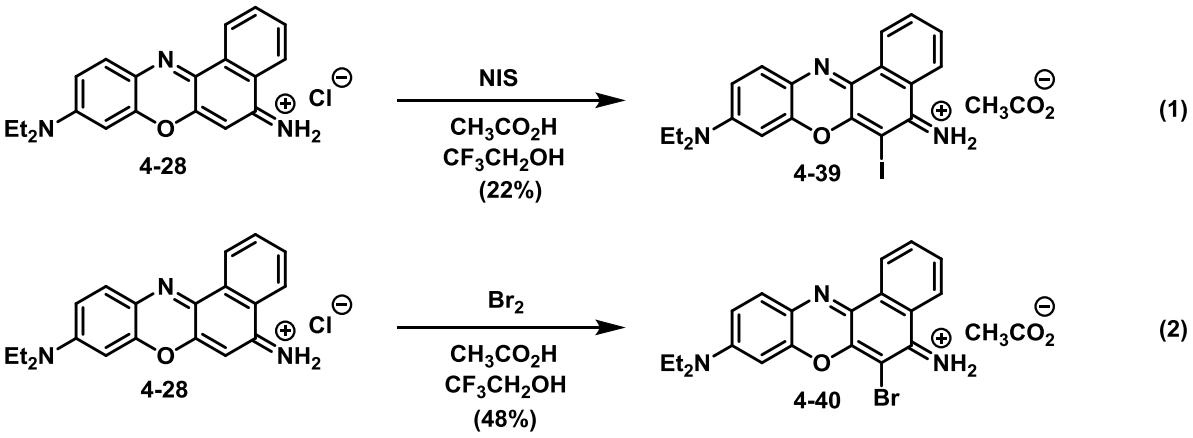

Direct halogenation of Nile Blue has also been reported (**Scheme 4.12**).[16] Although the reactions are limited by yields, treatment of Nile Blue with NIS in the presence acetic acid and trifluoroethanol yields iodo-Nile Blue **4-39** in 22% yield. Similarly, when Nile Blue is subjected to similar reaction conditions and mixed with bromine, bromo-Nile Blue **4-40** can be isolated in slightly higher yield (48%). These halogenated analogs of Nile Blue were could possibly serve as intermediates in the preparation of more functionalized analogs, but they were first prepared as photosensitizers to initiate processes that are cytotoxic to carcinogenic cells.

4.1.1.4. Other benzophenoxazine dyes

The synthesis of other benzophenoxazine-based dyes is underexplored, and most of the literature of this class of dyes is limited to the benzo[a]phenoxazines. The benzo[b]phenoxazine has been constructed starting from 2-aminophenol **4-41** and 2,3-dihydroxynaphthalene 4-42 (**Scheme 4.13**).[17] Condensation of 2-aminophenol **4-41** and 2,3-dihydroxynaphthalene **4-42** was accomplished under an atmosphere of carbon dioxide to give the linear benzo[b]phenoxazine **4-43** in 55% yield. Nitration with sodium nitrite led to compound **4-44** which was reduced tin(II)chloride under acidic conditions to **4-45**. Compound **4-45** has the potential to be strongly fluorescent, but the authors chose to neutralize the compound to **4-46** before examining this benzophenoxazines fluorescent properties.

Scheme 4.13. Synthesis of benzo[b]phenoxazine analogs

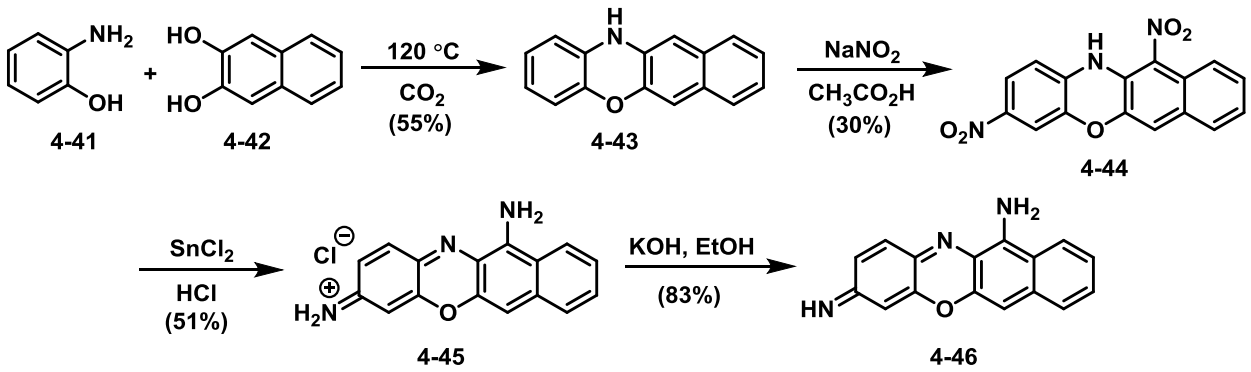

Only one example exists in the literature on the synthesis of a benzo[c]phenoxazine (Scheme 4.14).[18] For this lone example, 4-nitroso phenol **4-47** was condensed with 1-napthol **4-5** in the presence of Zn(II)Cl to give benzo[c]phenoxazine **4-48** in 2-3% yield. Unfortunately, the fluorescent properties of **4-48** were not reported, and the molecule does not contain an electron donating group in conjugation with the carbonyl, a property essentially conserved in most fluorescent molecules.

Scheme 4.14. Synthesis of benzo[c]phenoxazine

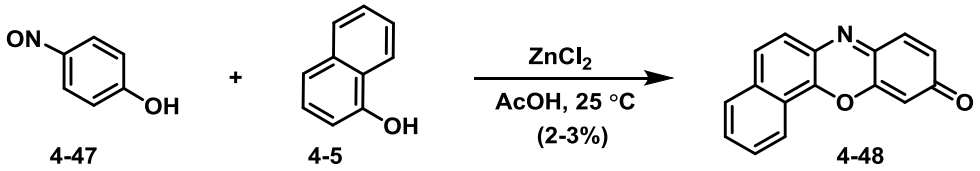

4.1.2. TCF and ITCF analogs

The 2-dicyanomethylene-3-cyano-2,5-dihydrofuran (DCDHF) or tricyanofuran (TCF) moiety has evolved into one of the most useful π-acceptors in the design of push-pull fluorophores. These accepting structures are separated from the electron donating unit by a π-electon rich conjugated linker as shown in **Figure 4.3**, and they are frequently used in nonlinear optical applications.[19] The use of these chromophores in fluorescence single-molecule imaging has only recently emerged.[20]

Figure 4.3. General TCF (DCDHF) fluorophore structure

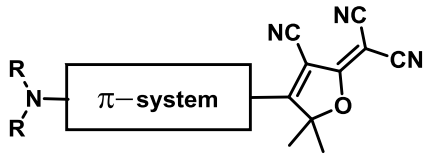

The earliest synthesis of TCF **4-51** was reported by the Melikian group when they reacted 3-hydroxy-3-methylbutan-2-one **4-49** with two equivalents of malonitrile **4-50** in the presence of sodium ethoxide (**Scheme 4.15**).[21] Melikian further demonstrated that TCF **4-51** could be condensed with aromatic aldehydes into the chromophore **4-52** although its properties were not further investigated.

Scheme 4.15. Early synthesis of TCF fluorophore

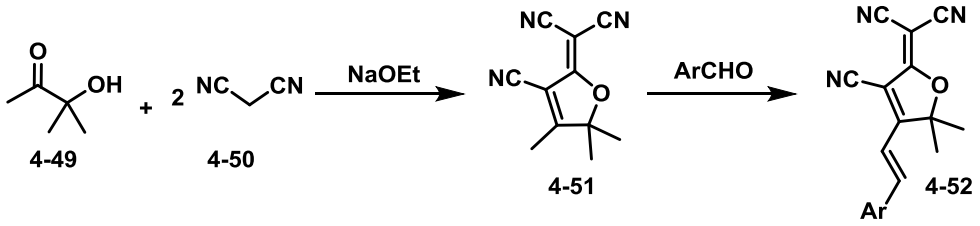

The group of Villemin later showed that the rate, simplicity and efficiency of the reaction could be improved by using microwave irradiation (**Scheme 4.16**).[22] In their study, the authors observed imidate **4-53**, the intermediate condensation product from the reaction of one equivalent **4-50** with **4-49**.

Scheme 4.16. Improved synthesis of TCF fluorophore

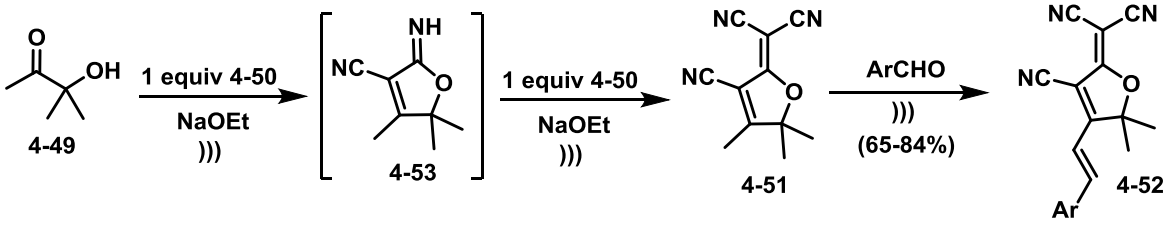

Application of the TCF fluorophore in single-molecule imaging studies was first demonstrated by Moerner.[23] In their study, a series of DCDHF fluorophores were synthesized utilizing the general process

Table 4.2. TCF fluorophores for single molecule imaging

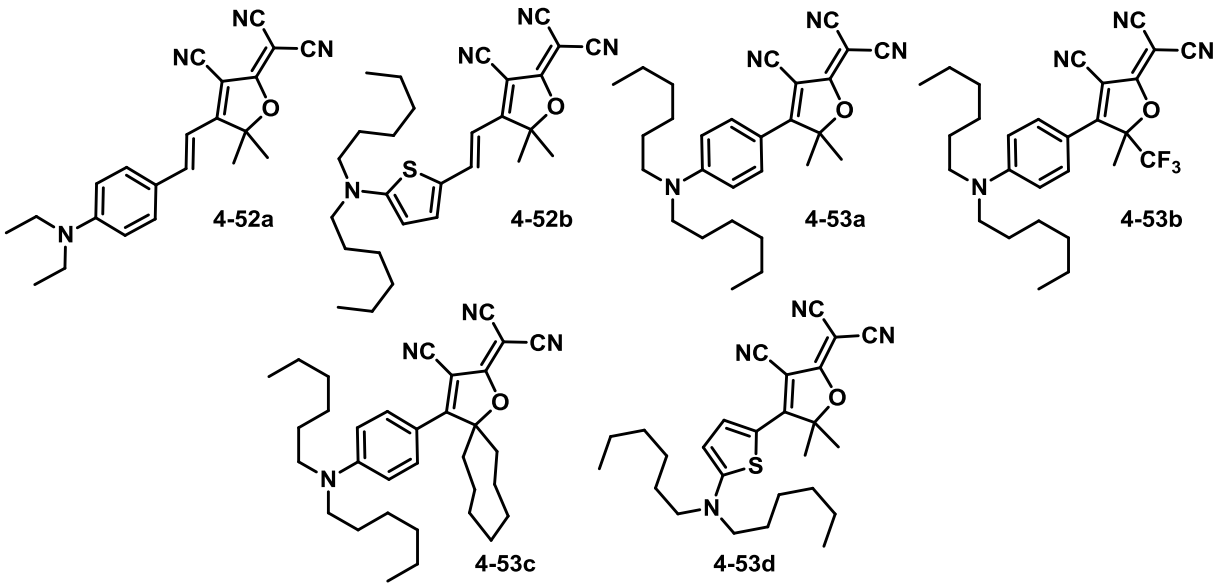

shown in **Scheme 4.15** (**Table 4.2**). Compounds 2-52a and 2-52b were the consequence of tandem condensation followed by treatment with the corresponding aromatic aldehyde. Alternatively, the electron donating aromatic ring could be appended directly to the TCF moiety using the appropriate α-hydroxy ketone (compounds **4-53a** to **4-53d**). Furthermore, in this report, Moerner reported the photophysical parameters of this new class of fluorophore. It was found that the fluorescence quantum yield (Φ_F) was moderate and below that of the rhodamines, but this value was highly dependent on concentration.

In a subsequent report, Moerner investigated some lipid-like TCF fluorophores **4-53** in their diffusion into the cell membrane (**Table 4.3**).[24] In this study, several new TCF fluorophores were constructed with favorable characteristics for membrane diffusion. Long greasy, nonpolar alkyl chains were used on the donor end of the fluorophore to aid in diffusion into the lipophilic membranes (compounds **4-53e** and **4-53f**). Two charged fluorophores were also synthesized, **4-53g** and **4-53h**, but these compounds displayed the lowest diffusion coefficients. This implies that the electrostatic effects affect diffusion of the TCF fluorophore into the Chinese hamster ovary cell plasma membranes that were investigated. This is

not unexpected, though, because the electrostatic nature of the probe would attract hydrophilic entities which are not conducive for diffusion into a plasma membrane.

Table 4.3. TCF fluorophores for membrane diffusion studies

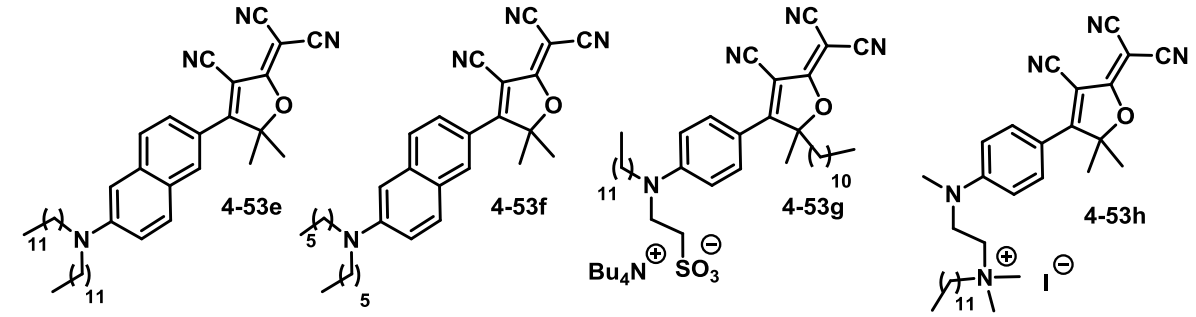

Later, Moerner and Lord investigated the effect of tetrahydroquinoline rings in the TCF fluorophore structure (Table 4.4).[25] Introduction of the first tetrahydroquinoline ring increased the fluorescence quantum yield (compounds 4-52c and 4-53i). When the second tetrahydroquinoline ring was introduced, a smaller effect was observed (compounds 4-52d and 4-53j). In general, when the donor ring is annulated to a benzene or naphthalene ring, a bathochromic shift in absorption was observed. Overall, the fluorescence properties of the TCF fluorophores were retained with these changes, but the solubility in aqueous systems was decreased.

Table 4.4. TCF fluorophores containing tetrahydroquinoline and related structures

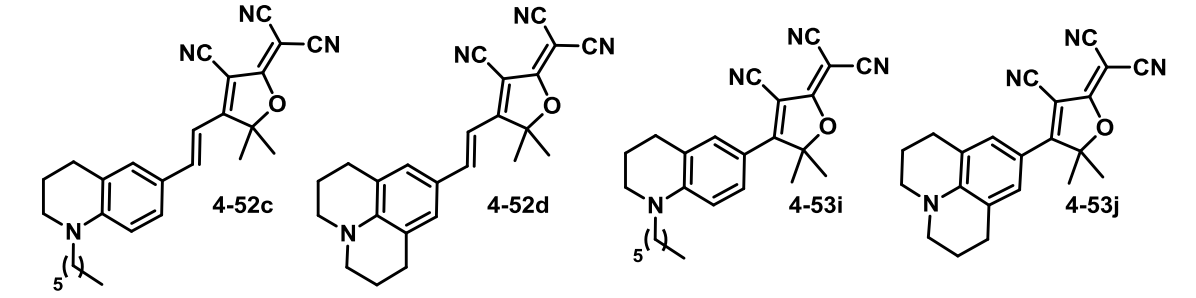

Shortly after, Lord and Moerner synthesized an acene TCF fluorophore (Scheme 4.17).[26] Starting from 2-bromo-6-dihexylaminoanthracene 4-54, a-hydroxy ketone 4-55 was synthesized in two steps via treatment with *n*-BuLi followed by trapping with TMS-protected acetone cyanohydrin and acidic hydrolysis. Condensation with malonitrile in the presence of pyridine led to 4-53k in 37% yield over 3 steps. This fluorophore exhibited favorable fluorescent properties including photostability, emission wavelength dependent on solvent polarity, and quantum yield relative to solvent viscosity. Likewise, absorption and emission occurred at longer wavelengths which was favorable for cellular imaging. Moreover, this new class of TCF fluorophore was found to be less photolabile in aqueous environment. Finally, the group was able to image single copies of the TCF acene fluorophore diffusing into the plasma membrane of living cells.

Scheme 4.17. Synthesis of acene DCDHF fluorophore

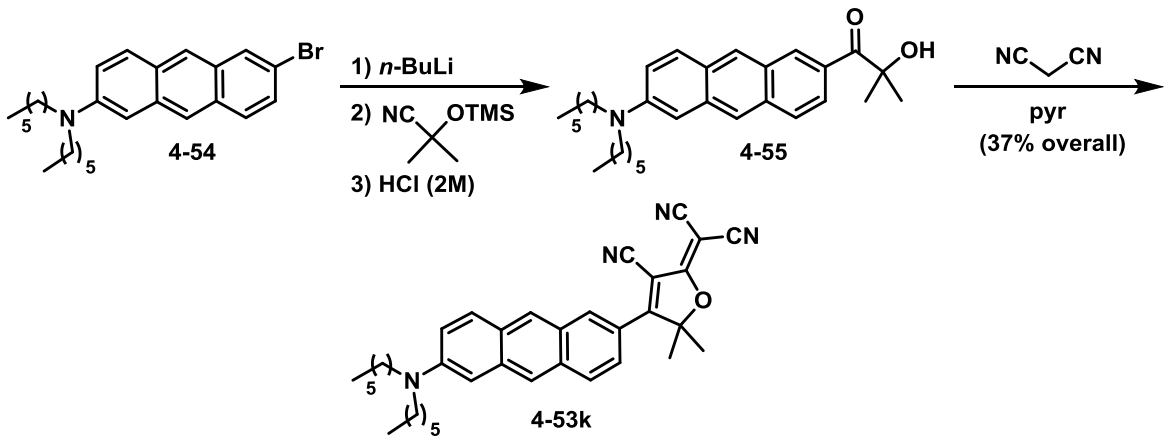

Also utilizing the DCDHF probe, Moerner and coworkers developed an improved molecular beacon for nucleic acid detection (**Figure 4.4**).[27] The group refers to their new probe as a self-quenched intramolecular dimer (SQuID) molecular beacon (MB). These MBs are single-stranded, "stem-loop" oligonucleotide probes which are utilized to detect particular nucleic acid sequences in solution. In this particular system, quenching occurs in the closed hairpin conformation because of an excitonic interaction between the two fluorophores which dimerize forming a non-emissive product.[28] Some advantages of this novel molecular beacon are one-pot labeling, visible colorimetric target detection and single molecule two-

step photobleaching behavior which allows for the discrimination of functional MBs and background fluorescence.

Figure 4.4. Structure of NHS ester-functionalized TCF fluorophore molecular beacon

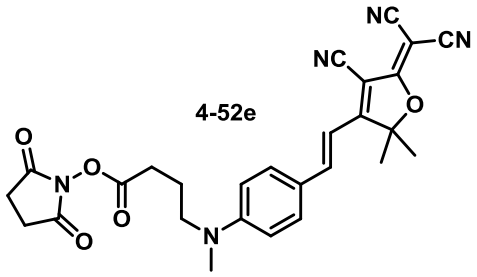

Lord and Moerner later modified the TCF fluorophore with appendages aimed at increasing water solubility (**Table 4.5**).[29] Modification of the disubstituted aniline portion of the fluorophore via nucleophilic aromatic substitution led to a variety oxygenated TCF analogs. Installation of hydroxyl groups led to compounds **4-53l** and **4-53m** which had water solubilities of 0.40 and 1.40 ppm respectively. When carboxylic acid groups were installed, solubility increased dramatically. Compound **4-53n** and **4-53o** had water solubilities of 3.80 and 2800 respectively.

Table 4.5. Water soluble TCF fluorophores

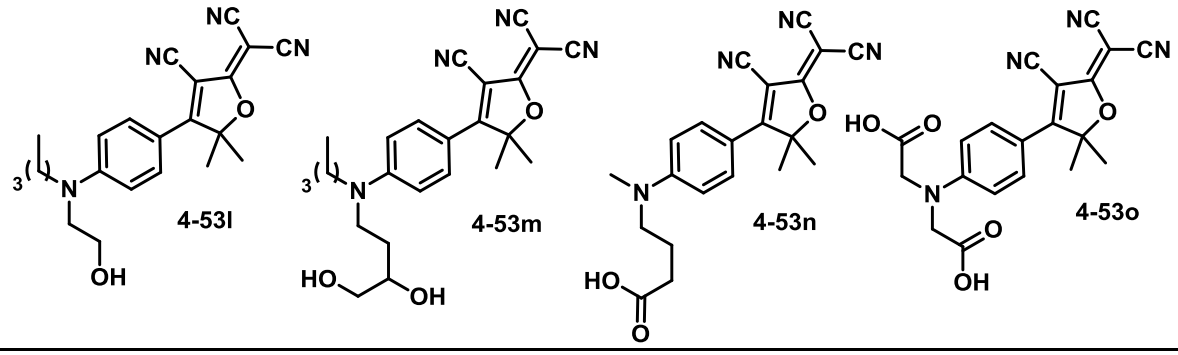

In a recent study, Moerner and Lord disclosed "a photoactivatable push-pull fluorophore for single molecule imaging in live cells" (**Scheme 4.18**).[30] Using Chinese hamster ovary (CHO) cells the scientists demonstrated that compound **4-52e** could diffuse into the CHO cell plasm membrane. When a short flash

of diffuse violet light is exerted on the cell, the fluorescence in the cytosol turns on. The activation is based on conversion of the azide in **4-52e** into the amine of **4-52f** when exposed to low intensity violet light. This photoactivation shifts absorption to long wavelengths and creates a bright red emitter.

Scheme 4.18. Photoactivatable TCF fluorophore for imaging in live cells

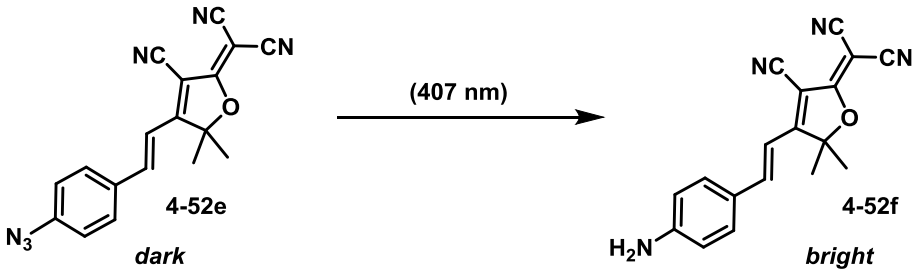

4.2. Results and discussion

The design plan for construction of a new thiol-selective fluorophore is outlined in **Figure 4.5**. Utilizing hydroxyl group (shown) or other heteroatom handle, a linker can be attached to the fluorophore which would then be tethered to a Michael acceptor for the thiol residue of the biomolecule. In this regard, 2-hydroxy Nile Red **4-11** is an optimal candidate for further exploration.

Figure 4.5. General strategy for fluorophore design

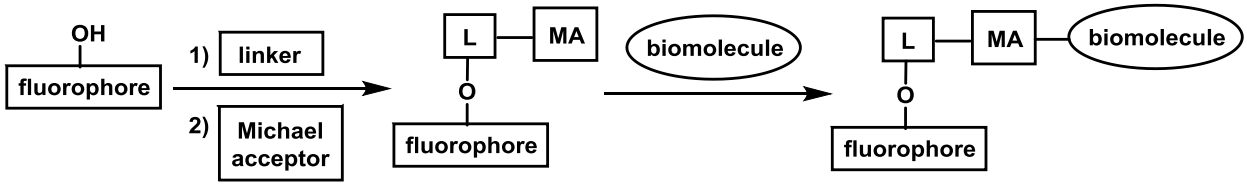

4.2.1. Nile Red analogs

By adapting the above strategy (**Figure 4.5**), a general approach for synthesis of a fluorophore probe involving the benzophenoxazine Nile Red can be envisioned (**Figure 4.6**). By attaching a linker to and Michael acceptor to **4-11**, the new thiol-selective probe can be realized.

Figure 4.6. General strategy for Nile Red-based fluorophore design

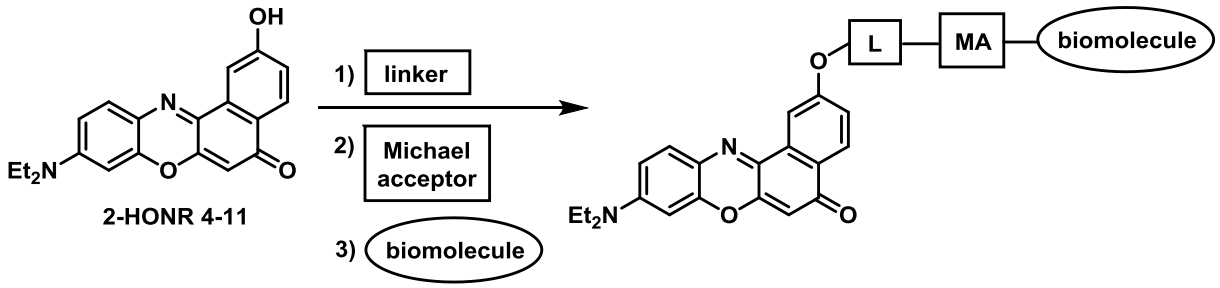

The first generation Nile Red-based fluorophore synthesis is shown in **Scheme 4.19**. Following the general procedures discussed earlier (**Section 4.11**), 2-hydroxy Nile Red **4-11** could be isolated from the reaction of nitroso compound **4-4** and 1,6-dihydroxy naphthalene **4-10**. When considering the linker, the shortest and simplest would be a carbon-oxygen σ-bond. In this regard, the acrylate Michael acceptor was attached directly to **4-11** producing Nile Red acrylate **4-54**. Delightfully, compound **4-54** behaved well in the microscopy experiments and fluoresced immensely in an orthogonal manner to the commercially available Acrylodan.[31] The big limitation to this first generation fluorophore was it was extremely "sticky" and adhered to all surfaces including glass and plastic. Also, the dye was impossible to remove from the biomolecules, and it could not be simply washed away. To confirm that the thiol residue of the biomolecule was indeed binding to the probe in a covalent manner, an NMR study was undertaken (**Figure 4.7**).

Scheme 4.19. Synthesis of Nile Red acrylate

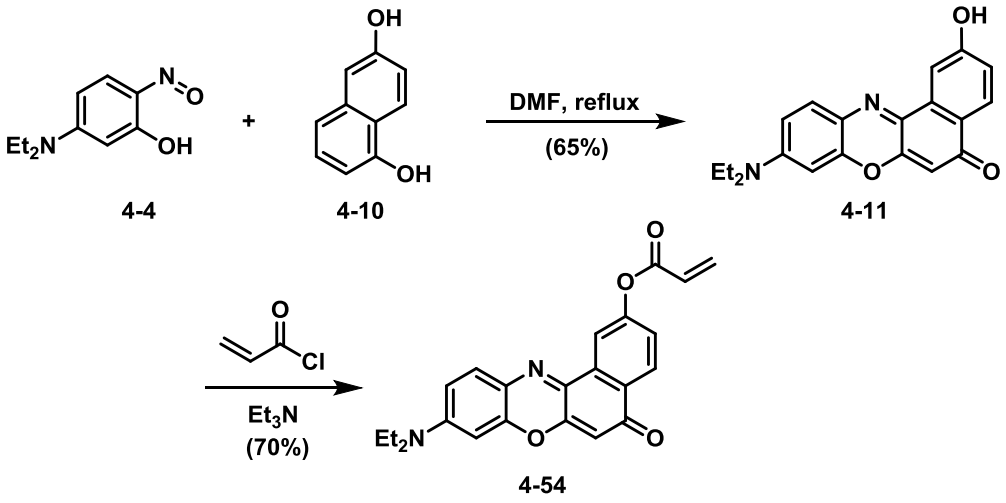

Figure 4.7. Probe binding NMR study

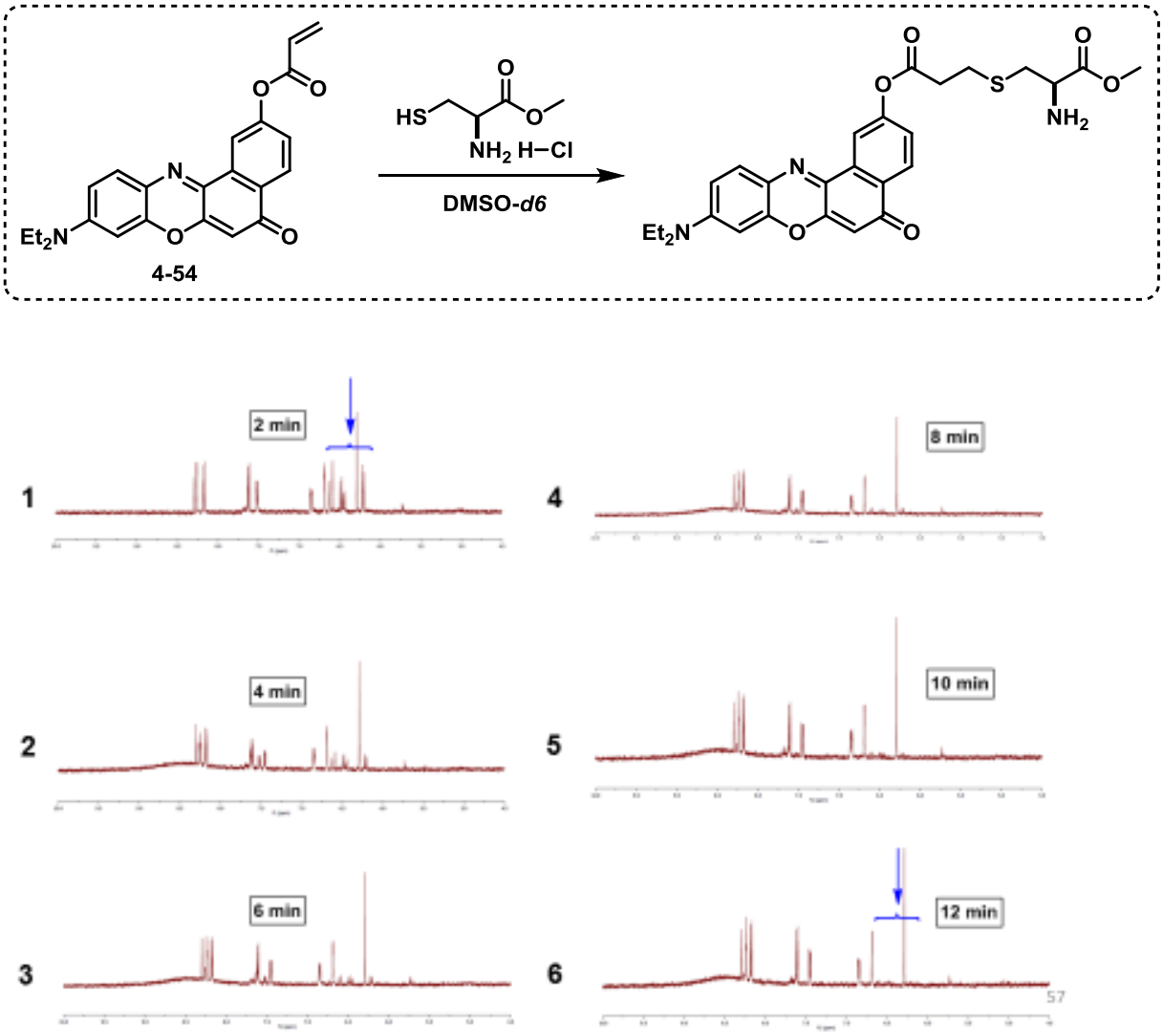

When Nile Red acrylate **4-54** was dissolved in DMSO and then exposed to L-Cysteine methyl ester hydrochloride, clear indication of Michael addition of the thiol residue to acrylate of 4-54 was apparent (**Figure 4.7**). During the time scale of six NMR experiments, the acrylate signals disappeared as the Michael addition took place. This simple series of experiments verified a covalent bonding interaction of the newly designed probe and thiol residue. Although the above experiments solidified the understanding of probe-thiol residue interaction, the problem still existed of fluorophore removal and its tendency to leech onto surfaces of all different compositions.

Scheme 4.20. Nile Red linker installation

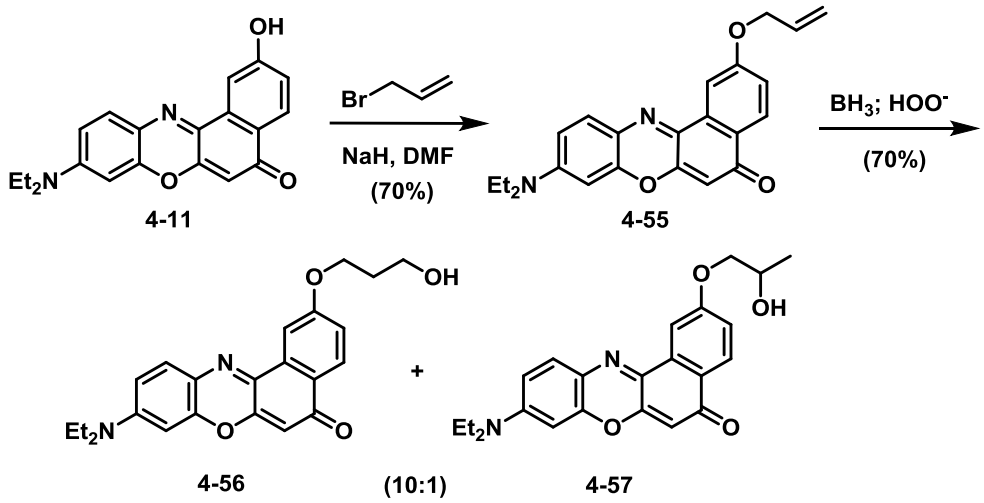

In order to circumvent the above mentioned limitations of probe **4-54**, linker installation was commenced (**Scheme 4.20**). Benzophenoxazine **4-11** was exposed to sodium hydride in DMF and then treated with allyl bromide generating 2-alloxy Nile Red **4-55** in 70% yield. Hydroboration of the resulting allylic ether gave **4-56** and **4-57** in a 10:1 mixture of regioisomers. These compounds were then treated with acryloyl chloride in the presence of triethylamine the same way as before to generate two new probes **4-58** and **4-59** in 72 and 75% yields respectively.

Scheme 4.21. Nile Red acrylate with linker

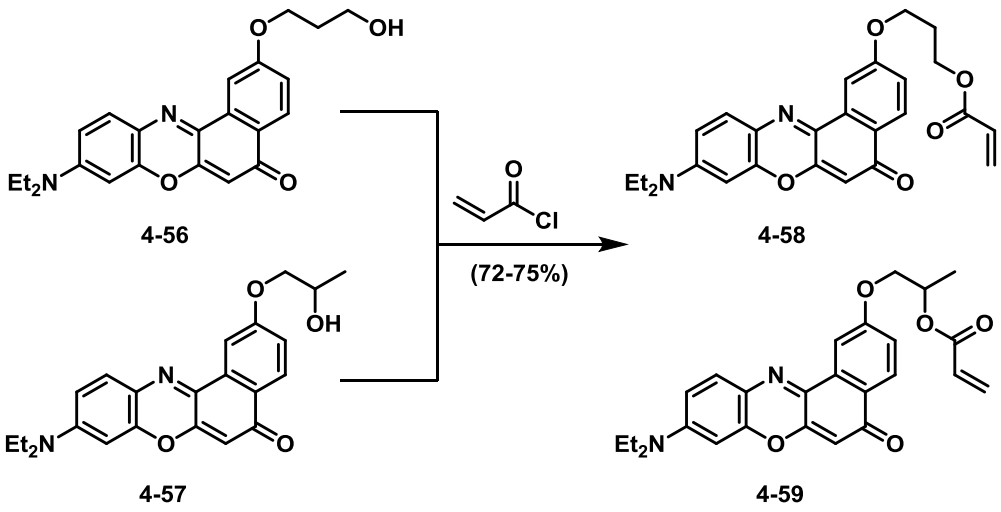

In an effort to increase water solubility, the donor end of Nile Red fluorophore was modified with ester functionality (**Scheme 4-22**). When 3-aminophenol was treated with excess acrylic acid and then esterified under acidic condition, phenol **4-60** was produced in 55% over two steps. Following the standard procedures, fluorophore **4-61** was synthesized in a three step sequence consisting of nitration, condensation with 1,6-dihydroxynaphthalene and acrylation in 33% overall yield. When compared to Nile red acrylate **4-54**, the three newly generated fluorophores (**4-58**, **4-59**, **4-61**) did not exhibit any significant improvement on water solubility or removal. At this juncture, attention was turned to the design of a fluorophore probe that contained a hydroxy group which could aid in both water solubility and removal.

Scheme 4.22. Modification of the donor end of fluorophore

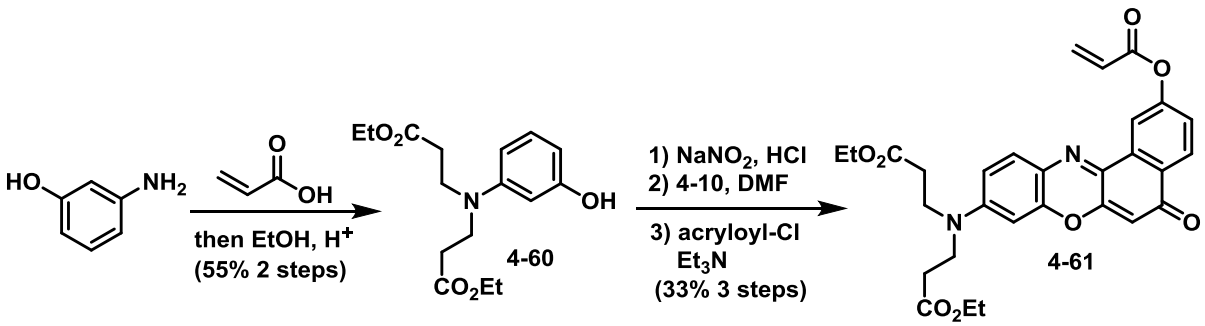

To this end, 2-allyloxy Nile red **4-55** was treated with catalytic osmium tetroxide and NMO to produce Nile Red diol **4-62** (**Scheme 4.23**). Nile Red diol **4-62** was exposed to sodium hydride and tosyl chloride generating epoxide **4-63** in 60% yield. This epoxide was opened with sodium hexamethyldisilazide to afford the 1,2-amino alcohol after chromatography on silica gel. Finally, acrylamide **4-64** was generated by treatment with acryloyl chloride and triethylamine. This fluorophore exhibited some favorable properties, but the lengthy synthesis made it uneconomical to scale for the microscopy studies. To overcome this, Nile Red diol **4-62** was treated with substoichiometric acryloyl chloride in the presence of triethylamine (**Scheme 4.24**). This process generated a separable mixture of both mono- (**4-65**) and bisacrylated Nile Red (**4-66**).

Scheme 4.23. Synthesis of Nile Red acrylamide

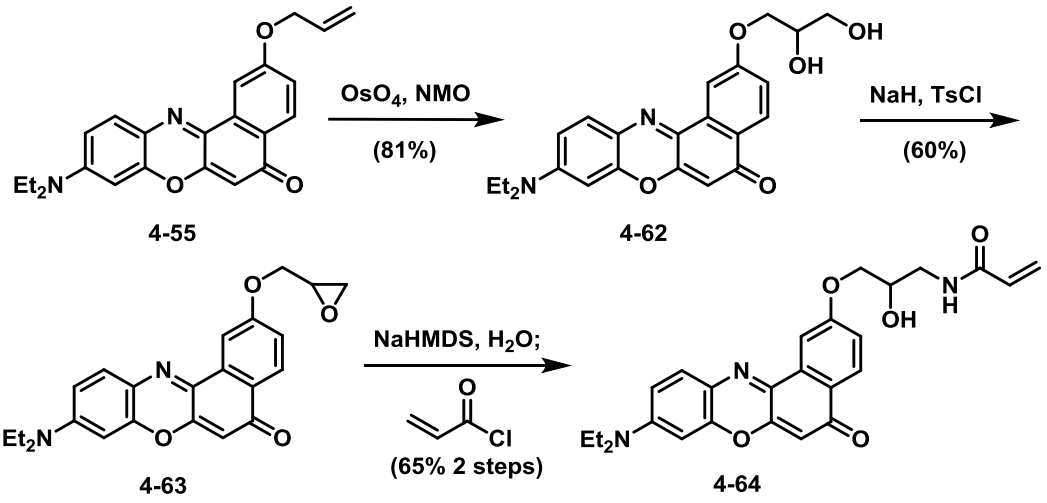

The properties of compound 4-65 were found to be highly desirable in both fluorophore performance and removal, the properties of which will be discussed in detail in Section 4.2.3.

Scheme 4.24. Direct acrylation of Nile Red diol

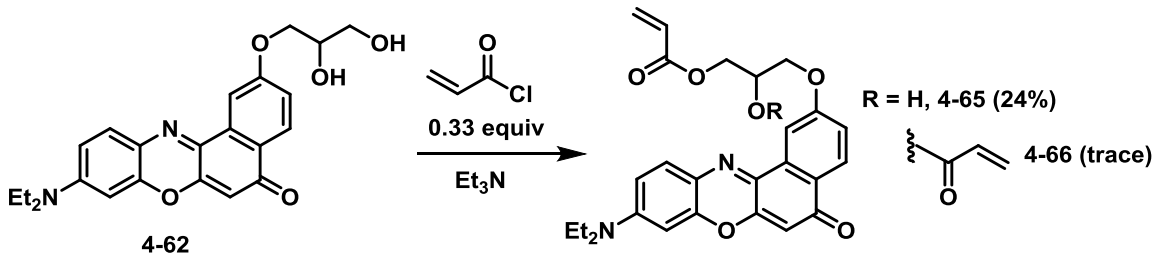

In summary, a series of benzo[a]phenoxazines based on the Nile Red core have been synthesized for use in microscopy studies as thiol-selective probes; several of these examples are summarized in **Table 4.6**. Compound **4-65** was found to be the best fluorophore in terms of its ease of synthesis and performance, and it was utilized successfully in a study on the dual quantification of two different lipid pools using orthogonal sensors.[32] The Nile Red-based fluorophore **4-65** was found to have minimal spectral overlap with the commercially available Acrylodan, and this property allowed for the accurate, spatiotemporally

resolved quantification of two different lipids on the same leaflet of the plasma membrane or a single lipid on two opposite leaflets of the plasma membrane of live mammalian cells.

Table 4.6. Summary of Nile Red analogs

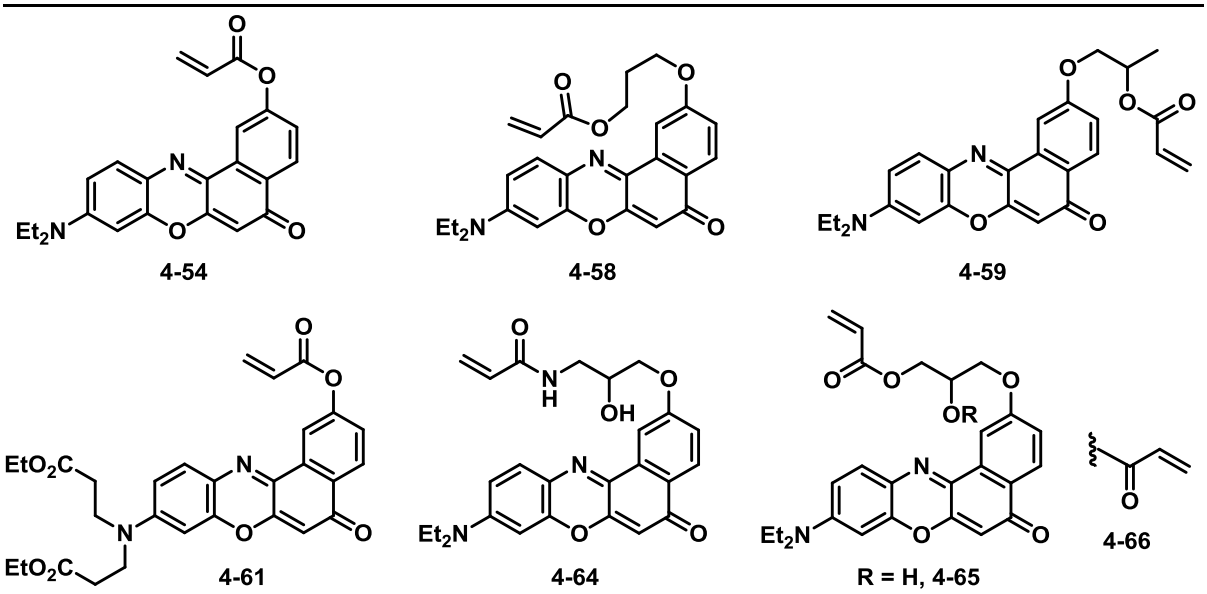

4.2.2. TCF and ITCF analogs

The second class of fluorophores examined were the tricyanofurans (TCF) and the interrupted tricyanofurans (ITCF).[33] As shown in **Scheme 4.25**, it was envisioned that intermediate **4-53** could be utilized to explore two different reaction pathways depending on the number of equivalents of malonitrile **4-50** were used. In the top, the traditional TCF fluorophore could be generated in a similar manner to that described previously in **Section 4.1.2**. A suitable R group on **4-67** could then be utilized as a handle to further attach a linker and Michael acceptor. In the second case, it was hypothesized that the intermediate imidate **4-53** could be generated from the addition of one equivalent of **4-50**. After condensation with an appropriate aldehyde, the acrylate linker could then be covalently attached to the imidate nitrogen of **4-68**. Either of these two pathways would lead to novel fluorophore structures which could be evaluated as probes for attachment to biomolecules via their cysteine residue. The first tricyanofuran class evaluated was the interrupted TCF.

Scheme 4.25. Tricyanofuran (TCF) and interrupted tricyanofuran (ITCF) fluorophores

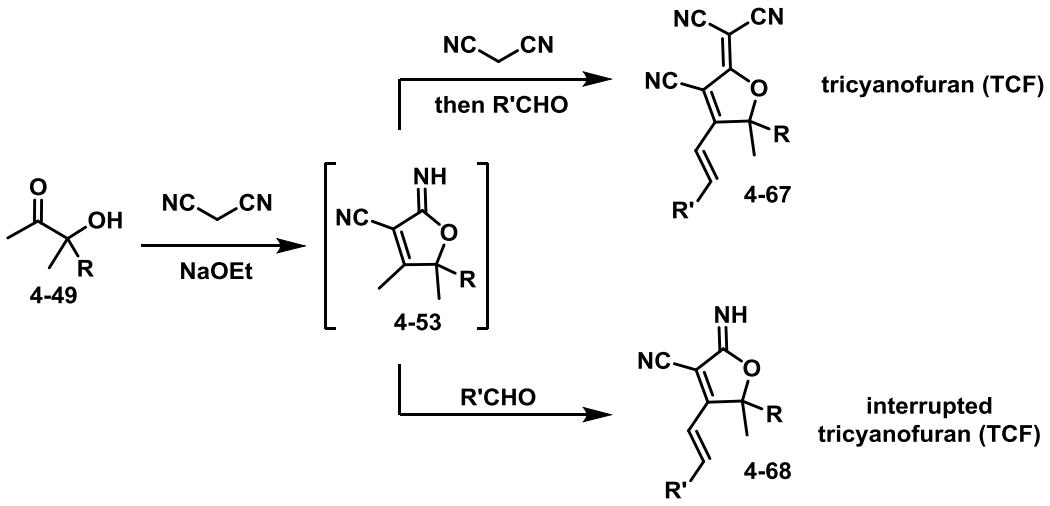

Starting from either methyl or allyl substituted a-hydroxy ketone **4-49**, condensation with one equivalent of malonitrile **4-50** led to the intermediate imidate **4-53** which was not isolated but directly condensed with 4-(dimethylamino)benzaldehyde (DMAB). Interestingly, two major brightly colored spots were visible on the TLC plate during the reaction which turned out to be cyano imidate **4-68** and its oxidized counterpart amide **4-68'**, the structure of which was confirmed via X-ray diffraction analysis. Although they could be carefully and tediously separated, this was not necessary because amide **4-68'** gets oxidized back to the nitrile after treatment with excess alkylating agent.

Scheme 4.26. Interrupted tricyanofuran (ITCF) fluorophores

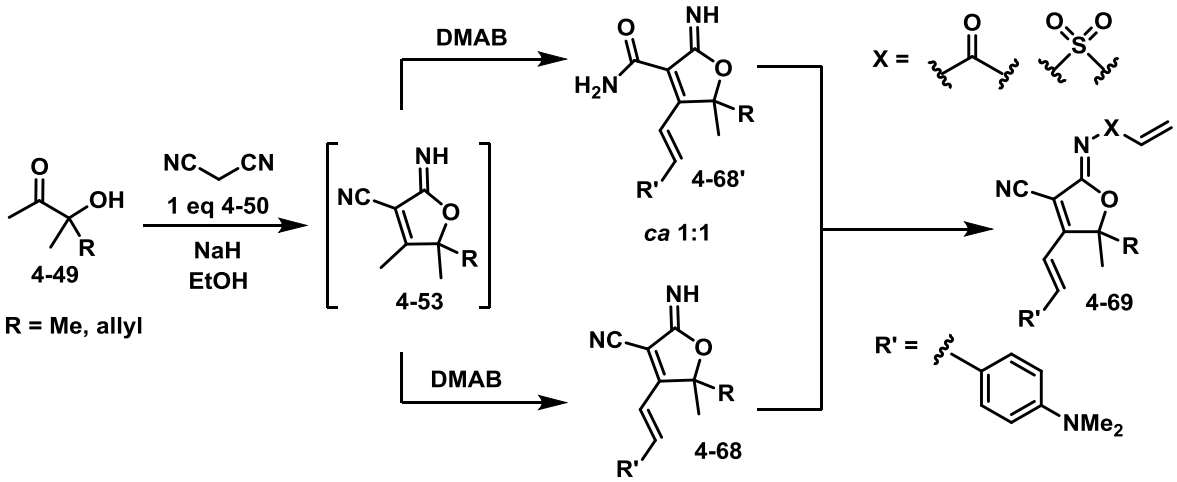

Scheme 4.27. Tricyanofuran (TCF) fluorophore

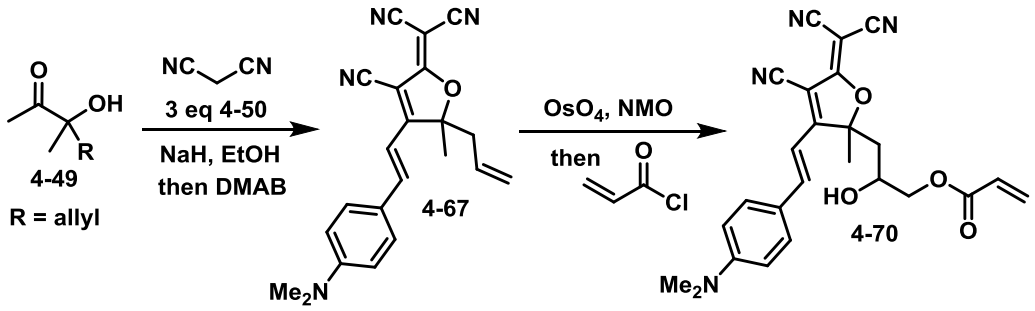

The tricyanofuran (TCF) fluorophore was synthesized by treatment of **4-49** (R = allyl) with excess malonitrile **4-50** and sodium hydride in ethanol. In a tandem, one-pot process, DMAB is added followed by sodium hydride to generate **4-67**. The linker was attached in a two-step process consisting of osmylation followed by acrylation, similar to that of the Nile Red analogs. In a modified procedure, TCF lactone **4-72** was synthesized. The process consisted of condensation of **4-49** under the standard condition, and then the crude imidate was treated with a mixture of pyridine and acetic acid in the presence of DMAB to generate **4-71**. The linker was attached in an analogous method to that shown above.

Scheme 4.28. TCF lactone fluorophore

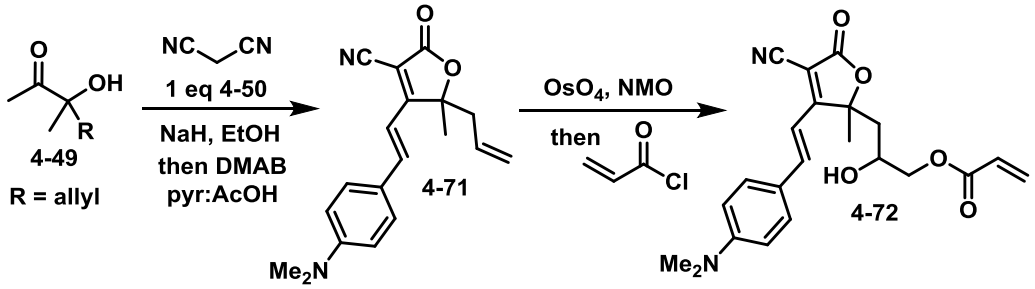

In summary, a variety of tricyanofuran-inspired fluorophores were synthesized as potential probes for microscopy experimentation, and they are shown in Table 4.7. The interrupted series includes fluorophores containing the acryl linker (**4-69a**, **4-69b**, **4-69e**, **4-69f**) and those containing the vinylsulfonyl linker (**4-69c** and **4-69d**). For the uninterrupted TCF, diastereomers **4-70a** and **4-70b** were isolated. Also, using the modified procedure, lactone **4-72** containing the acryl linker was synthesized. In general, these

fluorophores did not perform well in labeling studies when compared to the Nile Red series of dyes discussed in **Section 4.2.1**.

Table 4.7. Summary of TCF-based fluorophores

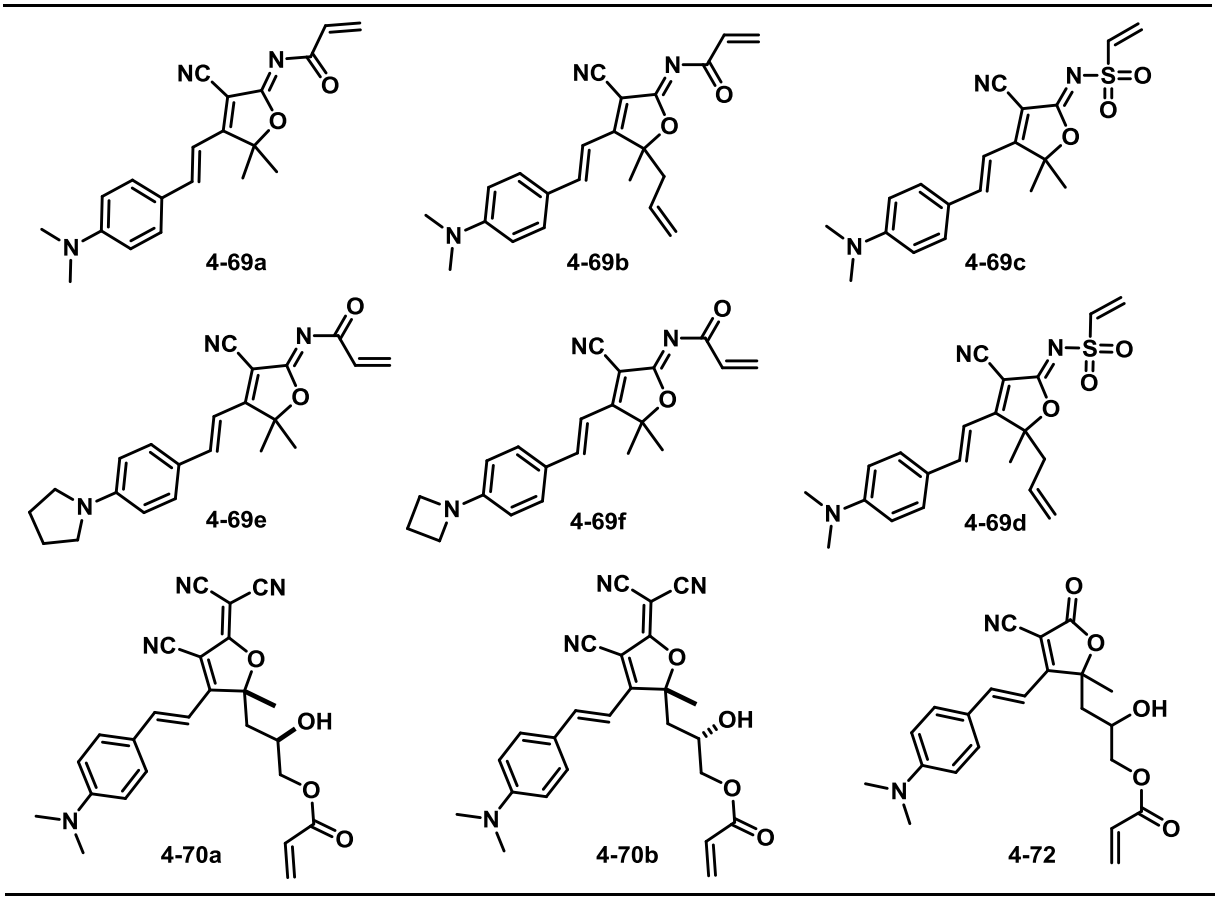

4.2.3. Fluorescence data

As mentioned above, in general, the TCF and interrupted TCF fluorophores did not generate satisfactory results from the microscopy study in terms of their fluorescence properties, so focus was on the Nile Red class of fluorophores. Out of all of the benzophenoxazines tested, compound **4-65** was superior in terms of fluorescence intensity and ease of removal from the engineered signaling domain (eENTH or eLactC2) after the microscopy experiments.[31] The fluorescence plot for fluorophore **4-65** can be seen in **Figure 4.8**. As shown in the figure, a concentration dependent increase in intensity is observed when

Figure 4.8. Fluorescence plot for fluorophore **4-65**

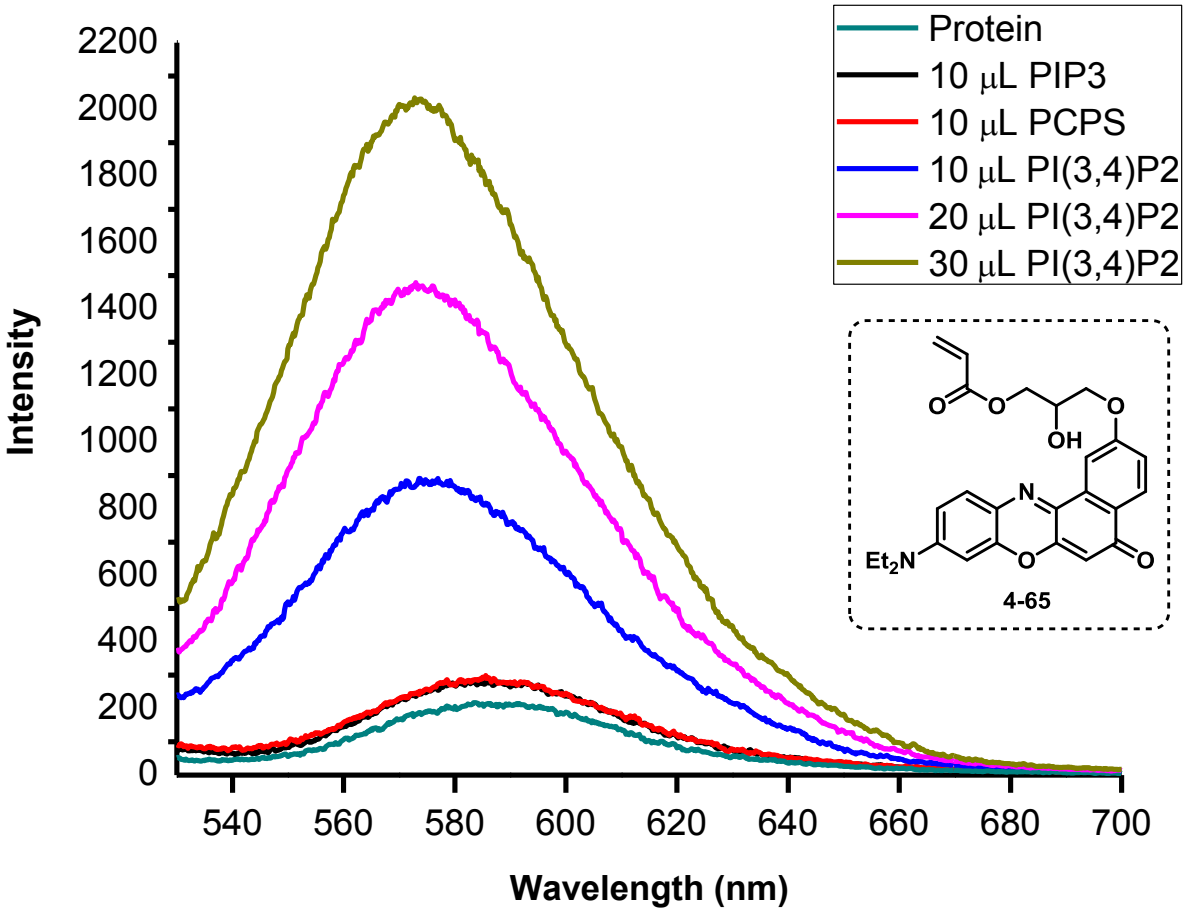

fluorophore **4-65** is evaluated with the different signaling lipids including phosphatidylinositol-3,4,5-trisphosphate (PIP3), and phosphatidylinositol-4,5-bisphosphate (PIP2). Compound **4-65** also showed other favorable properties including a low tendency to self-associate in solution and to nonspecifically absorb to lipid membranes and glass surfaces.

To prepare the sensor, **4-65** was attached to an engineered lactadherin C2 domain (eLactC2) which is widely used as a specific phosphatidylserine (PS) cellular probe.[34] The **4-65**-eLactC2 sensor showed characteristic spectral changes upon binding to vesicles in a PS concentration dependent manner as shown in **Figure 4.9A**. The sensor was then calibrated via in vitro ratiometric calibration (**Figure 4.9B**).

Figure 4.9. Evaluation and calibration of fluorophore **4-65**

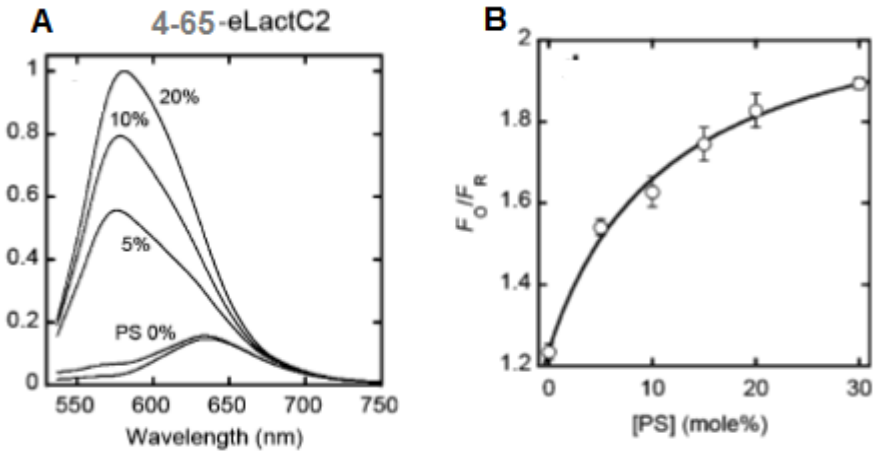

Utilizing the newly developed sensor, simultaneous in situ quantification of PS in the inner and outer plasma membrane (PM) of mouse embryonic fibroblast cells (NIH 3T3 cells) was achieved using the commercially available DAN as the orthogonal sensor. The Time-dependent changes of spatially averaged PIP2 and PIP3 concentrations in the outer and inner PM can be seen in **Figure 4.10**.[31]

Figure 4.10. Change of PS concentration in PM over time

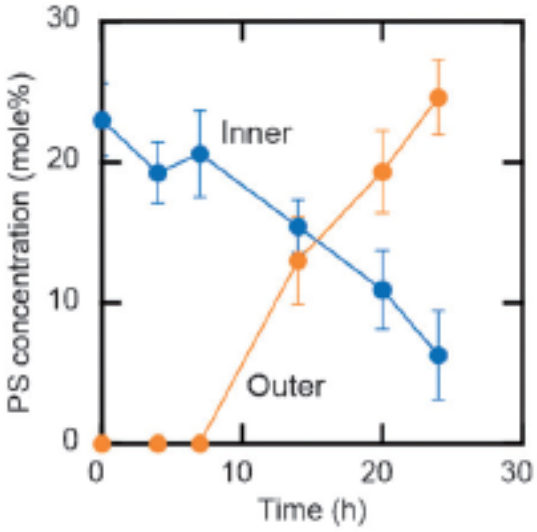

4.3. Conclusion

In summary, a variety of Nile Red and tricyanofuran (TCF) fluorophores were designed and synthesized for evaluation of their properties for quantification of cellular lipids using two photon microscopy. The Nile red analog **4-65** was found to be the optimal fluorophore for this purpose, and it was used in a study for simultaneous quantification of two lipid pools.[31] This dual quantification protocol using orthogonal sensors serves as an important technological advancement in developing new methods for understanding the role of lipids in cell regulation processes.

4.4. Experimental details

4.4.1. General information

All reactions were carried out under an inert nitrogen atmosphere, unless otherwise indicated. Flasks were oven-dried and cooled under a stream of nitrogen. Compounds were purchased from Aldrich unless otherwise noted. CH_2Cl_2, THF, Et_2O were purified based on standard procedures. Flash chromatography was performed using silica gel 60 Å (32-63 mesh) purchased from SiliCycle. Analytical thin layer chromatography (TLC) was performed on 0.25 mm SiliCycle precoated silica gel 60 (particle size 0.040-0.063 mm). 1H NMR and 13C NMR spectra were recorded on a Bruker AV-500 spectrometer. 1H and 13C chemical shifts were referenced to internal solvent resonances and reported relative to SiMe4; multiplicities are indicated by s (singlet), d (doublet), t (triplet), q (quartet), qn (quintet), m (multiplet) and br (broad). Coupling constants, J, are reported in Hz (Hertz). Electrospray ionization (ESI) mass spectra were recorded on a Micromass LCT equipped with a time-of-flight analyzer on a Waters Micromass Q-Tof Ultima in the University of Illinois at Urbana-Champaign. Electron impact (EI) mass spectra were obtained using a Micromass AutoSpecTM. Fast atom bombardment (FAB) mass spectra were taken at the Mass Spectrometry Laboratory in the University of Illinois at Urbana-Champaign, using a Micromass 70-VS-4F and 70-VSE for HRFAB and LRFAB, respectively. IR spectra were recorded using JASCO FT/IR-4100.

4.4.2. Synthesis of Nile red analogs

Select characterization data:

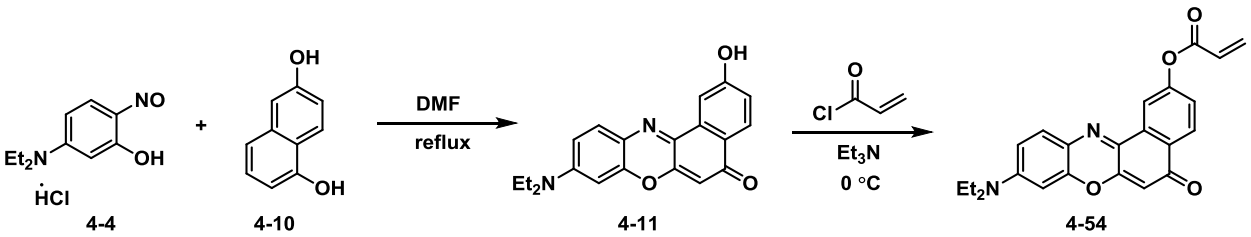

Procedure: 5-Diethylamino-2-nitrosophenol hydrochloride **4-4** (2.3 g, 10 mmol) and 1,6-hydroxynaphthalene **4-10** (1.6 g, 10 mmol) were heated under reflux in DMF (50 mL) for 4 h. After cooling to room temperature, SiO_2 (6 g) was added, and the DMF was removed under reduced pressure. The crude solid was flashed through an SiO_2 column (ethyl acetate–isopropanol, 100–50%), and the major purple band was collected as a single fraction to yield **4-11**, a dark purple solid. **4-11** (334 mg, 1 mmol) was suspended in 10 mL dichloromethane (CH_2Cl_2) and triethylamine was added (210 µL, 1.5 mmol); the homogenous solution was cooled to 0 °C, and 1.2 equivalents of acryloyl chloride (97 µL, 1.2 mmol) was slowly added. Progress of the reaction was followed by TLC, and after completion (~30 minutes), 0.5 g SiO_2 was added and the volatiles were removed by rotary evaporation. Flash chromatography (hexanes:EtOAc, 4:1) of the resulting solid gave **4-54** as a purple solid (85%). 1H NMR (500 MHz, $CDCl_3$) δ 8.35 (s, 1H), 8.31 (d, J = 8.40 Hz, 1H), 7.50 (d, J = 8.92 Hz, 1H), 7.38 (d, J = 8.07 Hz, 1H), 6.66 (d, J = 17.34 Hz, 1H), 6.40-6.31(m, 3H), 6.07 (d, J = 10.31 Hz, 1H), 3.40 (q, J = 6.83 Hz, 1H), 1.22 (t, J = 6.78, 6.78 Hz, 1H); 13C NMR (125 MHz, $CDCl_3$) δ 182.8, 164.2, 153.1, 152.4, 151.0, 146.9, 139.0, 133.7, 133.1, 131.3, 129.5, 127.7, 127.6, 125.0, 123.4, 116.3, 109.9, 105.5, 96.2, 45.2, 12.7; IR (neat): 2928, 1740, 1620, 1584, 1493, 1402.

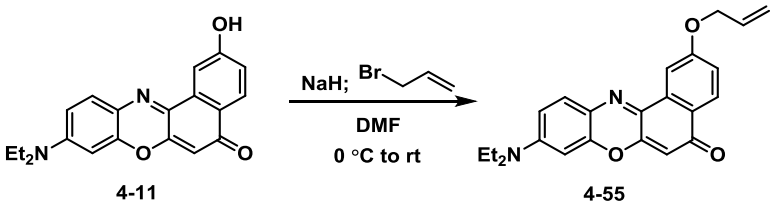

To an ice cold solution of **4-11** (500 mg, 1.5 mmol) in 15 mL dimethylformamide (DMF) was added NaH (66 mg, 1.65 mmol of a 60% dispersion in mineral oil). The suspension is stirred at 0 °C until gas evolution has ceased (~30 minutes) and allyl bromide (400 µL, 4.5 mmol) is added dropwise over 1 minute. The solution is allowed to warm to room temperature and stirred for 3 hours until TLC showed consumption of the starting material. The reaction mixture was quenched with saturated ammonium chloride (1 mL), diluted with water (45 mL) and extracted with chloroform (5 x 10 mL). The combined organic extracts were then washed with water (5 x 15 mL), brine (15 mL) and then dried (Mg_2SO_4). After filtration, the volatiles were removed by rotary evaporation, and flash chromatography (hexanes:EtOAc, 4:1) yielded **4-55** as a purple solid (72%). 1H NMR (500 MHz, $CDCl_3$) δ 8.14 (d, J = 8.64 Hz, 1H), 7.95 (s, 1H), 7.45 (d, J = 8.95 Hz, 1H), 7.11 (d, J = 7.07 Hz, 1H), 6.53 (d, J = 7.51 Hz, 1H), 6.31 (s, 1H), 6.19 (s, 1H), 6.10 (m, 1H), 5.48 (d, J = 17.20 Hz, 1H), 5.33 (d, J = 10.46 Hz, 1H), 5.28 (s, 2H), 4.68 (d, J = 4.46 Hz, 2H), 3.37 (q, J = 6.64 Hz, 4H), 1.21 (t, J = 6.92 Hz, 6H); 13C NMR (125 MHz, CDCl3) δ 183.1, 161.1, 152.0, 150.7, 146.7, 139.6, 134.0, 132.8, 131.0, 127.6, 125.7, 124.6, 118.3, 118.1, 109.5, 106.7, 105.1, 96.1, 69.0, 45.0, 12.6; IR (neat): 1721, 1464, 1370; HRMS (ESI) calcd for $C_{23}H_{23}N_2O$ $[M+H]^+$ 375.1709, found 375.1707.

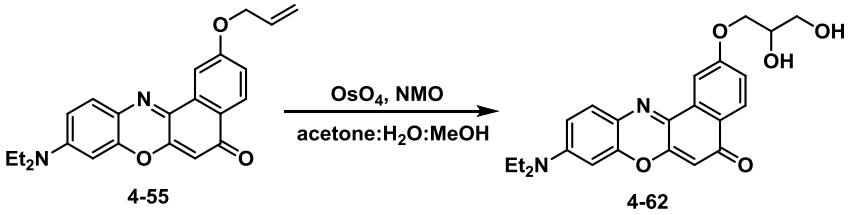

To a solution of **4-55** (500 mg, 1.34 mmol) in 22 mL acetone:H_2O:MeOH (8:2:1) was added NMO (313 mg, 2.68 mmol) followed by 6 drops of a 5% aqueous OsO_4 solution. The resulting mixture is allowed to stir at room temperature until TLC showed full consumption of the starting material (~36 hours). After completion of the reaction, $Na_2S_2O_4$ (0.5 g) and magnesium silicate (0.5 g) were added, and the suspension was stirred for one hour at room temperature. Additional SiO_2 (1 g) was added, and the volatiles were removed by rotary evaporation. The crude solid was chromatographed on silica gel (EtOAc:CH_2Cl_2:MeOH,

2:1:2%) providing **4-62** (65%). 1H NMR (500 MHz, $CDCl_3$) δ 8.08 (d, J = 8.71 Hz, 1H), 7.92 (d, J = 2.31 Hz, 1H), 7.48 (d, J = 9.04 Hz, 1H), 7.08 (dd, J = 8.72, 2.37 Hz, 1H), 6.58 (dd, J = 9.14, 2.39 Hz, 1H), 6.39 (d, J = 2.40 Hz, 1H), 6.23 (s, 1H), 4.24-4.19 (m, 3H), 3.89 (ddd, J = 16.36, 11.54, 4.23 Hz, 1H), 3.44 (q, J = 7.00 Hz, 4H), 1.26 (t, J = 7.04 Hz, 6H); 13C NMR (125 MHz, CDCl3) δ 183.3, 161.2, 152.1, 150.7, 147.0, 139.4, 133.9, 131.2, 124.9, 118.3, 109.7, 106.7, 105.1, 96.2, 70.3, 69.3, 63.5, 45.1, 12.7; IR (neat): 3360, 3182, 2971, 2922, 2607, 1721, 1643, 1584, 1568, 1428, 1400; HRMS (ESI) calcd for $C_{23}H_{25}N_2O_5$ $[M+H]^+$ 409.1763, found 409.1767.

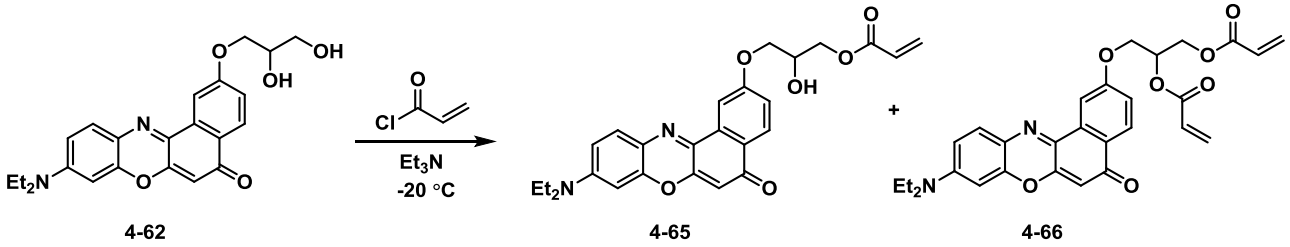

4-62 4-65 4-66

To a suspension of **4-62**(54 mg, 0.13 mmol) in 8 mL dichloromethane (CH_2Cl_2) was added triethylamine (100 µL); the mixture is stirred until a homogenous solution was obtained (about 10 minutes). After cooling to -20 °C, acryloyl chloride (4 µL, 0.33 equiv) was added slowly. After 10 minutes, SiO_2 (250 mg) was added, and the volatiles were removed. The resulting solid was chromatographed on silica gel affording **4-65** (25%) and recovered **4-62** (60%). ^{1}H NMR (500 MHz, $CDCl_3$) δ 8.21 (d, J = 8.71 Hz, 1H), 8.05 (d, J = 2.52 Hz, 1H), 7.58 (d, J = 9.03 Hz, 1H), 7.17 (dd, J = 8.73, 2.59 Hz, 1H), 6.65 (dd, J = 9.07, 2.66 Hz, 1H), 6.49 (dd, J = 17.31, 1.02 Hz, 1H), 6.45 (d, J = 2.62 Hz, 1H), 6.29 (s, 1H), 6.20 (dd, J = 17.32, 10.44 Hz, 1H), 5.90 (dd, J = 10.45, 1.04 Hz, 1H), 4.45 (ddd, J = 17.27, 11.52, 5.17 Hz, 2H), 4.38 (td, J = 10.31, 5.05, 5.05 Hz, 1H), 4.31-4.23 (m, 2H), 3.47 (q, J = 7.10, 7.08, 7.08 Hz, 4H), 1.26 (t, J = 7.09 Hz, 6H); ^{13}C NMR (125 MHz, CDCl3) δ 183.3, 161.1, 152.1, 150.9, 146.8, 139.8, 134.2, 131.7, 131.1, 127.9, 126.2, 124.8, 118.1, 109.6, 106.8, 105.3, 96.3, 69.0, 68.6, 65.5, 45.1, 12.6; IR (neat): 3305, 2922, 2854, 1717, 1591, 1549, 1400; HRMS (ESI) calcd for $C_{26}H_{27}N_2O_6$ $[M+H]^+$ 463.1869, found 463.1872.

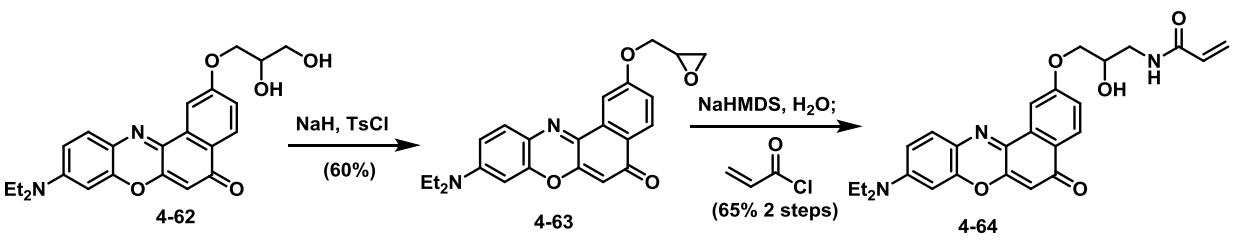

To a solution of **4-62** (13.5 mg, 0.03305 mmol) in DMF (0.5 mL) was added tosyl chloride (6.3 mg, 1 equiv). The resulting suspension was cooled to 0 °C, and sodium hydride was added (2.1 equiv). The mixture was followed by TLC and then quenched with silica gel. The resulting solids we purified over SiO_2, and the resulting purple band (**4-63**) was isolated and dissolved in THF. The resulting solution was cooled to 0 °C, and 3 eq NaHMDS was added. The mixture was stirred overnight and then water was added. After loading onto SiO_2, the purple band was isolated to yield **4-64**. ^{1}H NMR (500 MHz, $CDCl_3$) δ 8.42 (d, 1H, J=2.2Hz) ppm 8.35 (d, 1H, J=8.6Hz) ppm 7.60 (d, 1H, J=9.1Hz) ppm 7.07 (m, 1H) ppm 6.68 (m, 1H) ppm 6.39 (m, 1H) ppm 6.09 (m, 3H) ppm 4.21 (dd, 2H, J=7.2Hz, J=14.3Hz) ppm 4.11 (dd, 2H, J=1.2Hz, J=10.3Hz) ppm 3.48 (dd, 4H, J=7.1Hz, J=14.2Hz) ppm 1.27 (t, 6H).

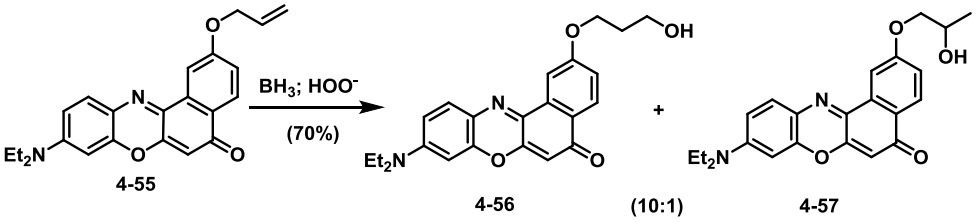

A solution of **4-55** (0.3 mmol) in THF 5 mL was treated with BH_3 dimethylsulfide complex (0.31 mmol) at 0 °C. After completion of the reaction by TLC, the mixture is quenched with silica gel and then chromatographed yielding **4-56** and **4-57** in a 10:1 mixture of regioisomers. **4-56** ^{1}H NMR (500 MHz, $CDCl_3$) δ 8.20 (d, 1H, J=8.7Hz) ppm 8.06 (d, 1H, J=2.3Hz) ppm 7.59 (d, 1H, J=9.0Hz) ppm 7.16 (dd, 1H, J=2.3Hz, J=8.7Hz) ppm 6.65 (dd, 1H, J=2.5Hz, J=9.0Hz) ppm 6.45 (d, 1H, J=2.4Hz) ppm 6.29 (s, 1H) ppm 4.34 (t, 2H, J=5.9Hz) ppm 3.93 (t, 2H, J=5.9Hz) ppm 3.47 (q, 4H, J=7.1Hz) ppm 2.14 (m, 2H) ppm 1.26

(m, 6H). ^{13}C NMR (125 MHz, CDCl3) δ 131.08, 127.80, 118.22, 109.53, 106.70, 105.31, 96.33, 65.87, 60.16, 45.08, 32.05, 29.71, 12.63. **4-57** ^{1}H NMR 8.24 (d, 1H, J=8.8Hz) ppm 8.08 (d, 1H, J=2.5Hz) ppm 7.63 (d, 1H, J=9.1Hz) ppm 7.20 (dd, 1H, J=2.5Hz, J=8.7Hz) ppm 6.46 (m, 1H) ppm 6.34 (s, 1H) ppm 6.16 (dd, 1H, J=10.3Hz, J=17.3Hz) ppm 5.85 (dd, 1H, J=1.3Hz, J=10.5Hz) ppm 5.42 (m, 1H) ppm 4.27 (dd, 2H, J=4.9Hz, J=6.7Hz) ppm 3.48 (dd, 4H, J=6.1Hz, J=13.5Hz) ppm 1.48 (d, 3H, J=6.5Hz) ppm 1.27 (m, 6H).

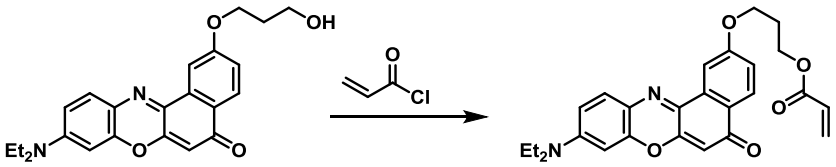

The general acrylation procedure for the synthesis of 4-54 was followed. **4-56** ^{1}H NMR (500 MHz, $CDCl_3$) δ 8.23 (d, 1H, J=8.7Hz) ppm 8.07 (d, 1H, J=2.6Hz) ppm 7.62 (d, 1H, J=9.1Hz) ppm 7.18 (dd, 1H, J=2.6Hz, J=8.7Hz) ppm 6.46 (dd, 1H, J=10.0Hz, J=24.9Hz) ppm 6.33 (s, 1H) ppm 6.15 (dd, 1H, J=10.4Hz, J=17.3Hz) ppm 5.85 (dd, 1H, J=1.1Hz, J=10.4Hz) ppm 4.42 (t, 12H, J=6.3Hz) ppm 4.30 (t, 2H, J=6.0Hz) ppm 3.48 (q, 4H, J=7.1Hz) ppm 2.26 (m, 2H) ppm 1.27 (m, 6H).

4.4.3. Synthesis of TCF analogs

General procedure of interrupted TCF analogs (ITCF):

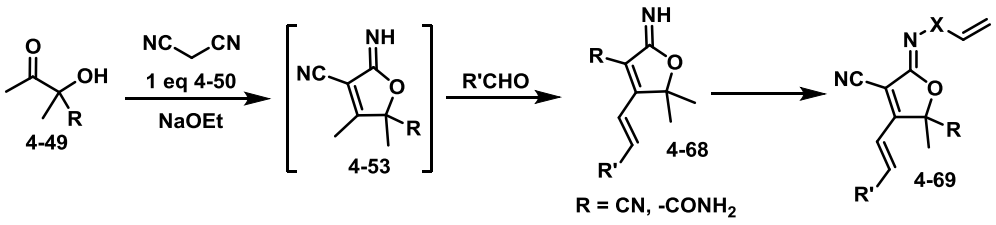

To a stirred solution of hydroxy ketone **4-49** (3 mmol) and malonitrile **4-50** (3 mmol) in 5 mL Ethanol is added sodium hydride (ca 0.1 g). The reaction is followed by TLC, and two new deeply colored spots

become visible instantaneously. After consumption of **4-49**, 1 equivalent DMAB is added followed by addition sodium hydride (ca 0.1 g). The reaction is run to completion and then loaded onto SiO_2 and purified. Compounds **4-68** and **4-68′** are isolated as a mixture and used directly in the acylation step. Acylation of **4-68** is achieved by dissolving 1 mmol **4-68** in 5 mL DCM and adding Et_3N (2.5 equiv). The solution is cooled to 0 °C, and the appropriate acylating agent is added. A.fter completion of the reaction, the mixture is purified over silica gel to yield **4-69**.

Select characterization data:

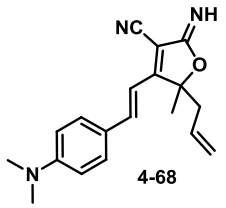

4-68

^{1}H NMR (500 MHz, $CDCl_3$) δ 7.47 (dd, 3H, J=3.5Hz, J=12.5Hz) ppm 6.68 (d, 2H, J=8.9Hz) ppm 6.62 (d, 1H, J=16.3Hz) ppm 5.63 (m, 1H) ppm 5.11 (m, 2H) ppm 3.07 (s, 6H) ppm 2.69 (dd, 1H, J=7.4Hz, J=14.5Hz) ppm 2.59 (dd, 1H, J=7.0Hz, J=14.5Hz) ppm 1.61 (s, 3H). ^{13}C NMR (125 MHz, $CDCl_3$) δ 169.16, 166.21, 152.40, 143.61, 130.35, 130.28, 122.20, 120.30, 113.38, 111.94, 110.12, 90.89, 43.54, 40.12, 25.16.

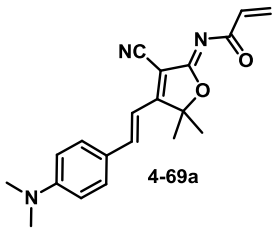

4-69a

^{1}H NMR (500 MHz, $CDCl_3$) δ 7.55 (d, 1H, J=16.2Hz) ppm 7.50 (d, 2H, J=8.9Hz) ppm 6.69 (dd, 3H, J=5.3Hz, J=12.6Hz) ppm 6.35 (dq, 2H, J=5.8Hz, J=17.3Hz) ppm 5.87 (dd, 1H, J=2.1Hz, J=9.7Hz) ppm 3.10 (s, 6H) ppm 1.67 (s, 6H).

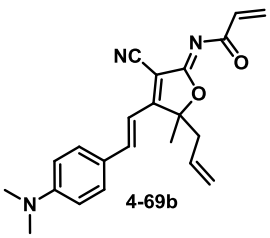

4-69b

^{1}H NMR (500 MHz, $CDCl_3$) δ 7.59-7.49 (m, 3H), 6.73-6.65 (m, 3H), 6.35-6.29 (m, 2H), 5.87-5.85 (m, 1H), 5.57-5.54 (m, 1H), 5.15-5.10 (m, 2H), 3.09 (s, 6H), 2.64-2.60 (m, 2H), 1.65 (s, 3H) . ^{13}C NMR (125 MHz, $CDCl_3$) δ 176.90, 171.28, 158.68, 152.62, 145.20, 145.13, 133.33, 130.87, 130.15, 129.66, 122.36, 121.03, 112.70, 112.27, 109.74, 97.22, 93.09, 43.40, 40.32, 25.06.

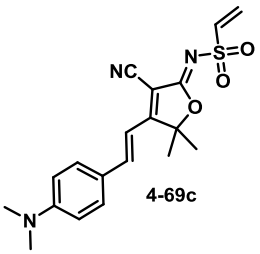

^{1}H NMR (500 MHz, $CDCl_3$) δ 7.71 (d, 1H, J=16.0Hz) ppm 7.56 (d, 1H, J=8.9Hz) ppm 6.84 (s, 1H) ppm 6.73 (d, 1H, J=9.0Hz) ppm 6.68 (d, 1H, J=16.0Hz) ppm 6.42 (d, 1H, J=16.6Hz) ppm 5.96 (d, 1H, J=10.0Hz) ppm 3.15 (s, 6H) ppm 1.78 (s, 6H). ^{13}C NMR (125 MHz, $CDCl_3$) δ 175.03, 166.17, 153.44, 147.85, 137.68, 131.72, 125.67, 121.75, 112.25, 112.11, 108.64, 95.26, 40.20, 26.44.

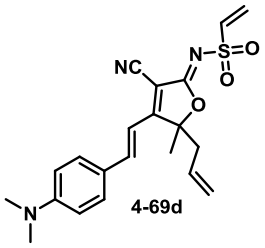

^{1}H NMR (500 MHz, $CDCl_3$) δ 7.73 (d, 1H, J=16.0Hz) ppm 7.56 (d, 1H, J=9.0Hz) ppm 6.83 (dd, 1H, J=10.0Hz, J=16.6Hz) ppm 6.74 (d, 1H, J=9.0Hz) ppm 6.68 (d, 1H, J=16.0Hz) ppm 6.42 (d, 1H, J=16.6Hz) ppm 5.96 (d, 1H, J=10.0Hz) ppm 5.61 (tdd, 1H, J=7.2Hz, J=9.7Hz, J=17.2Hz) ppm 5.22 (m, 1H) ppm 3.16 (s, 6H) ppm 2.89 (dd, 1H, J=7.5Hz, J=14.5Hz) ppm 2.69 (dd, 1H, J=7.0Hz, J=14.5Hz) ppm 1.77 (s, 3H). ^{13}C NMR (125 MHz, $CDCl_3$) δ 173.46, 153.44, 147.59, 137.67, 128.98, 125.73, 121.78, 112.16, 112.11, 108.72, 96.98, 43.40, 40.21, 24.90.

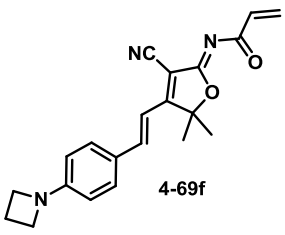

^{1}H NMR (500 MHz, $CDCl_3$) δ 7.54 (d, 1H, J=16.2Hz) ppm 7.46 (d, 2H, J=8.5Hz) ppm 6.66 (d, 1H, J=16.2Hz) ppm 6.34 (ddd, 4H, J=9.2Hz, J=15.8Hz, J=27.0Hz) ppm 5.87 (dd, 1H, J=1.9Hz, J=9.7Hz) ppm 4.04 (t, 4H, J=7.3Hz) ppm 2.46 (m, 2H) ppm 1.66 (s, 6H). ^{13}C NMR (125 MHz, $CDCl_3$) δ 176.91, 172.96, 153.52, 145.60, 133.54, 130.12, 122.53, 112.73, 110.71, 109.53, 51.54, 29.70, 26.46, 16.46.

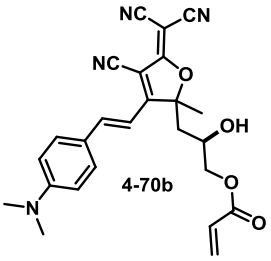

^{1}H NMR (500 MHz, $CDCl_3$) δ 7.68 (d, 1H, J=15.7Hz) ppm 7.54 (d, 2H, J=8.9Hz) ppm 6.75 (d, 1H, J=15.9Hz) ppm 6.70 (d, 2H, J=8.9Hz) ppm 6.46 (d, 1H, J=17.2Hz) ppm 6.15 (dd, 1H, J=10.5Hz, J=17.4Hz) ppm 5.90 (d, 1H, J=11.1Hz) ppm 4.11 (ddd, 2H, J=5.3Hz, J=11.4Hz, J=18.2Hz) ppm 3.94 (bs, 1H) ppm 3.14 (s, 6H) ppm 2.30 (t, 2H, J=5.3Hz) ppm 2.15 (m, 1H) ppm 1.76 (s, 3H).

4.5. ORTEP

ORTEP of 4-68-lactone (via imidate hydrolysis)

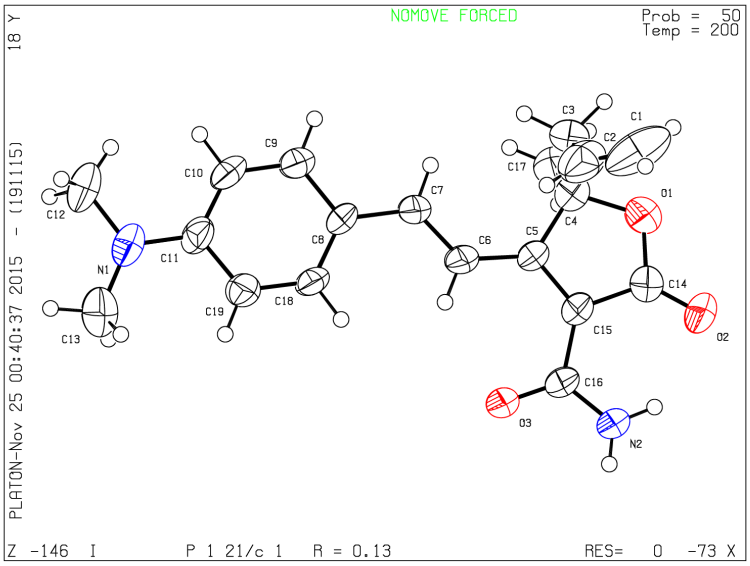

4.6. References

[1] Sahoo, H. *RSC Adv.* **2012**, *2*, 7017.

[2] Wichmann, C. F.; Liesch, J. M.; Schwartz, R. E. *J. Antibiot.* **1989**, *42*, 168.

[3] Ottawa, N.; Schafer, G. U.S. 3,655,601, **1972**.

[4] Zinger, B.; Shier, P. *Sens. Actuators, B* **1999**, *B56*, 206.

[5] a) Abayomi, L. A.; Terry, L. A.; White, S. F.; Warner, P. J. *Biosens. Bioelectron.* **2006**, *21*, 2176 10. b) Ignacio, D. V.;Matias, I. R.; Arregui, F. J.; Claus, R. O. *IEEE Sens. J.* **2005**, *5*, 365. c) Alonso Lomillo, M. A.; Ruiz, J. G.; Pascual, F.J. M. *Anal. Chim. Acta* **2005**, *547*, 209. d) Forrow, N. J.; Sanghera, G. S.; Walters, S. J.; Watkin, J. L. *Biosens. Bioelectron.* **2005**, *20*, 1617. e) Kerman, K.; Oezkan, D.; Kara, P.; Karadeniz, H.; Oezkan, Z.; Erdem, A.; Jelen, F.; Oezsoez, M. *Turk. J. Chem.* **2004**, *28*, 523.

[6] Long, J.;Wang, Y.-M.; Matsuura, T.; Meng, J.-B. *J. Heterocycl. Chem.* **1999**, *36*, 895.

[7] Briggs, M. S. J.; Bruce, I.; Miller, J. N.; Moody, C. J.; Simmonds, A. C.; Swann, E. *J. Chem. Soc., Perkin Trans. 1* **1997**, *7*, 1051. b) Alekseev, N. N.; Gorelenko, A. Y.; Vasil'ev, N. N. SU1109393, **1984**.

[8] Sherman, D. B.; Pitner, J. B.; Ambroise, A.; Thomas, K. J. *Bioconjugate Chem.* **2006**, *17*, 387.

[9] Moerner, W. E. *J. Phys. Chem. B* **2005**, *109*, 24517.

[10] Gerasimova, T. N.; Kolchina, E. F.; Kargapolova, I. Y.; Fokin, E. P. *Russ. J. Org. Chem.* **1997**, *33*, 735.

[11] Nakanishi, J.; Nakajima, T.; Sato, M.; Ozawa, T.; Tohda, K.; Umezawa, Y. *Anal. Chem.* **2001**, *73*, 2920.

[12] Jose, J.; Burgess, K. *J. Org. Chem.* **2006**, *71*, 7835.

[13] Mohlau, R.; Uhlmann, K. *Justus Liebigs Ann. Chem.* **1896**, *289*, 94.

[14] Kanitz, A.; Hartmann, H. *Eur. J. Org. Chem.* **1999**, 923.

[15] a) Fries, J.; Lopez-Calle, E. EP10236, **2002**. b) Lopez-Calle, E.; Fries, J. R.; Mueller, A.; Winkler, D. *Innovation Perspect. Solid Phase Synth. Comb. Libr: Collect. Pap., Int. Symp. 7th*, **2002**, 129. c) Ho, N.-H.; Weissleder, R.; Tung, C.-H. *Tetrahedron* **2006**, *62*, 578.

[16] a) Becker, R. S.; Chakravorti, S.; Das, S. Photochem. Photobiol. **1990**, *51*, 533. b) Foley, J. W.; Cincotta, L. U.S. 4,962,197, **1990**.

[17] Kehrmann, F.; Neil, A. A. Ber. **1914**, *47*, 3102.

[18] Afanas'eva, G. B.; Pashkevich, K. I.; Postovskii, I. Y. *Khim. Geterotsikl. Soedin.* **1971**, *7*, 742.

[19] a) Nicoud, J. F.; Twieg, R. J. *Nonlinear Optical Properties of Organic Molecules and Crystals* (Eds: D. S. Chemla, J. Zyss), Academic Press, New York, **1987**, 227. b) Prasad, P. N.; Williams, D. J. *Introduction to Nonlinear Optical Effects in Molecules and Polymers*, Wiley, New York, **1991**. c) Zyss, J. *Molecular Nonlinear Optics*, Academic Press, New York, **1994**.

[20] Willets, K. A.; Ostroverkhova, O.; He, M.; Twieg, R. J.; Moerner, W. E. *J. Am. Chem. Soc.* **2003**, *125*, 1174; b) Lord, S. J.; Conley, N. R.; Hsiao-lu, Lee, D.; Nishimura, S. Y.; Pomerantz, A. K.; Willets, K. A.; Lu, Z.; Wang, H.; Liu, N.; Samuel, R.; Weber, R.; Semyonov, A.; He, M.; Twieg, R. J.; Moerner, W. E. *ChemPhysChem* **2009**, *10*, 55.

[21] Melikian, G.; Rouessac, F.P. and Alexandre, C. *Synth. Commun.* **1995**, *25*, 3045.

[22] Villemin, D.; Liang, L. *Synth. Commun.* **2001**, *31*, 1771.

[23] Willets, K. A.; Ostroverkhova, O.; He, M.; Twig, R. W.; Moerner, W. E. *J. Am. Chem. Soc.* **2003**, *125*, 1174.

[24] Nishimura, S. Y.; Lord, S. J. ; Klein, L. O.; Willets, K. A.; he, M.; Lu, Z.; Twieg, R. J.; Moerner, W. E. *J. Phys. Chem. B* **2006**, *110*, 8151.

[25] Wang, H.; Lu, Z.; Lord, S. J.; Willets, K. A.; Bertke, J. A. ; Bunge, S. D. ; Moerner, W. E. ; Twieg, R. J. *Tetrahedron* **2007**, *63*, 103.

[26] Lord, S. J.; Lu, Z.; Wang, H.; Willets, K. A. ; Schuck, P. J. ; Lee, H. D. ; Nishimura, S. Y.; Twieg, R. J. ; Moerner, W. E. *J. Phys. Chem. A* **2007**, *111*, 8934.

[27] Conley, N.; Kurtz, R.; Pomerantz, A.; Wang, H.; Twieg, R. J.; Moerner, W. E. *J. Phys. Chem. B*, **2007**, *111*, 7929.

[28] a) McRae, E. G.; Kasha, M. *Physical Processes in Radiation Biology*; Augenstein, L., Rosenberg, B., Mason, R., Eds.; Academic: New York, **1964**, 23. b) Hernando, J.; van der Schaaf, M.; van Dijk, E. M. H. P.; Sauer, M.; Garcı´a-Parajo´, M. F.; van Hulst, N. F. *J. Phys. Chem. A* **2003**, *107*, 43.

[29] Wang, H.; Lu, Z.; Lord, S. J. ; Moerner, W. E.; Twieg, R. J. *Tetrahedron Letters* **2007**, *48*, 3471.

[30] Lord, S. J.; Conley, N. R.; Lee, H. D.; Samuel, R.; Liu, N.; Twig, R. J.; Moerner, W. E. *J. Am. Chem. Soc.* **2008**, *130*, 9204.

[31] Prendergast, F. G.; Meyer, M.; Carlson, G. L.; Iida, S.; Potter, J. D. *J Biol Chem.* **1983**, *258*, 7541.

[32] Liu, S.; Sheng, R.; O'Connor, M. J.; Cui, Y. ; Yoon, Y. ; Kurilova, S. ; Lee, D.; Cho, W. *Angew. Chem. Int. Ed*. **2014**, *53*, 14387.

[33] Avetisyan, A. *Russ. J. Org. Chem.*, **2011** , *47*, 433.

[34] Leventis, P. A.; Grinstein, S. *Annu. Rev. Biophys.* **2010**, *39*, 407.

APPENDIX I: Selected NMR Spectra

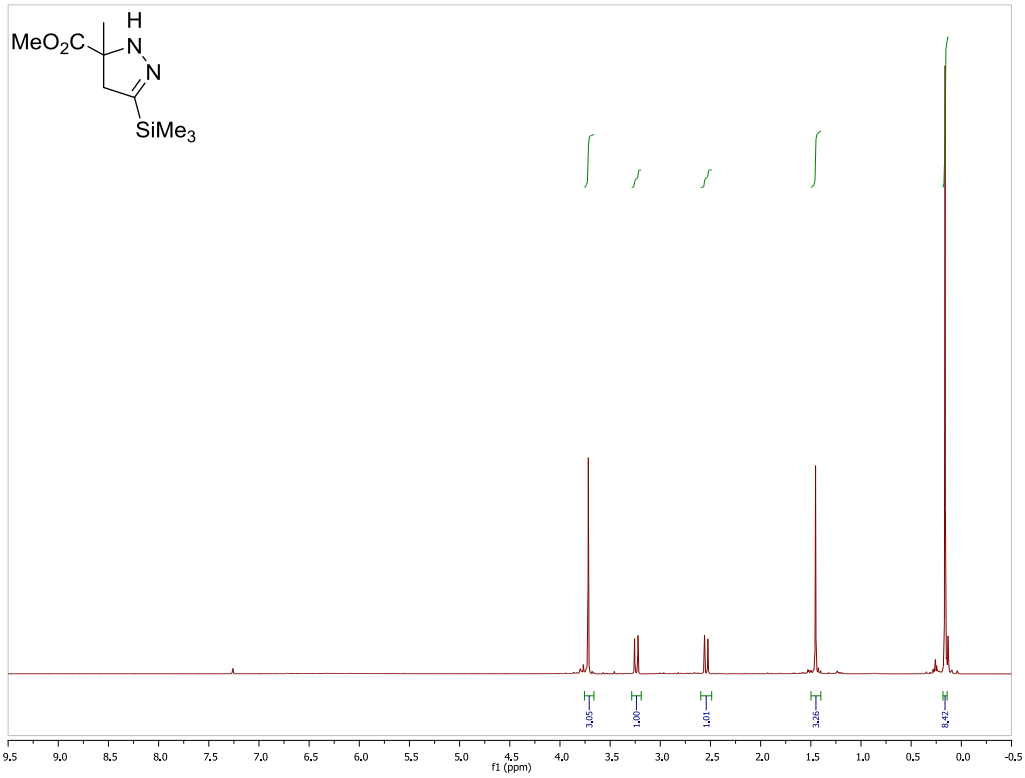

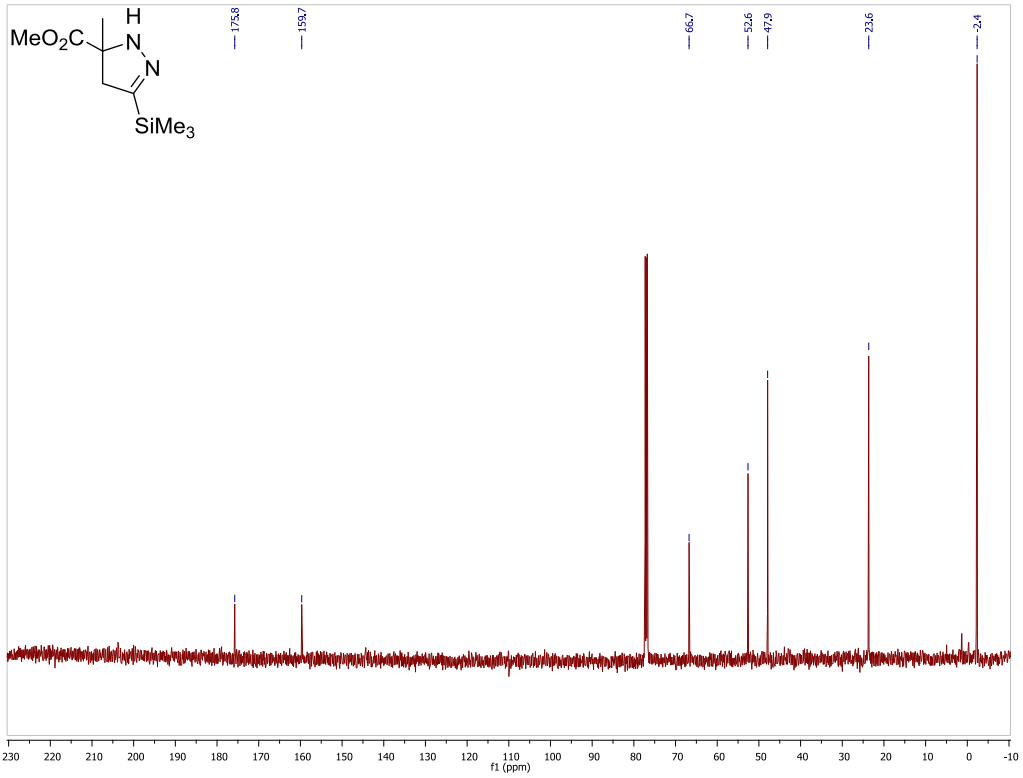

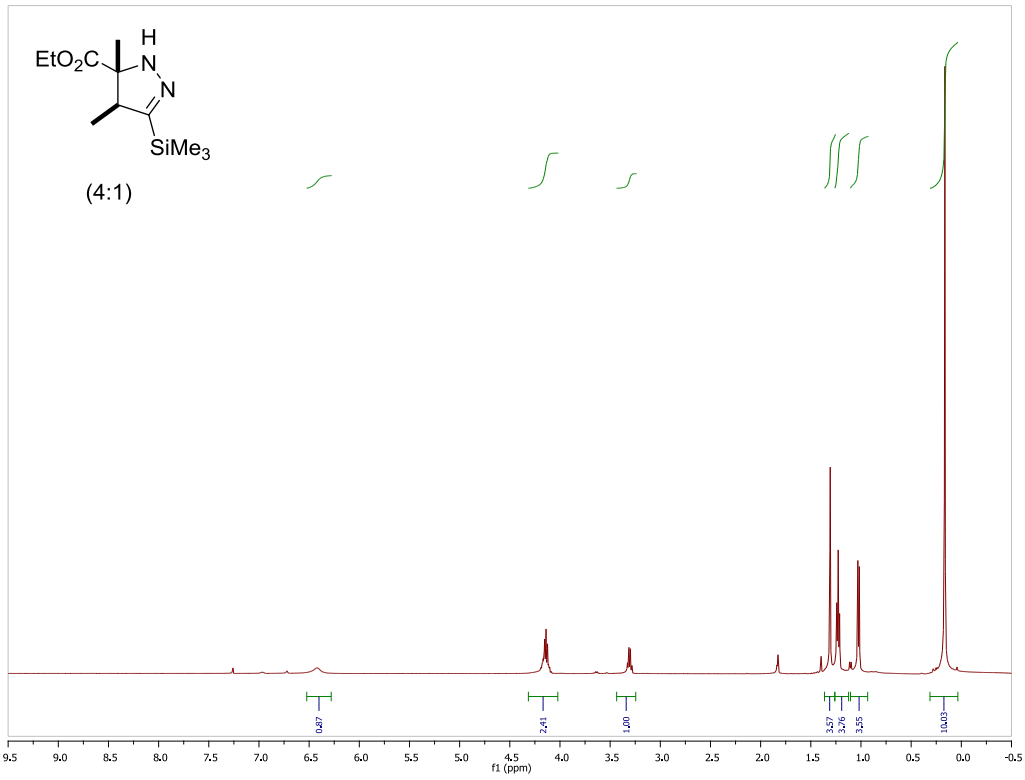
EtO2C
H
N
N
SiMe3
(4:1)
0.87
2.41
1.00
3.57
3.76
3.55
16.03
f1 (ppm)

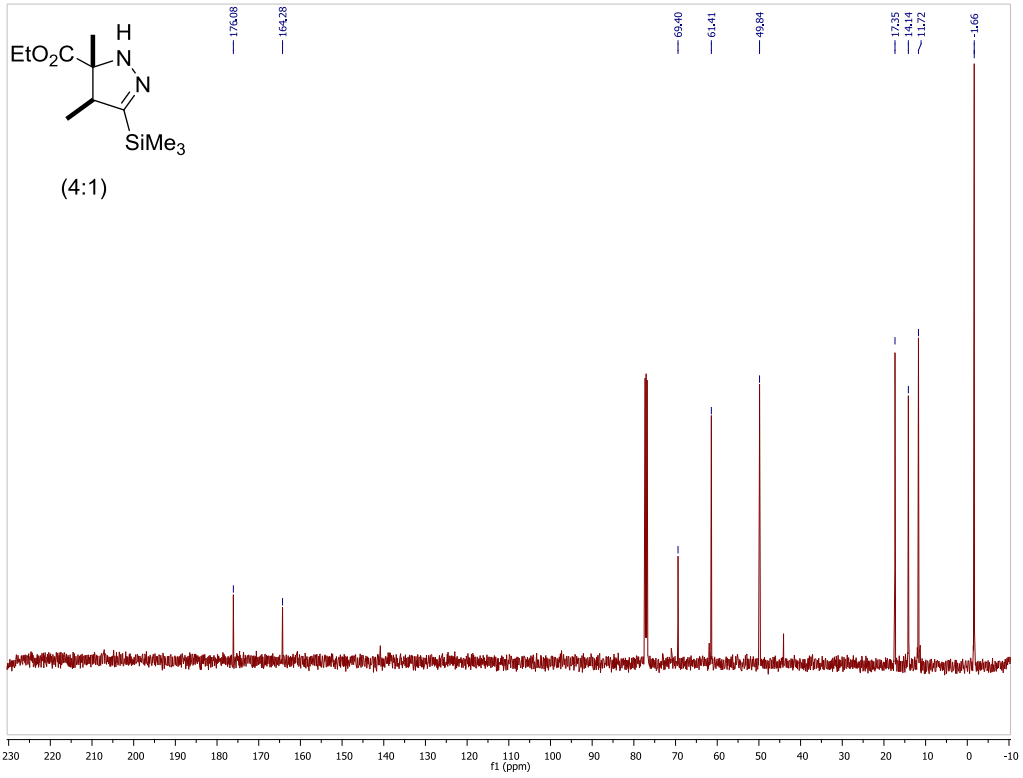
EtO2C
H
N
N
SiMe3
(4:1)
176.08
164.28
69.40
61.41
49.84
17.35
14.14
11.72
-1.66
f1 (ppm)

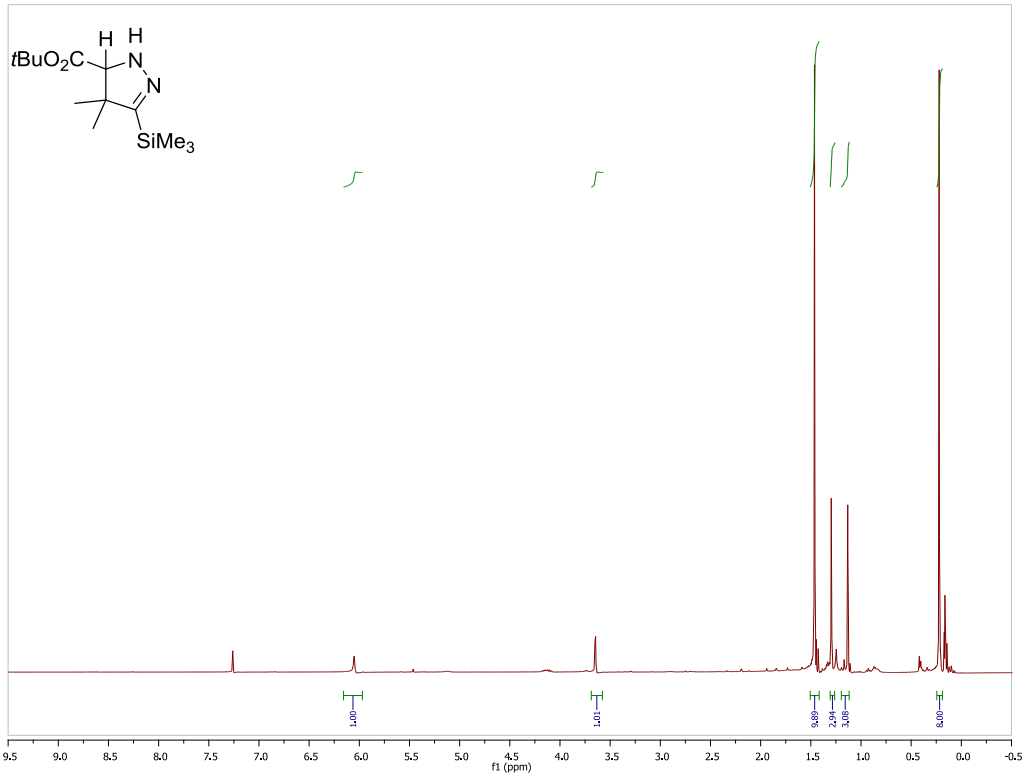
H H
tBuO2C
N
N
SiMe3
1.00
1.01
9.89
2.94
3.08
8.00
9.5 9.0 8.5 8.0 7.5 7.0 6.5 6.0 5.5 5.0 4.5 4.0 3.5 3.0 2.5 2.0 1.5 1.0 0.5 0.0 -0.5
f1 (ppm)

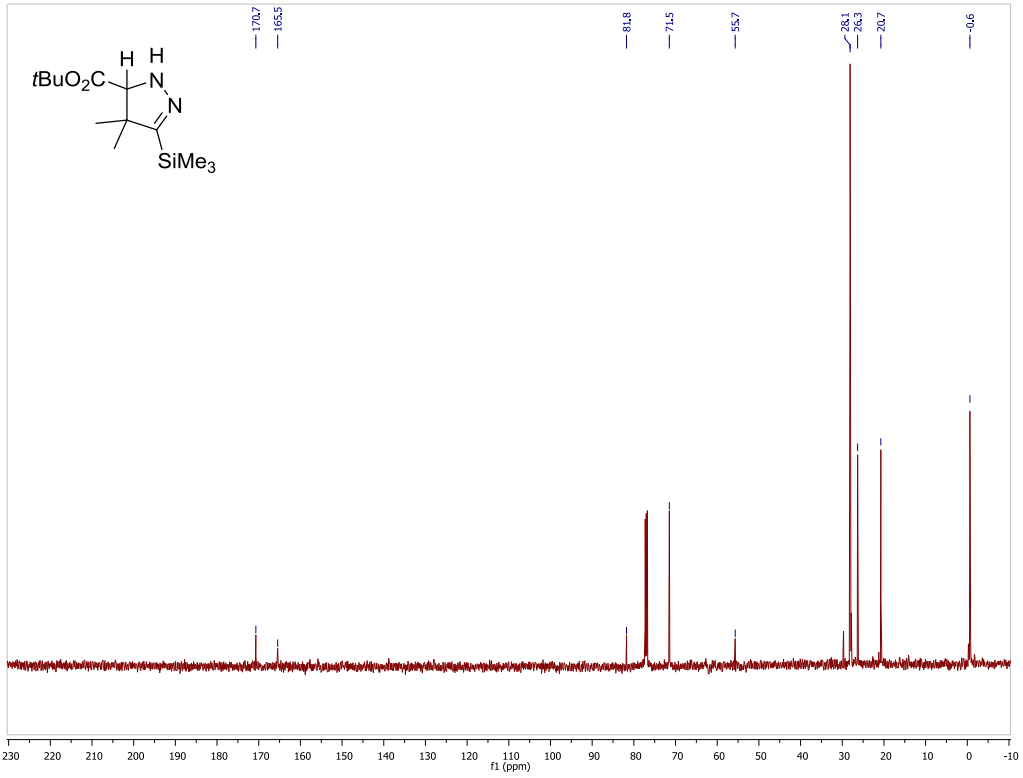
170.7
165.5
81.8
71.5
55.7
28.1
26.3
20.7
-0.6
H H
tBuO2C
N
N
SiMe3
230 220 210 200 190 180 170 160 150 140 130 120 110 100 90 80 70 60 50 40 30 20 10 0 -10
f1 (ppm)

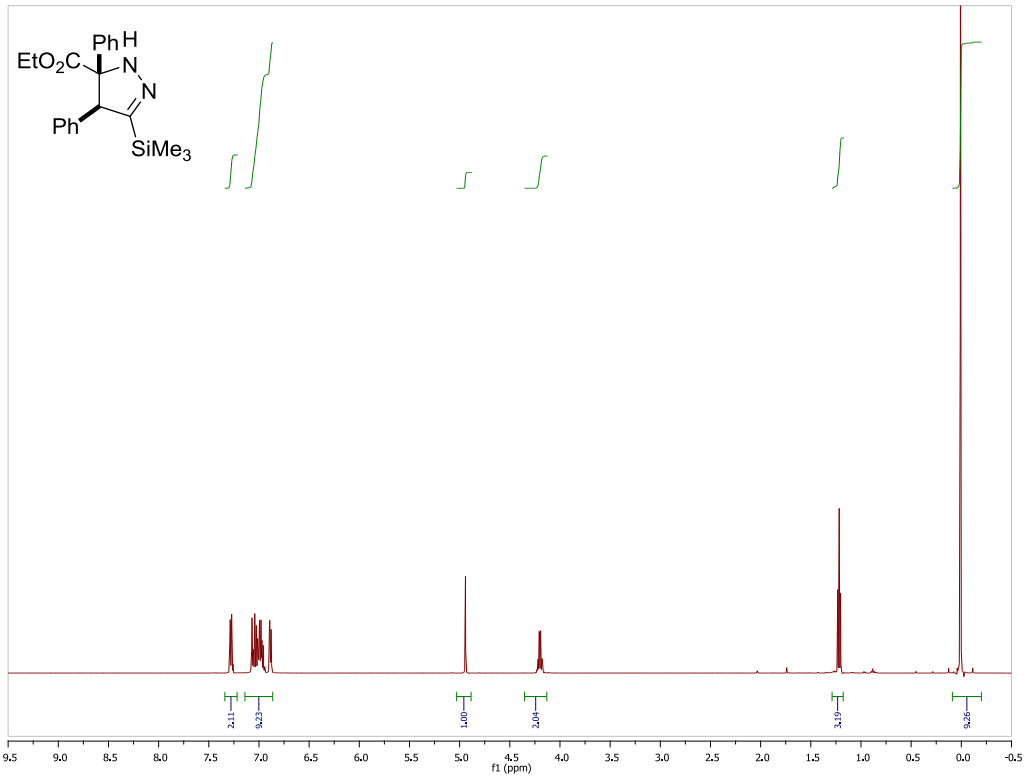
Ph H
EtO2C
N
N
Ph
SiMe3
2.11
9.23
1.00
2.04
3.19
9.26
f1 (ppm)

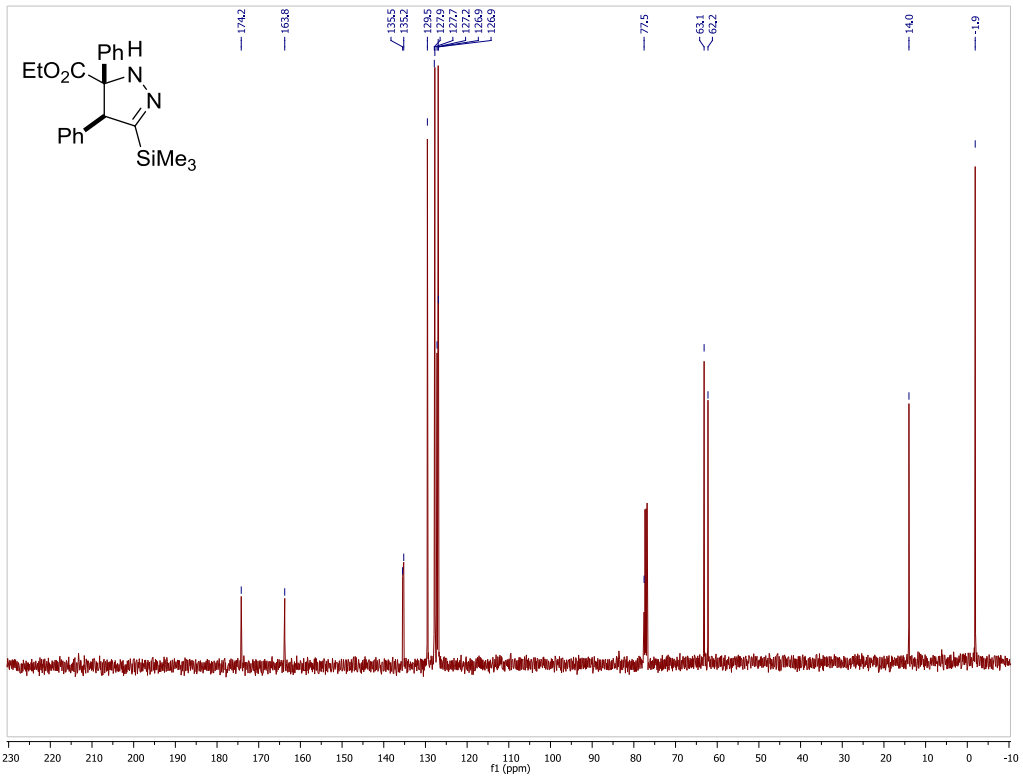
Ph H
EtO2C
N
N
Ph
SiMe3
174.2
163.8
135.5
135.2
129.5
127.9
127.7
127.2
126.9
126.9
77.5
63.1
62.2
14.0
-1.9
f1 (ppm)

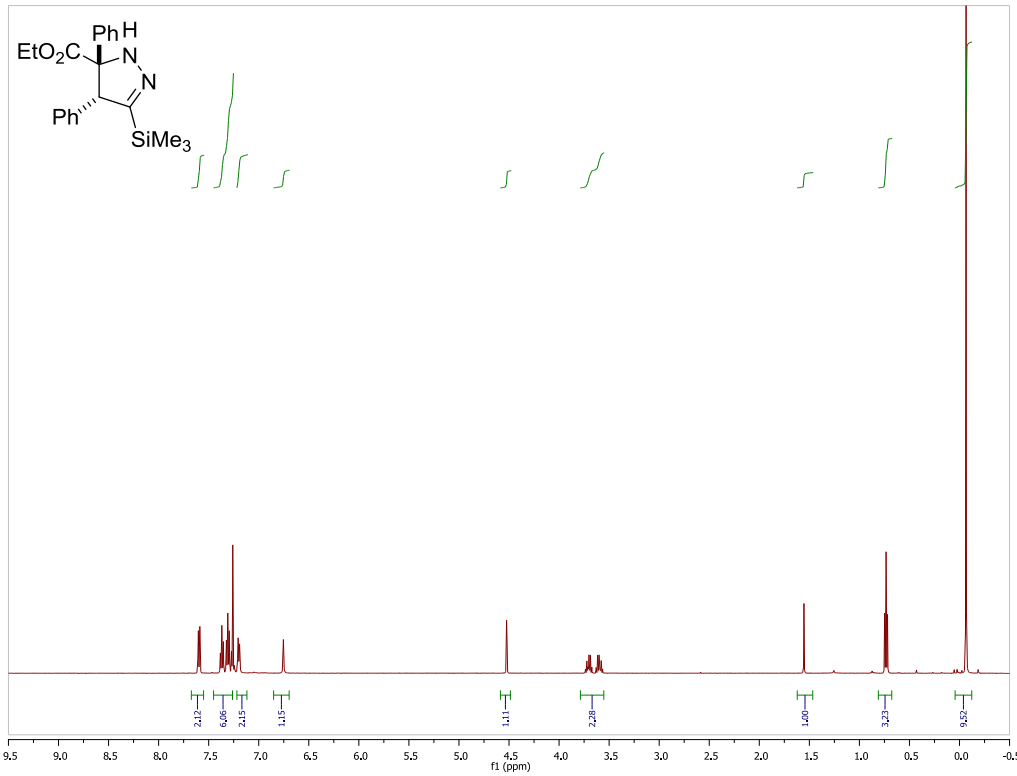
Ph H
EtO2C
N
N
Ph
SiMe3
2.12
6.06
2.15
1.15
1.11
2.28
1.00
3.23
9.52
f1 (ppm)

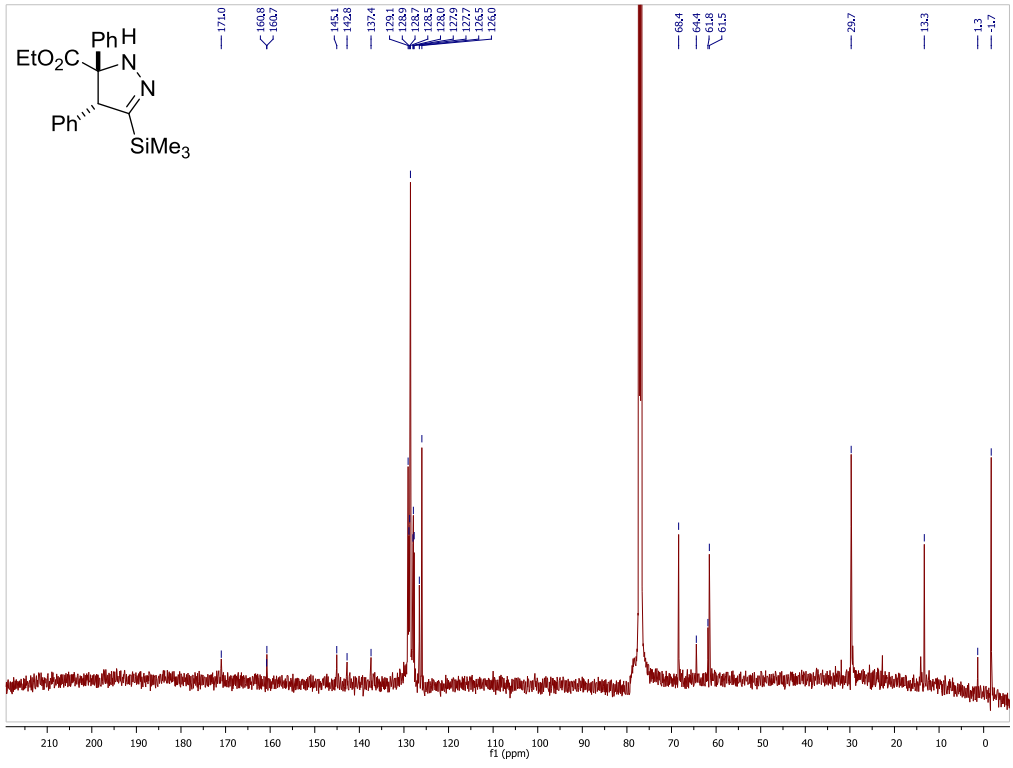
Ph H
EtO2C
N
N
Ph
SiMe3
171.0
160.8
160.7
145.1
142.8
137.4
129.1
128.9
128.7
128.5
128.0
127.9
127.7
126.5
126.0
68.4
64.4
61.8
61.5
29.7
13.3
1.3
-1.7
f1 (ppm)

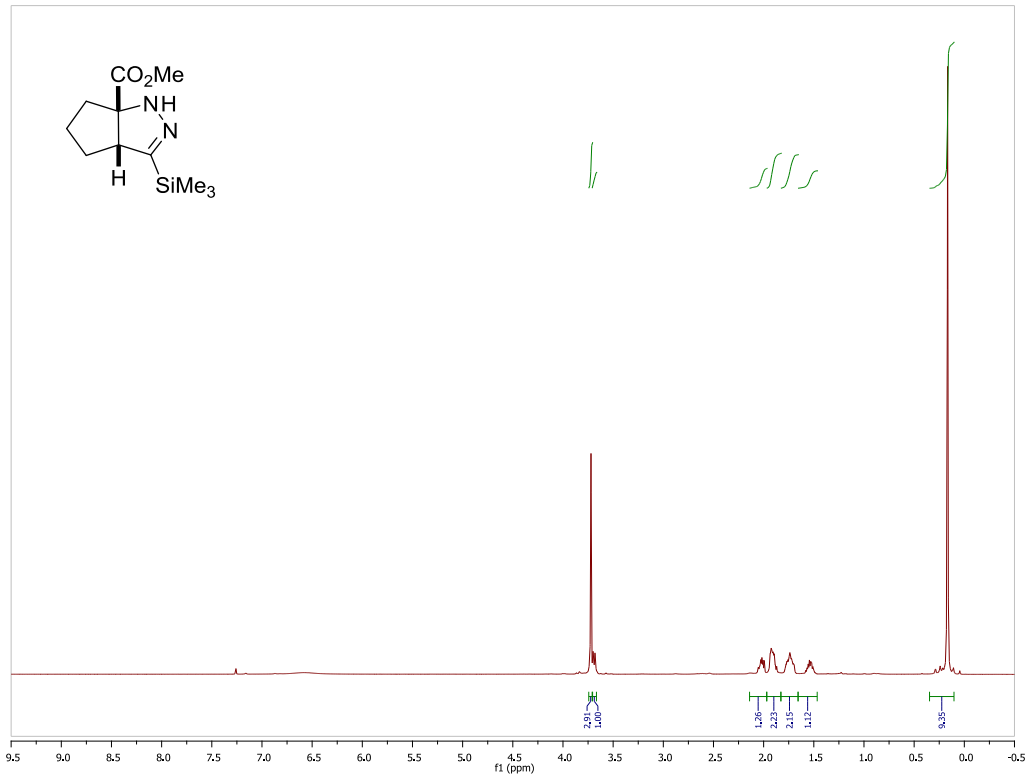
CO2Me
NH
N
H
SiMe3
2.91
1.00
1.26
2.23
2.15
1.12
9.35
f1 (ppm)

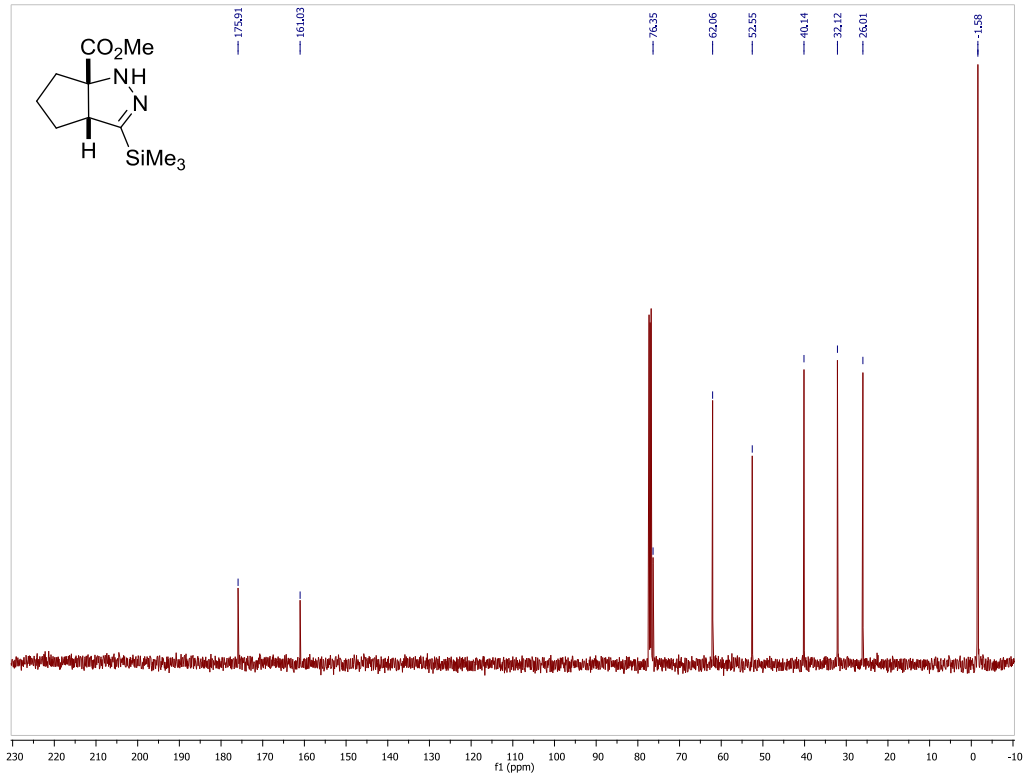
CO2Me
NH
N
H
SiMe3
175.91
161.03
76.35
62.06
52.55
40.14
32.12
26.01
-1.58
f1 (ppm)

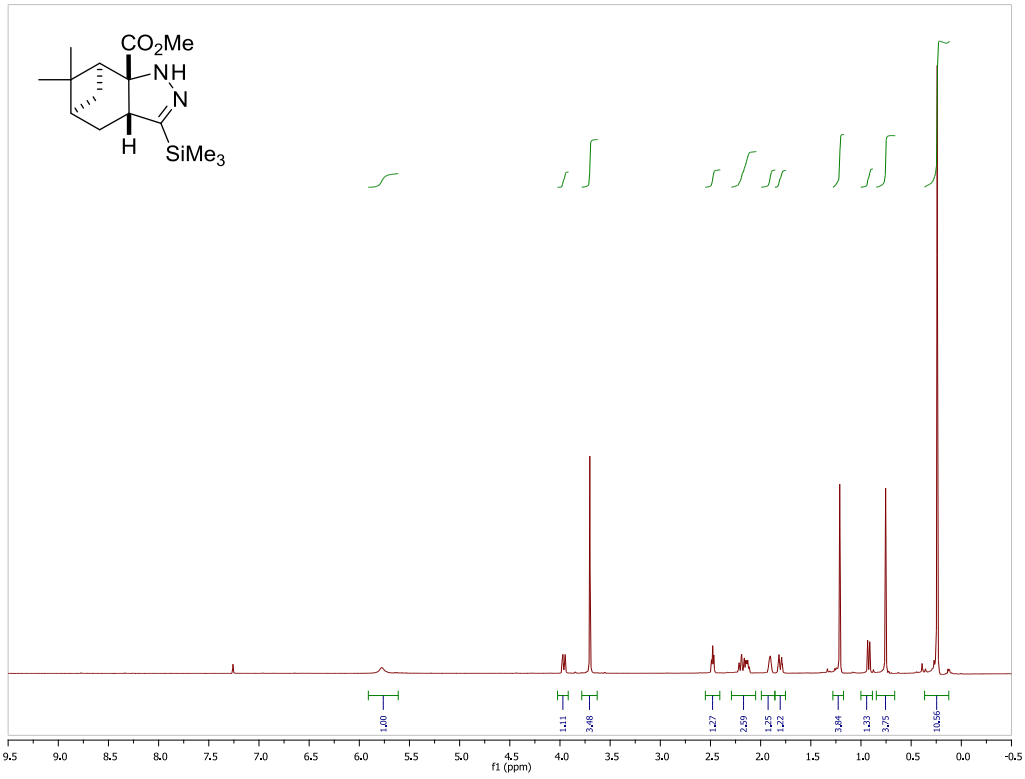
CO2Me
NH
N
H
SiMe3
1.00
1.11
3.48
1.27
2.59
1.25
1.22
3.84
1.33
3.75
10.56
f1 (ppm)

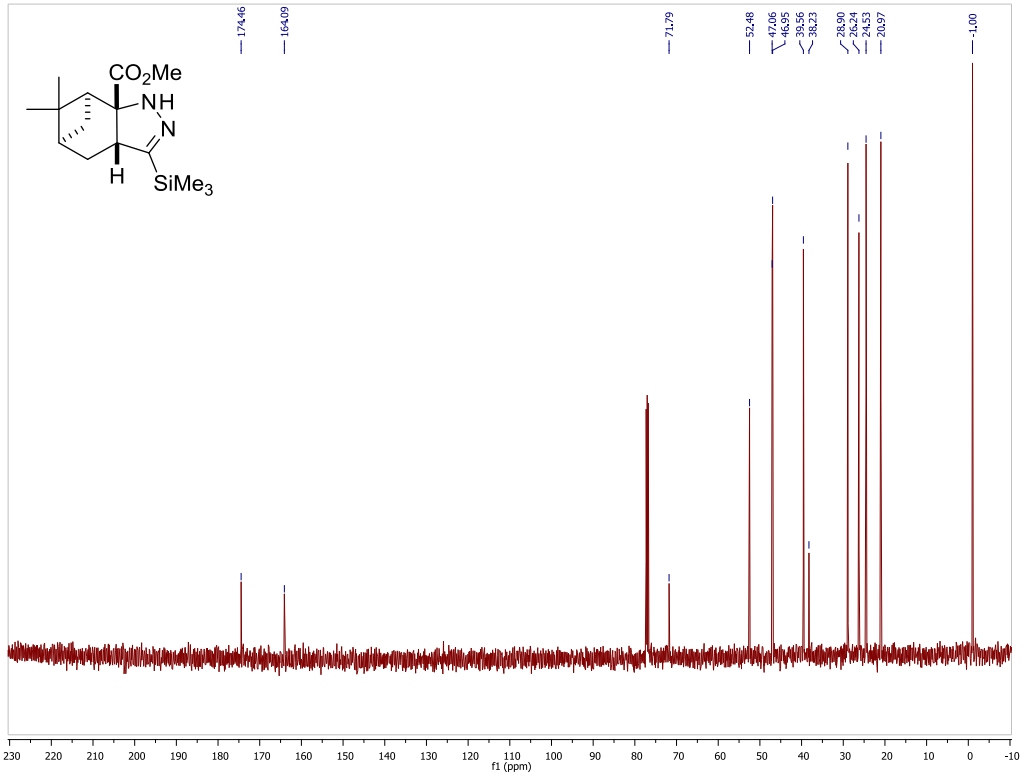
174.46
164.09
71.79
52.48
47.06
46.95
39.56
38.23
28.90
26.24
24.53
20.97
-1.00
CO2Me
NH
N
H
SiMe3
f1 (ppm)

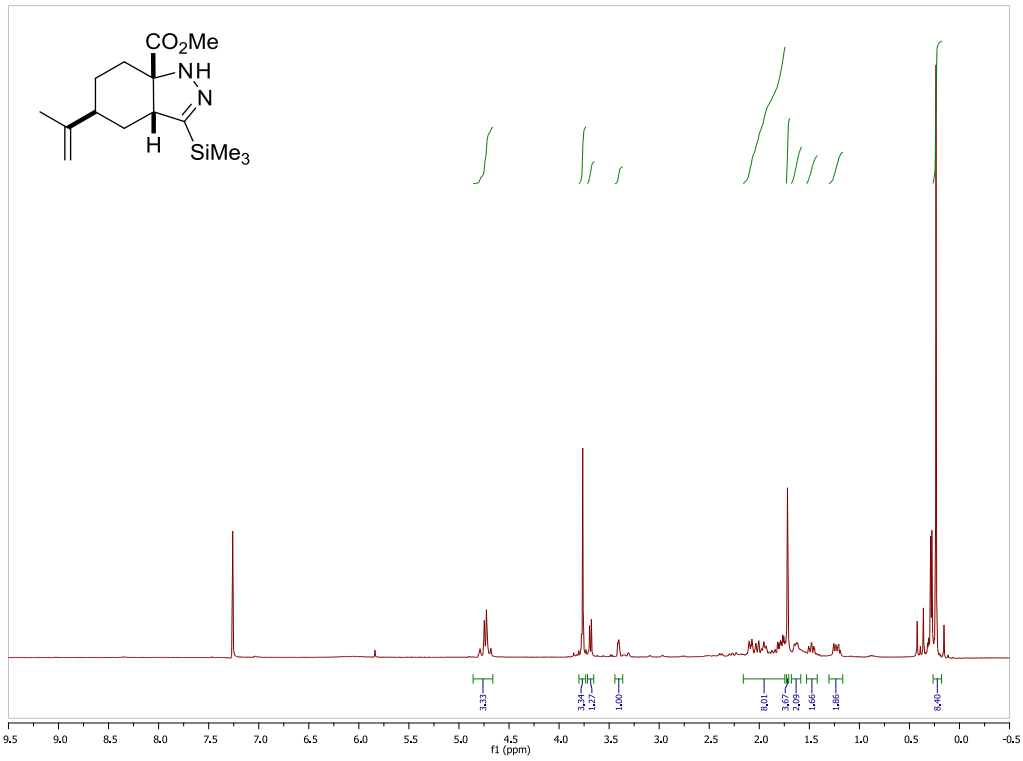
CO2Me
NH
N
H
SiMe3
3.33
3.34
1.27
1.00
8.01
3.67
2.09
1.66
1.86
8.40
f1 (ppm)

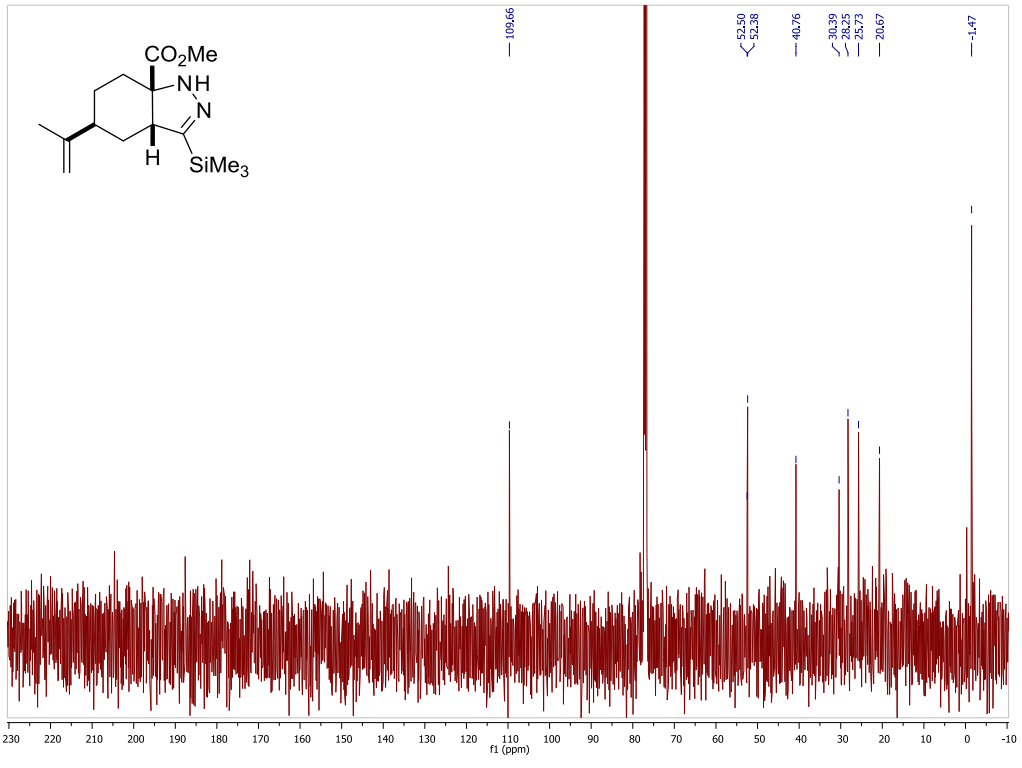
CO2Me
NH
N
H
SiMe3
109.66
52.50
52.38
40.76
30.39
28.25
25.73
20.67
-1.47
f1 (ppm)

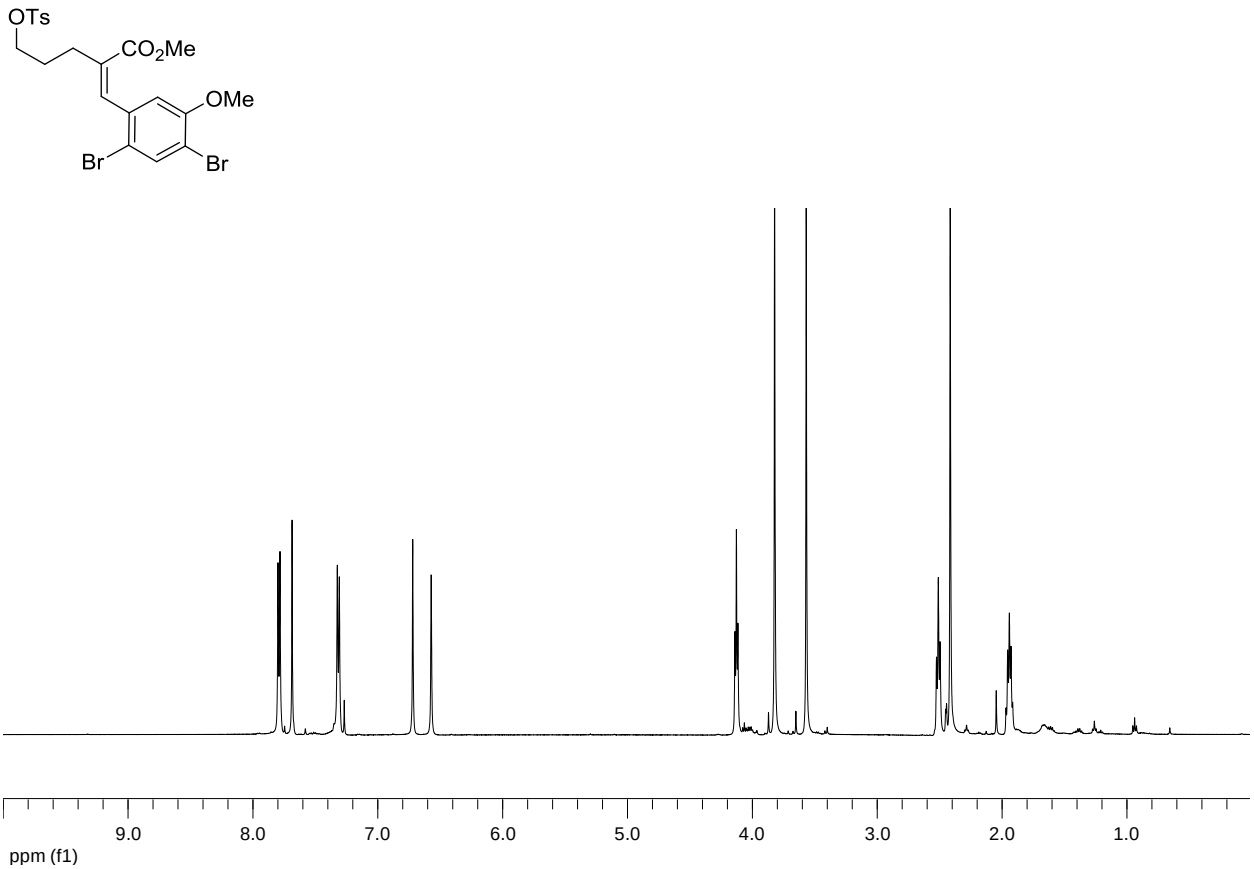
OTs
CO2Me
OMe
Br
Br
9.0
8.0
7.0
6.0
5.0
4.0
3.0
2.0
1.0
ppm (f1)

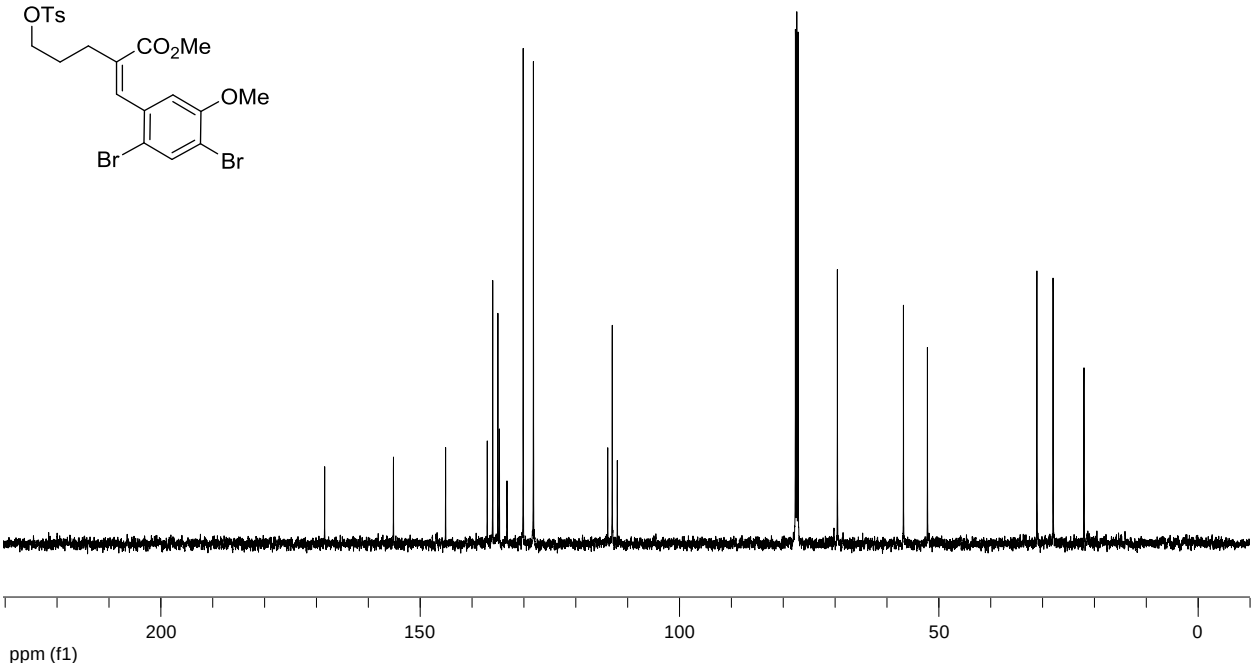
OTs
CO2Me
OMe
Br
Br
200
150
100
50
0
ppm (f1)

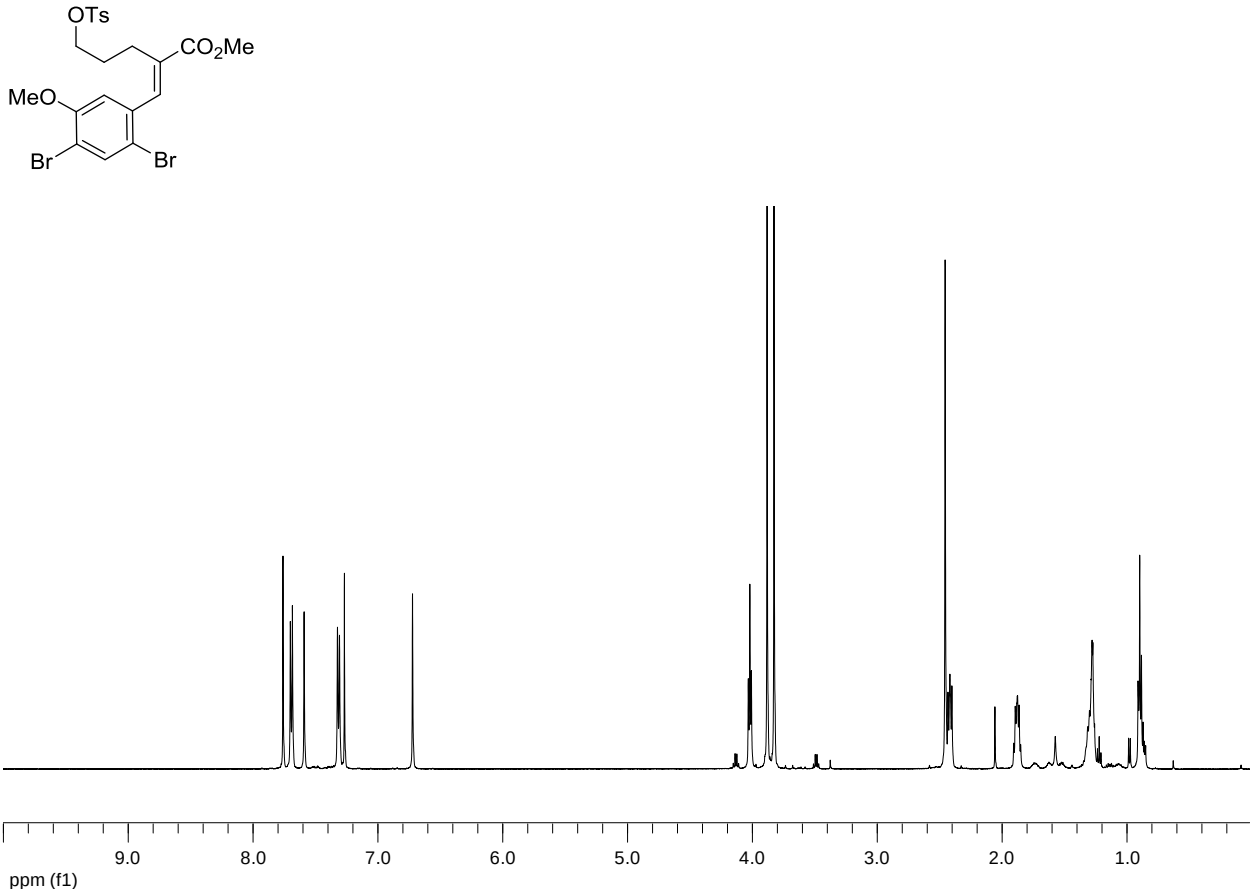
OTs
CO2Me
MeO
Br
Br
9.0
8.0
7.0
6.0
5.0
4.0
3.0
2.0
1.0
ppm (f1)

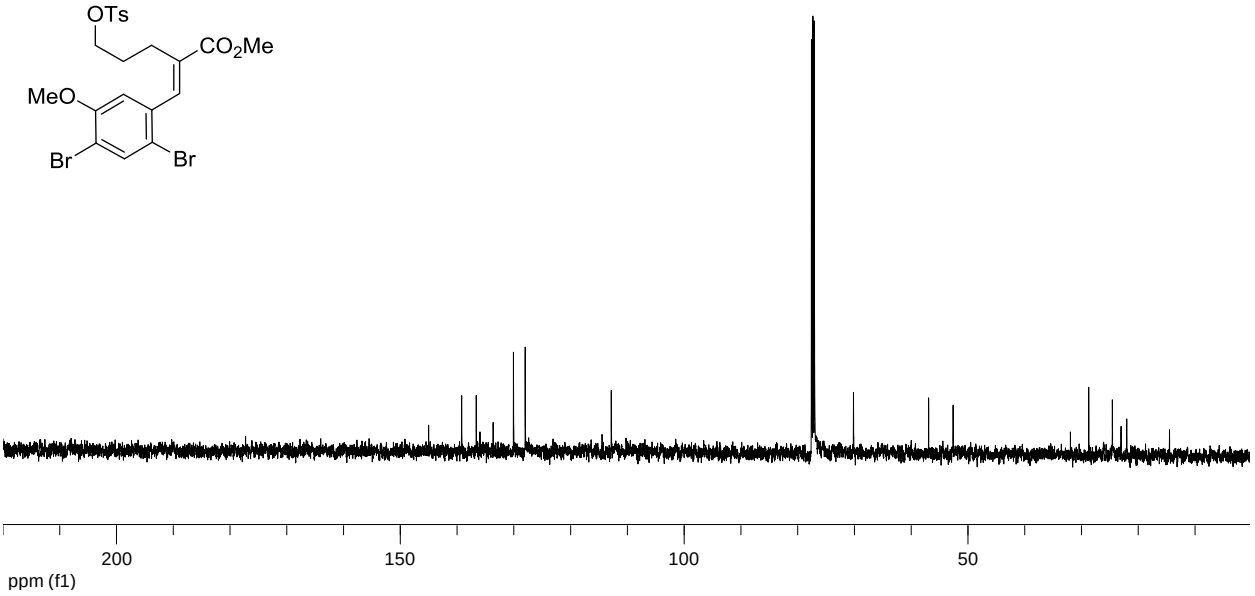
OTs
CO2Me
MeO
Br
Br
200
150
100
50
ppm (f1)

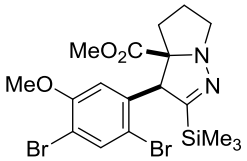
MeO2C
N
N
MeO
Br
Br
SiMe3

β-aryl

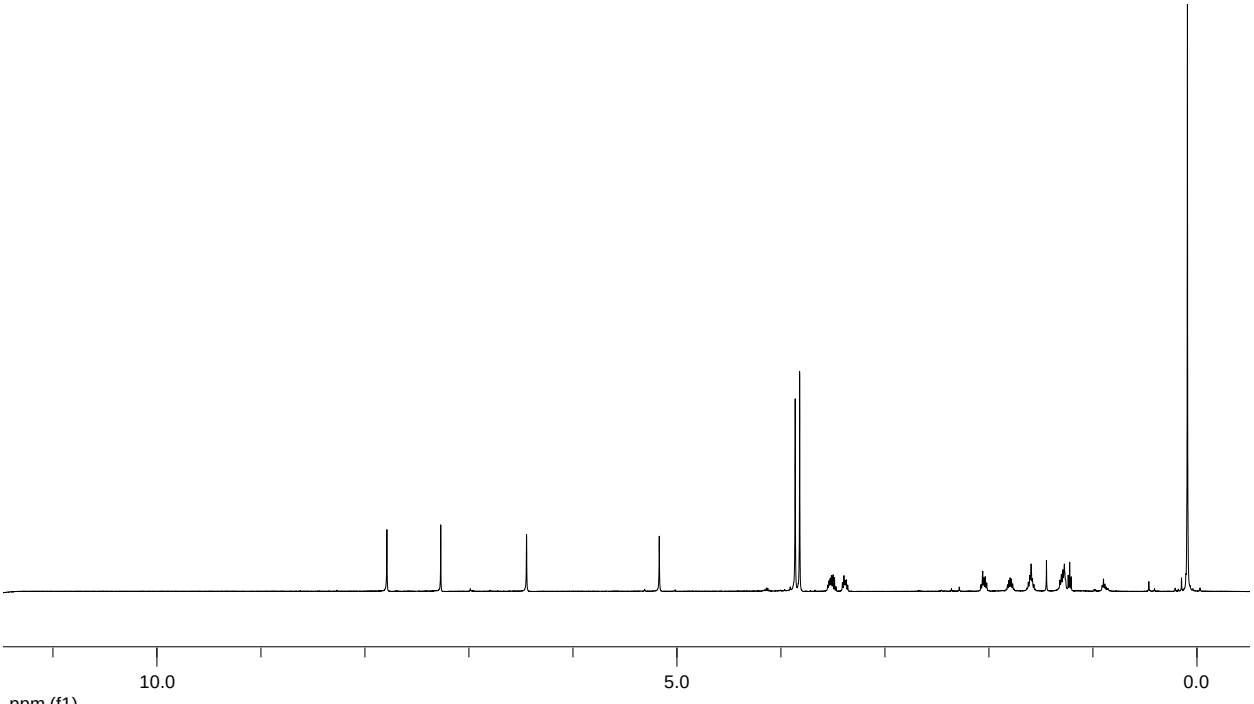
10.0
5.0
0.0
ppm (f1)

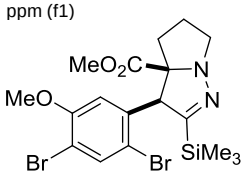
MeO2C
N
N
MeO
Br
Br
SiMe3

β-aryl

200
150
100
50
0
ppm (f1)

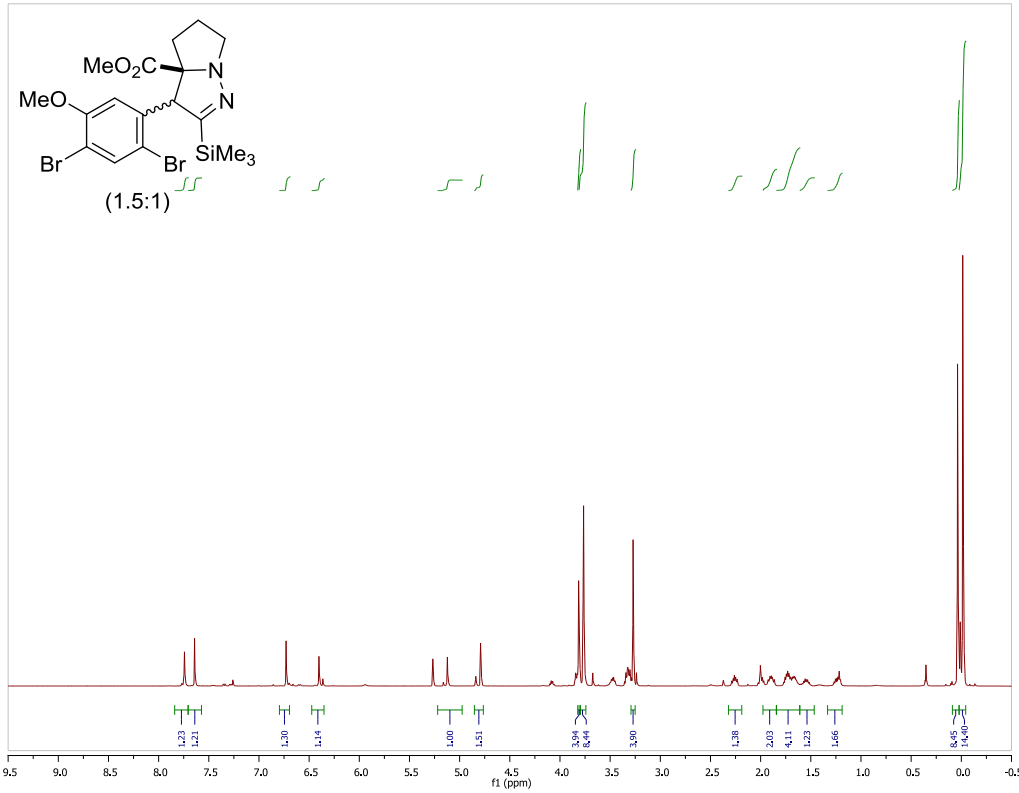
MeO2C
N
MeO
N
Br
Br
SiMe3
(1.5:1)
f1 (ppm)

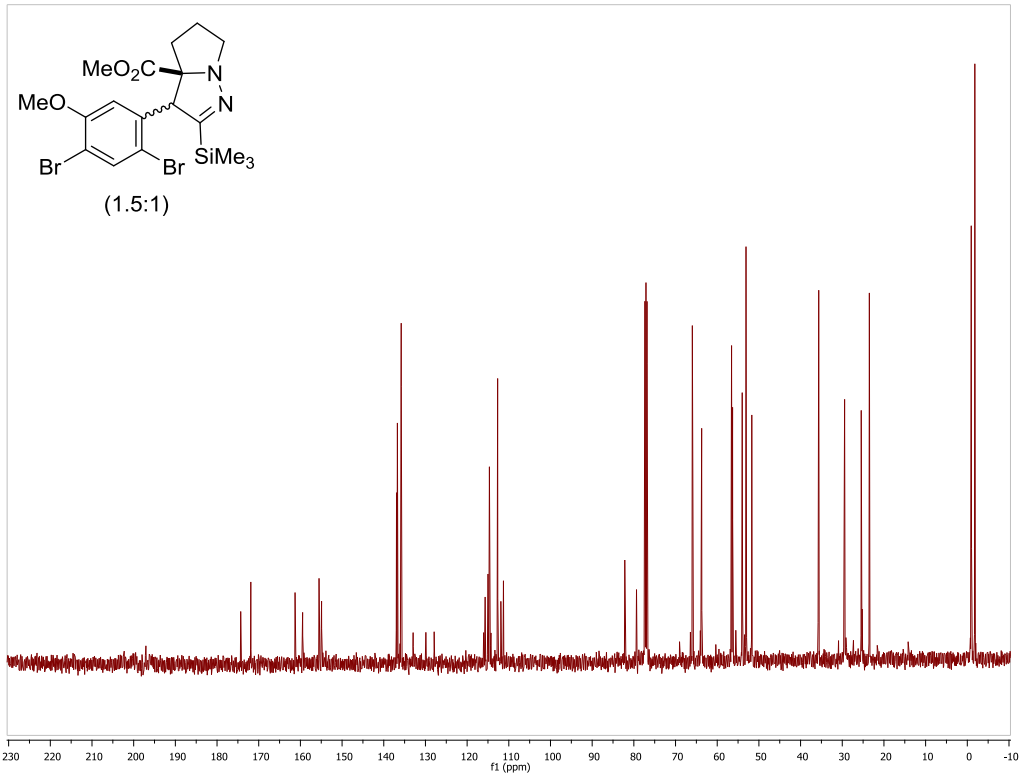
MeO2C
N
MeO
N
Br
Br
SiMe3
(1.5:1)
f1 (ppm)

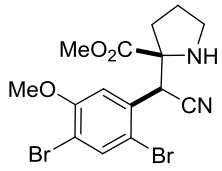
MeO2C
NH
MeO
CN
Br
Br

(β-Aryl)

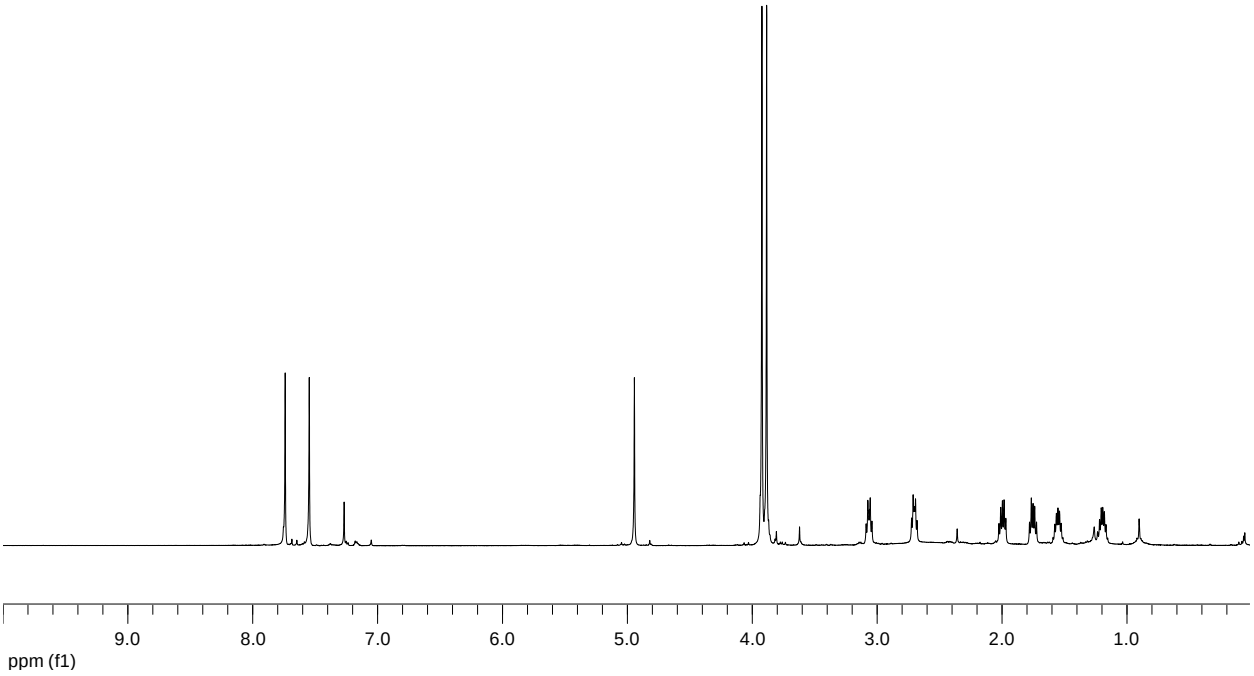
9.0
8.0
7.0
6.0
5.0
4.0
3.0
2.0
1.0
ppm (f1)

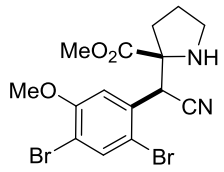
MeO2C
NH
MeO
CN
Br
Br

(β-Aryl)

200
150
100
50
0
ppm (f1)

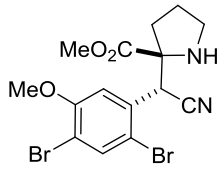
MeO2C
NH
MeO
CN
Br
Br

(α-Aryl)

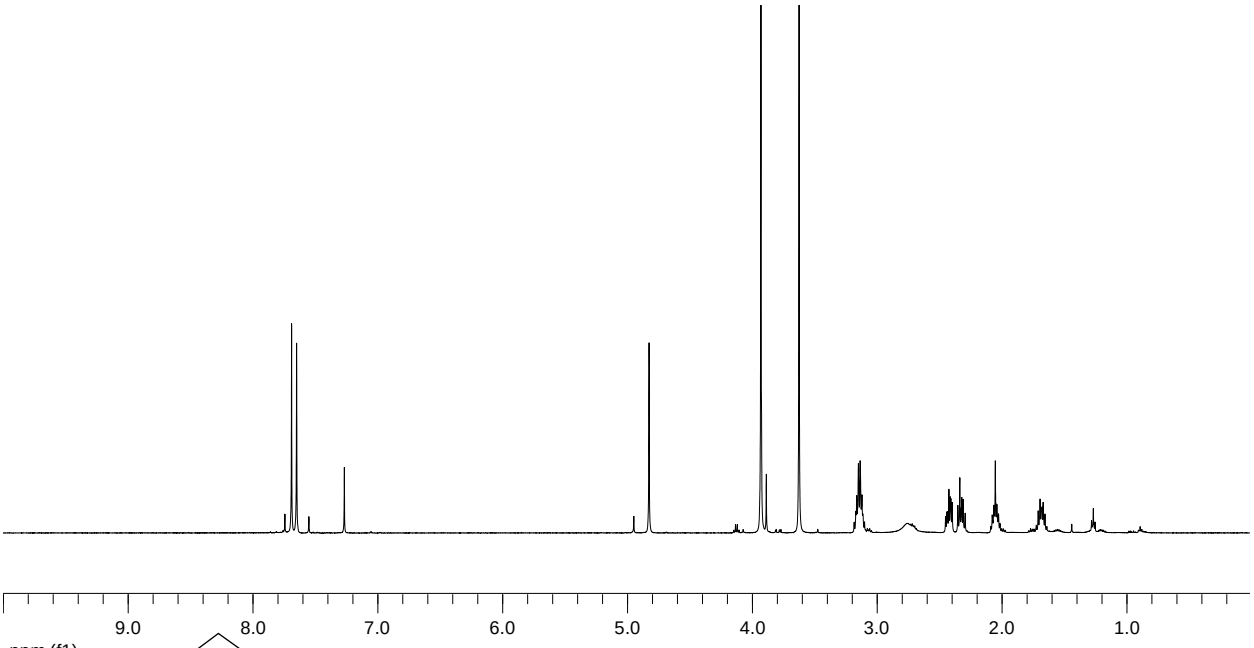
9.0
8.0
7.0
6.0
5.0
4.0
3.0
2.0
1.0
ppm (f1)

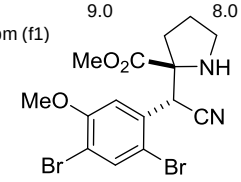
MeO2C
NH
MeO
CN
Br
Br

(α-Aryl)

200
150
100
50
0
ppm (f1)

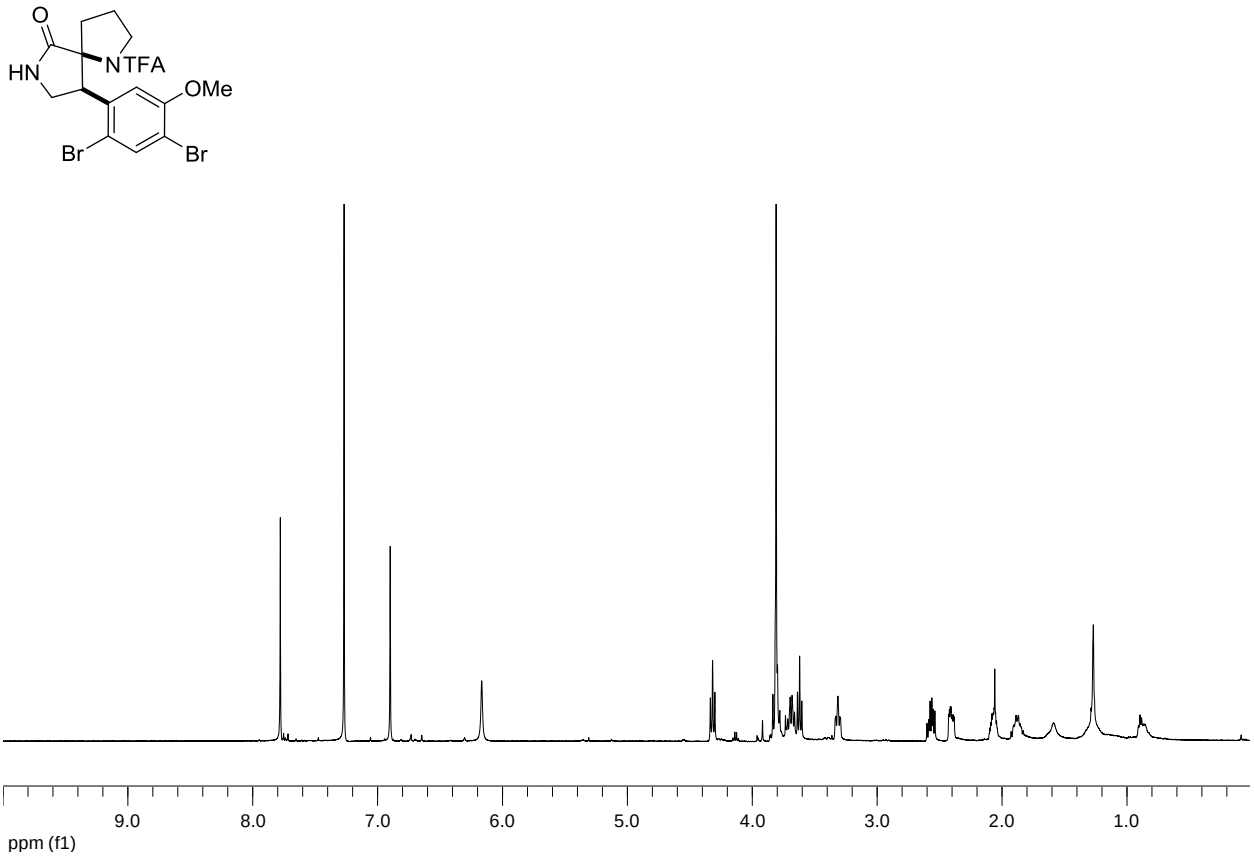
O
HN
NTFA
OMe
Br
Br
9.0
8.0
7.0
6.0
5.0
4.0
3.0
2.0
1.0
ppm (f1)

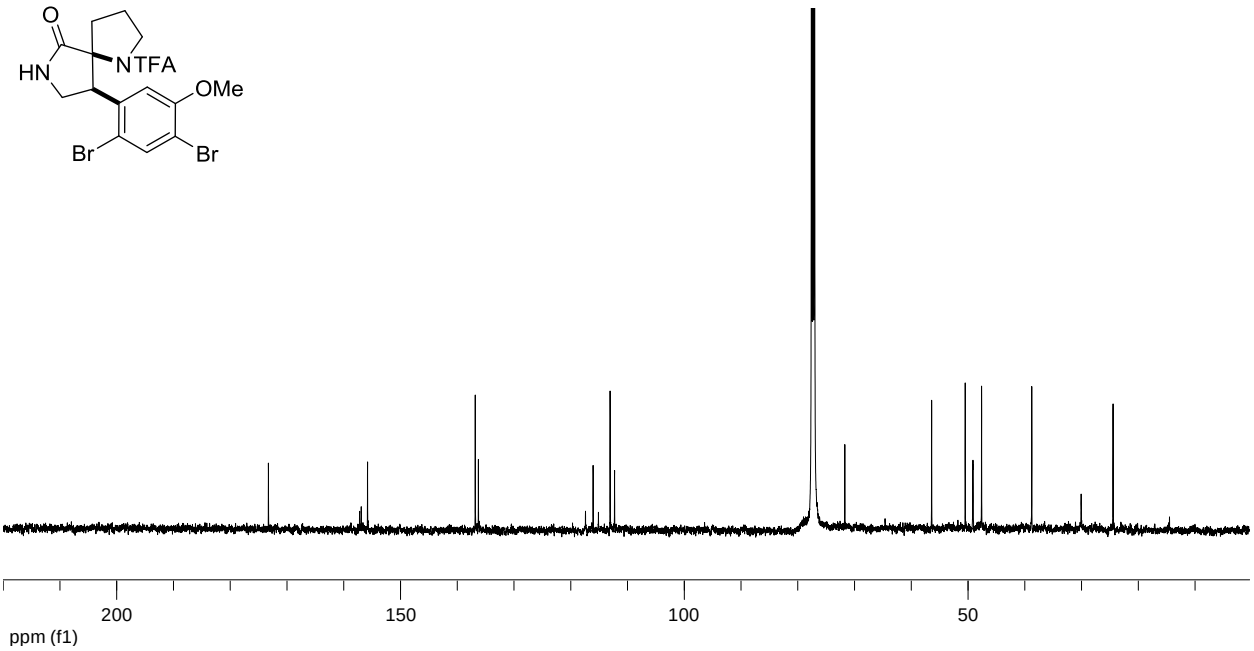
O
HN
NTFA
OMe
Br
Br
200
150
100
50
ppm (f1)

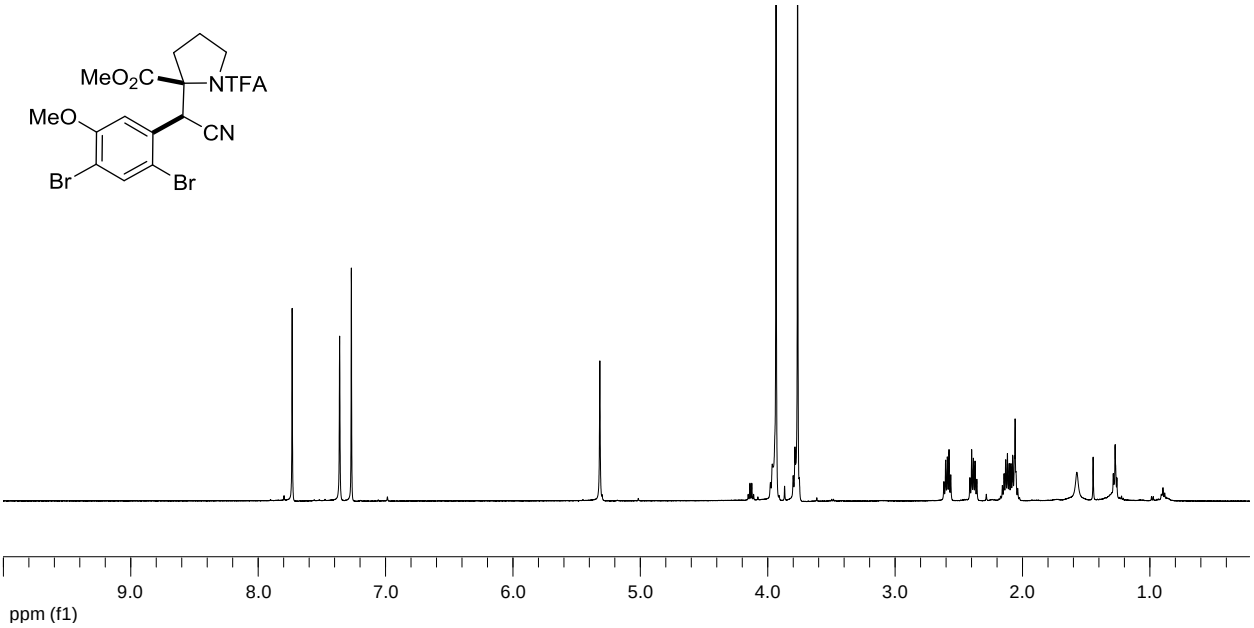
MeO2C
NTFA
MeO
CN
Br
Br
9.0
8.0
7.0
6.0
5.0
4.0
3.0
2.0
1.0
ppm (f1)

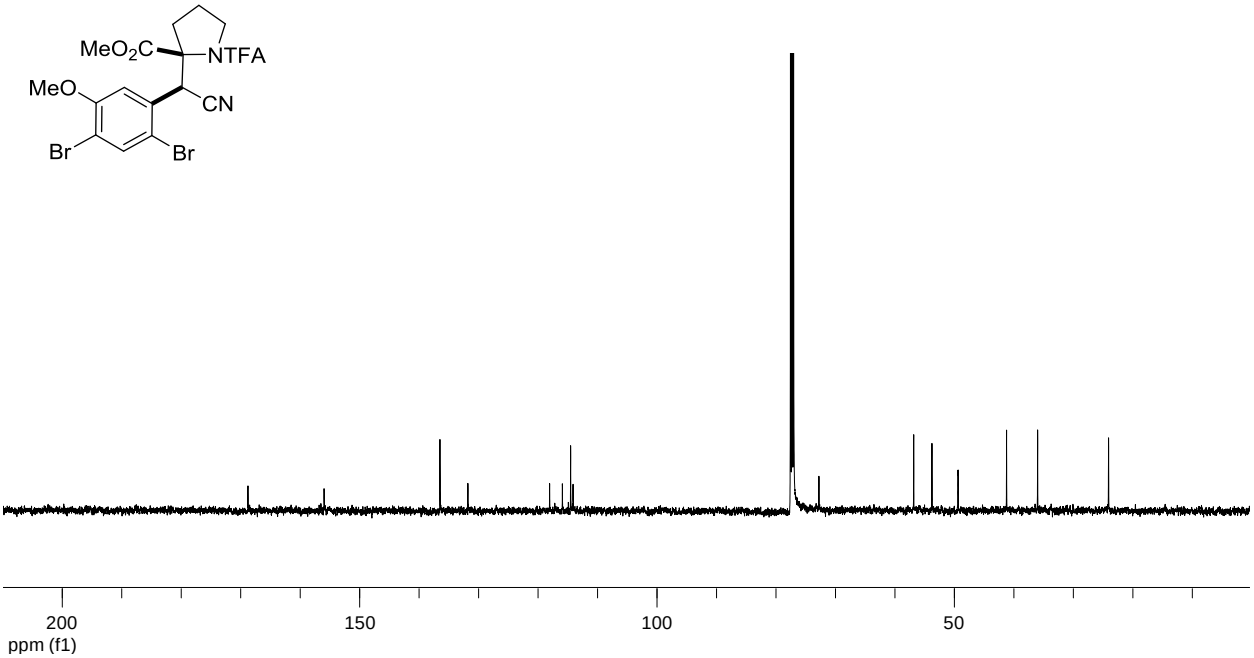
MeO2C
NTFA
MeO
CN
Br
Br
200
150
100
50
ppm (f1)

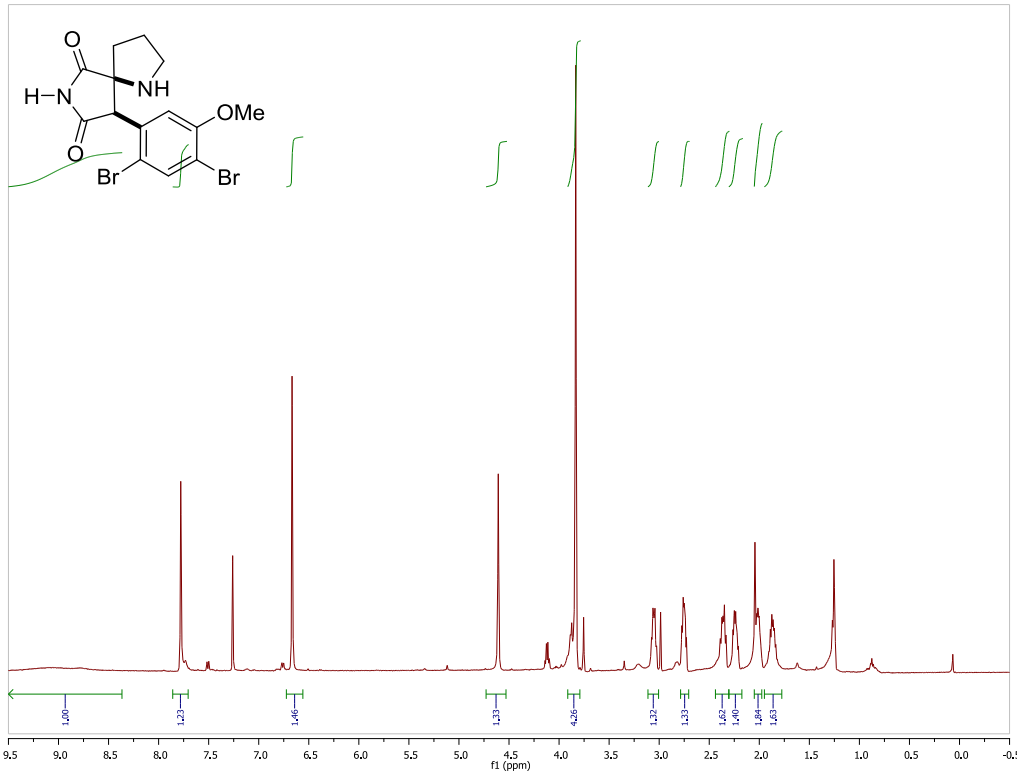
O
H–N
NH
O
OMe
Br
Br
1.00
1.23
1.46
1.23
4.26
1.32
1.33
1.62
1.40
1.84
1.63
9.5 9.0 8.5 8.0 7.5 7.0 6.5 6.0 5.5 5.0 4.5 4.0 3.5 3.0 2.5 2.0 1.5 1.0 0.5 0.0 -0.5
f1 (ppm)

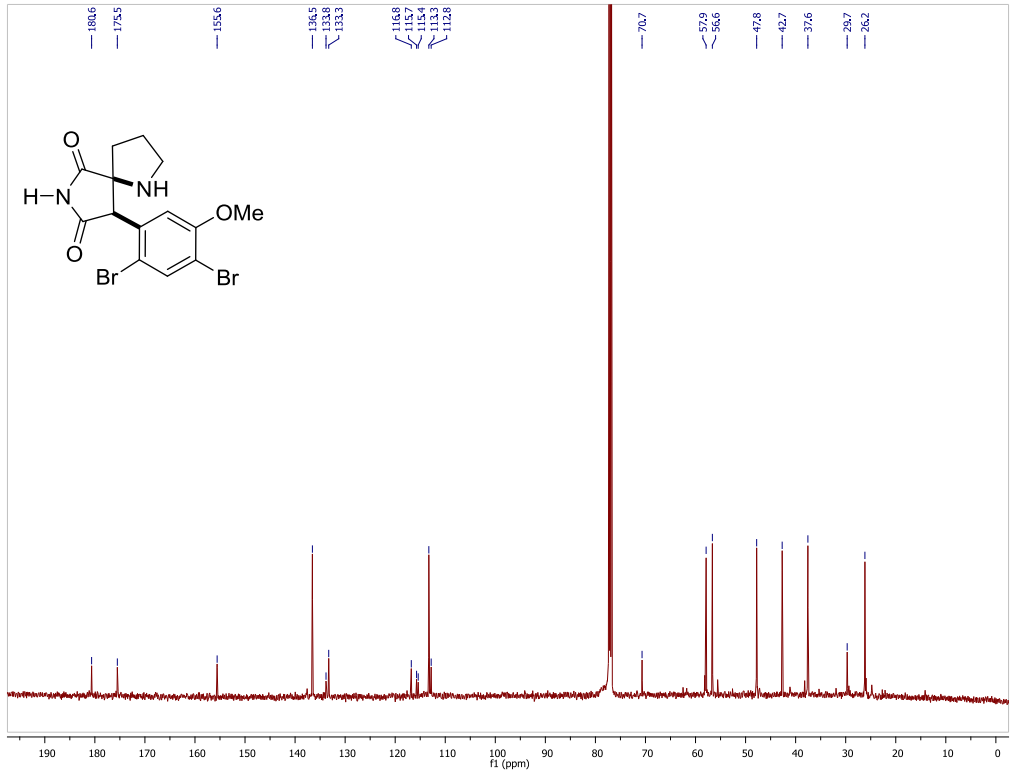
180.6
175.5
155.6
136.5
133.8
133.3
116.8
115.7
115.4
113.3
112.8
70.7
57.9
56.6
47.8
42.7
37.6
29.7
26.2
O
H–N
NH
O
OMe
Br
Br
190 180 170 160 150 140 130 120 110 100 90 80 70 60 50 40 30 20 10 0
f1 (ppm)

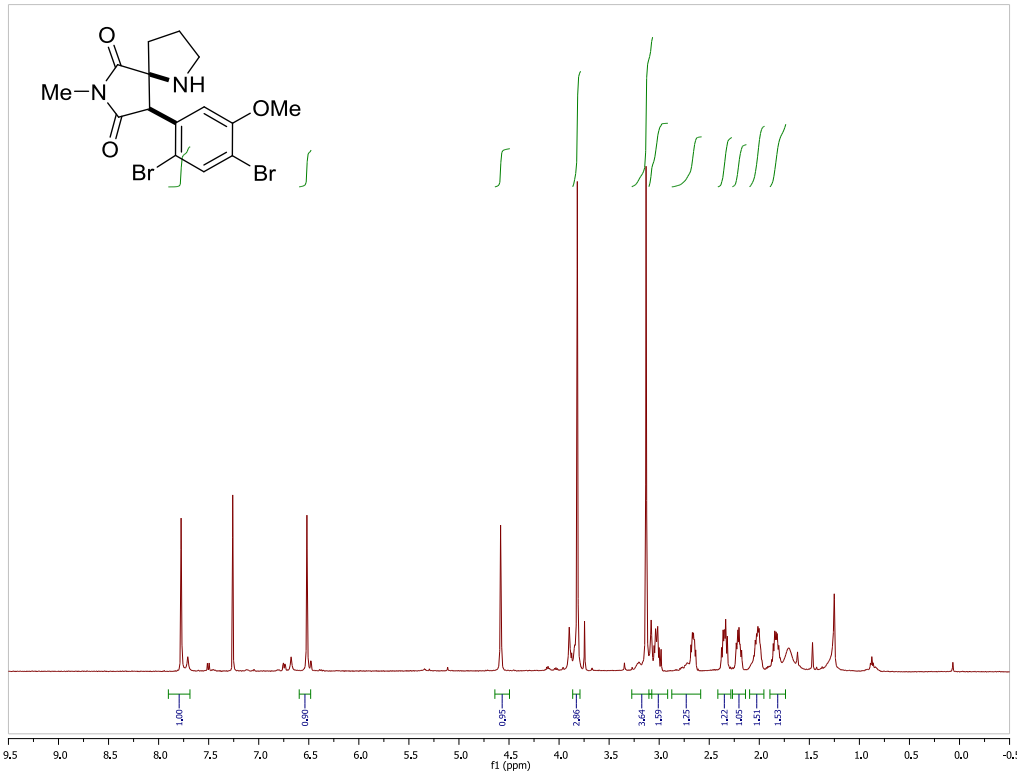
O
Me–N
NH
OMe
O
Br
Br
1.00
0.90
0.95
2.86
3.64
1.59
1.25
1.22
1.45
1.51
1.53
9.5 9.0 8.5 8.0 7.5 7.0 6.5 6.0 5.5 5.0 4.5 4.0 3.5 3.0 2.5 2.0 1.5 1.0 0.5 0.0 -0.5
f1 (ppm)

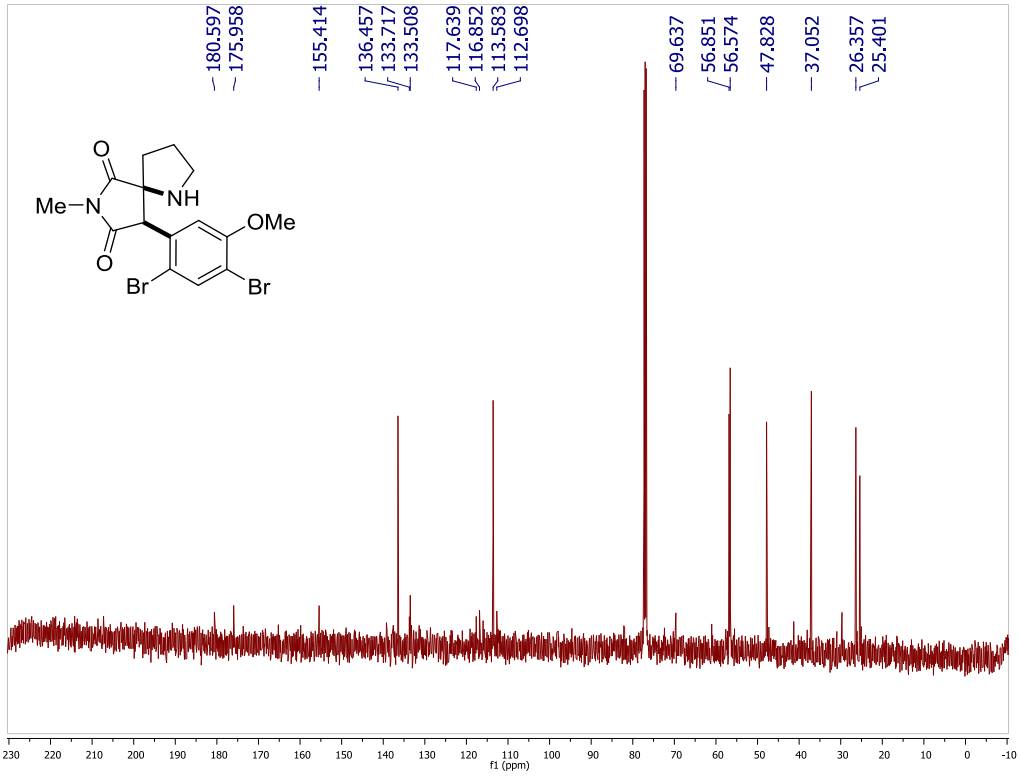
180.597
175.958
155.414
136.457
133.717
133.508
117.639
116.852
113.583
112.698
69.637
56.851
56.574
47.828
37.052
26.357
25.401
O
Me–N
NH
OMe
O
Br
Br
230 220 210 200 190 180 170 160 150 140 130 120 110 100 90 80 70 60 50 40 30 20 10 0 -10
f1 (ppm)

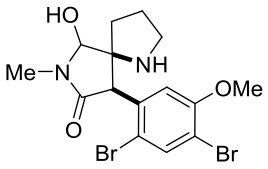
HO
Me–N
NH
OMe
O
Br
Br

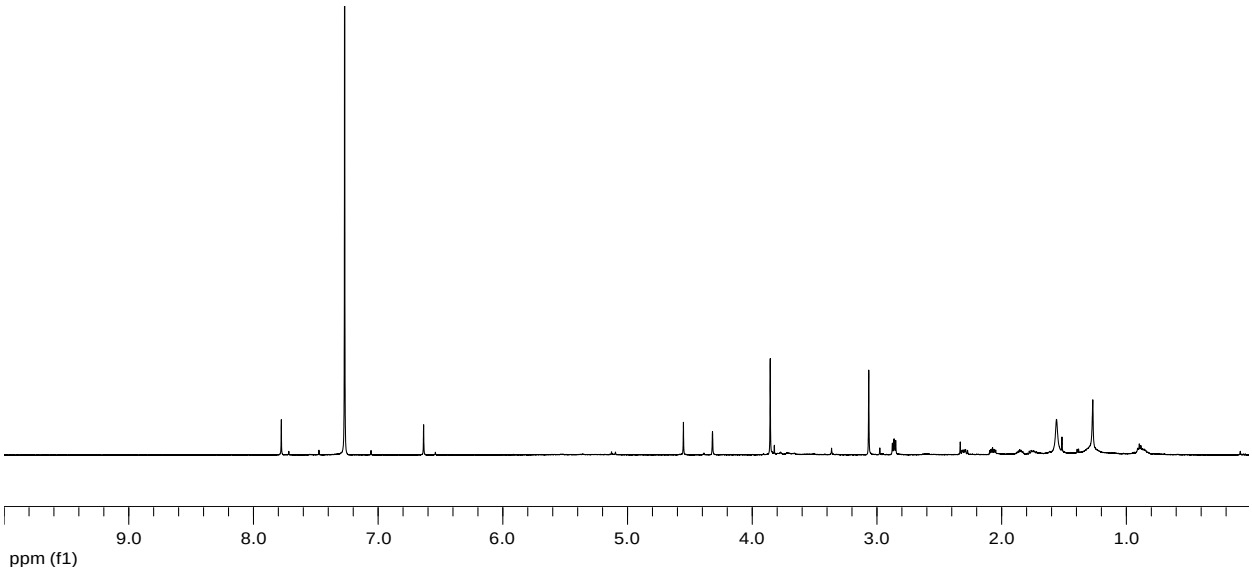
9.0
8.0
7.0
6.0
5.0
4.0
3.0
2.0
1.0
ppm (f1)

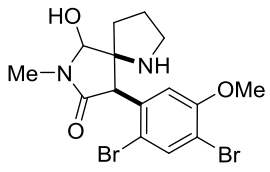
HO
Me–N
NH
OMe
O
Br
Br

epi

9.0
8.0
7.0
6.0
5.0
4.0
3.0
2.0
1.0
ppm (f1)

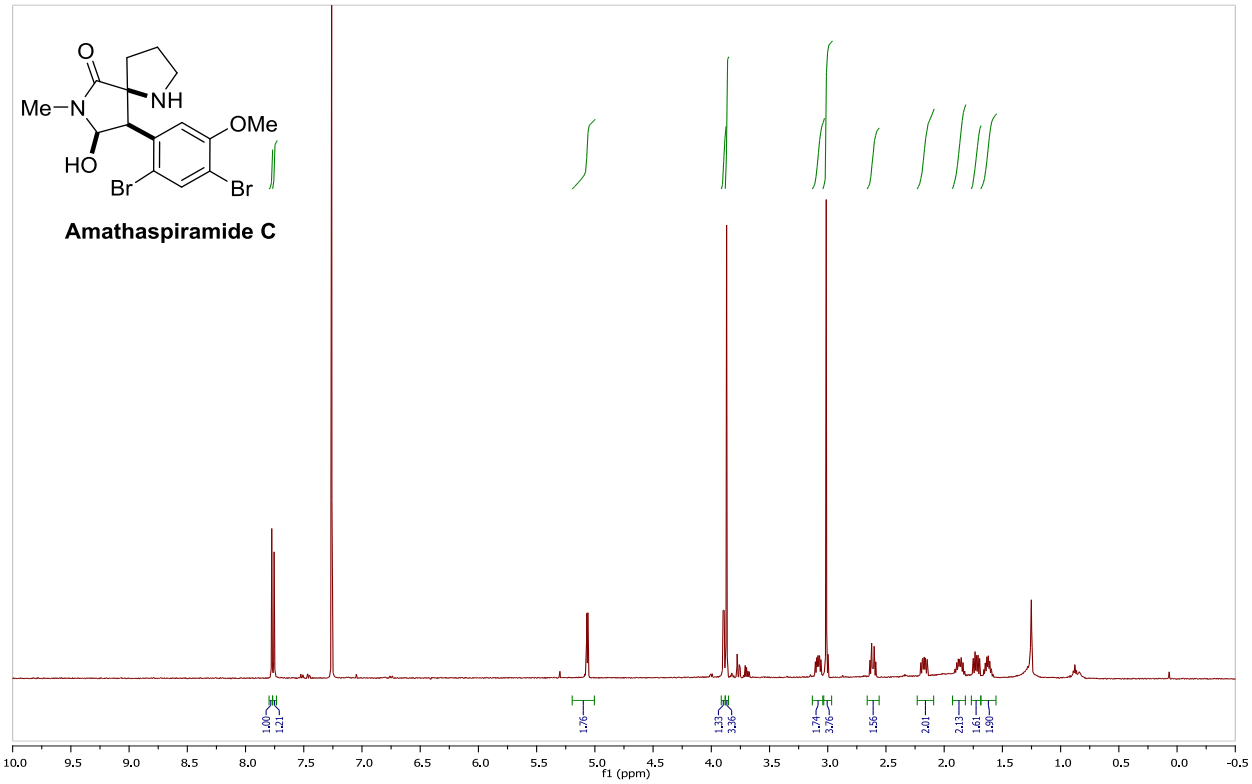

Authentic NMR of amathaspiramide C

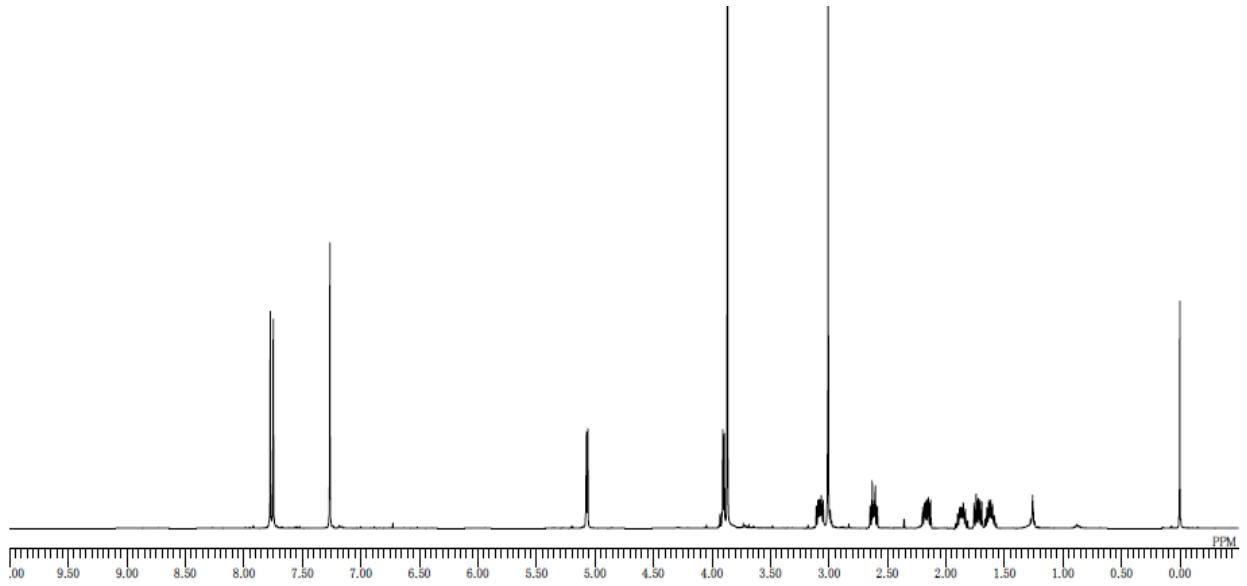

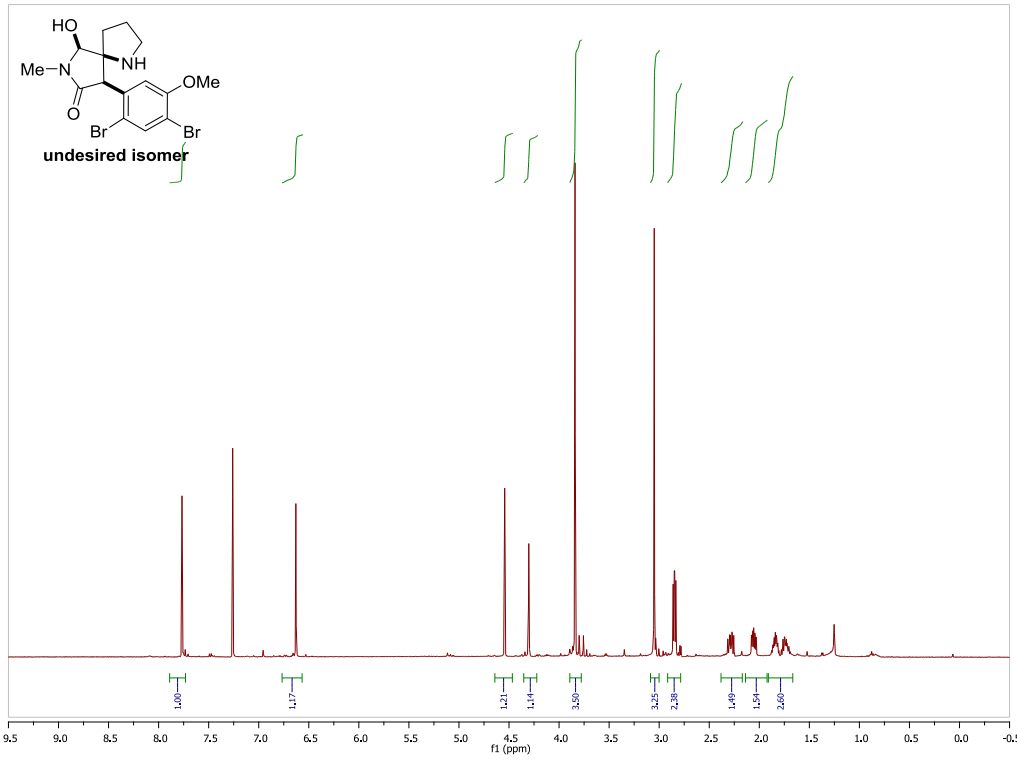
HO
Me–N
NH
O
OMe
Br
Br
undesired isomer
1.00
1.17
1.21
1.14
3.50
3.25
2.38
1.49
1.54
2.60
f1 (ppm)

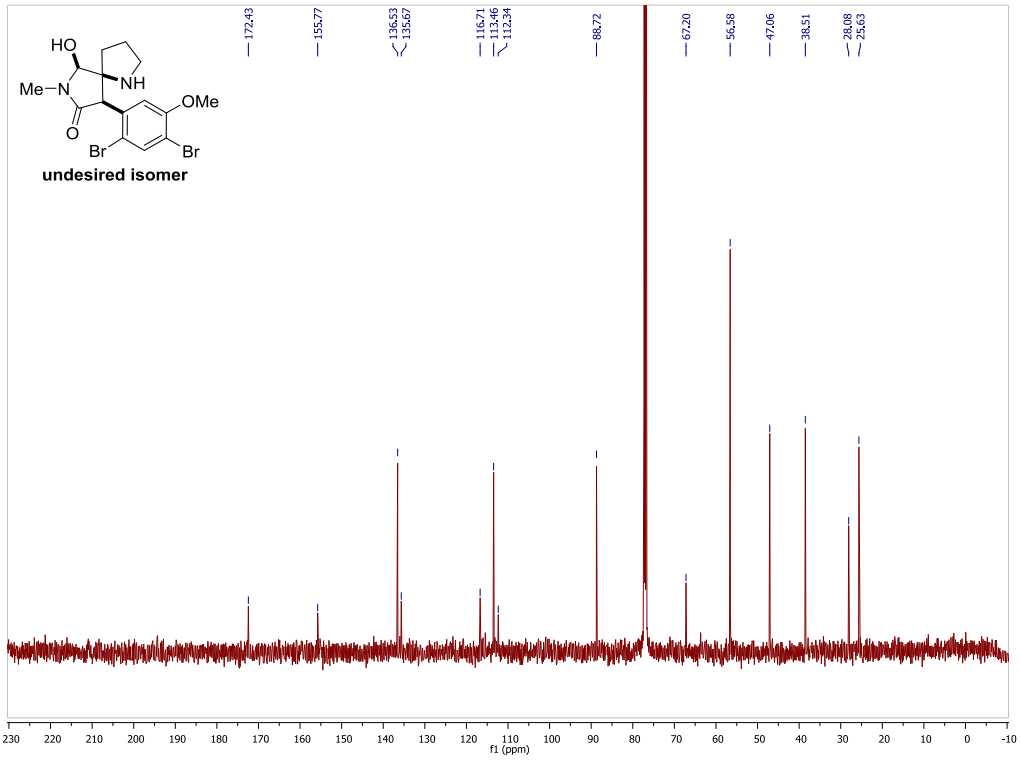
HO
Me–N
NH
O
OMe
Br
Br
undesired isomer
172.43
155.77
136.53
135.67
116.71
113.46
112.34
88.72
67.20
56.58
47.06
38.51
28.08
25.63
f1 (ppm)

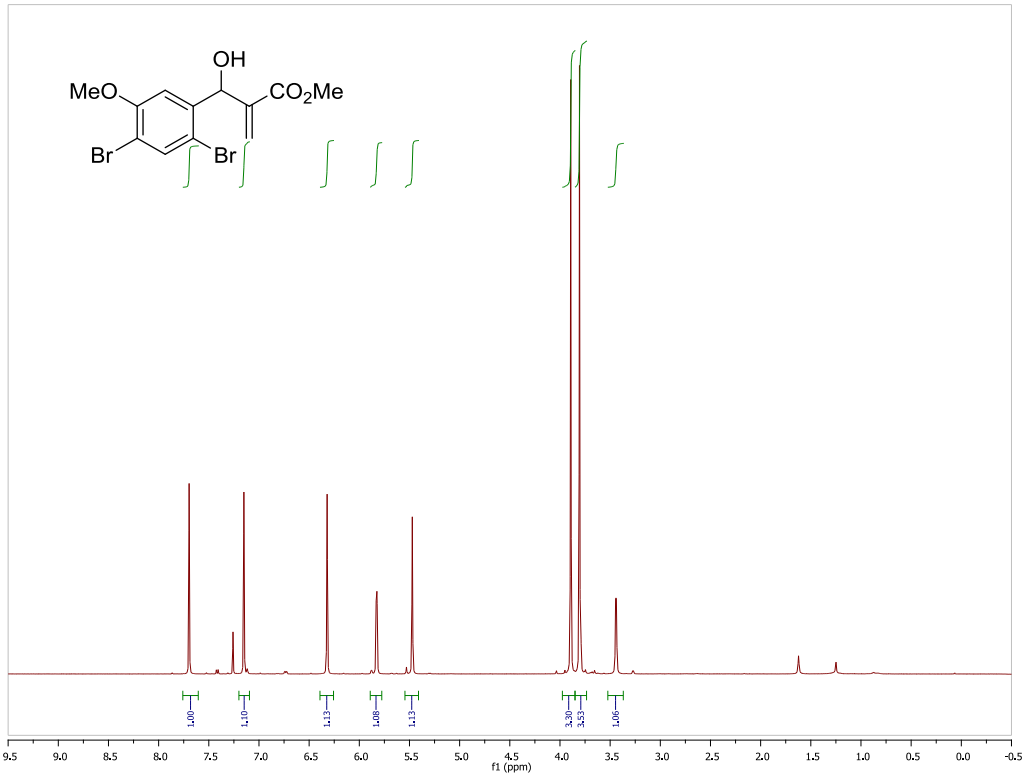
OH
MeO
CO2Me
Br
Br
1.00
1.10
1.13
1.08
1.13
3.30
3.53
1.06
f1 (ppm)

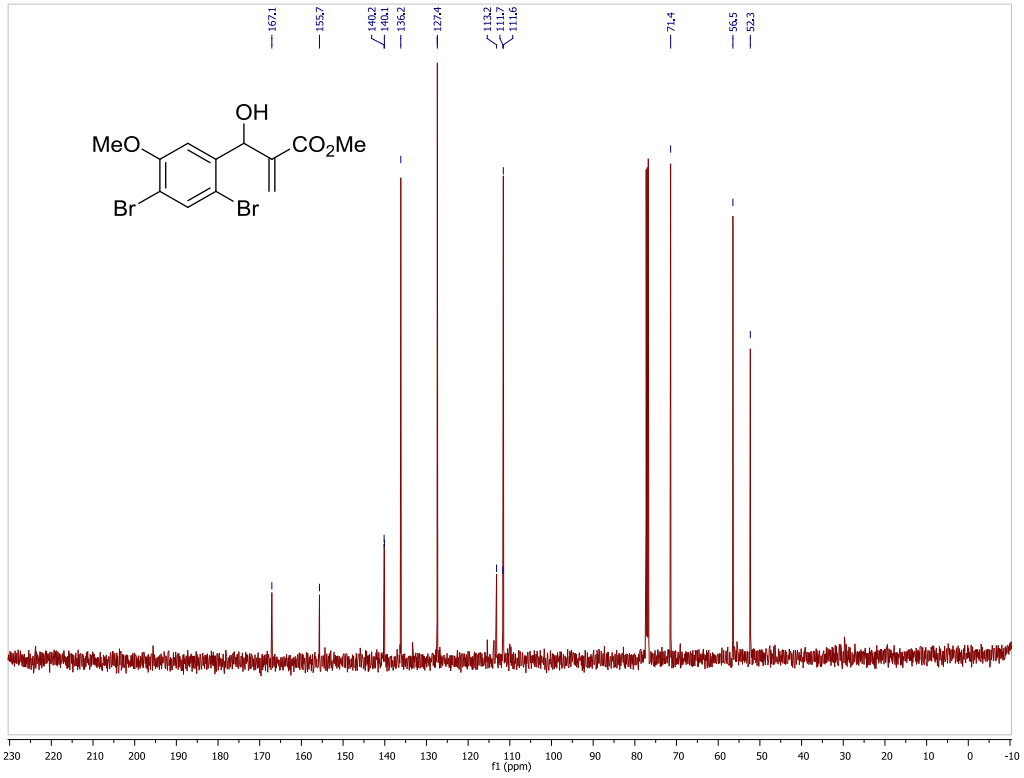
167.1
155.7
140.2
140.1
136.2
127.4
113.2
111.7
111.6
71.4
56.5
52.3
OH
MeO
CO2Me
Br
Br
f1 (ppm)

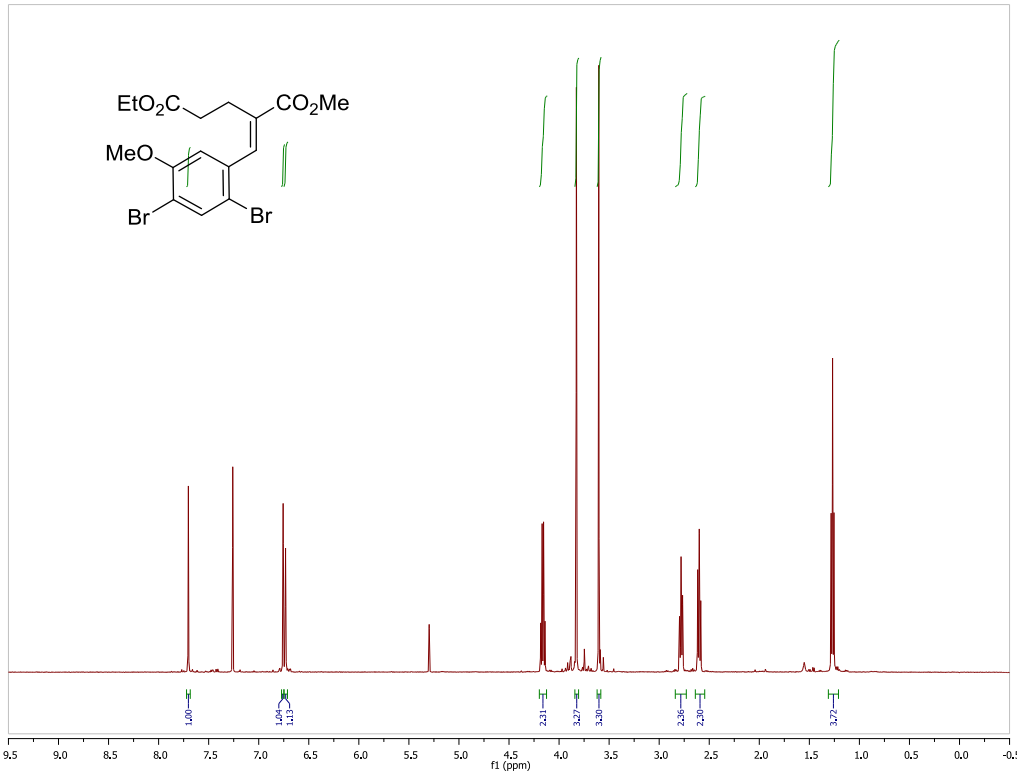
EtO2C
CO2Me
MeO
Br
Br
f1 (ppm)

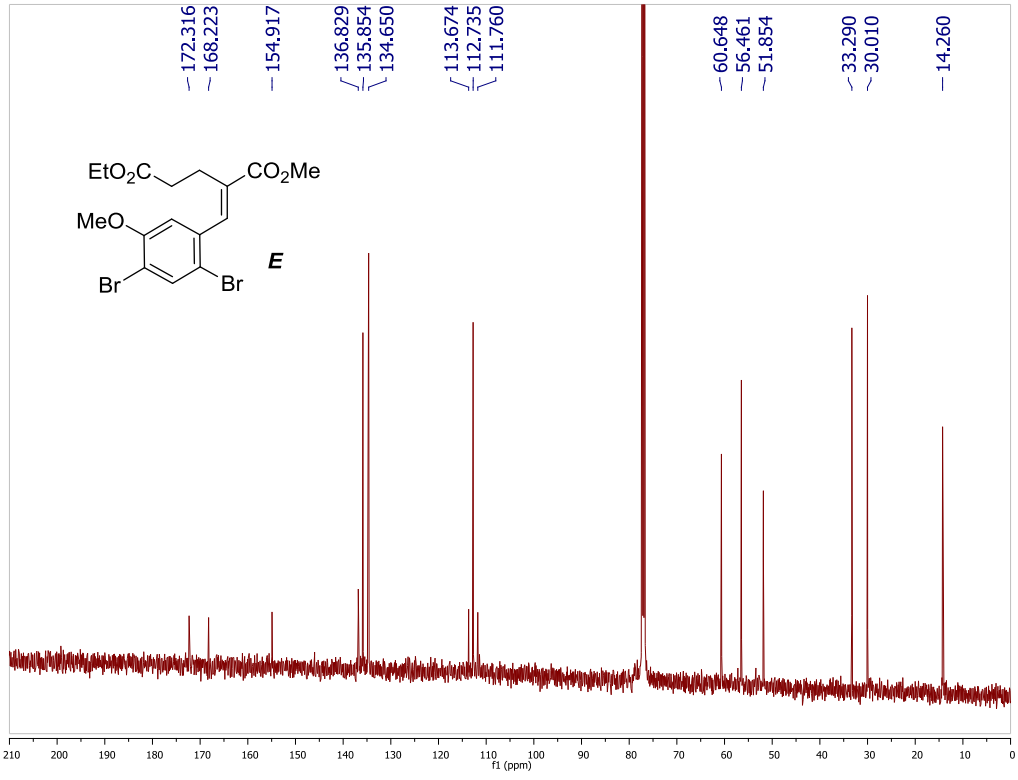
172.316
168.223
154.917
136.829
135.854
134.650
113.674
112.735
111.760
60.648
56.461
51.854
33.290
30.010
14.260
EtO2C
CO2Me
MeO
Br
Br
E
f1 (ppm)

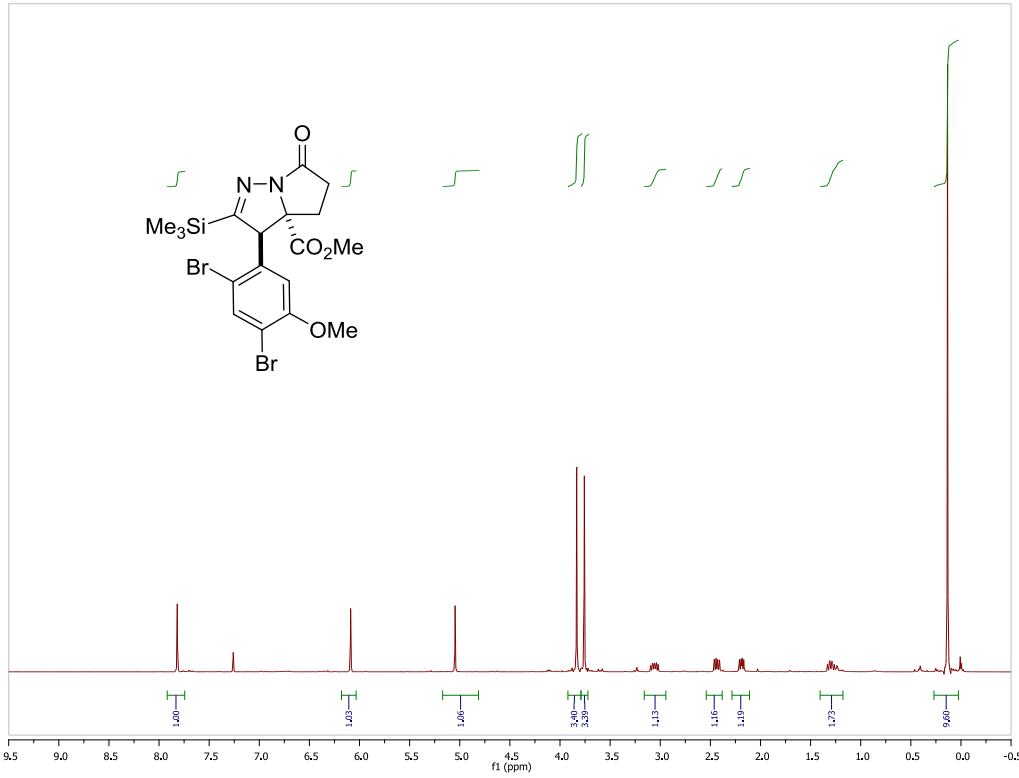
O
N–N
Me3Si
CO2Me
Br
OMe
Br
1.00
1.03
1.06
3.40
3.39
1.13
1.16
1.19
1.73
9.60
f1 (ppm)

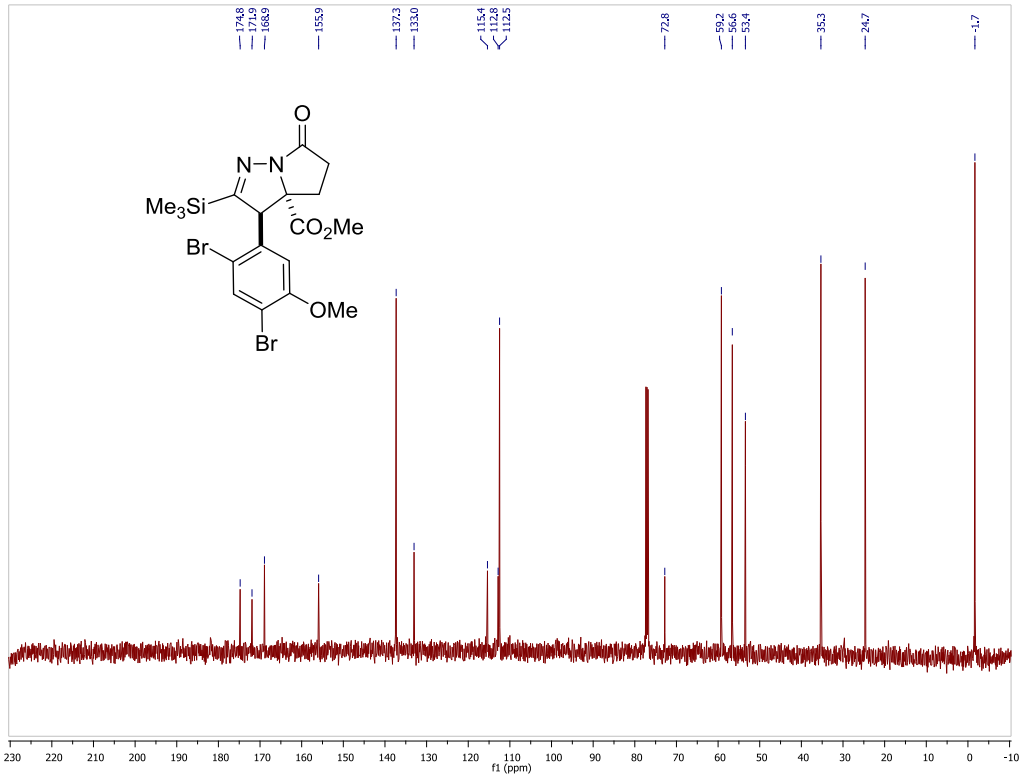
174.8
171.9
168.9
155.9
137.3
133.0
115.4
112.8
112.5
72.8
59.2
56.6
53.4
35.3
24.7
-1.7
O
N–N
Me3Si
CO2Me
Br
OMe
Br
f1 (ppm)

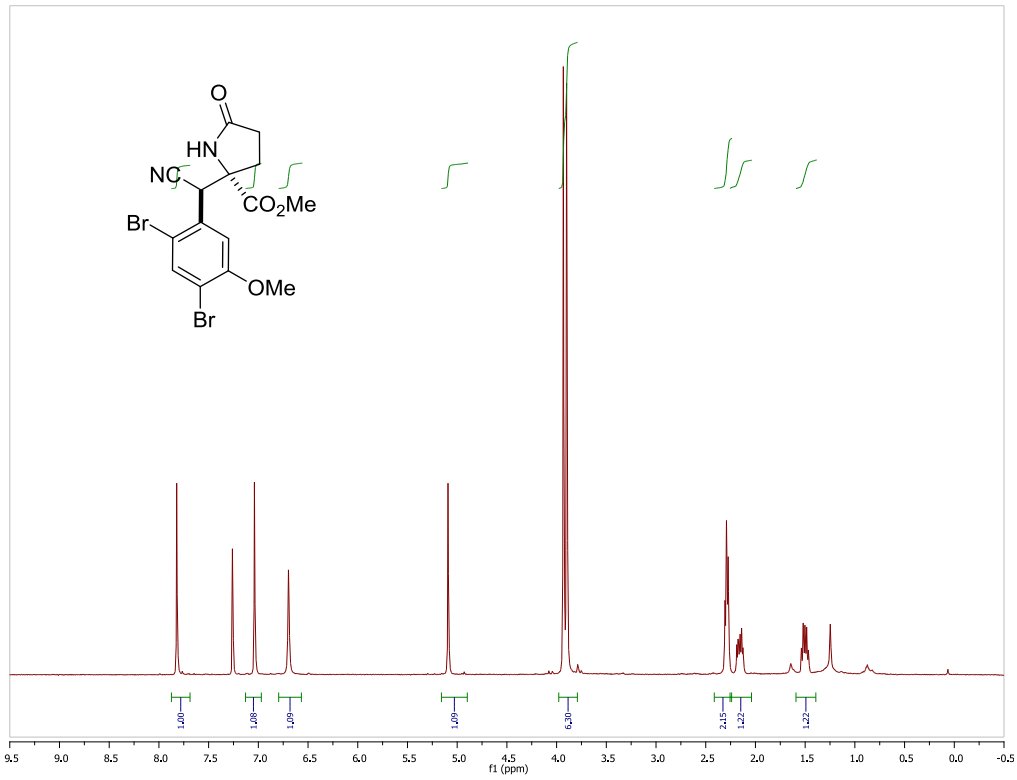
O
HN
NC
CO2Me
Br
OMe
Br
1.00
1.08
1.09
1.09
6.30
2.15
1.22
1.22
9.5 9.0 8.5 8.0 7.5 7.0 6.5 6.0 5.5 5.0 4.5 4.0 3.5 3.0 2.5 2.0 1.5 1.0 0.5 0.0 -0.5
f1 (ppm)

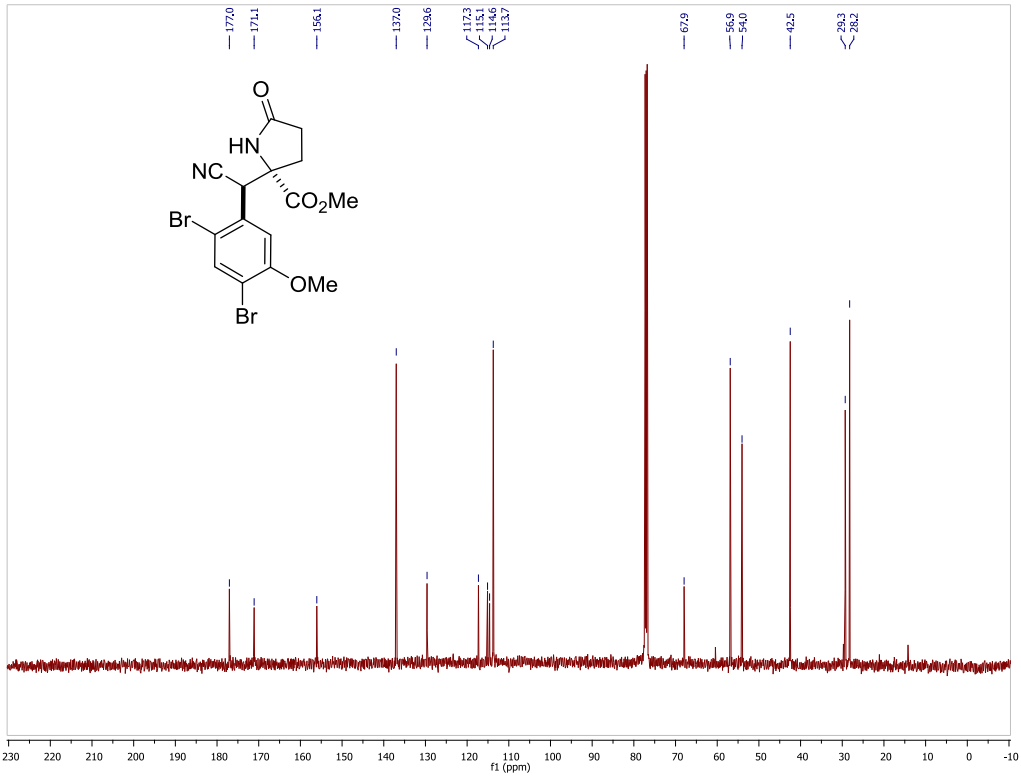
177.0
171.1
156.1
137.0
129.6
117.3
115.1
114.6
113.7
67.9
56.9
54.0
42.5
29.3
28.2
O
HN
NC
CO2Me
Br
OMe
Br
230 220 210 200 190 180 170 160 150 140 130 120 110 100 90 80 70 60 50 40 30 20 10 0 -10
f1 (ppm)

^{1}H NMR of imide

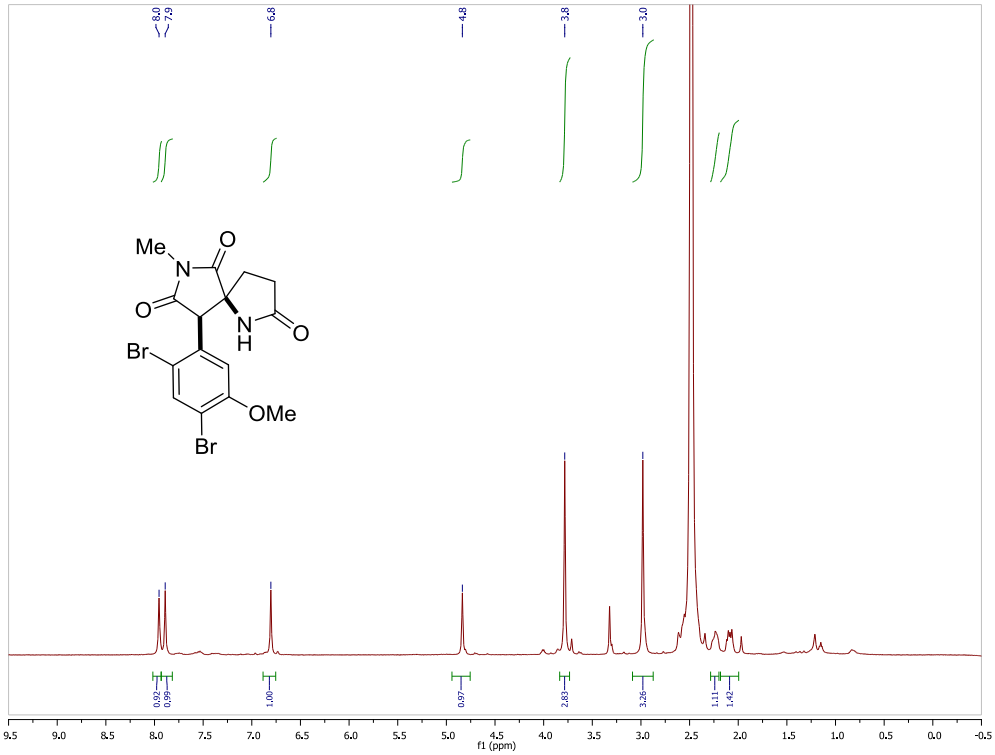

^{1}H NMR of Fukuyama Intermediate

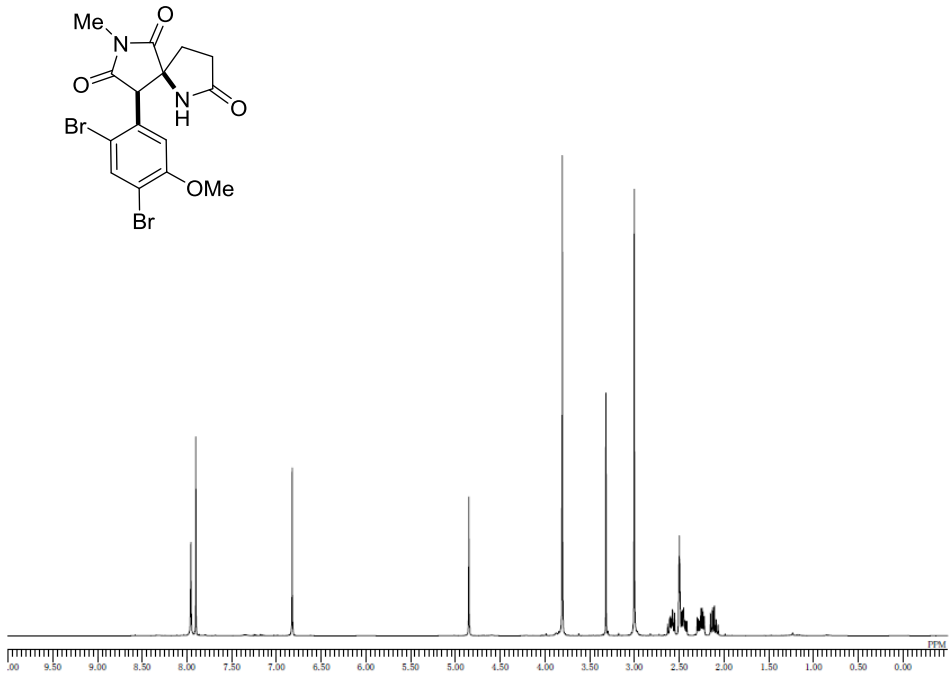

^{13}C NMR of imide

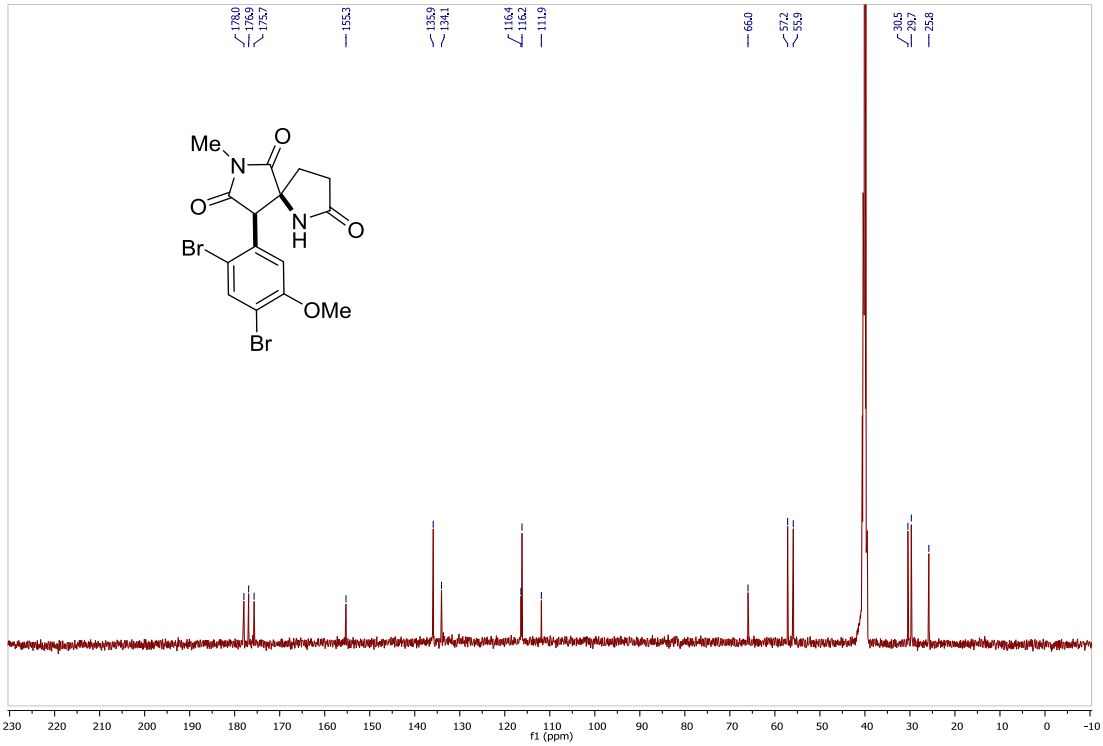

^{13}C NMR of Fukuyama Intermediate

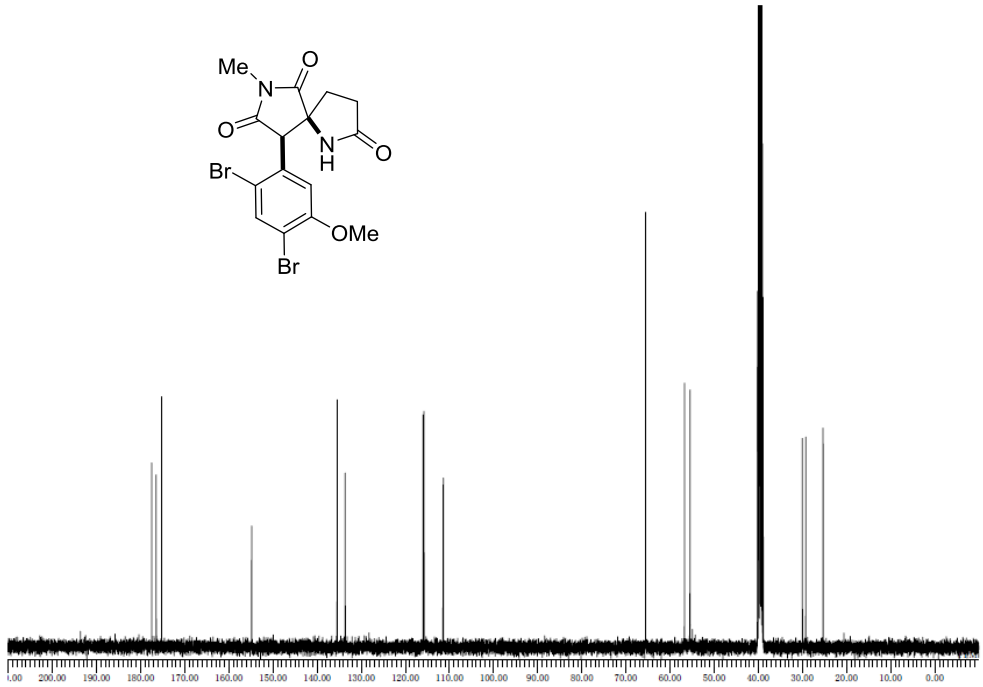

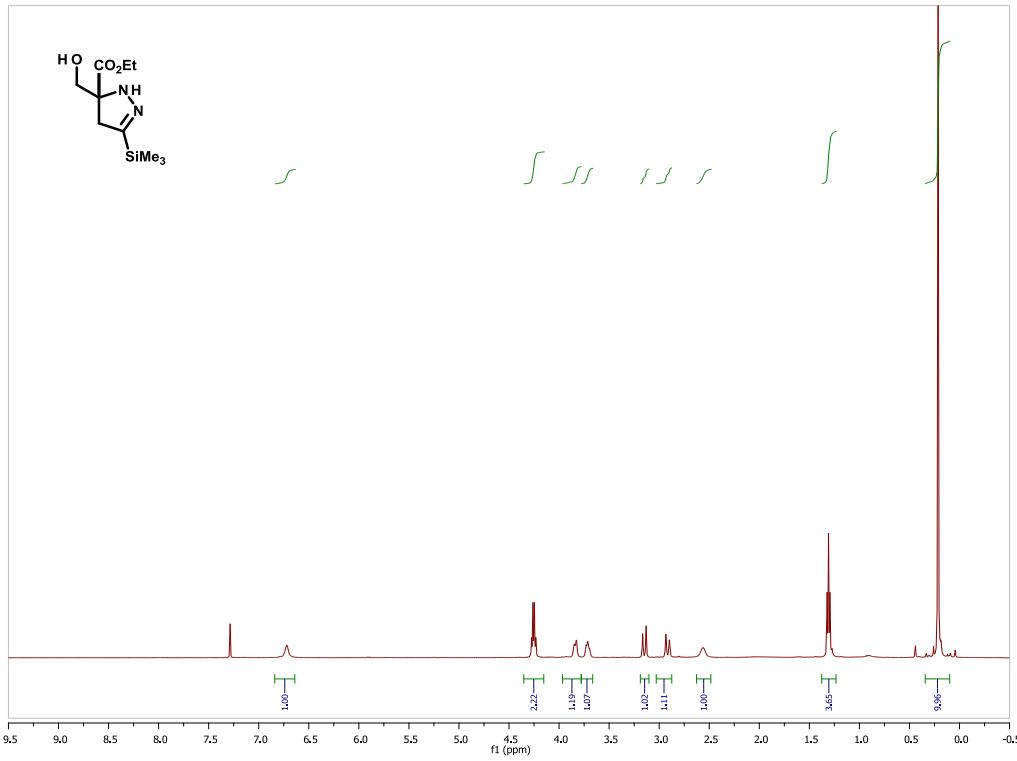
HO
CO2Et
NH
N
SiMe3
1.00
2.22
1.19
1.07
1.02
1.11
1.00
3.65
9.86
f1 (ppm)

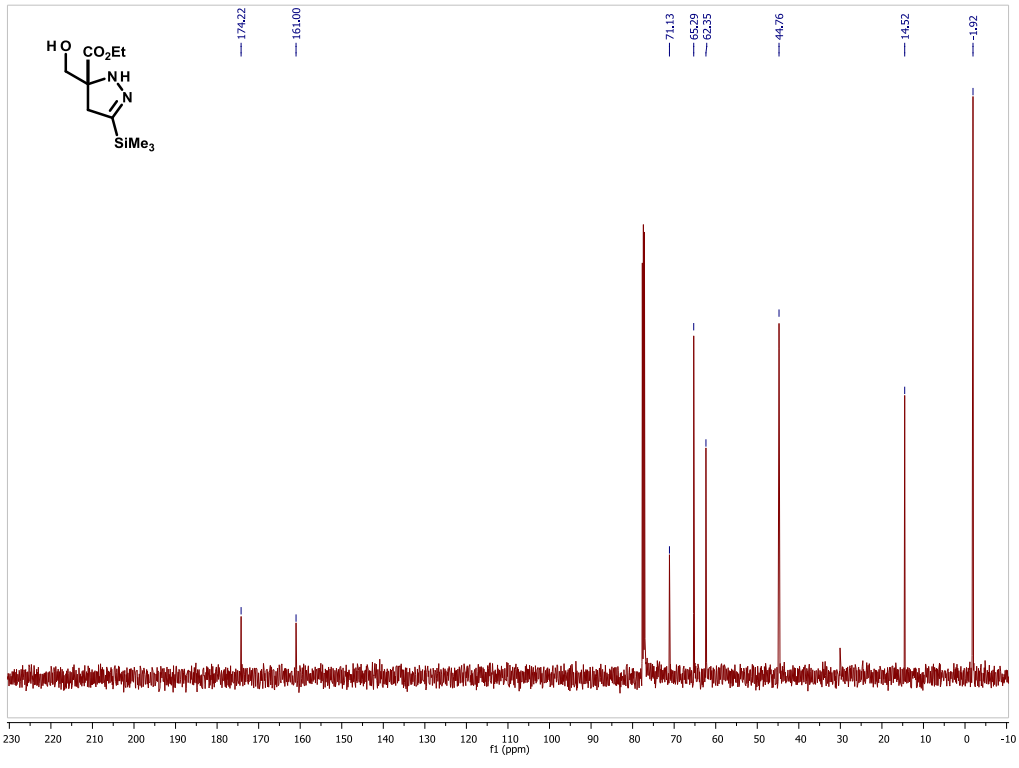
HO
CO2Et
NH
N
SiMe3
174.22
161.00
71.13
65.29
62.35
44.76
14.52
-1.92
f1 (ppm)

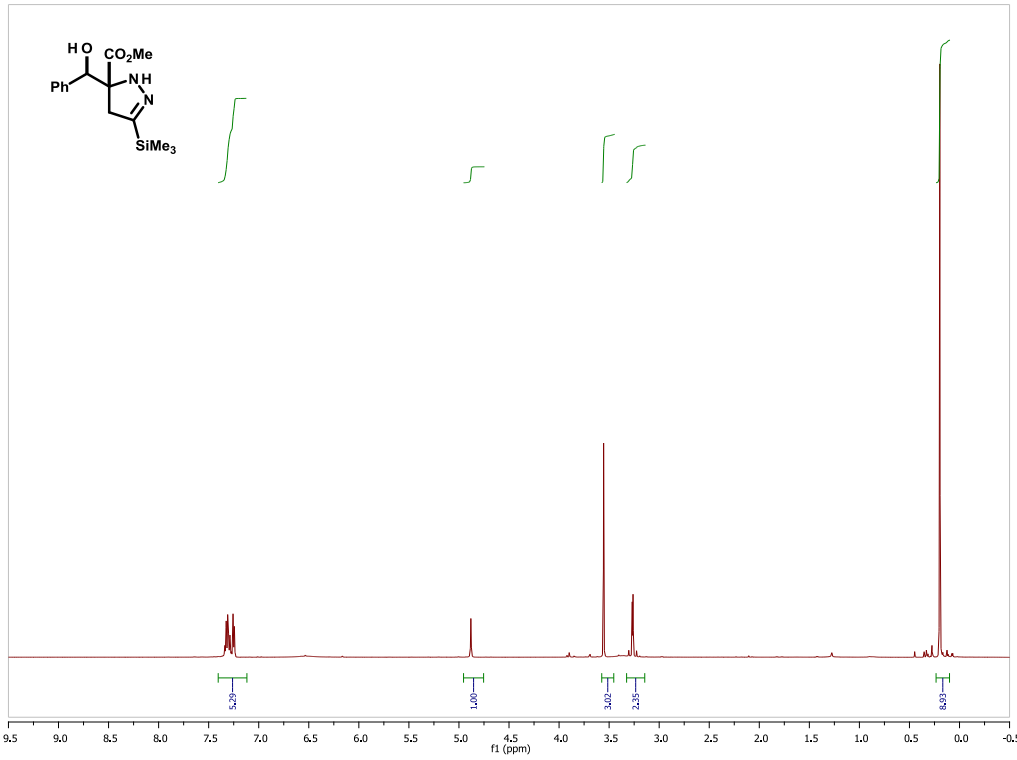
HO
CO2Me
Ph
NH
N
SiMe3
5.29
1.00
3.02
2.35
8.93
f1 (ppm)

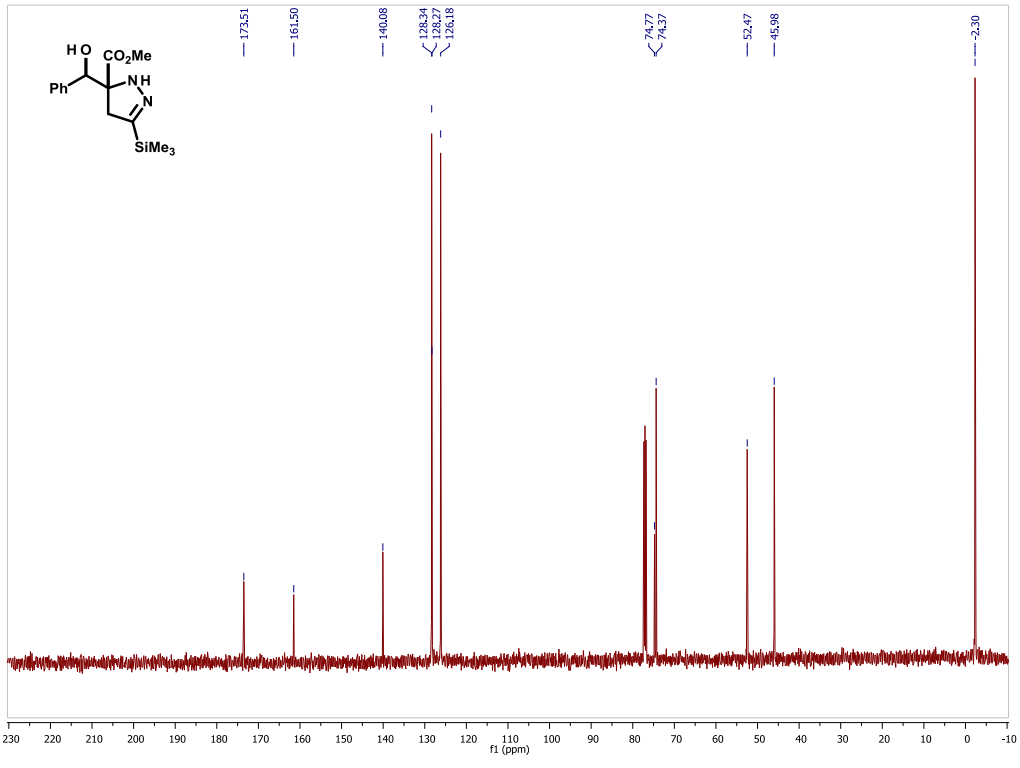
HO
CO2Me
Ph
NH
N
SiMe3
173.51
161.50
140.08
128.34
128.27
126.18
74.77
74.37
52.47
45.98
-2.30
f1 (ppm)

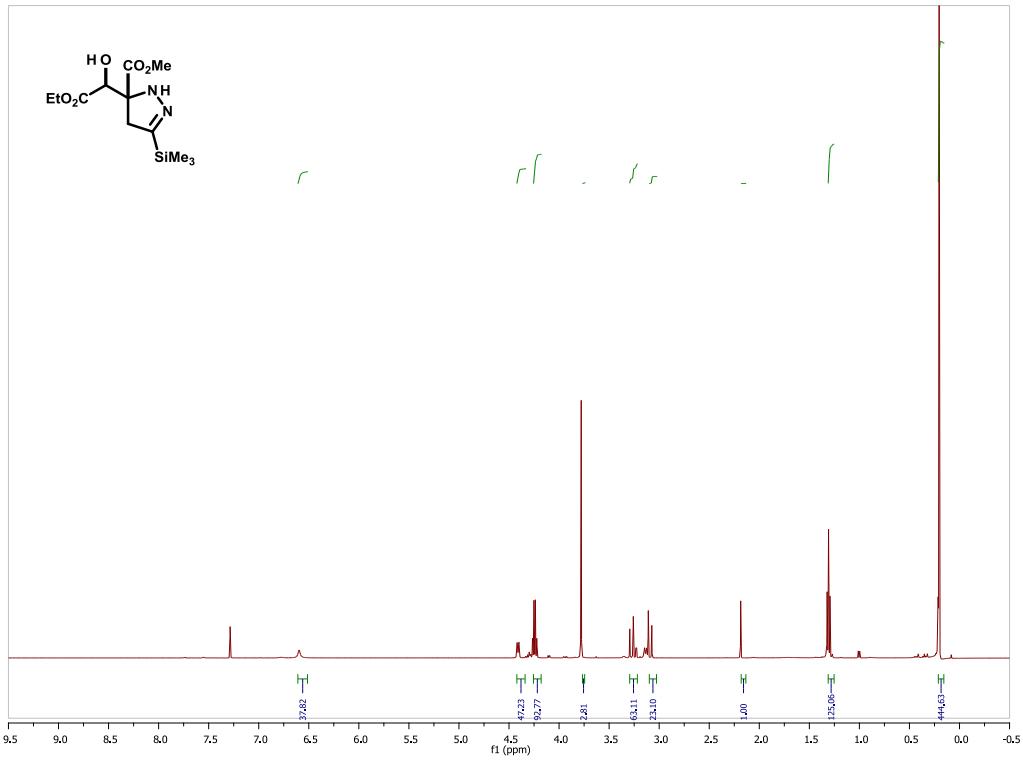
HO
CO2Me
EtO2C
NH
N
SiMe3
3.82
47.23
92.77
2.81
63.11
23.10
1.00
125.06
444.83
f1 (ppm)

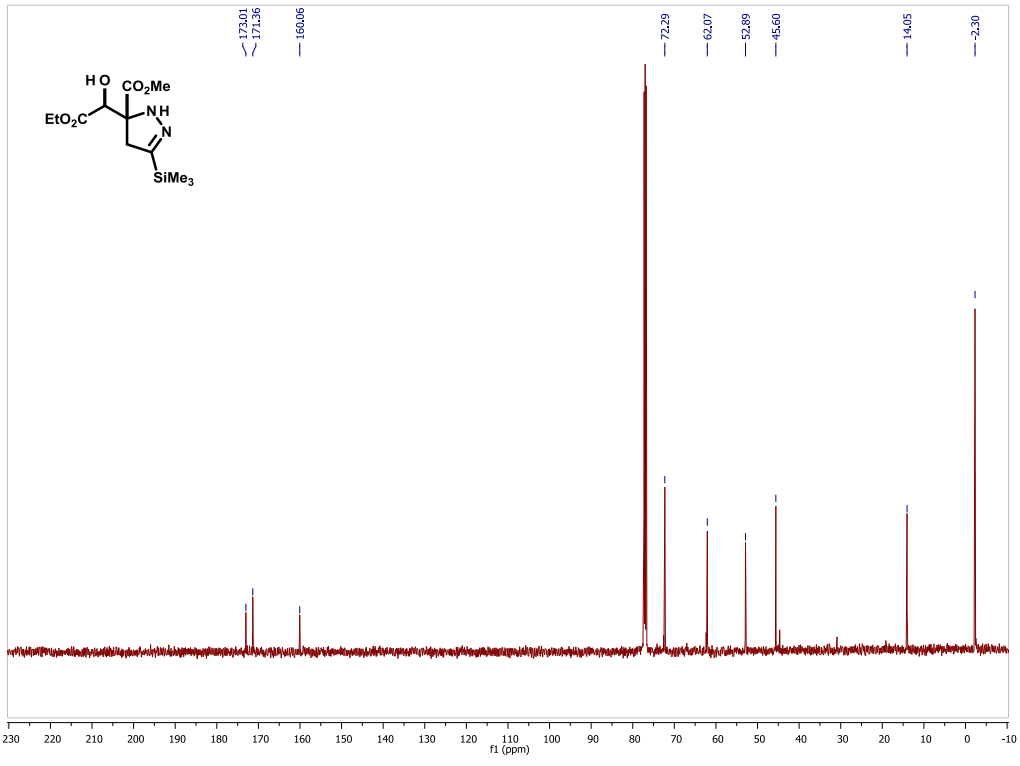
173.01
171.36
160.06
72.29
62.07
52.89
45.60
14.05
-2.30
HO
CO2Me
EtO2C
NH
N
SiMe3
f1 (ppm)

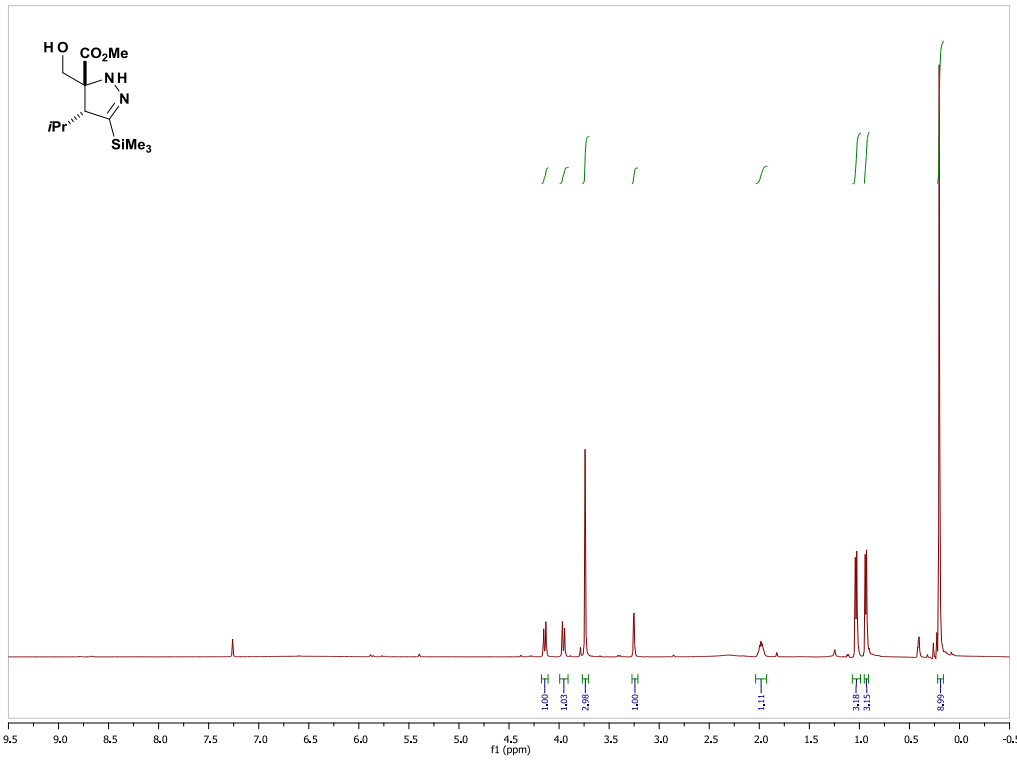
HO
CO2Me
NH
N
iPr
SiMe3
1.00
1.03
2.98
1.00
1.11
3.18
3.15
8.99
f1 (ppm)

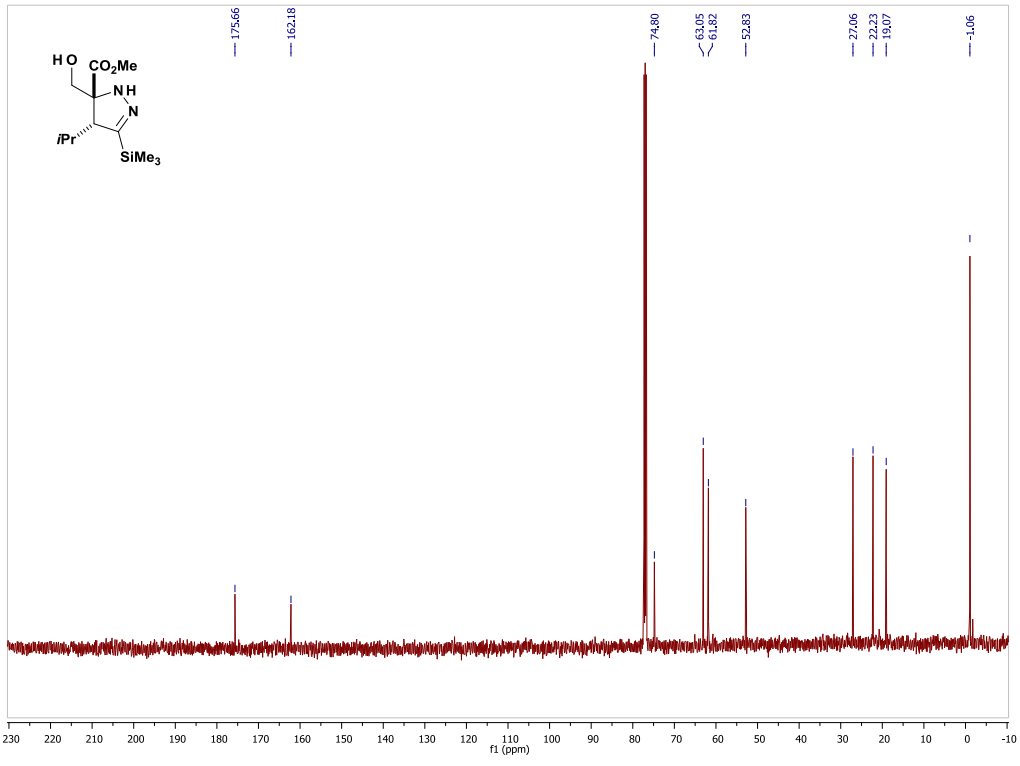
HO
CO2Me
NH
N
iPr
SiMe3
175.66
162.18
74.80
63.05
61.82
52.83
27.06
22.23
19.07
-1.06
f1 (ppm)

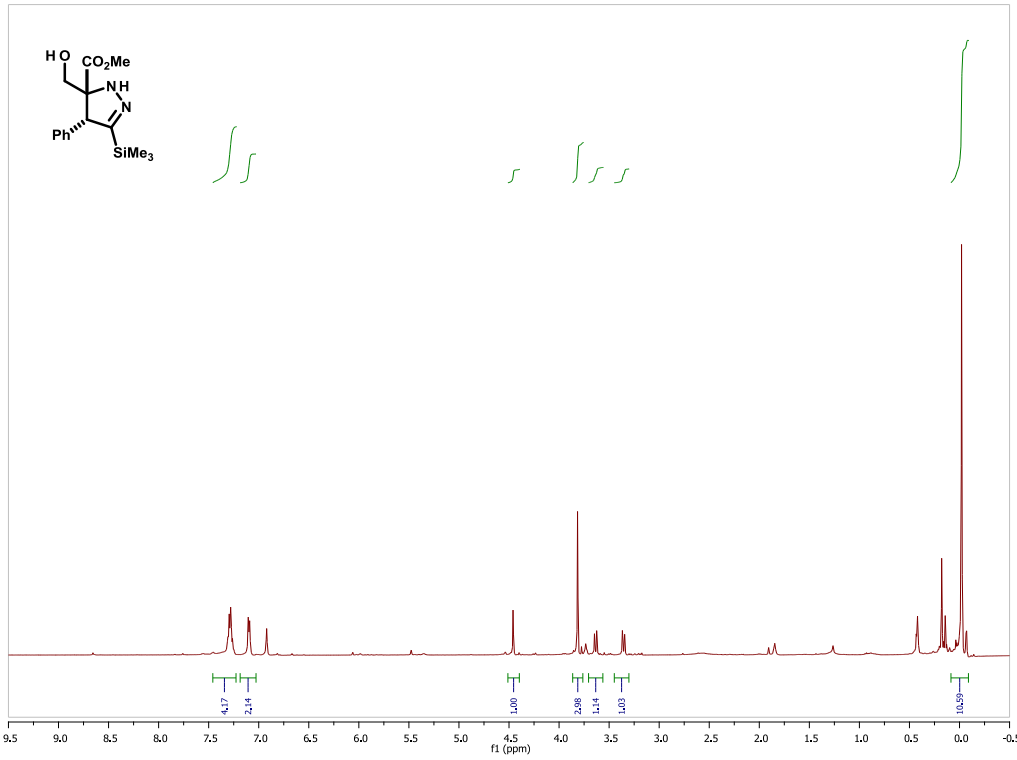
HO
CO2Me
NH
N
Ph
SiMe3
4.17
2.14
1.00
2.98
1.14
1.03
10.59
f1 (ppm)

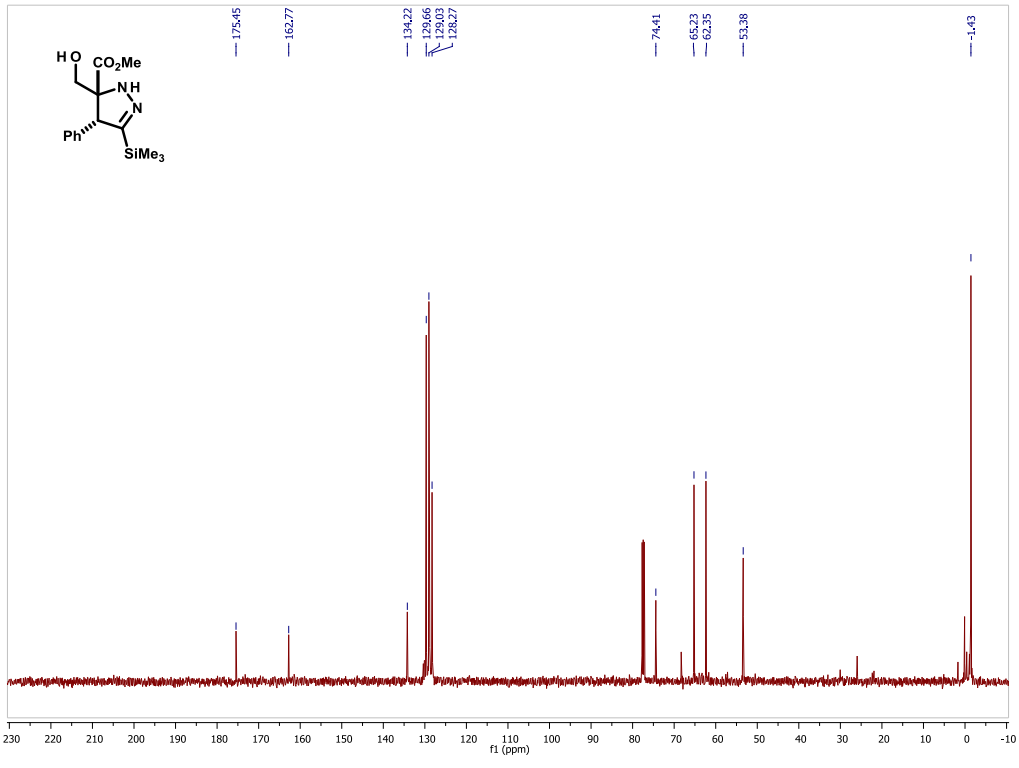
HO
CO2Me
NH
N
Ph
SiMe3
175.45
162.77
134.22
129.66
129.03
128.27
74.41
65.23
62.35
53.38
-1.43
f1 (ppm)

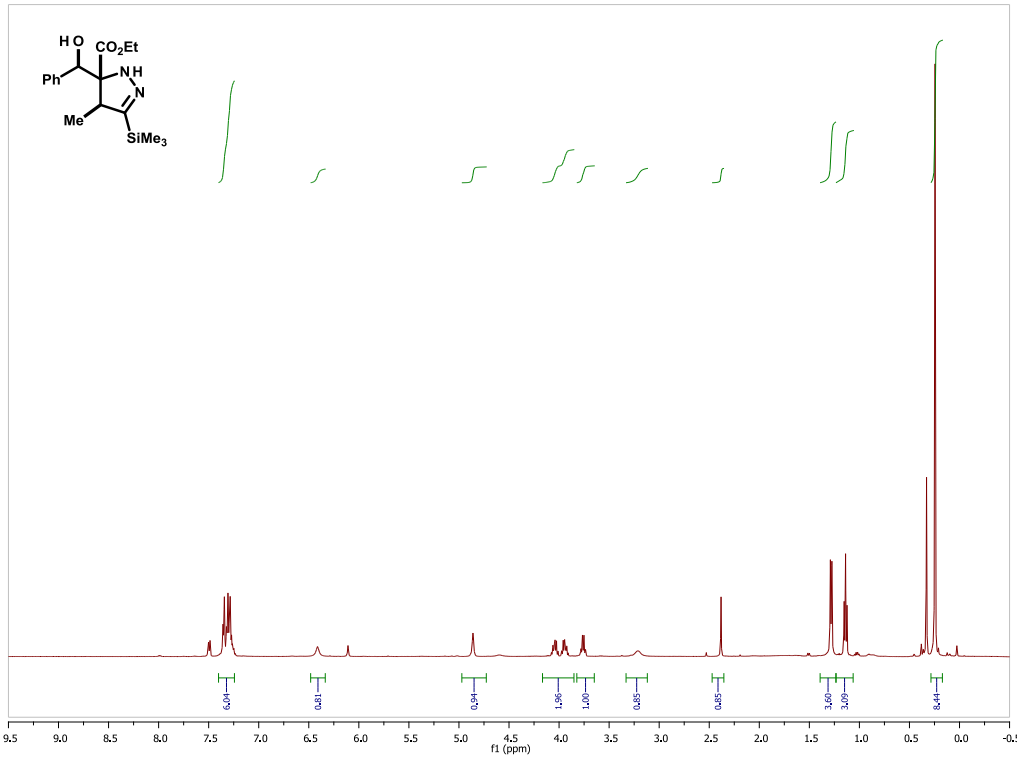
HO
CO2Et
Ph
NH
N
Me
SiMe3
6.04
0.81
0.94
1.96
1.00
0.85
0.85
3.60
3.09
8.44
f1 (ppm)

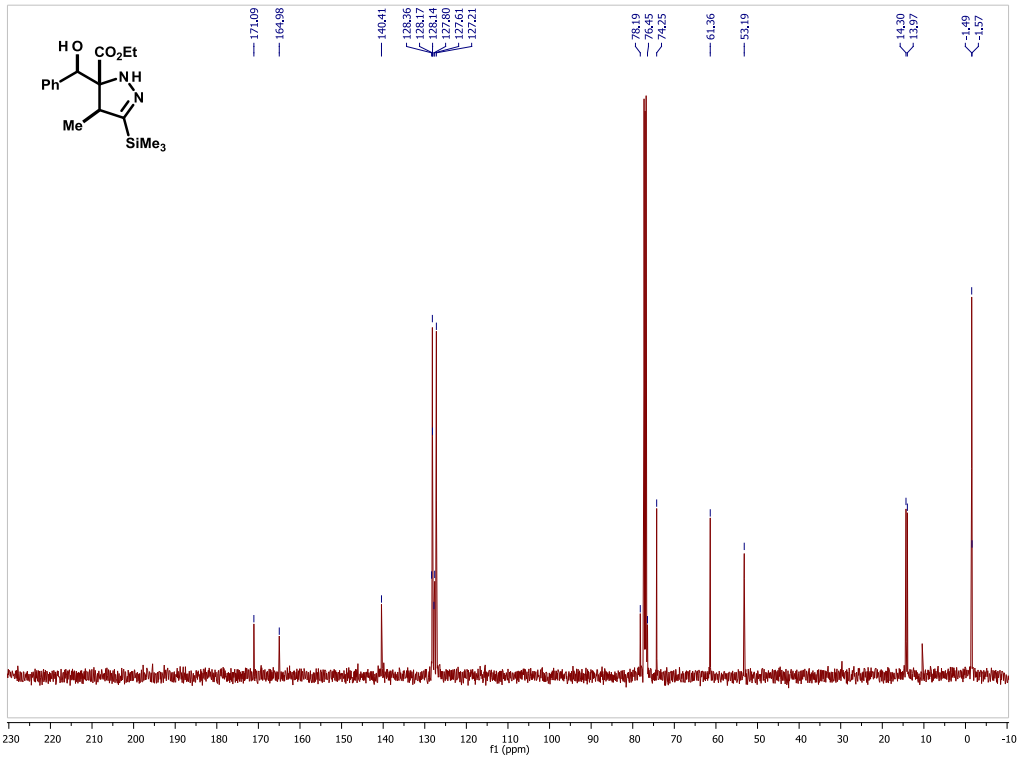
HO
CO2Et
Ph
NH
N
Me
SiMe3
171.09
164.98
140.41
128.36
128.17
128.14
127.80
127.61
127.21
78.19
76.45
74.25
61.36
53.19
14.30
13.97
-1.49
-1.57
f1 (ppm)

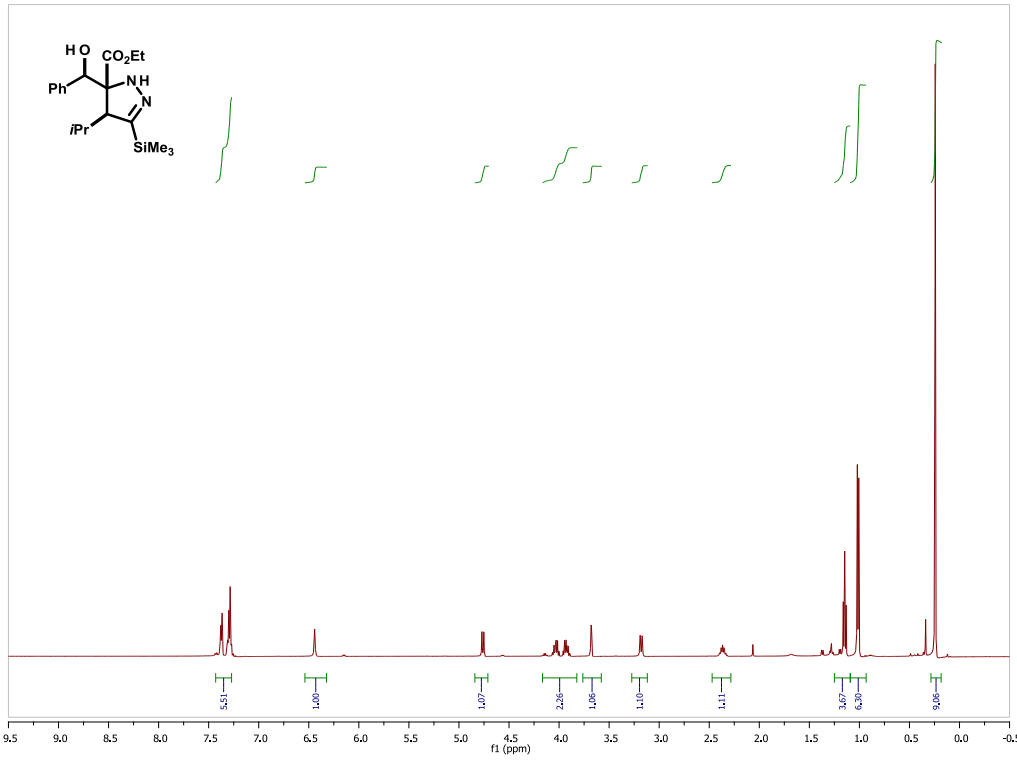
HO
CO2Et
Ph
NH
N
iPr
SiMe3
5.51
1.00
1.07
2.26
1.05
1.10
1.11
3.67
6.30
9.06
f1 (ppm)

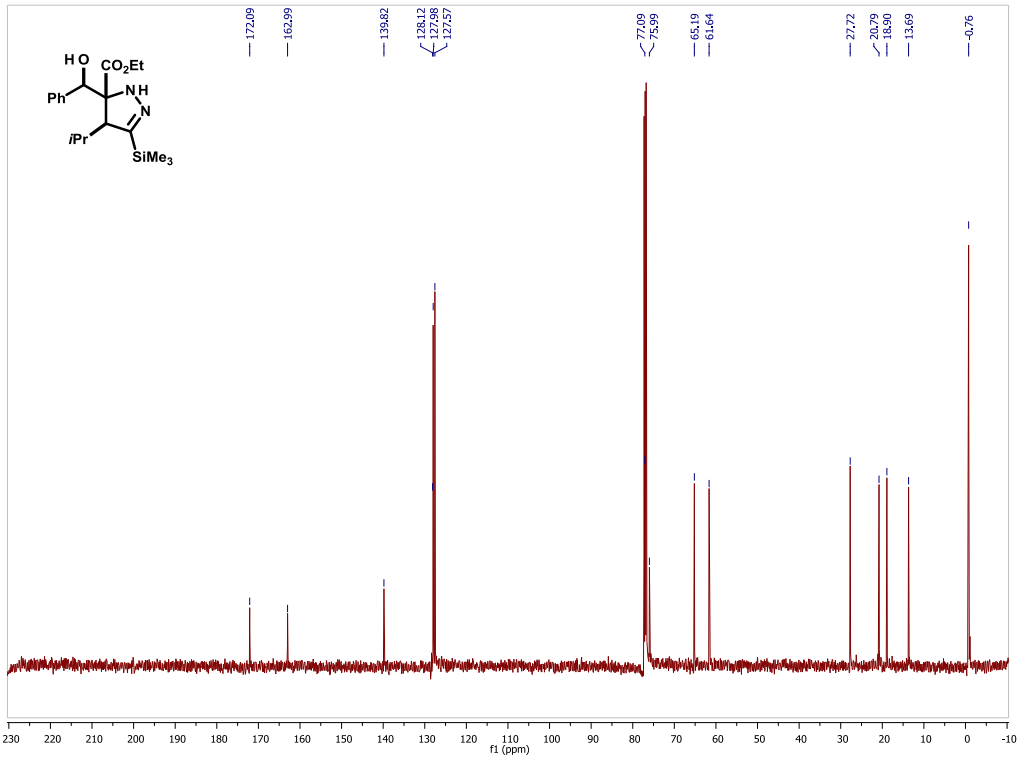
HO
CO2Et
Ph
NH
N
iPr
SiMe3
172.09
162.99
139.82
128.12
127.98
127.57
77.09
75.99
65.19
61.64
27.72
20.79
18.90
13.69
-4.76
f1 (ppm)

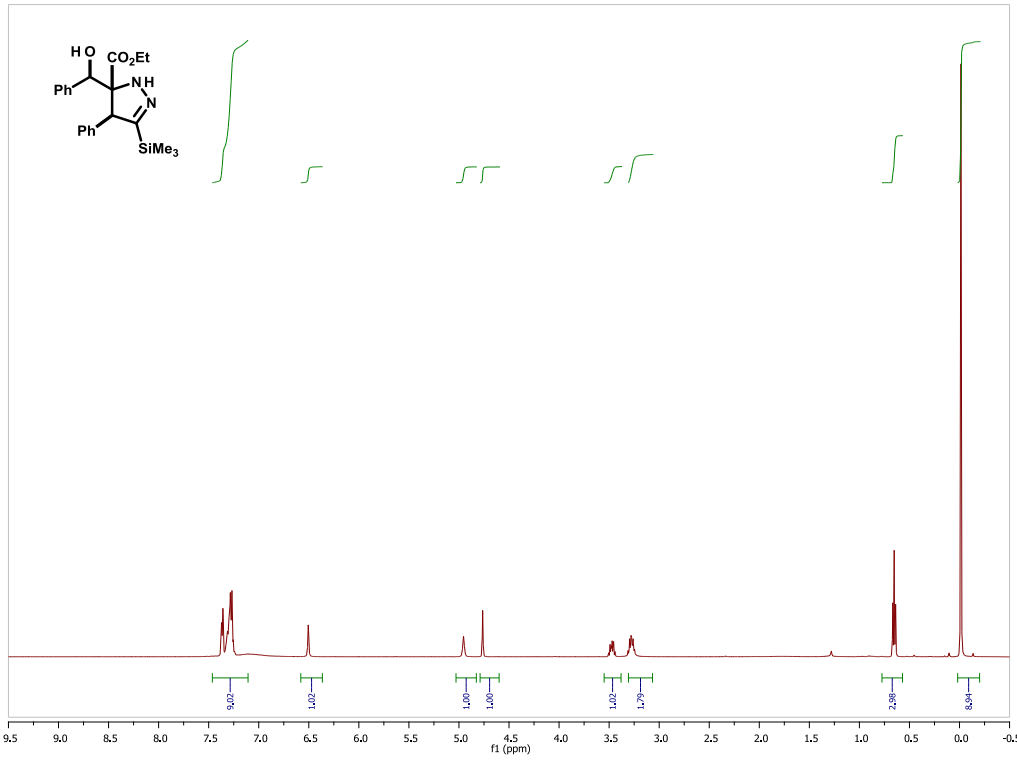
HO
CO2Et
Ph
NH
N
Ph
SiMe3
9.02
1.02
1.00
1.00
1.02
1.79
2.98
8.84
f1 (ppm)

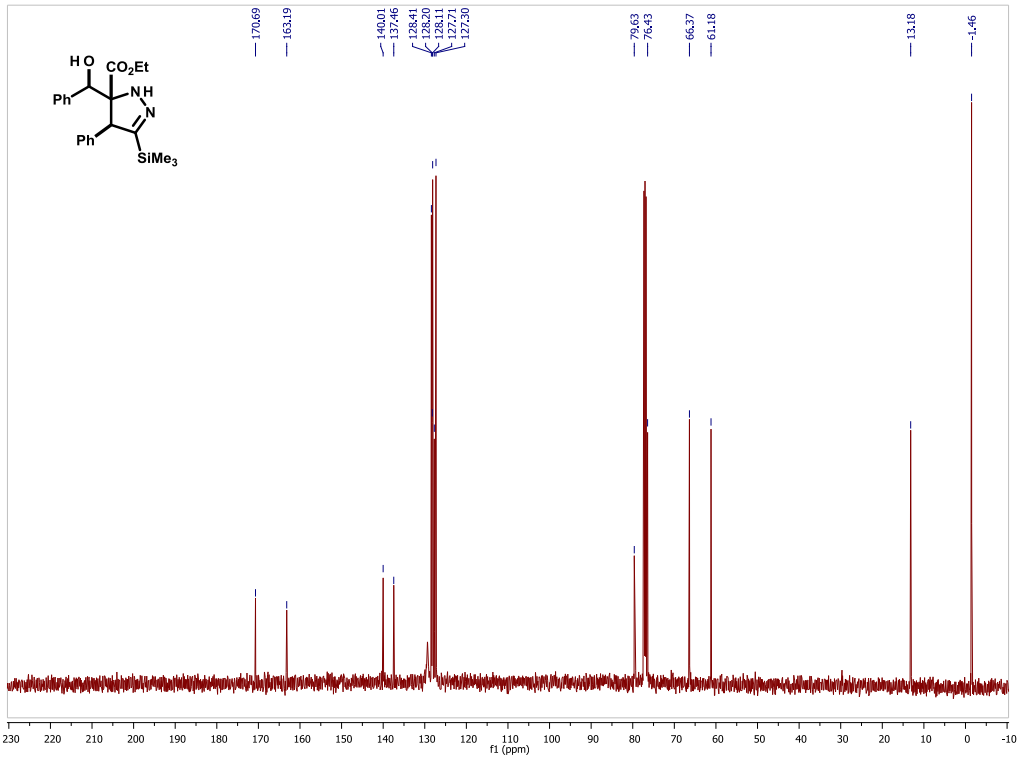
170.69
163.19
140.01
137.46
128.41
128.20
128.11
127.71
127.30
79.63
76.43
66.37
61.18
13.18
-1.46
HO
CO2Et
Ph
NH
N
Ph
SiMe3
f1 (ppm)

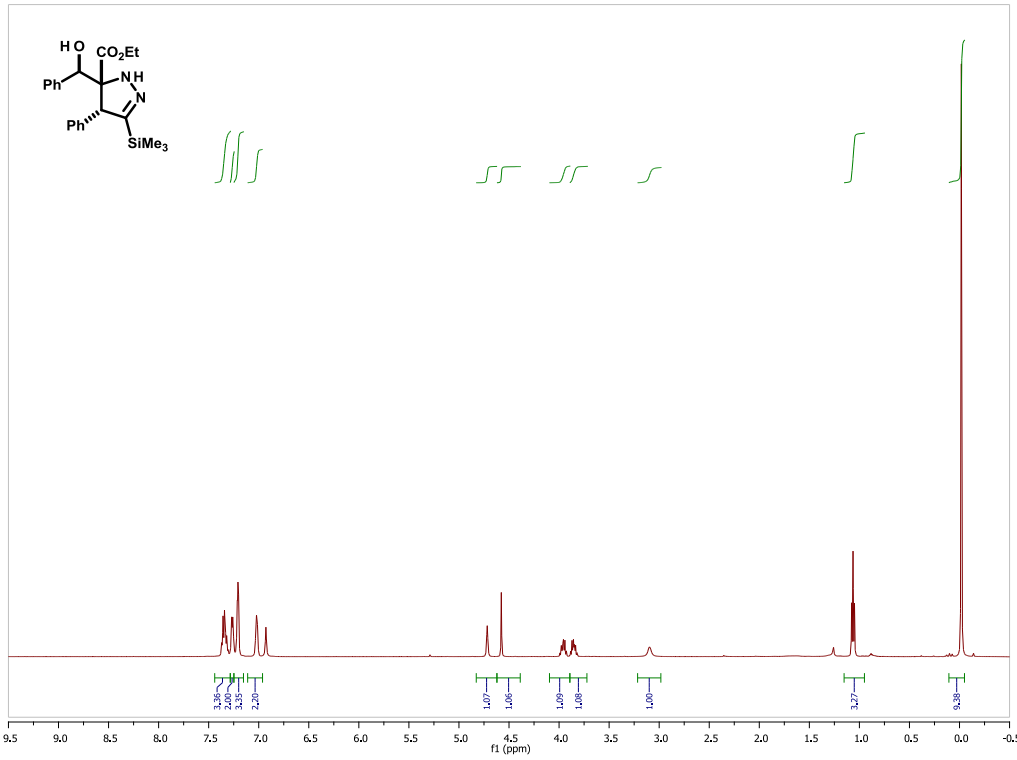
HO
CO2Et
Ph
NH
N
Ph
SiMe3
3.36
2.09
3.15
2.20
1.07
1.06
1.09
1.08
1.00
3.27
9.38
f1 (ppm)

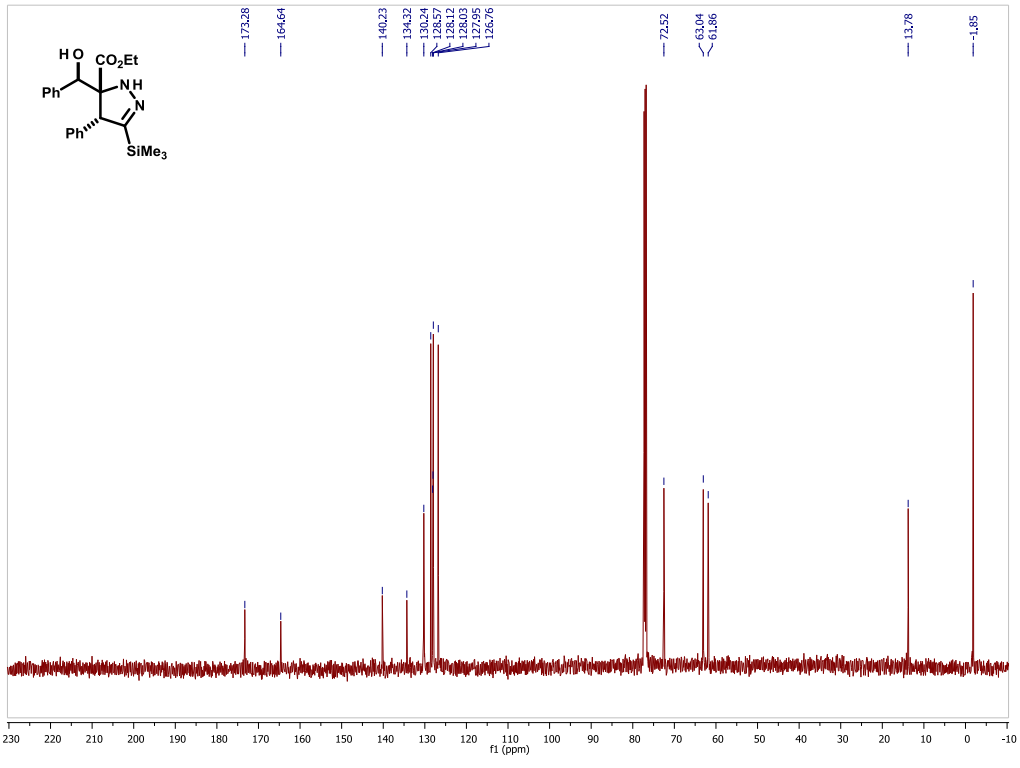
HO
CO2Et
Ph
NH
N
Ph
SiMe3
173.28
164.64
140.23
134.32
130.24
128.57
128.12
126.03
127.95
126.76
72.52
63.04
61.86
13.78
-1.85
f1 (ppm)

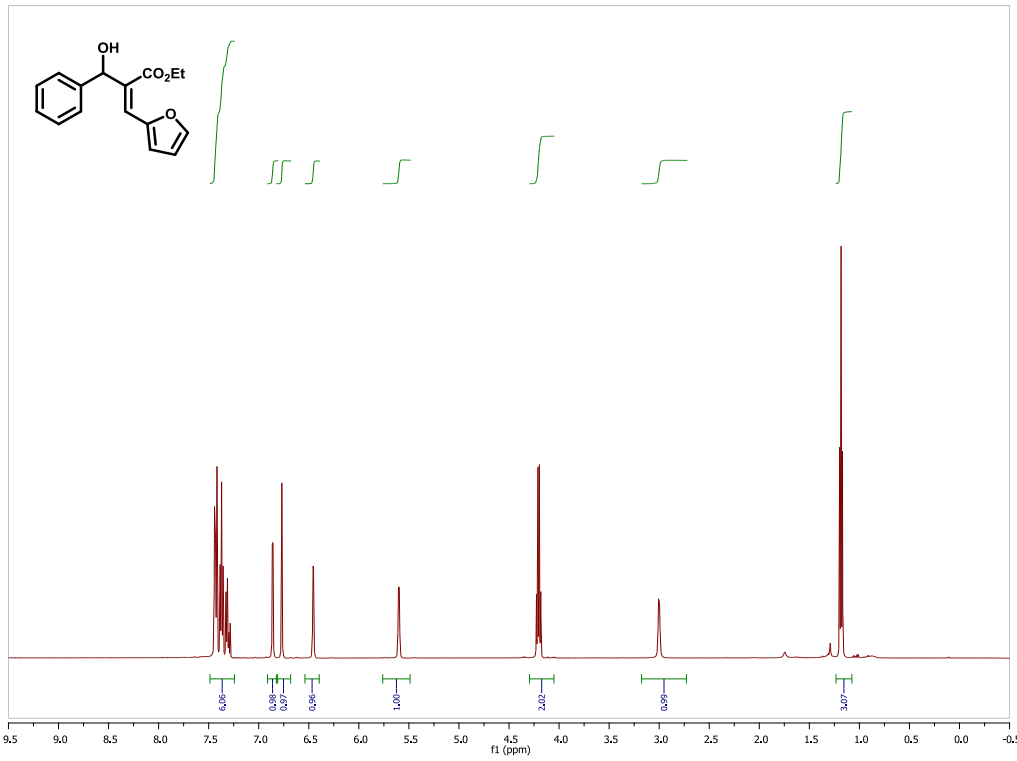
OH
CO2Et
O
6.06
0.88
0.97
0.96
1.00
2.02
0.99
3.07
f1 (ppm)

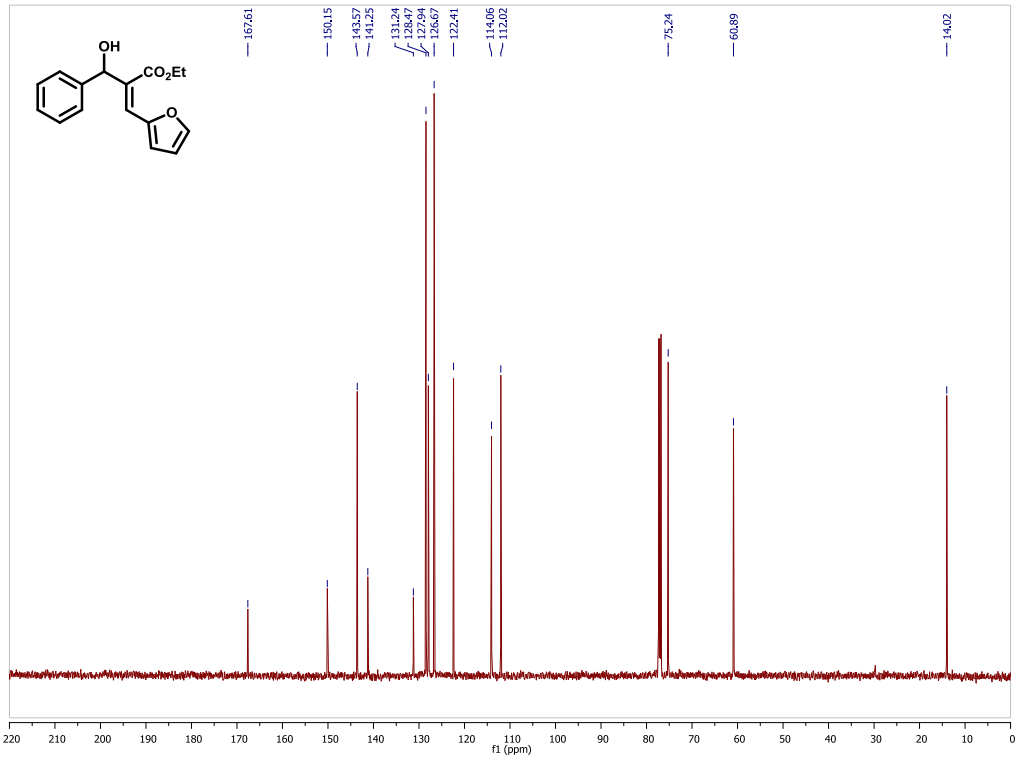
OH
CO2Et
O
167.61
150.15
143.57
141.25
131.24
128.47
127.94
126.67
122.41
114.06
112.02
75.24
60.89
14.02
f1 (ppm)

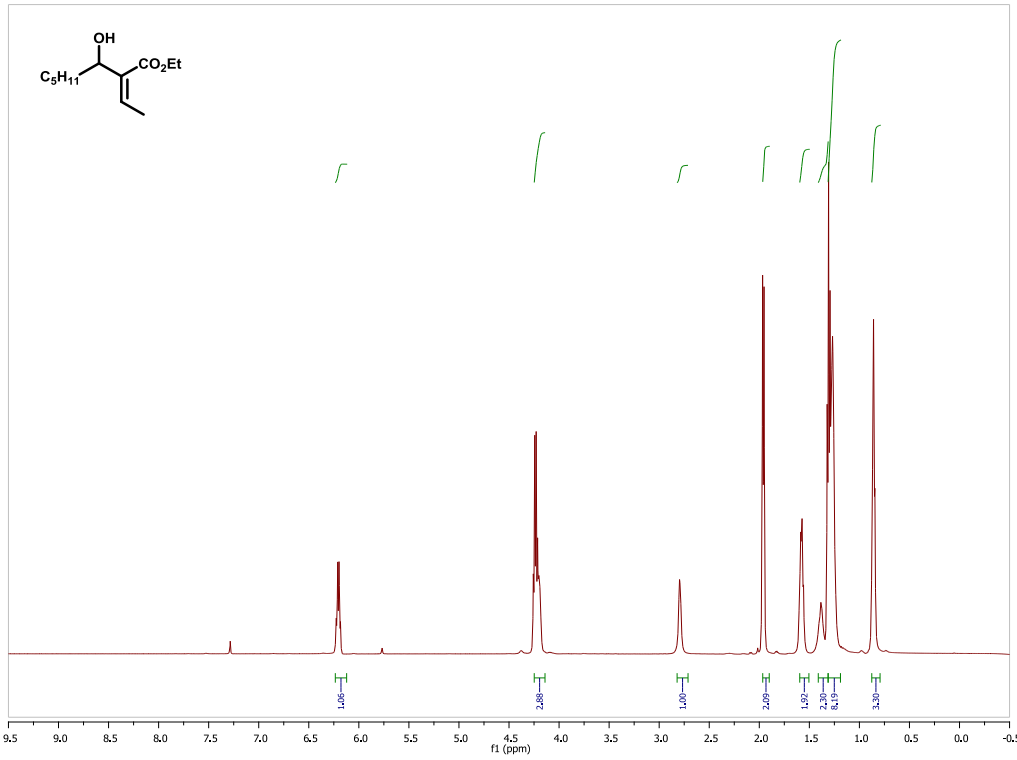
OH
C_5H_{11}
CO_2Et
1.06
2.88
1.00
2.09
1.92
2.20
8.19
3.30
f1 (ppm)

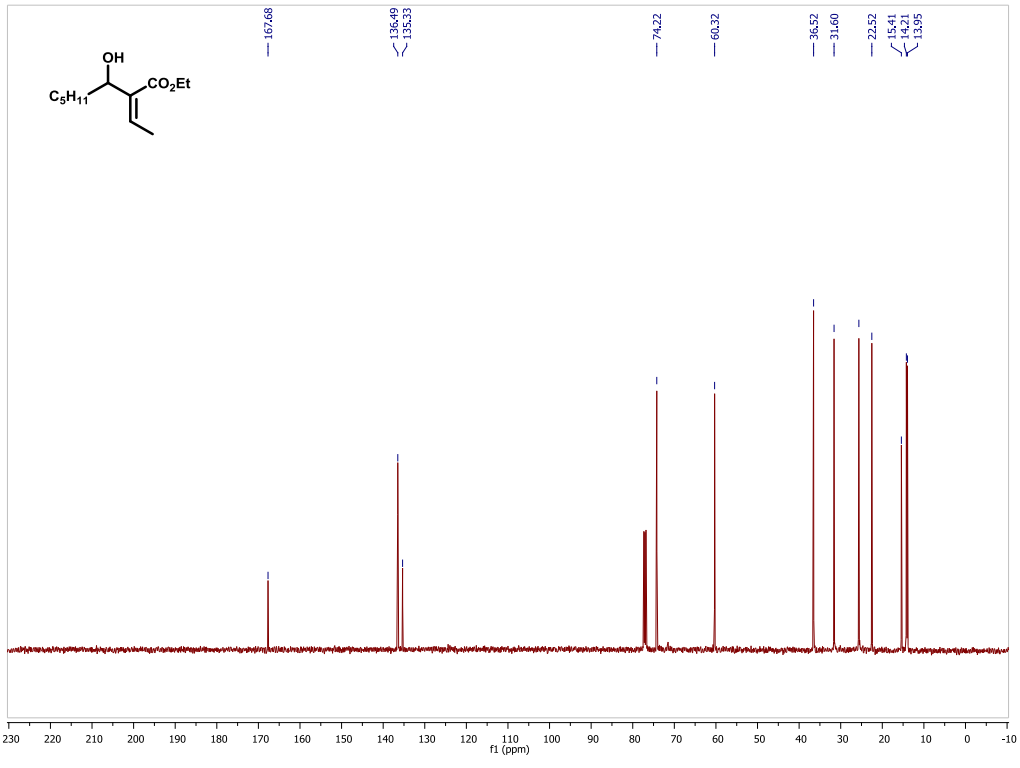
OH
C_5H_{11}
CO_2Et
167.68
136.49
135.33
74.22
60.32
36.52
31.60
22.52
15.41
14.21
13.95
f1 (ppm)

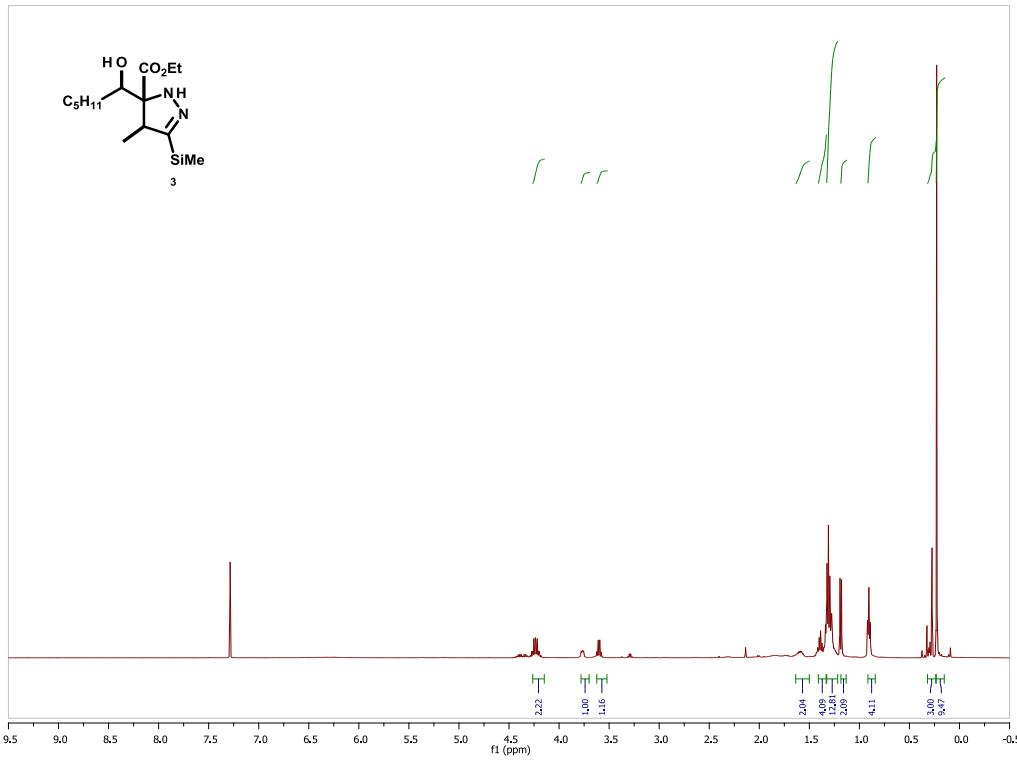
HO
CO2Et
C5H11
NH
N
SiMe
3
2.22
1.00
1.16
2.04
4.09
12.81
2.09
4.11
3.00
9.47
f1 (ppm)

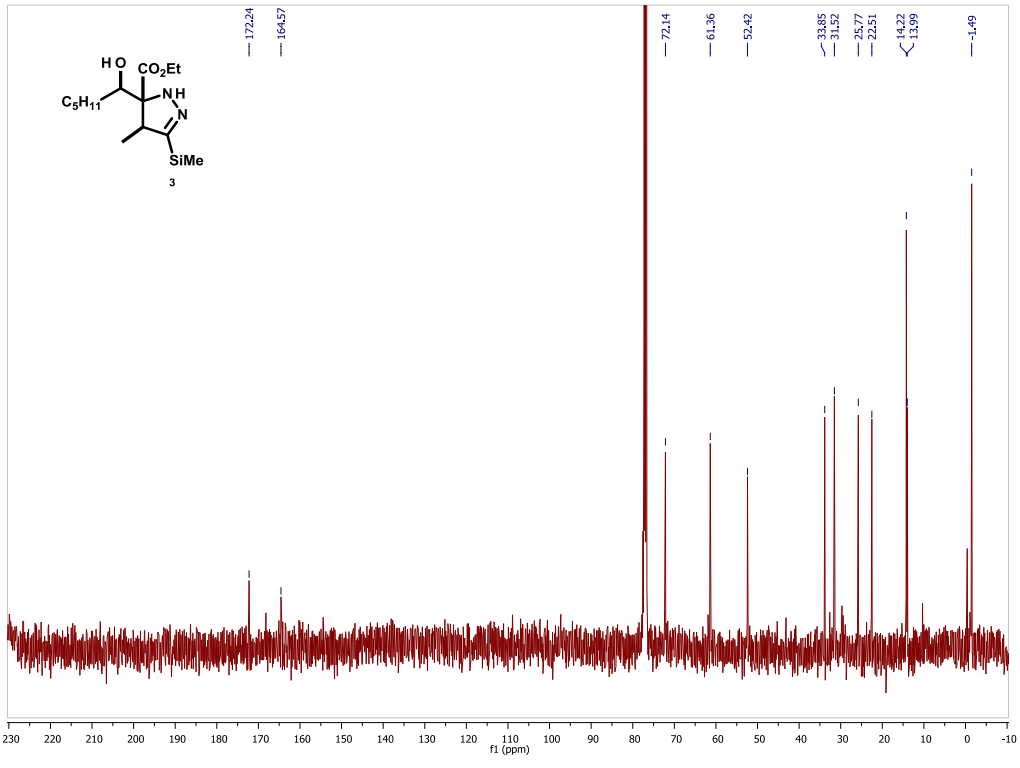
172.24
164.57
72.14
61.36
52.42
33.85
31.52
25.77
22.51
14.22
13.99
-1.49
HO
CO2Et
C5H11
NH
N
SiMe
3
f1 (ppm)

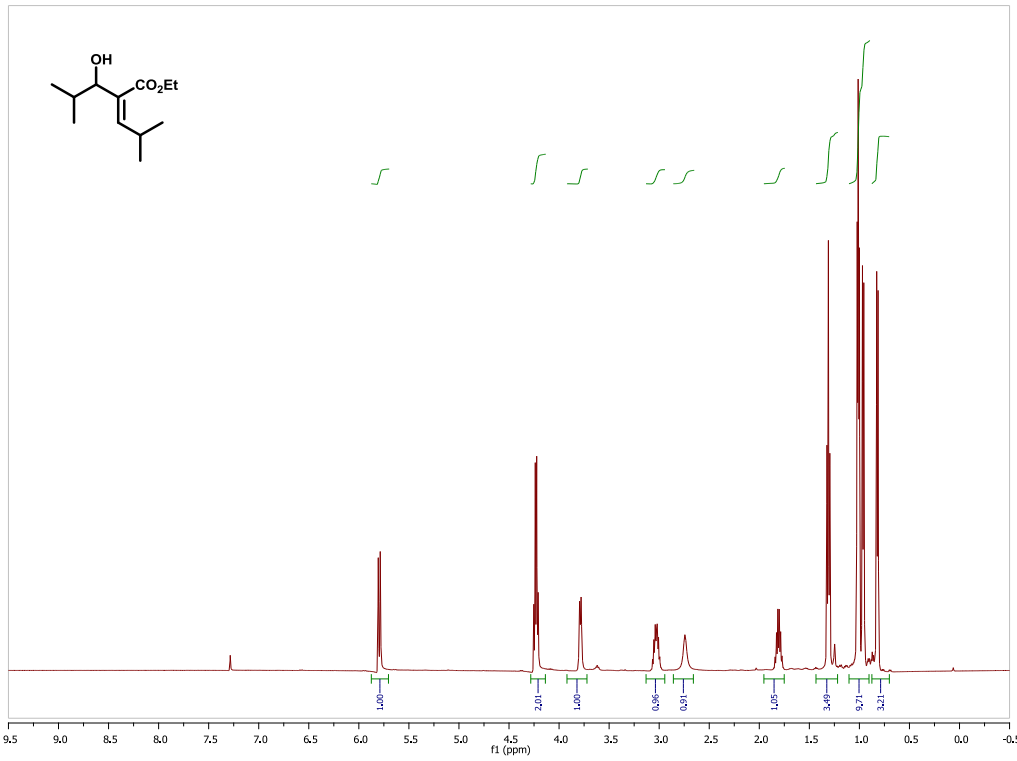
OH
CO2Et
1.00
2.01
1.00
0.96
0.91
1.05
3.49
9.71
3.21
f1 (ppm)

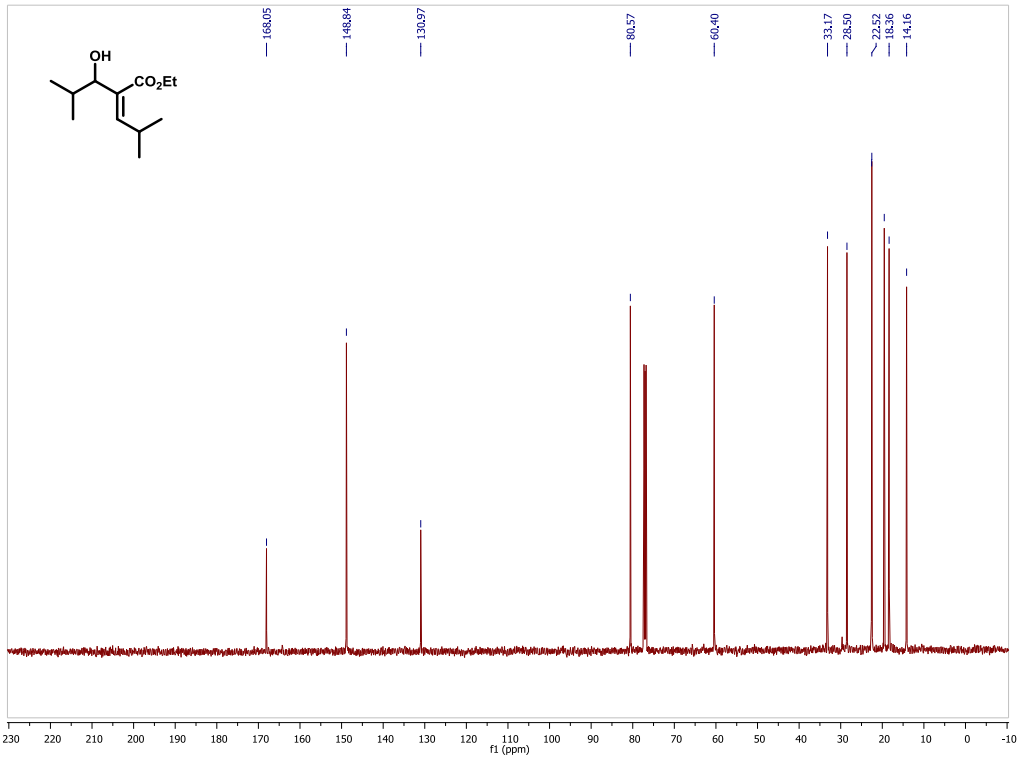
OH
CO2Et
168.05
148.84
130.97
80.57
60.40
33.17
28.50
22.52
18.36
14.16
f1 (ppm)

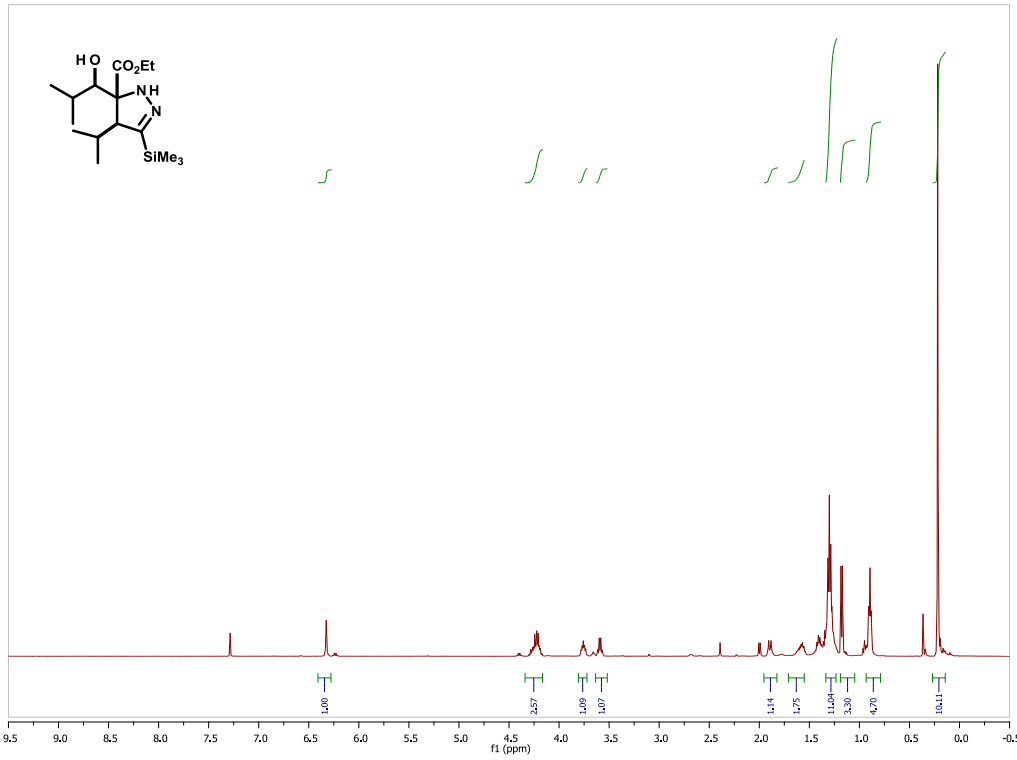
HO
CO2Et
NH
N
SiMe3
1.00
2.57
1.09
1.07
1.14
1.75
11.04
3.30
4.70
10.11
f1 (ppm)

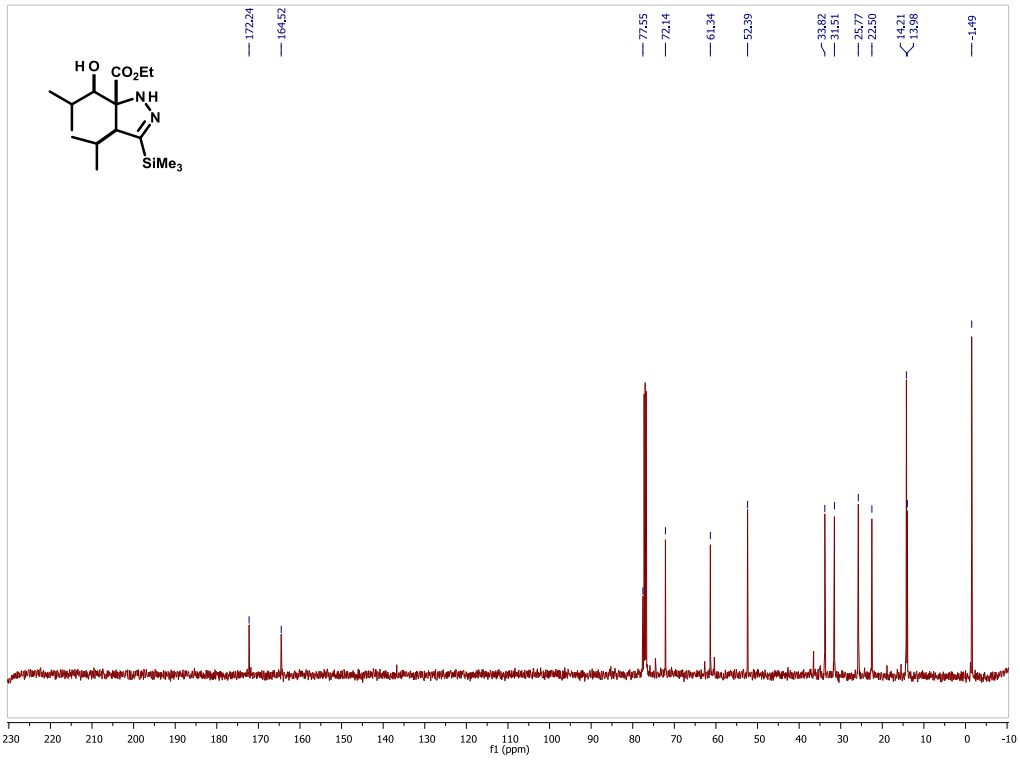
172.24
164.52
77.55
72.14
61.34
52.39
33.82
31.51
25.77
22.50
14.21
13.98
-1.49
HO
CO2Et
NH
N
SiMe3
f1 (ppm)

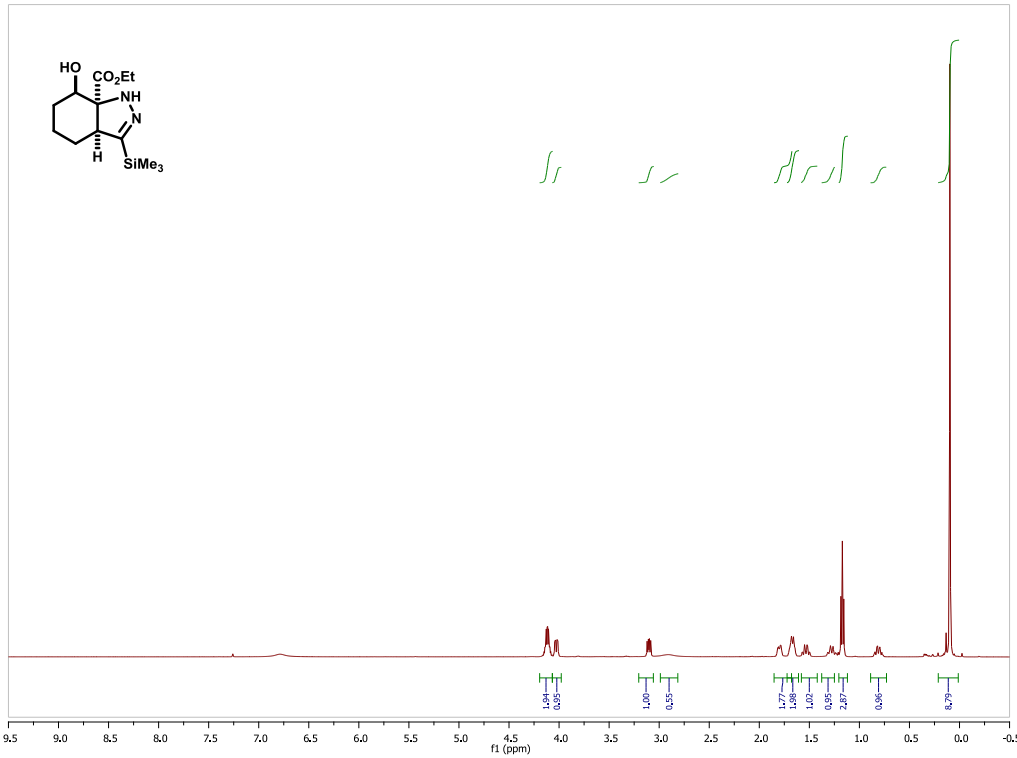
HO
CO2Et
NH
N
H
SiMe3
1.94
0.95
1.00
0.55
1.77
1.98
1.02
0.95
2.87
0.96
8.79
f1 (ppm)

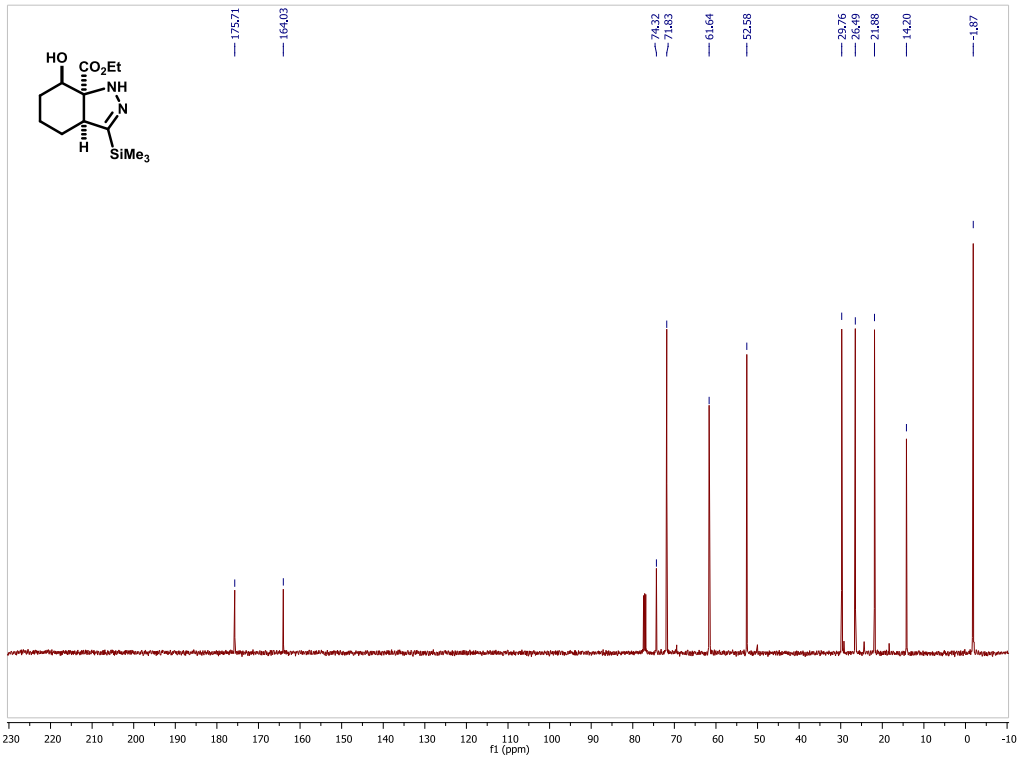
HO
CO2Et
NH
N
H
SiMe3
175.71
164.03
74.32
71.83
61.64
52.58
29.76
26.49
21.88
14.20
-1.87
f1 (ppm)

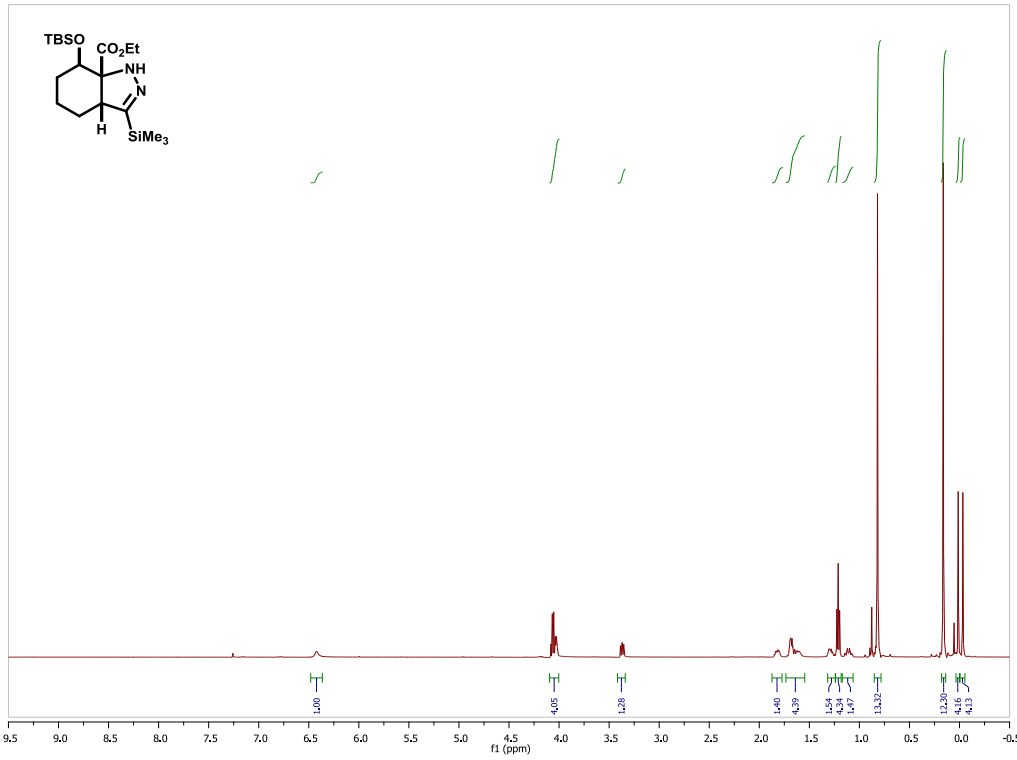
TBSO
CO2Et
NH
N
H
SiMe3
1.00
4.05
1.28
1.40
4.39
1.54
4.34
1.47
13.22
12.30
4.16
4.13
f1 (ppm)

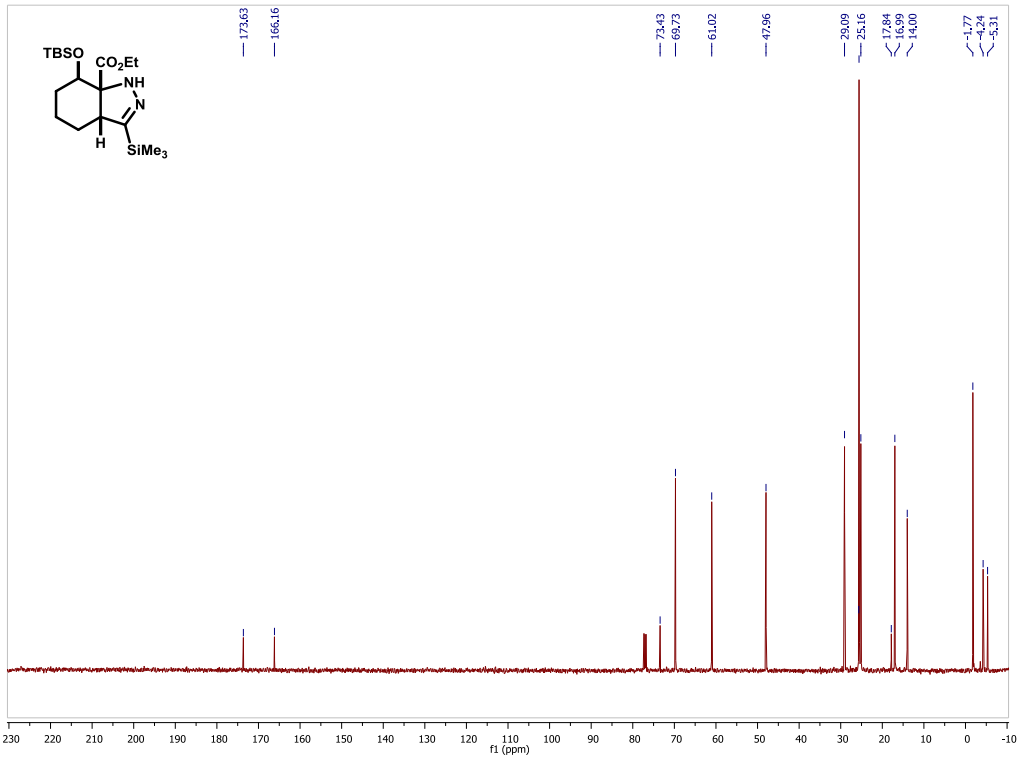
TBSO
CO2Et
NH
N
H
SiMe3
173.63
166.16
73.43
69.73
61.02
47.96
29.09
25.16
17.84
16.99
14.00
-1.77
-4.24
-5.31
f1 (ppm)

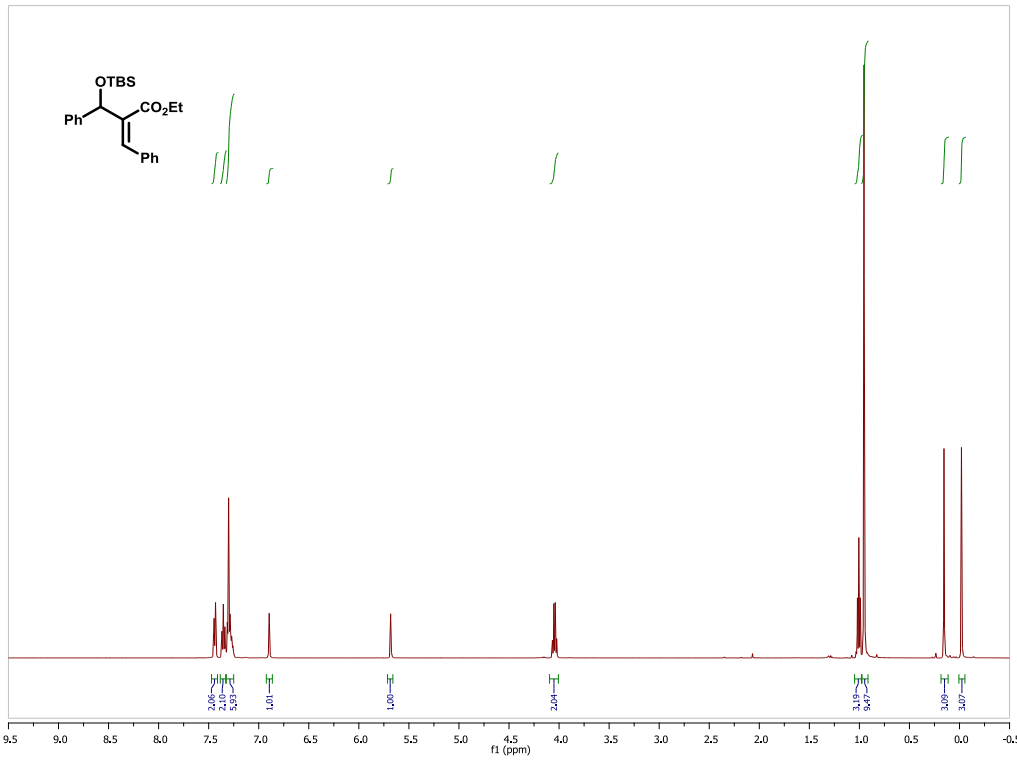
OTBS
Ph
CO2Et
Ph
2.05
2.10
5.93
1.01
1.00
2.04
3.19
3.47
3.09
3.07
f1 (ppm)

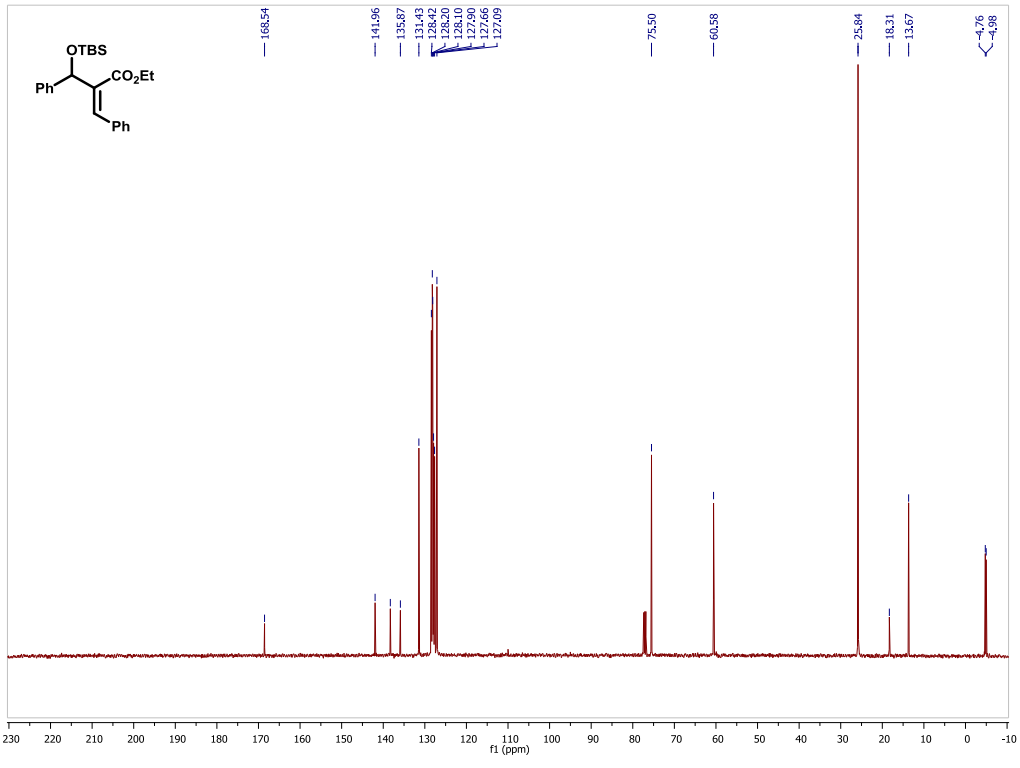
OTBS
Ph
CO2Et
Ph
168.54
141.96
135.87
131.43
128.42
128.20
128.10
127.90
127.66
127.09
75.50
60.58
25.84
18.31
13.67
-4.76
-4.98
f1 (ppm)

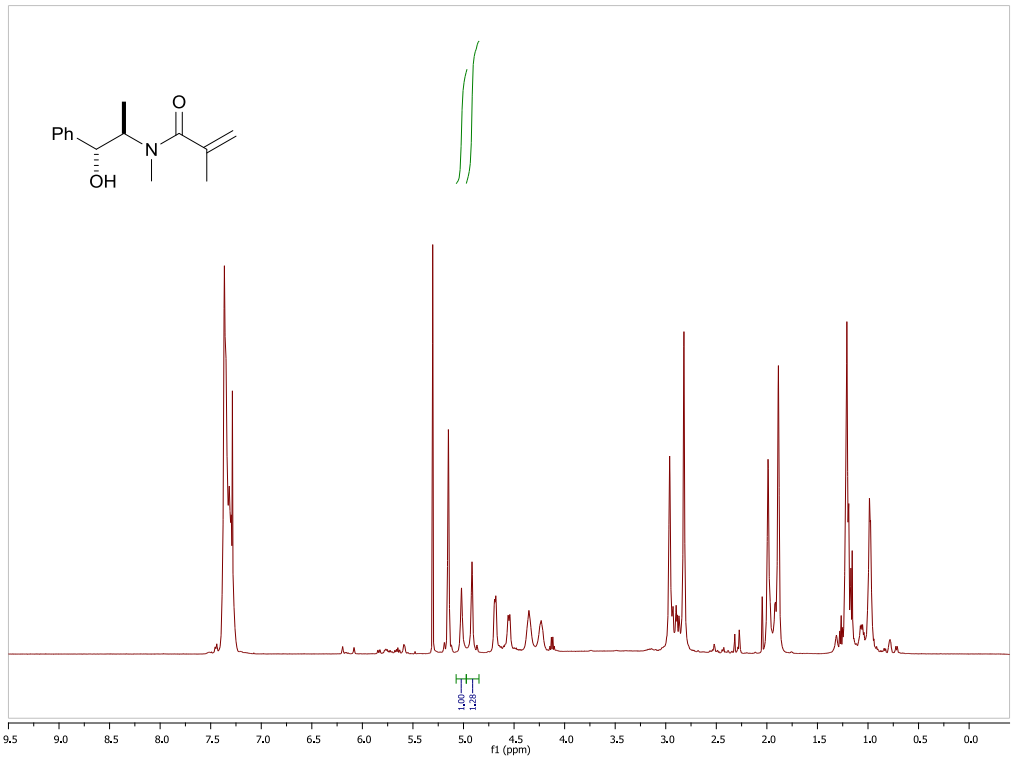
Ph
OH
N
O
1.00
1.28
f1 (ppm)

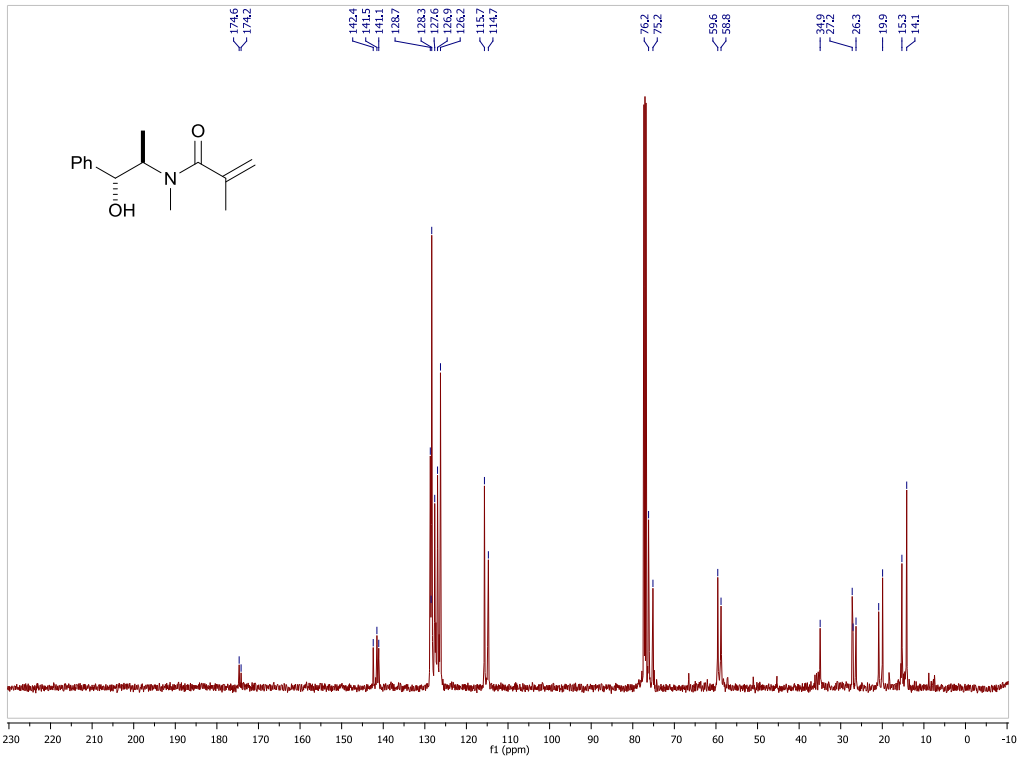
174.6
174.2
142.4
141.5
141.1
128.7
128.3
127.6
126.9
126.2
115.7
114.7
76.2
75.2
59.6
58.8
34.9
27.2
26.3
19.9
15.3
14.1
Ph
OH
N
O
f1 (ppm)

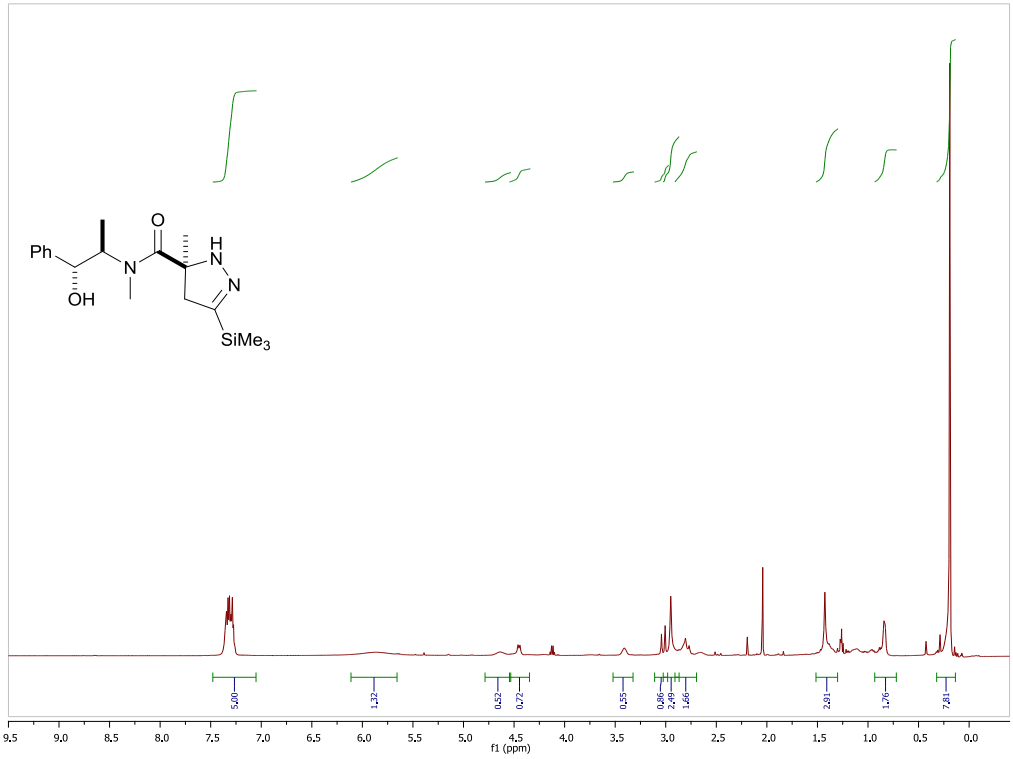
Ph
OH
N
O
H
N
N
SiMe3
5.00
1.32
0.52
0.72
0.55
0.86
2.88
1.66
2.01
1.76
7.81
f1 (ppm)

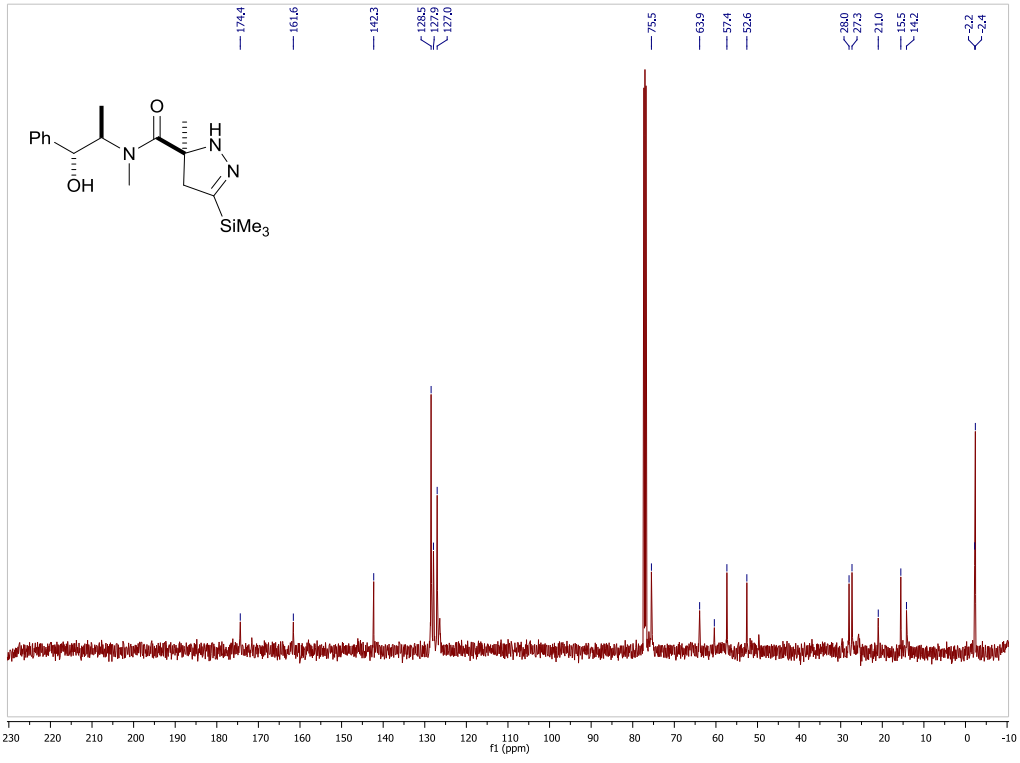
174.4
161.6
142.3
128.5
127.9
127.0
75.5
63.9
57.4
52.6
28.0
27.3
21.0
15.5
14.2
-2.2
-2.4
Ph
OH
N
O
H
N
N
SiMe3
f1 (ppm)

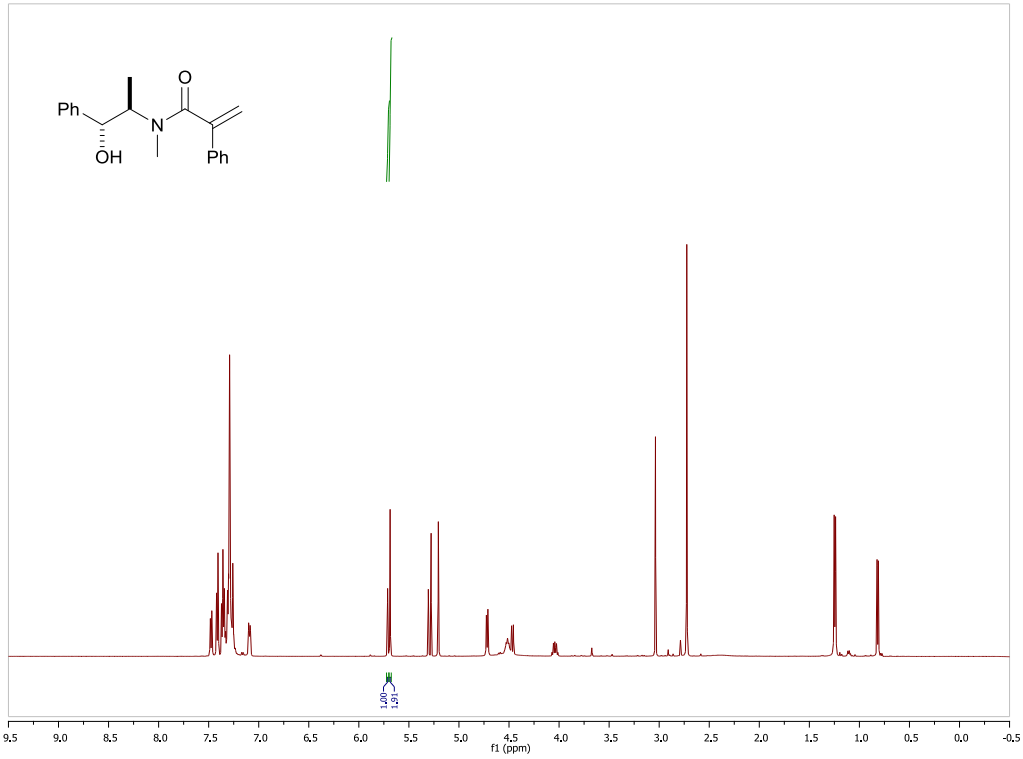
Ph
OH
N
O
Ph
1.00
1.91
9.5 9.0 8.5 8.0 7.5 7.0 6.5 6.0 5.5 5.0 4.5 4.0 3.5 3.0 2.5 2.0 1.5 1.0 0.5 0.0 -0.5
f1 (ppm)

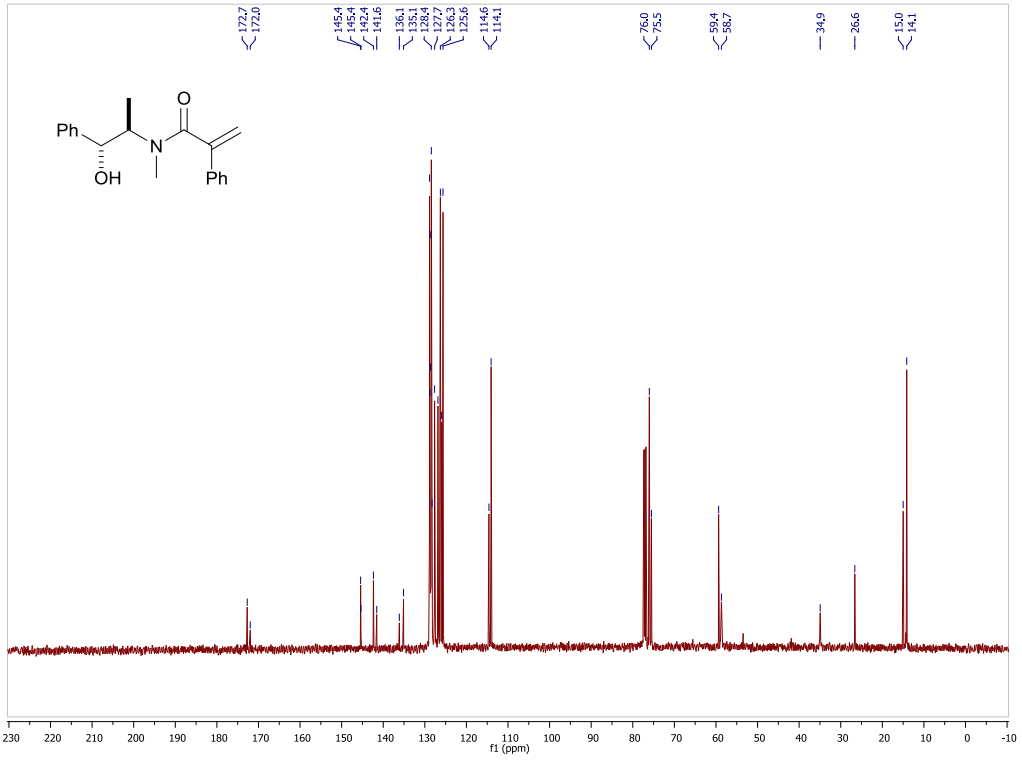
172.7
172.0
145.4
145.4
142.4
141.6
136.1
135.1
128.4
127.7
126.3
125.6
114.6
114.1
76.0
75.5
59.4
58.7
34.9
26.6
15.0
14.1
Ph
OH
N
O
Ph
230 220 210 200 190 180 170 160 150 140 130 120 110 100 90 80 70 60 50 40 30 20 10 0 -10
f1 (ppm)

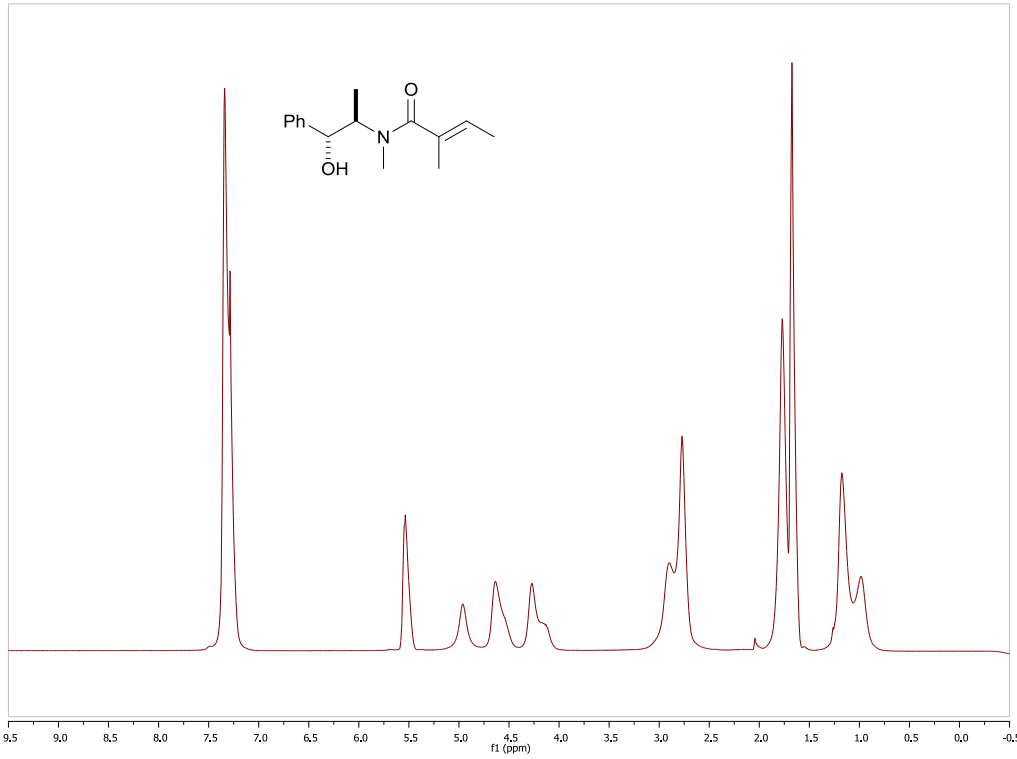
Ph
OH
N
O
9.5 9.0 8.5 8.0 7.5 7.0 6.5 6.0 5.5 5.0 4.5 4.0 3.5 3.0 2.5 2.0 1.5 1.0 0.5 0.0 -0.5
f1 (ppm)

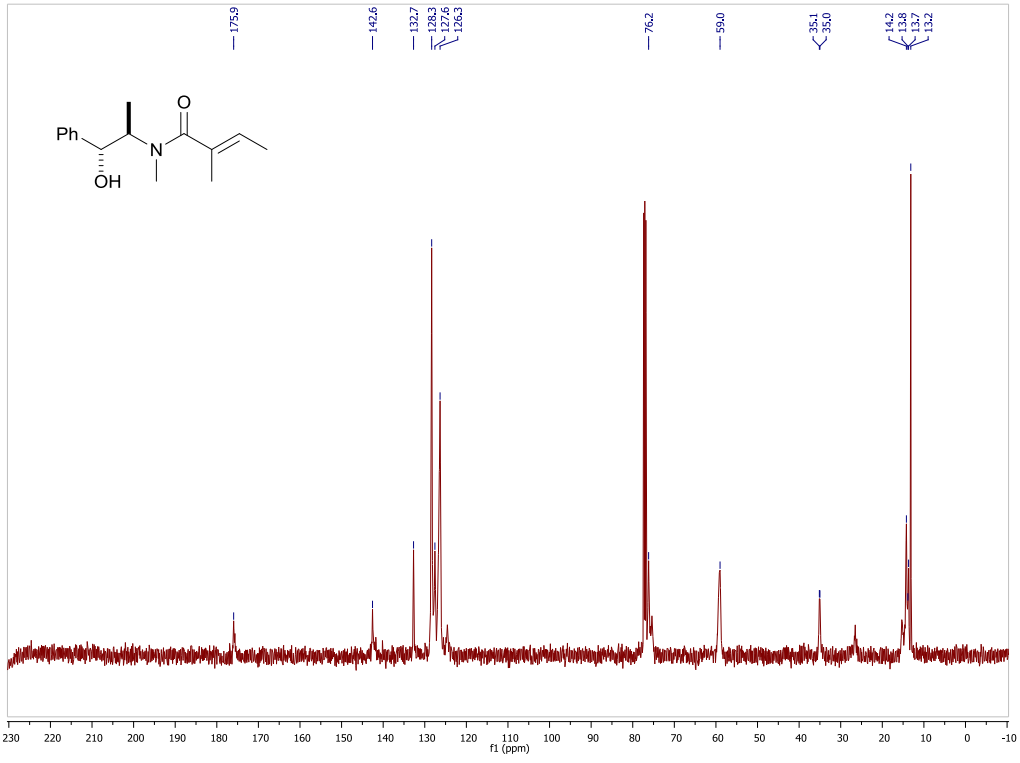
175.9
142.6
132.7
128.3
127.6
126.3
76.2
59.0
35.1
35.0
14.2
13.8
13.7
13.2
Ph
OH
N
O
230 220 210 200 190 180 170 160 150 140 130 120 110 100 90 80 70 60 50 40 30 20 10 0 -10
f1 (ppm)

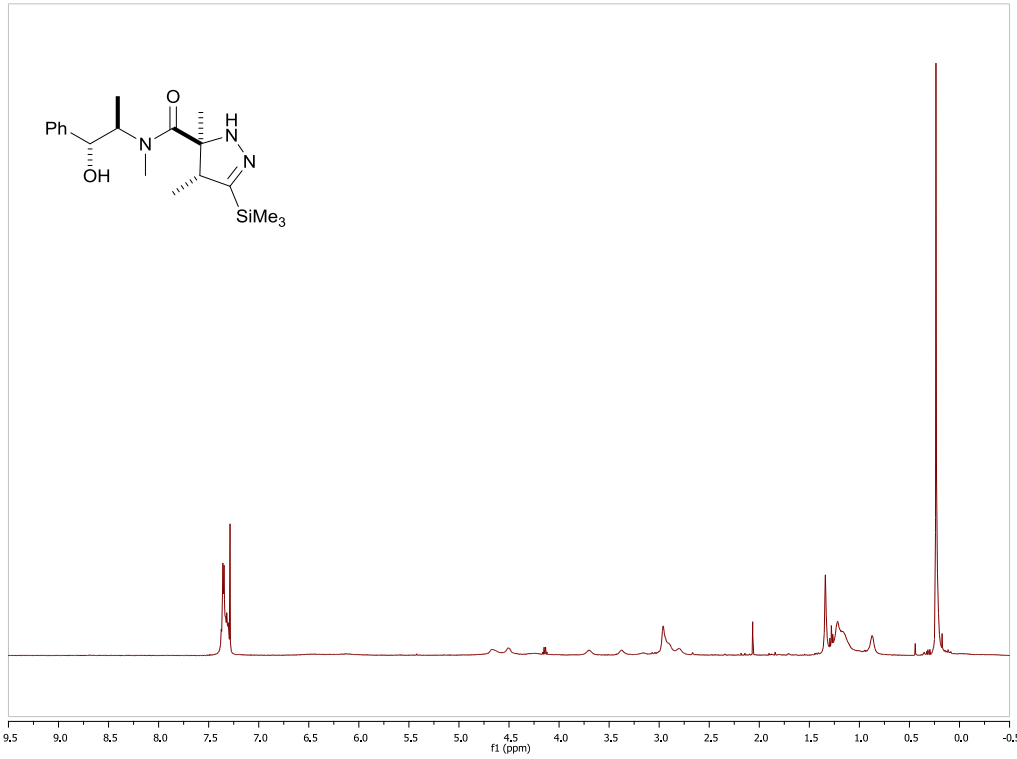
Ph
OH
N
O
H
N
N
SiMe3
9.5 9.0 8.5 8.0 7.5 7.0 6.5 6.0 5.5 5.0 4.5 4.0 3.5 3.0 2.5 2.0 1.5 1.0 0.5 0.0 -0.5
f1 (ppm)

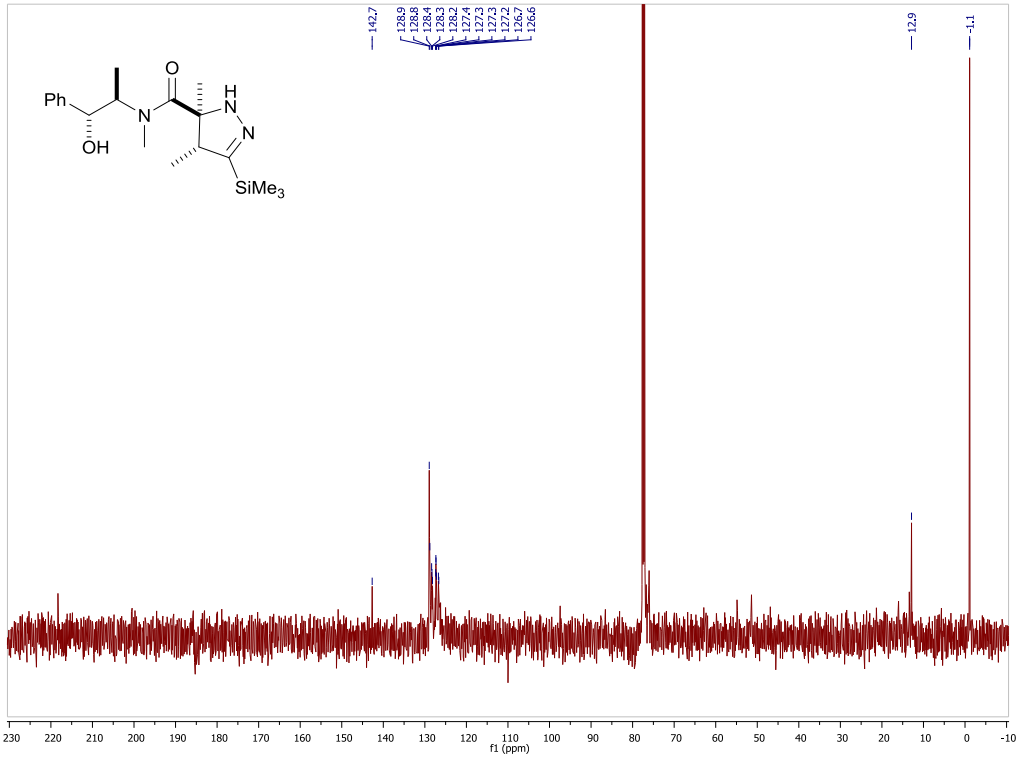
142.7
128.9
128.8
128.4
128.3
128.2
127.4
127.3
127.3
127.2
126.7
126.6
12.9
-1.1
Ph
OH
N
O
H
N
N
SiMe3
230 220 210 200 190 180 170 160 150 140 130 120 110 100 90 80 70 60 50 40 30 20 10 0 -10
f1 (ppm)

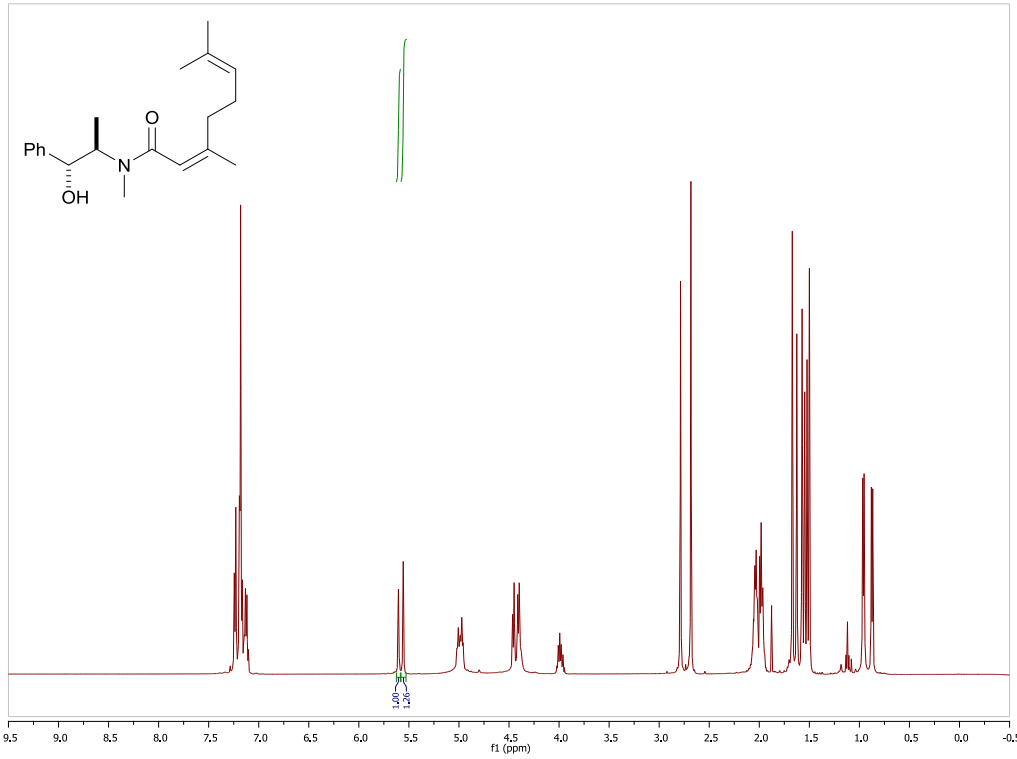
Ph
N
O
OH
1.00
1.26
9.5 9.0 8.5 8.0 7.5 7.0 6.5 6.0 5.5 5.0 4.5 4.0 3.5 3.0 2.5 2.0 1.5 1.0 0.5 0.0 -0.5
f1 (ppm)

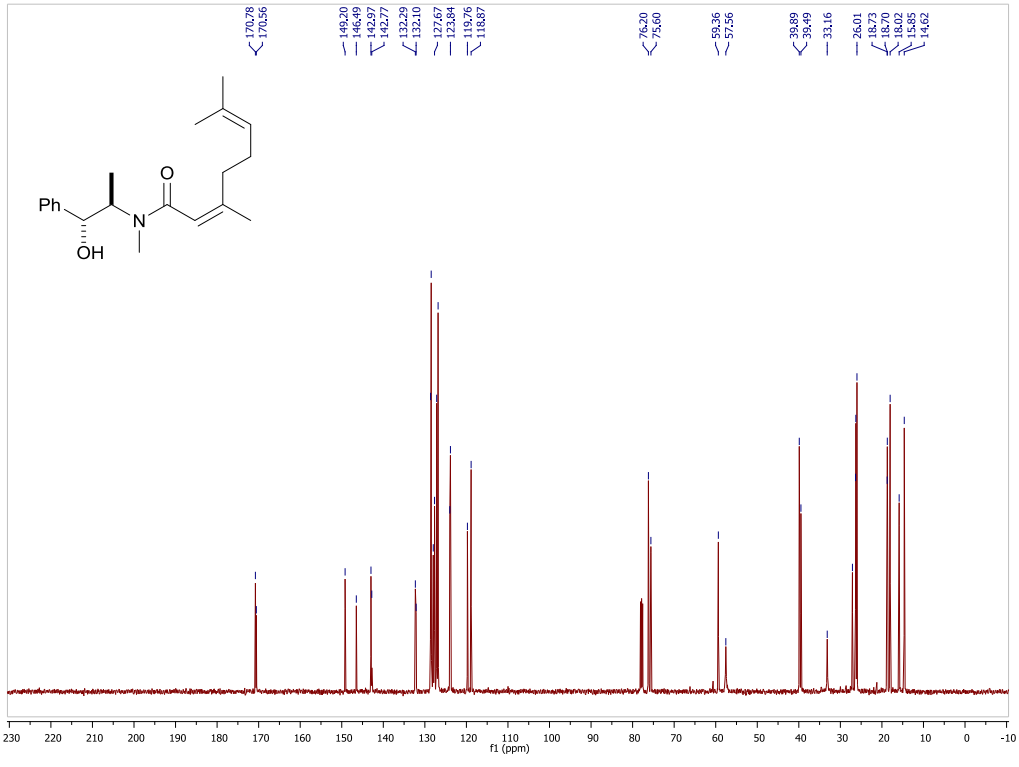
170.78
170.56
149.20
146.49
142.97
142.77
132.29
132.10
127.67
123.84
119.76
118.87
76.20
75.60
59.36
57.56
39.89
39.49
33.16
26.01
18.73
18.70
18.02
15.85
14.62
Ph
N
O
OH
230 220 210 200 190 180 170 160 150 140 130 120 110 100 90 80 70 60 50 40 30 20 10 0 -10
f1 (ppm)

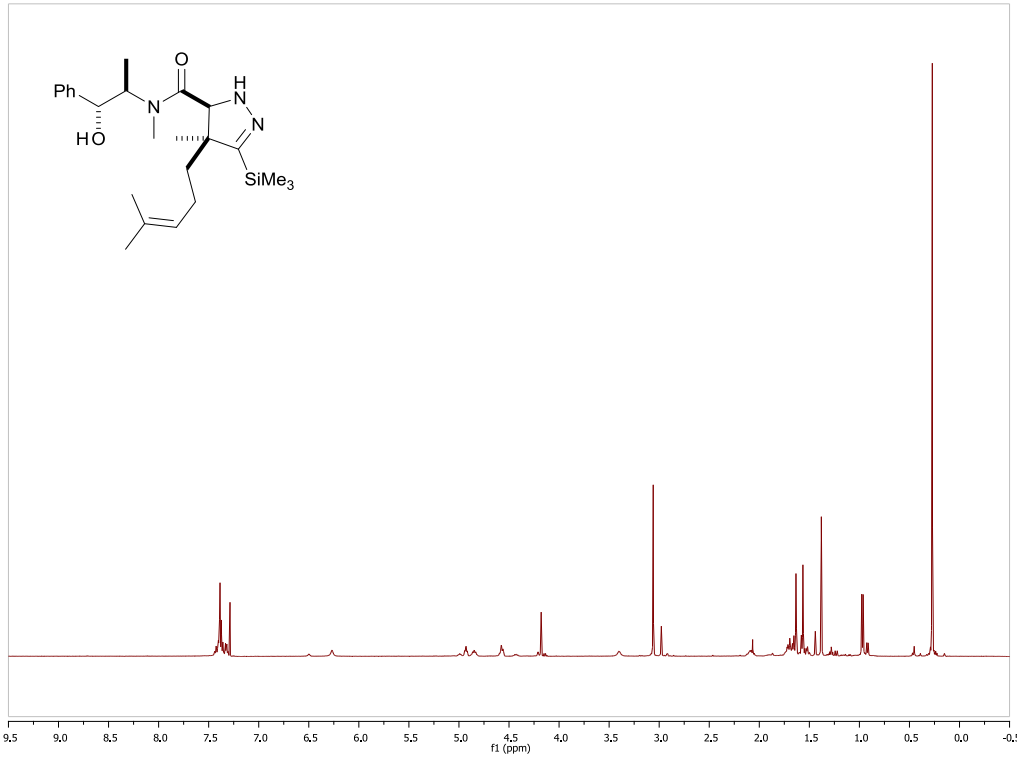
Ph
HO
N
O
H
N
N
SiMe3
9.5 9.0 8.5 8.0 7.5 7.0 6.5 6.0 5.5 5.0 4.5 4.0 3.5 3.0 2.5 2.0 1.5 1.0 0.5 0.0 -0.5
f1 (ppm)

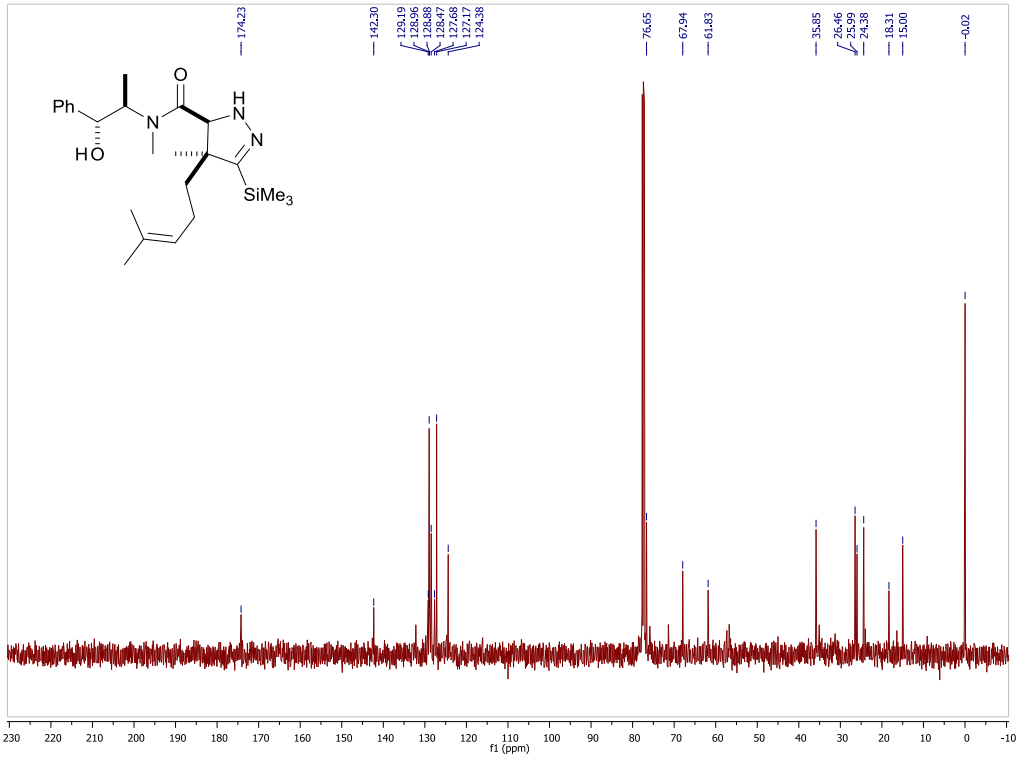
174.23
142.30
129.19
128.96
128.88
128.47
127.68
127.17
124.38
76.65
67.94
61.83
35.85
26.46
25.99
24.38
18.31
15.00
-0.02
Ph
HO
N
O
H
N
N
SiMe3
230 220 210 200 190 180 170 160 150 140 130 120 110 100 90 80 70 60 50 40 30 20 10 0 -10
f1 (ppm)

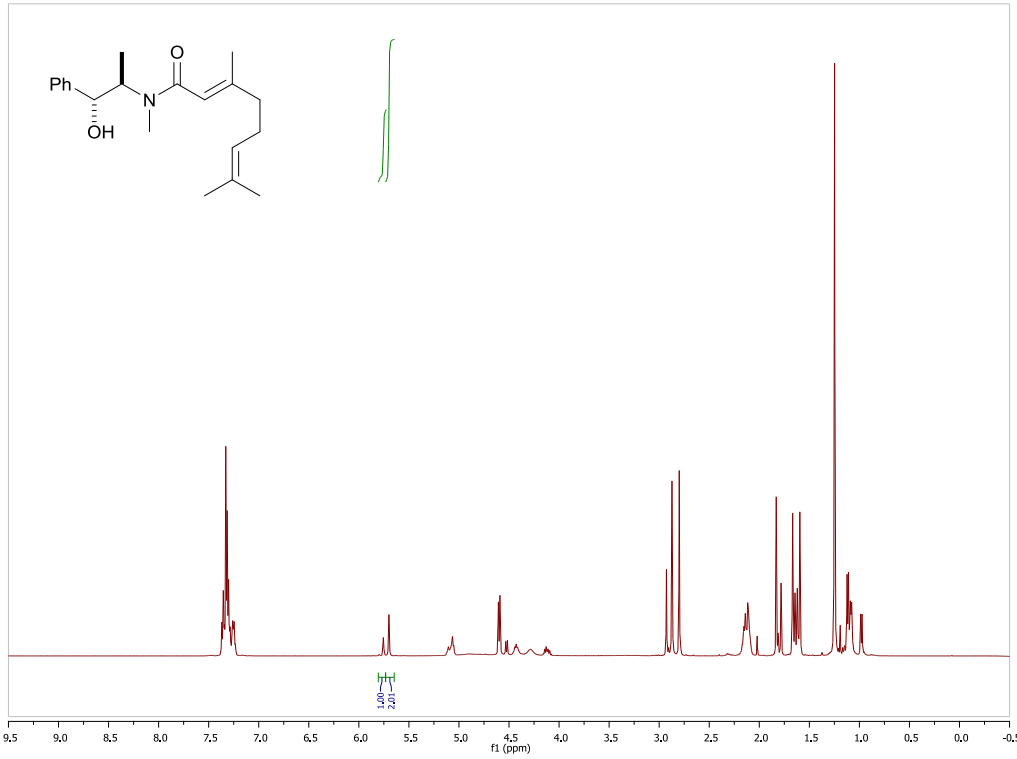
Ph
OH
N
O
1.00
2.01
9.5 9.0 8.5 8.0 7.5 7.0 6.5 6.0 5.5 5.0 4.5 4.0 3.5 3.0 2.5 2.0 1.5 1.0 0.5 0.0 -0.5
f1 (ppm)

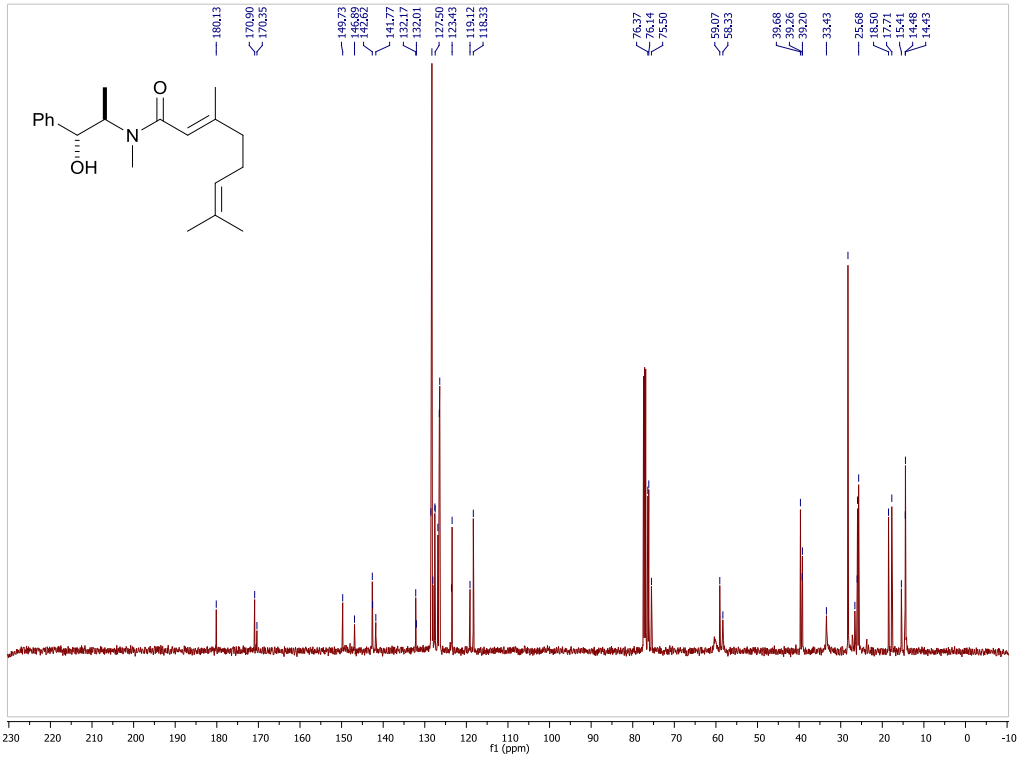
180.13
170.90
170.35
149.73
146.89
142.62
141.77
132.17
132.01
127.50
123.43
119.12
118.33
76.37
76.14
75.50
59.07
58.33
39.68
39.26
39.20
33.43
25.68
18.50
17.71
15.41
14.48
14.43
Ph
OH
N
O
230 220 210 200 190 180 170 160 150 140 130 120 110 100 90 80 70 60 50 40 30 20 10 0 -10
f1 (ppm)

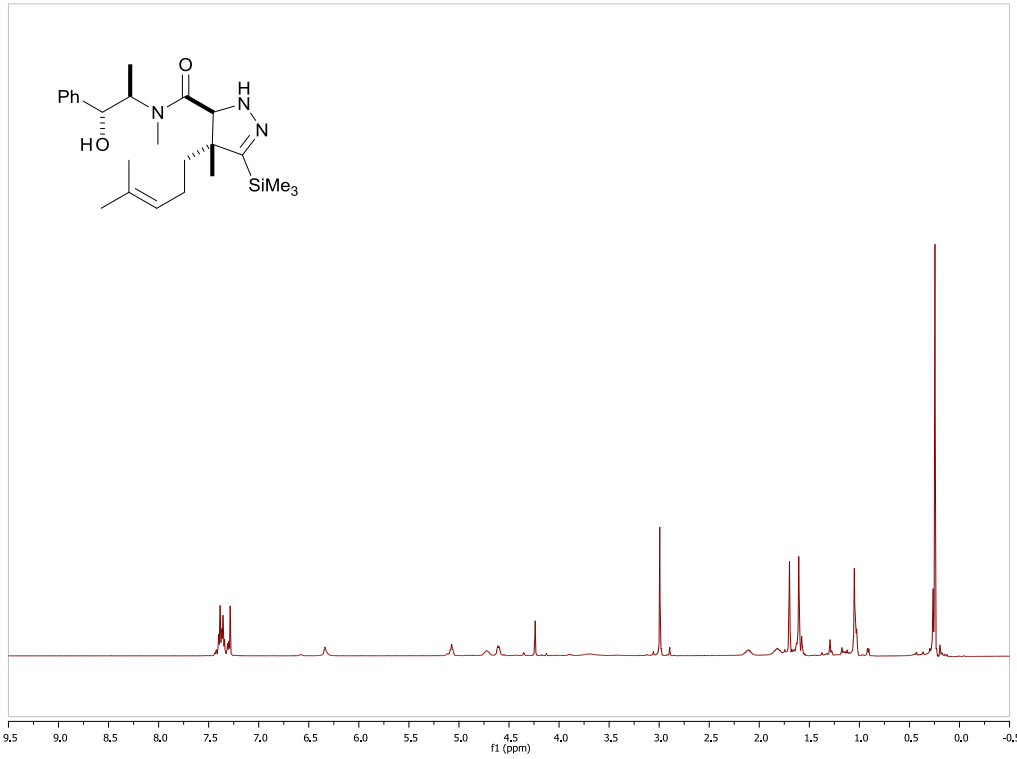
Ph
HO
N
O
H
N
N
SiMe3
9.5 9.0 8.5 8.0 7.5 7.0 6.5 6.0 5.5 5.0 4.5 4.0 3.5 3.0 2.5 2.0 1.5 1.0 0.5 0.0 -0.5
f1 (ppm)

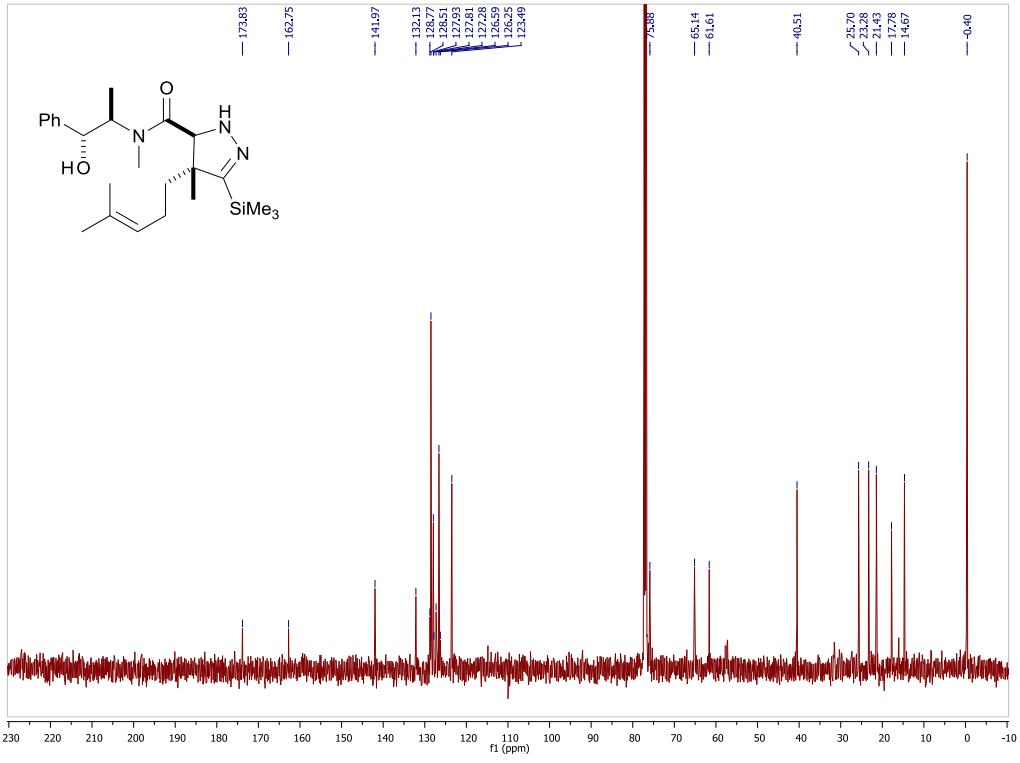
173.83
162.75
141.97
132.13
128.77
128.51
127.93
127.81
127.28
126.59
126.25
123.49
75.88
65.14
61.61
40.51
25.70
23.28
21.43
17.78
14.67
-0.40
Ph
HO
N
O
H
N
N
SiMe3
230 220 210 200 190 180 170 160 150 140 130 120 110 100 90 80 70 60 50 40 30 20 10 0 -10
f1 (ppm)

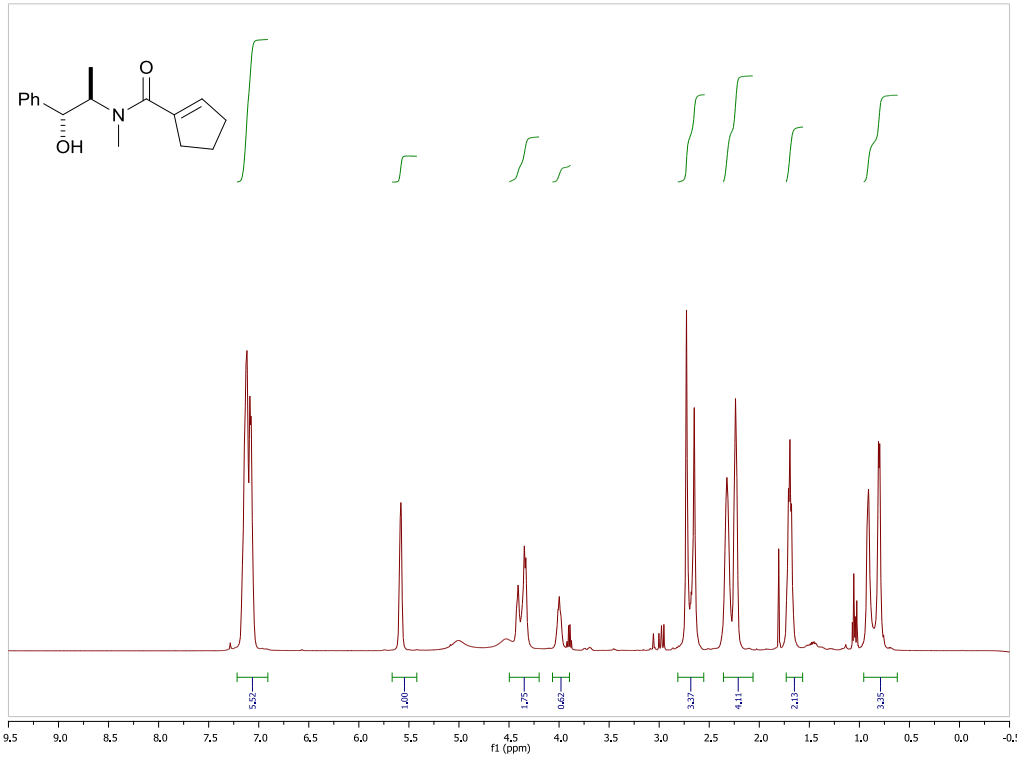
Ph
OH
N
O
5.52
1.00
1.75
0.62
3.27
4.11
2.13
3.35
f1 (ppm)

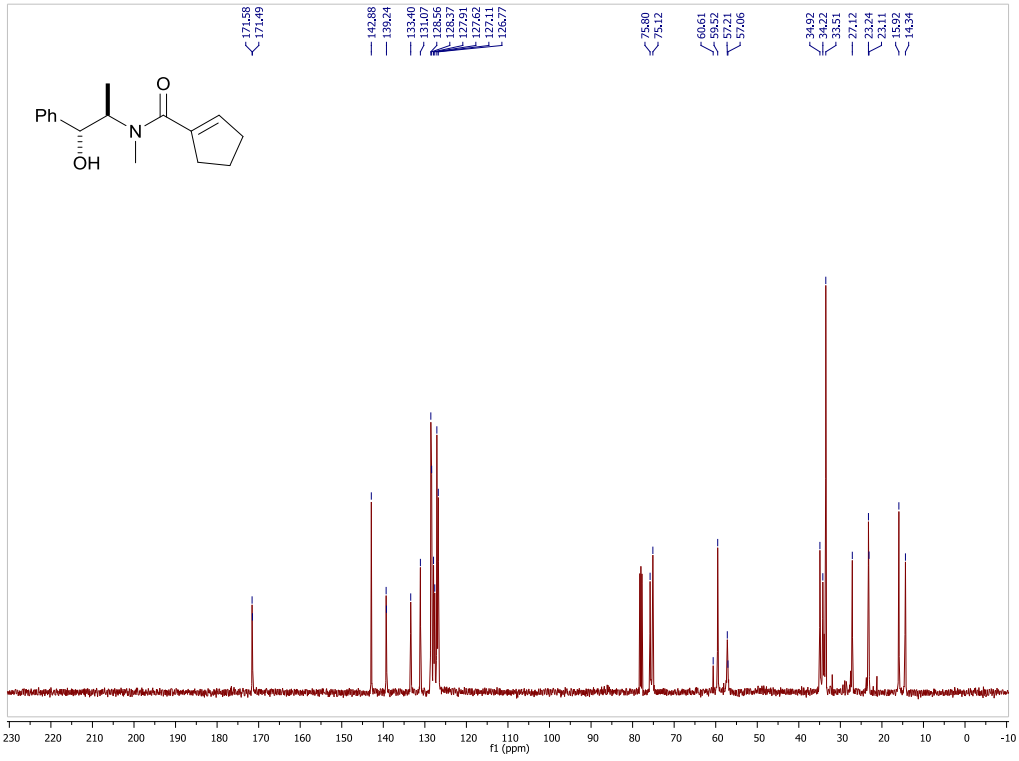
171.58
171.49
142.88
139.24
133.40
131.07
128.56
128.37
127.91
127.62
127.11
126.77
75.80
75.12
60.61
59.52
57.21
57.06
34.92
34.22
33.51
27.12
23.24
23.11
15.32
14.34
Ph
OH
N
O
f1 (ppm)

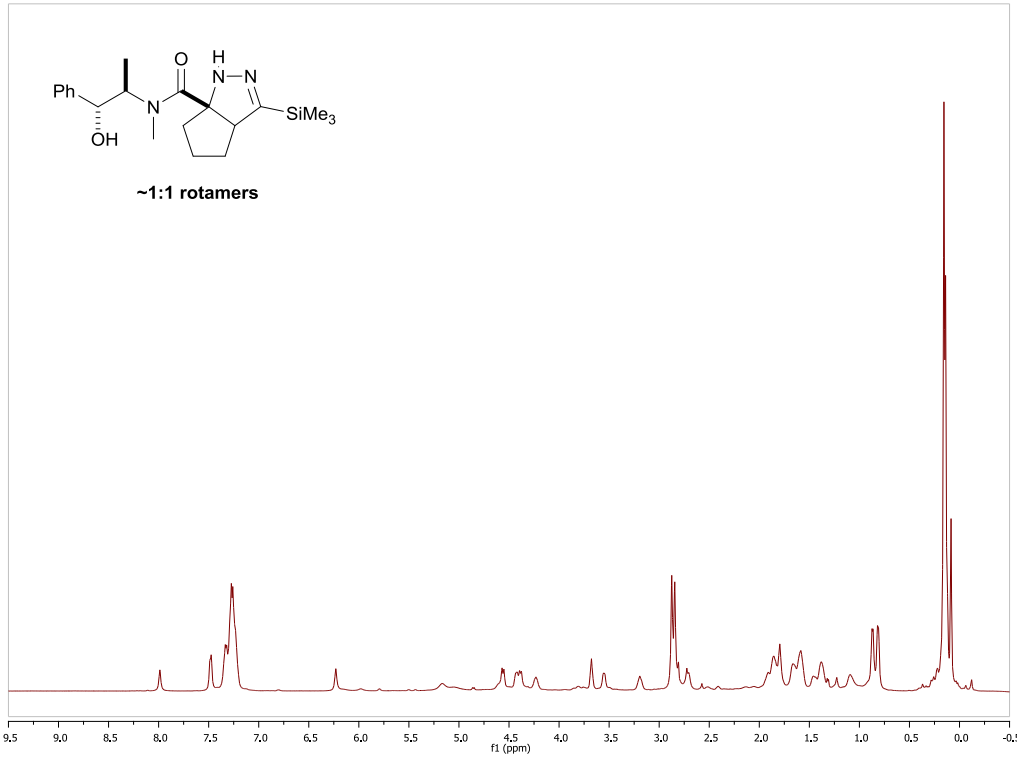
Ph
OH
N
O
H
N–N
SiMe3
~1:1 rotamers
f1 (ppm)

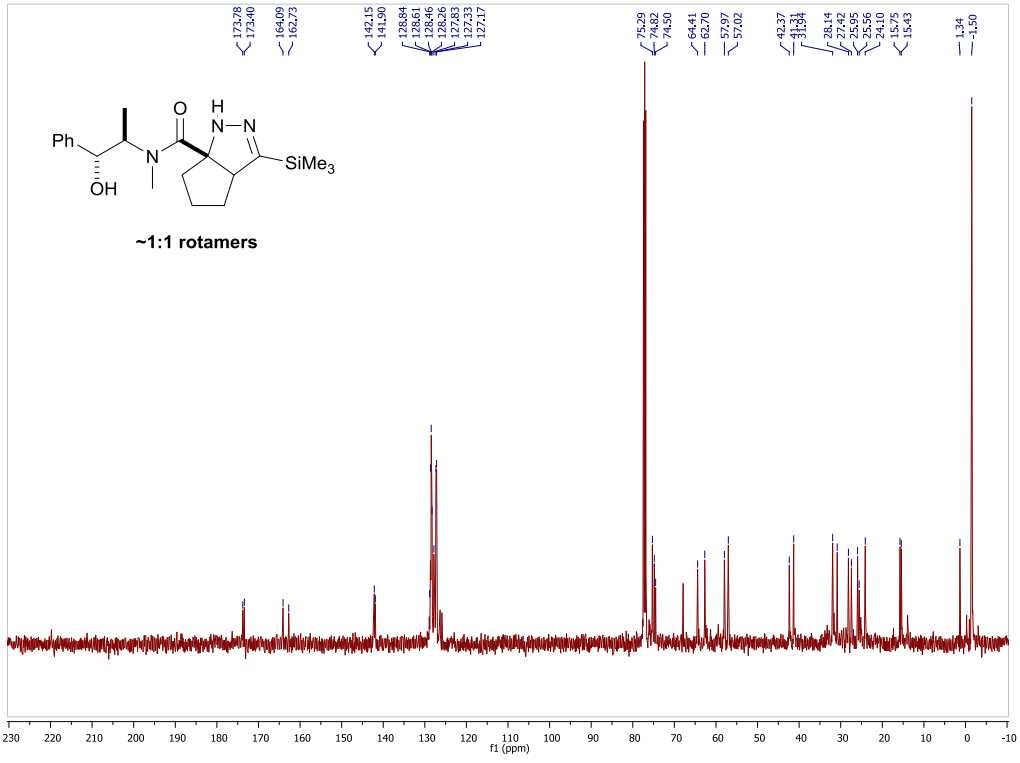
173.78
173.40
164.09
162.73
142.15
141.90
128.84
128.61
128.46
128.26
127.83
127.33
127.17
75.29
74.82
74.50
64.41
62.70
57.97
57.02
42.37
41.31
31.94
28.14
27.42
25.95
25.56
24.10
15.75
15.43
1.34
-1.50
Ph
OH
N
O
H
N–N
SiMe3
~1:1 rotamers
f1 (ppm)

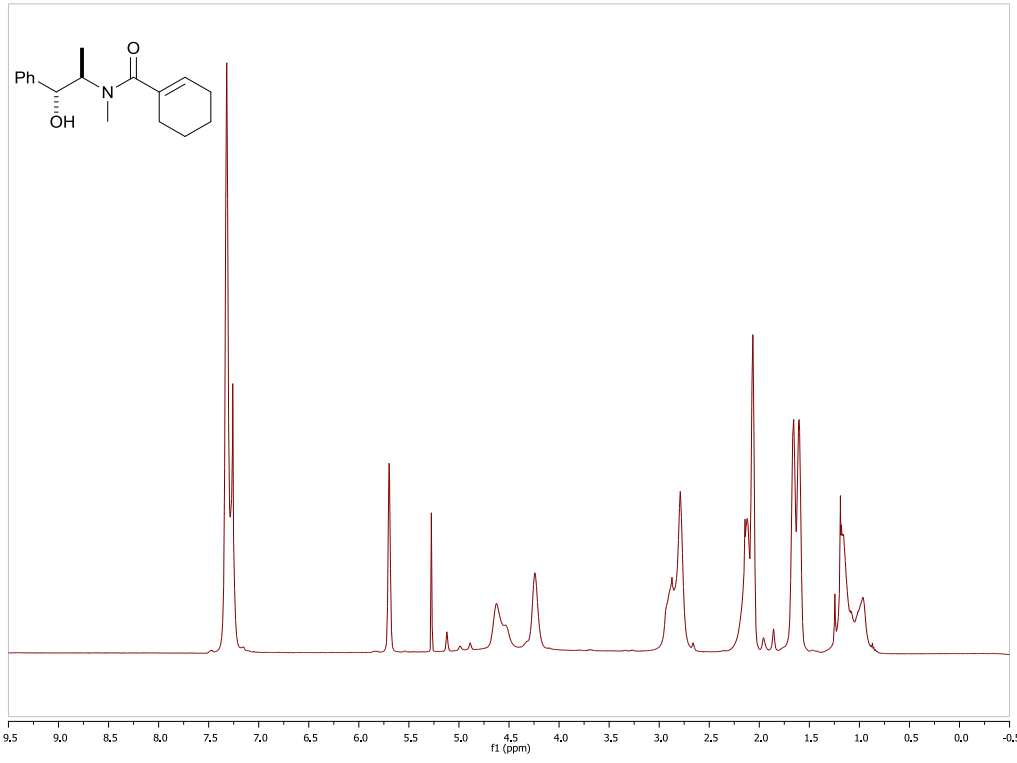
Ph
OH
N
O
9.5 9.0 8.5 8.0 7.5 7.0 6.5 6.0 5.5 5.0 4.5 4.0 3.5 3.0 2.5 2.0 1.5 1.0 0.5 0.0 -0.5
f1 (ppm)

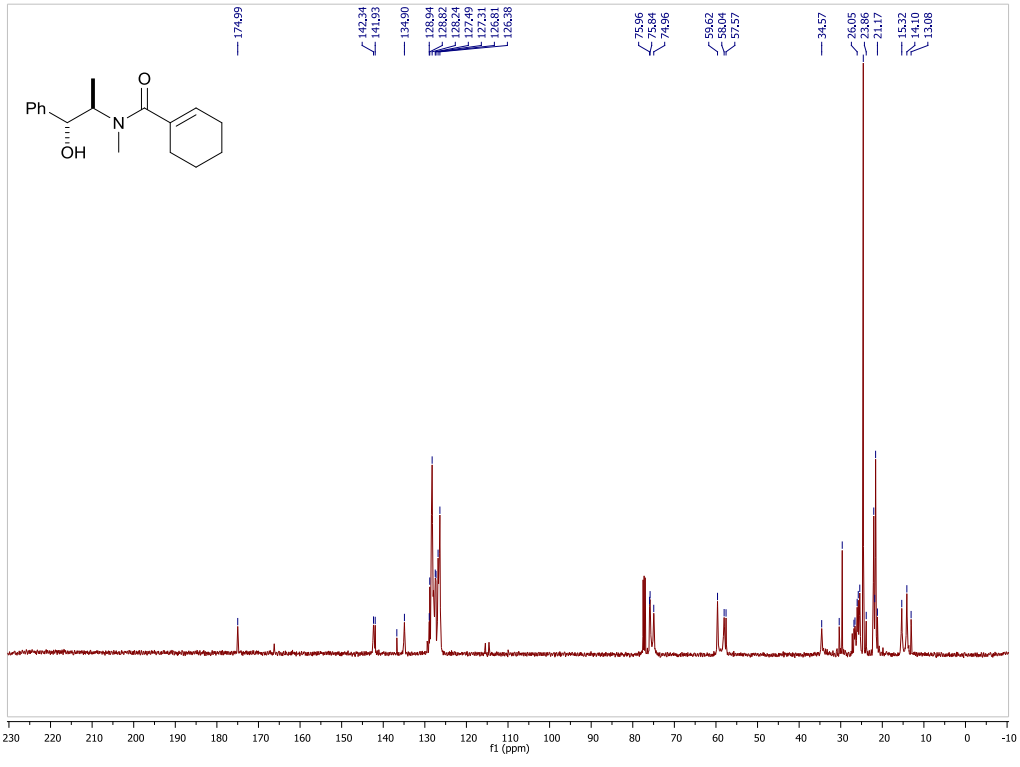
174.99
142.34
141.93
134.90
128.94
128.82
128.24
127.49
127.31
126.81
126.38
75.96
75.84
74.96
59.62
58.04
57.57
34.57
26.05
23.86
21.17
15.32
14.10
13.08
Ph
OH
N
O
230 220 210 200 190 180 170 160 150 140 130 120 110 100 90 80 70 60 50 40 30 20 10 0 -10
f1 (ppm)

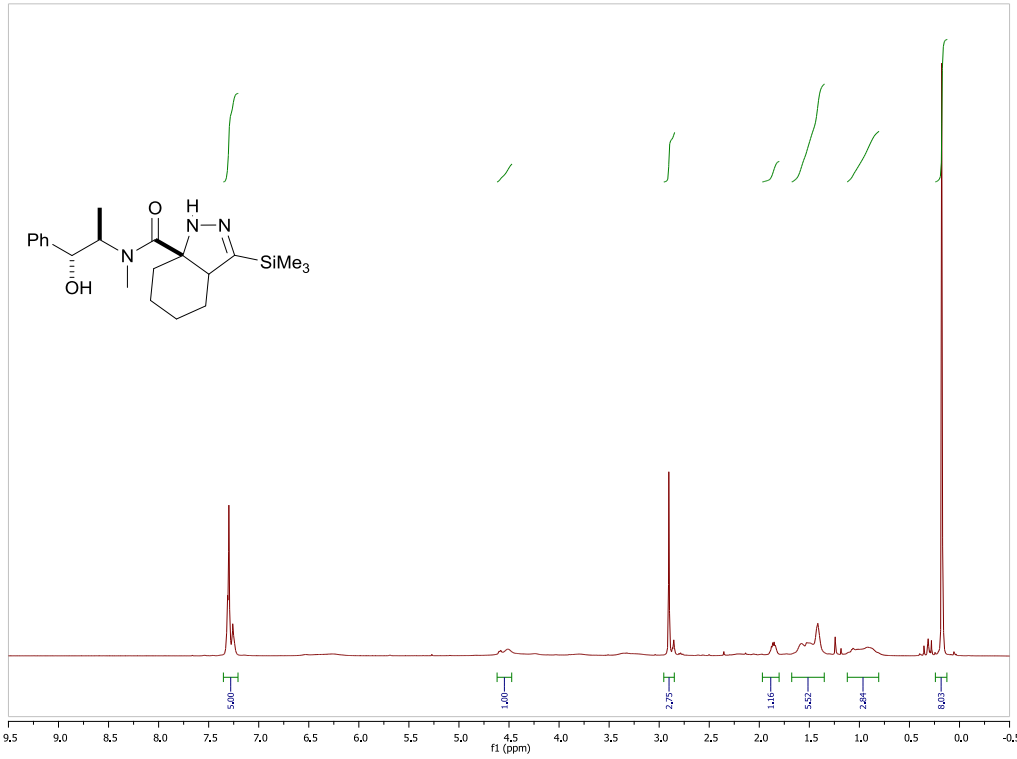
Ph
OH
N
O
H
N—N
SiMe3
5.00
1.00
2.75
1.16
5.52
2.84
8.03
f1 (ppm)

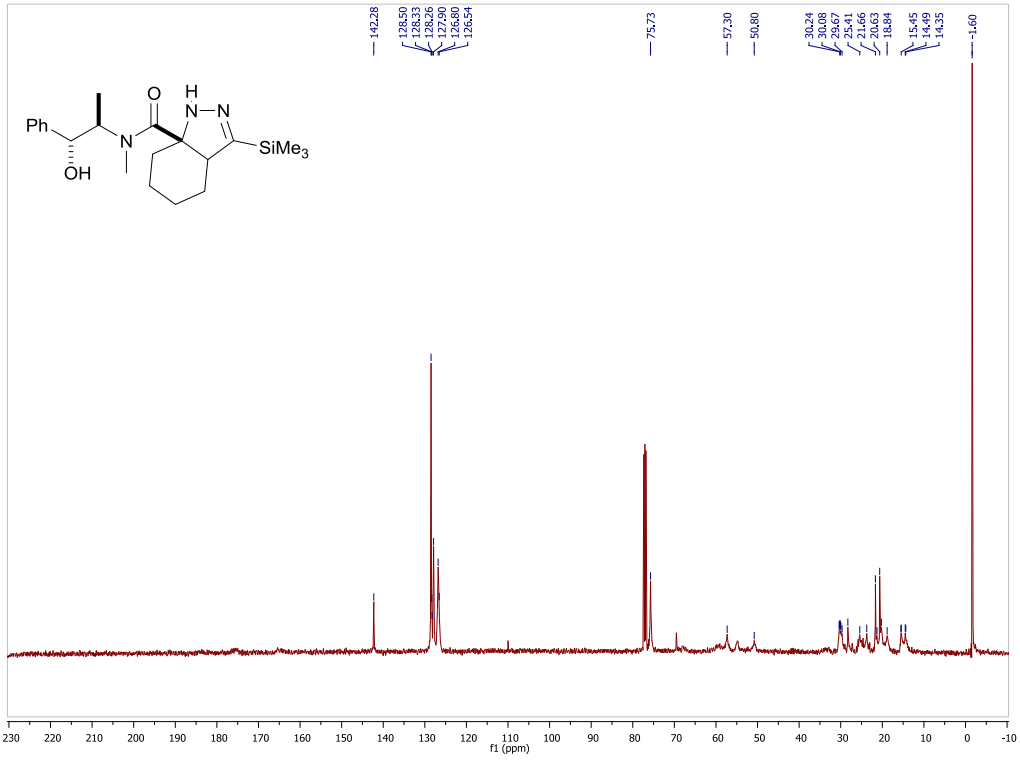
142.28
128.50
128.33
128.26
127.90
126.80
126.54
75.73
57.30
50.80
30.24
30.08
29.67
25.41
21.66
20.63
18.84
15.45
14.49
14.35
-1.60
Ph
OH
N
O
H
N—N
SiMe3
f1 (ppm)

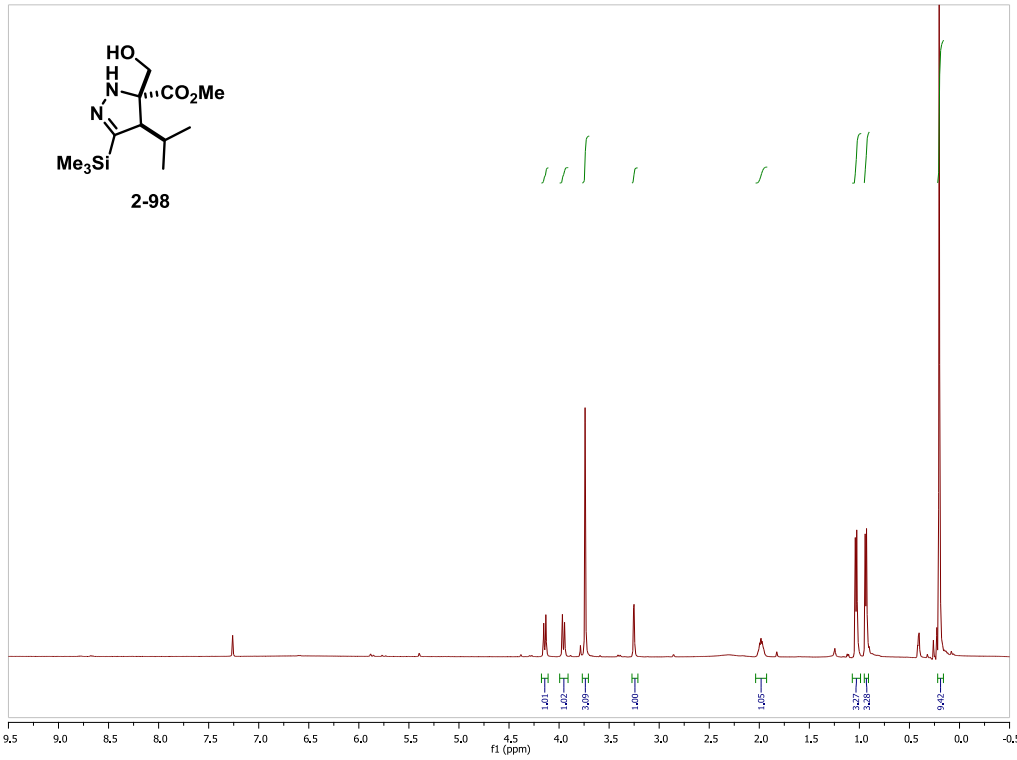
HO
H
N
N
CO2Me
Me3Si
2-98
1.01
1.22
3.09
1.20
1.05
3.27
3.28
9.42
f1 (ppm)

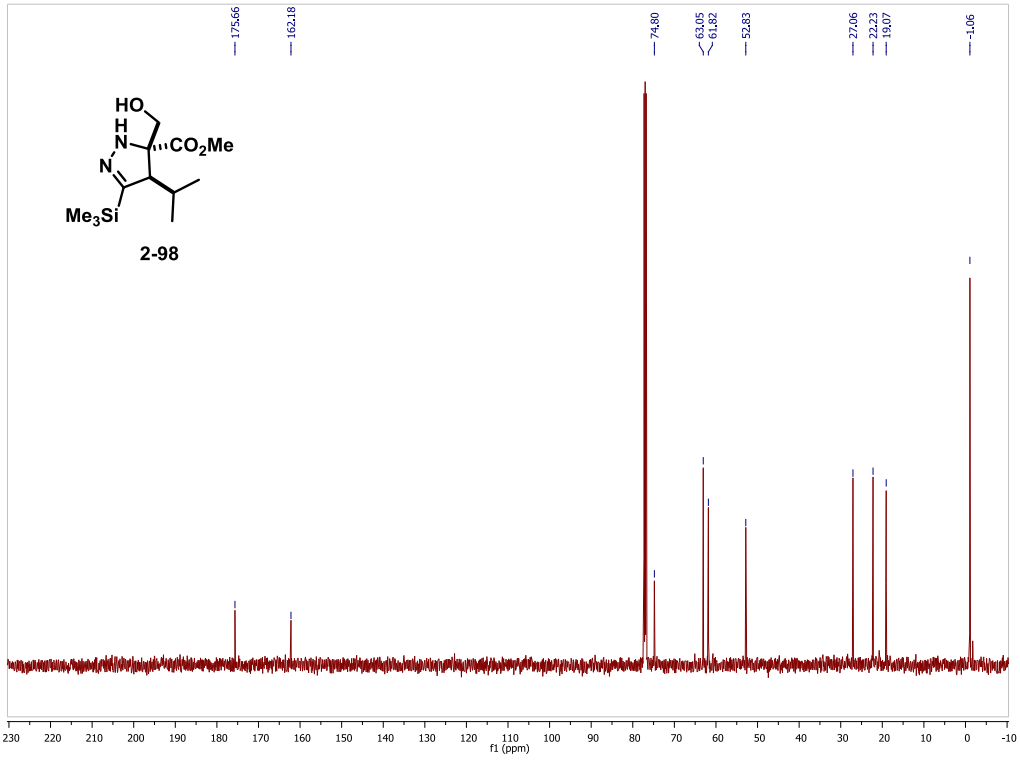
175.66
162.18
74.80
63.05
61.82
52.83
27.06
22.23
19.07
-1.06
HO
H
N
N
CO2Me
Me3Si
2-98
f1 (ppm)

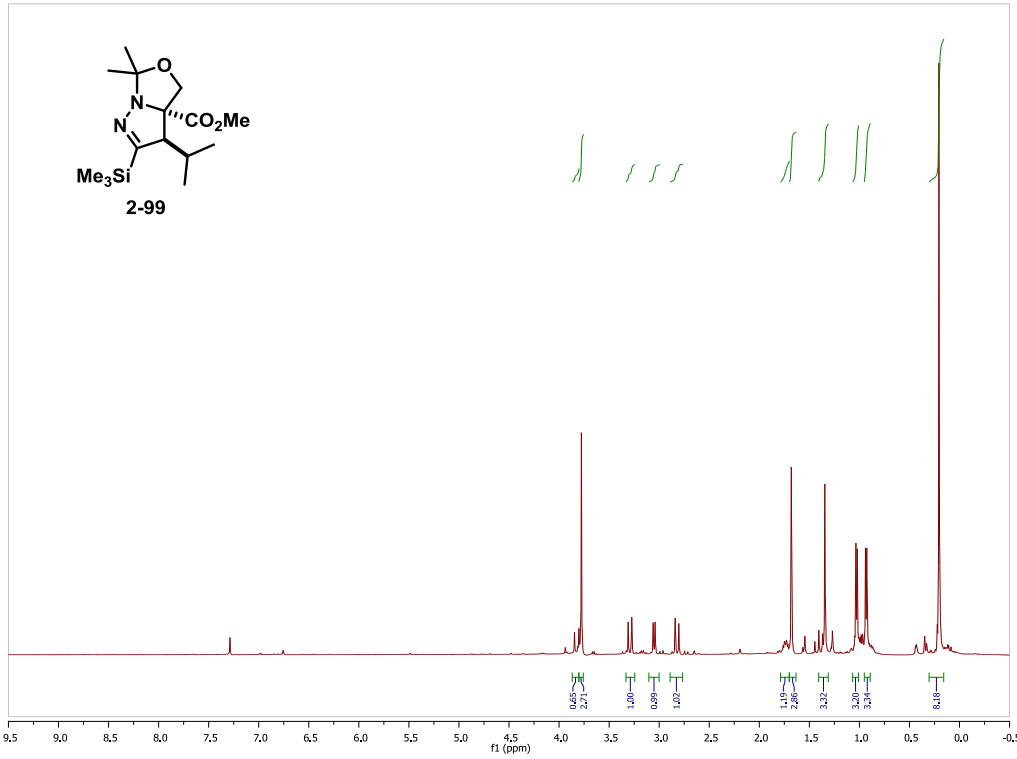
O
N
N
CO2Me
Me3Si
2-99
0.65
2.71
1.00
0.99
1.02
1.19
2.86
3.22
3.20
3.34
8.18
f1 (ppm)

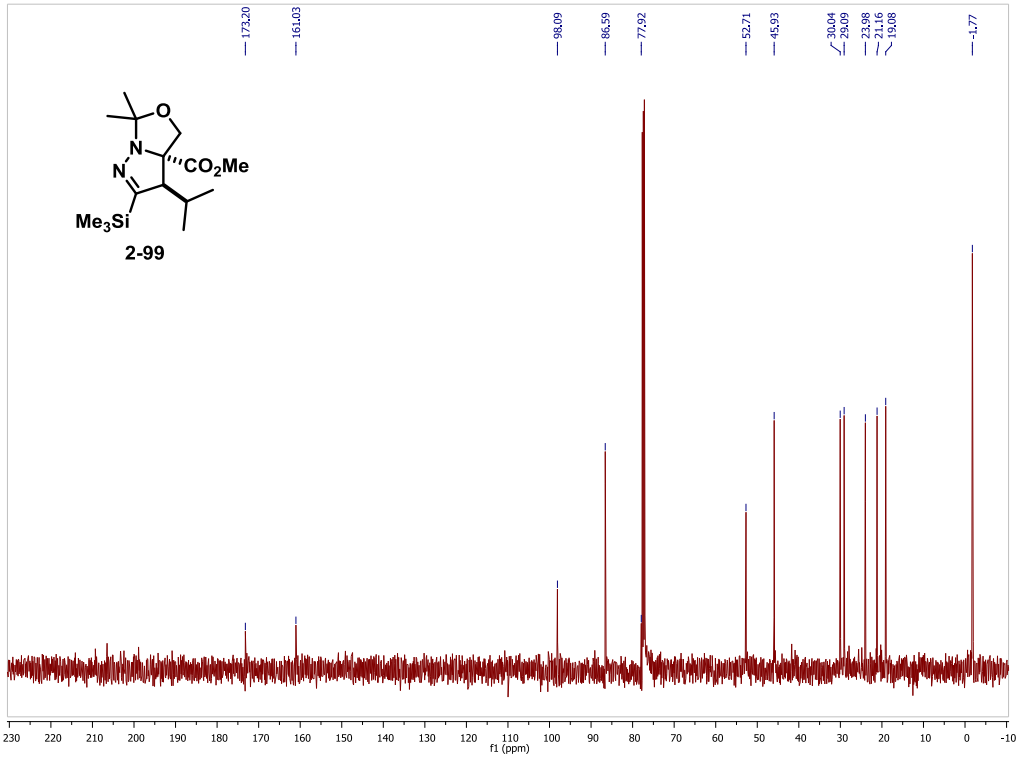
173.20
161.03
98.09
86.59
77.92
52.71
45.93
30.04
29.09
23.98
21.16
19.08
-1.77
O
N
N
CO2Me
Me3Si
2-99
f1 (ppm)

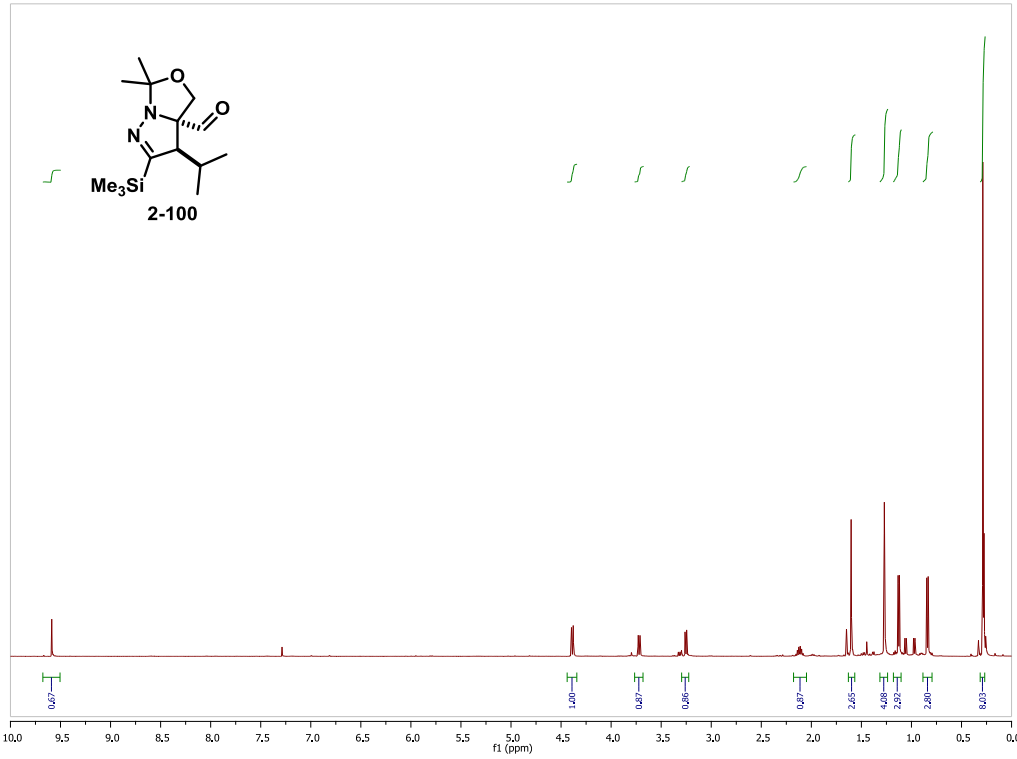
Me3Si
2-100
f1 (ppm)

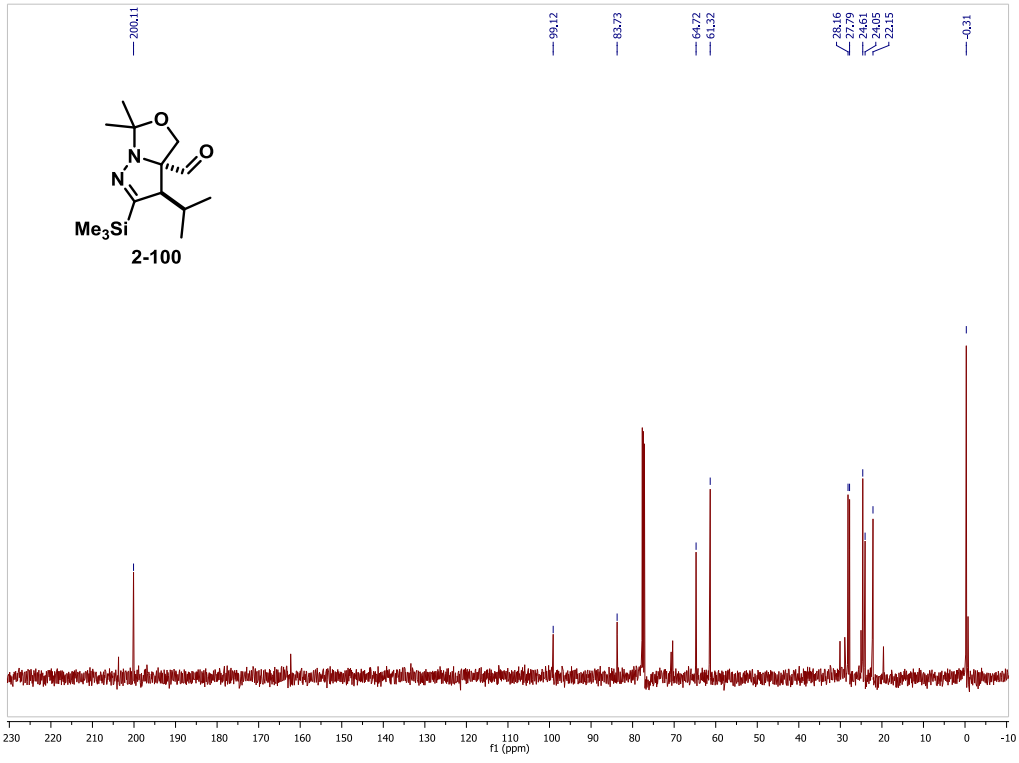
200.11
99.12
83.73
64.72
61.32
28.16
27.79
24.61
24.05
22.15
-0.31
Me3Si
2-100
f1 (ppm)

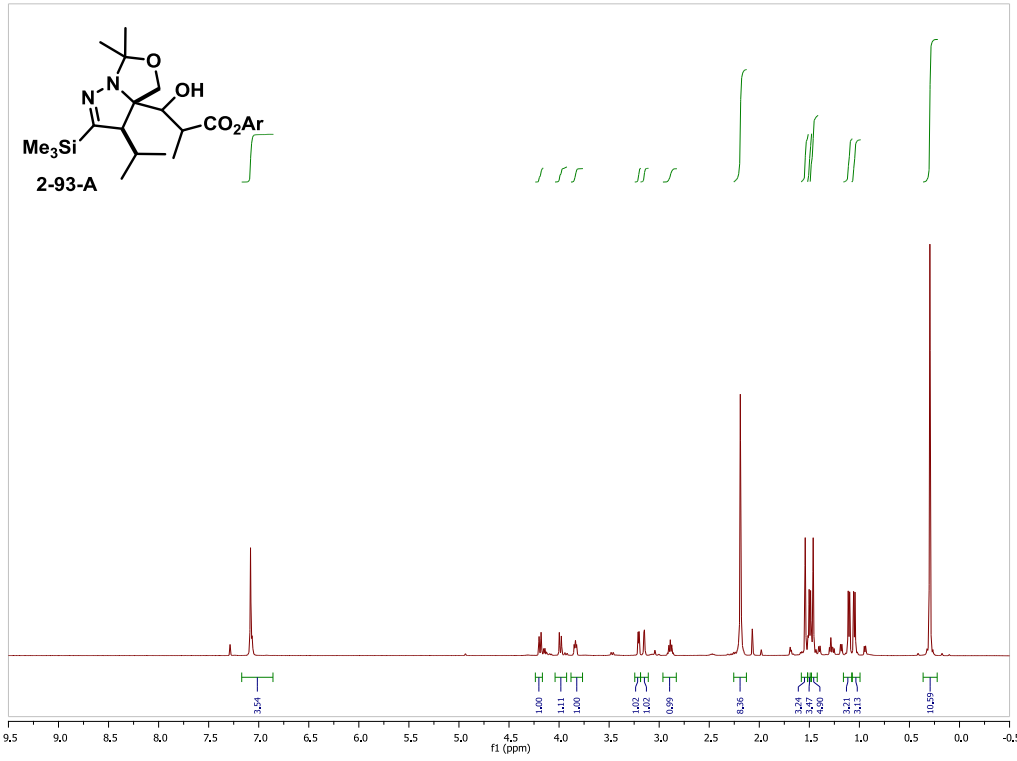
Me3Si
OH
CO2Ar
2-93-A
f1 (ppm)

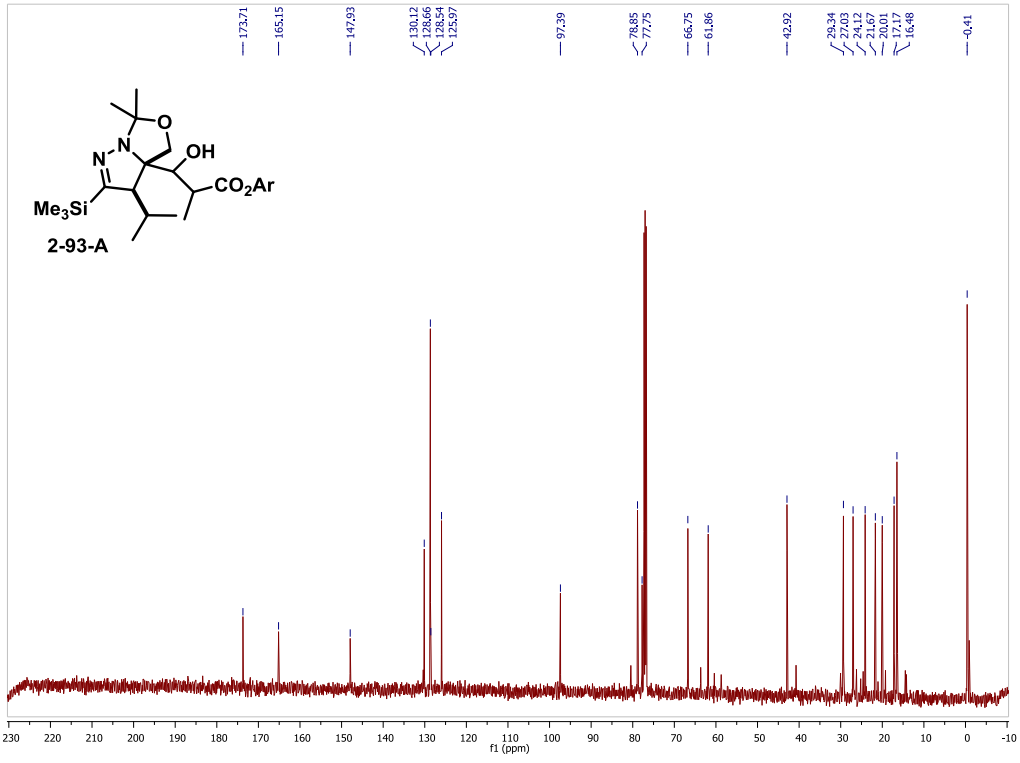
Me3Si
OH
CO2Ar
2-93-A
f1 (ppm)

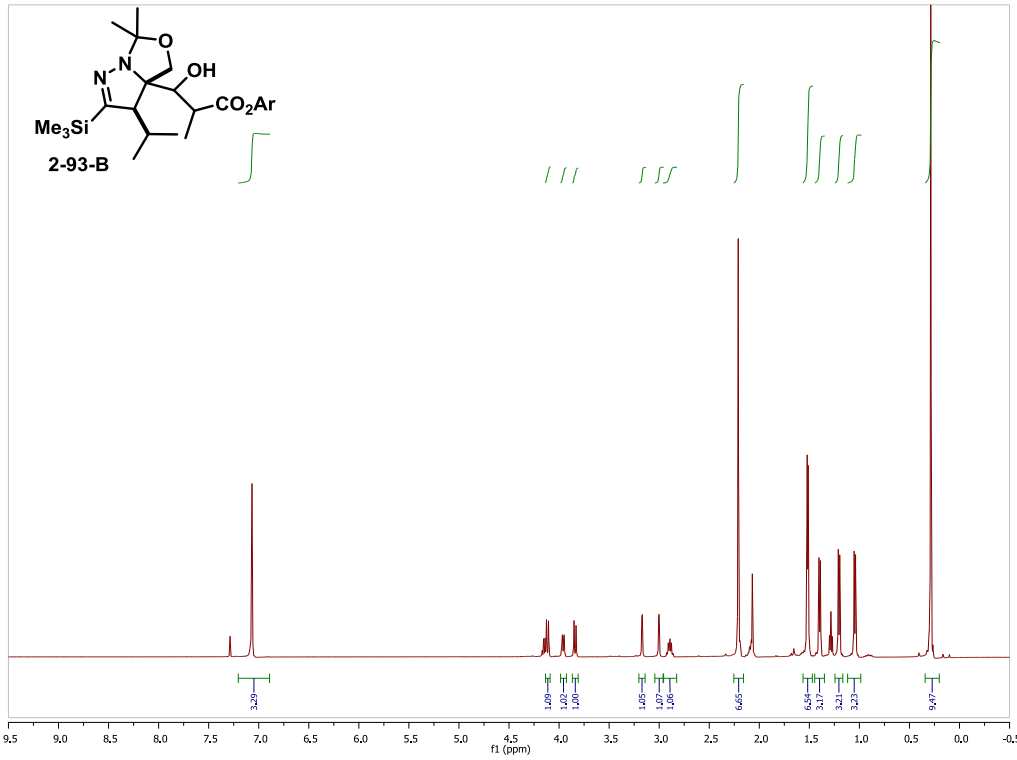
Me3Si
2-93-B
OH
CO2Ar
f1 (ppm)

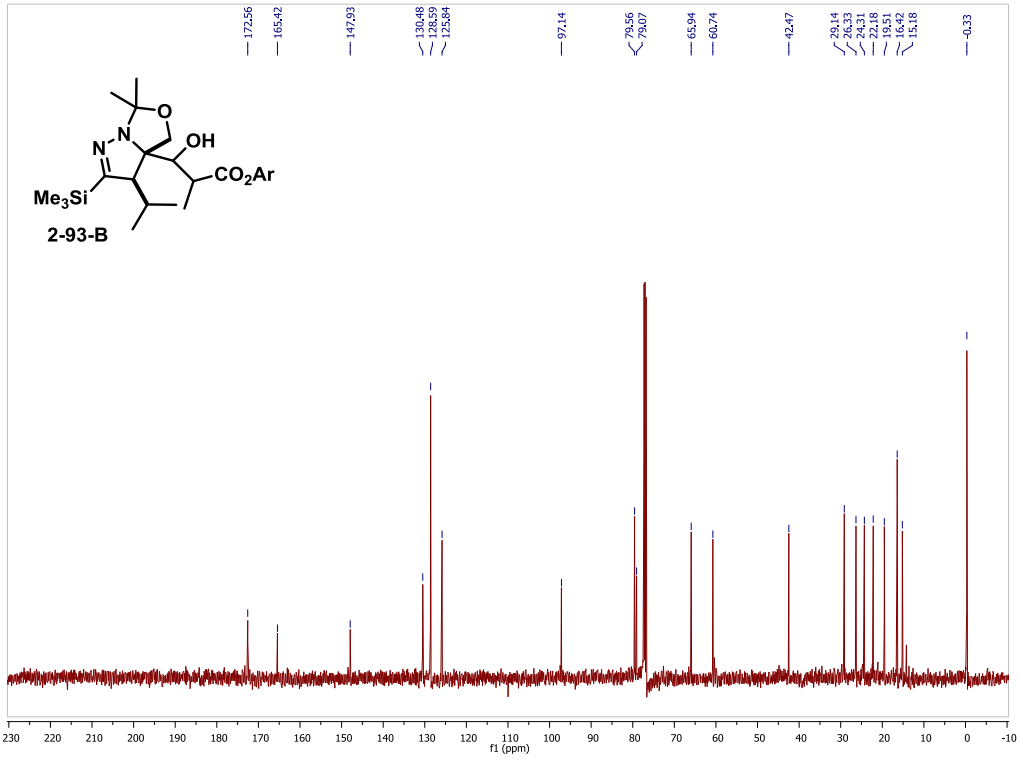
172.56
165.42
147.93
130.48
128.59
125.84
97.14
79.56
79.07
65.94
60.74
42.47
29.14
26.33
24.31
22.18
19.51
16.42
15.18
-0.33
Me3Si
2-93-B
OH
CO2Ar
f1 (ppm)

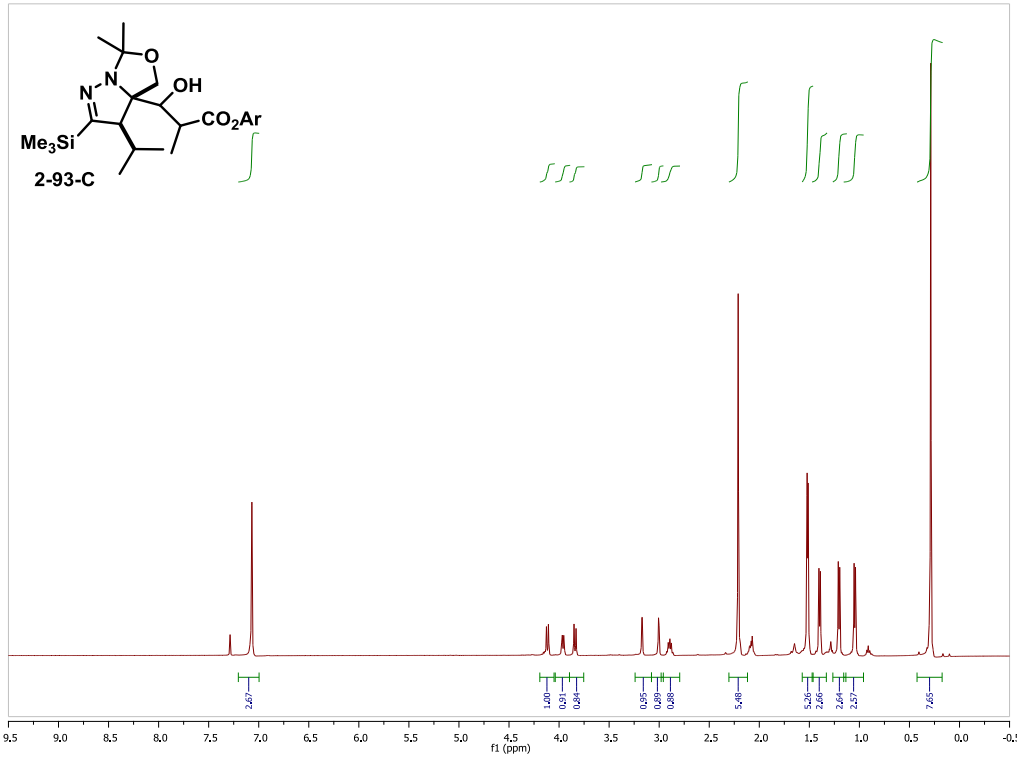
Me3Si
OH
CO2Ar
2-93-C
f1 (ppm)

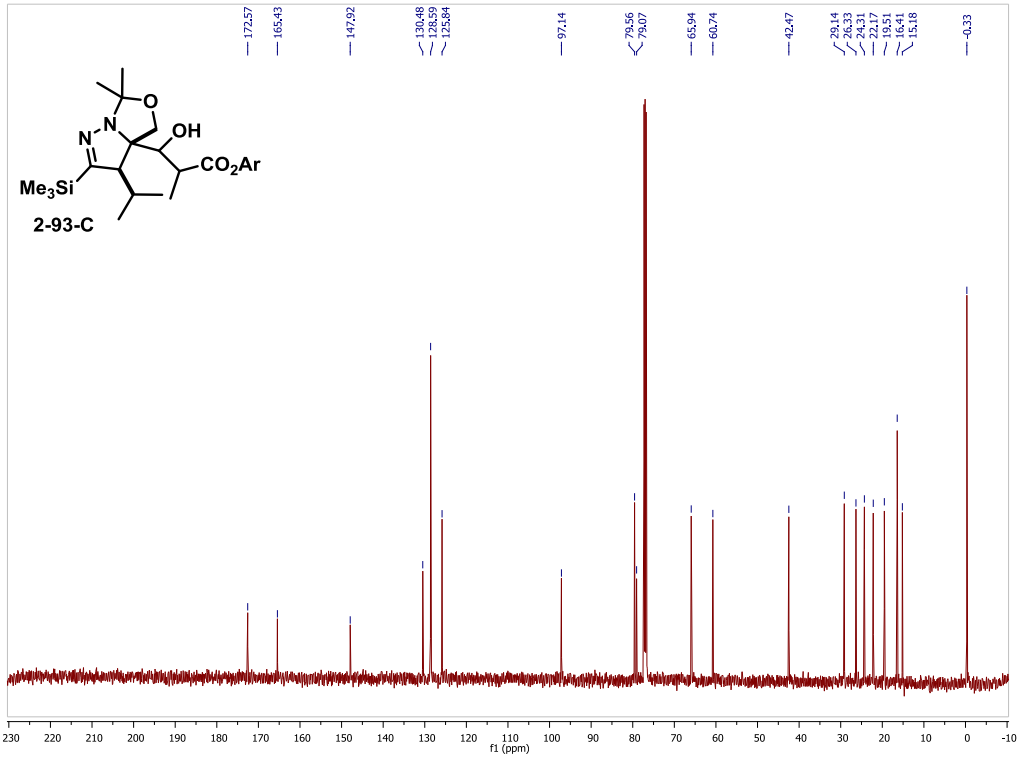
172.57
165.43
147.92
130.48
128.59
125.84
97.14
79.56
79.07
65.94
60.74
42.47
29.14
26.33
24.31
22.17
19.51
16.41
15.18
-0.33
Me3Si
OH
CO2Ar
2-93-C
f1 (ppm)

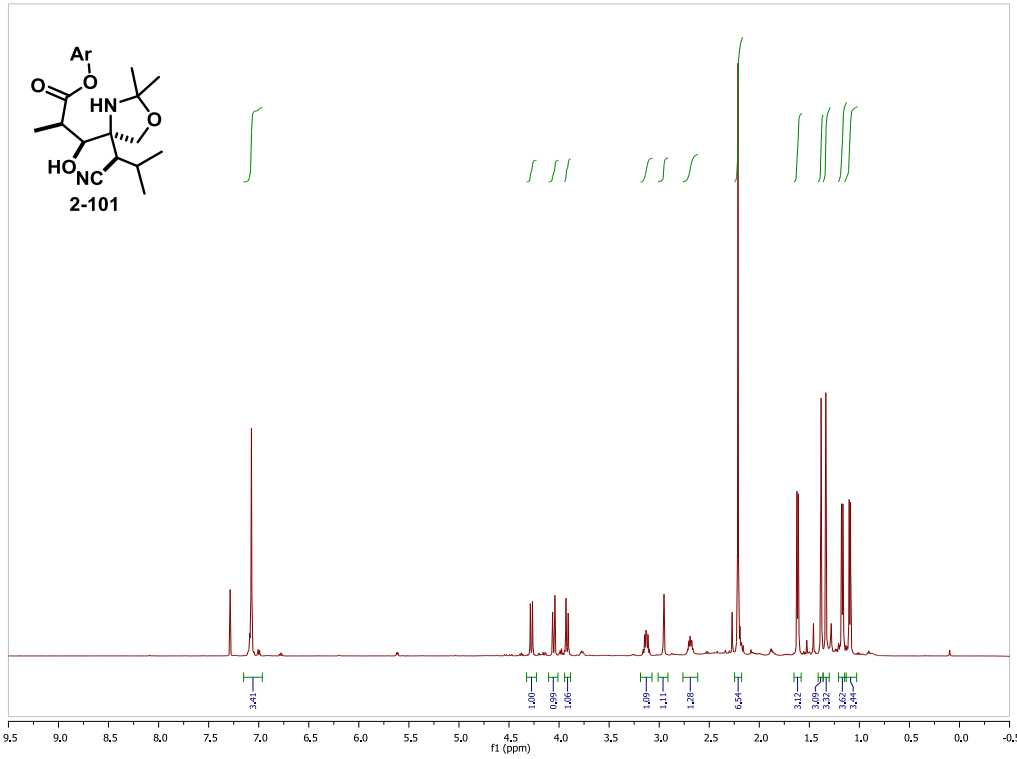
Ar
O
O
HN
O
HO
NC
2-101
3.41
1.00
0.99
1.06
1.09
1.11
1.28
6.54
3.12
3.09
3.12
3.04
3.04
f1 (ppm)

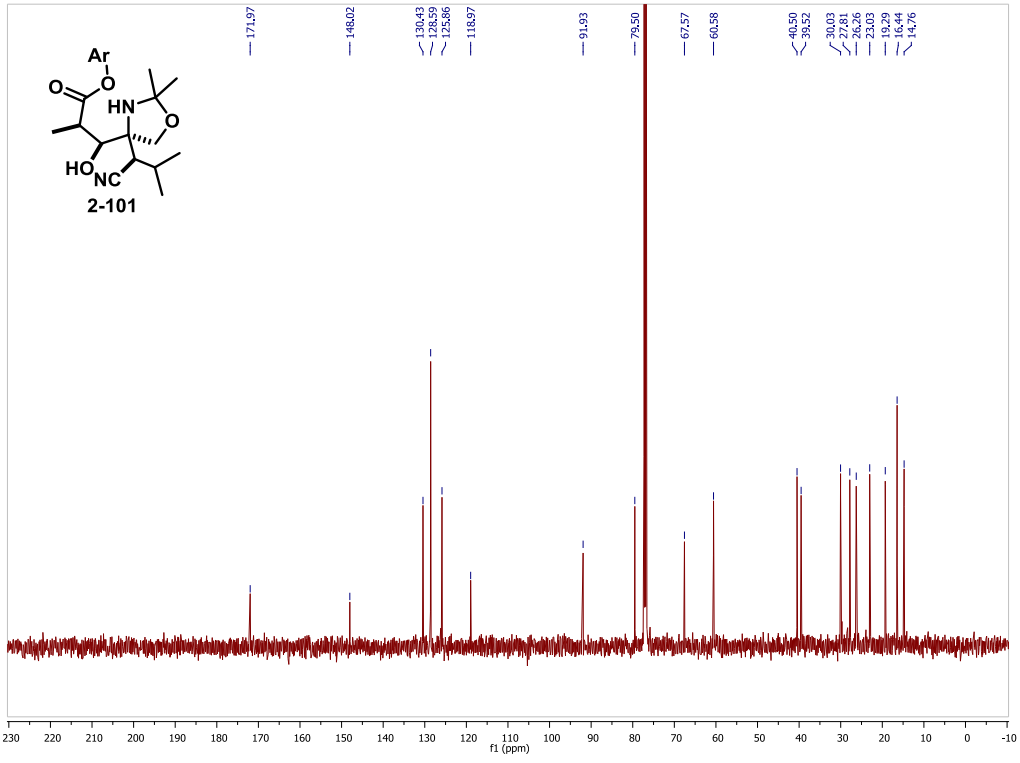
Ar
O
O
HN
O
HO
NC
2-101
171.97
148.02
130.43
128.59
125.86
118.97
91.93
79.50
67.57
60.58
40.50
39.52
30.03
27.81
26.26
23.03
19.29
16.44
14.76
f1 (ppm)

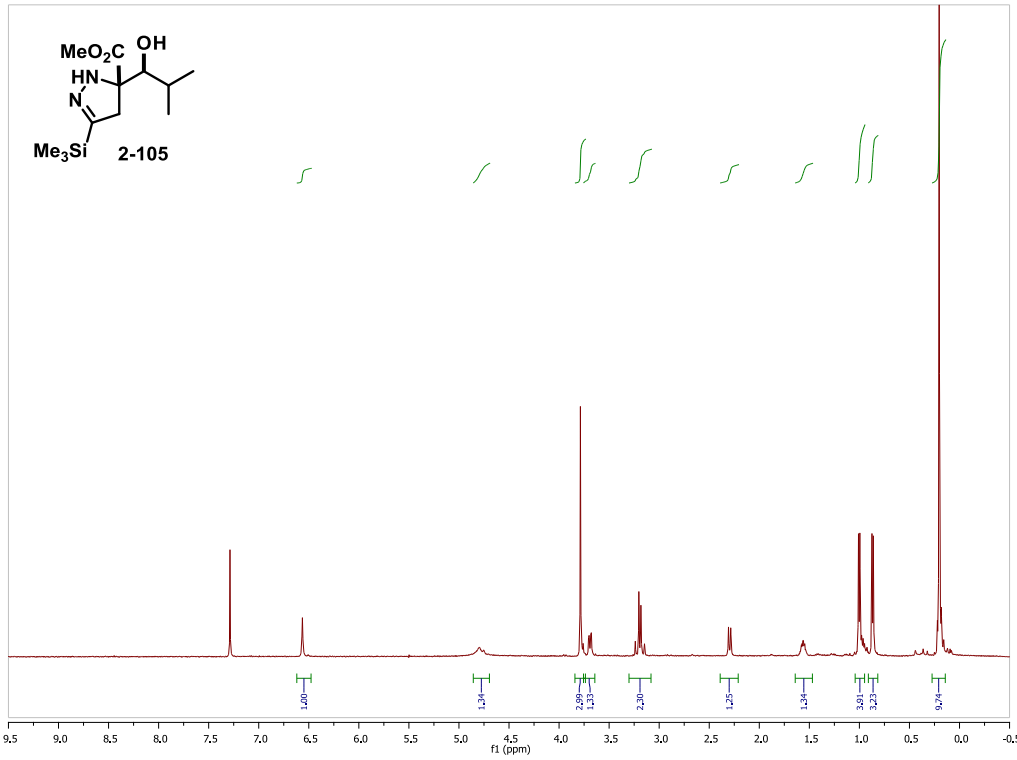
MeO2C
OH
HN
N
Me3Si
2-105
f1 (ppm)

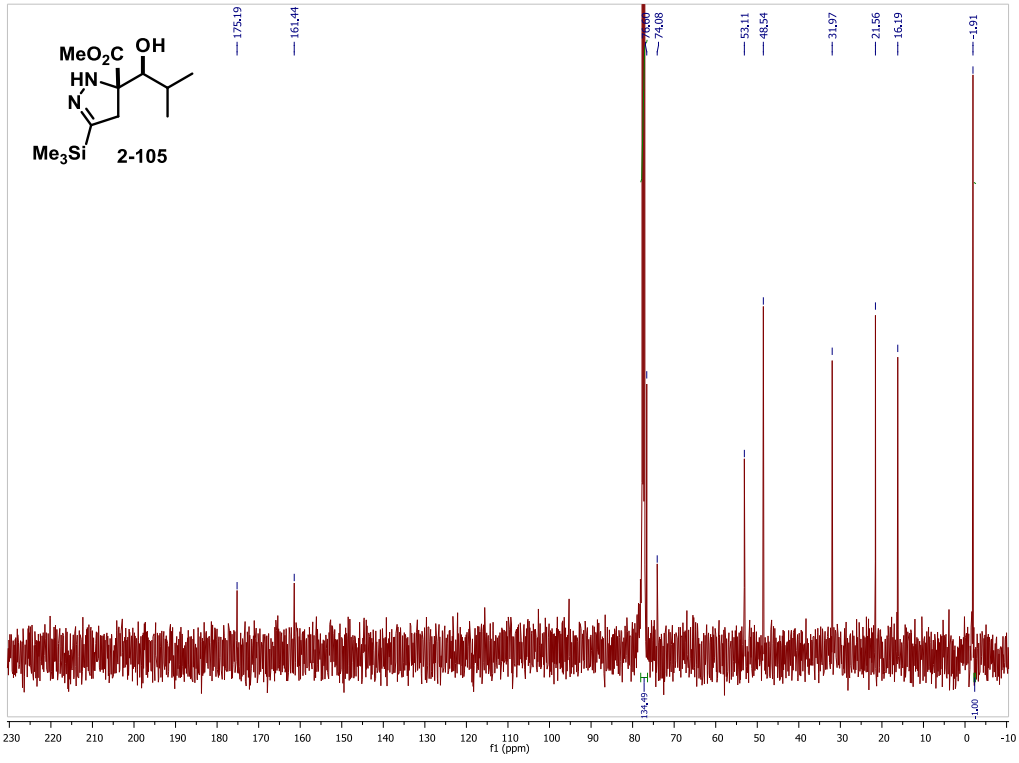
MeO2C
OH
HN
N
Me3Si
2-105
175.19
161.44
78.00
74.08
53.11
48.54
31.97
21.56
16.19
-1.91
f1 (ppm)

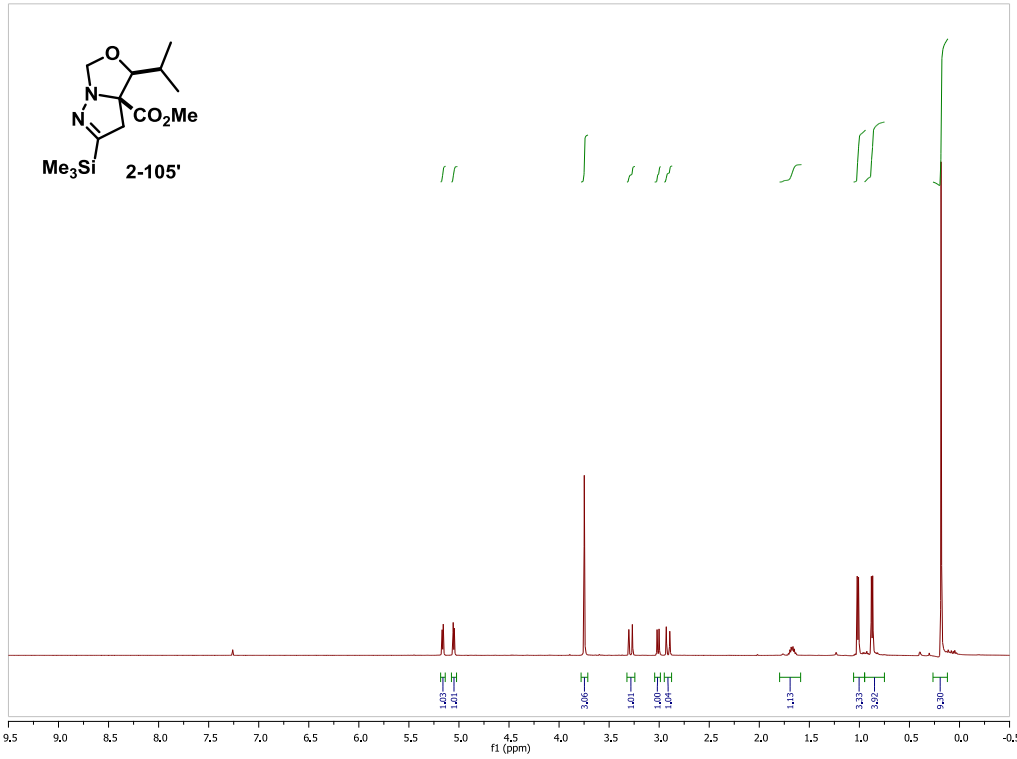
O
N
N
CO2Me
Me3Si
2-105'
1.03
1.01
3.06
1.01
1.00
1.04
1.13
3.13
3.02
9.20
f1 (ppm)

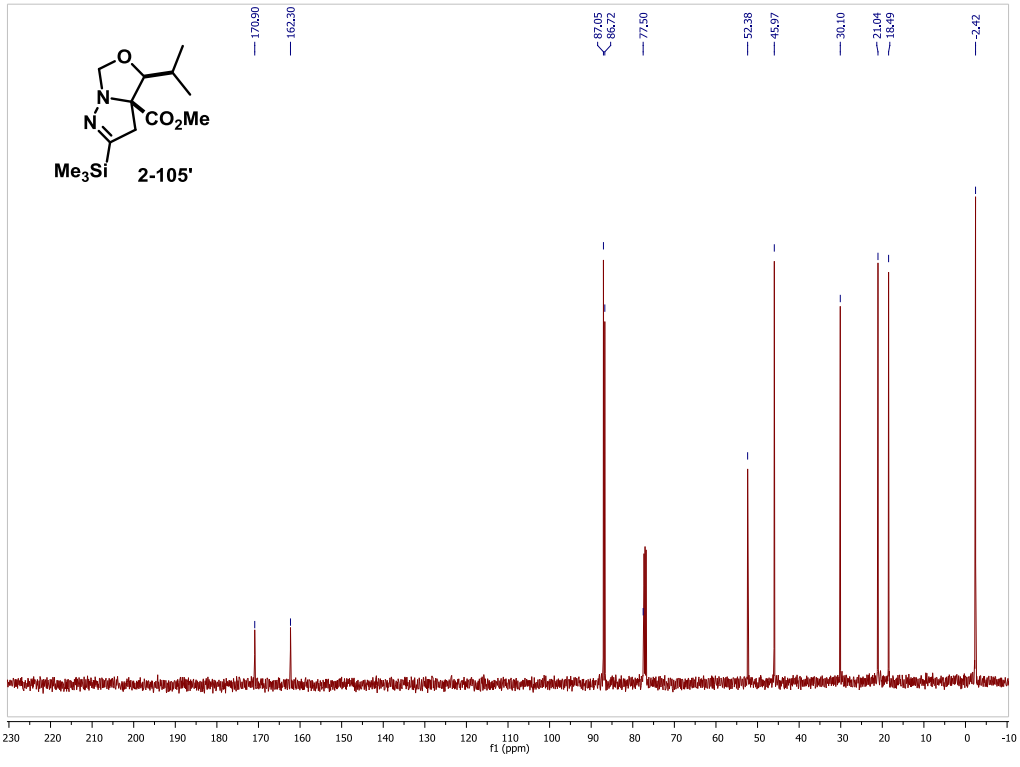
170.90
162.30
87.05
86.72
77.50
52.38
45.97
30.10
21.04
18.49
-2.42
O
N
N
CO2Me
Me3Si
2-105'
f1 (ppm)

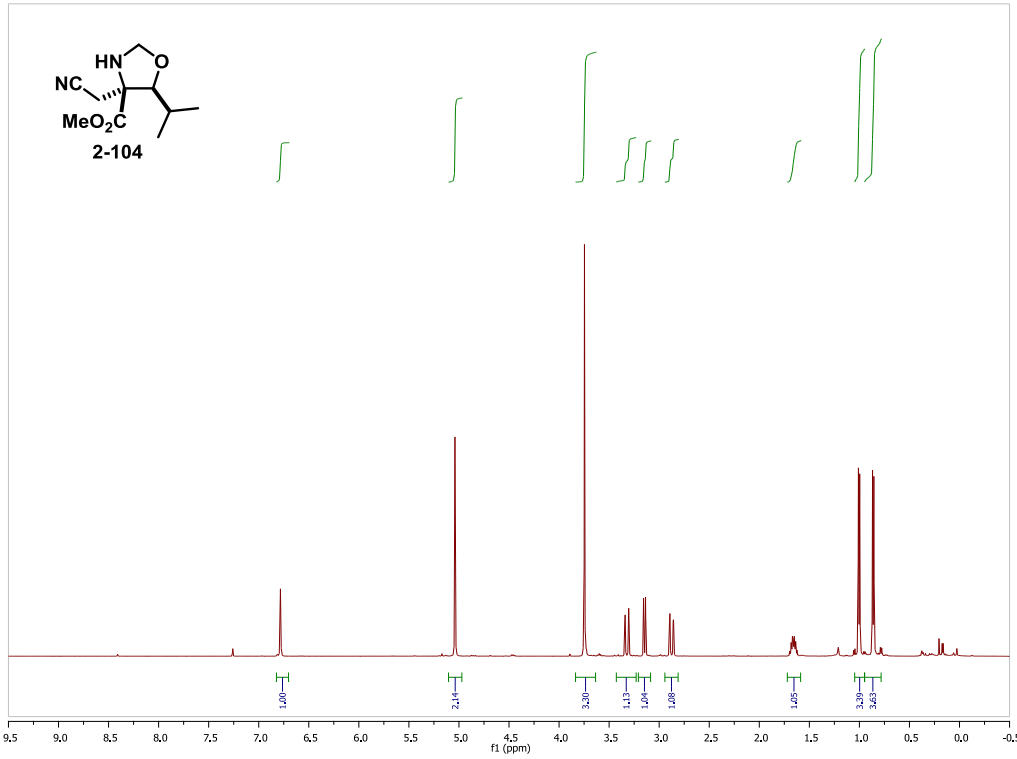
HN
O
NC
MeO2C
2-104
1.00
2.14
3.20
1.13
1.04
1.08
1.05
3.29
3.63
f1 (ppm)

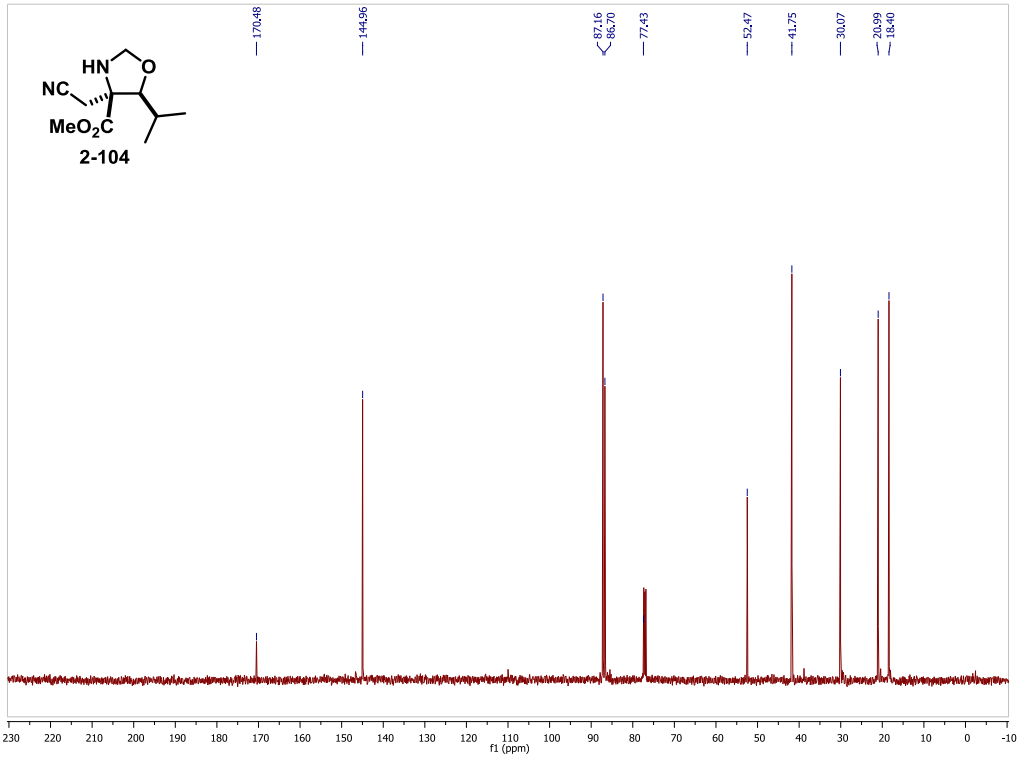
170.48
144.96
87.16
86.70
77.43
52.47
41.75
30.07
20.99
18.40
HN
O
NC
MeO2C
2-104
f1 (ppm)

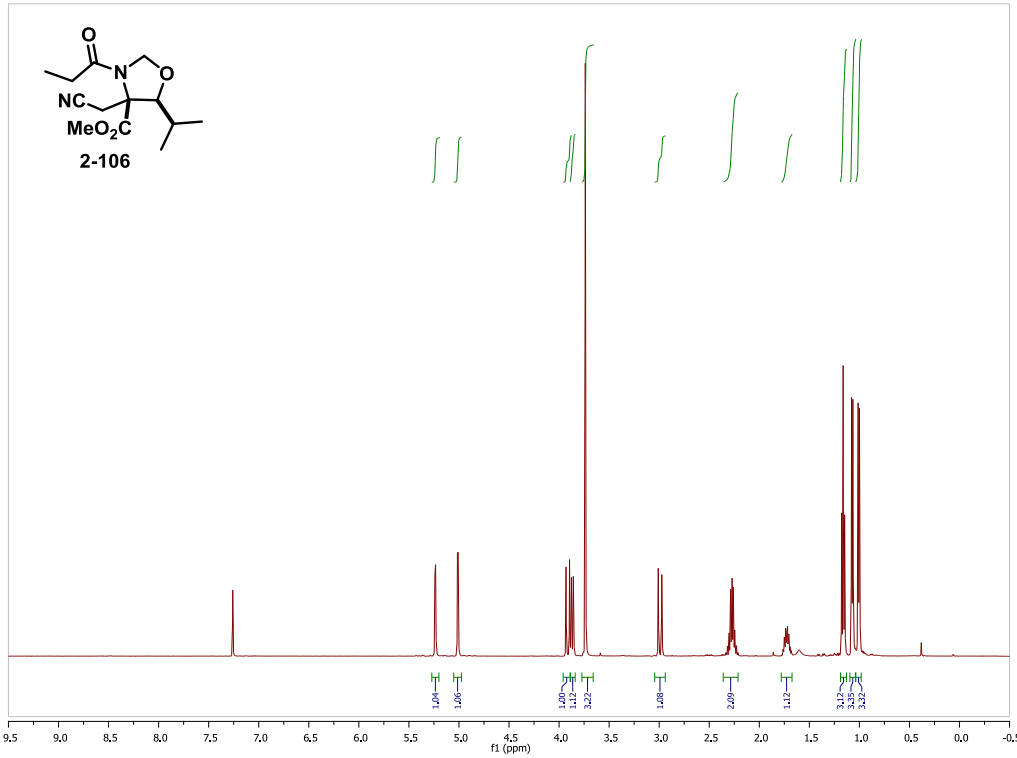
O
N
O
NC
MeO2C
2-106
1.04
1.06
1.00
1.12
3.22
1.08
2.09
1.12
3.13
3.25
3.32
9.5 9.0 8.5 8.0 7.5 7.0 6.5 6.0 5.5 5.0 4.5 4.0 3.5 3.0 2.5 2.0 1.5 1.0 0.5 0.0 -0.5
f1 (ppm)

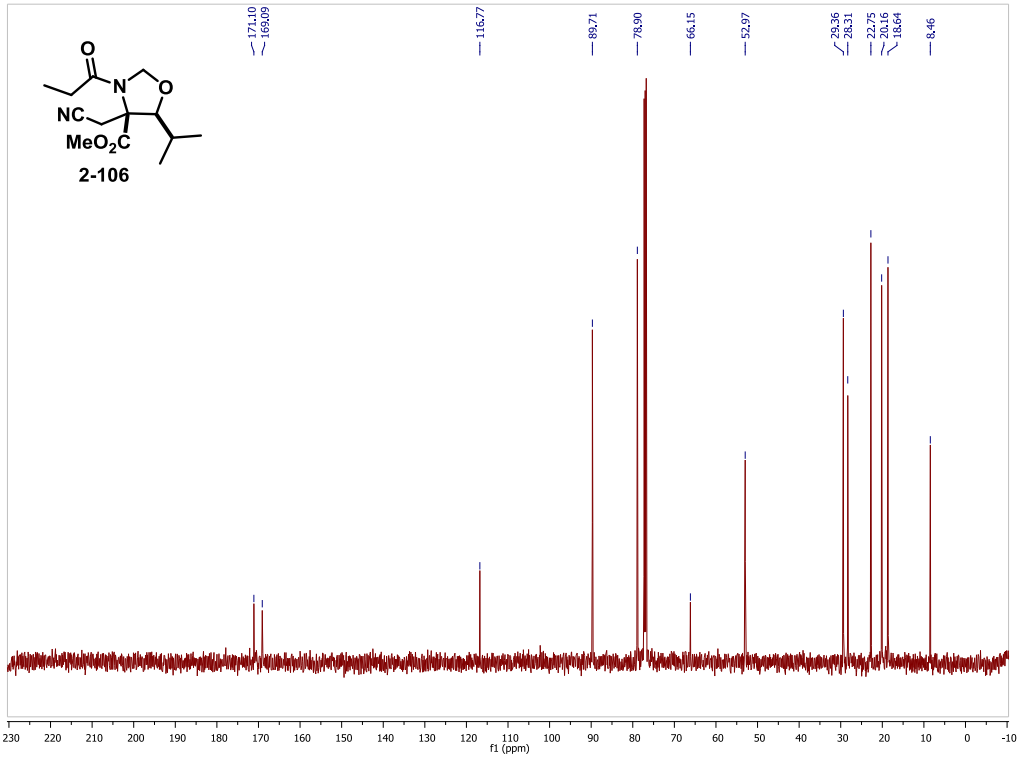
O
N
O
NC
MeO2C
2-106
171.10
169.09
116.77
89.71
78.90
66.15
52.97
29.36
28.31
22.75
20.16
18.64
8.46
230 220 210 200 190 180 170 160 150 140 130 120 110 100 90 80 70 60 50 40 30 20 10 0 -10
f1 (ppm)

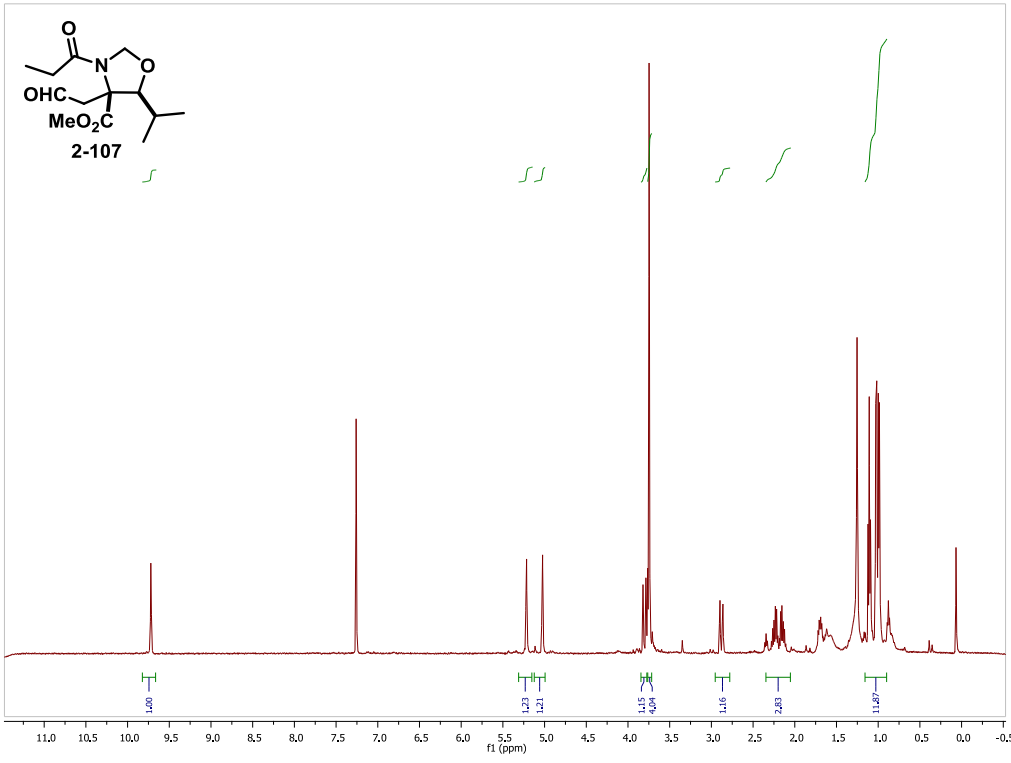
O
N
O
OHC
MeO2C
2-107
1.00
1.23
1.21
1.15
4.04
1.16
2.83
11.87
11.0 10.5 10.0 9.5 9.0 8.5 8.0 7.5 7.0 6.5 6.0 5.5 5.0 4.5 4.0 3.5 3.0 2.5 2.0 1.5 1.0 0.5 0.0 -0.5
f1 (ppm)

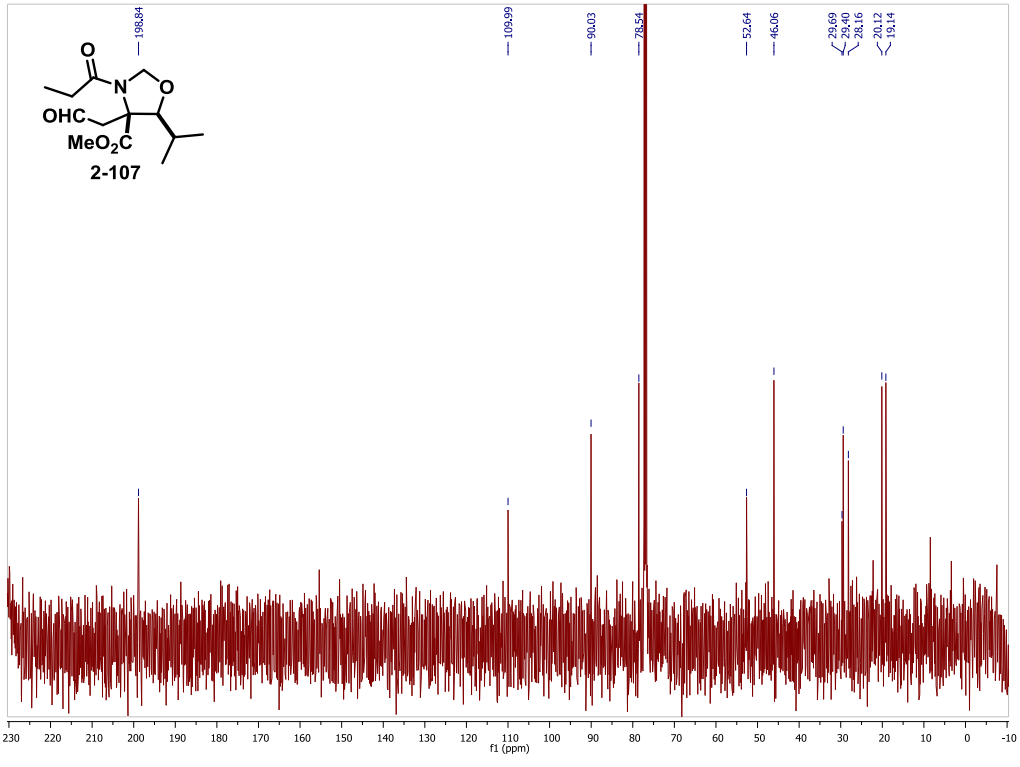
198.84
109.99
90.03
78.54
52.64
46.06
29.69
29.40
28.16
20.12
19.14
O
N
O
OHC
MeO2C
2-107
230 220 210 200 190 180 170 160 150 140 130 120 110 100 90 80 70 60 50 40 30 20 10 0 -10
f1 (ppm)

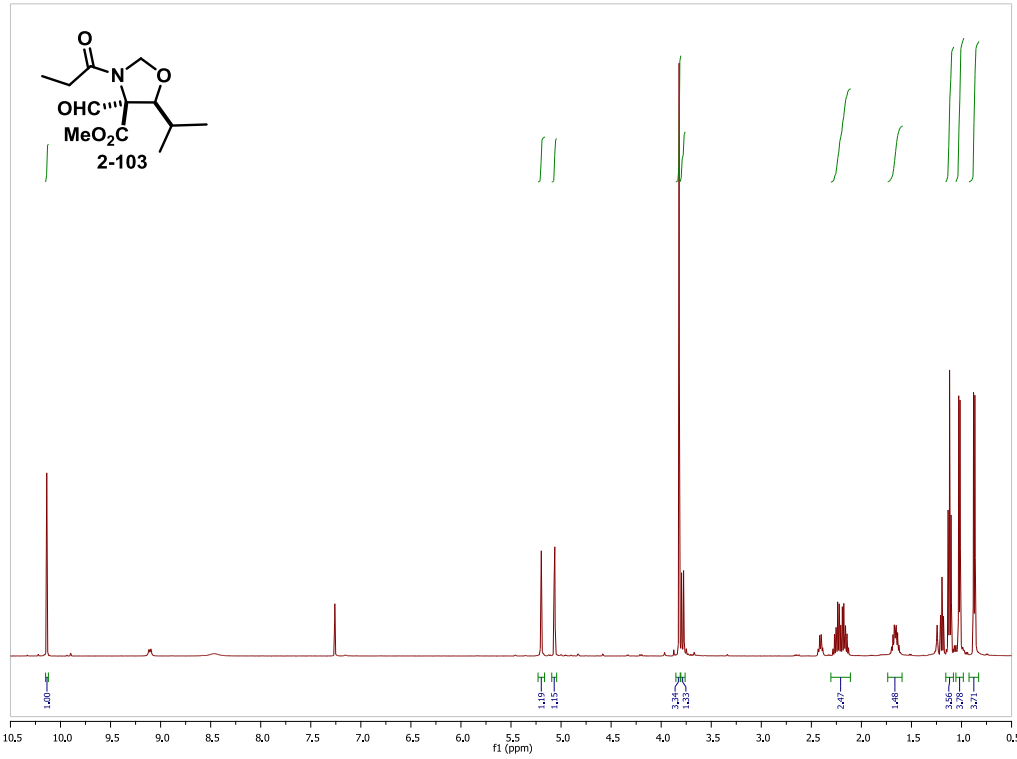
O
N
O
OHC
MeO2C
2-103
1.00
1.19
1.15
3.34
1.33
2.47
1.48
3.56
3.78
3.71
10.5 10.0 9.5 9.0 8.5 8.0 7.5 7.0 6.5 6.0 5.5 5.0 4.5 4.0 3.5 3.0 2.5 2.0 1.5 1.0 0.5
f1 (ppm)

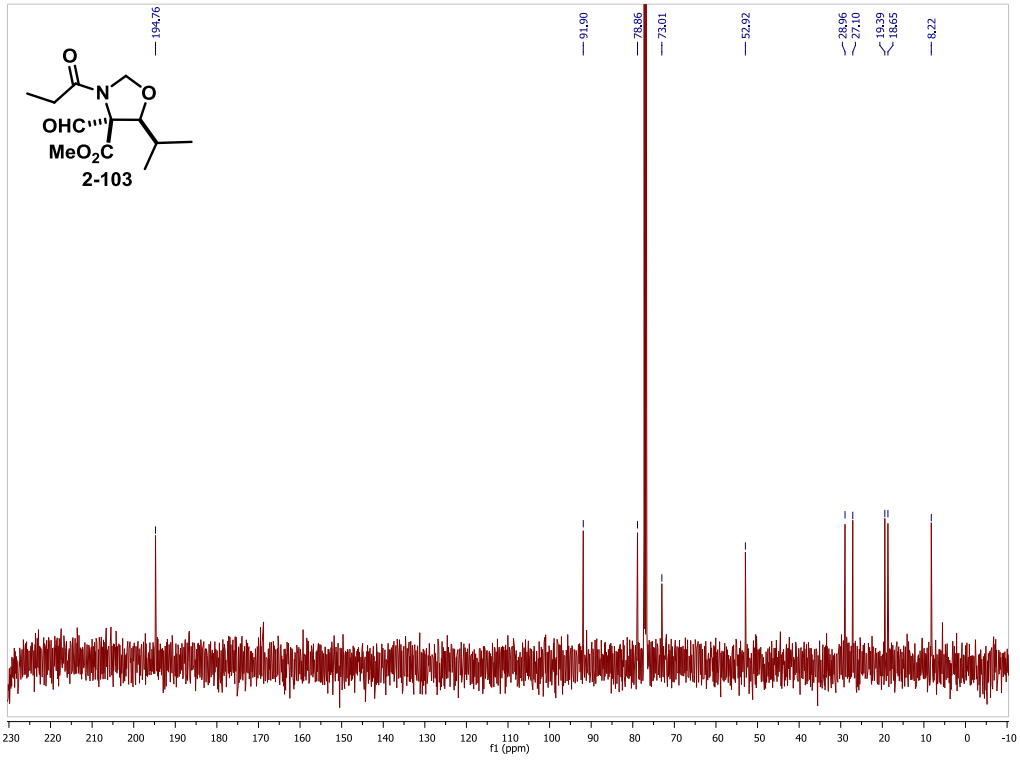
O
N
O
OHC
MeO2C
2-103
194.76
91.90
78.86
73.01
52.92
28.96
27.10
19.39
18.65
8.22
230 220 210 200 190 180 170 160 150 140 130 120 110 100 90 80 70 60 50 40 30 20 10 0 -10
f1 (ppm)

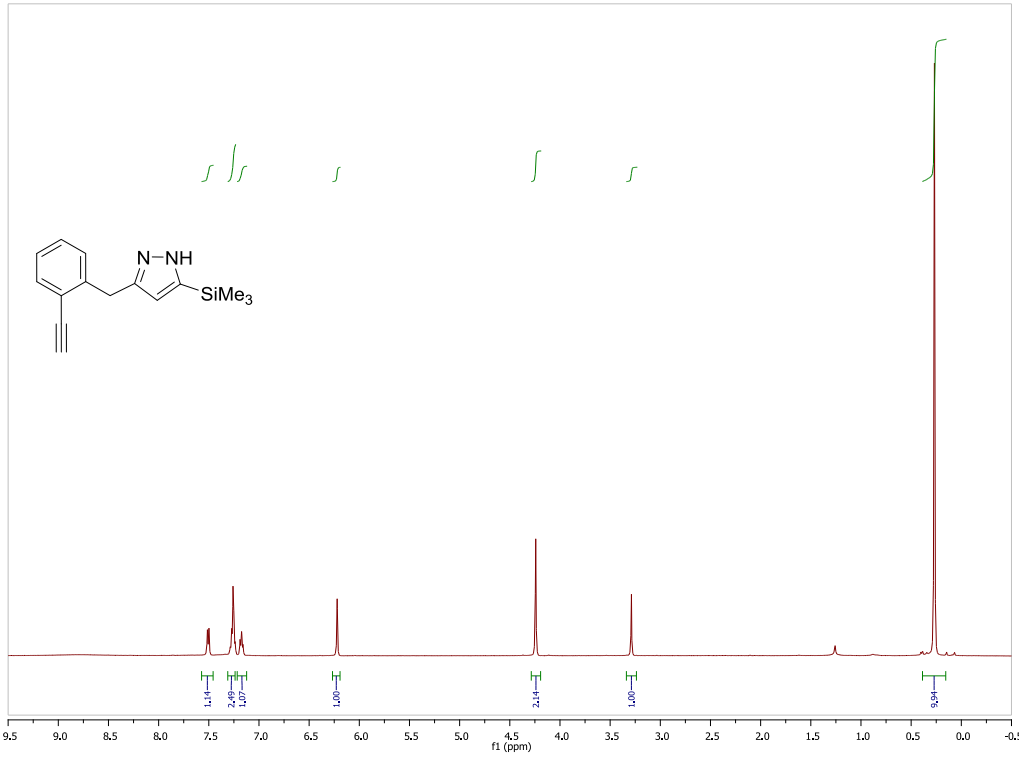
N–NH
SiMe3
1.14
2.49
1.07
1.00
2.14
1.00
9.94
f1 (ppm)

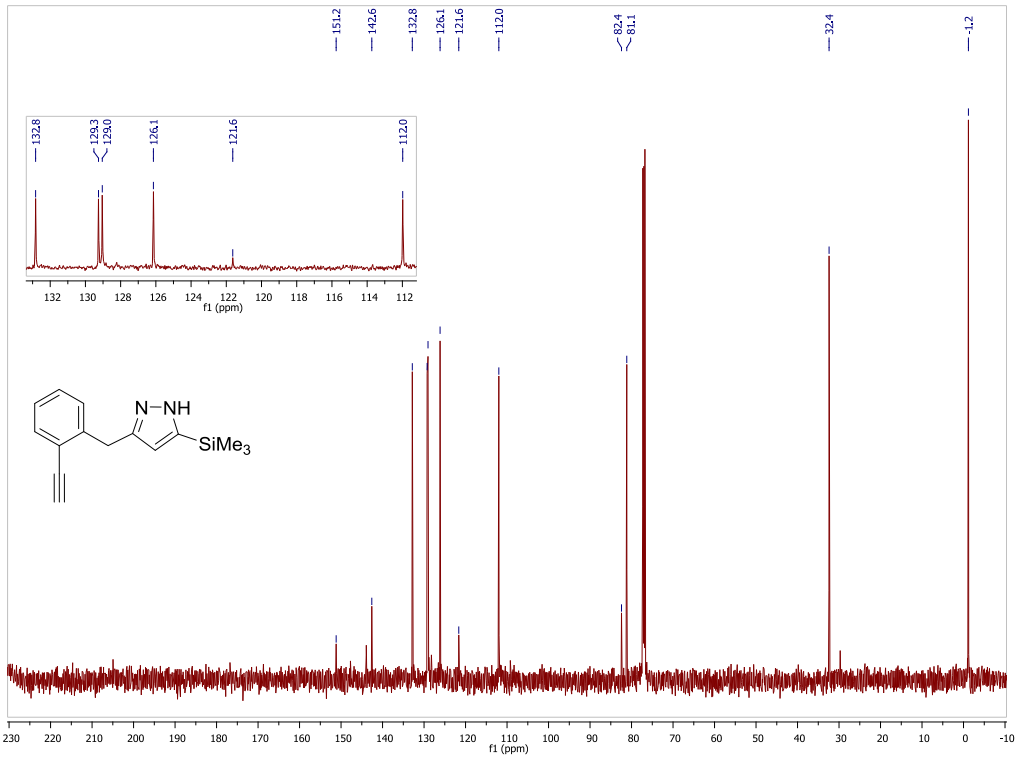
151.2
142.6
132.8
126.1
121.6
112.0
82.4
81.1
32.4
-1.2
132.8
129.3
129.0
126.1
121.6
112.0
f1 (ppm)
N–NH
SiMe3
f1 (ppm)

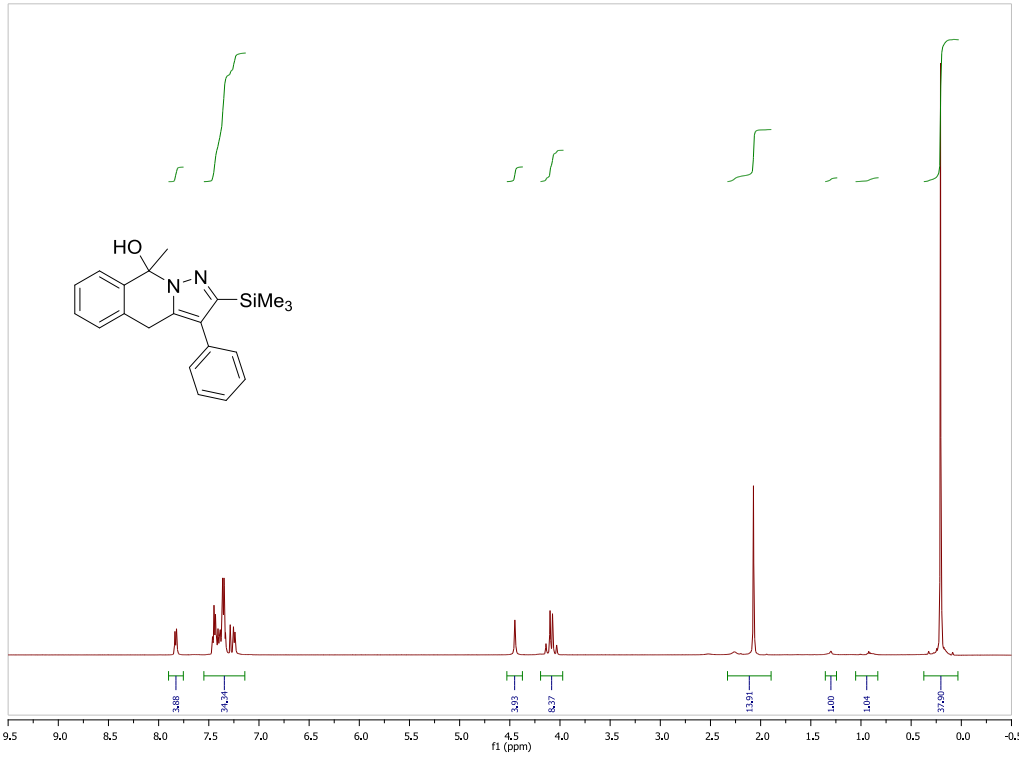
HO
N
N
SiMe3
5.88
34.34
3.93
6.37
13.91
1.00
1.04
37.60
f1 (ppm)

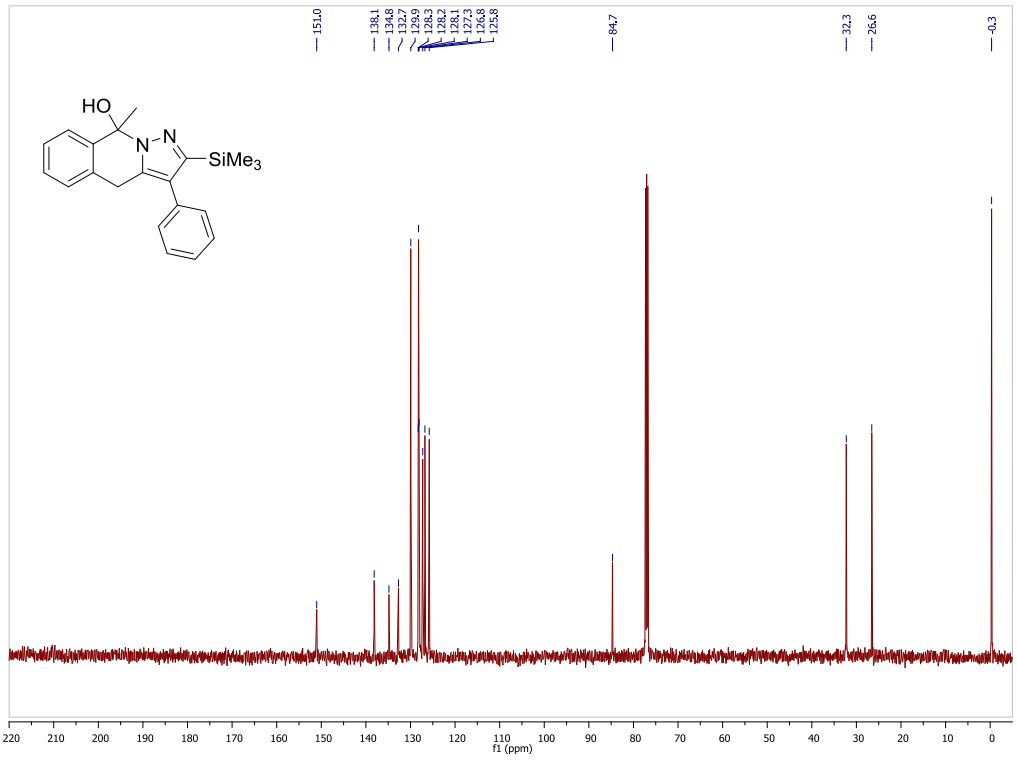
151.0
138.1
134.8
132.7
129.9
128.3
128.2
128.1
127.3
126.8
125.8
84.7
32.3
26.6
0.3
HO
N
N
SiMe3
f1 (ppm)

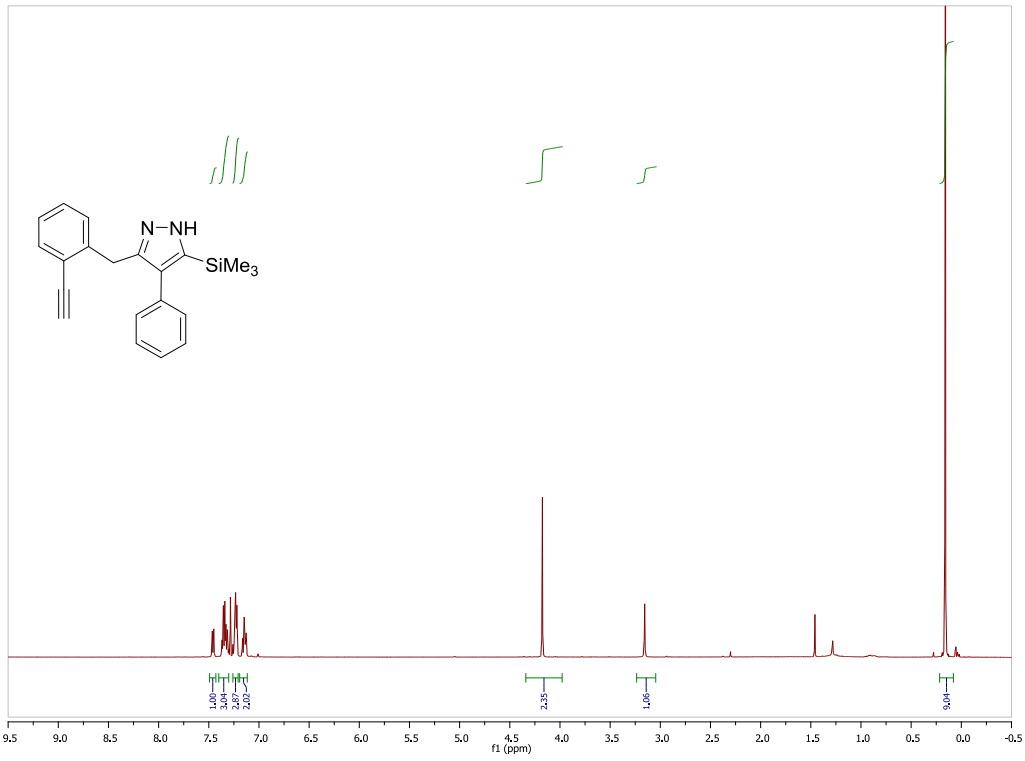
N–NH
SiMe3
1.00
3.04
2.87
2.02
2.35
1.06
9.04
f1 (ppm)

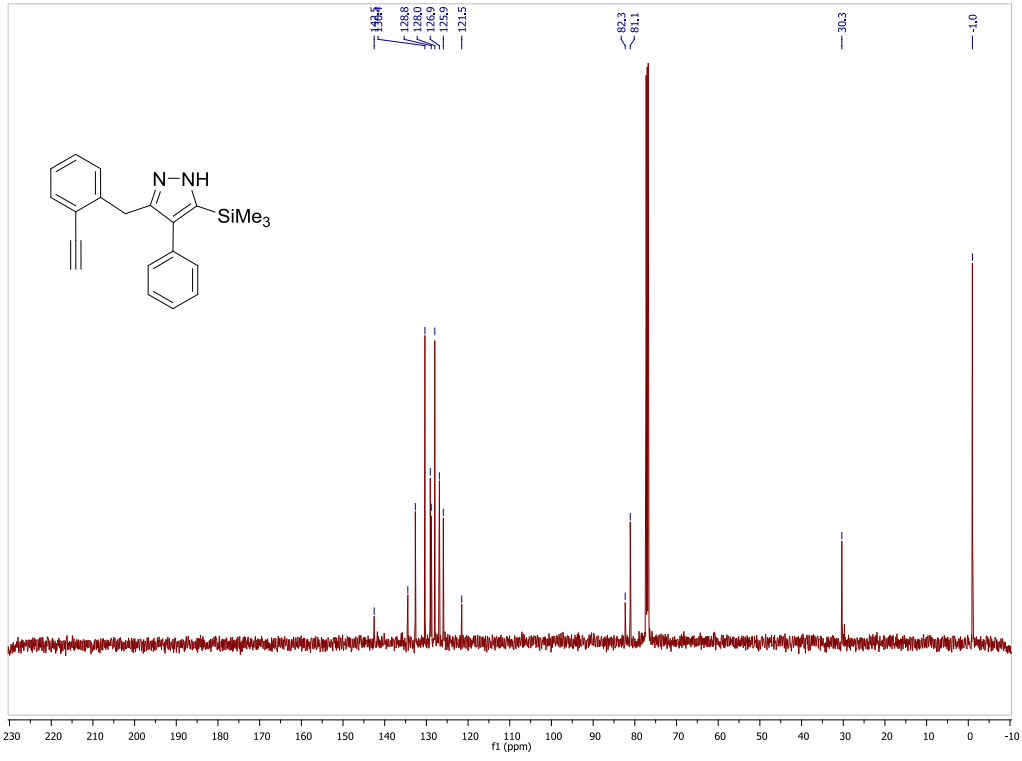
N–NH
SiMe3
128.8
128.0
126.9
125.9
121.5
82.3
81.1
30.3
-1.0
f1 (ppm)

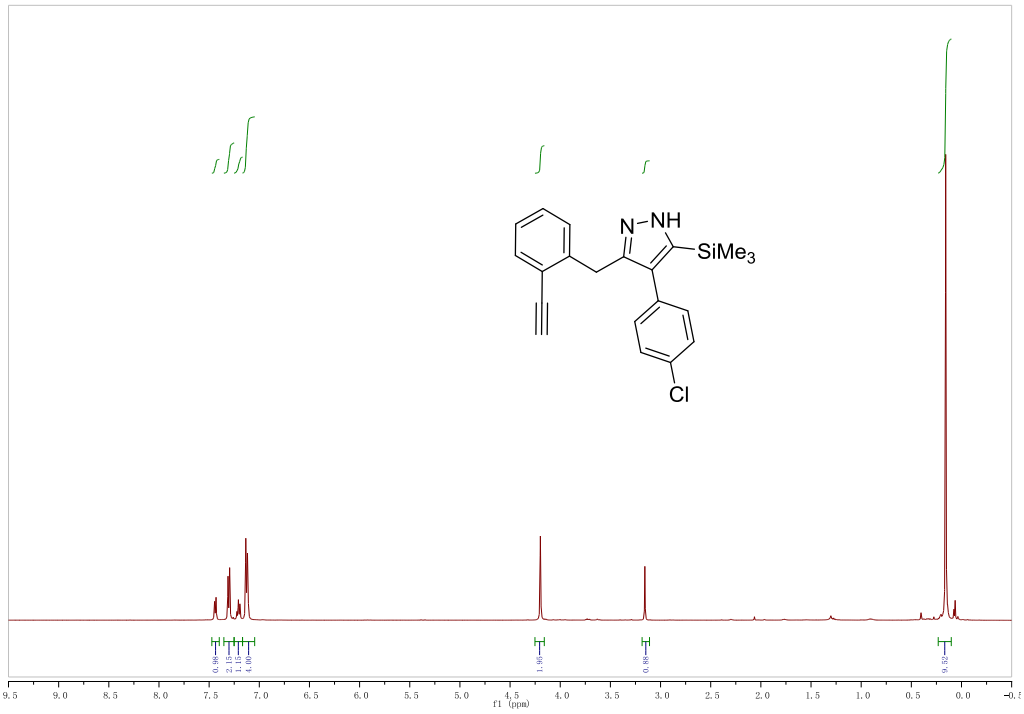
N–NH
SiMe3
Cl
f1 (ppm)

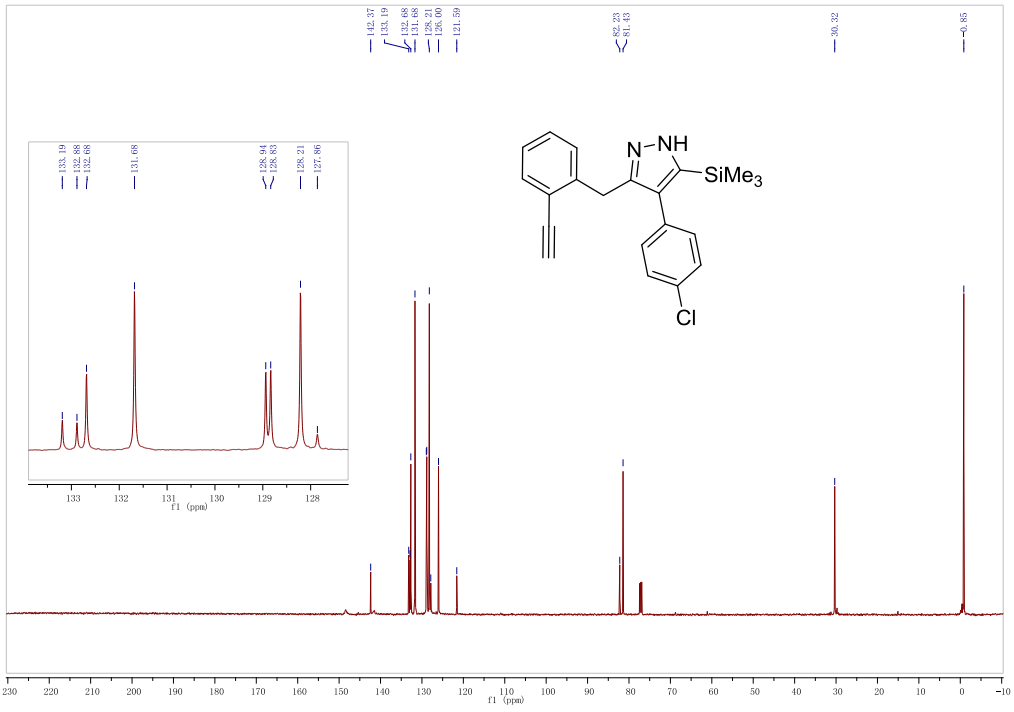
142.37
133.19
132.68
131.68
128.71
126.00
121.59
82.23
81.43
30.32
0.85
N–NH
SiMe3
Cl
f1 (ppm)

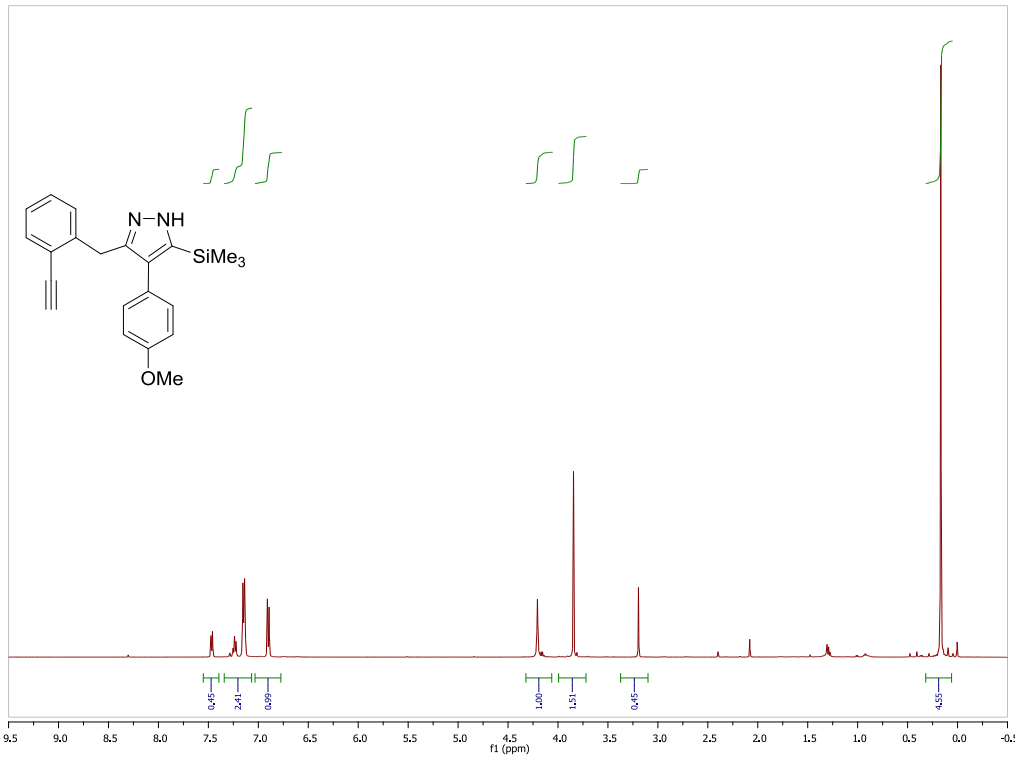
N–NH
SiMe3
OMe
0.45
2.41
0.99
1.00
1.51
0.45
4.55
9.5 9.0 8.5 8.0 7.5 7.0 6.5 6.0 5.5 5.0 4.5 4.0 3.5 3.0 2.5 2.0 1.5 1.0 0.5 0.0 -0.5
f1 (ppm)

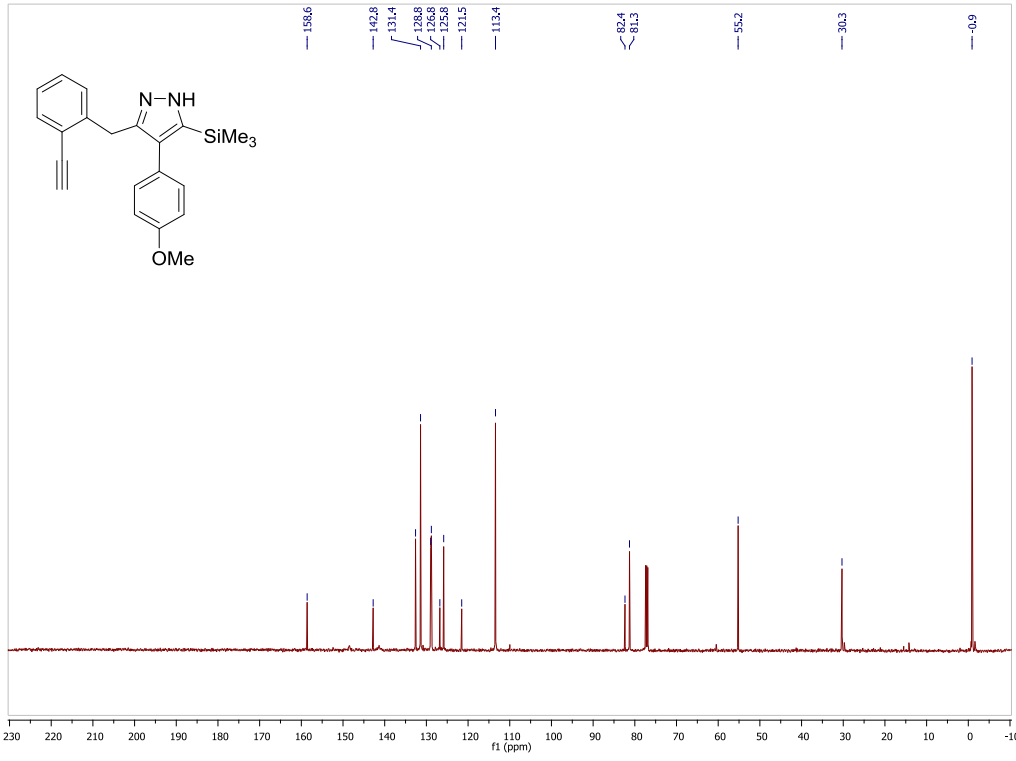
158.6
142.8
131.4
128.8
126.8
125.8
121.5
113.4
82.4
81.3
55.2
30.3
-0.9
N–NH
SiMe3
OMe
230 220 210 200 190 180 170 160 150 140 130 120 110 100 90 80 70 60 50 40 30 20 10 0 -10
f1 (ppm)

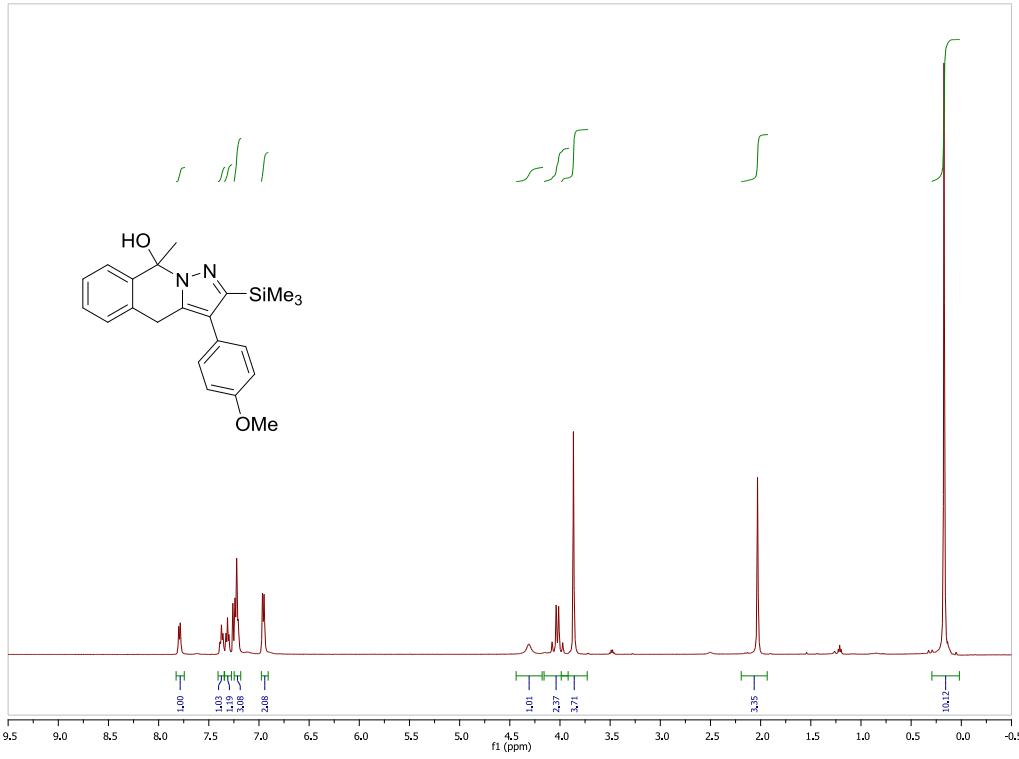
HO
N
N
SiMe3
OMe
1.00
1.03
1.19
3.08
2.08
1.01
2.37
3.71
3.35
10.12
f1 (ppm)

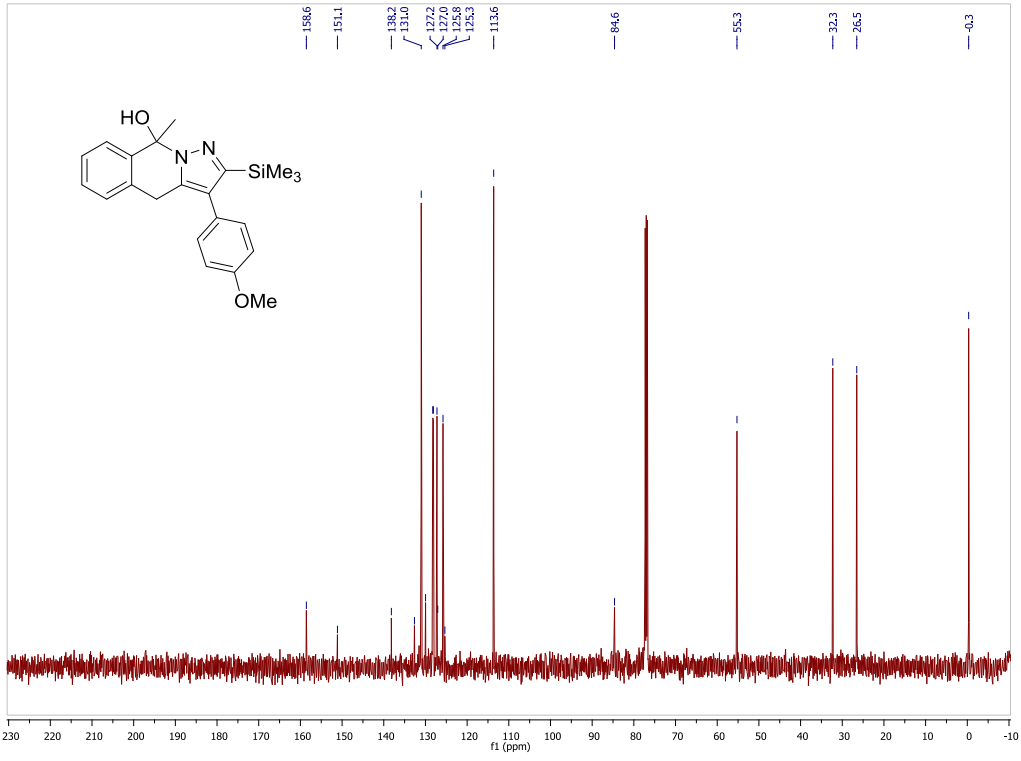
158.6
151.1
138.2
131.0
127.2
127.0
125.8
125.3
113.6
84.6
55.3
32.3
26.5
-0.3
HO
N
N
SiMe3
OMe
f1 (ppm)

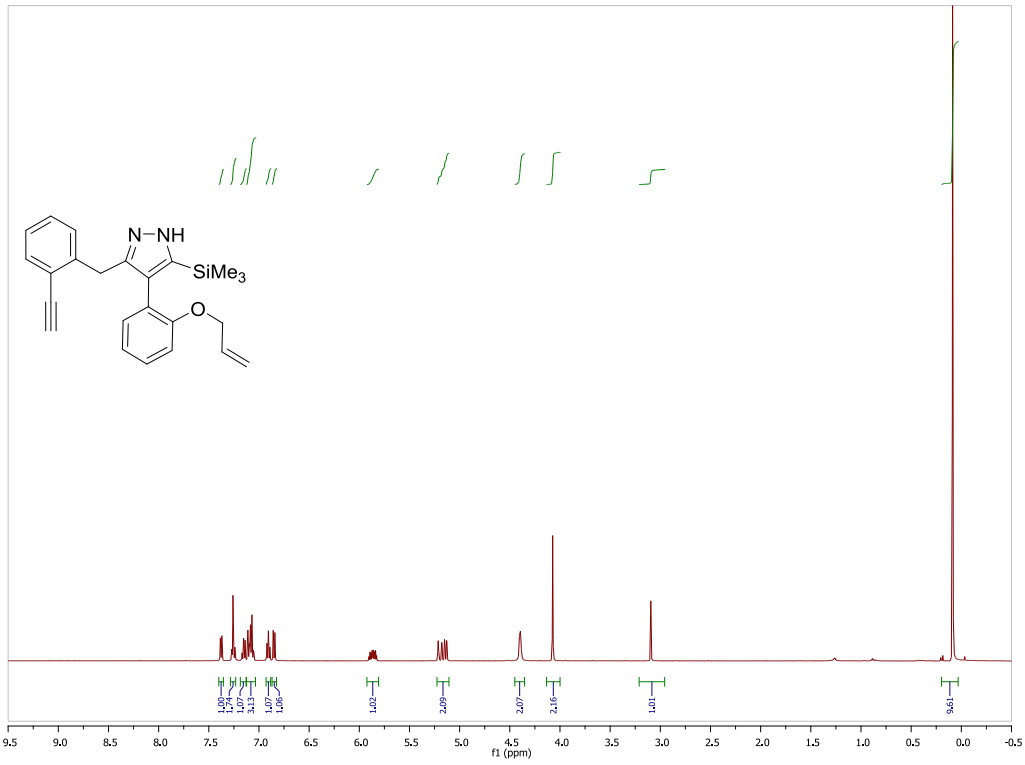
N–NH
SiMe3
O
1.00
1.74
1.03
3.13
1.07
1.06
1.02
2.09
2.07
2.16
1.01
9.61
f1 (ppm)

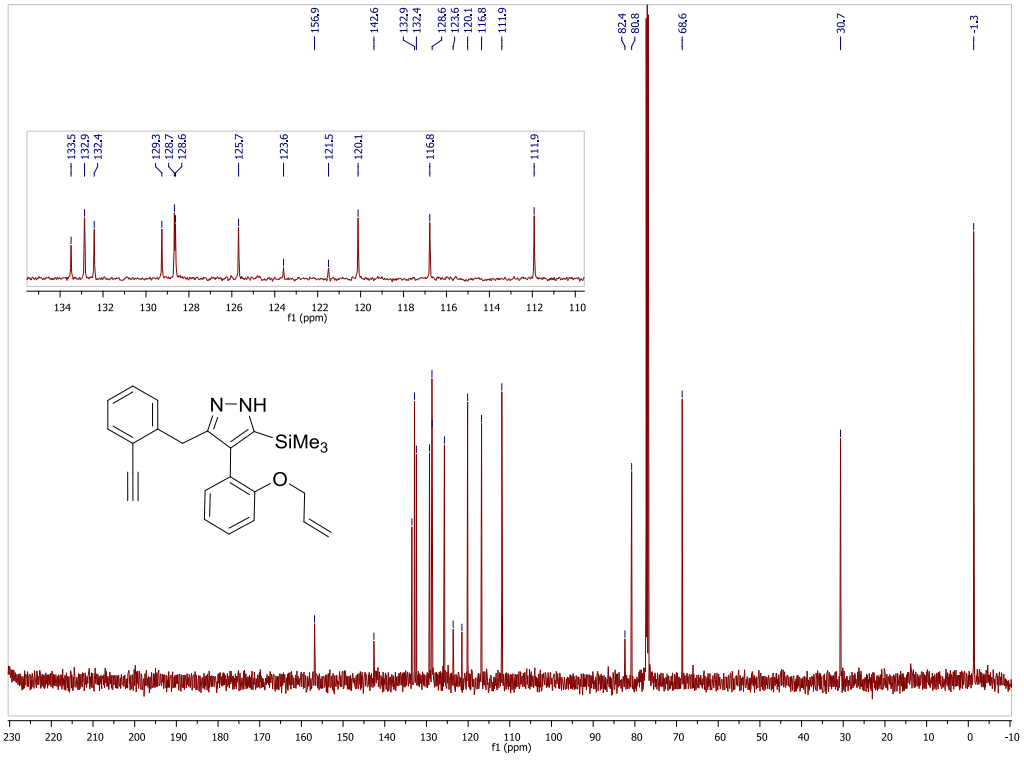
156.9
142.6
132.9
132.4
128.6
123.6
120.1
116.8
111.9
82.4
80.8
68.6
30.7
-1.3
133.5
132.9
132.4
129.3
128.7
128.6
125.7
123.6
121.5
120.1
116.8
111.9
f1 (ppm)
N–NH
SiMe3
O
f1 (ppm)

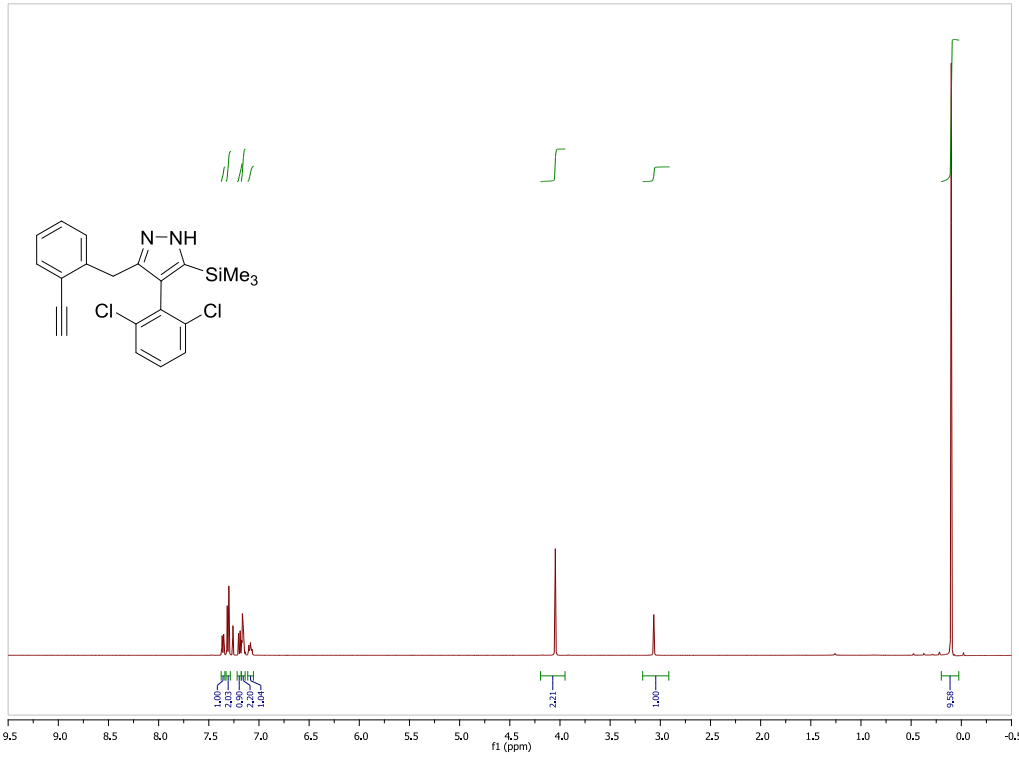
N–NH
SiMe3
Cl
Cl
1.00
2.03
0.99
2.20
1.04
2.21
1.00
9.58
f1 (ppm)

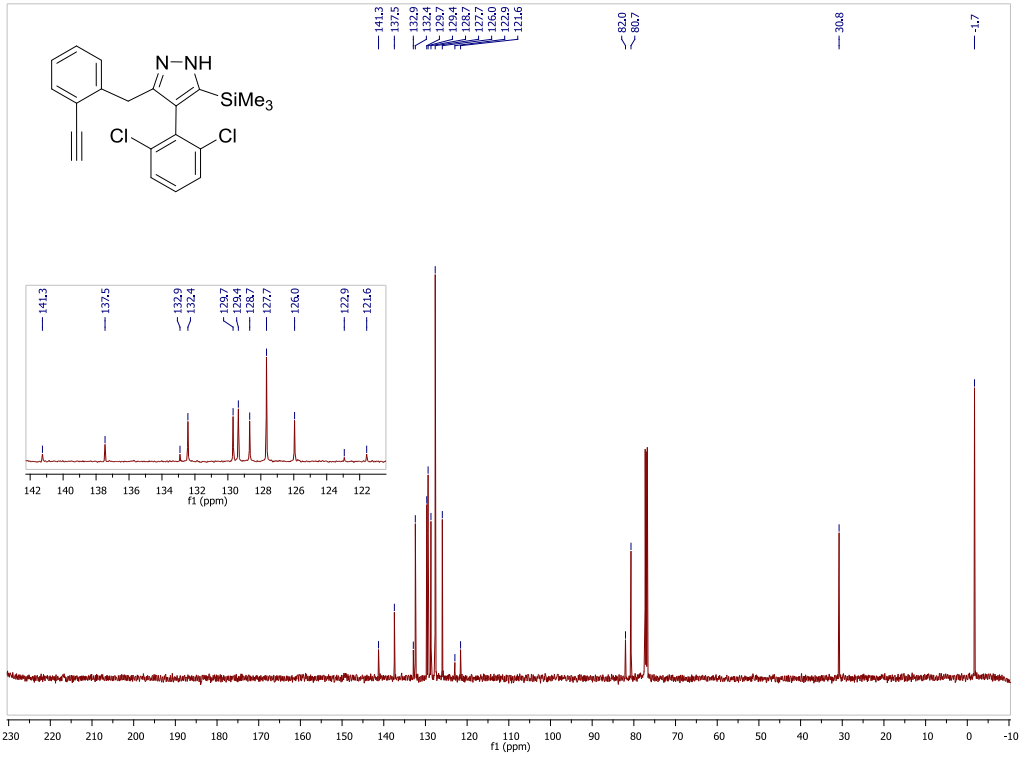
141.3
137.5
132.9
132.4
129.7
129.4
128.7
127.7
126.0
122.9
121.6
82.0
80.7
30.8
-1.7
N–NH
SiMe3
Cl
Cl
f1 (ppm)

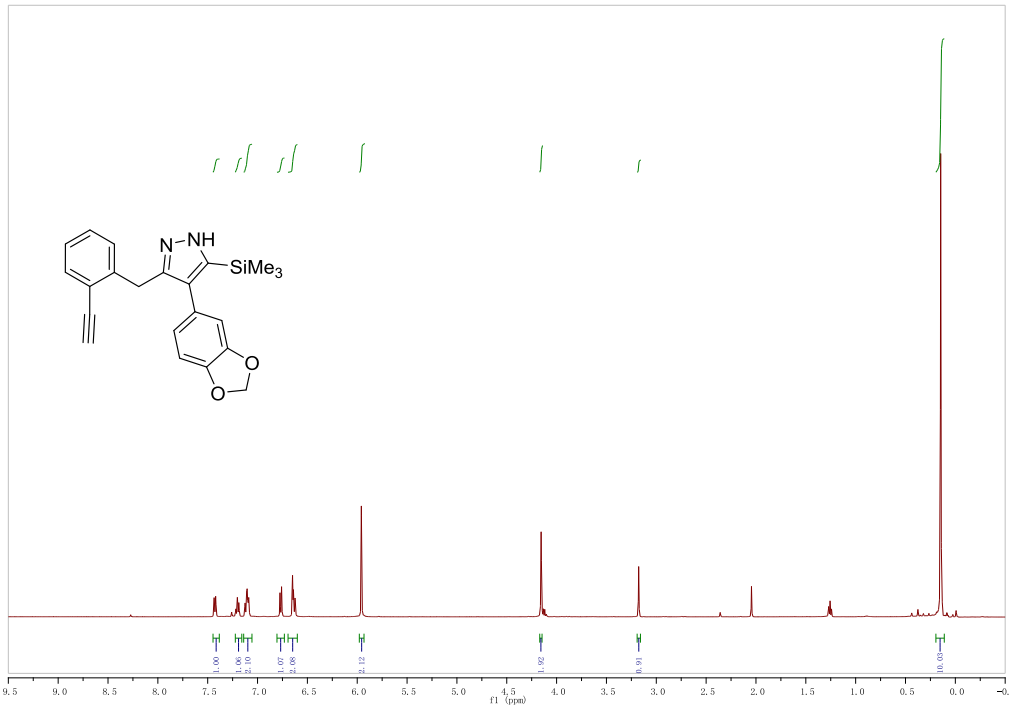
N
NH
SiMe3
O
O
1.00
1.06
2.10
1.07
2.08
2.12
1.92
0.91
10.03
f1 (ppm)

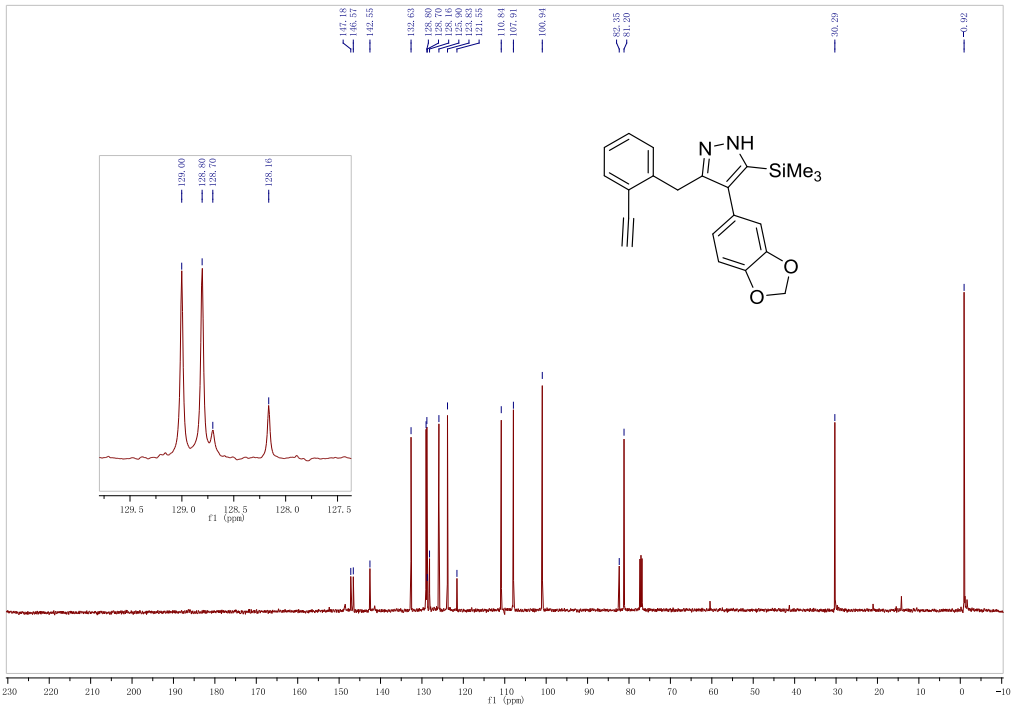
147.18
146.57
142.55
132.63
128.89
128.70
128.16
125.90
124.85
121.55
110.84
107.91
100.94
82.35
81.20
30.29
0.92
129.00
128.80
128.70
128.16
N
NH
SiMe3
O
O
f1 (ppm)

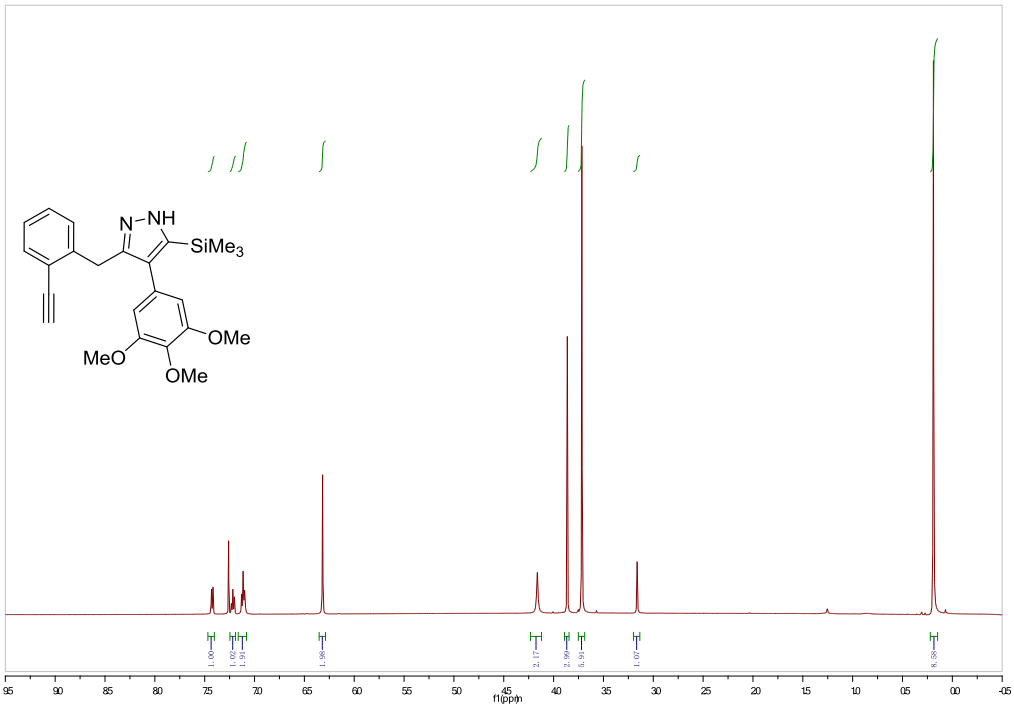
N-NH
SiMe3
OMe
MeO
OMe
f1(ppm)

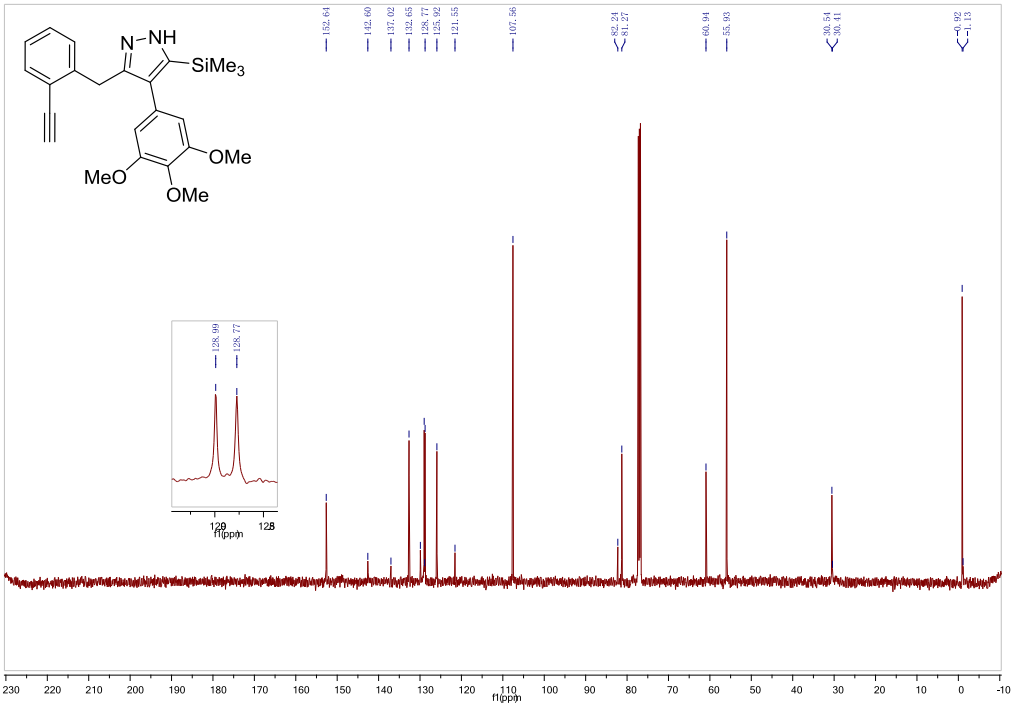
N-NH
SiMe3
OMe
MeO
OMe
152.64
142.60
137.02
132.65
128.77
125.92
121.55
107.56
82.24
81.27
60.94
55.93
30.54
30.41
0.92
-1.13
128.99
128.77
f1(ppm)

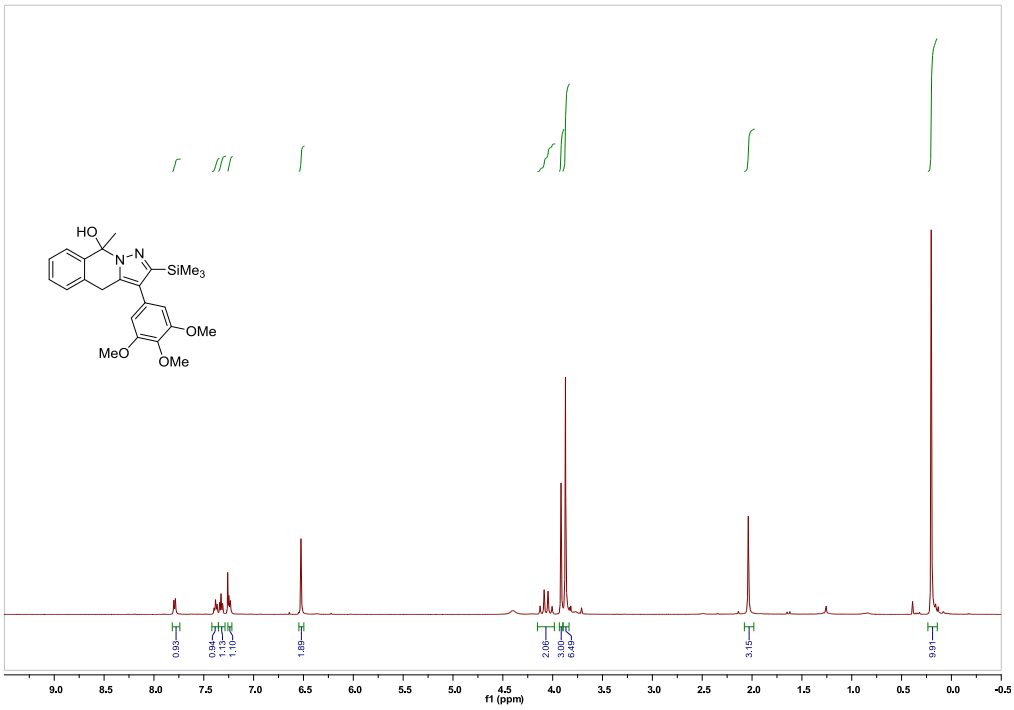
HO
N
N
SiMe3
OMe
MeO
OMe
0.93
0.94
1.13
1.10
1.89
2.06
3.00
6.49
3.15
9.91
f1 (ppm)

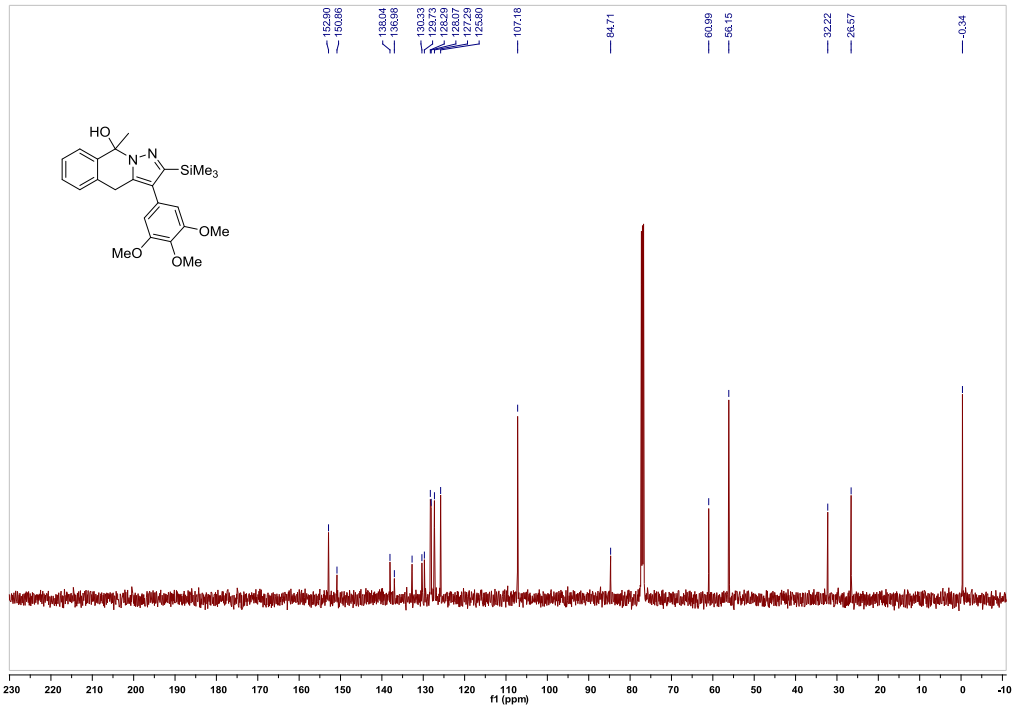
152.90
150.86
138.04
136.98
130.33
129.73
128.29
128.07
127.29
125.80
107.18
84.71
60.99
56.15
32.22
26.57
-0.34
HO
N
N
SiMe3
OMe
MeO
OMe
f1 (ppm)

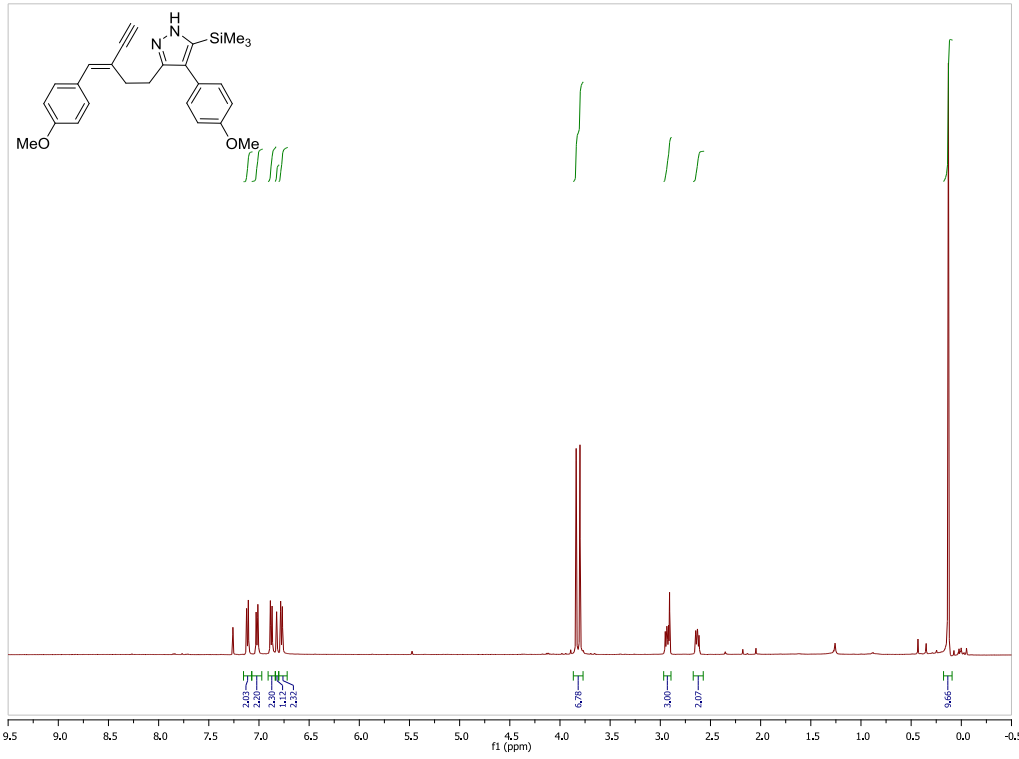
H
N
N
SiMe3
MeO
OMe
2.03
2.20
2.30
1.13
2.22
6.78
3.00
2.07
9.65
9.5 9.0 8.5 8.0 7.5 7.0 6.5 6.0 5.5 5.0 4.5 4.0 3.5 3.0 2.5 2.0 1.5 1.0 0.5 0.0 -0.5
f1 (ppm)

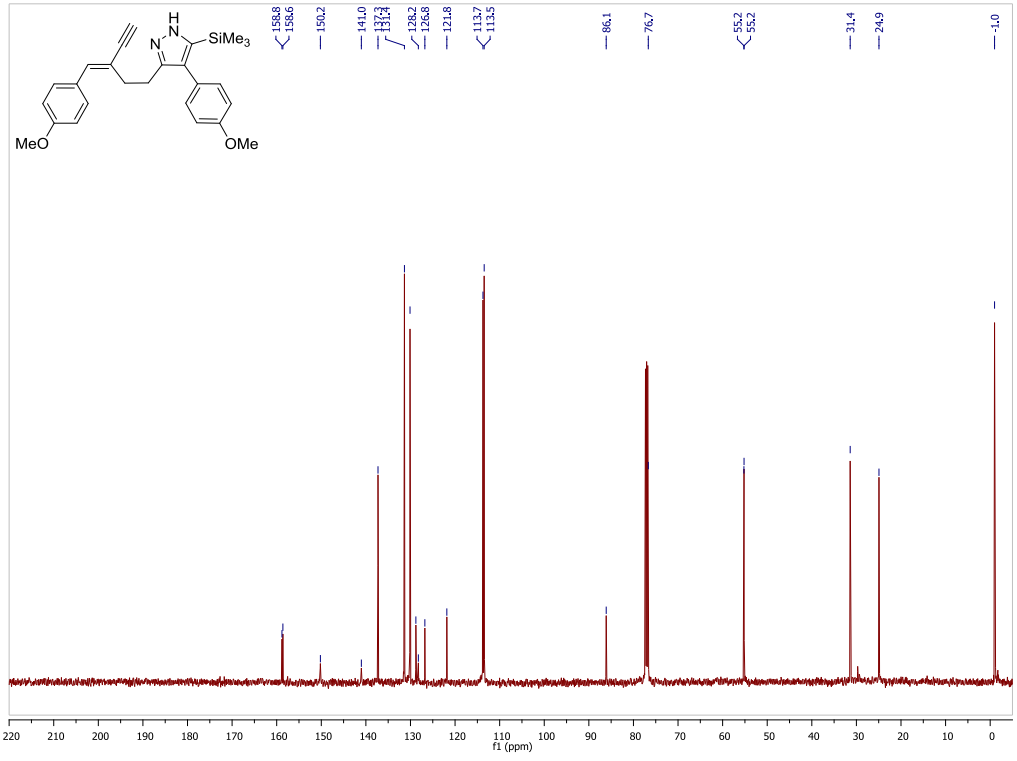
H
N
N
SiMe3
MeO
OMe
158.8
158.6
150.2
141.0
137.3
131.4
128.2
126.8
121.8
113.7
113.5
86.1
76.7
55.2
55.2
31.4
24.9
-1.0
220 210 200 190 180 170 160 150 140 130 120 110 100 90 80 70 60 50 40 30 20 10 0
f1 (ppm)

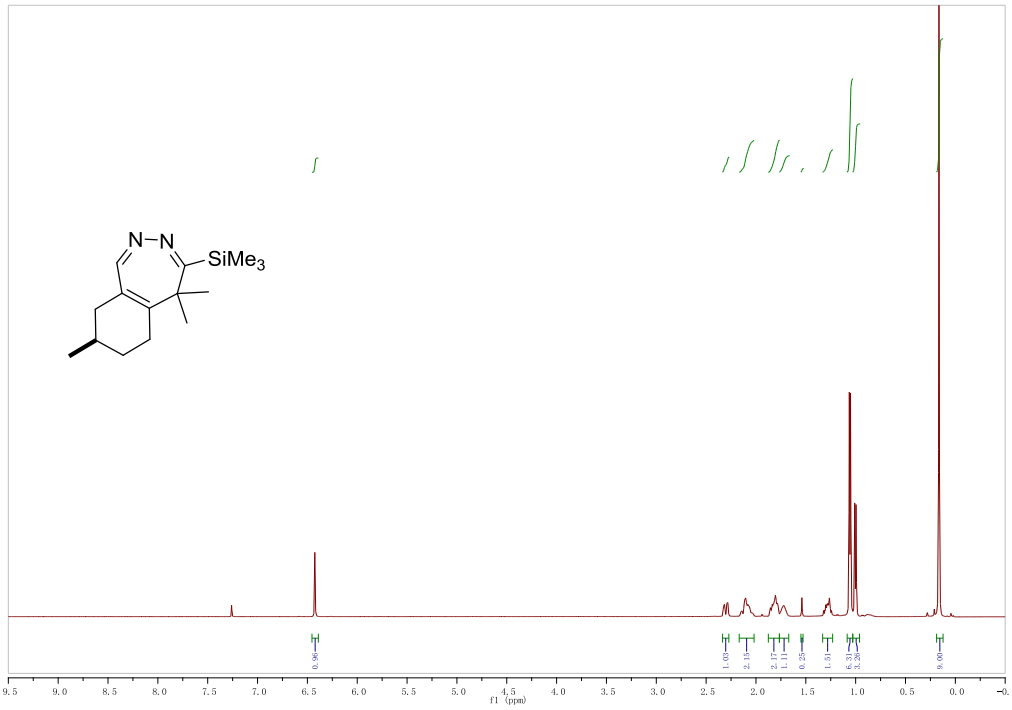
N–N
SiMe3
0.96
1.03
2.10
2.17
1.11
0.25
1.51
6.31
3.26
9.00
f1 (ppm)

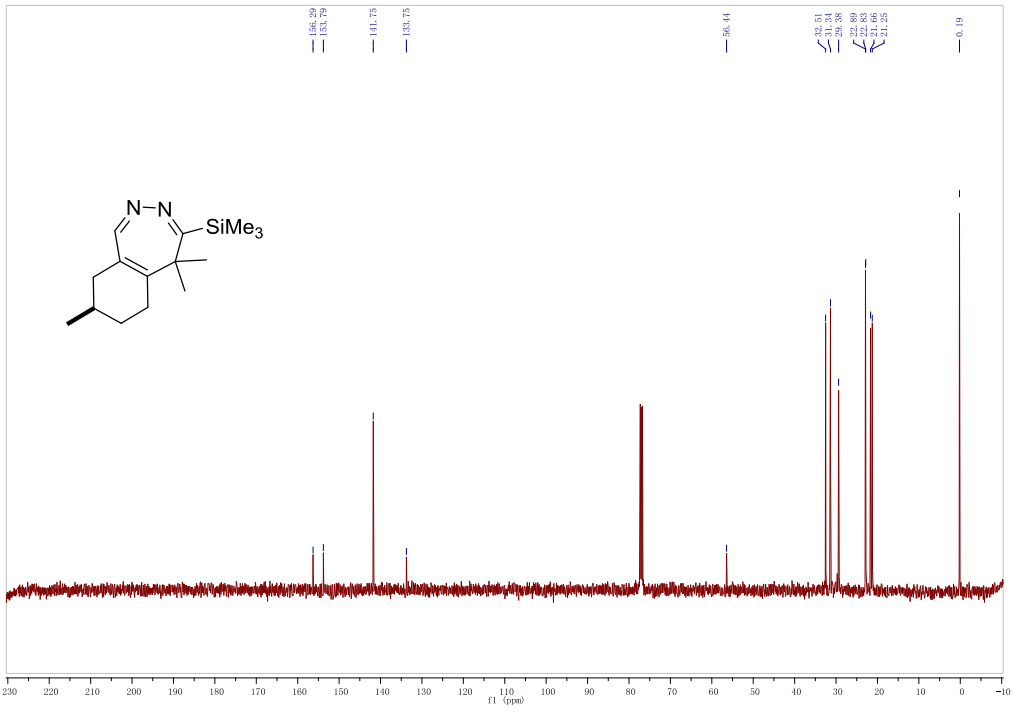
156.29
153.79
141.75
133.75
56.44
32.51
31.34
29.38
22.89
22.63
21.46
21.25
0.19
N–N
SiMe3
f1 (ppm)

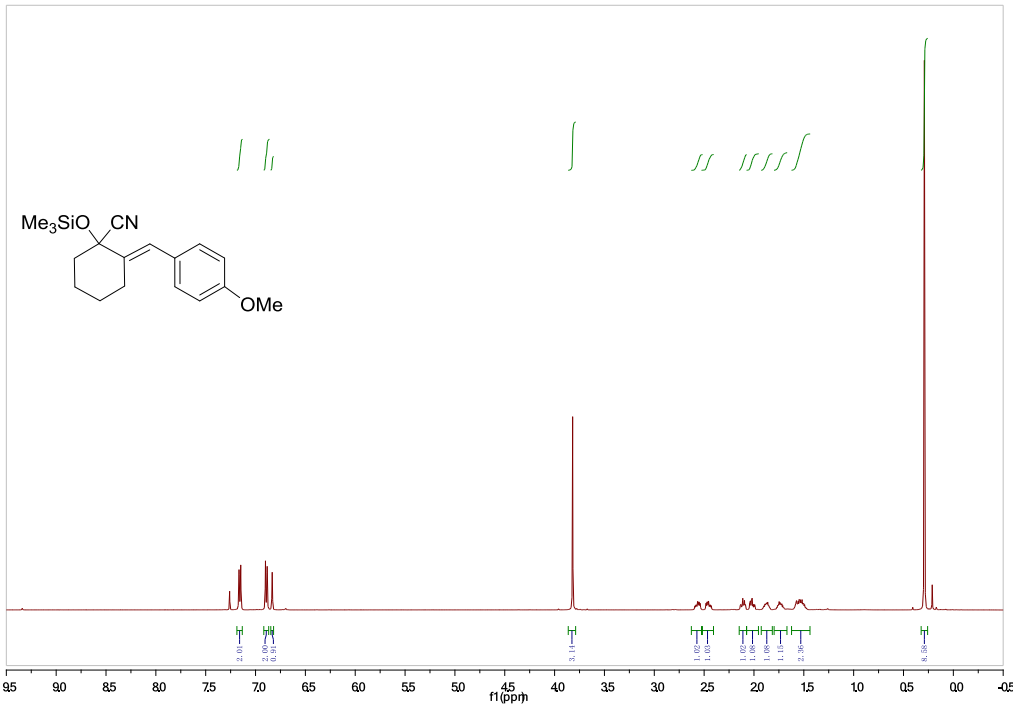
Me3SiO CN
OMe
f1(ppm)

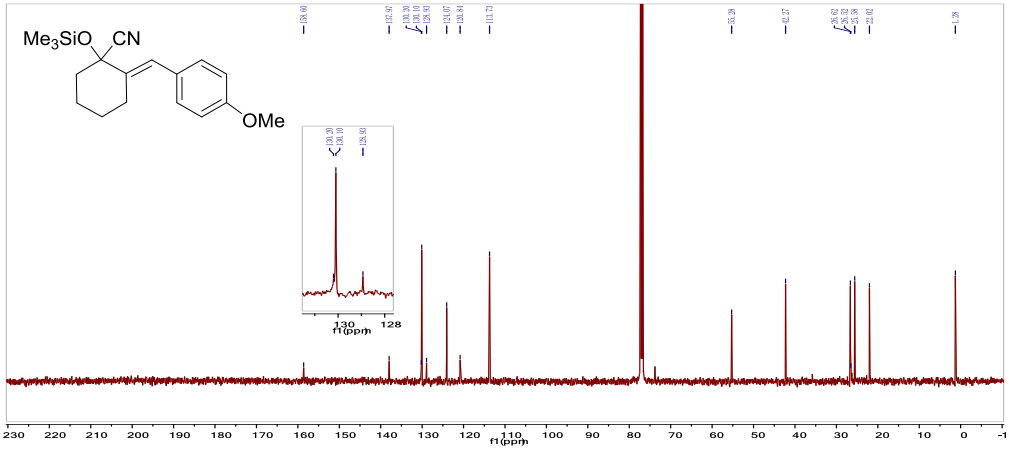
Me3SiO CN
OMe
f1(ppm)

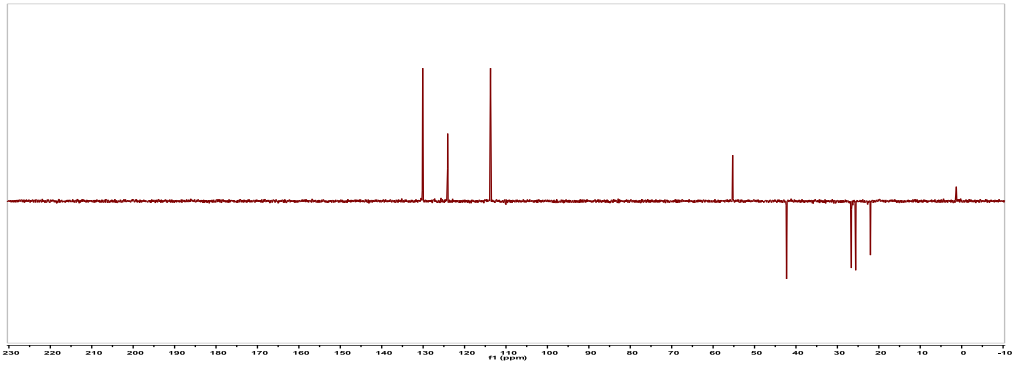
f1 (ppm)

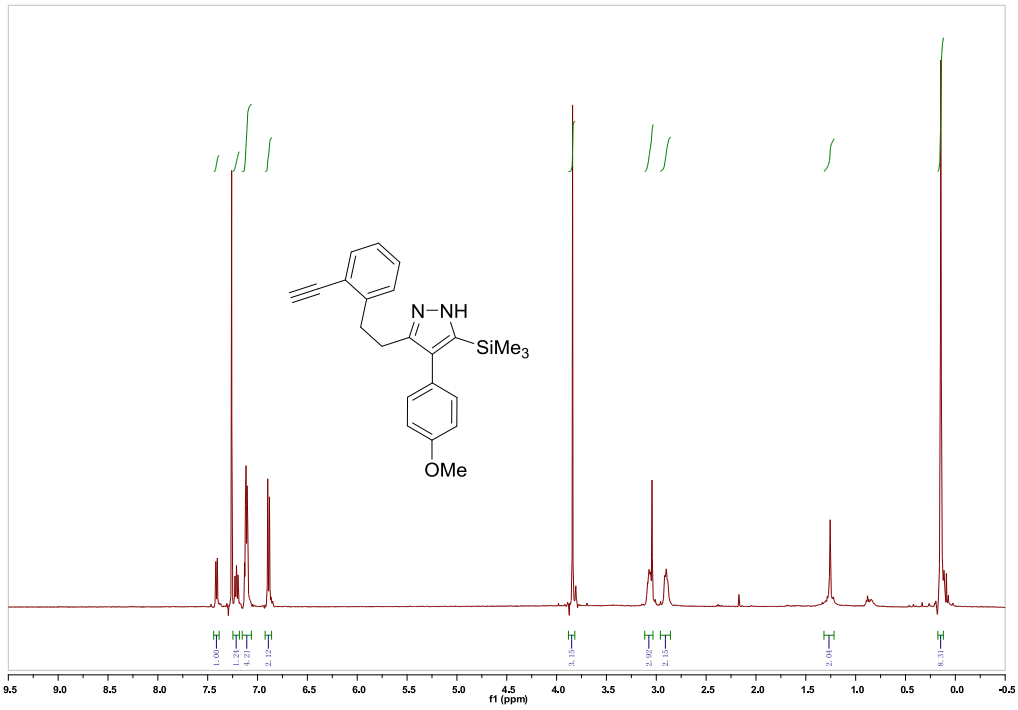
N–NH
SiMe3
OMe
1.00
1.23
4.21
2.12
3.15
2.92
2.15
2.04
8.31
f1 (ppm)

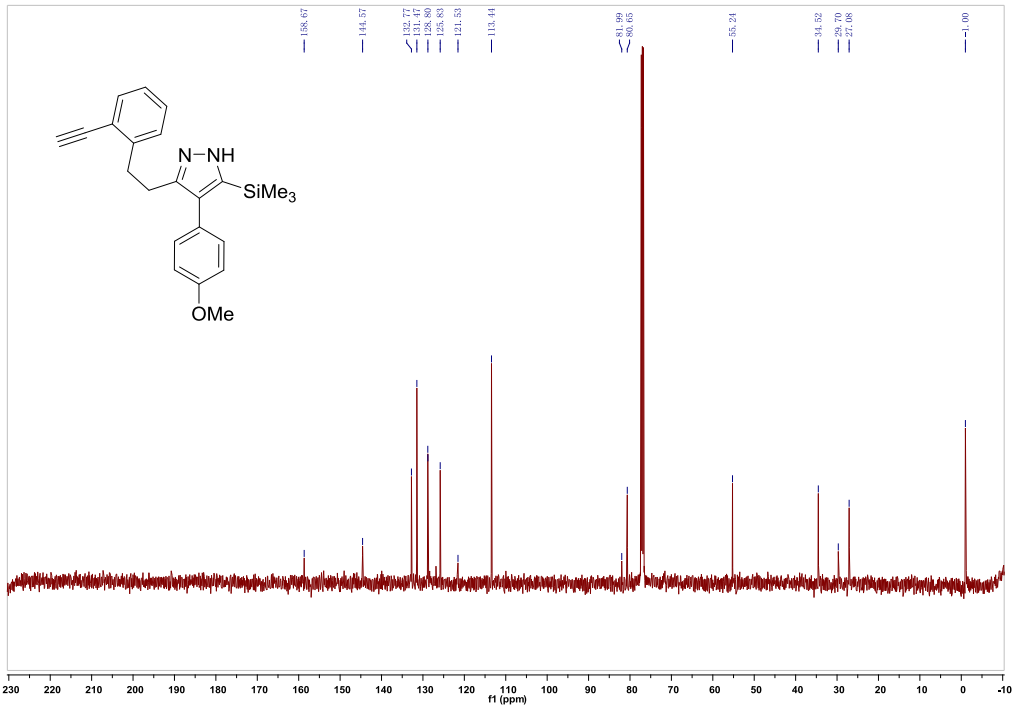
158.67
144.57
132.77
131.47
130.80
125.83
121.53
113.44
81.89
80.65
55.24
34.52
29.70
27.08
1.00
N–NH
SiMe3
OMe
f1 (ppm)

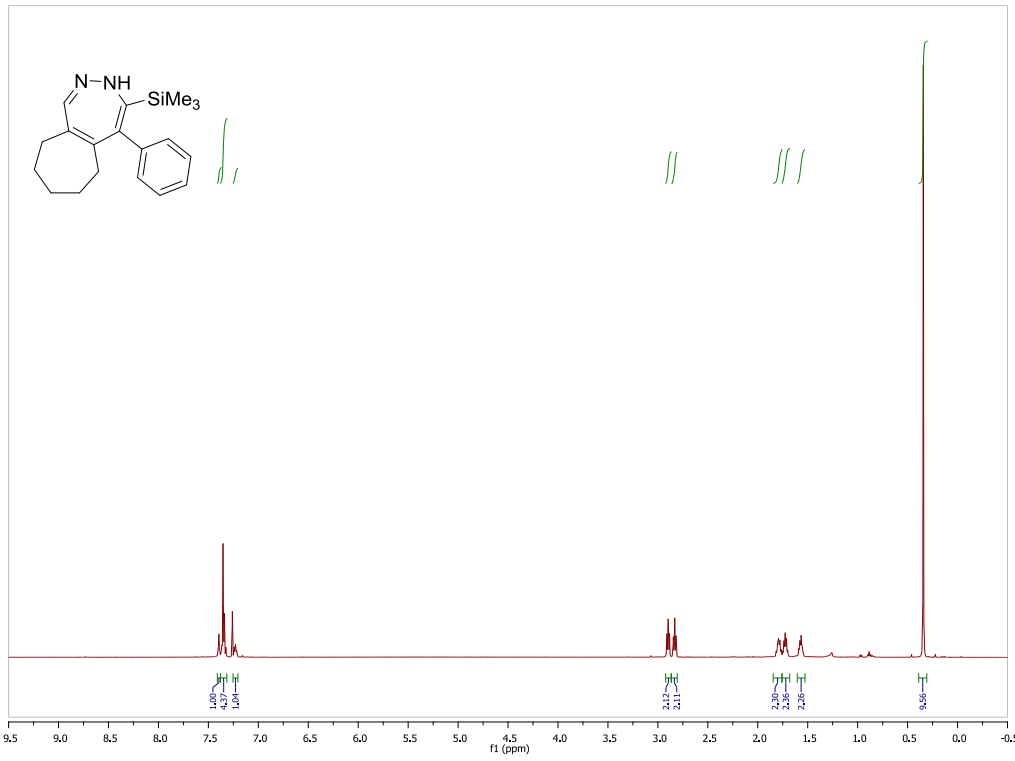
N–NH
SiMe3
1.09
4.57
1.04
2.12
2.11
2.30
2.26
2.26
9.66
f1 (ppm)

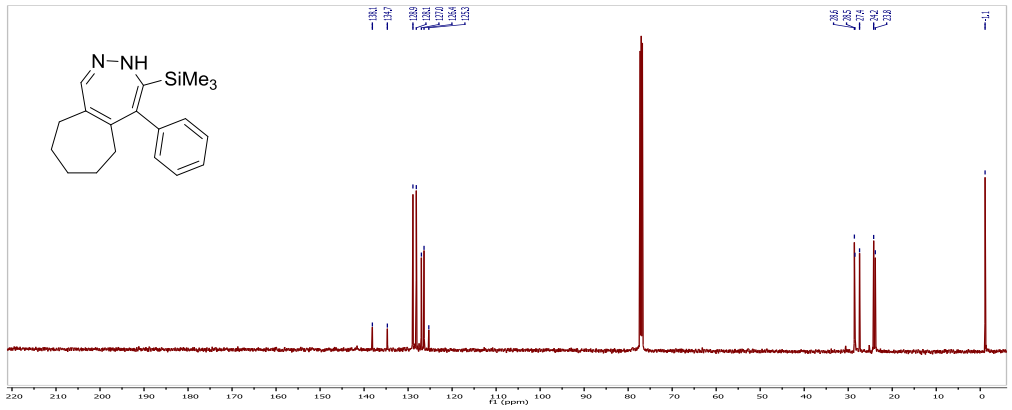
N–NH
SiMe3
f1 (ppm)

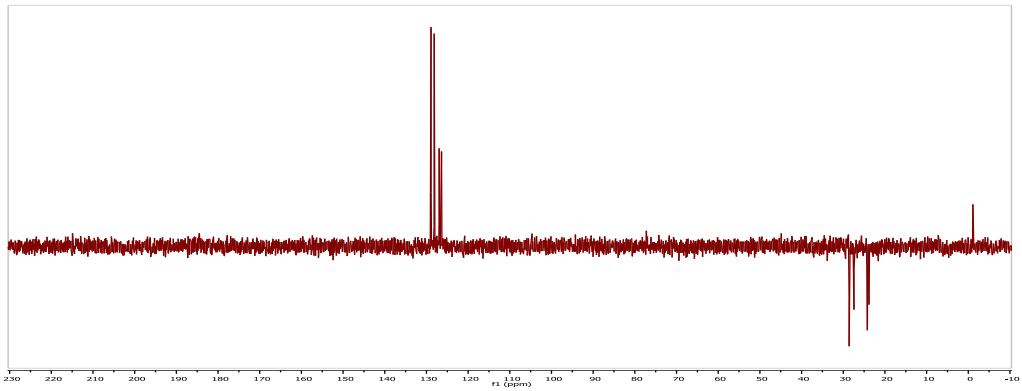
f1 (ppm)

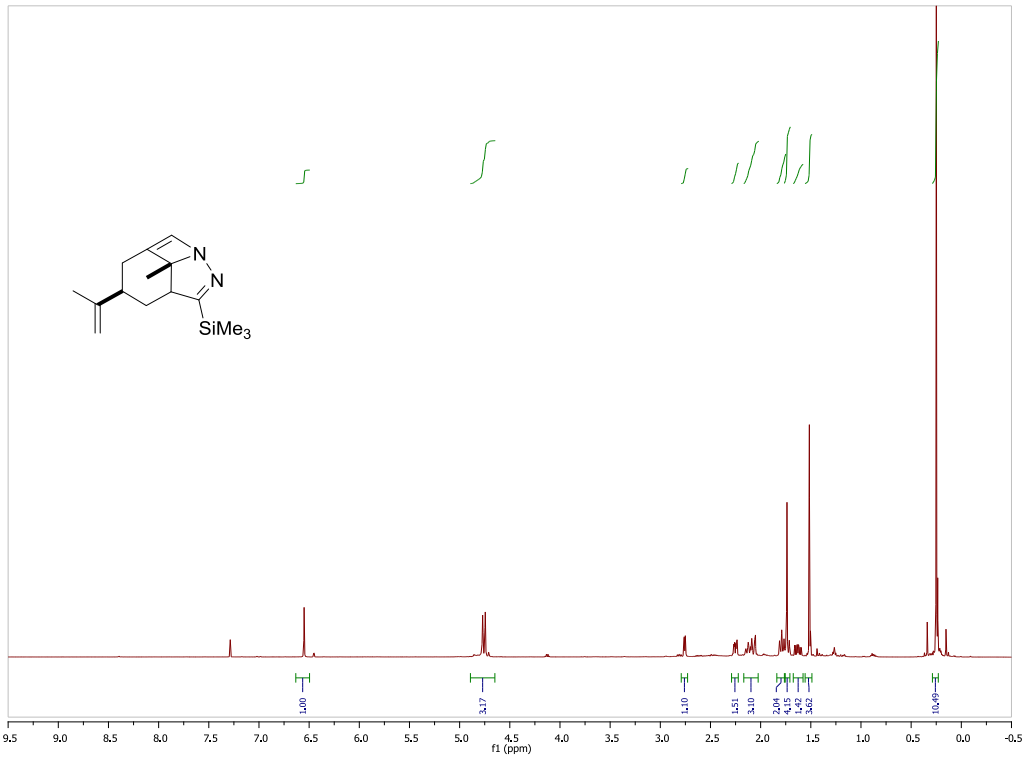
N
N
SiMe3
1.00
3.17
1.10
1.51
3.10
2.04
4.15
3.62
10.49
f1 (ppm)

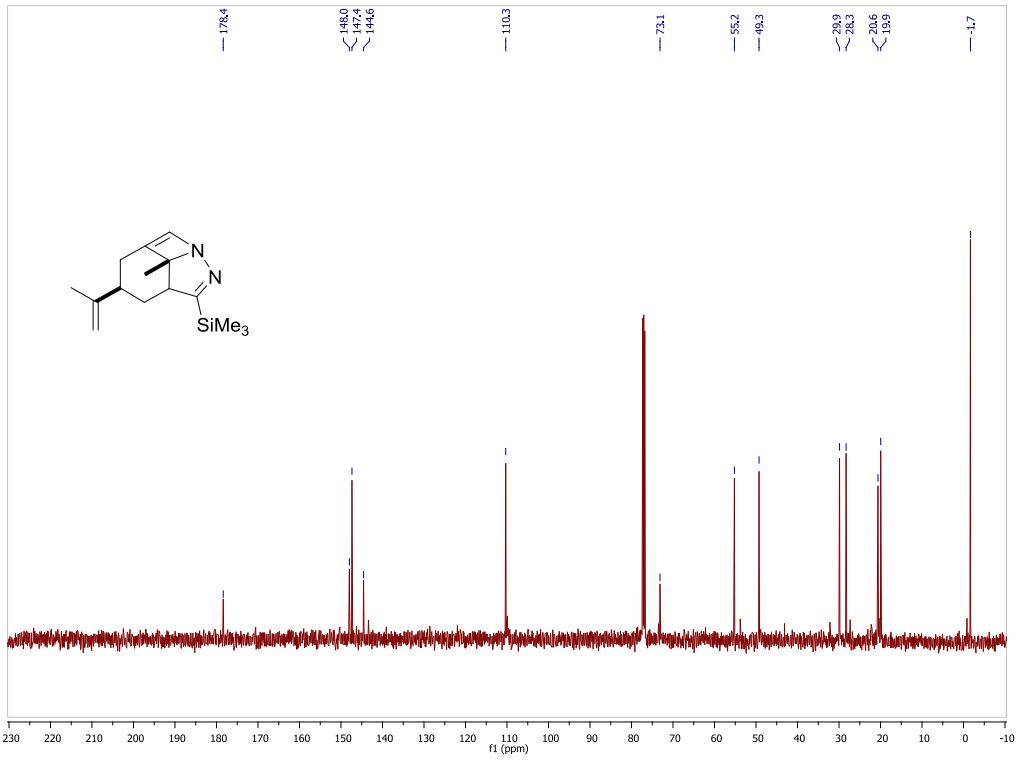
178.4
148.0
147.4
144.6
110.3
73.1
55.2
49.3
29.9
28.3
20.6
19.9
-1.7
N
N
SiMe3
f1 (ppm)

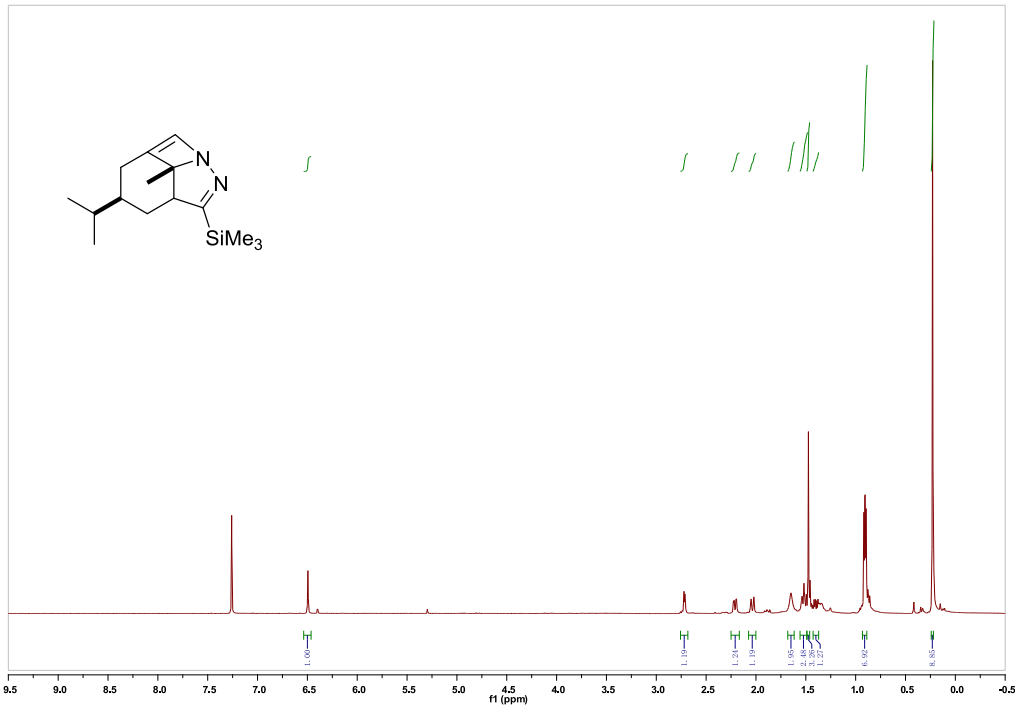
N
N
SiMe3
1.00
1.19
1.21
1.19
1.65
2.49
3.26
1.27
6.62
8.85
9.5 9.0 8.5 8.0 7.5 7.0 6.5 6.0 5.5 5.0 4.5 4.0 3.5 3.0 2.5 2.0 1.5 1.0 0.5 0.0 -0.5
f1 (ppm)

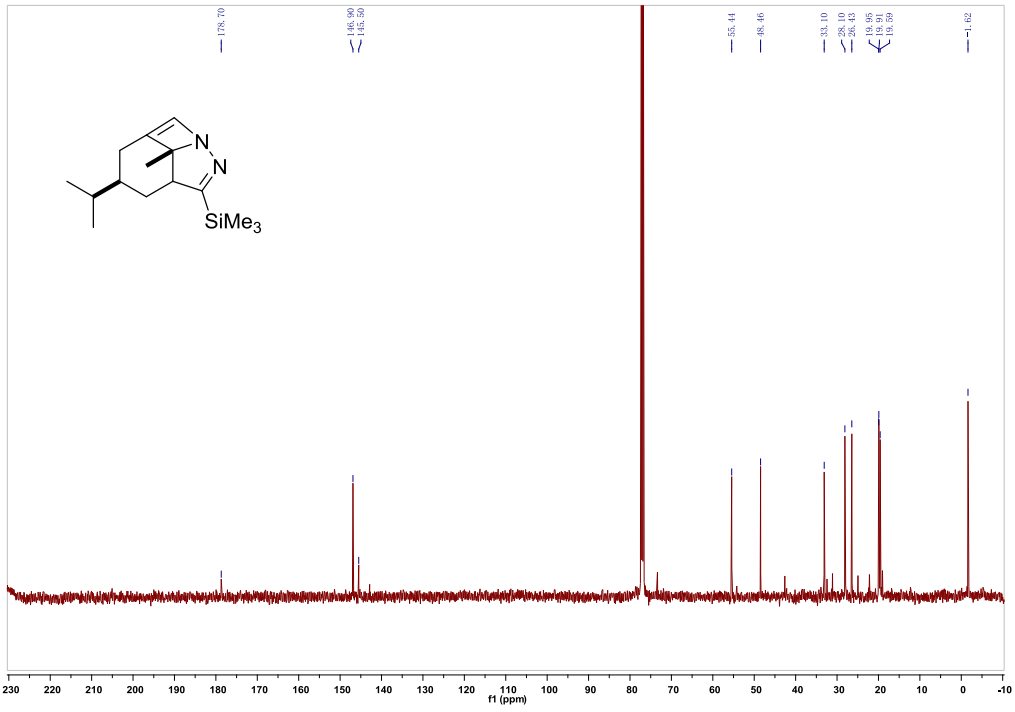
178.70
146.90
145.50
55.44
48.46
33.10
28.10
26.43
19.95
19.91
19.89
-1.62
N
N
SiMe3
230 220 210 200 190 180 170 160 150 140 130 120 110 100 90 80 70 60 50 40 30 20 10 0 -10
f1 (ppm)

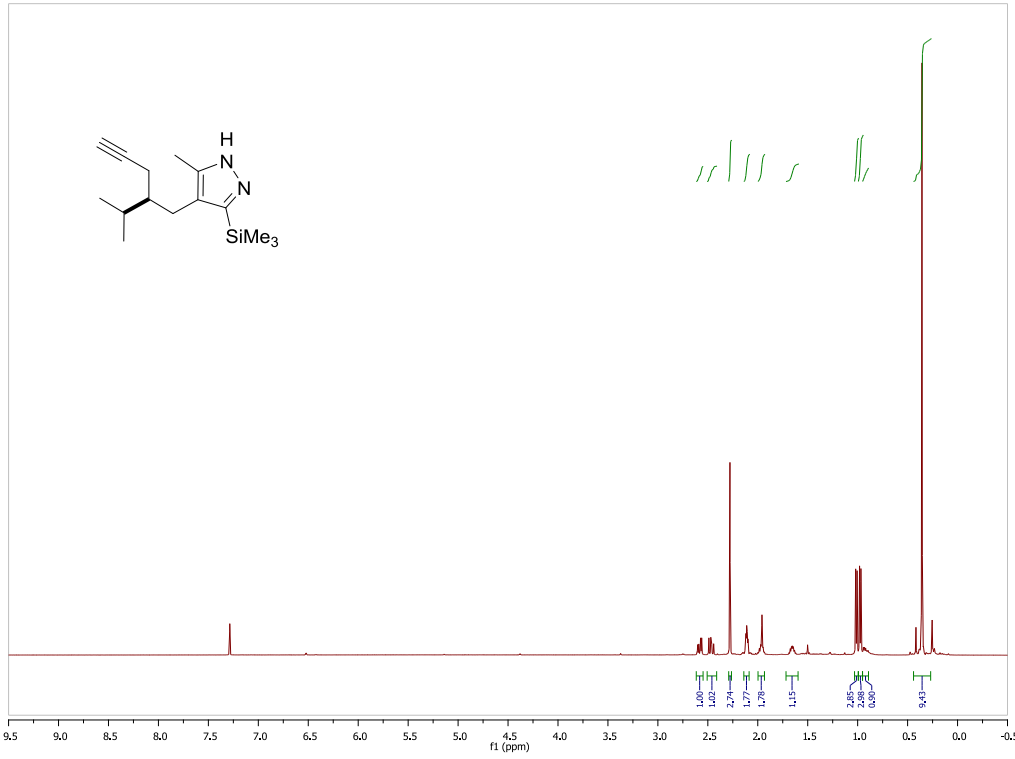
H
N
N
SiMe3
1.00
1.02
2.74
1.77
1.78
1.15
2.85
2.88
6.90
9.43
9.5 9.0 8.5 8.0 7.5 7.0 6.5 6.0 5.5 5.0 4.5 4.0 3.5 3.0 2.5 2.0 1.5 1.0 0.5 0.0 -0.5
f1 (ppm)

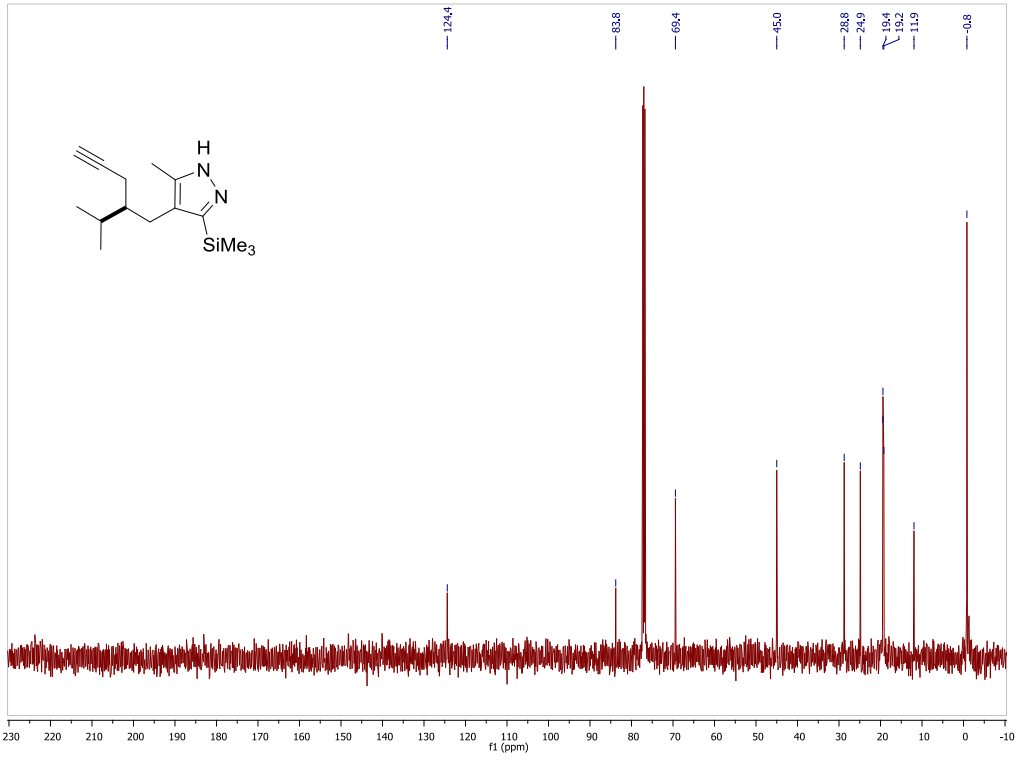
124.4
83.8
69.4
45.0
28.8
24.9
19.4
19.2
11.9
-0.8
H
N
N
SiMe3
230 220 210 200 190 180 170 160 150 140 130 120 110 100 90 80 70 60 50 40 30 20 10 0 -10
f1 (ppm)

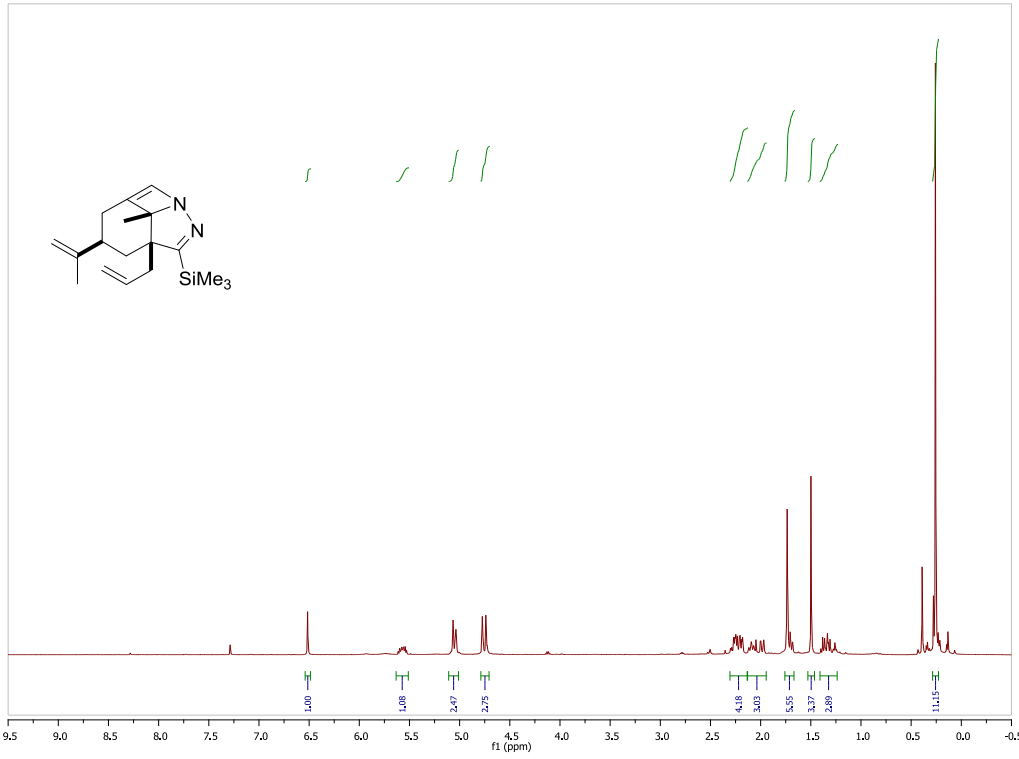
N
N
SiMe3
1.00
1.08
2.47
2.75
4.18
3.03
5.55
3.37
2.89
11.15
9.5 9.0 8.5 8.0 7.5 7.0 6.5 6.0 5.5 5.0 4.5 4.0 3.5 3.0 2.5 2.0 1.5 1.0 0.5 0.0 -0.5
f1 (ppm)

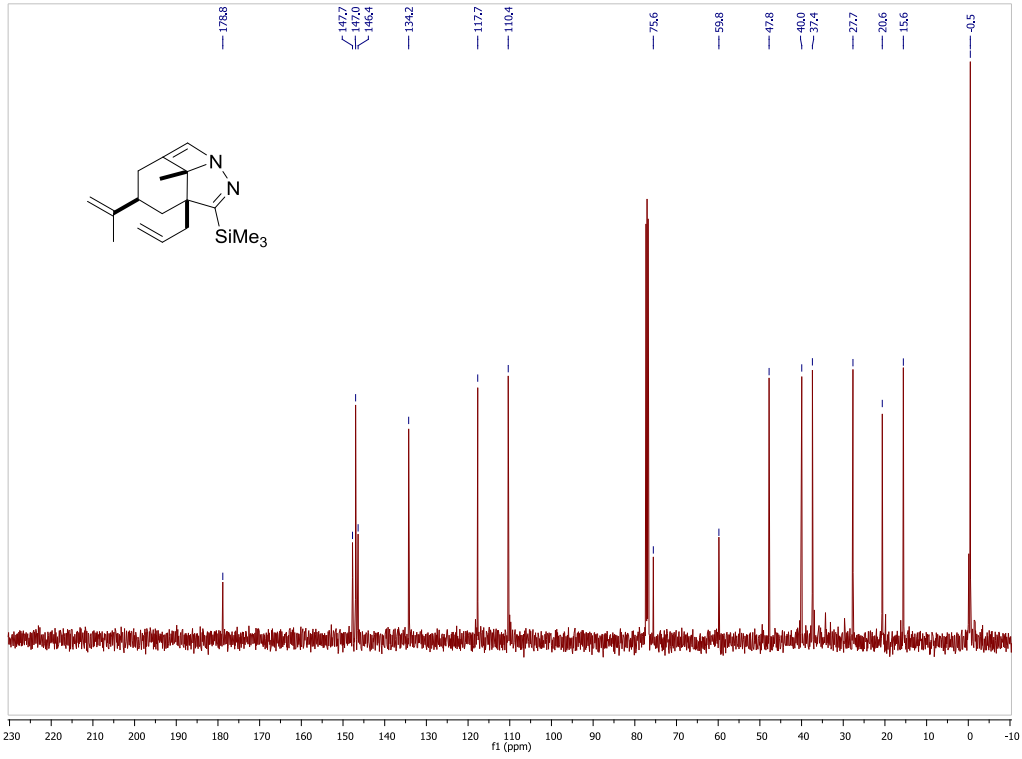
178.8
147.7
147.0
146.4
134.2
117.7
110.4
75.6
59.8
47.8
40.0
37.4
27.7
20.6
15.6
-0.5
N
N
SiMe3
230 220 210 200 190 180 170 160 150 140 130 120 110 100 90 80 70 60 50 40 30 20 10 0 -10
f1 (ppm)

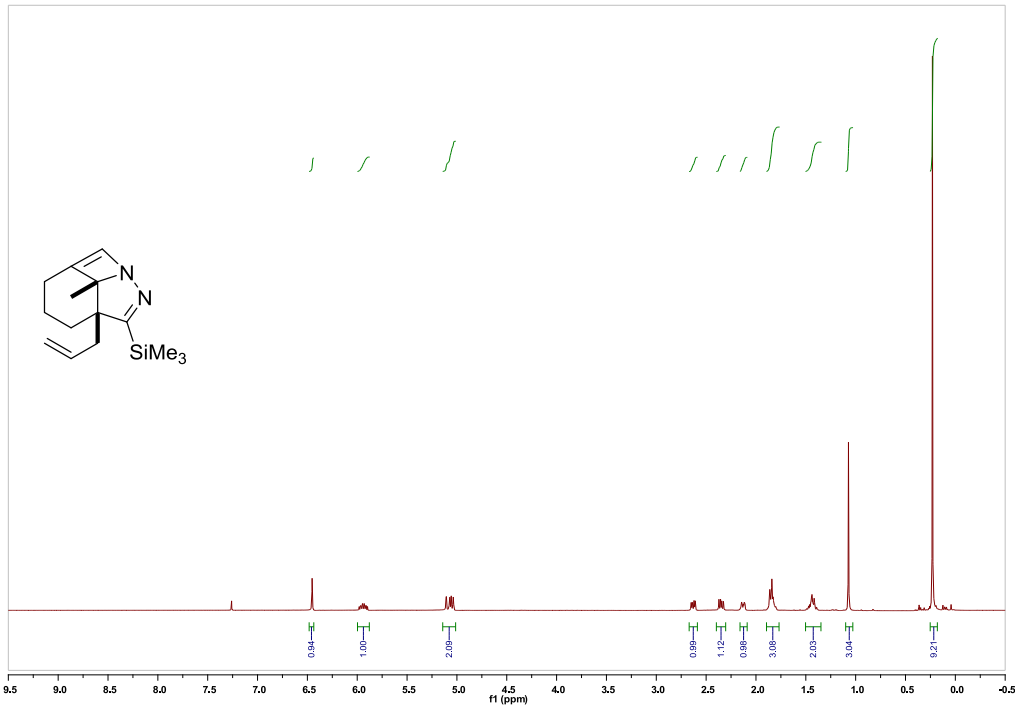
N
N
SiMe3
0.94
1.00
2.09
0.99
1.12
0.98
3.08
2.03
3.04
9.21
f1 (ppm)

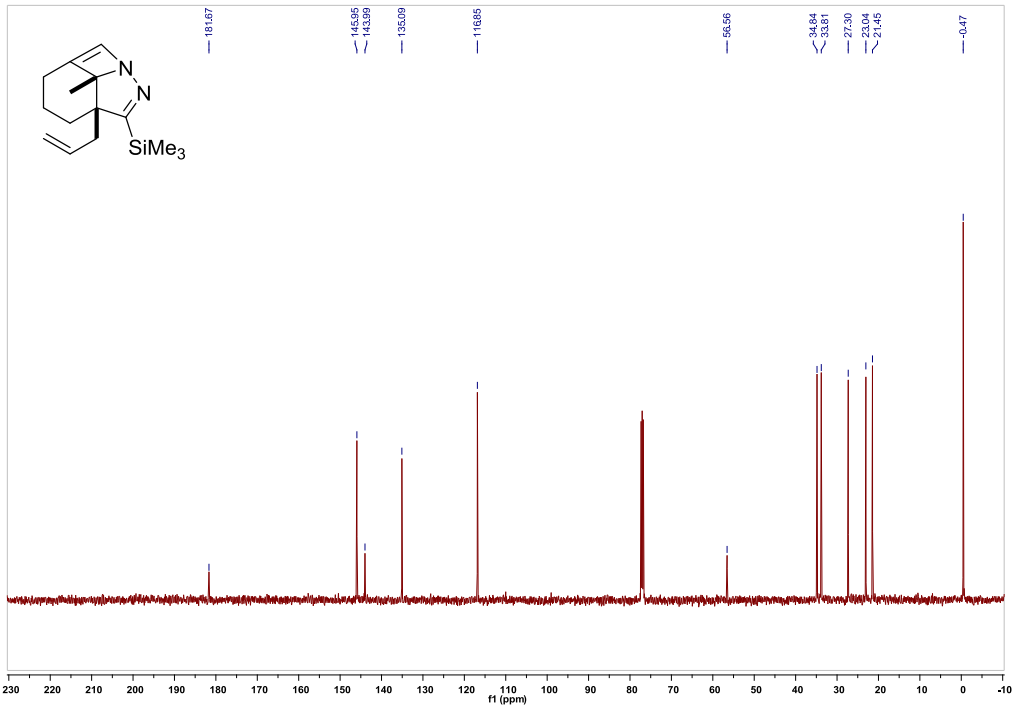
181.67
145.95
143.99
135.09
116.85
56.56
34.84
33.81
27.30
23.04
21.45
-0.47
N
N
SiMe3
f1 (ppm)

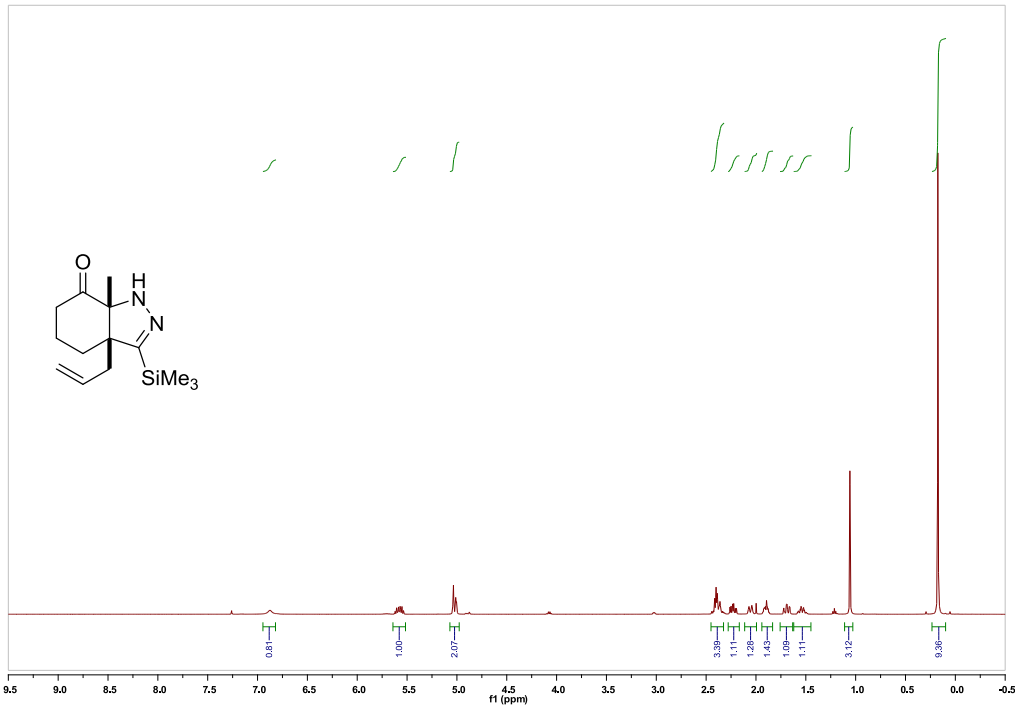
O
H
N
N
SiMe3
0.81
1.00
2.07
3.39
1.11
1.28
1.43
1.09
1.11
3.12
9.36
9.5 9.0 8.5 8.0 7.5 7.0 6.5 6.0 5.5 5.0 4.5 4.0 3.5 3.0 2.5 2.0 1.5 1.0 0.5 0.0 -0.5
f1 (ppm)

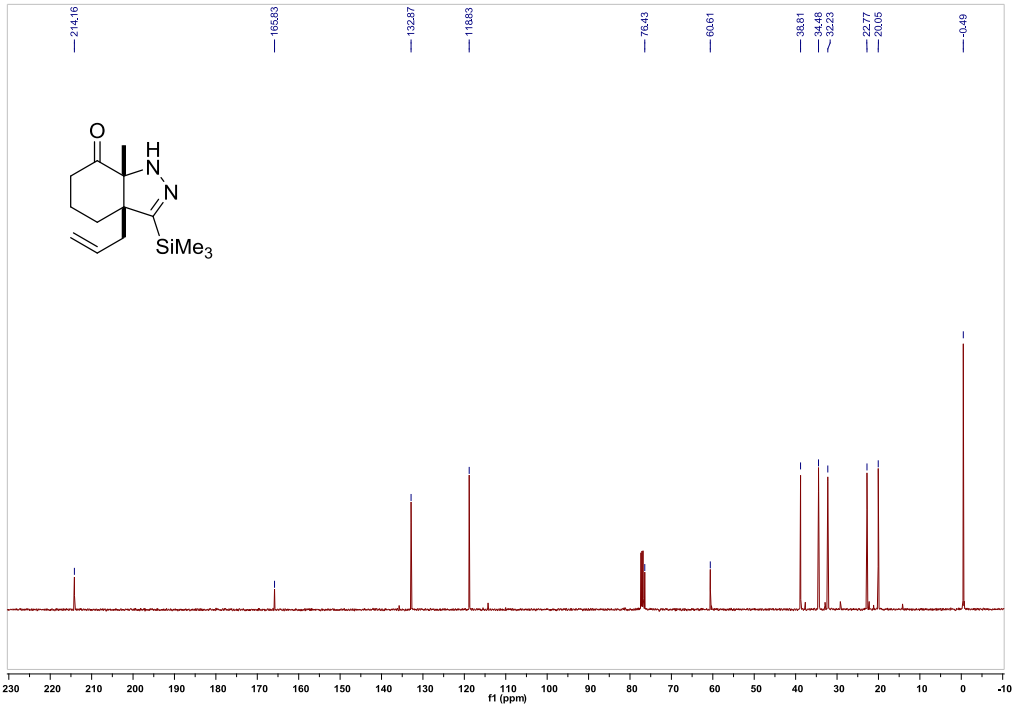
214.16
165.83
132.87
118.83
76.43
60.61
38.81
34.48
32.23
22.77
20.05
-0.49
O
H
N
N
SiMe3
230 220 210 200 190 180 170 160 150 140 130 120 110 100 90 80 70 60 50 40 30 20 10 0 -10
f1 (ppm)

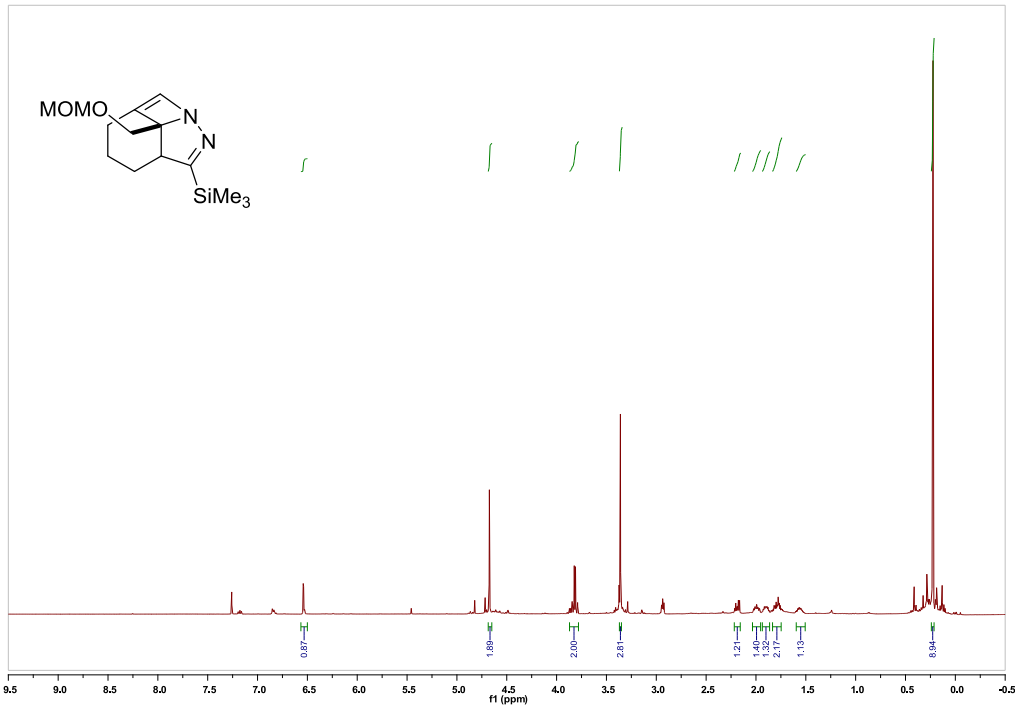
MOMO
N
N
SiMe3
0.87
1.89
2.00
2.81
1.21
1.40
3.57
2.17
1.13
8.94
f1 (ppm)

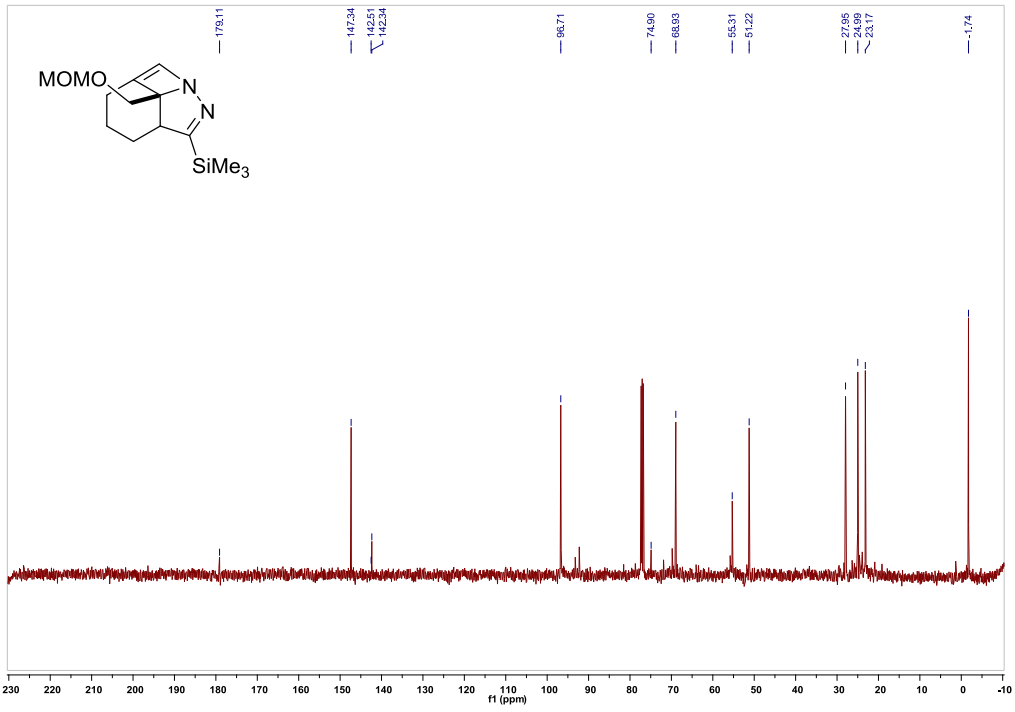
179.11
147.34
142.51
142.34
96.71
74.90
68.93
55.31
51.22
27.95
24.99
23.17
-1.74
MOMO
N
N
SiMe3
f1 (ppm)

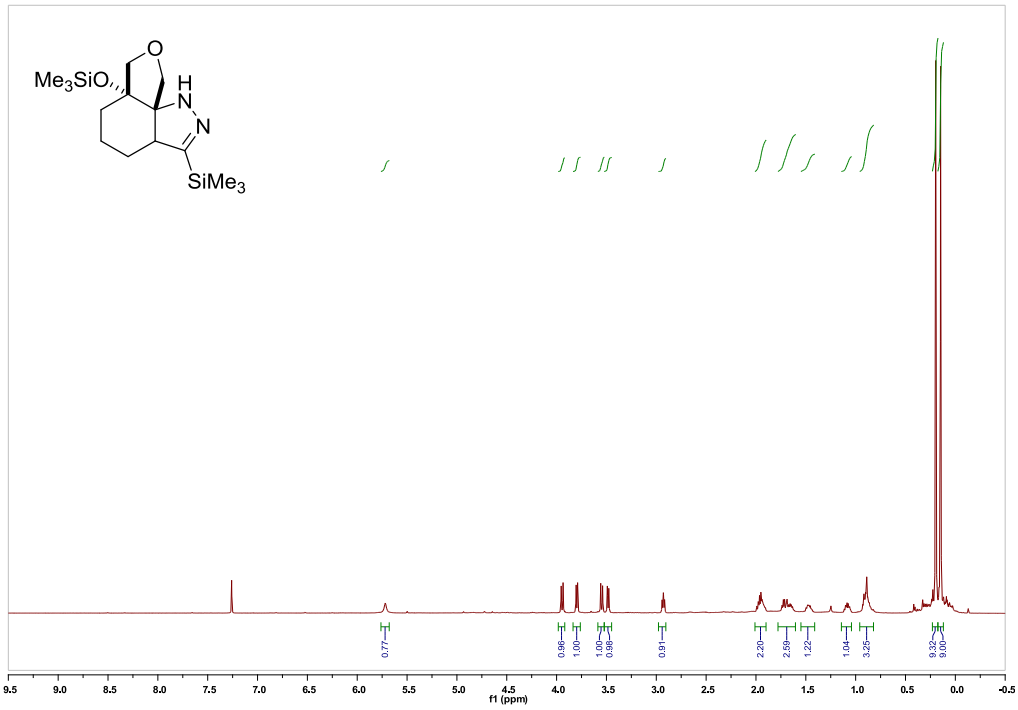
Me3SiO
O
H
N
N
SiMe3
0.77
0.96
1.00
1.02
0.98
0.91
2.20
2.59
1.22
1.04
3.28
9.32
9.00
f1 (ppm)

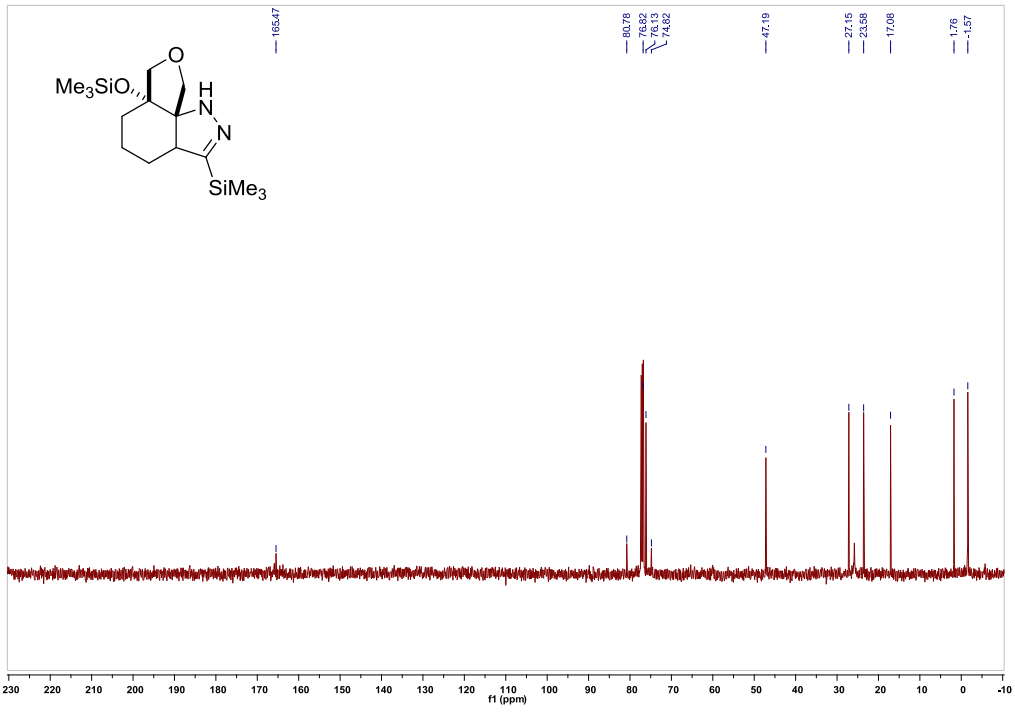
165.47
80.78
76.82
76.13
74.82
47.19
27.15
23.58
17.08
1.76
-1.57
Me3SiO
O
H
N
N
SiMe3
f1 (ppm)

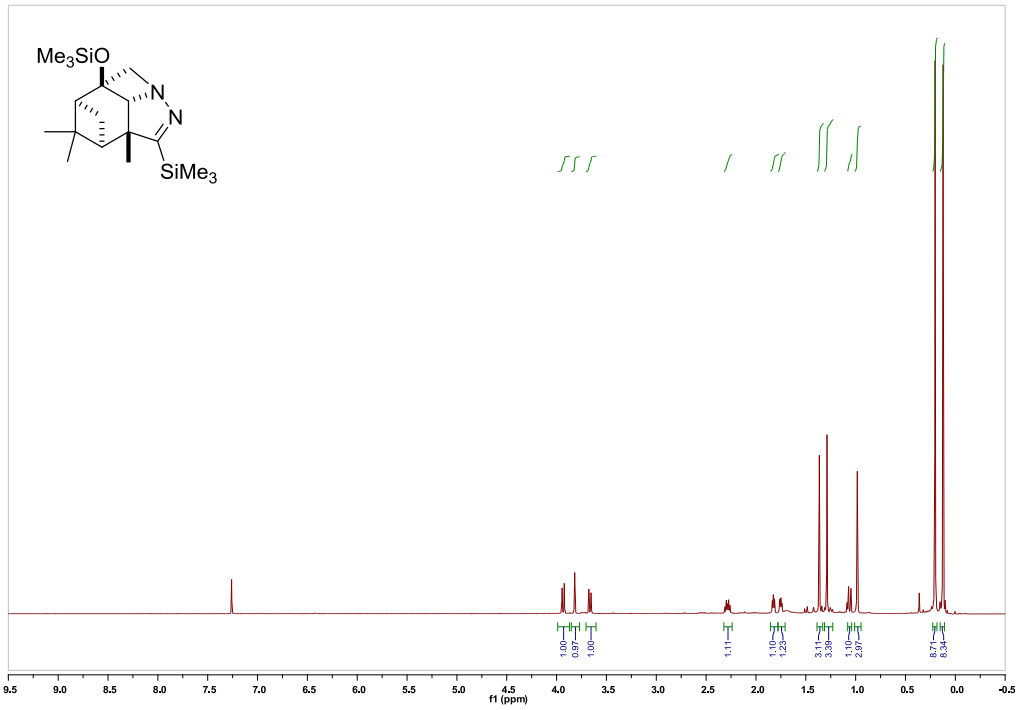
Me3SiO
N
N
SiMe3
1.00
0.97
1.00
1.11
1.10
1.23
3.11
3.39
1.10
2.97
8.71
8.34
f1 (ppm)

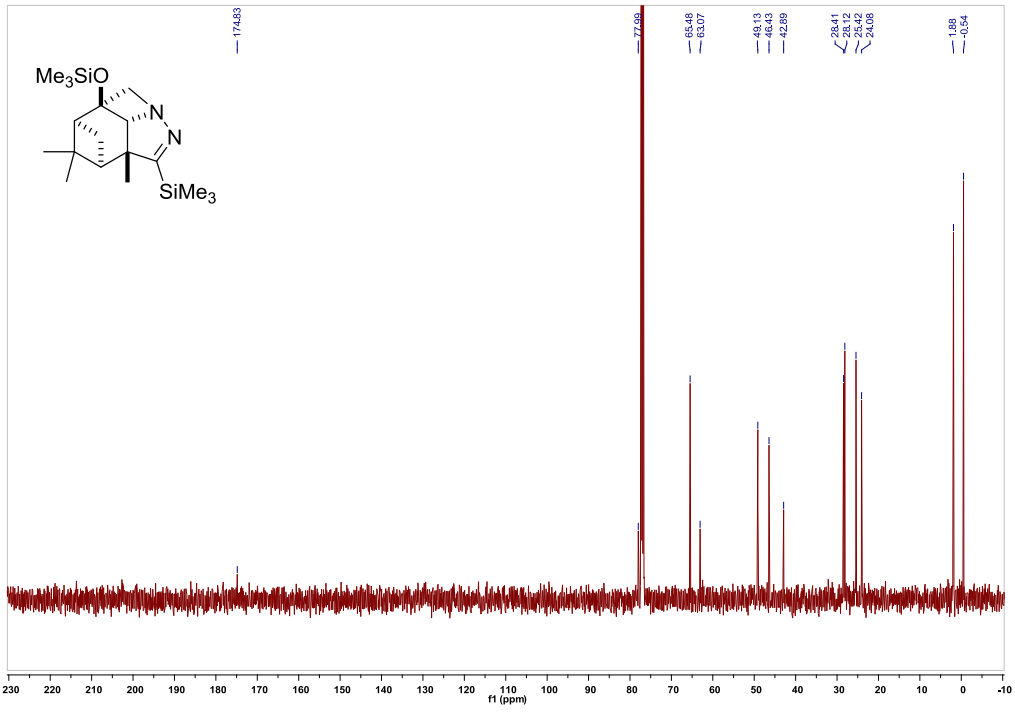
Me3SiO
N
N
SiMe3
174.483
77.699
65.48
63.07
49.13
46.43
42.89
28.41
28.12
25.42
24.08
1.88
-0.54
f1 (ppm)

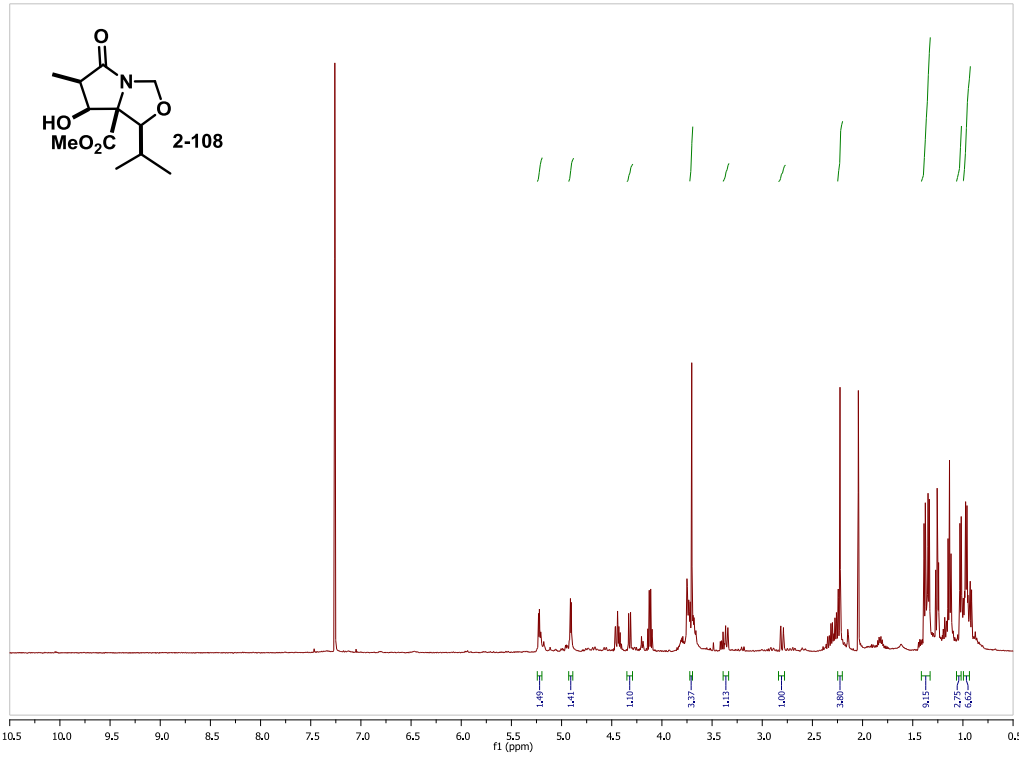
O
N
O
HO
MeO2C
2-108
1.49
1.41
1.10
3.37
1.13
1.00
3.80
9.15
2.75
6.62
f1 (ppm)

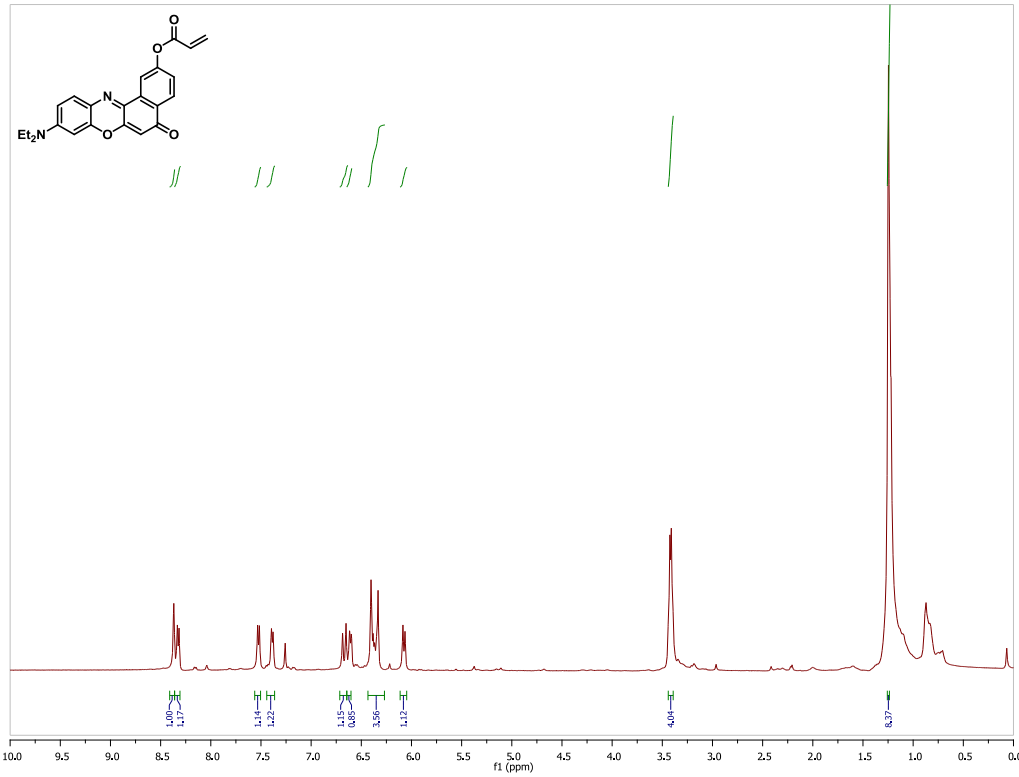
O
O
N
Et2N
O
O
1.00
1.17
1.14
1.22
1.15
0.85
3.56
1.12
4.04
8.37
f1 (ppm)

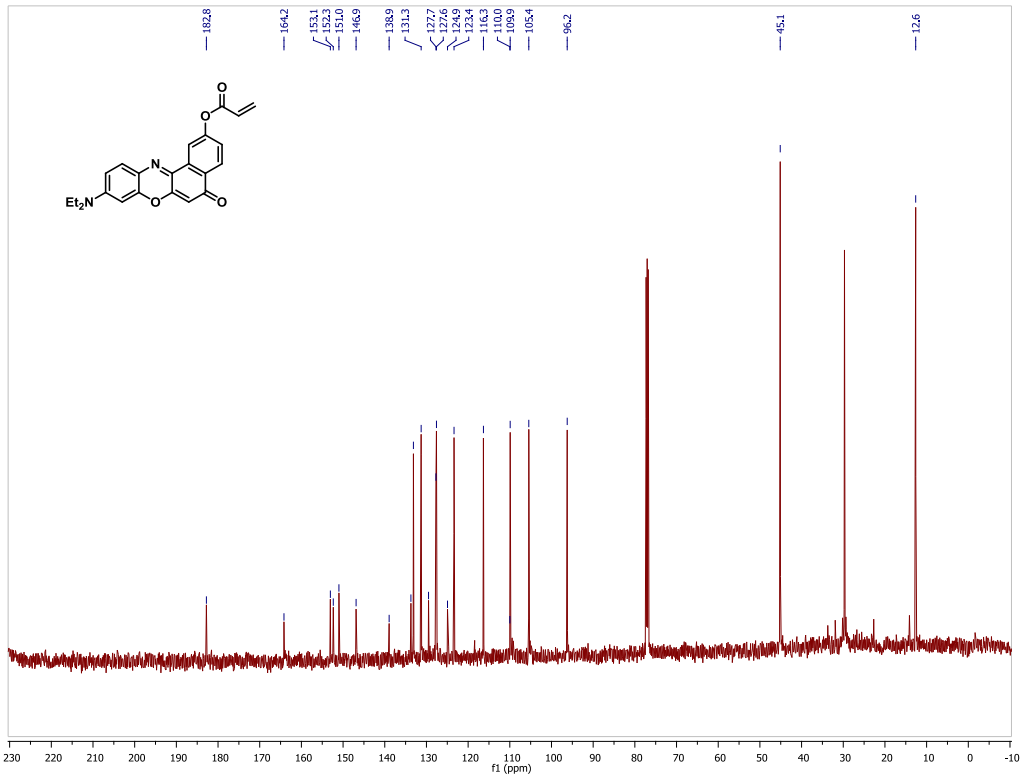
182.8
164.2
153.1
152.3
151.0
146.9
138.9
131.3
127.7
127.6
124.9
123.4
116.3
110.0
109.9
105.4
96.2
45.1
12.6
Et2N
O
N
O
O
f1 (ppm)

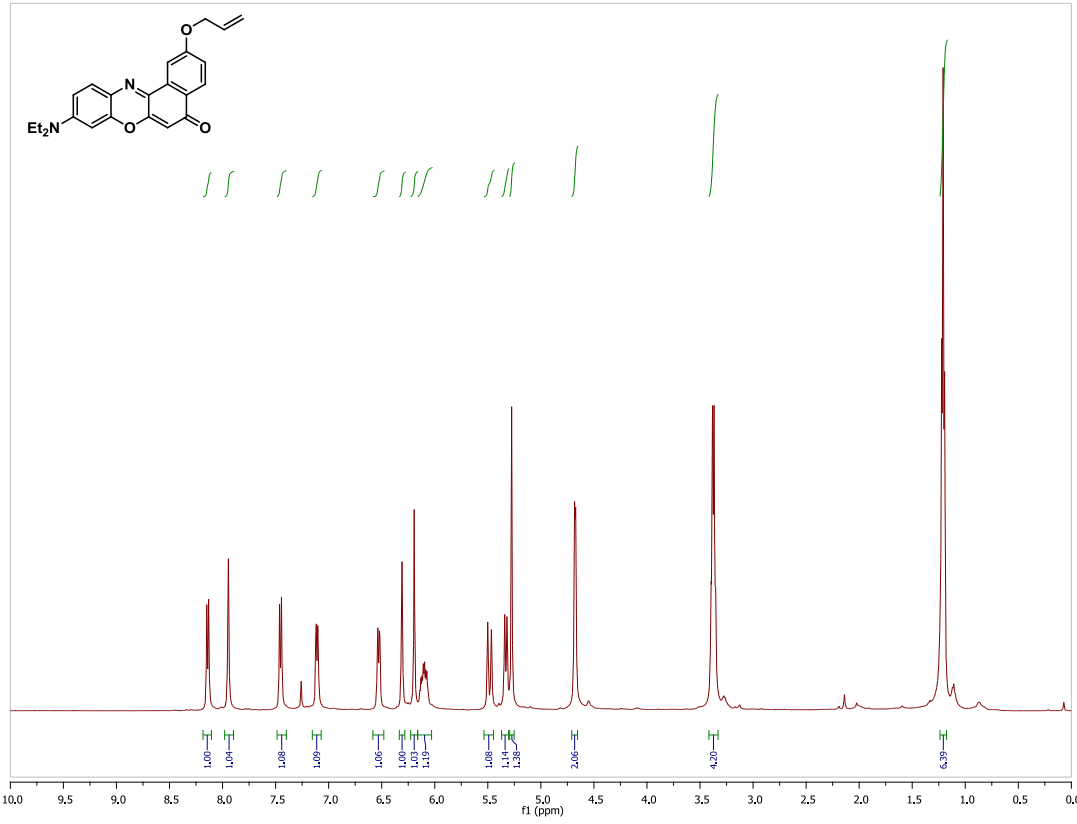
Et2N
O
N
O
O
1.00
1.04
1.08
1.09
1.06
1.00
1.03
1.19
1.08
1.14
1.38
2.06
4.20
6.39
f1 (ppm)

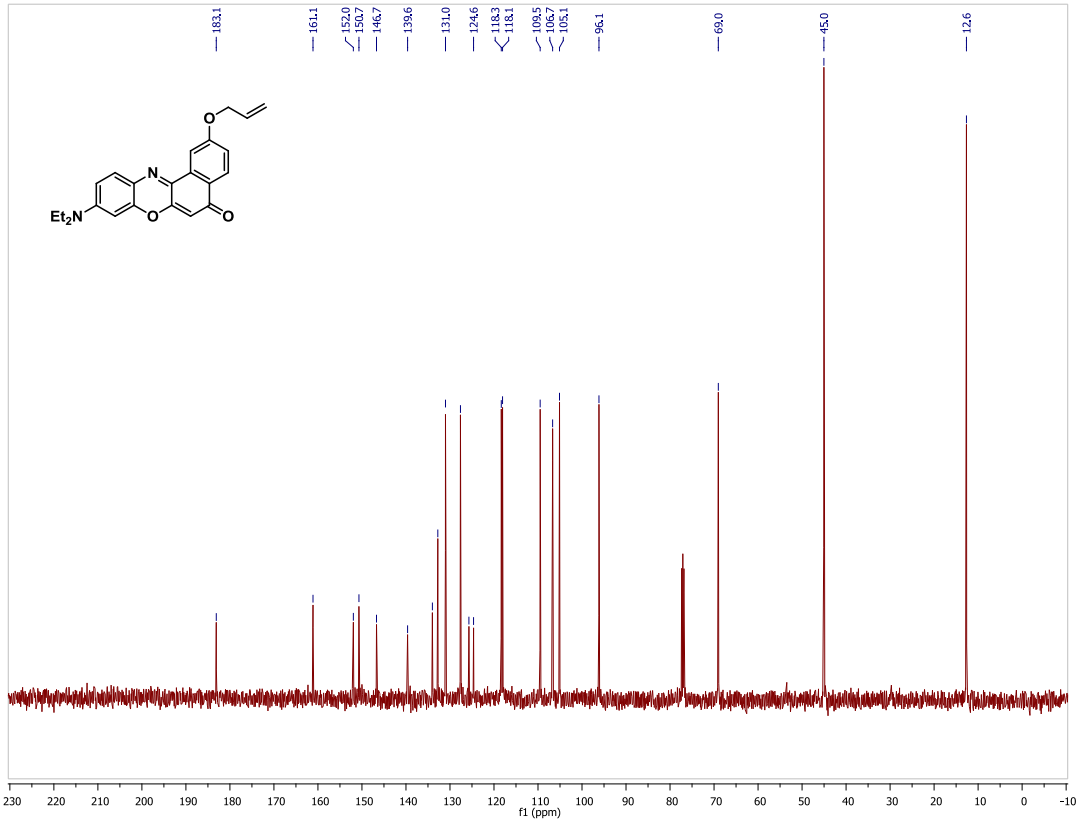
183.1
161.1
152.0
150.7
146.7
139.6
131.0
124.6
118.3
118.1
109.5
106.7
105.1
96.1
69.0
45.0
12.6
Et2N
O
N
O
O
f1 (ppm)

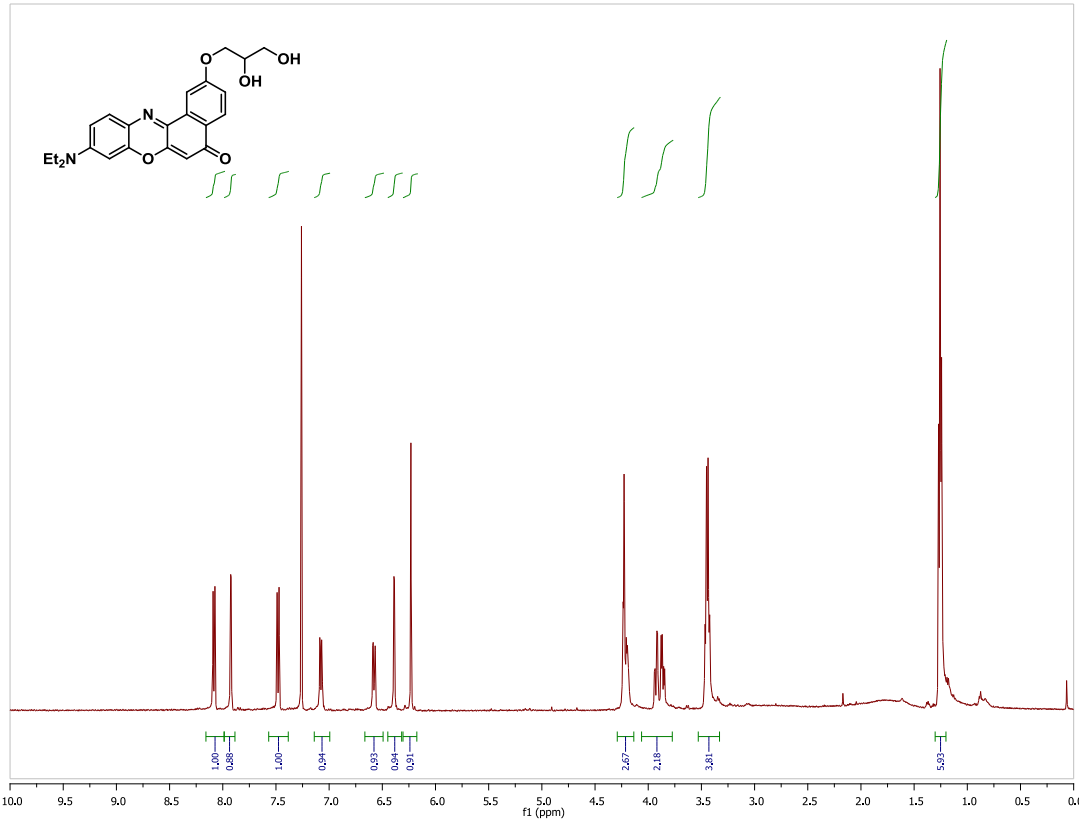
OH
OH
Et2N
1.00
0.88
1.00
0.94
0.93
0.94
0.91
2.67
2.18
3.81
5.93
f1 (ppm)

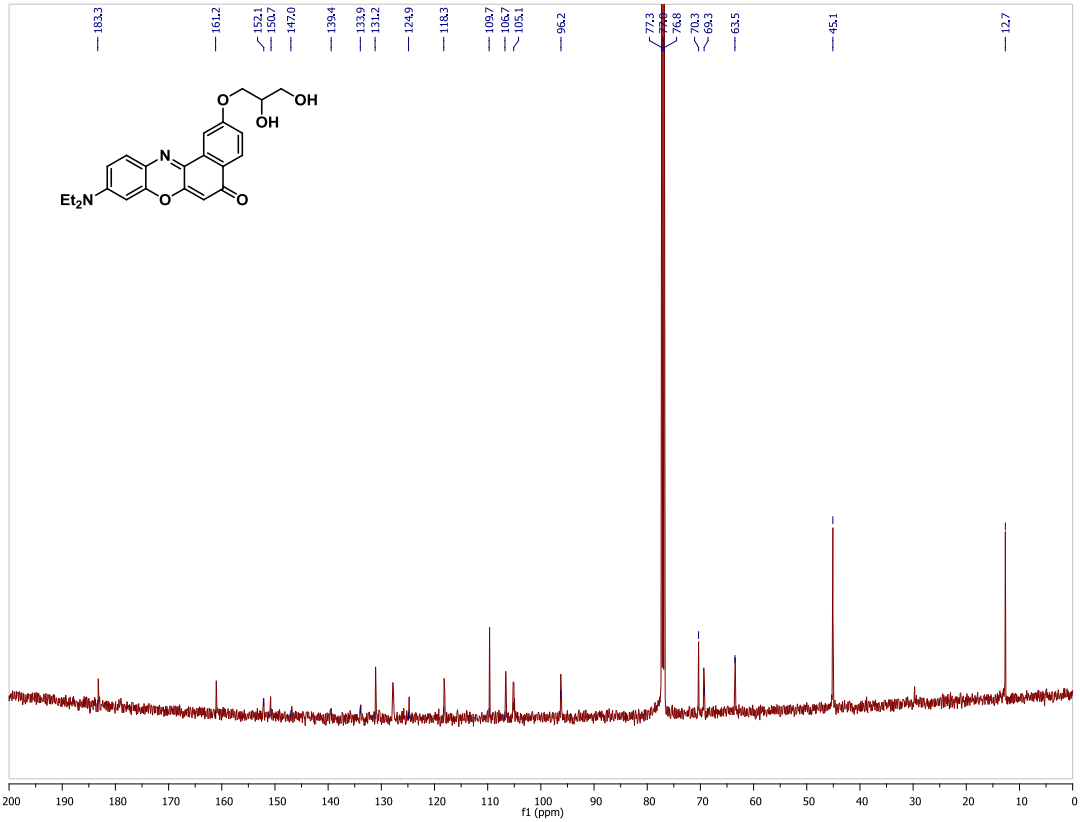
183.3
161.2
152.1
150.7
147.0
139.4
133.9
131.2
124.9
118.3
109.7
106.7
105.1
96.2
77.3
76.8
70.3
69.3
63.5
45.1
12.7
OH
OH
N
O
O
Et2N
O
200 190 180 170 160 150 140 130 120 110 100 90 80 70 60 50 40 30 20 10 0
f1 (ppm)

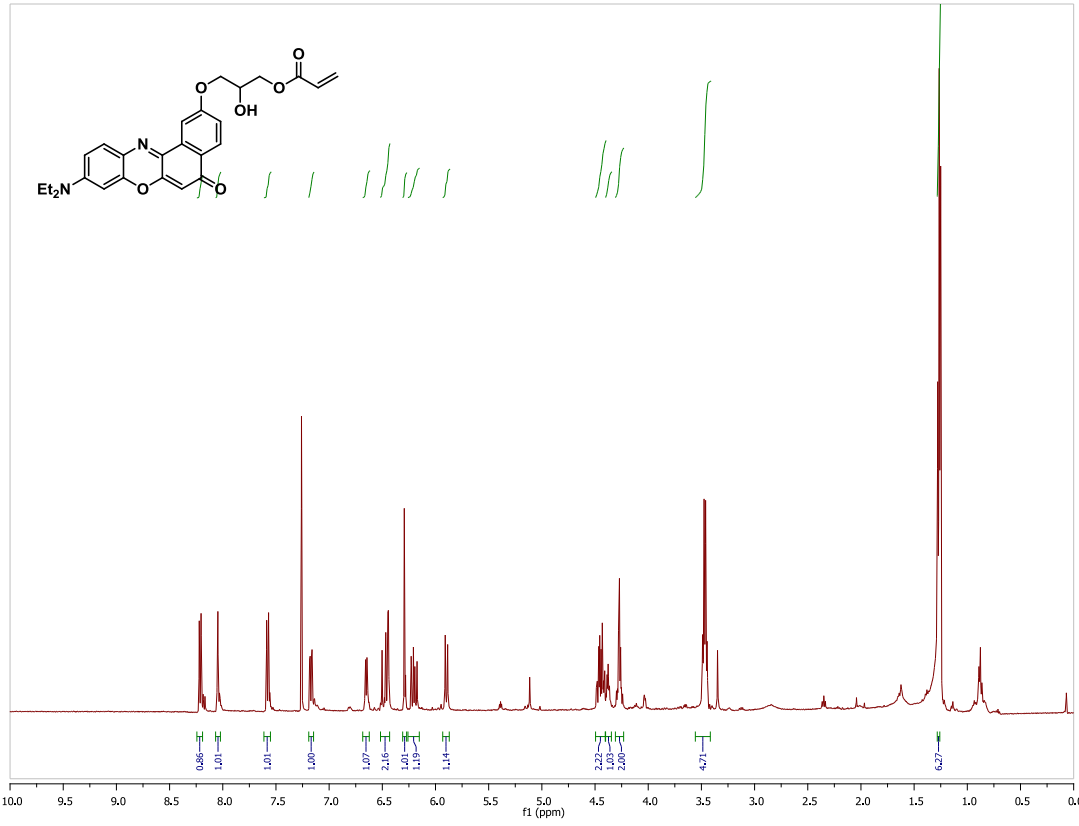
O
O
OH
O
N
O
Et2N
O
0.86
1.01
1.01
1.00
1.07
2.16
1.01
1.19
1.14
2.22
1.03
2.08
4.71
6.27
10.0 9.5 9.0 8.5 8.0 7.5 7.0 6.5 6.0 5.5 5.0 4.5 4.0 3.5 3.0 2.5 2.0 1.5 1.0 0.5 0.0
f1 (ppm)

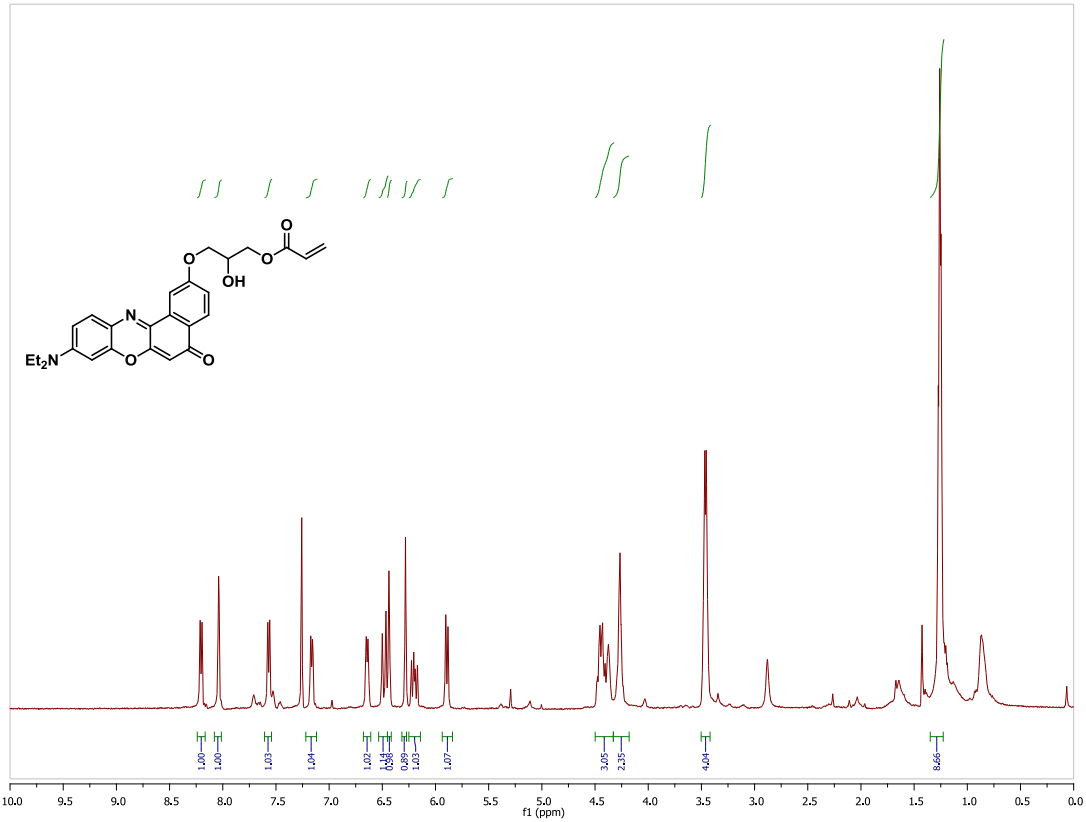
Et2N
O
OH
N
O
O
O
1.00
1.00
1.03
1.04
1.02
1.14
0.98
0.89
1.03
1.07
3.05
2.35
4.04
8.66
f1 (ppm)

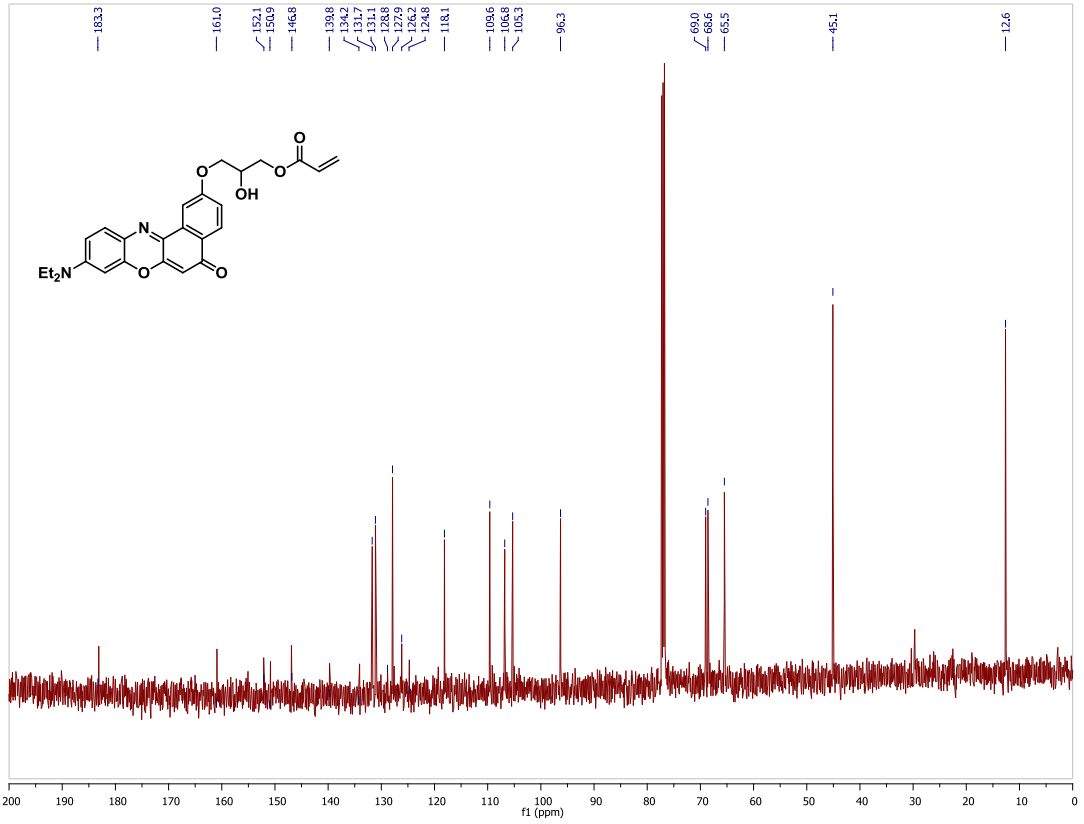
183.3
161.0
152.1
150.9
146.8
139.8
134.2
131.7
131.1
128.8
127.9
126.2
124.8
118.1
109.6
106.8
105.3
96.3
69.0
68.6
65.5
45.1
12.6
Et2N
O
OH
N
O
O
O
f1 (ppm)

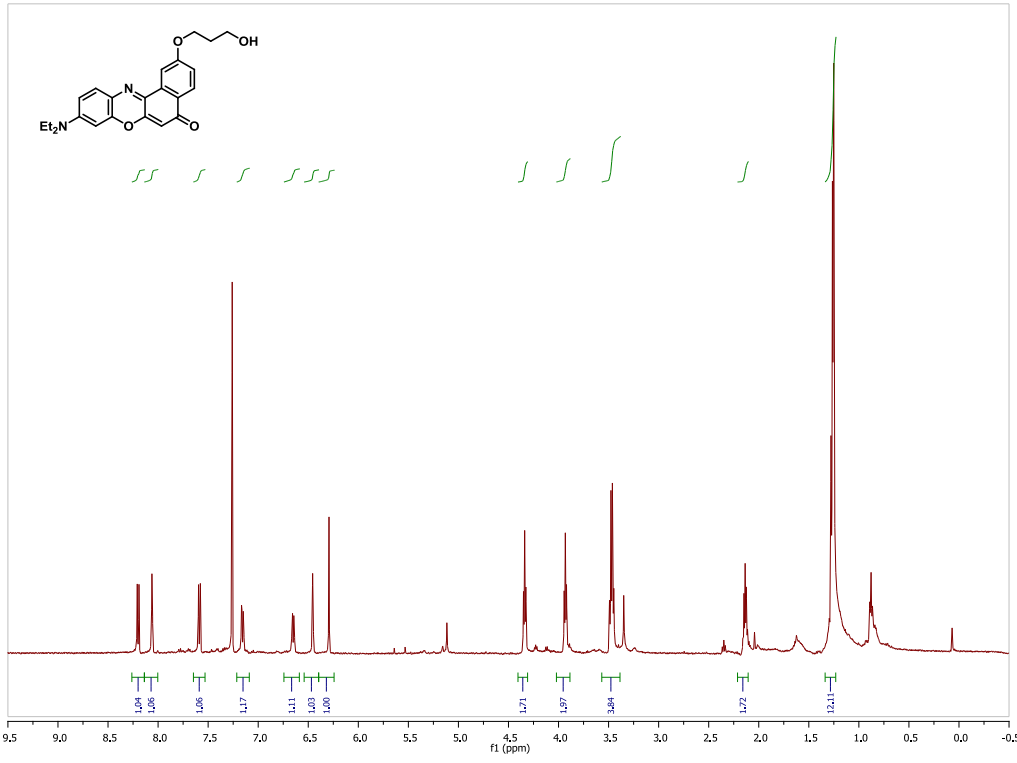
O
OH
N
Et2N
O
O
1.04
1.06
1.06
1.17
1.11
1.03
1.00
1.71
1.97
3.84
1.72
12.11
9.5 9.0 8.5 8.0 7.5 7.0 6.5 6.0 5.5 5.0 4.5 4.0 3.5 3.0 2.5 2.0 1.5 1.0 0.5 0.0 -0.5
f1 (ppm)

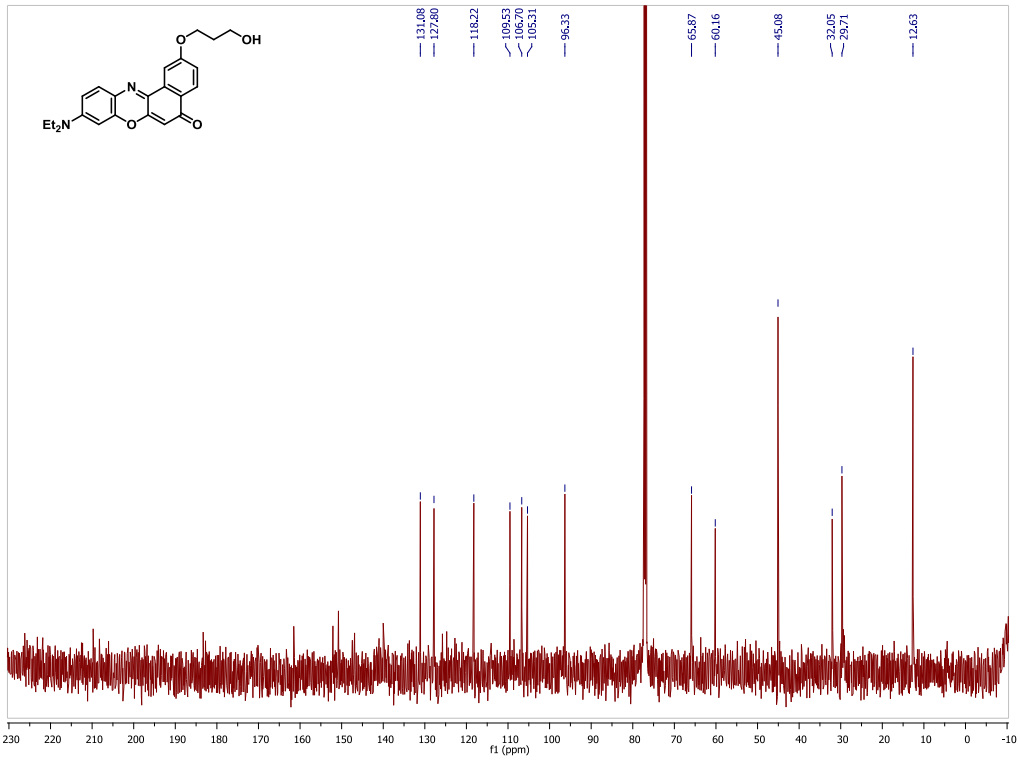
O
OH
N
Et2N
O
O
131.08
127.80
118.22
109.53
106.70
105.31
96.33
65.87
60.16
45.08
32.05
29.71
12.63
230 220 210 200 190 180 170 160 150 140 130 120 110 100 90 80 70 60 50 40 30 20 10 0 -10
f1 (ppm)

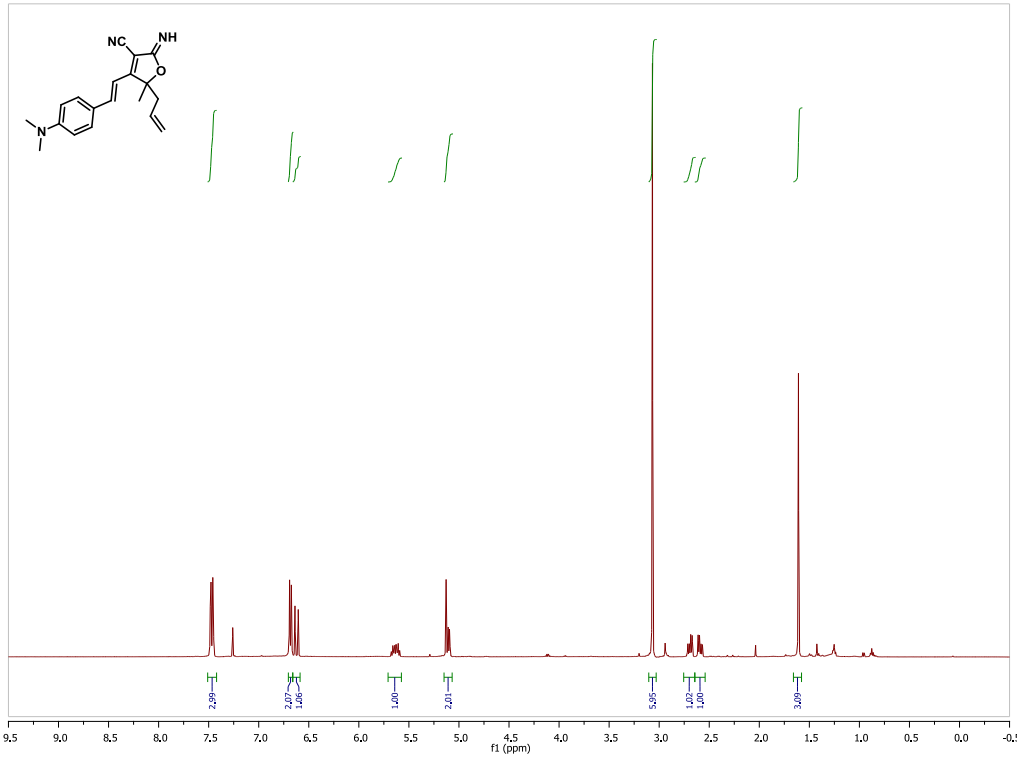
NC
NH
O
N
2.99
2.07
1.26
1.00
2.01
5.95
1.02
1.00
3.09
f1 (ppm)

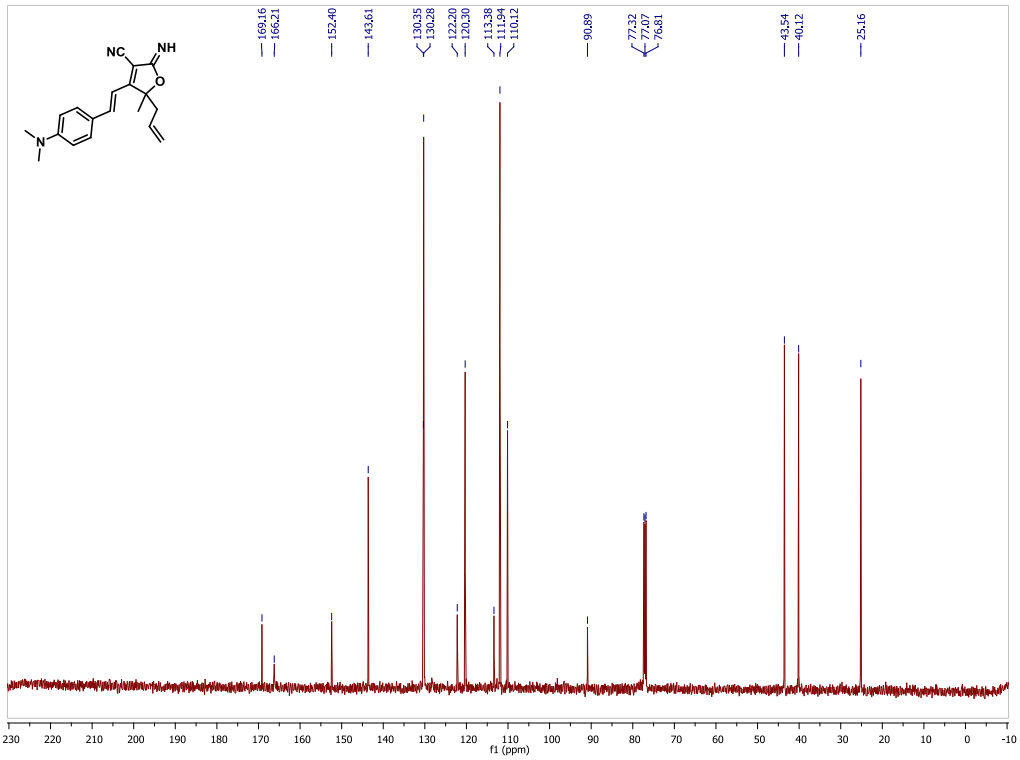
NC
NH
O
N
169.16
166.21
152.40
143.61
130.35
130.28
122.20
120.30
113.38
111.94
110.12
90.89
77.32
77.07
76.81
43.54
40.12
25.16
f1 (ppm)

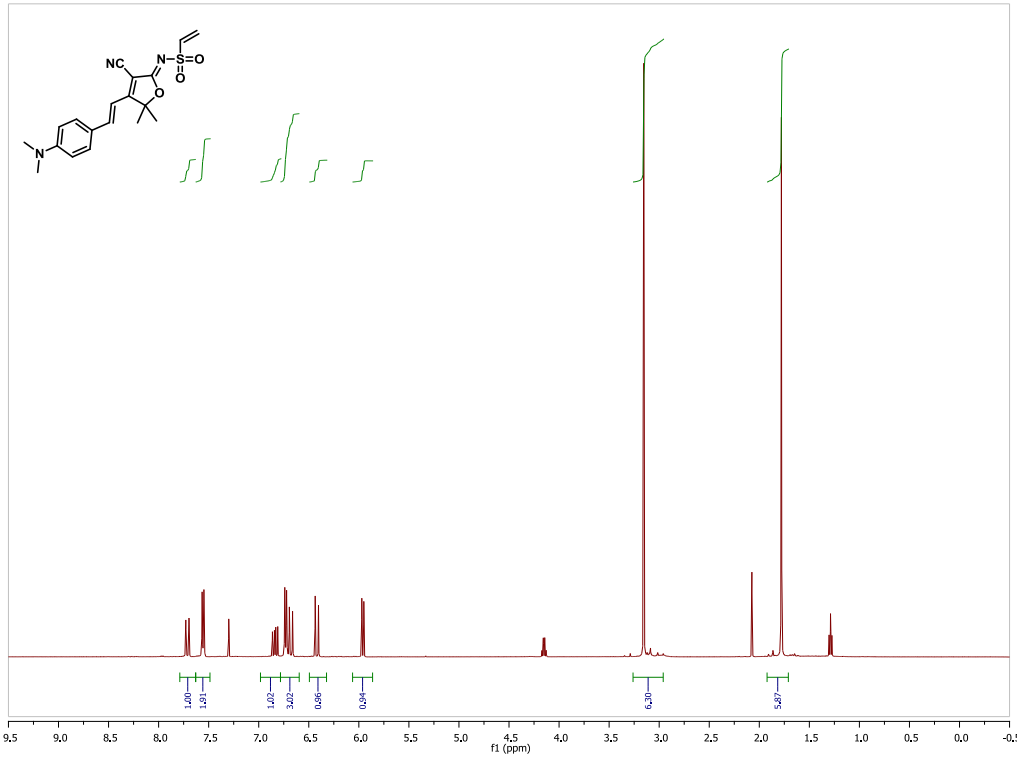
NC
N
S
O
O
O
N
1.00
1.91
1.02
3.02
0.96
0.94
6.20
5.87
9.5 9.0 8.5 8.0 7.5 7.0 6.5 6.0 5.5 5.0 4.5 4.0 3.5 3.0 2.5 2.0 1.5 1.0 0.5 0.0 -0.5
f1 (ppm)

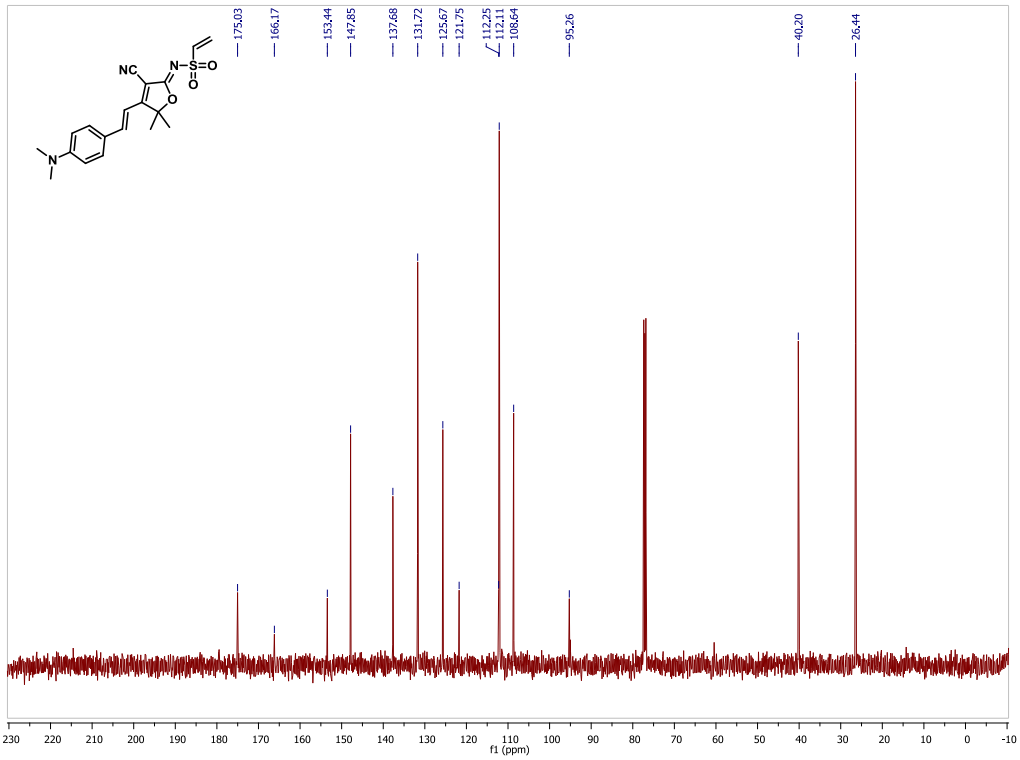
175.03
166.17
153.44
147.85
137.68
131.72
125.67
121.75
112.25
112.11
108.64
95.26
40.20
26.44
NC
N
S
O
O
O
N
230 220 210 200 190 180 170 160 150 140 130 120 110 100 90 80 70 60 50 40 30 20 10 0 -10
f1 (ppm)

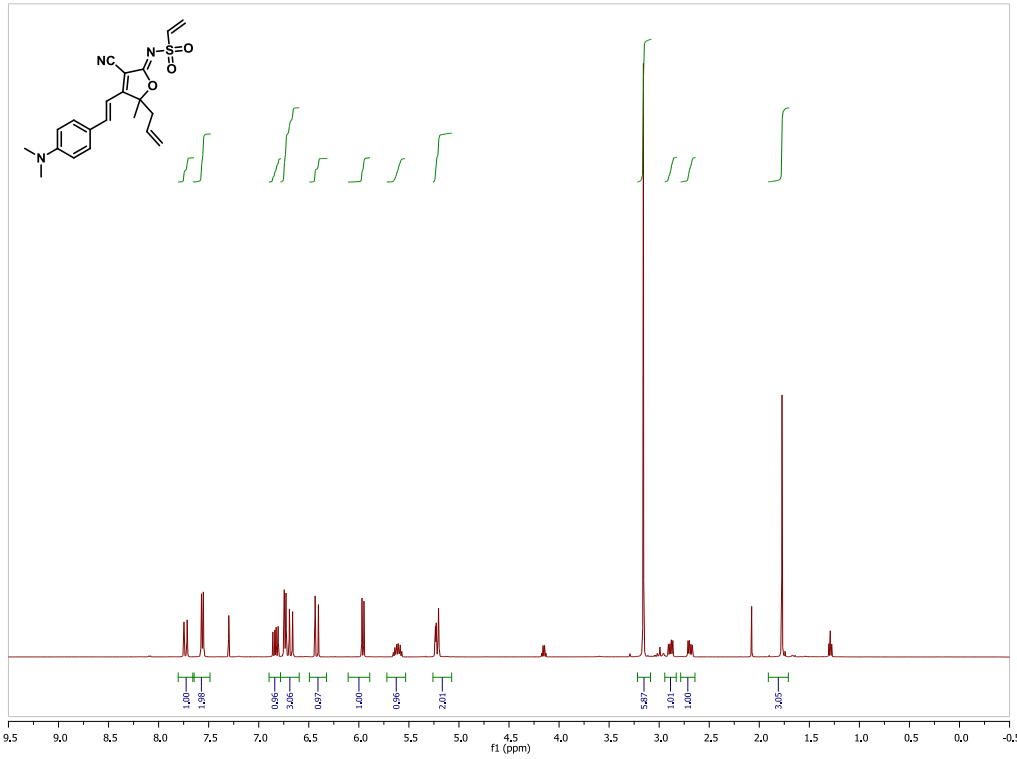
NC
N
S
O
O
O
N
1.00
1.98
0.96
3.06
0.97
1.00
0.96
2.01
5.87
1.01
1.00
3.05
9.5
9.0
8.5
8.0
7.5
7.0
6.5
6.0
5.5
5.0
4.5
4.0
3.5
3.0
2.5
2.0
1.5
1.0
0.5
0.0
-0.5
f1 (ppm)

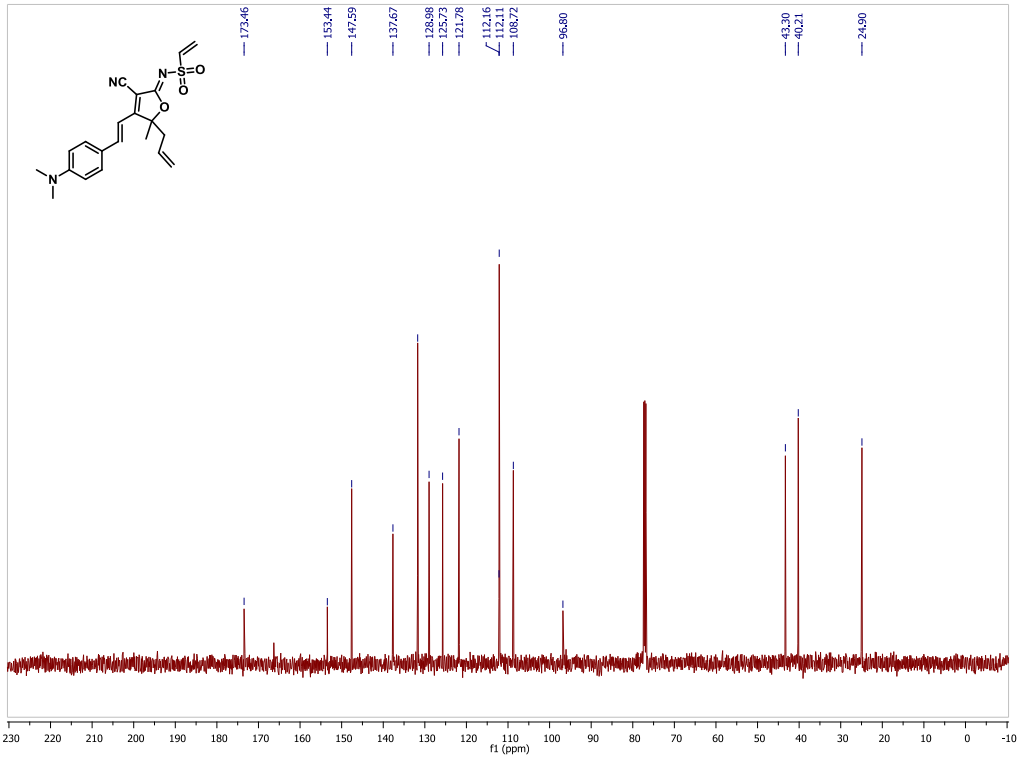
173.46
153.44
147.59
137.67
128.98
125.73
121.78
112.16
112.11
108.72
96.80
43.30
40.21
24.90
NC
N
S
O
O
O
N
230
220
210
200
190
180
170
160
150
140
130
120
110
100
90
80
70
60
50
40
30
20
10
0
-10
f1 (ppm)

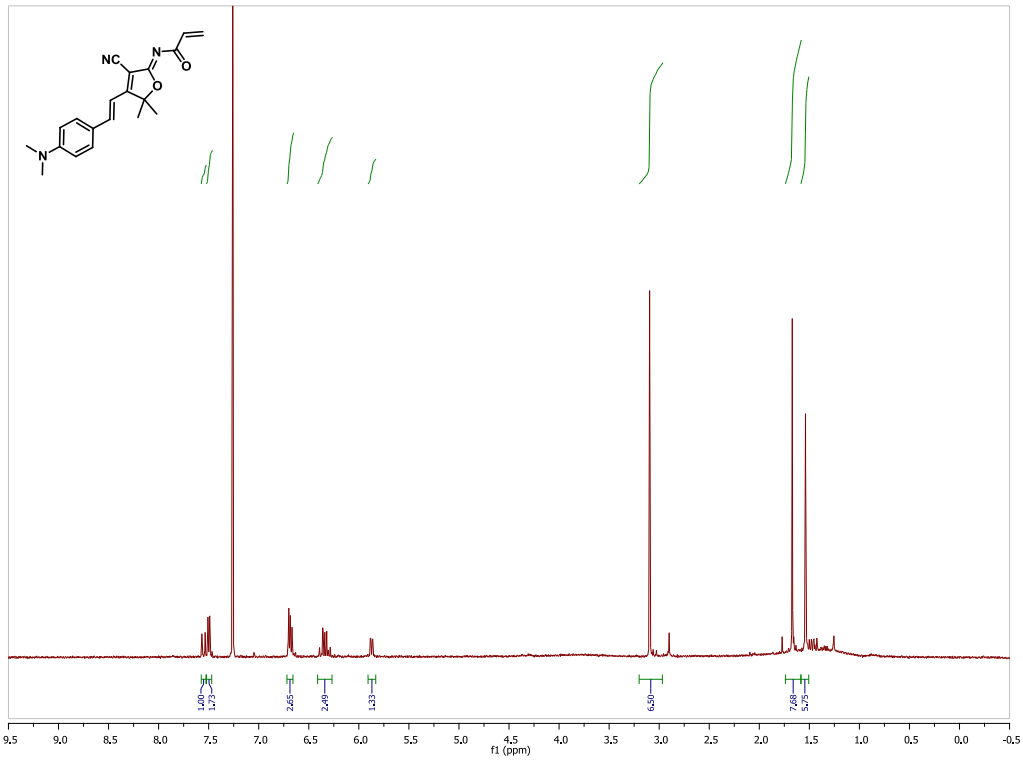
NC
N
O
O
N
1.40
1.73
2.65
2.49
1.33
6.50
7.68
5.75
f1 (ppm)

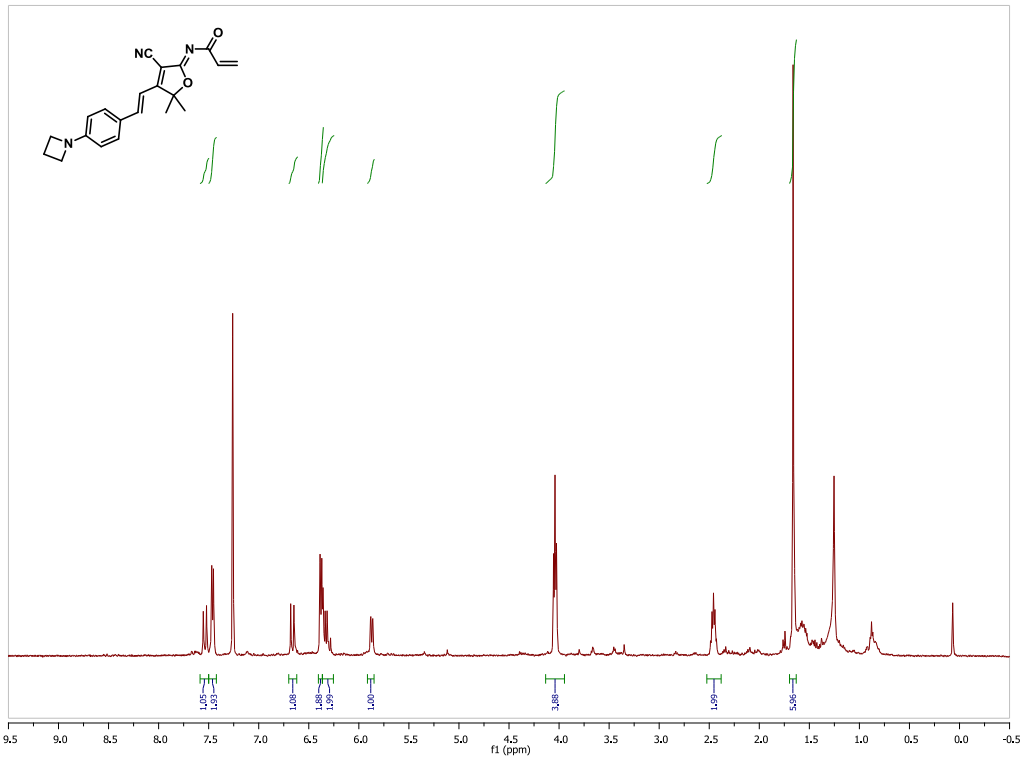
NC
N
O
O
N
1.05
1.03
1.08
1.88
1.99
1.00
3.88
1.93
5.96
f1 (ppm)

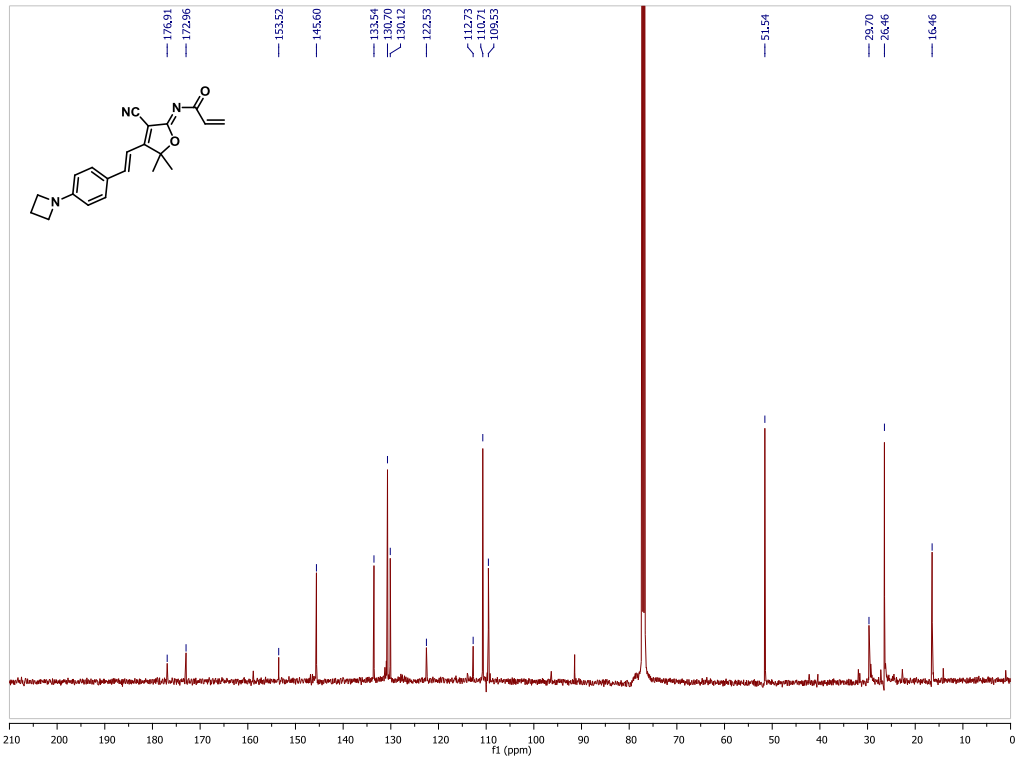
176.91
172.96
153.52
145.60
133.54
130.70
130.12
122.53
112.73
110.71
109.53
51.54
29.70
26.46
16.46
NC
N
O
O
N
f1 (ppm)

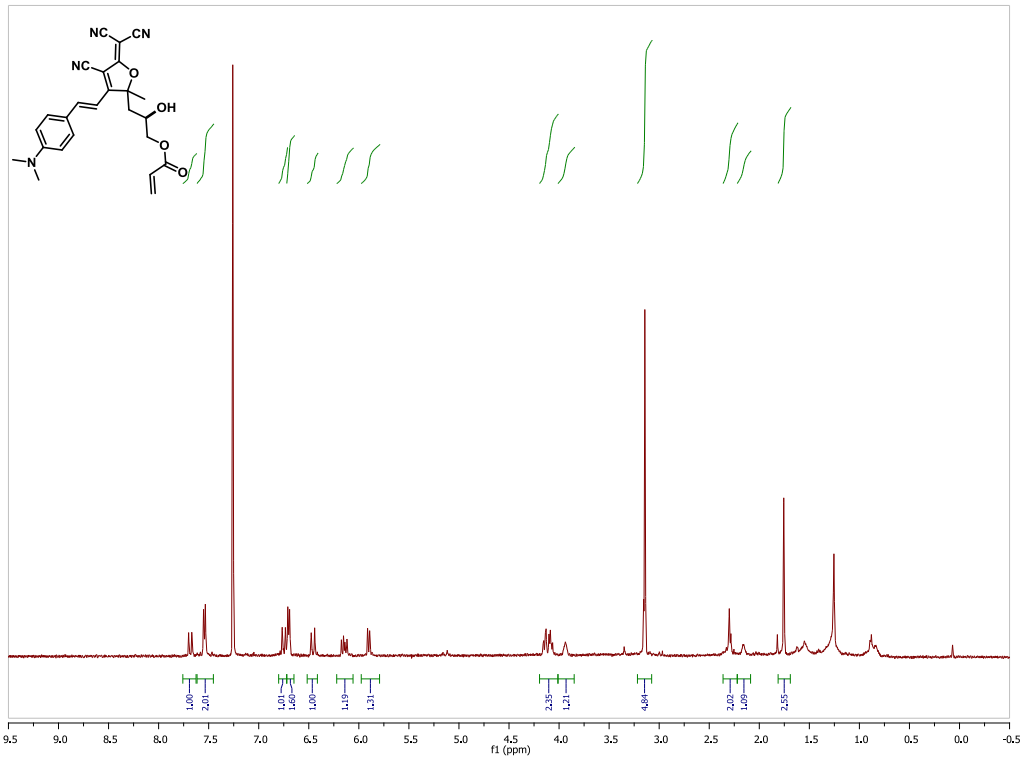
NC
CN
NC
O
OH
N
O
O
1.00
2.01
1.01
1.60
1.00
1.19
1.31
2.35
1.21
4.84
2.02
1.09
2.55
f1 (ppm)

APPENDIX II: Copyright Permissions

Chapter 1 original source:

Chapter 3 original source:

VITA

NAME: Matthew J. T. O'Connor

EDUACTION: B.S., Biochemistry, Northern Illinois University, DeKalb, IL, 2007

M.S., Organic Chemistry, Northern Illinois University, DeKalb, IL, 2010

Ph.D., Organic Chemistry, University of Illinois at Chicago, Chicago, IL, 2015

TEACHING： Department of Chemistry, Northern Illinois University, DeKalb, IL
General Chemistry, and General Chemistry Laboratory for Undergraduates, 2004-2006

Department of Chemistry, University of Illinois at Chicago, Chicago, IL
Organic Chemistry, and Organic Chemistry Laboratory for Undergraduates, 2010-2015

PUBLICATIONS: **Matthew J. O'Connor**, Chunrui Sun, Xinyu Guan, Venkata Sabbasani and Daesung Lee* "Sequential 1,4-/1,2-Addition of Lithiumtrimethylsilydiazomethane onto Cyclic Enones to Induce C–C Fragmentation and N–Li Insertion" *Angew. Chem., Int. Ed.* **2016**, *55*, 2222.

Matthew J. O'Connor, Chunrui Sun, Daesung Lee* "Synthesis of Amathaspiramides via Aminocyanation of Enoates" *Angew. Chem., Int. Ed.* **2015**, *54*, 9963.

Shu-Lin Liu, Ren Sheng, **Matthew J. O'Connor**, Yang Cui, Youngdae Yoon+, Svetlana Kurilova, Daesung Lee*, and Wonhwa Cho* "Simultaneous In Situ Quantification of Two Cellular Lipid Pools Using Orthogonal Fluorescent Sensors" *Angew. Chem., Int. Ed.* **2014**, *52*, 14387.

Chunrui Sun, **Matthew J. O'Connor**, Daesung Lee*, Donald J. Wink, and Robert D.Milligan "Formal Aminocyanation of α,β-Unsaturated Cyclic Enones as an Efficinet Entry to the Synthesis of α-Amino Ketones" *Angew. Chem., Int. Ed.* **2014**, *53*, 3197.

Huaqing Liu, **Matthew J. O'Connor**, Chunrui Sun, Donald J. Wink, and Daesung Lee* "Sequential Reactions of Trimethylsilyldiazomethane with Carbonyls & Tethered Alkenes Catalyzed by Lewis Bases" *Org. Lett.* **2013**, *15*, 2974.

Sai, K. K. S.; **O'Connor, M. J.**; Klumpp, D. A. "Aza-Nazarov Cyclization Cascades." Tetrahedron Lett. **2011**, *52*, 2195.

O'Connor, M. J.; Boblak, K. N.; Spitzer, A. D; Gucciardo, P. A.; Baumann, A. M.; Peter, J. W.; Chen, C. Y.; Ronald Peter, R.; Mitton, A. A.; Klumpp, D. A..

"Condensations of aryl trifluoromethyl ketones with arenes in acidic media". *Tetrahedron Letters*. **2010**. *51*, 4984.

O'Connor, Matthew. J.; Boblak, Ken. N.; Topinka, M. J.; Kindelin, P. J.; Briski, J. M.; Zheng, C.; Klumpp, D. A. "Superelectrophiles and the Effects of Trifluoromethyl Substituents". *J. Am. Chem. Soc.* **2010**. *132*, 3266.

Zhang, Y.; **O'Connor, M.**; Esteves, P.; de Almeida, L.; Klumpp, D.; "Aza-Nazarov Reaction and the Role of Superelectrophiles". *Organic Letters*. **2007**, *9*, 3085.

PRESENTATIONS: **O'Connor, M.**; Sun, C.; Lee, D. "Synthesis of Amathaspiramides via Aminocyanation of Enoates." Abstracts of Papers, Poster Presentation, 6th Chicago Organic Symposium, Chicago, IL 60607, **2015**.

O'Connor, M.; Sun, C.; Lee, D. "Pyrazoline and Pyrazole Synthesis Using Lithiumtrimethylsilyldiazomethane." Abstracts of Papers, Poster Presentation, 5th Chicago Organic Symposium, Notre Dame, IN 46556, **2014**.

O'Connor, M.; Sun, C.; Lee, D. "Diastereoselective [3+2] Dipolar Cycloadditions with Lithiumtrimethylsilyldiazomethane as an Activated Dipole." Abstracts of Papers, Poster Presentation, 4th Chicago Organic Symposium, Chicago, IL, **2012**.

O'Connor, M. J.; Klumpp, D. A.; Zhang, Y.; Kindelin, P. J.; Esteves, P. M.; de Almeida, L. S. "Superacid-catalyzed Aza-Nazarov Reactions." Abstract of Papers, 233rd National Meeting of the American Chemical Society, Chicago, IL, March, **2007**; Abstract ORGN 172.

O'Connor, M. J.; Klumpp, D. A.; Zhang, Y.; de Almeida, L. S. Esteves, P. M."Superacid-catalyzed Aza-Nazarov Reactions."; Abstracts of Papers, Joint Meeting of the Eighteenth Annual Argonne Symposium for Undergraduates in Science, Engineering, and Mathmatics & The Central States Universities, Incorporated Research Conference; Argonne National Lab, Argonne, IL; **2007**; Abstract 12.

HONORS:

Peer Orientation Leader, *UIC*, **2010-2013**
Kevin Cull Memorial Teaching Award, *NIU*, **2009-2010**
Outstanding Undergraduate Research Award, *NIU*, **2007-2008**
Trustee Leadership Scholar, *ECC*, **2003-2004**